POLISH PUBLICATIONS IN MEDITERRANEAN ARCHAEOLOGY 10

Marta Osypińska and Piotr Osypiński

KOBS, AUROCHS AND CLAMS

Human Behavior in Late Pleistocene sub-Saharan Africa
The Middle Stone Age in the Affad Basin, Sudan

PEETERS

KOBS, AUROCHS AND CLAMS

POLISH PUBLICATIONS IN MEDITERRANEAN ARCHAEOLOGY 10

KOBS, AUROCHS AND CLAMS

Human Behavior in Late Pleistocene sub-Saharan Africa

The Middle Stone Age in the Affad Basin, Sudan

By

Marta OSYPIŃSKA, Piotr OSYPIŃSKI

with the contribution of

Sallie BUROUGH, Krzysztof KIERSNOWSKI, Michał KUC, Lenka LISA, Katarzyna PYŻEWICZ, Jerzy RACZYK, Krzysztof RĘKAS, Robert RYNDZIEWICZ, Anne SKINNER, Karol STANDZIKOWSKI, Paweł WIKTOROWICZ

PEETERS
LEUVEN – PARIS – BRISTOL, CT.
2025

The open access version of this book has been made possible thanks to funding from the University of Wrocław IDUB program.

Series Editor: Iwona Zych
Volume Editor: Iwona Zych
Cover photo: Michał Sita

A catalogue record for this book is available from the Library of Congress.

ISBN 978-90-429-5419-9
eISBN 978-90-429-5420-5
doi: 10.2143/9789042954205
D/2025/0602/66

CONTENTS

REFERENCES

Adamiec, G. and Aitken, M. (1998). Dose-rate conversion factors: Update. *Ancient TL*, 16(2), 37–50

Adamson, D.A., Gasse, F., Street, T.A., and Williams, M.A.J. (1980). Late Quaternary history of the Nile. *Nature*, 288, 50–55

Almond, D.C. (1974). The composition of basaltic lavas from Bayuda, Sudan and their place in the cainozoic volcanic history of north-east Africa. *Bulletin Volcanologique*, 38(1), 345–360

Andrefsky, W. (2005). *Lithics: Macroscopic approaches to analysis* (2nd ed.). Cambridge: Cambridge University Press

Arkell, A.J. (1949). *The Old Stone Age in the Anglo-Egyptian Sudan*. Khartoum: Sudan Antiquities Service

Arnold, L.J., Roberts, R.G., Galbraith, R.F., and DeLong, S.B. (2009). A revised burial dose estimation procedure for optical dating of youngand modern-age sediments. *Quaternary Geochronology*, 4(4), 306–325

Bailey, G. and Milner, N. (2008). Molluscan archives from European Prehistory. In A. Antczak and R. Cipriani (eds), *Early human impact on megamolluscs* (=*BAR International Series* 1865) (pp. 111–134). Oxford: Archaeopress

Banks, K.M., Snortland, J.S., Cummings, L.S., Gatto, M.C., and Usai, D. (2015). The Terminal Late Palaeolithic in Wadi Kubbaniya, Egypt. *Antiquity*, 346(89). Retrieved from http://antiquity.ac.uk/projgall/banks346 (accessed: 26.03.2023)

Bar-Yosef, O. and Van Peer, P. (2009). The *chaîne opératoire* approach in Middle Paleolithic archaeology. *Current Anthropology*, 50(1), 103–131

Bar-Yosef Mayer, D.E. (2005). The exploitation of shells as beads in the Palaeolithic and Neolithic of the Levant. *Paléorient*, 31(1), 176–185

Barker, P. (1993). *Techniques of archaeological excavation* (3rd ed.). London: Routledge

Bate, D.M.A. (1951). The mammals from Singa and Abu Hugar. *Fossil Mammals of Africa*, 2, 1–28

Bird, D.W. and O'Connell, J.F. (2006). Behavioral ecology and archaeology. *Journal of Archaeological Research*, 14(2), 143–188

Boëda, E. (1986). *Approche technologique du concept Levallois et évaluation de son champ d'application. Étude de trois gisements saaliens et weichseliens de la France septentrionale* (Ph.D. diss.). Université Paris X-Nanterre

Boëda, E. (1995). Levallois: A volumetric construction, methods, a technique. In H.L. Dibble and O. Bar-Yosef, *The definition and interpretation of Levallois technology* (=*Monographs in World Archaeology* 23) (pp. 41–70). Madison, WI: Prehistory Press

Brain, C.K. (1981). *The hunters or the hunted? An introduction to African cave taphonomy*. Chicago: University of Chicago Press

Broughton, J.M. and Grayson, D.K. (1993). Diet breadth, adaptive change, and the White Mountains faunas. *Journal of Archaeological Science*, 20(3), 331–336

Burow, C. (2019). calc_MinDose(): Apply the (un-)logged minimum age model (MAM) after Galbraith et al. (1999) to a given De distribution. Function version 0.4.4. In S. Kreutzer, C. Burow, M. Dietze, M.C. Fuchs, C. Schmidt, M. Fischer, and J. Friedrich, *Luminescence: Comprehensive Luminescence Dating Data Analysis. R package version 0.9.5*

Butzer, K.W. (1980). The Holocene lake plain of North Rudolph, East Africa. *Physical Geography*, 1(1), 42–58

Cain, C.R. (2006). Human activity suggested by the taphonomy of 60 ka and 50 ka faunal remains from Sibudu Cave. *Southern African Humanities*, 18(1), 241–260

Caton-Thompson, G. (1946). The Levalloisian industries of Egypt. *Proceedings of the Prehistoric Society*, 12, 57–120

Chaix, L., Faure, M., Guerin, C., and Honegger, M. (2000). Kaddanarti, a Lower Pleistocene assemblage from Northern Sudan. In L. Krzyżaniak, K. Kroeper, and M. Kobusiewicz (eds), *Recent research into the Stone Age of Northeastern Africa* (=*Studies in African Archaeology* 7) (pp. 33–46). Poznań: Poznań Archaeological Museum

Chłodnicki, M., Bagińska, D., and Polkowski, P. (2015). *Archaeology of the Sudan: Catalogue of the exhibition in the Poznań Archaeological Museum*. Poznań: Poznań Archaeological Museum

Chmielewski, W. (1968). Early and Middle Palaeolithic sites near Arkin, Sudan. In F. Wendorf (ed.), *The prehistory of Nubia* I (pp. 110–147). Dallas, TX: Fort Burgwin Research Center

Clark, J.L. and Kandel, A.W. (2013). The evolutionary implications of variation in human hunting strategies and diet breadth during the Middle Stone Age of Southern Africa. *Current Anthropology*, 54(S8), S269–S287

Close, A.E. (ed.). (1984). *Cattle-keepers of the Eastern Sahara: The Neolithic of Bir Kiseiba*. Dallas, TX: Department of Anthropology, Southern Methodist University

Cziesla, E., Eickhoff, S., Arts, N., and Winter, D. (eds). (1990). *The big puzzle: International Symposium on Refitting Stone Artefacts, Monrepos, 1987* (=*Studies in Modern Archaeology* 1). Bonn: Holos

Dal Sasso, G., Zerboni, A., Maritan, L., Angelini, I., Compostella, C., Usai, D., and Artioli, G. (2018). Radiocarbon dating reveals the timing of formation and development of pedogenic calcium carbonate concretions in Central Sudan during the Holocene. *Geochimica et Cosmochimica Acta*, 238, 16–35

de Heinzelin, J. (1968a). Geological history of the Nile Valley in Nubia. In F. Wendorf (ed.), *The prehistory of Nubia* I (pp. 19–55). Dallas, TX: Fort Burgwin Research Center

de Heinzelin, J. (1968b). Survey in the Debba-Korti Area. *Kush*, 15, 59–69

Dietze, M., Kreutzer, S., Burow, C., Fuchs, M.C., Fischer, M., and Schmidt, C. (2016). The abanico plot: Visualising chronometric data with individual standard errors. *Quaternary Geochronology*, 31, 12–18

Duller, G.A.T. (2003). Distinguishing quartz and feldspar in single grain luminescence measurements. *Radiation Measurements*, 37(2), 161–165

Estes, R.D. (1974). Social organization of the African Bovidae. In V. Geist and F. Walther (eds), *The behaviour of ungulates and its relation to management: The papers of an international symposium held at the University of Calgary, Alberta, Canada, 2–5 November 1971*, I (pp. 166–205). Morges: International Union for Conservation of Nature and Natural Resources

Falchetti, E. and Mostacci, B. (1993). The Nile lechwe *Kobus megaceros*: PVA factors and guidelines to captive management. *International Zoo Yearbook*, 32(1), 60–69

Fedorowicz, S., Łanczont, M., Mroczek, P., Bogucki, A., Standzikowski, K., Moska, P., Kusiak, J., and Bluszcz, A. (2018). Luminescence dating of the Volochysk section – a key Podolian loess site (Ukraine). *Geological Quarterly*, 62(3), 729–744

Folk, R.L. and Ward, W.C. (1957). Brazos River bar: A study in the significance of grain size parameters. *Journal of Sedimentary Petrology*, 27(1), 3–26

Gagnon, M. and Chew, A.E. (2000). Dietary preferences in extant African Bovidae. *Journal of Mammalogy*, 81(2), 490–511

Galbraith, R.F. and Green, P.F. (1990). Estimating the component ages in a finite mixture. *International Journal of Radiation Applications and Instrumentation. Part D. Nuclear Tracks and Radiation Measurements*, 17(3), 197–206

Gautier, A. (1968). Mammalian remains of the northern Sudan and southern Egypt. In F. Wendorf (ed.), *The prehistory of Nubia* I (pp. 80–99). Dallas, TX: Fort Burgwin Research Center

Gautier, A. (1987). Fishing, fowling and hunting in Late Palaeolithic times in the Nile Valley in Upper Egypt. *Palaeoecology of Africa and Surrounding Islands*, 18, 429–440

Gautier, A. (1988). The final demise of *Bos Ibericus*? *Sahara*, 1, 37–48

Gautier, A., Makowiecki, D., Paner, H., and Van Neer, W. (2012). Palaeolithic big game hunting at HP766 in Wadi Umm Rahau, Northern Sudan. *Journal of African Archaeology*, 10(2), 165–174

Gifford-Gonzalez, D. (1989). Ethnographic analogues for interpreting midified bones: Some cases from East Africa. In R. Bonnichsen and M.H. Sorg (eds), *Bone modification* (pp. 179–246). Orono, ME: Center for the Study of the First Americans, Institute for Quaternary Studies, University of Maine

Ginter, B. and Kozłowski, J.K. (1990). *Technika obróbki i typologia wyrobów kamiennych paleolitu, mezolitu i neolitu* (Processing techniques and typology of Paleolithic, Mesolithic and Neolithic stone objects) (3rd rev. ed.). Warsaw: Państwowe Wydawnictwo Naukowe (in Polish)

Goder-Goldberger, M. (2013). The Khormusan: Evidence for an MSA East African industry in Nubia. *Quaternary International*, 300, 182–194

GROUCUTT, H.S. and BLINKHORN, J. (2013). The Middle Palaeolithic in the desert and its implications for understanding hominin adaptation and dispersal. *Quaternary International*, 300, 1–12

GUÉRIN, G., MERCIER, N., and ADAMIEC, G. (2011). Dose-rate conversion factors: Update. *Ancient TL*, 29(1), 5–8

GUÉRIN, G., MERCIER, N., NATHAN, R., ADAMIEC, G., and LEFRAIS, Y. (2012). On the use of the infinite matrix assumption and associated concepts: A critical review. *Radiation Measurements*, 47(9), 778–785

GUICHARD, J. and GUICHARD, G. (1968). Contributions to the study of the Early and Middle Paleolithic of Nubia. In F. Wendorf (ed.), *The prehistory of Nubia* I (pp. 148–193). Dallas, TX: Fort Burgwin Research Center

HAPPOLD, D. and LOCK, J.M. (2013). The biotic zones of Africa. In J. Kingdon, D. Happold, T. Butynski, M. Hoffmann, M. Happold, and J. Kalina (eds), *Mammals of Africa* I (pp. 57–74). London: Bloomsbury

HODDER, I. and ORTON, C. (1976). *Spatial analysis in archaeology*. Cambridge: Cambridge University Press

HONG, D.G., KIM, M.J., CHOI, J.H., EL-FARAMAWY, N.A., and GÖKSU, H.Y. (2006). Equivalent dose determination of single aliquot regenerative-dose (SAR) protocol using thermoluminescence on heated quartz. *Nuclear Instruments and Methods in Physics Research Section B: Beam Interactions with Materials and Atoms*, 243(1), 174–178

INIZAN, M.-L., ROCHE, H., and TIXIER, J. (1992). *Technology of knapped stone* (=*Préhistoire de la pierre taillée* 3). Meudon: CREP

INMAN, D.L. (1952). Measures for describing the size distribution of sediments. *Journal of Sedimentary Research*, 22(3), 125–145

ISSMER, K. (2000). Optical methods in the grain-size analysis of fine-grained sediments. *Geological Quarterly*, 44(2), 205–210

KALICKI, T. and OLSZAK, I. (2016). Supplementary materials for: P. Osypiński, M.W. Morley, M. Osypińska, A.M. Kotarba-Morley, Affad 23: Settlement structures and palaeoenvironments in the Terminal Pleistocene of the Middle Nile Valley, Sudan. *Antiquity*, 90(352), 894–913

KAPLAN, H. and HILL, K. (1992). The evolutionary ecology of food acquisition. In E.A. Smith and B. Winterhalder (eds), *Evolutionary ecology and human behavior* (pp. 167–201). New York: Aldine de Gruyter

KELLY, R.L. (1995). *The foraging spectrum: Diversity in hunter-gatherer lifeways*. Washington, DC: Smithsonian Institution Press

KINGDON, J., HAPPOLD, D., BUTYNSKI, T., HOFFMANN, M., HAPPOLD, M., and KALINA, J. (eds). (2013). *Mammals of Africa* I–VI. London: Bloomsbury

KUC, M. (2017). *Chronologia i lito-strukturalny zapis zmian środowiska w osadach wydm dorzecza Baryczy między Żmigrodem a Miliczem* (Chronology and litho-structural record of environmental changes in the dune sediments of the Barycz River basin between Zmigrod and Milicz) (unpubl. Ph.D. diss.). University of Wrocław (in Polish)

ŁANCZONT, M., MADEYSKA, T., BOGUCKI, A., MROCZEK, P., HOŁUB, B., ŁĄCKA, B., FEDOROWICZ, S., NAWROCKI, J., FRANKOWSKI, Z., and STANDZIKOWSKI, K. (2015). Środowisko abiotyczne paleolitycznej ekumeny strefy pery- i metakarpackiej (Abiotic environment of the Paleolithic ecumene of the Peri- and Metacarpathic zones). In M. Łanczont and T. Madeyska (eds), *Paleolityczna ekumena strefy pery- i metakarpackiej* (pp. 55–458). Lublin: Wydawnictwo Uniwersytetu Marii Curie-Skłodowskiej (in Polish)

LASOTA-MOSKALEWSKA, A. (2005). *Zwierzęta udomowione w dziejach ludzkości* (Domesticated animals in human history). Warsaw: Wydawnictwa Uniwersytetu Warszawskiego (in Polish)

LASOTA-MOSKALEWSKA, A. (2008). *Archeozoologia: ssaki* (Archaeozoology: Mammals). Warsaw: Wydawnictwa Uniwersytetu Warszawskiego (in Polish)

LEPLONGEON, A., GODER-GOLDBERGER, M., and PLEURDEAU, D. (eds). (2020). *Not just a corridor: Human occupation of the Nile Valley and neighbouring regions between 75,000 and 15,000 years ago* (=*Natures en sociétés* 3). Paris: Publications scientifiques du Muséum

LEROI-GOURHAN, A. (1964). *Le geste et la parole*. Paris: Albin Michel

LINSEELE, V. (2004). Size and size change of the African aurochs during the Pleistocene and Holocene. *Journal of African Archaeology*, 2(2), 165–185

LOMBARD, M. (2012). Thinking through the Middle Stone Age of sub-Saharan Africa. *Quaternary International*, 270, 140–155

LOMBARD, M. and CLARK, J.L. (2008). Variability and change in Middle Stone Age hunting behaviour: Aspects from the lithic and faunal records. In S. Badenhorst, P. Mitchell, and J.C. Driver (eds), *Animals and people: Archaeozoological papers in honour of Ina Plug* (=*BAR International Series* 1849) (pp. 46–56). Oxford: Archaeopress

LUPO, K.D. (2007). Evolutionary foraging models in zooarchaeological analysis: Recent applications and future challenges. *Journal of Archaeological Research*, 15(2), 143–189

LUPO, K.D. and SCHMITT, D.N. (2005). Small prey hunting technology and zooarchaeological measures of taxonomic diversity and abundance: Ethnoarchaeological evidence from Central African forest foragers. *Journal of Anthropological Archaeology*, 24(4), 335–353

LYMAN, R.L. (1987). Archaeofaunas and butchery studies: A taphonomic perspective. *Advances in Archaeological Method and Theory*, 10, 249–337

LYMAN, R.L. (1994). *Vertebrate taphonomy*. Cambridge: Cambridge University Press

MACDONALD, D.W. (1984). *The encyclopaedia of mammals*. London: Allen & Unwin

MAREAN, C.W., ABE, Y., FREY, C.J., and RANDALL, R.C. (2000). Zooarchaeological and taphonomic analysis of the Die Kelders Cave 1 Layers 10 and 11 Middle Stone Age larger mammal fauna. *Journal of Human Evolution*, 38(1), 197–233

MARKS, A.E. (1968a). The Halfan industry. In F. Wendorf (ed.), *The prehistory of Nubia* I (pp. 392–460). Dallas, TX: Fort Burgwin Research Center

MARKS, A.E. (1968b). The Khormusan: An Upper Pleistocene industry in Sudanese Nubia. In F. Wendorf (ed.), *The prehistory of Nubia* I (pp. 315–391). Dallas, TX: Fort Burgwin Research Center

MARKS, A.E. (1968c). The Mousterian industries of Nubia. In F. Wendorf (ed.), *The prehistory of Nubia* I (pp. 194–314). Dallas, TX: Fort Burgwin Research Center

MARKS, A.E. (1968d). The Sebilian industry of the Second Cataract. In F. Wendorf (ed.), *The prehistory of Nubia* I (pp. 461–531). Dallas, TX: Fort Burgwin Research Center

MARKS, A.E., HAYS, T.R., and DE HEINZELIN, J. (1968). Preliminary report of the Southern Methodist University Expedition in the Dongola Reach. *Kush*, 15, 165–192

MARKS, A.E. and MOHAMMED-ALI, A.S. (1991). *The late prehistory of the eastern Sahel: The Mesolithic and Neolithic of Shaqadud, Sudan*. Dallas, TX: Southern Methodist University Press

MARTÍNEZ-NAVARRO, B., KAROUI-YAAKOUB, N., OMS, O., AMRI, L., LÓPEZ-GARCÍA, J.M., ZERAI, K., … PALMQVIST, P. (2014). The early Middle Pleistocene archeopaleontological site of Wadi Sarrat (Tunisia) and the earliest record of *Bos primigenius*. *Quaternary Science Reviews*, 90, 37–46

MARTÍNEZ-NAVARRO, B., PÉREZ-CLAROS, J.A., PALOMBO, M.R., ROOK, L., and PALMQVIST, P. (2007). The Olduvai buffalo *Pelorovis* and the origin of *Bos*. *Quaternary Research*, 68(2), 220–226

MEADOW, R.H. (1980). Animal bones: Problems for the archaeologist together with some possible solutions. *Paléorient*, 6(1), 65–77

MEDANI, A.H. (1975). Nubian Sandstone Formation (Sudan): Distribution and typical section. *AAPG Bulletin*, 59(2), 345–347

MEJDAHL, V. (1979). Thermoluminescence dating: Beta-dose attenuation in quartz grains. *Archaeometry*, 21(1), 61–72

MOHAMMED, A.E. and MOHAMMED, N.Z. (2013). WGS84 to Adindan-Sudan datum transformation manipulated by ITRF96. *International Journal of Multidisciplinary Sciences and Engineering*, 4(5), 60–64

MURRAY, A.S. and WINTLE, A.G. (2000). Luminescence dating of quartz using an improved single-aliquot regenerative-dose protocol. *Radiation Measurements*, 32(1), 57–73

MURRAY, A.S. and WINTLE, A.G. (2003). The single aliquot regenerative dose protocol: Potential for improvements in reliability. *Radiation Measurements*, 37(4), 377–381

NOE-NYGAARD, N., PRICE, T.D., and HEDE, S.U. (2005). Diet of aurochs and early cattle in southern Scandinavia: Evidence from ^{15}N and ^{13}C stable isotopes. *Journal of Archaeological Science*, 32(6), 855–871

NOWAK, R.M. (1999). *Walker's mammals of the world* (6th ed.). Baltimore, MD: Johns Hopkins University Press

OSYPIŃSKA, M. (2003). Faunal remains from the Southern Dongola Reach. In B. Żurawski (ed.), *Survey and excavations between Old Dongola and Ez-Zuma* (=*Nubia* 2; *Southern Dongola Reach Survey* 1) (pp. 490–493). Warsaw: Neriton

Osypińska, M. (2018). *Krowie królestwa: zwierzęta w historii doliny Środkowego Nilu. Studium archeozoologiczne* (Cattle kingdoms: The animals in the history of Middle Nile Valley. Archaeozoological study). Warsaw: Wydawnictwo Instytutu Archeologii i Etnologii Polskiej Akademii Nauk (in Polish)

Osypińska, M. and Osypiński, P. (2003). SDRS Site Gazetteer – Affad 23. In B. Żurawski (ed.), *Survey and excavations between Old Dongola and Ez-Zuma* (=*Nubia* 2; *Southern Dongola Reach Survey* 1) (pp. 270–273). Warsaw: Neriton

Osypińska, M. and Osypiński, P. (2012). Epigones of the Levallois Tradition in the Middle Nile Valley: The first season of a new prehistoric project in Affad, Northern Sudan. *Nyame Akuma*, 78, 17–22

Osypińska, M. and Osypiński, P. (2013). Middle Palaeolithic research in the Middle Nile Valley – 2013 field season in Affad, Northern Sudan. *Nyame Akuma*, 80, 14–21

Osypińska, M. and Osypiński, P. (2015). Levallois Tradition epigones in the Middle Nile Valley: Survey in the Affad basin. *Polish Archaeology in the Mediterranean*, 24(1), 601–626

Osypińska, M. and Osypiński, P. (2016). Animal exploitation and behaviour of the latest Middle Stone Age societies in the Middle Nile Valley: Archaeozoological and taphonomic analysis of Late Pleistocene fauna from the Affad Basin, Sudan. *African Archaeological Review*, 33(2), 107–127

Osypińska, M., Osypiński, P., Bełka, Z., Chłodnicki, M., Wiktorowicz, P., Ryndziewicz, R., and Kubiak, M. (2021). Wild and domestic cattle in the ancient Nile Valley: Marks of ecological change. *Journal of Field Archaeology*, 46(7), 429–447

Osypińska, M., Osypiński, P., Chłodnicki, M., Kuc, M., Wiktorowicz, P., and Ryndziewicz, R. (2020). The PalaeoAffad Project and the prehistory of the Middle Nile. *Archaeologia Polona*, 58, 79–97

Osypiński, P. (2003). Southern Dongola Reach in prehistory. In B. Żurawski (ed.), *Survey and excavations between Old Dongola and Ez-Zuma* (=*Nubia* 2; *Southern Dongola Reach Survey* 1) (pp. 463–467). Warsaw: Neriton

Osypiński, P. (2010). A corpus of lithic raw material from the inventories of the Fourth Cataract. *Gdańsk Archaeological Museum African Reports*, 6, 139–146

Osypiński, P. (2012). The lithic traditions of Late-Pleistocene settlement at Affad, Sudan. In J. Kabaciński, M. Chłodnicki, and M. Kobusiewicz (eds), *Prehistory of northeastern Africa: New ideas and discoveries* (=*Studies in African Archaeology* 11) (pp. 213–221). Poznań: Poznań Archaeological Museum

Osypiński, P. (2014). Prehistory of the Fourth Cataract. In J.R. Anderson and D.A. Welsby (eds), *The Fourth Cataract and beyond: Proceedings of the 12th International Conference for Nubian Studies* (=*British Museum Publications on Egypt and Sudan* 1) (pp. 9–18). Leuven–Paris–Walpole, MA: Peeters

Osypiński, P. (2016). *Najpóźniejsze tradycje lewaluaskie Środkowej Doliny Nilu. Technologia wytwórczości kamiennej na przykładzie mikroregionu Affad w Sudanie* (Latest Levallois traditions in the Middle Nile Valley. The lithic technology on the example of the microregion Affad in Sudan) (unpubl. Ph.D. diss.). Adam Mickiewicz University in Poznań (in Polish)

Osypiński, P. (2020). Upper Nubia and beyond during the Terminal Pleistocene: New premises for the late occurrence of the Middle Stone Age. In A. Leplongeon, M. Goder-Goldberger, and D. Pleurdeau (eds), *Not just a corridor: Human occupation of the Nile valley and neighbouring regions between 75,000 and 15,000 years ago* (=*Natures en sociétés* 3) (pp. 115–137). Paris: Publications scientifiques du Muséum

Osypiński, P., Burrough, S., Skinner, A., and Standzikowski, K. (2021). Re-examining the age of the Affad MSA deposits in the Middle Nile Valley. *Archaeometry*, 63(6), 1405–1420

Osypiński, P., Morley, M.W., Osypińska, M., and Kotarba-Morley, A.M. (2016). Affad 23: Settlement structures and palaeoenvironments in the Terminal Pleistocene of the Middle Nile Valley, Sudan. *Antiquity*, 90(352), 894–913

Osypiński, P. and Osypińska, M. (2016). Optimal adjustment or cultural backwardness? New data on the latest Levallois industries in the Nile Valley. *Quaternary International*, 408, 90–105

Osypiński, P., Osypińska, M., and Gautier, A. (2011). Affad 23, a late Middle Palaeolithic site with refitted lithics and animal remains in the Southern Dongola reach, Sudan. *Journal of African Archaeology*, 9(2), 177–188

Peters, J. (1986). *Osteomorphology and osteometry of the appendicular skeleton of Grant's Gazelle, Gazella granti Brooke, 1872, Bohor Reedbuck, Redunca redunca (Pallas, 1767) and Bushbuck, Tragelaphus scriptus (Pallas, 1766)*. Ghent: Laboratorium, Rijksuniversiteit

PETERS, J. (1989a). Faunal remains and environmental change in Central and Eastern Sudan from Terminal Pleistocene to Middle Holocene times. *Academiae Analecta*, 51(4), 123–148

PETERS, J. (1989b). Osteomorphological features of the appendicular skeleton of gazelles, genus *Gazella* Blainville 1816, bohor reedbuck, *Redunca redunca* (Pallas, 1767) and bushbuck, *Tragelaphus scriptus* (Pallas, 1766). *Anatomia, Histologia, Embryologia*, 18(2), 97–113

PETERS, J. (1992). Late Quaternary mammalian remains from Central and Eastern Sudan and their palaeoenvironmental significance. In K. Heine (ed.), *Palaeoecology of Africa and the surrounding islands* XXIII (pp. 91–115). Rotterdam: A.A. Balkema

PETERS, J., GAUTIER, A., BRINK, J.S., and HAENEN, W. (1994). Late Quaternary extinction of ungulates in sub-Saharan Africa: A reductionist's approach. *Journal of Archaeological Science*, 21(1), 17–28

PLUG, I. (2014). *What bone is that? A guide to the identification of southern African mammal bones*. Wierda Park: Rosslyn Press

PRESCOTT, J.R. and HUTTON, J.T. (1994). Cosmic ray contributions to dose rates for luminescence and ESR dating: Large depths and long-term time variations. *Radiation Measurements*, 23(2), 497–500

RACINOWSKI, R., SZCZYPEK, T., and WACH, J. (2001). *Prezentacja i interpretacja wyników badań uziarnienia osadów czwartorzędowych* (Presentation and interpretation of the results of grain size studies of Quaternary sediments) (2nd rev. ed.). Katowice: Wydawnictwo Uniwersytetu Śląskiego (in Polish)

REED, K.E. (1998). Using large mammal communities to examine ecological and taxonomic structure and predict vegetation in extant and extinct assemblages. *Paleobiology*, 24(3), 384–408

REIMER, P.J., AUSTIN, W.E.N., BARD, E., BAYLISS, A., BLACKWELL, P.G., RAMSEY, C.B., … TALAMO, S. (2020). The IntCal20 Northern Hemisphere radiocarbon age calibration curve (0–55 cal kBP). *Radiocarbon*, 62(4), 725–757

REVEL, M., DUCASSOU, E., GROUSSET, F.E., BERNASCONI, S.M., MIGEON, S., REVILLON, S., MASCLE, J., MURAT, A., ZARAGOSI, S., and BOSCH, D. (2010). 100,000 years of African monsoon variability recorded in sediments of the Nile margin. *Quaternary Science Reviews*, 29(11), 1342–1362

ROBERTS, R.G., GALBRAITH, R.F., YOSHIDA, H., LASLETT, G.M., and OLLEY, J.M. (2000). Distinguishing dose populations in sediment mixtures: A test of single-grain optical dating procedures using mixtures of laboratory-dosed quartz. *Radiation Measurements*, 32(5), 459–465

SAID, R. (1993). *The river Nile: Geology, hydrology and utilization*. Oxford: Pergamon Press

SCERRI, E.M.L. (2013). The Aterian and its place in the North African Middle Stone Age. *Quaternary International*, 300, 111–130

SCHILD, R. (1980). Introduction to dynamic technological analysis of chipped stone assemblages. In R. Schild (ed.), *Unconventional archaeology: New approaches and goals in Polish archaeology* (pp. 57–85). Wrocław: Zakład Narodowy im. Ossolińskich

SCHILD, R., HILL, C.L., and BLUSZCZ, A. (2020). Age of the Late Middle Palaeolithic Nile aggradation. The Khormusan and the Atmur El Kibeih Aterian. In A. Leplongeon, M. Goder-Goldberger, and D. Pleurdeau (eds), *Not just a corridor: Human occupation of the Nile valley and neighbouring regions between 75,000 and 15,000 years ago* (=*Natures en sociétés* 3) (pp. 71–91). Paris: Publications scientifiques du Muséum

SCHILD, R. and WENDORF, F. (2010). Late Palaeolithic hunter-gatherers in the Nile Valley of Nubia and Upper Egypt. In E.A.A. Garcea (ed.), *South-eastern Mediterranean peoples between 130,000 and 10,000 years ago* (pp. 89–125). Oxford: Oxbow Books

SKINNER, A.R. (2015). General principles of Electron Spin Resonance (ESR) dating. In W.J. Rink and J.W. Thompson (eds), *Encyclopedia of scientific dating methods* (pp. 246–255). Dordrecht: Springer

STERN, R.J. and KRÖNER, A. (1993). Late Precambrian crustal evolution in NE Sudan: Isotopic and geochronologic constraints. *The Journal of Geology*, 101(5), 555–574

STUART, C. and STUART, T. (2006). *Field guide to the larger mammals of Africa*. Cape Town: Struik

THOMPSON, J.C. (2010). Taphonomic analysis of the Middle Stone Age faunal assemblage from Pinnacle Point Cave 13B, Western Cape, South Africa. *Journal of Human Evolution*, 59(3–4), 321–339

THOMPSON, J.C. and HENSHILWOOD, C.S. (2011). Taphonomic analysis of the Middle Stone Age larger mammal faunal assemblage from Blombos Cave, southern Cape, South Africa. *Journal of Human Evolution*, 60(6), 746–767

THOMSEN, K.J., MURRAY, A.S., and BØTTER-JENSEN, L. (2005). Sources of variability in OSL dose measurements using single grains of quartz. *Radiation Measurements*, 39(1), 47–61

TOMASZEWSKI, A.J. (1986). Metoda składanek wytworów kamiennych i jej walory poznawcze (The method of refittings of chipped stone artefacts and its research value). *Archeologia Polski*, 31(2), 239–277 (in Polish with English summary)

UDDEN, J.A. (1914). Mechanical composition of clastic sediments. *Geological Society of America Bulletin*, 25(1), 655–744

URBANIAK-BIERNACKA, U. (1975). Propozycja terminologii dla przedziałów klasowych stopniowanej skali wielkości okruchów skalnych. *Przegląd Geograficzny*, 47(1), 147–152 (in Polish)

USIK, V.I., ROSE, J.I., HILBERT, Y.H., VAN PEER, P., and MARKS, A.E. (2013). Nubian Complex reduction strategies in Dhofar, southern Oman. *Quaternary International*, 300, 244–266

VAN DAMME, D. and VAN BOCXLAER, B. (2009). Freshwater molluscs of the Nile Basin, past and present. In H.J. Dumont (ed.), *The Nile: Origin, environments, limnology and human use* (pp. 585–629). Dordrecht: Springer Netherlands

VAN NEER, W. (1989). *Contribution to the archaeozoology of Central Africa*. Tervuren: Vertebrate Section, Royal Museum of Central Africa

VAN NEER, W. (2004). Evolution of prehistoric fishing in the Nile Valley. *Journal of African Archaeology*, 2(2), 251–269

VAN NEER, W., AUGUSTYNEN, S., and LINKOWSKI, T. (1993). Daily growth increments on fish otoliths as seasonality indicators on archaeological sites: The tilapia from Late Palaeolithic Makhadma in Egypt. *International Journal of Osteoarchaeology*, 3(4), 241–248

VAN NEER, W., PAULISSEN, E., and VERMEERSCH, P.M. (2000). Chronology, subsistence and environment at the Late Palaeolithic fishing sites of Makhadma 2 and 4. In P.M. Vermeersch (ed.), *Palaeolithic living sites in Upper and Middle Egypt* (pp. 271–287). Leuven: Leuven University Press

VAN PEER, P. (1991). Interassemblage variability and Levallois styles: The case of the Northern African Middle Palaeolithic. *Journal of Anthropological Archaeology*, 10(2), 107–151

VAN PEER, P. (1998). The Nile Corridor and the Out-of-Africa model: An examination of the archaeological record. *Current Anthropology*, 39(S1), S115–S140

VAN PEER, P. and VERMEERSCH, P.M. (2007). The place of northeast Africa in the early history of modern humans: New data and interpretations on the Middle Stone Age. In P. Mellars (ed.), *Rethinking the human revolution: New behavioural and biological perspectives on the origin and dispersal of modern humans* (pp. 187–198). Cambridge: McDonald Institute for Archaeological Research

VAN PEER, P., VERMEERSCH, P.M., MOEYERSONS, J., and VAN NEER, W. (1996). Palaeolithic sequence of Sodmein Cave, Red Sea Mountains, Egypt. In G. Pwiti and R. Soper (eds), *Aspects of African archaeology: Papers from the 10th Congress of the PanAfrican Association for Prehistory and Related Studies* (pp. 149–156). Harare: University of Zimbabwe

VAN PEER, P., VERMEERSCH, P.M., and PAULISSEN, E. (2010). *Chert quarrying, lithic technology and a modern human burial at the Palaeolithic site of Taramsa 1, Upper Egypt*. Leuven: Leuven University Press

VAN REYBROUCK, D. (2016). *Kongo: opowieść o zrujnowanym kraju* (Congo: a tale of a ruined country) (2nd ed.; J. Jędryas, trans.). Warsaw: Grupa Wydawnicza Foksal (Polish translation of: *Congo: Een Geschiedenis*)

VAN VUURE, T. (2005). *Retracing the aurochs: History, morphology and ecology of an extinct wild ox*. Sofia: Pensoft

VERMEERSCH, P.M., PAULISSEN, E., and HUYGE, D. (2000). Makhadma 4, a Late Palaeolithic fishing site. In P.M. Vermeersch (ed.), *Palaeolithic living sites in Upper and Middle Egypt* (pp. 227–270). Leuven: Leuven University Press

VERMEERSCH, P.M. and VAN NEER, W. (2015). Nile behaviour and Late Palaeolithic humans in Upper Egypt during the Late Pleistocene. *Quaternary Science Reviews*, 130, 155–167

VIGNARD, E. (1928). Une nouvelle industrie lithique: le Sébilien. *Bulletin de la Société préhistorique française*, 25(4), 200–240

VON DEN DRIESCH, A. (1976). *A guide to the measurement of animal bones from archaeological sites* (=*Peabody Museum Bulletin* 1). Cambridge, MA: Peabody Museum of Archaeology and Ethnology, Harvard University

WALKER, R. (1985). *A guide to post-cranial bones of East African animals*. Norwich: Hylochoerus Press

WALTHER, F.R. (1990). Reedbucks, waterbucks and impalas. In B. Grzimek (ed.), *Grzimek's encyclopedia of mammals* V (pp. 448–461). New York: McGraw-Hill Publishing Company

WARREN, G. (1974). Simplified form of the Folk-Ward skewness parameter. *Journal of Sedimentary Research*, 44(1), 259

WENDORF, F. (ed.). (1968). *The prehistory of Nubia*. Dallas, TX: Fort Burgwin Research Center

WENDORF, F. and SCHILD, R. (1989). Summary and synthesis. In F. Wendorf, R. Schild, and A.E. Close (eds), *The prehistory of Wadi Kubbaniya* III. *Late Paleolithic archaeology* (pp. 768–824). Dallas, TX: Southern Methodist University Press

WENDORF, F. and SCHILD, R. (1992). The Middle Palaeolithic of North Africa: A status report. In F. Klees and R. Kuper (eds), *New light on the Northeast African past: Current prehistoric research* (pp. 39–80). Cologne: Heinrich-Barth-Institut

WENDORF, F., SCHILD, R., and ISSAWI, B. (1976). *Prehistory of the Nile Valley*. New York: Academic Press

WENTWORTH, C.K. (1922). A scale of grade and class terms for clastic sediments. *The Journal of Geology*, 30(5), 377–392

WHITEMAN, A.J. (1971). *The geology of the Sudan Republic*. Oxford: Clarendon Press

WILLIAMS, M.A.J. (2009). Late Pleistocene and Holocene environments in the Nile basin. *Global and Planetary Change*, 69(1), 1–15

WILLIAMS, M.A.J. (2019). *The Nile Basin: Quaternary geology, geomorphology and prehistoric environments*. Cambridge: Cambridge University Press

WILLIAMS, M., TALBOT, M., AHARON, P., ABDL SALAAM, Y., WILLIAMS, F., and INGE BRENDELAND, K. (2006). Abrupt return of the summer monsoon 15,000 years ago: New supporting evidence from the lower White Nile valley and Lake Albert. *Quaternary Science Reviews*, 25(19), 2651–2665

WILLIAMS, M.A.J., USAI, D., SALVATORI, S., WILLIAMS, F.M., ZERBONI, A., MARITAN, L., and LINSEELE, V. (2015). Late Quaternary environments and prehistoric occupation in the lower White Nile valley, central Sudan. *Quaternary Science Reviews*, 130, 72–88

WILLIAMS, M.A.J., WILLIAMS, F.M., DULLER, G.A.T., MUNRO, R.N., EL TOM, O.A.M., BARROWS, T.T., MACKLIN, M., WOODWARD, J., TALBOT, M.R., HABERLAH, D., and FLUIN, J. (2010). Late Quaternary floods and droughts in the Nile valley, Sudan: New evidence from optically stimulated luminescence and AMS radiocarbon dating. *Quaternary Science Reviews*, 29(9–10), 1116–1137

WOLFHEIM, J.H. (1983). *Primates of the world: Distribution, abundance, and conservation*. Seattle: University of Washington Press

WOODWARD, J.C., MACKLIN, M.G., KROM, M.D., and WILLIAMS, M.A.J. (2007). The Nile: Evolution, Quaternary river environments and material fluxes. In A. Gupta (ed.), *Large rivers: Geomorphology and management* (pp. 261–292). Chichester: John Wiley

ŻURAWSKI, B. (ed.). (2003). *Survey and excavations between Old Dongola and Ez-Zuma* (=*Nubia* 2; *Southern Dongola Reach Survey* 1). Warsaw: Neriton

INTRODUCTION

Affad first riveted our attention when we were on Bogdan Żurawski's Polish Joint Archaeological Mission to the Middle Nile Valley (1999–2003), better known as the SDRS – Southern Dongola Reach Survey, which carried out archaeological prospection along a section of the right bank of the Nile, working in cooperation with several Polish institutions. A member of the Poznań school of prehistory, Piotr Osypiński was directly involved in discovering the Pleistocene sites at Affad. Marta Osypińska also took part in the SDRS project, thereby gaining formative experience in the study of the archaeozoology and palaeontology of northeastern Africa.

Due to a series of fortunate circumstances, not the least thanks to the generous support of experienced senior colleagues and mentors, suggestions from valued experts, and the scientific inspiration of other academics, we both came to perceive the scientific potential of the sites at Affad. A few years later we returned with our own comprehensive research program, aimed at a holistic investigation of this microregion located in the Great Bend of the Nile in Sudan. Our funding came from two successive grants from Poland's National Science Centre: "Epigones of Levallois traditions in the Middle Nile Valley" (NCN 2011/01/D/HS3/04125) (2012–2014) and "Epigones and Forerunners – Adaptation strategies of the sub-Saharan societies in Terminal Pleistocene and Early Holocene. Case study of the region of the Affad Basin, Southern Dongola Reach, Sudan" (NCN 2015/18/E/HS3/00416) (2015–2021). Marta Osypińska was the Principal Investigator in both instances. Fieldwork in the Sudanese interior was supplemented with extensive specialist analyses of the bone and lithic material, performed between 2016 and 2022 in laboratories in Poland, the United Kingdom, Belgium and the United States.

This volume brings together the results of more than a decade of our research in the Affad Basin, a microregion, which has fully proved its potential for studies of the Middle Stone Age as a key period in the emergence of human culture and its expansion beyond Africa. The material has already been presented in part in a number of scientific articles and chapters in post-conference materials and, to an extent, in the published post-doctoral dissertation of Marta Osypińska (2018). Piotr Osypiński's (2016) unpublished doctoral dissertation on stone processing from the Affad Basin constitutes the core of the discussion presented here. Working on this monograph, we have decided to divide the material. The Pleistocene phase of settlement in the Affad Basin is the theme of the first of two volumes, the second being intended for the significantly later Holocene sources. The division was dictated by the sheer quantity of raw data for both periods accumulated in the course of the project, which we have decided to present *en bloc* in view of the massive and progressing devastation of the region that is being carried out in the name of agricultural development—most of the archaeological sites that we investigated in the course of this project have simply ceased to exist. In 2018, enormous industrial-scale farms overran almost all of the alluvial soils reaching the limits of the Mesozoic heights above the river valley. The horrible civil war, ongoing since April 2023, has not affected the Affad region, but it has interfered with any new scientific research in Sudan. Two years later, there is still no optimistic perspective for a change of this situation…

Samples left over from the various different laboratory analyses, as well as all the finds are kept in storage, with the agreement of the National Corporation for Antiquities and Museums in Sudan, in the storerooms of the Banganarti Archaeological Station (BAS), established by Bogdan T. Żurawski from the Polish Academy of Sciences in Warsaw, at the site of Banganarti (just 50 km from the place of their discovery), as well as at the Polish Academy of Science's Institute of Archaeology and Ethnology in Poznań, Poland. A small part of this collection is also on display at the Poznań Archaeological Museum, one of the few places in the world presenting the complex prehistory of the Middle Nile Valley.

A few words are in order about the make-up of this volume. The discovery and research on Palaeolithic sites in the Affad region is briefly reviewed in Chapter 1, including the current state of publications. Chapter 2 is dedicated to a presentation of the palaeoenvironmental background essential to a discussion of adaptation strategies of Pleistocene communities whose lithic artifacts have been found at Affad. It reviews the current state of knowledge on geomorphological changes in the Affad Basin over a span of 70,000 years, formed on the basis of the evidence—as complete as humanly possible—teased from the raw results of lab-based analyses. The temporal framework for the data comes from a broad-spectrum analysis harnessing the luminescence, ESR and radiocarbon methods (Osypiński et al. 2021). A reconstruction of the palaeochannel river network is supported by the results of magnetic prospection and a Digital Elevation Model (DEM) analysis.

No less important for picturing the ecosystem in which the late Pleistocene communities from Affad functioned are the results of archaeozoological studies discussed in Chapter 3. The regional composition of fauna and the apparent seasonal changes it underwent are directly related to human hunting strategies and butchering practices, both of which have a strong impact on the functional interpretation of lithic artifacts used by communities inhabiting this area.

The collection of lithic artifacts, discussed in depth in Chapter 4, encompasses the assemblages from AFD23, which were at the core of Osypiński's doctoral dissertation, as well as groups of finds, unpublished or published in part, from other sites in the microregion, namely: Affad 111, Affad 24, Affad 131, Affad 122, as well as a few smaller sets. The spatial and temporal contexts of these assemblages are precisely determined as a result of lab-based analyses (including a revision of some early OSL dating results that were published prematurely in the first years of the project), thus enabling an assessment of the relationship between historical artifacts and, in consequence, the degree of homogeneity of individual assemblages. The different groups of finds were characterized in morphological and metric terms, and compared with the known and defined lithic industries of northeastern Africa. The characteristic follows recognized methods and standards in this field, but the extensive illustrative material accompanying the discussion of the finds is hardly a standard approach in African archaeology. This concerns in particular the concept of *chaine opératoire* and refitting methods. The presentation in this chapter, which has identified characteristic features of the Affad lithic tradition in terms of individual creativity, should also foster studies on the technological aspects of stone-tool making over time. Moreover, the functional approach to the study of these artifacts should also be appreciated. By comparing assemblages from four separate locations (zones) within the AFD23 site, as well as a range of other sites in the Affad Basin, the author was able to identify functionally diverse settlement zones. The conclusions drawn from this are supplemented by the results of use-wear analysis, covering both residual waste products as well as formal tools.

Added to this is unique evidence of light wooden structures, hearths and small pits—the oldest example of this kind of encampment remains in the Middle Nile region—presented in Chapter 5. Coupled with analyses of the dispersal of lithic artifacts and animal bone remains, this material gives grounds for a singular consideration of spatial organization in a human settlement from this period.

The central research question concerning MSA human adaptation strategies to life in a relatively small area over many millennia is discussed in the last chapter. The data issuing from the PalaeoAffad Project are summarized, providing a comprehensive picture of what can reliably be said of the life and activities of Late Pleistocene communities in the Affad Basin.

Acknowledgments

We would like to express our gratitude to several researchers who have worked with us at various stages of this project: archaeozoologists Achilles Gautier, Wim Van Neer and Veerle Linseele; prehistorians Romuald Schild and Andrzej Wiśniewski, whose comments as reviewers of Osypiński's doctoral dissertation were helpful in editing the final text for this volume; geoarchaeologists Mike and Anna Maria Kotarba Morley, who joined the project in its early stages (2013). The work of others have made them contributors to this volume: Michał Kuc (PalaeoAffad Project scholarship holder in 2016–2018, doctoral candidate in the Institute of Geography of Wrocław University), Katarzyna Pyżewicz (traseologist at the Adam Mickiewicz University in Poznań), Marek Chłodnicki (researcher of Neolithic sites in Sudan and successor of Lech Krzyżaniak at the Archaeological Museum in Poznań), Anne Skinner (ESR dating specialist, Williams College, USA), Paweł Wiktorowicz (archaeologist and GIS expert, Institute of Archaeology and Ethnology, Polish Academy of Sciences), Robert Ryndziewicz and Krzysztof Kiersnowski (magnetometric study, Institute of Archaeology and Ethnology, Polish Academy of Sciences), Karol Standzikowski (OSL and TL dating methods specialists, Maria Curie-Skłodowska University in Lublin), Sallie Burrough (OSL specialist, University of Oxford, UK), Zdzisław Bełka (leader of strontium isotope research, Adam Mickiewicz University in Poznań).

Fieldwork effectiveness in the Sudanese interior was gracefully ensured by the following NCAM inspectors: Mongira Khalid Madzoub (2012), Houyam Khalid Mohammed (2013, 2014, 2022), Fathiya Abdelrahman Ahmed (2016), Samael Mohammed (2017, 2018). Last but not least, there are our friends to thank—our host in Affad Fajsal Mohammed and our driver and wonderful cook Saleh Fadul.

CHAPTER 1

PALAEOLITHIC SITES AROUND AFFAD: DISCOVERY AND RESEARCH

The Nile Valley in its central part covers almost 1,600 km from the sixth cataract downstream of Khartoum to the first one at Aswan [*Fig. 1.1*]. For kilometers on end the river valley in this section, which is mostly in Sudan, meanders among erosion-resistant Precambrian rocks, mainly diorites and granites. The lowering of the land between the cataracts, where the river flows, dates to the Miocene (Said 1993). The system of Nile palaeochannels, tributaries and lakes, which came and went over the millennia, is still under discussion. Of particular interest is the section covering the so-called Great Bend, lying between the third and fourth cataracts, where the river changes its direction and flows for several hundred kilometers from northeast to southwest rather than from south to north [*Fig. 1.2*]. The western part of this area is called the Dongola Reach while from the point of view of state administration most of it lies in Sudan's Northern State or al-Shimaliya.

Three large, now-dry tributaries converge in this section of the valley: Wadi Howar from the southwest, and Wadi el-Melik and Wadi Muqqadam from the south. They continue to serve as major transportation and communication routes even today.

Herein the term "Affad Basin" (an alternative transcription of this Arabic name is al-Affat) is defined as the right-bank section of the Nile Valley in the Great Bend, stretching between two points marked by the southernmost extent of sandstone inselbergs. The medieval fortresses of Abkur and Diffar stood on hills near the present-day course of the Nile, about 20 km apart. They have long lost their importance as cultural and administrative centers and the villages are now peopled by farmers from the Shaigiya tribe, and a large number of nomads from several other tribes who have settled there. The landscape of the region beyond the zone under cultivation is dominated by sand dunes and sandstone hills (inselbergs; *jebel* in Arabic) often rising several dozen meters above the plain.

The way the valley looks today is a major obstacle to understanding the prehistoric human relationship with the environment. The desert landscape of contemporary northern Sudan, with a narrow strip of cultivated terraces (no more than 1.5 km wide on both sides of the river), is just one of the possible scenarios of how populations could have functioned in the past. Shifting climatic zones—in particular the extent of the monsoon rains—have significantly impacted the form of the landscape, in terms of its living elements, the flora and the fauna, as well as non-living ones, namely, hydrological network, exposure and erosion of ancient rock formations or, ultimately, sediment formation by river and wind (Williams 2019).

The archaeological sites around the village of Affad/Affat were discovered by the Polish Joint Archaeological Mission to the Middle Nile Valley directed by Bogdan T. Żurawski (see Żurawski 2003), which was responsible for the Southern Dongola Reach Survey (SDRS). Between 1998 and 2000, a team comprising mainly students from the University of Warsaw recorded over 800 archaeological sites from all periods on the right bank of the Nile between Old Dongola and

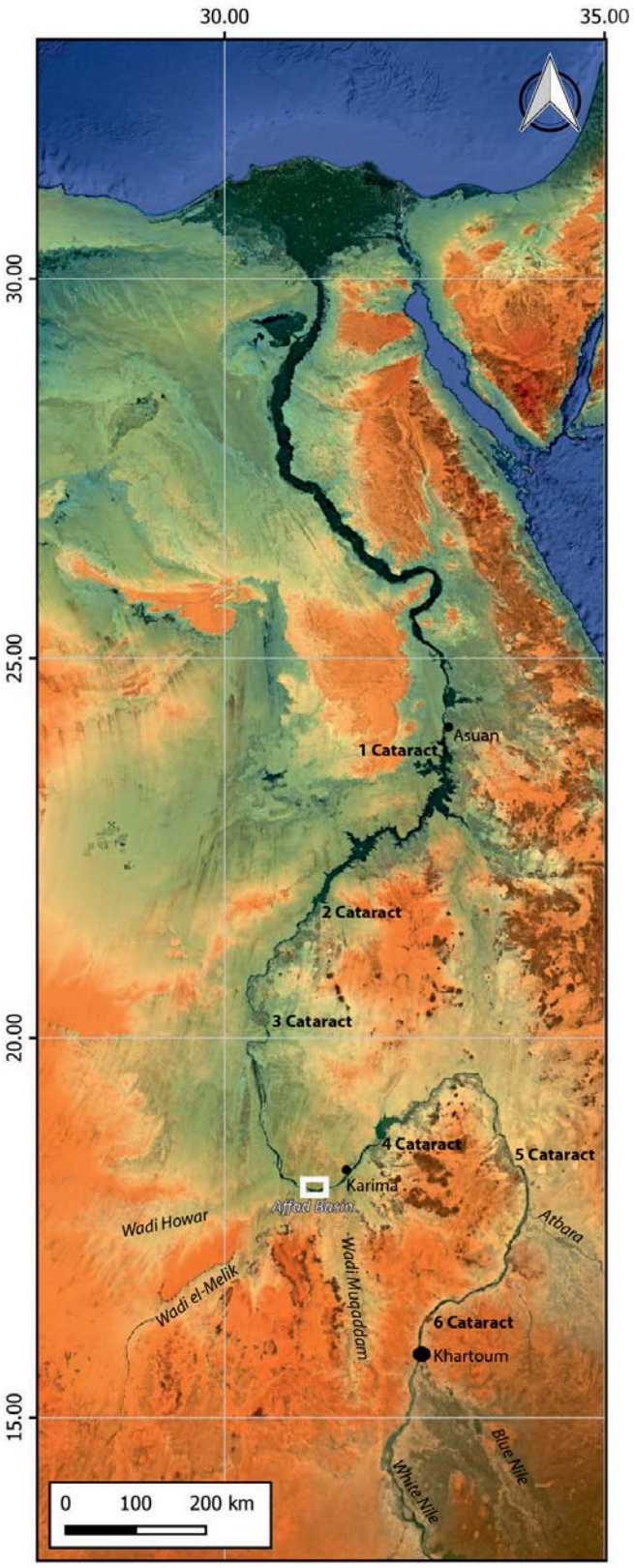

Fig. 1.1. The Nile Valley in satellite imagery
(Source: Google Maps + SRTM30 by NASA http://www.opentopography.org [September 28, 2022])

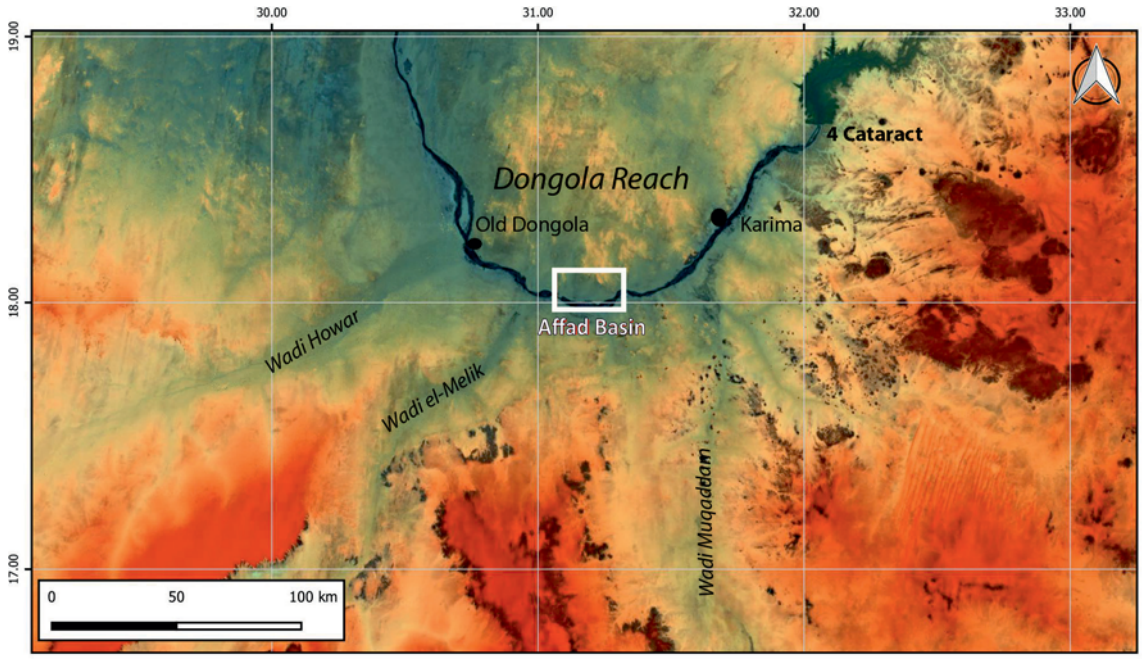

Fig. 1.2. Southwestern section of the Great Bend of the Nile and the location of the Affad Basin in satellite imagery (Source: Google Maps + SRTM30 by NASA http://www.opentopography.org [September 28, 2022])

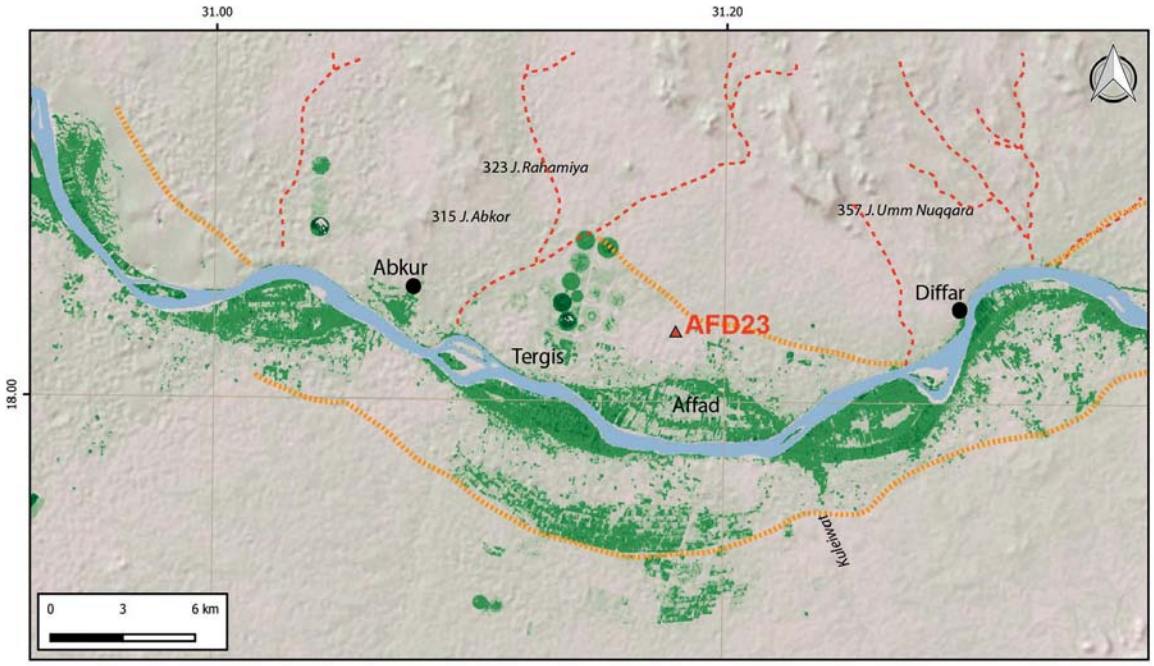

Fig. 1.3. Satellite image of the Affad Basin showing the extent of modern farming (green) and Pleistocene alluvial soils (grey, within orange borderline), as well as much later, Early Holocene(?) gorges (red dashed line). Location of the site AFD23 (Source: Esri Shaded Relief https://www.arcgis.com/home/item.html?id =f92b545ffa354d0699e48b47a0ea5ac5 + Landsat 8-9 OLI/TRIS C2 L2, http://www.earthexplorer.usgs.gov [September 28, 2022])

the suburbs of Karima (ancient Napata). The zone that was surveyed was several hundred meters wide, extending beyond the line of modern fields and buildings; field trips to the desert interior recorded the edge of the Mesozoic plains marked by a series of rocky elevations rising in the landscape. Clusters of artifacts and remains of buildings or tombs visible on the surface were given site numbers, GPS coordinates were recorded and the location described in terms of characteristic elements of the landscape; sites were sampled for artifacts (ceramics, lithics, bones, etc.). The numbering system, distinguishing sites with the initials of the surveyors during the fieldwork stage (e.g., KK67 meant that it was the 67th site discovered by Kazimierz Kotlewski), was standardized at a later stage of the study to reflect the location within a district (*mantiqa*) while simultaneously verifying site extent.

The area of drifting sand dunes between the medieval fortresses of Abkur and Diffar, north of the villages of Tergis and Affad, was surveyed in January 1999 [*Fig. 1.3*]. The surface artifact collection was dominated by products manufactured from fine crystalline raw materials, chert or flint, and represented both the Levallois manufacturing traditions as well as microlithic (Holocene) traditions. Many locations also revealed the presence of mineralized animal remains [*Fig. 1.4*]. Affad 23 (AFD23) turned out to be one of the most interesting locations, with a collection of perfectly preserved Levallois artifacts (11 altogether) made of chert and sandstone and heavily mineralized faunal remains. Similar discoveries were made at other sites visited by the SDRS team (Kuri 6, el-Nafab 8, Rekabija 9 Rekabija 11; after Osypińska 2003).

The authors of this monograph participated in this research, one of their tasks being the description and classification of lithic and bone finds according to their specialty (Osypiński 2003; Osypińska 2003). The examination at the time was preliminary and general owing to the authors' then still limited experience in studying African material, coupled with an unfamiliar local geology and the absence of absolute dating data. Among the basic research problems taken into account was the extraordinarily late survival of Middle Palaeolithic manufacturing traditions and a specific form of Late Palaeolithic inventory, different from that found in Europe or the Near East and described in the literature on the subject. Therefore, the presentation of finds

Fig. 1.4. SDRS ground survey: recording one of the sites on the alluvial plain between Abkur and Diffar, and an assemblage of mineralized animal bones gathered from the surface of site AFD23 (original location codenames KK66 and KK67)

from the SDRS survey project followed a division into four morphological-technological groups, avoiding precise dating of particular assemblages. Levallois products were sorted as Group II, being of every possible size and made of every possible local raw material. It appeared that this material could come just as well from the initial phase of the Middle Palaeolithic (over 120,000 years ago) as from the middle period (up to 40,000–30,000 years ago), and could even represent so-called epi-Levallois industries comprising a specific regional form of production from the Late Palaeolithic, which ultimately disappeared at the beginning of the Holocene, about 10,000 years ago.

In February 2003, a team directed by Piotr Osypiński, which also included archaeozoologist Marta Gauza-Osypińska, ethnologist Maciej Kurcz, a Sudanese inspector and a driver, spent five days in the field, verifying the current state of preservation and estimating the scientific potential of Palaeolithic settlement remains in the Affad basin. Geographical coordinates from the SDRS data facilitated the search for a small cluster of stone and animal bone artifacts set in a monotonous plain with just a few isolated sand dunes. Palaeolithic artifacts and mineralized bones covered an area of about four hectares (marked A–D in *Fig. 1.5*), which was treated as a single site given that no other sites had previously been recorded in the location. The site grid consisted of units 10 m by 10 m (ares). Four clear clusters of artifacts were noted: in the western part of Are 22 (=Southeastern cluster), at the junction of Ares 22, 23 and 32 (=Eastern cluster), in the southwestern part of Are 33 (=Western cluster), and in the central part of Are 23 (=Southwestern cluster). By far the greatest concentration was in the center, extending over an area 50 m by 50 m in size [*Fig. 1.5*; see below, *Fig. 4.1*]. Altogether, 1931 lithic artifacts were collected from the

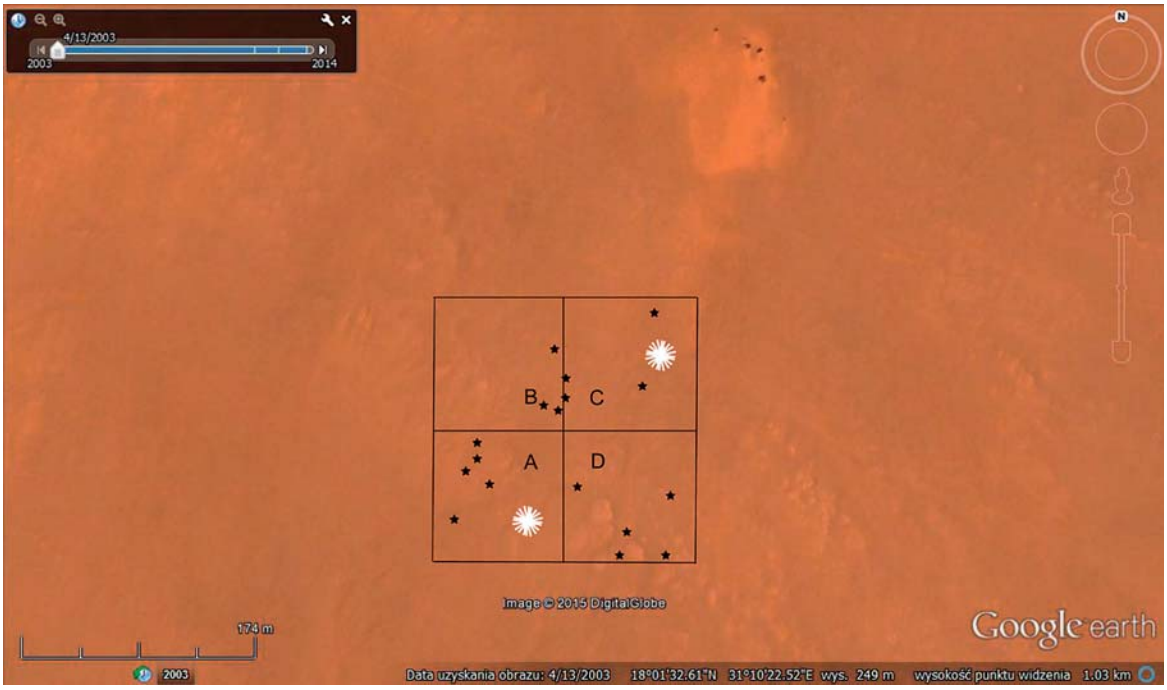

Fig. 1.5. AFD23 measurement framework in February 2003: hectares marked with the letters A–D; clusters of lithic artifacts in white, mineralized animal bone remains as black stars (Source: Google Earth V 6.2.2.6613 [April 13, 2003]. Sudan. 18°01'28"N, 31°10'21"W, eye altitude 1030 m. DigitalGlobe 2015. http://www.earth.google.com [April 26, 2015])

surface, in various states of preservation, from completely patinated and coated to relatively 'fresh' with no patina. Already at the recording stage, the relatively large size of the artifacts, their good state of preservation, and an easily recognizable raw material promised good results with a refitting of these fragments.

A test pit, 1 m by 1 m, was excavated on the spot of an assemblage of lithic artifacts collected from the surface, practically in the center of the largest cluster in Are A/34. The purpose was to establish the stratigraphy in this area, identifying the nature of the sediment yielding Palaeolithic artifacts. Below the loose surface sand, which was the setting for the surface collection of lithics from the area, was a sterile layer of friable silt, approximately 20 cm thick, overlying a more sandy layer, no thicker than 3–5 cm, which yielded a relatively numerous set of lithic artifacts of Palaeolithic origin (36 artifacts/1 m^2). The underlying layer of very hard silt, permeated with gypsum precipitation, was explored in one spot to a depth of 15 cm and found not to contain any lithic artifacts [*Fig. 1.6*]. Based on the recording of two separate layers of Palaeolithic artifacts, the Affad 23 site was identified as one of the few stratified open-air sites of Palaeolithic age in the Nile Valley.

In the summer of 2003, a large part of the lithic (1283 artifacts) and bone material from Affad 23 was transferred to Poznań, Poland, as part of a deposit of finds from B.T. Żurawski's research sent by the Sudan National Corporation for Antiquities and Museums to the Poznań Archaeological Museum. The first results of a refitting and examination of the lithic artifacts from Affad 23 were published in the SDRS project monograph (Osypińska and Osypiński 2003). They were also presented at an international symposium held in Poznań in July 2003, organized by the

Fig. 1.6. Baulk of test pit A/34 at site AFD23 (2003). Each unit on the scale bar = 10 cm

International Commission of the Later Prehistory of Northeastern Africa (LPNEA). The identification of the assemblage as a Middle Palaeolithic industry was critiqued by Romuald Schild, who considered a later dating more probable because of the placement on such low-lying alluvial soils (barely a few meters above the modern flood plain). A complete study appeared in 2011, covering the results of an analysis of both the lithic artifacts (including refittings) and the animal remains (Osypiński, Osypińska, and Gautier 2011). The archaeozoological research on the remains from site AFD23 entered a new stage when, thanks to the help and experience of Achilles Gautier, it became possible to work on collections of comparable African fauna kept at the Institut royal des Sciences naturelles de Belgique in Brussels and the Paleontology and Paleo Environments Research Unit at Ghent University.

At this point in the research the AFD23 site had been dated on the grounds of formal analogies and the contemporary state of knowledge concerning environmental changes in the central section of the Nile Valley. Given the archaic nature of the lithic assemblage (no correlates for microlithic production methods, as well as no tool forms typical of later manifestations of the Levallois tradition from Lower Nubia), a date corresponding to the period of the Khormusan industry in Nubia, namely MIS 4 (through approximately 60,000 years ago) was considered. Yet the location of the site, which was evidently not an example of redeposited earlier material but was intrinsically linked with the floor section of low-lying alluvial soils, argued in favor of a "young" assessment of its age. Following consultation with the Southern Methodist University Expedition investigating the opposite, right bank of the Nile, the riverine sediments above the Holocene terraces were attributed to the so-called Goshabi Formation (Marks, Hays, and de Heinzelin 1968). It was assumed to be contemporary with the Lower Nubian formations of Dibeira-Jer and Sahaba (de Heinzelin 1968b; Wendorf and Schild 1992). The latter is dated to between 20,000 and 10,000 years BCE. Even so, the lack of absolute dating constituted a major drawback.

A three-year research grant (Sonata 1, No. 2011/01/D/HS3/04125) from Poland's National Science Centre (NCN), awarded in 2011 to Marta Osypińska, then from the Institute of Archaeology and Ethnology of the Polish Academy of Sciences, constituted a breakthrough in the research on Affad. It provided the opportunity to verify the dating and attribution of sites in the Affad Basin discovered during the SDRS survey and to carry out archaeological excavations at the AFD23 site. The project also included geoarchaeological investigations (Michael Morley, Oxford Brookes University, UK) supported by an OSL dating series (see Chapter 2). The authors of this monograph continued their respective studies of lithic and osteological sources, while supervising archaeological fieldwork. Provisional reports from this work appeared successively in the *Nyame Akuma* bulletin (Osypińska and Osypiński 2012; 2013), as well as in the quarterly *Antiquity* (online Project Gallery, http://journal.antiquity.ac.uk/projgall/osypinska341). The results were publicized at several international symposia, including the "Stories written in stone" conference in Romania; 14th Congress of the Pan-African Archaeological Association for Prehistory and Related Studies in South Africa; 13th International Conference for Nubian Studies in Switzerland; The Middle Palaeolithic in the Desert II conference in France, as well as various lesser meetings in both Poland and Sudan. An exhibition of the Affad discoveries accompanied the "Desert and the Nile. Late Prehistory of the Nile Basin and the Sahara" symposium held in Poznań in 2015 and some artifacts from Affad are currently on display at the Poznań Archaeological Museum (Chłodnicki, Bagińska, and Polkowski 2015: 44, 50).

The three seasons of grant-funded fieldwork (2012–2014), beside verifying SDRS site location data, facilitated a systematic identification of the four zones of site AFD23 and enabled an investigation of two other sites: AFD110 and AFD111, both of which were particularly promising in terms of finds [*Figs 1.7, 1.8*]. A new site grid was established, the old one from ten years before having become obsolete. Trenches were 10 m by 10 m (the basic grid unit being the are as before), further subdivided into square meters. Arbitrary excavated levels were 10 cm thick, and sediments were sieved in justified cases.

An OSL dating of samples collected from layers recorded in several stratigraphic sequences, carried out by a laboratory in Kielce, Poland, gave the first series of absolute dates, placing the Affad settlement at the close of the 16th millennium, during a phase of milder climate following the peak of a very dry period (Last Glacial Maximum, LGM),which signified long-lasting improvement of environmental conditions (so-called African Humid Period). However, further testing of samples in Lublin and Oxford proved these initial findings to be in error as a result of the application of a minimum age-calculation model (Osypiński et al. 2021).

The systematic exploration of both horizontal and vertical stratigraphy at the Affad 23 site enabled a reinterpretation of the spatial distribution of artifacts from the surface collection made in 2003. The nature of the deposits, that is, whether primary or secondary, could now be sorted out [*Fig. 1.9*]. It was deemed expedient to adopt a uniform system of identifying contexts for the entire area under investigation (see Chapter 2). This system is as follows:

1a – site surface at Affad 23, indeterminate stratigraphic relationship when considering sediments related to settlement

1b-x – site surface at other sites in the Affad Basin, indeterminate stratigraphic relationship when considering sediments dated to the Late Pleistocene

2a – sediments related to the settlement episode in the southwestern sector of site AFD23 (trenches 2013/F–I and 2014/N,O,P,Q) regardless of the degree of natural exposure (modern erosion of the floor section, as well as the lower section covered by subsequent layers) – deposit 23.D.1

2b-x – sediments related to the settlement episode in the remaining sectors of site AFD23 (trenches 2013/L–M and 2014/R), as well as at other sites.

3 – preserved (subsurface) sediments post-dating the settlement episode – deposits 23.E.1 and 23.F.1.

Superimposition of the positioning of lithic artifacts recorded in 2003 on a mapping of geological deposits recorded just below the surface (at a depth of approximately 10 cm) [see *Fig. 1.9*] confirmed that the four initially identified clusters were indeed to a large extent zones of artifact deposition during the original settlement phase and not the result of secondary (natural) accumulation. The largest displacement affected elements from the floor section of sandy deposit 23.D.1 which had been subject to erosion, artifacts being found often above deposits of younger origin but lying on a lower level. This reflects the dynamics of the processes affecting the landscape in the area under investigation (see Chapter 2).

An analysis of horizontal stratigraphy revealed the presence of numerous postholes, pits and hearth remains exclusively in sediments defined as original deposits corresponding to the occupation period. This identified the functional zone of the camp, imbuing the cluster of lithic artifacts with a functional importance. A significantly enriched set of sources (adding 4521 artifacts)

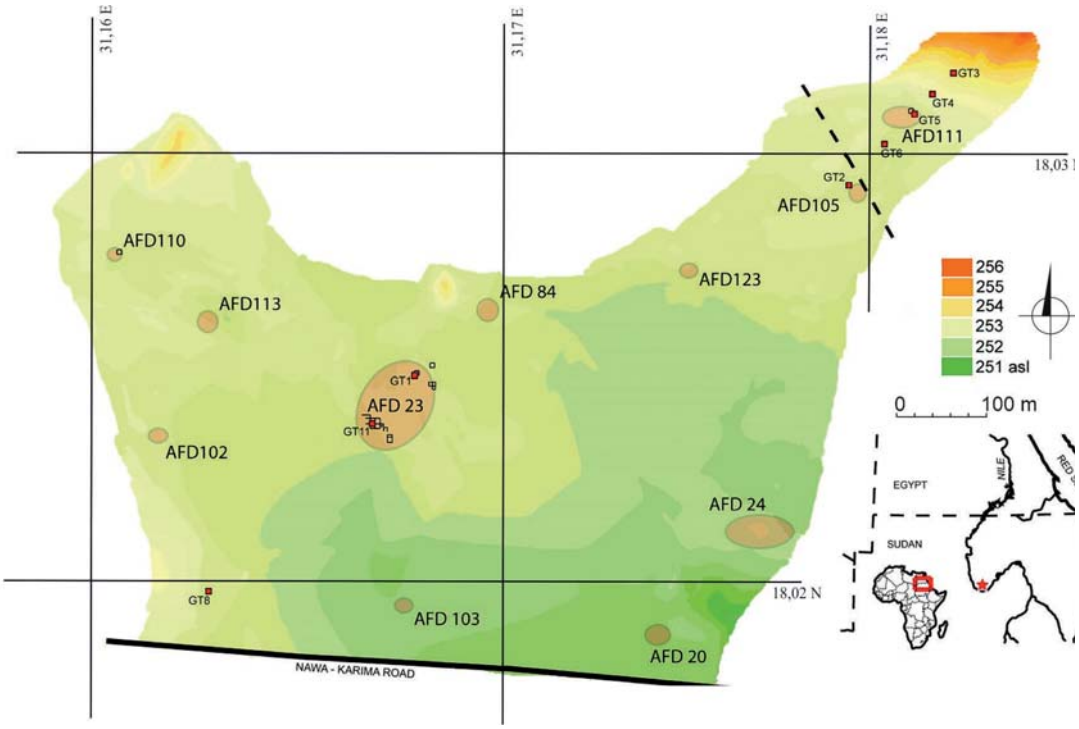

Fig. 1.7. Hypsometric map of the research area at Affad during the 2012–2014 seasons indicating the location of sites dated to the late Pleistocene and geological exposures (GT)

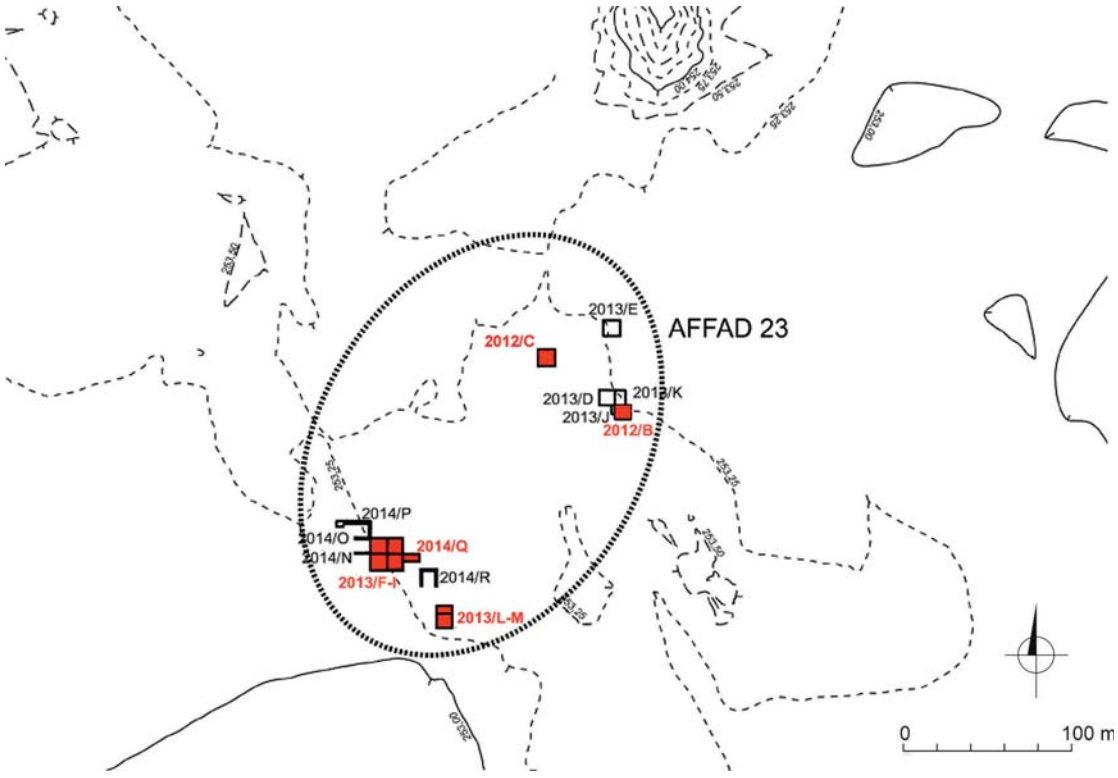

Fig. 1.8. Location of excavation trenches (marked in red) and surveys carried out in the four zones of the AFD23 site in 2012–2014

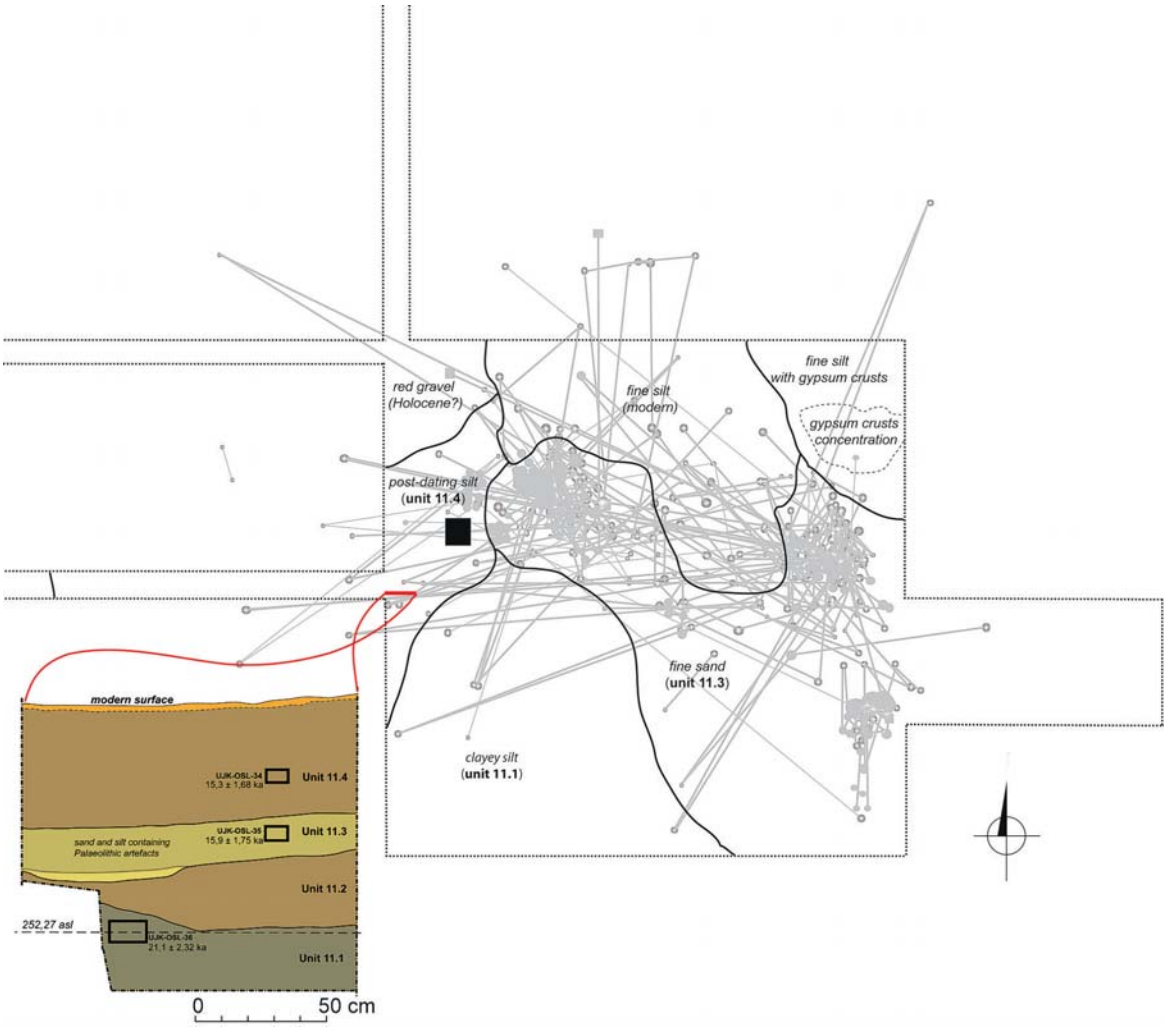

Fig. 1.9. Site AFD23: combined distribution of refittings of lithic artifacts collected from the surface in 2003 (marked in gray; see also *Figs 4.24–4.49*) in relation to the horizontal (at a depth of 10 cm, outlined in black) and vertical stratigraphy recorded in 2013 (location of section marked as a red line; OSL dates reviewed in Osypiński et al. 2021). Solid black square indicates location of test pit A/34 from 2003 [see *Fig. 1.6*].

made it possible to identify stone-processing methods in relation to the different phases of the encampment. Osypiński's doctoral dissertation was dedicated to a detailed consideration of this issue (Osypiński 2016).

The broad spectrum of new data from Affad continued to be studied thanks to another NCN research grant awarded Marta Osypińska in 2015 (Sonata-Bis 5; No. 2015/18/E/HS3/00416). The researchers concentrated now on identifying the factors shaping the various human adaptation strategies of the Pleistocene and early Holocene in an effort to describe the different ways in which a similar ecosystem (composition of fauna, and the morphology and hydrology of the terrain) would have been used by human groups living in the Middle Nile Valley in the two periods in question. The project aimed to reconstruct the evolutionary formation of this area through a multi-faceted analysis of sources, from sites already examined and newly explored ones, as well as a palaeo-environmental analysis, covering, among other things, magnetic prospection and dating

of deposits. The field team was extended to include other specialists: Neolithic researcher Marek Chłodnicki and geomorphologist Michał Kuc, as well as a team dealing with DEM measurement and analysis of the modern surface (Paweł Wiktorowicz) and subsurface levels (geophysicists Robert Ryndziewicz and Krzysztof Kiersnowski). Laboratory analyses included use-wear traces (Dr. Katarzyna Pyżewicz, Institute of Archaeology, Adam Mickiewicz University, Poznań), strontium isotope analysis of selected elements of the landscape (Prof. Zdzislaw Bełka, Isotope Laboratory, Adam Mickiewicz University, Poznań), radiocarbon dating (Tomasz Goslar, Poznań Radiocarbon Laboratory FUAM), ESR dating (Dr. Anne Skinner, Department of Chemistry, Williams College, USA), as well as TL and OSL dating in two laboratories (Dr. Karol Standzikowski, Faculty of Earth Sciences and Spatial Management, Maria Curie-Skłodowska University, Lublin, and Dr. Sallie Burrough, School of Geography and the Environment, University of Oxford).

The following four seasons of field research were devoted to completing the research at site AFD23, carrying out an extensive field survey identifying a whole range of interesting locations in the northwestern part of the Affad Basin, and excavations at a number of crucial Pleistocene sites in the region (see below). More importantly, the absolute dates for the AFD23 site were revised thanks to a reexamination of sediment samples; the results obtained for newly collected samples (often from the same sedimentary units dated by the Kielce laboratory) pointed toward the initial period of MIS3 (that is, approximately the 50th millennium BP). A discussion of the revised dating was published in *Archaeometry* (Osypiński et al. 2021). Dating with OSL methods (multi- and single-grain) gave results corresponding to the outcomes of a TL dating of the heated substratum from sites AFD23 and AFD134 and a radiocarbon dating of clam shells from site AFD134. Ultimately, the Nile alluvium, which is the layer containing all of the MSA sites from the Affad Basin, should be dated to the MIS3 period. Only the ESR dating of animal tooth enamel from Affad gave an even earlier date (MIS5), although the need for a better application of these methods to local conditions should be stressed. While this shift weakens the preliminary interpretation of "epigones of Levallois traditions in the Middle Nile Valley" (see Osypiński 2020), it permits a significantly more detailed analysis of adaptation strategies of human groups from the later MSA in the Nile Valley perceived in terms of the main migration corridor for the human species moving out of Africa. Indeed, the only information available on late MSA settlement in Nubia in particular comes from the research of the Combined Prehistoric Expedition in Nubia (Wendorf 1968; Wendorf and Schild 1989; Schild and Wendorf 2010; Schild, Hill, and Bluszcz 2020).

Among the Pleistocene sites where investigations commenced in 2016 several proved crucial to a reconstruction of the palaeo-environment and human adaptation strategies. Sites AFD24 and AFD131 turned out to be similar in nature to the AFD23 encampment, producing an extraordinarily rich collection of lithic sources (including further refittings), animal bone remains, as well as further evidence of Pleistocene communities using light wooden structures within the encampments. Other investigated locations demonstrated a lesser importance of production correlates and the use of stone tools, replaced instead by a greater presence of animal remains: mammals at AFD124, fish at AFD113, and clams at AFD134. Archaeologists usually tend not to examine sites that do not yield distinctive collections of artifacts, avoiding the issue of identifying such assemblages and their attribution to particular settlement periods. At Affad, a well-developed program of dating the alluvial-aeolian substratum allowed these sites to be included in the discussion.

To reconstruct the course of ancient river channels the project reached for a geophysical survey method, which has successfully been applied for almost a decade now at urban sites in the Nile Valley in Sudan (of Kerman through Funj date). Magnetic measurements were taken in four key sectors during the 2016 and 2017 seasons, revealing the extraordinary complexity of the Affad Basin structure, perceived up till then as a monotonous plain with just a few shifting sand dunes. The location of prehistoric sites was demonstrated to indicate with considerable precision the riverbank zones of late Pleistocene river channels, with the bottom zones used during the temporary (seasonal?) drying-out of these channels, and at the beginning of the Holocene also above or below periodic river inundations. Modern ground relief was studied through satellite imagery and RTK measurements taken on the ground in order to compare the results with the magnetic mapping. In effect, the course of Pleistocene river channels as presented on maps in this monograph, is a unique proxy for dynamic modelling of changing terrain in the Affad Basin over the last 70 millennia.

Last but not least, the last phase of the project yielded numerous and diagnostically indisputable remains of the African auroch (*Bos primigenius*). The discovery of these remains at sites AFD124, AFD131, AFD24 and AFD120 is undoubtedly one of the most important outcomes of the project, previous surface finds being limited to not very distinctive bone fragments of these large ruminants. The first reconstructions of the environment of the AFD23 encampment had indicated a dense riparian forest and the research on the range of aurochs as a species had also suggested that the African buffalo (*Syncerus caffer*) could have been the only animal of this size to live at this geographical latitude. However, in 2017, investigations in the Affad Basin revealed sites with a clearly different composition of the hunted animal species. Apart from aurochs, the newly examined sites yielded remains of zebras, giraffes and antelopes. This demonstrated a significantly more open ecosystem of a woodland and savannah. Insofar as all of these sites are dated to the same period (MIS3), the evidence can be explained not so much as a complete change of ecosystem, but as seasonal change and flexible adaptation on the part of MSA human groups capable of exploiting both the riparian biome when the level of water in the Nile was low and the savannah surrounding the river when the water levels rose. To date, the finds of auroch remains at Affad are the oldest evidence, complete with absolute dating, of the presence of this species on the Nile, while simultaneously indicating the southernmost extent of this species in Africa. A more detailed presentation of this discovery appeared in the *Journal of Field Archaeology* (Osypińska et al. 2021), including the first results of a strontium isotope analysis of the tooth enamel of both animals—aurochs, zebras, hippopotamuses and kob antelopes (all Pleistocene fauna) and reference sediment samples (as well as the fill of one of the postholes from site AFD24) and domestic Neolithic fauna—and people. Given the small number of samples, these results should be treated as pioneering work heralding a very interesting study. Among others, the results have shown that none of the sampled individuals originated from an area of decidedly different geological character, thus contradicting theories about the migration of Neolithic herders and Pleistocene zebras (currently a migratory species).

SITE GAZETTEER

Affad 23 (AFD23)

N 18°01'29.2", E 31°10'26.5"; 253 m asl
Ground survey and site excavation through 2018: Osypińska and Osypiński 2003; Osypiński, Osypińska, and Gautier 2011; Osypiński et al. 2016; Osypińska and Osypiński 2015: 607; 2016

Research after 2015:

Exploration of the Northwestern Zone, supplementing research in the Southwestern Zone (including the gathering of additional samples for verification of OSL/TL dating results). Magnetometric prospection covering the western sector of the site. Sr isotope analysis of hippopotamus and Kob antelope tooth enamel, supplementing work done on lithic and osteological collections.

Sources discussed in this volume:

lithic material (Chapter 4: pp. 150ff.)
use-wear study results (Chapter 4: pp. 361ff.)
osteological material (Chapter 3: p. 104);
geomorphological samples (Chapter 2: pp. 25ff.)
sediment sample dating results (Chapter 2: pp. 82ff.)
magnetic prospection results (Chapter 2: pp. 78ff.)

Affad 24 (AFD24)

N 18°01'33.7", E 31°10'58.5"; 253 m asl
Surface survey through 2014: Żurawski 2003: 274; Osypińska and Osypiński 2015: 607

Research after 2015:

Exploration of the central sector of the site covering a cluster of postholes and hearths; examination of collections of lithic artifacts and bone remains, sedimentological description. Dating of auroch and equid tooth enamel with the ESR method. Sr isotope analysis of two subsurface sediments.

Sources discussed in this volume:

lithic material (Chapter 4: pp. 349ff.)
use-wear evidence (Chapter 4: pp. 361ff.)
osteological material (Chapter 3: p. 112)
geomorphological samples (Chapter 2: pp. 33ff.)
ESR dating results (Chapter 2: pp. 90ff.)
cut features (Chapter 5: pp. 374ff.)

Affad 110 (AFD110)

N 18°01'42.1", E 31°10'00.4"; 253 m asl

Research after 2015:

Study of bone collections. The site was excavated in 2013 (Osypińska and Osypiński 2015: 617; Osypińska and Osypiński 2016: 115)

Sources discussed in this volume:

osteological material (Chapter 3: pp. 113ff.)

Affad 111 (AFD111)

N 18°01'54.2", E 31°11'05.6"; 253 m asl
Excavated in 2014: Osypińska and Osypiński 2015: 618; 2016

Research after 2015:

Study of lithic collections.

Sources discussed in this volume:

lithic material (Chapter 4: pp. 303ff.)
osteological material (Chapter 3: p. 114)
sediment samples dating (Chapter 4: p. 304)

Affad 113 (AFD113)

N 18°01'38.6", E 31°10'07.5"; 253 m asl
Surface survey through 2014: Osypińska and Osypiński 2015: 607

Research after 2015:

Site excavation, magnetic prospection, sedimentological description, study of animal bone remains.

Sources discussed in this volume:

lithic material (Chapter 4: pp. 353ff.)
osteological material (Chapter 3: p. 121)
geomorphological samples (Chapter 2: pp. 40ff.)
magnetic prospection results (Chapter 2: pp. 78ff.)

Affad 120 (AFD120)

N 18°02'22.1"; E 31°09'54.1"; 253 m asl
Surface survey through 2014: Osypińska and Osypiński 2015: 621

Research after 2015:

Site excavation/systematic surface collection, study of lithic artifacts and animal bone remains.

Sources discussed in this volume:

lithic material (Chapter 4: pp. 338ff.)
osteological material (Chapter 3: p. 115)

Affad 122 (AFD122)

N 18°01'57.20", E 31°09'55.8"; 253 m asl
Surface survey through 2014: Osypińska and Osypiński 2015: 621

Research after 2015:

Site excavation, magnetic prospection, study of collections of lithic artifacts and animal bone remains, sedimentological description. OSL dating of the substratum.

Sources discussed in this volume:

lithic material (Chapter 4: pp. 338ff.)
osteological material (Chapter 3: p. 115)

geomorphological samples (Chapter 2: pp. 38ff.)
magnetic prospection results (Chapter 2: pp. 78ff.)
OSL dating results (Chapter 2: pp. 82ff.)

Affad 124 (AFD124)

N 18°02'02", E 31°09'36"; 253 m asl

Research after 2015:

Ground survey and site excavation, study of collections of lithic artifacts and animal bone remains; Sr isotope analysis of auroch enamel; OSL dating of substratum layers.

Sources discussed in this volume:

lithic material (Chapter 4: pp. 353ff.)
osteological material (Chapter 3: p. 116)
OSL dating results (Chapter 2: pp. 82ff.)

Affad 131 (AFD131)

N 18°02'12", E 31°09'34"; 253 m asl

Research after 2015:

Ground survey and site excavation, study of collections of lithic artifacts and animal bone remains, Sr isotope analysis of and zebra tooth enamel; sedimentological description, magnetic prospection, OSL dating of the substratum.

Sources in this volume:

lithic material (Chapter 4: pp. 317ff.)
osteological material (Chapter 3: p. 119)
geomorphological samples (Chapter 2: pp. 35ff.)
magnetic prospection results (Chapter 2: pp. 78ff.)
OSL dating results (Chapter 2: pp. 82ff.)

Affad 134 (AFD134)

N 18°02'23", E 31°09'35"; 253 m asl

Research after 2015:

Ground survey and site excavation, study of collections of lithic artifacts and malacological remains, radiocarbon dating of malacological remains, TL dating of the substratum.

Sources in this volume:

lithic material (Chapter 4: pp. 353ff.)
malacological material (Chapter 3: p. 123)
TL dating results (Chapter 2: pp. 82ff.)

CHAPTER 2

NON-LIVING COMPONENTS OF THE AFFAD BASIN ENVIRONMENT IN THE PAST

(with the contribution of Michał Kuc)

A reconstruction of the late Pleistocene landscape, which was the natural environment in which Palaeolithic human groups functioned in the Affad Basin, was deemed a prerequisite to studies of prehistoric settlement in this specific part of the Middle Nile Valley. Initial observations of the sedimentation in the study area came from a meter-wide test pit A/34 excavated in 2003, supported by the state of preservation of artifacts discovered at the time. Aiming for a more comprehensive and coherent picture, the authors launched a series of studies and laboratory analyses of the non-living components of the environment, the results of which complemented the findings from fieldwork following standard archaeological practice, conducted within the frame of the PalaeoAffad Project starting from 2013.

The most important research task was a geomorphological and geological reconnaissance. A partial geomorphological assessment by Michael Morley from Oxford Brookes University has already been published (Osypiński et al. 2016). The buried topographical relief, that is, the palaeochannels of the late Pleistocene landscape were mapped with magnetic prospection and Digital Elevation Models (DEMs) were generated from ground data recorded with RTK GPS (for both see the reports included in appendices to this chapter). Macroscopic determination of sediment structure was carried out on selected trench sections at individual archaeological sites or extant natural or anthropogenic exposures.

In order to anchor the findings in a temporal framework, the project implemented a program of analyses designed to date the landscape components and anthropogenic remains of late Pleistocene and early Holocene settlement at Affad. The method of age determination—optically stimulated luminescence (OSL)—was chosen because of the assumed MIS4 chronology extending beyond the range of the radiocarbon method. In 2016–2017, new samples were sent for OSL dating: to the laboratory of the Maria Curie-Skłodowska University in Lublin (Poland), which had resumed OSL dating under the supervision of Karol Standzikowski, and to the Oxford Luminescence Dating Laboratory at Oxford University (UK) (one sample); the lab reports are presented as appendices to this chapter. The results of these successive analyses have contributed substantially to the discussion of settlement and landscape periodization in the Affad Basin (Osypiński et al. 2021).

Alternative methods were considered as new data accumulated. For radiocarbon dating the project has cooperated with the University of Poznań Foundation laboratory throughout the course of the investigations, while ESR dating was performed at the Williams College laboratory (USA) (see reports presented in the appendices section at the end of the chapter).

2.1 GEOLOGICAL STRUCTURE AND GROUND RELIEF

The Desert (or Middle) Nile, which is the part of the river between the first and sixth cataracts, drains a geological substratum that includes rocks and sediments from the Precambrian to the Holocene [*Fig. 2.1*]. Its oldest part, which lies exposed in the eastern and northern sections of the area, is formed by a Proterozoic basement composed of various igneous and metamorphic rocks, mainly gneisses and amphibolites, intruded by granites (Stern and Kröner 1993). These rocks are overlain in an unconformable way by horizontal strata of Nubian sandstone, a lithological unit widespread across northern Africa, which includes mainly sandy continental, estuarine and marine sediments (Medani 1975). The age of Nubian sandstone is not well established; in central Sudan, it is considered to be predominantly Cretaceous. Nubian sandstone forms extensive exposures in the Bayuda Desert and the area west of the Nile. North of the Nile valley, in the Nubian desert, it is covered by Quaternary sands, weathered rock material and some dunes. South of the Desert Nile, between Wadi Abu Dom and Wadi Abu Ghidian, there are outcrops

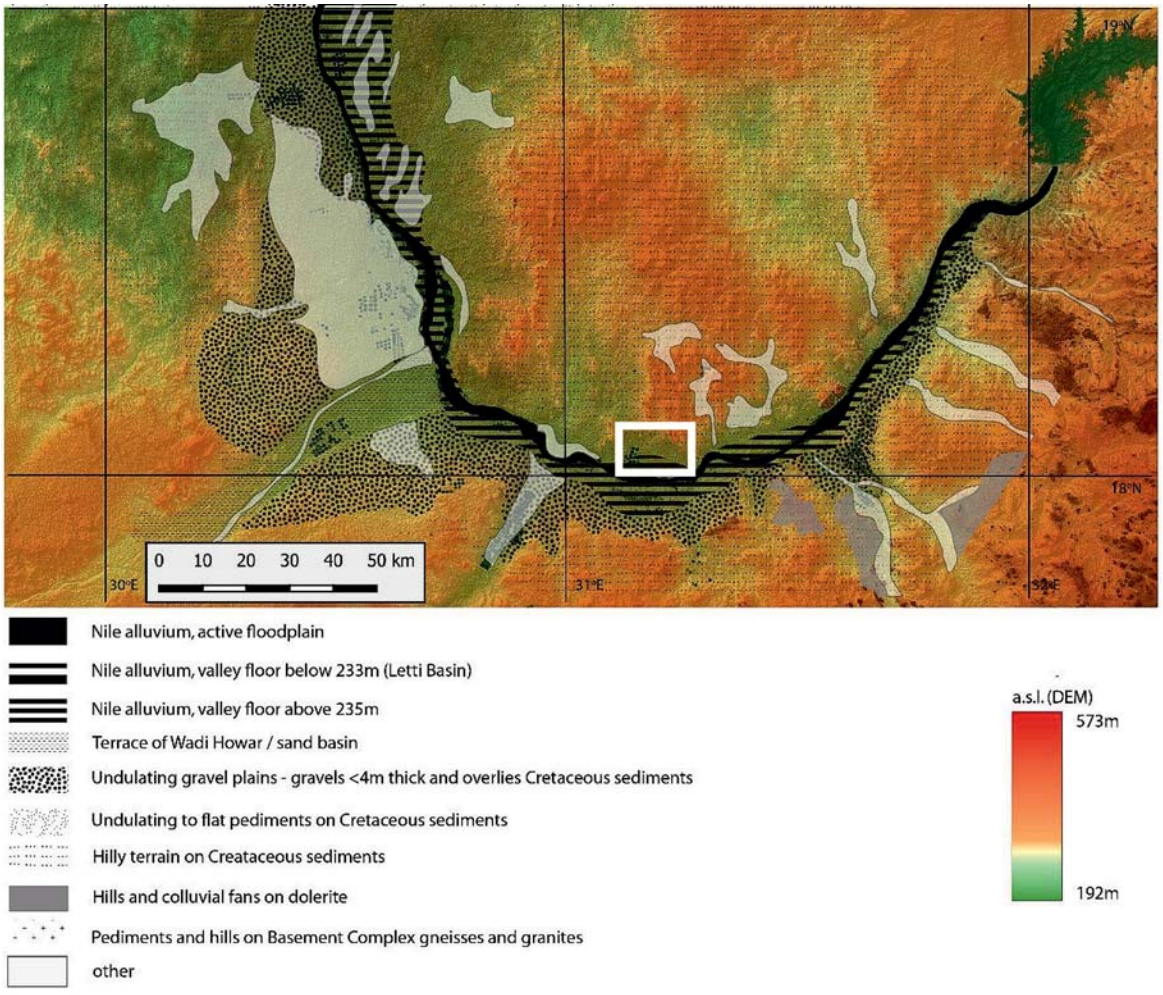

Fig. 2.1. Middle Nile region: geological/geomorphological sketch (after Williams et al. 2010: Fig. 3) superimposed on a Digital Elevation Model (DEM) (source: Sentinel); area presented in *Fig. 2.2* framed in white box

of basalts (dolerites) which represent records of volcanic eruptions in the Tertiary period (Almond 1974), related to the activity of the East Africa–Red Sea rift system. The youngest sediments in the study area are the alluvial Holocene muds, silts and sands forming the floodplains in the Desert Nile valley, as well as infillings of tributary wadis.

Nowadays, the Nile valley, in the part studied by the project, is filled with fluvial and aeolian sediments of various grain size. There are two terraces in this part of the valley [*Fig. 2.2*]. The surface of the lower/younger terrace is made up of mainly silts and sandy silts, and has been strongly transformed by aeolian processes, attested by a growing percentage of the sandy fraction in the roof layer of the analyzed sections. The second, higher terrace is made up of gravel with a small admixture of sandy and silty fractions in the roof layer sections. Today, the upper/older terrace is preserved in the form of gravel inselbergs left standing as a result of denudation. Some of them were additionally transformed when the gravel was exploited in the construction of an asphalt road in 2009. The terrain on both terraces is not very diversified in shape. Denivelations reach a few meters, mainly within young single dunes and small fields of aeolian sands that are partly covered with dunes (on the lower terrace).

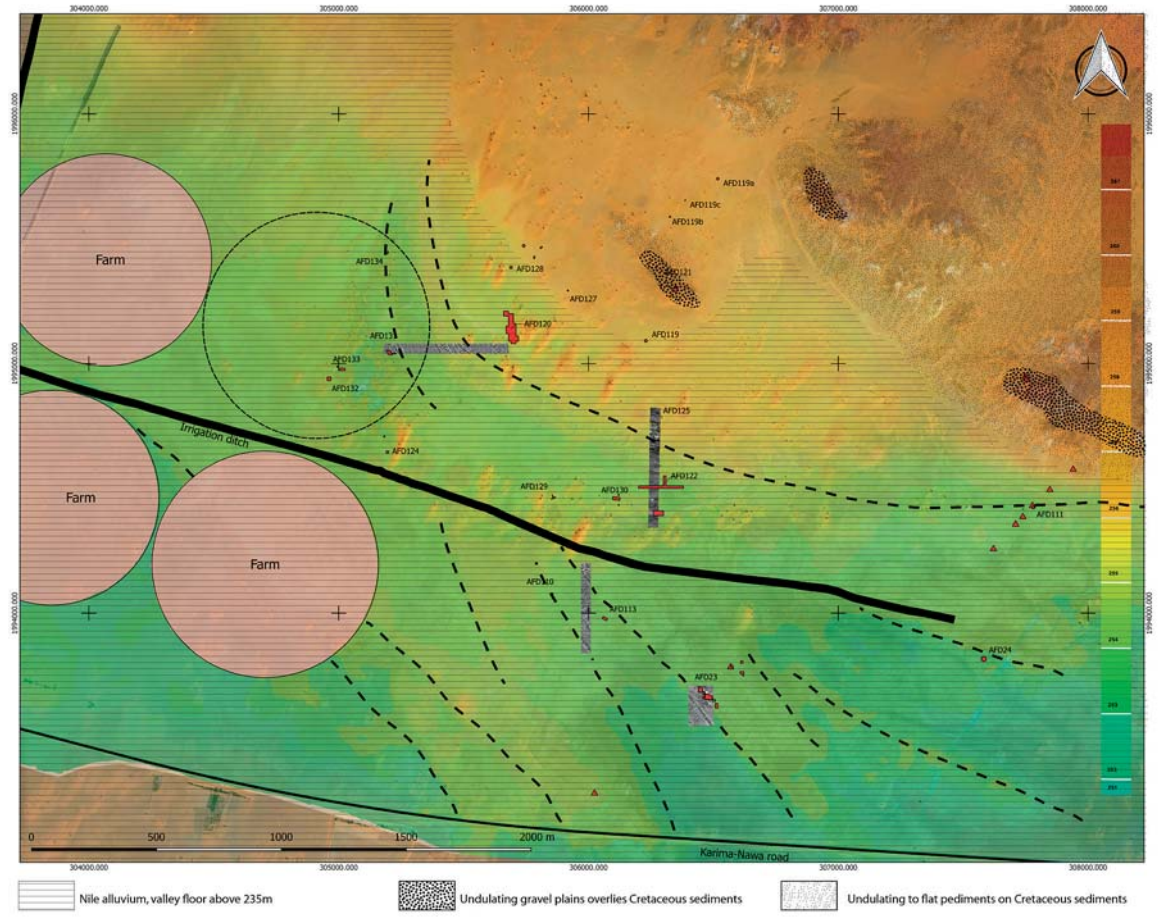

Fig. 2.2. Digital Elevation Model (DEM) of the investigated area with labelled geomorphological components of different chronology. Dashed lines indicate restored banks of palaeochannels from the sediment aggradation stage within the lower terrace (MIS3)

2.2 RESEARCH METHODS AND LABORATORY ANALYSES (2017–2019)

Geological and geomorphological mapping was done in the field. Documentation (macroscopic observations of the variability of sediment, structures, etc.) and sampling for laboratory studies were carried out at selected archaeological sites and on extant exposures.

Laboratory analyses of sediment samples concentrated on sediment granulometry, organic content and magnetic susceptibility. Analyses of granulometric composition using the laser diffractometry method were performed at the Soil Science Laboratory of the Department of Physical Geography at the Institute of Geography and Regional Development of the University of Wrocław (see Appendix 2.A1). Organic content was also determined there by the roasting method. Magnetic susceptibility was tested in a laboratory at the Czech Research Institute in Prague (see Appendix 2.A1). Dating of selected sediments with luminescent methods (OSL and TL) was done (after 2017) in the laboratories in Lublin (see Appendix 2.A3) and Oxford (see Appendix 2.A4).

The laser diffractometry method measures the size of particles in suspension at the time of measurement (Issmer 2000). The advantage of this method is the large measuring range of 0.002–2000 μm, a high reproducibility of the results, as well as its speed and the low sample weight required (Kuc 2017). In cases where grains with a diameter exceeding 2000 μm were noted, measurements were supplemented with sieving. Knowing the granulometric composition of sediments allows statistical lithodynamic indicators to be used to reconstruct the transportation and sedimentation conditions of loose sediments. This leads, in turn, to conclusions concerning changes in the dynamics of these processes. Indirectly, this can also be used to reconstruct general environmental conditions. Basic statistical indices are calculated following the analysis of the granulometric composition of the samples (Racinowski, Szczypek, and Wach 2001):

Mean size diameter

$$M_z = \frac{\varnothing 16 + \varnothing 50 + \varnothing 84}{3}$$

Kurtosis

$$K_G = \frac{\varnothing 95 + \varnothing 5}{2{,}44 \cdot (\varnothing 75 - \varnothing 25)}$$

according to R.L. Folk and W.C. Ward (1957)

The following classes of kurtosis were adopted for the distribution curves: 0.41–0.67 very platykurtic distribution; 0.67–0.90 platykurtic distribution; 0.90–1.11 mesokurtic distribution; 1.11–1.5 leptokurtic distribution; 1.50–3.0 very leptokurtic/extremely leptokurtic distribution.

Standard deviation

$$\delta_I = \frac{\varnothing 84 - \varnothing 16}{4} - \frac{\varnothing 95 - \varnothing 5}{6{,}6}$$

according to R.L. Folk and W.C. Ward (1957)

For the standard deviation value, the following sorting ranges were adopted: <0.35 very good; 0.35–0.5 good; 0.5–1.0 moderate (medium); 1.0–2.0 weak; 2.0–4.0 very weak; >4.0 extremely weak.

Skewness

$$Sk_I = \frac{\varnothing 84 - \varnothing 50}{\varnothing 84 - \varnothing 16} - \frac{\varnothing 50 - \varnothing 5}{\varnothing 95 - \varnothing 5}$$

according to R.L. Folk and W.C. Ward (1957), modified by G. Warren (1974)

The following ranges were adopted for the skewness of the distribution: -1.0– -0.3 very negatively skewed; -0.3– -0.1 negatively skewed; -0.1–0.1 symmetrical; 0.1–0.3 positively skewed; 0.3–1.0 very positively skewed.

Median

$$Md_{\varphi} = \varnothing 50$$

(Inman 1952)

The indicators of the mean grain diameter **Mz** and **Md** are a measure of mean grain size, which allows for a reconstruction of the dynamics of the transport stream (in this case a fluvial stream). Standard deviation $\boldsymbol{\delta_I}$ is a measure of the sorting of material in loose sediment tests (Racinowski et al. 2001). It is assumed that the greater variability of the energy of the transport stream translates into less sediment being sorted. The graphical kurtosis of $\mathbf{K_G}$ is a measure of the stability of the current environment (Racinowski et al. 2001). The skewness of the $\mathbf{Sk_I}$, in turn, informs of increased content of coarser or finer fractions compared with the most common fraction. It is assumed that a positively skewed graph records a larger percentage of a finer fraction, that is, a tendency to decrease the speed/energy of the stream relative to the mean value, while a negatively skewed plot records higher speeds/energies (Kuc 2017).

2.3 SEDIMENT STUDY RESULTS

The results from four sites (AFD23, AFD24, AFD131 and AFD113) will be discussed on a site by site basis, followed by a discussion of exposures PG1, PG2 and PG3 in the riverbank zone (PG= Profil Geologiczny [=geological section]), the well and channel, and, finally, exposures GT20, GT21 and GT24 (GT=Geological Testpit). For the sake of clarity, OSL dates from an earlier series of analyses, which have appeared in previously published articles and which have since been proved in error (see page 12), are referenced after the datings in this section.

2.3.1 SITE AFD23

Given the special importance of archaeological finds from the southwestern sector of site AFD23, the formation of sediment in this area will be discussed in detail, mainly on the basis of stratigraphic analyses conducted before 2016 and limited data from the northern part of the site.

Additional granulometric analyses in 2018 were carried out on exposure GT23P, which had a depth of 1.20 m, the purpose being to document the stratigraphic context and sediment characteristics of a sample taken for TL dating; this location was situated approximately 15 m northwest of exposure GT11 that had been analyzed in 2014 [*Fig. 2.3*].

2.3.1.1 Facies A

The earliest deposits to be recorded were found in exposure GT1 (area of trench 2012/C) [*Fig. 2.4*]. The total thickness of this layer was not established because exploration stopped at a depth of 3.60 m. However, the top of the layer was recorded at 250.80 m asl (approximately 2.60 m below the modern surface). This sediment, with a predominance of sand over fine-grained

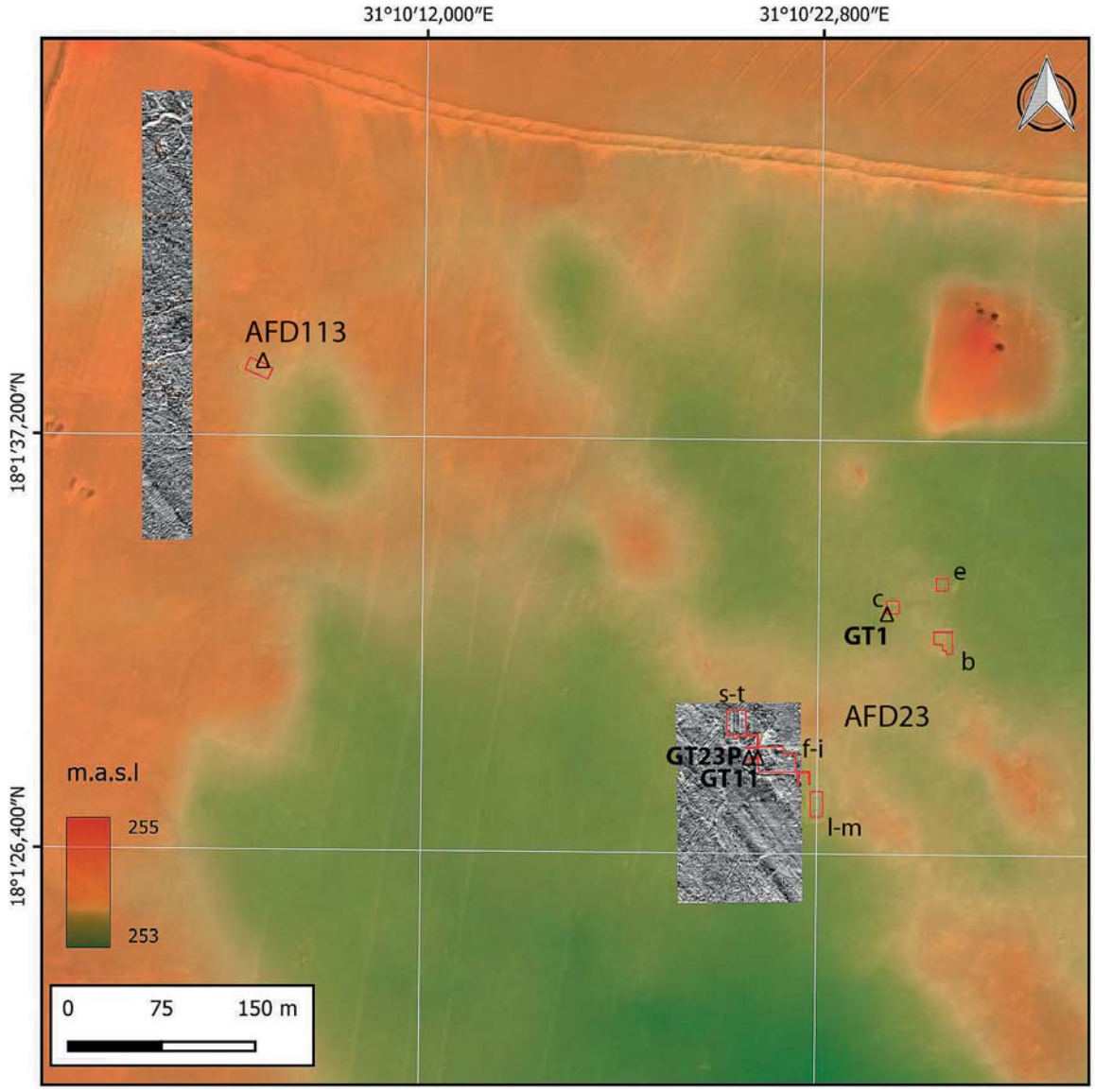

Fig. 2.3. Location of geological exposures (GT) at sites AFD23 and AFD113, superimposed on a DEM image of the site including the results of magnetic mapping

fractions and a relatively high magnetic susceptibility, constitutes evidence for a wetland ecosystem with periodic flooding.

2.3.1.2 Facies B

An accumulation of silt characterized by a high degree of magnetic susceptibility indicates a wetland environment also in the next layer recorded in exposure GT1 [see *Fig. 2.4*]. This facies accumulated up to a level of ~252.4 m asl. It corresponds to a period of increased water levels.

2.3.1.3 Facies C

The third and final series of silts from the pluvial recorded in the sections was at the same time the bottommost layer in all of the archaeological trenches explored at AFD23, as well as the geological test pits GT11 and GT23P [*Fig. 2.5*]. These silts, marked as sedimentation unit 23.C.1, formed an undulating surface with elevation differences exceeding 1 m in the exposures (outside the trenches, the top of this hardened layer of silts would be subject to denudation processes wherever it appeared on the surface). These silts are a predominantly light gray in color (10YR7/2 dry; 10YR6/3 wet). A sample from 253.0 m asl was dated to 60.11 ± 8.70 ka (Lub-5657, OSL-MG-CAM); the initial dating, later revised, was 21.1 ± 2.32 ka (UJK-OSL-36, OSL-MG-MAM).

Depressions in the surface of this facies were filled with brownish sandy silts (10YR7/4 dry), which were characterized by increased magnetic susceptibility (sedimentation unit 23.C.2). This sediment was dated to 57.83 ± 9.69 ka (Lub-5656, OSL-MG-CAM).

2.3.1.4 Facies D

A drying and cooling of the climate resulted in increased aeolian activity corresponding to an accumulation of a series of sand layers. At Affad, this process was observed in the form of very sandy brown silts (10YR5/3 dry, 10YR4/4 wet) deposited over the entire surface of the site (sedimentation unit 23.D.1) [*Figs 2.6, 2.7*]. The dating of a sample from a depth of 0.65 m, that is, 252.62 m asl, is 57.9 ± 4.9 ka (Lub-6431, OSL-MG-CAM) and 50.02 ± 5.58 (L018, OSL-SG-FMMc3); the initial published date, now rejected, was 15.9 ± 1.75 ka (UJK-OSL-35, OSL-MG-MAM).

On lower ground, the color of deposits from this facies was slightly darker (10YR7/3 dry; sedimentation unit 23.D.1a), probably indicating slightly wetter sedimentation conditions (palaeochannel beds?). However, the chronology of this deposit was confirmed in the G–H section [*Fig. 2.6*], where the marginal zone and the overlapping of the two deposits were observed. A zone of overheated substratum, recorded in the basement section of this stratification in 2017, was interpreted as the remains of a hearth related to Palaeolithic settlement as suggested by a TL date of 46.4 ± 4.0 ka (Lub-6432). This indicates settlement during a dry period, when fires could be lit even on lower ground. Meriting attention is a clear peak in the value of organic substances in samples from the GT23P exposure, corresponding to the Palaeolithic settlement.

However, the finest-grained variety of facies D deposits (yellowish-brown in color, 2.5Y6/3 dry, 2.5Y5/3–4/4 wet) lay in the higher parts of the studied area, the layer reaching 0.40 m in thickness. Remains of Palaeolithic settlement were recorded mostly within this sediment. Cut features (postholes, pits) also appeared in the top of the facies D sands.

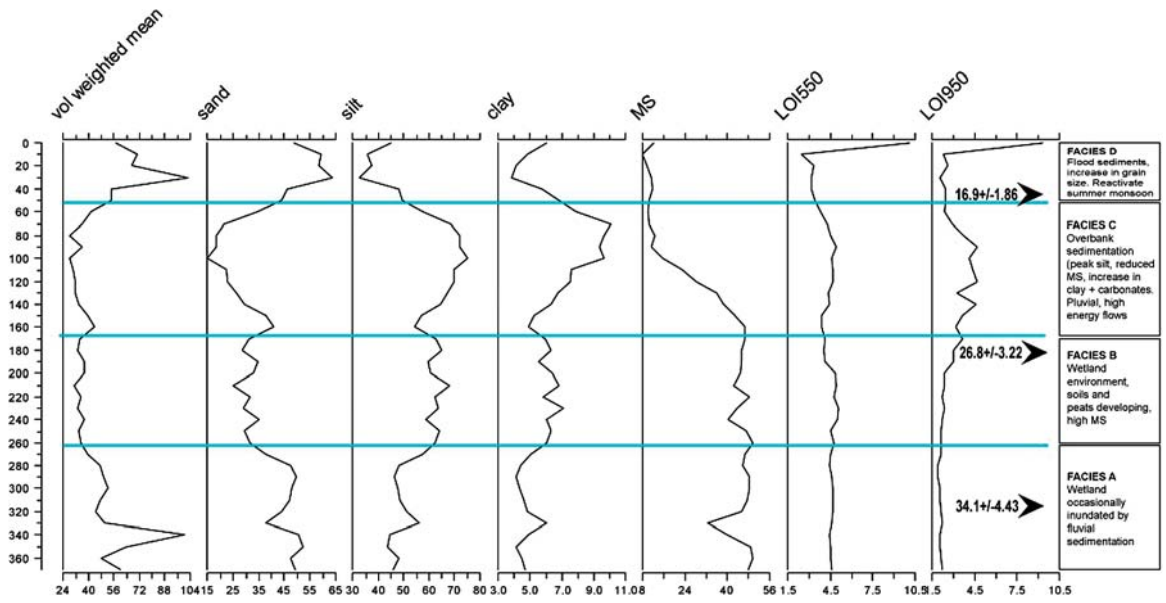

Fig. 2.4. GT1 exposure: granulometric comparison (sand-silt-clay), magnetic susceptibility (MS), and content of organic (LOI550) and inorganic (LOI950) fractions. Absolute dates were obtained with the multigrain technique (MG), using the MAM model, hence they reflect only the mean minimum age of the layers. See Appendix 2.A1 for an explanation of units on the horizontal scale

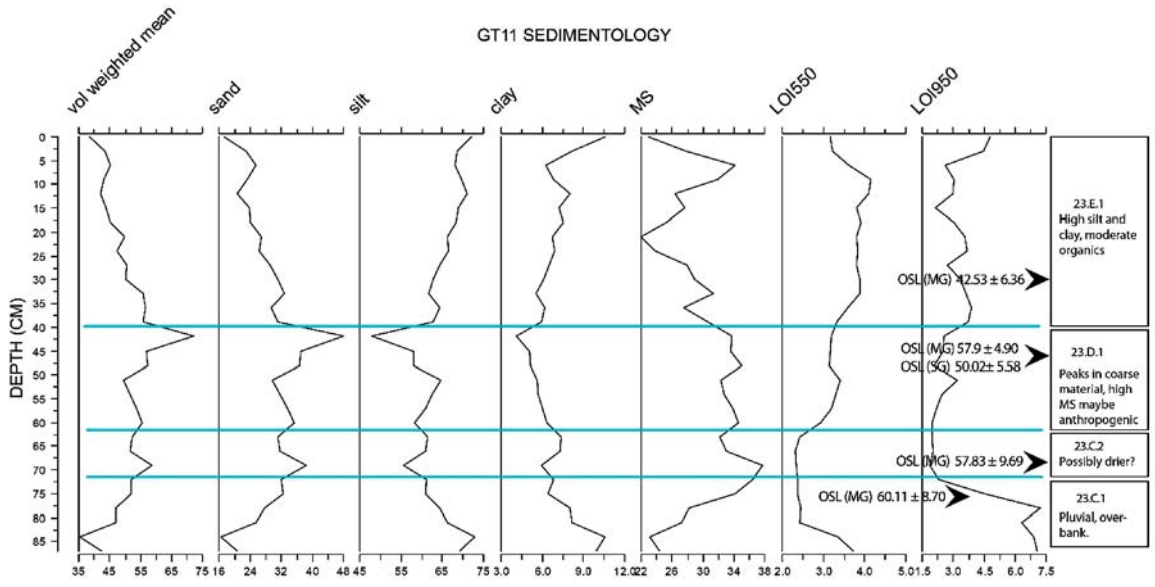

Fig. 2.5. GT11 exposure: granulometric comparison (sand-silt-clay), magnetic susceptibility (MS), and content of organic (LOI550) and inorganic (LOI950) fractions. Absolute dates were obtained by the multigrain (MG) method, applying the CAM model, and, in one case, single-grain (SG) applying the FMM model. See Appendix 2.A1 for an explanation of units on the horizontal scale

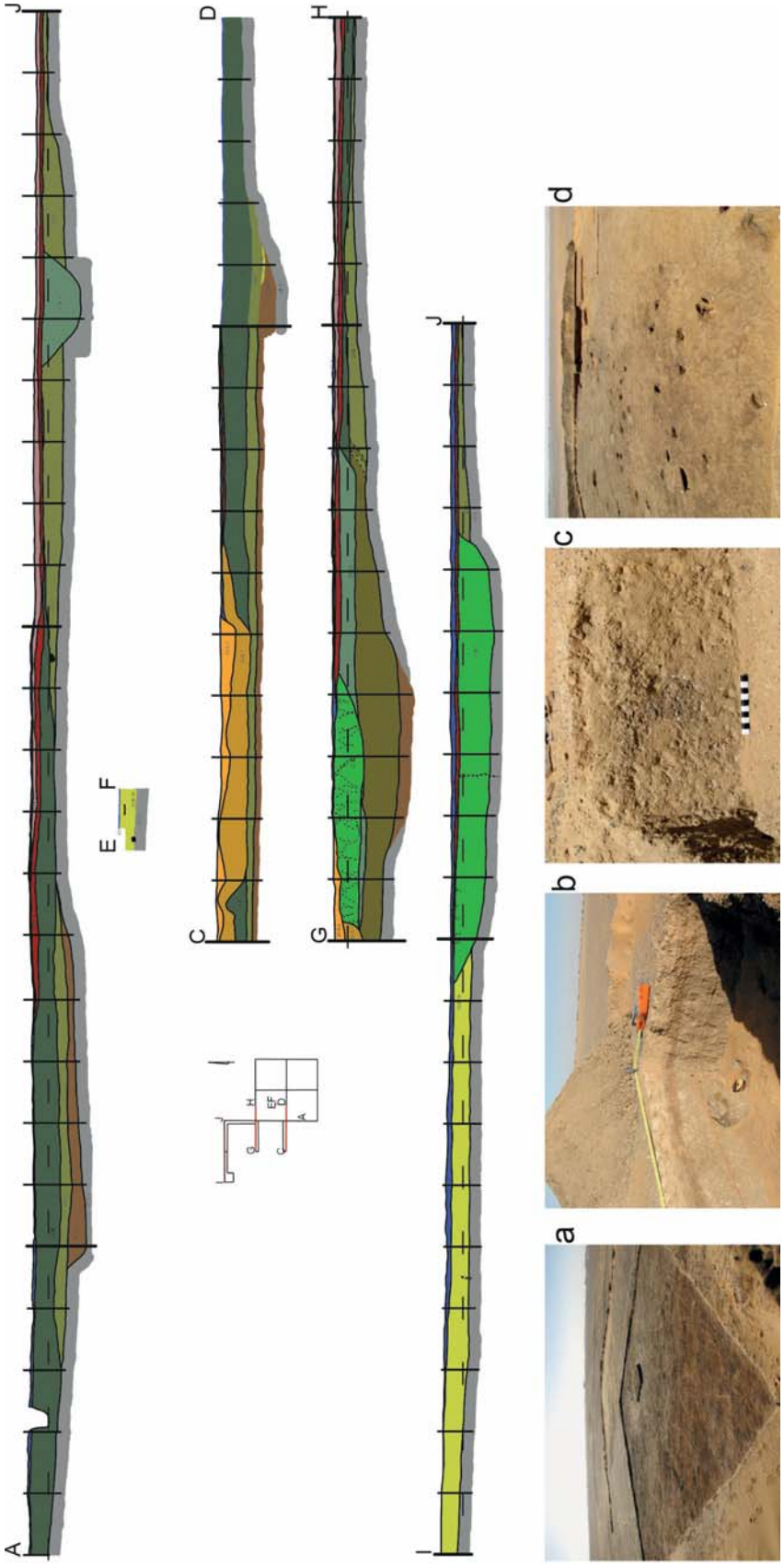

Fig. 2.6. Stratigraphic sections in the southwestern zone of site AFD23 illustrated with a selection of views of sediment exploration: a – gravel roof layer 23.F.1 in the foreground, in trench 2013/I from the northwest; b – stratigraphy in the northwestern corner of trench 2013/I with visible layer 23.F.1, below it silt (23.E.1) and a large chert concretion in sandy silt (23.D.1); c – evidence of cut features (postholes) from the roof layer of aeolian silt (23.D.1b) in trench 2013/I/54; d – partly explored basement sections of postholes intersecting silt (23.C.1) in trench 2013/FI and a relief depression (in the background) filled with alluvial layers (facies D, E and F). Section colors correspond to those appearing in *Figs 2.7* through *2.9*

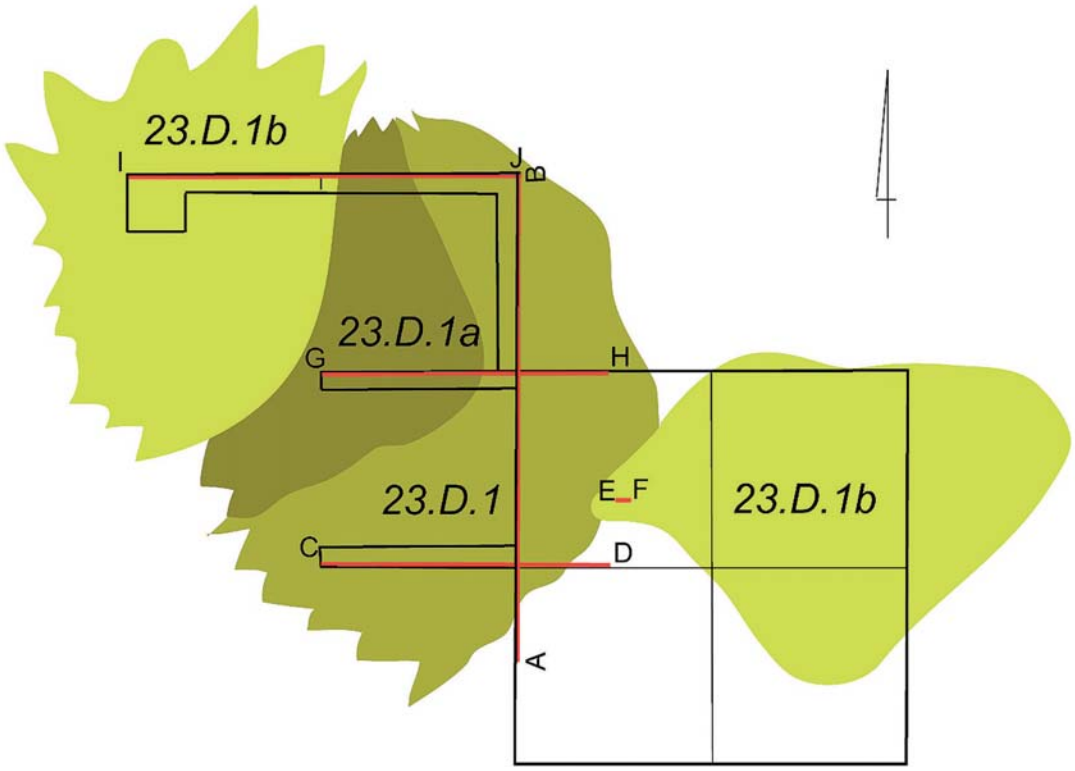

Fig. 2.7. Facies D sediments deposited around the southwestern zone of site AFD23

2.3.1.5 Facies E [*Fig. 2.8*]

Episodes of renewed high-water levels are attested by a series of silt deposits filling the numerous relief depressions [*Fig. 2.8*]. The earliest of these, sedimentation unit 23.E.1 (brownish in color, 10YR7/3 dry), is dated to 42.53 ± 6.36 ka (Lub-5658, OSL-MG-CAM); the previously published date was 15.3 ± 1.68 ka (UJK-OSL-34, OSL-MG-MAM).

New erosion channels with a depth not exceeding 1 m and the brown (10YR5/3 dry, 10YR4/3 wet) gravel filling them (sedimentation unit 23.E.2) probably mark an intermediate stage of changing environmental conditions (greater river energy indicated by significantly increased MS indices in exposure GT23P). The simultaneous accumulation of dark yellowish-brown sediment (10YR3/4 dry, 10YR4/4 wet) in these channels (sedimentation unit 23.E.3) marks a return to a wetland environment. These deposits also reveal numerous mineral precipitates around ancient plant root systems. Single fragments of bones and stone artifacts recorded in the basement of these deposits signify the washing away and erosion of upper parts of older sediments related to occupation in the late Pleistocene. Significantly, no Holocene artifacts (whether pottery or microlithic debris) were noted in these deposits.

2.3.1.6 Facies F (Fe-rich pluvial?)

Sedimentation unit 23.F.1 marks the next phase of denudation of the remains of the wetland and the accumulation of gravel saturated with iron precipitates [*Fig. 2.9*]. It filled an extensive albeit shallow hollow in a former, partly filled erosion channel. Up to 0.10 m thick, this sediment had

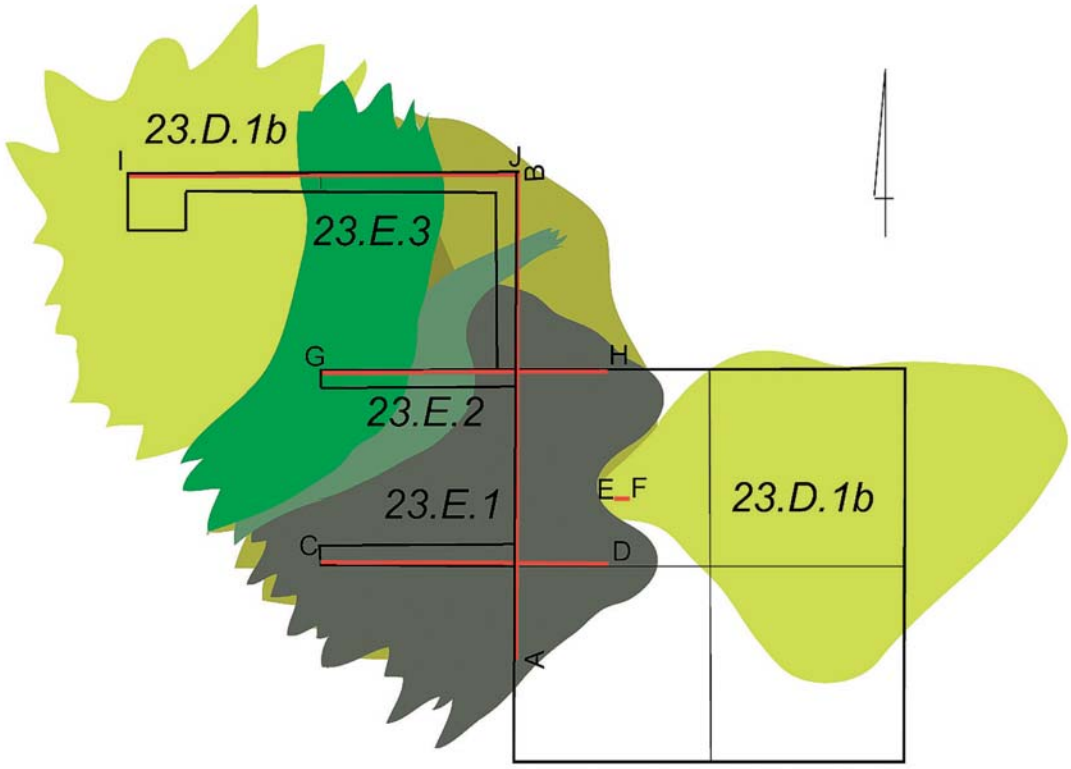

Fig. 2.8. Facies E sediments deposited around the southwestern zone of site AFD23

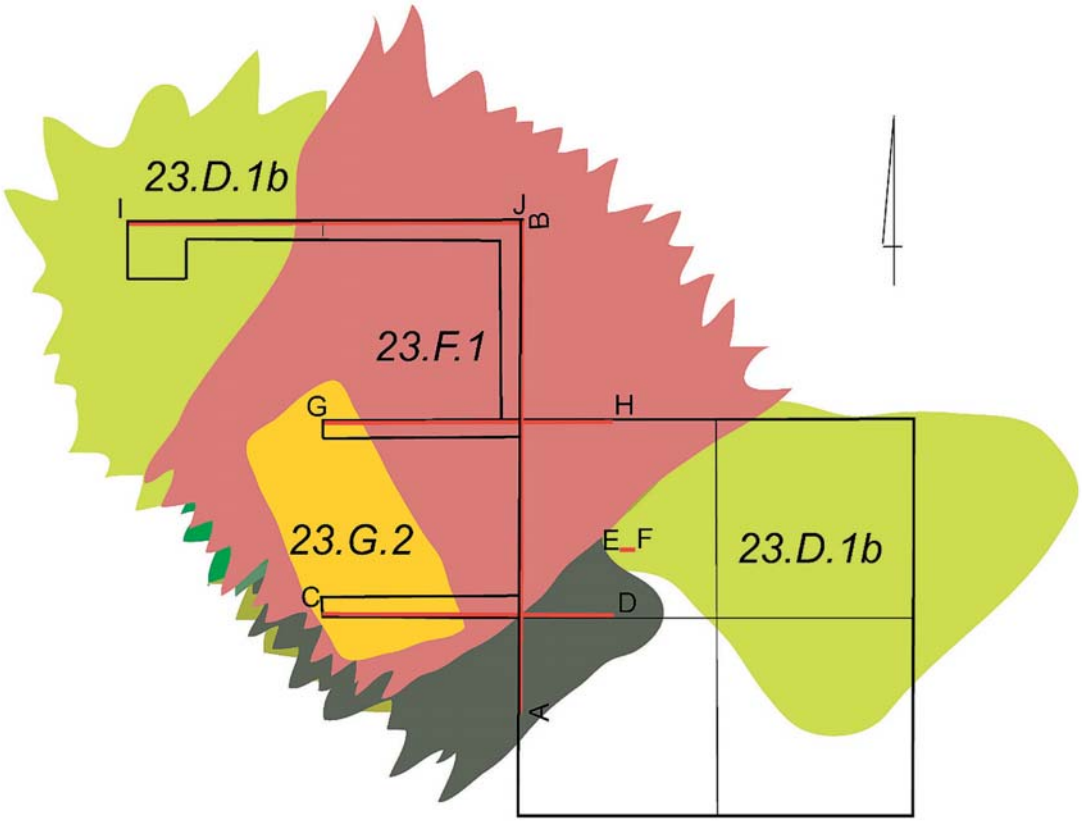

Fig. 2.9. Facies F and G sediments deposited around the southwestern zone of site AFD23

an intensely dark reddish-brown color (2.5YR4/4 dry), while above it there was sometimes a thin layer of fine-grained silt of slightly pinkish, almost white color (2.5YR8/1 dry; sedimentation unit 23.F.2). Although the gravel accumulation is of fluvial origin, the formation of a layer of silt means the end of this process and the domination of aeolian sedimentation. Both strata of this facies mark the beginning of the degradation of the wetland environment associated with the desiccation of the climate following the Early Holocene period. A lowered magnetic susceptibility of these sediments and the low percentage of organic substances recorded in the GT23P exposure should also be noted.

2.3.1.7 Facies G and X

A large cut recorded in the western part of the test pits in the 2014/N area reached the top of the sandy silts of facies D at a depth of 0.70 m. Filling it was sand with fine-grained concretions (sedimentation unit 23.G.1), as well as laminates of aeolian sands (sedimentation unit 23.G.2). The cut is assumed to be of anthropogenic origin and relatively young (modern?) in age. Silt was most likely extracted here for construction purposes (mud-brick production?), probably not the road construction project of 2009 because the contours of the trench cannot be seen on the surface, while the most recent exposures, made with bulldozers, were until recently (2018) still visible both as cuts and as accompanying piles of sand.

The entire surface (except for modern cuts) is covered with a thin layer (up to 5 cm) of aeolian material (sedimentation unit 23.X). Progressive erosion of the sediments containing archaeological artifacts (facies D) left objects dispersed over the modern surface, that is, over sediments of later date (facies E and F).

2.3.1.8 Geological test pit GT23P (2018)

The basic fraction in this exposure (75–87%) comprises silt with some clay (7–4%), sand (6–10%) and very fine gravel (0.16–11%). The dominance of the silty fraction is evident, with slight declines in favor of sands and very fine gravel [*Fig. 2.10*]. An exception is a sample from a depth of 1.10 m, where the recorded gravel content was relatively the highest in the whole exposure (approximately 10%). At the same time, analysis of a sample from a depth of 0.10 m indicated a very clear drop in silt content and corresponding rise in that of sand (27.85%) and very fine gravel (8.87%), as well as clay (3.92%). The Md and Mz values are in the range of 5.17–6.62 and 5.40–6.71, respectively. The standard deviation ranges from 1.79 to 1.75 to a depth of 0.80 m. It drops to 1.55–1.61 going up to the roof layer, where it rises sharply to 2.40. The situation is similar in the case of skewness (Sk_I): a symmetrical distribution of values up to a depth of 0.80 m, then positively skewed towards the roof layer and again positively skewed in the roof layer itself.

To a depth of 0.70 m, K_G takes on very slightly differentiated values from 0.84 to 0.89 (very platykurtic); towards the roof layer the flattening of the distribution turns into a platykurtic curve, and in the roof layer itself into a mesokurtic curve.

Exposure GT23P is located in fluvial sediments (silts) in a sandy roof layer section with a slight addition of very fine gravel (facies 23.F). The values of the lithodynamic indices indicate that all sediments correspond to a low-energy environment. The sediments are poorly sorted, the Mz and

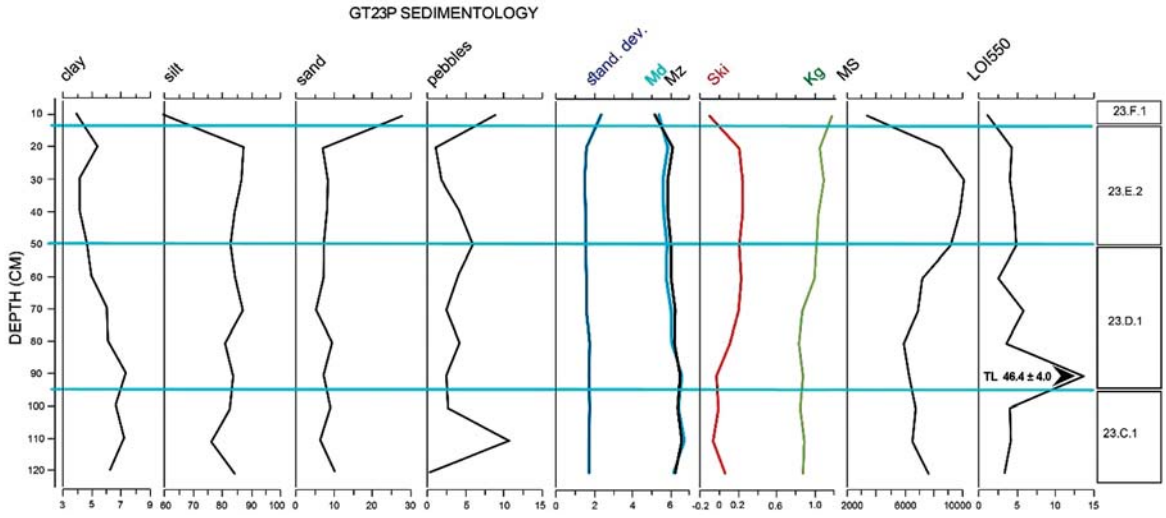

Fig. 2.10. Exposure GT23P: comparison of granulometry (clay-silt-sand-pebbles), lithodynamic indicators (standard deviation, Md, Mz, Sk_I, K_G), magnetic susceptibility (MS) and content of organic fractions (LOI550). Far right column and blue lines represent stratigraphy recorded macroscopically in the exposure. See Appendix 2.A1 for an explanation of units on the horizontal scale

Md values indicate that they are quite homogeneous, while the flattening of the distribution (very platykurtic and platykurtic) also suggests low-energy conditions and high saturation with mineral material. Therefore, it should be concluded that these are non-channel sediments deposited under flood conditions. The significant increase in the content of sand and very fine gravel in the basement is related to the deposition of intensely red sediments of facies 23.F. The very poor sorting of the material in the latter sediment may indicate a sediment trap.

2.3.2 Site AFD24

Detailed analyses of site AFD24, which is comparable to site AFD23, were carried out on a 0.50-m-deep section in the northwestern wall of trench A [*Fig. 2.11*]. The site was located on a slight elevation of the ground, probably surrounded by wetlands during the late Pleistocene. As at AFD23, numerous postholes and locally overheated ground, interpreted as the remains of a seasonal campsite, were recorded here (see below, § 5.1.2). Anthropogenic features consisted of cuts sliced through hard stratifications corresponding to facies C sediment at site AFD23. Relief depressions in this surface were filled with much looser sand and dust (analogous to the facies D sediment at site AFD23). However, no layers indicating the return of a wetland environment (corresponding to facies E at AFD23) were recorded, which is also confirmed by the uniform diagram of a decrease in magnetic susceptibility towards the roof layer of the section.

The dominant fraction in the AFD24 section [*Fig. 2.12*] is silt: from 78% to 65%. The content of sand increases towards the roof layer from 15.24% to 32.58%, while the content of fine gravel is small, exceeding 5% (depth of 0.30 m) in only one case. However, sand in the roof layer itself comprises 2.13%. There was also a drop in clay content ranging from 5.5% to 2%. The values of

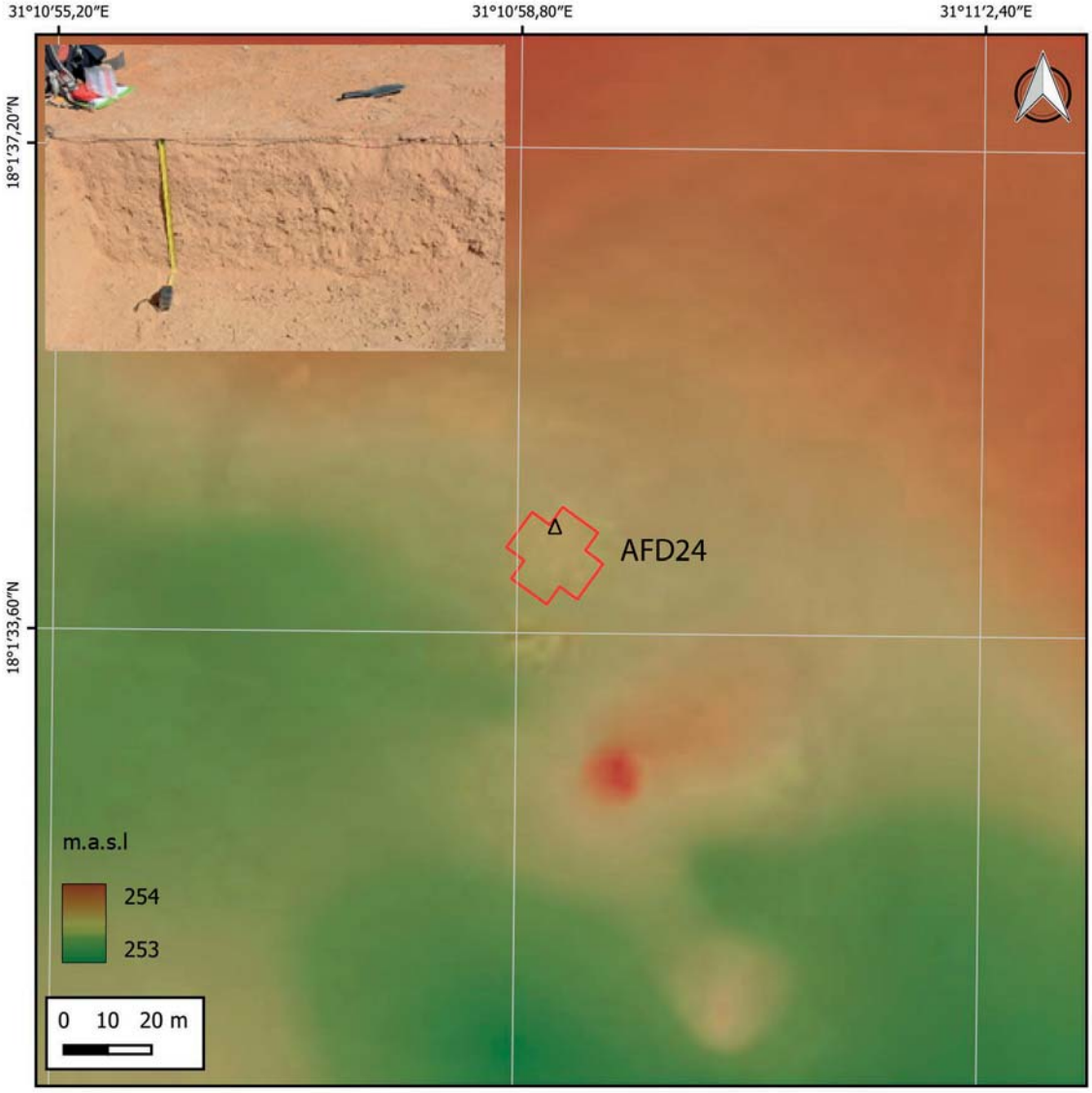

Fig. 2.11. Location of the sections examined at site AFD24 (trench marked with a red contour line); inset, view of the documented section

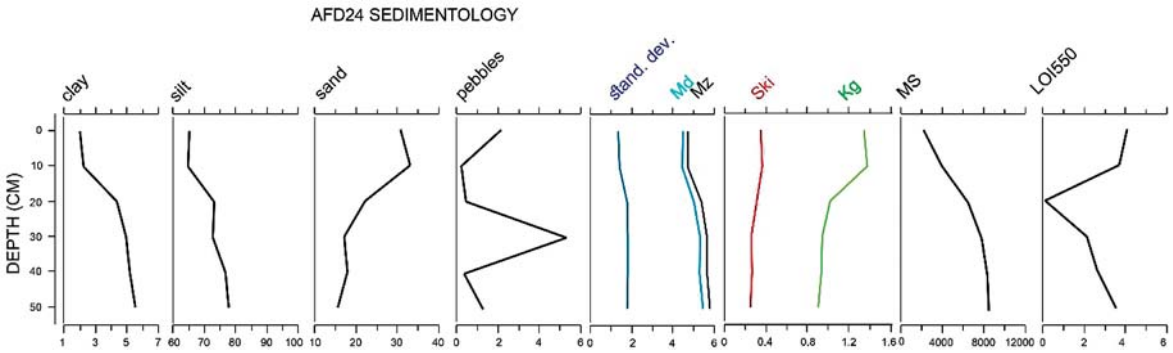

Fig. 2.12. AFD24 exposure: comparison of granulometry (clay-silt-sand-pebbles), lithodynamic indices (standard deviation, Md, Mz, Sk_I, K_G), magnetic susceptibility (MS) and content of organic fractions (LOI550). See Appendix 2.A1 for an explanation of units on the horizontal scale

the indices successively decrease towards the roof layer. The Md and Mz values are in the range of 5.46–4.45 and 5.77–4.73, respectively. Standard deviation is within the range of 1.83–1.40, which indicates poor sorting of the material. At the same time, skewness (Sk_I) values at 0.25–0.36 increase in the direction of the roof layer. Although to a depth of 0.30 m the distribution is symmetrical, in the direction of the basement it changes into a positively skewed one. Similarly, in the case of K_G, the values increase towards the roof layer from 0.90 (mesokurtic) to 1.37 (leptokurtic).

The exposure is located within sandy silts with a marginal addition of very fine gravel. The same as at site AFD23, these sediments represent a low-energy environment indicated by the values of the lithodynamic indices. Sediment is poorly sorted and quite homogeneous to judge by the Mz and Md values, and the flattening of distribution (mesokurtic and leptokurtic) also suggests low-energy conditions. Therefore, it should be concluded that these are non-channel sediments deposited under flood conditions, generally corresponding to the sediments representing facies D and E at AFD23. The significant increase in the content of sand and very fine gravel in the roof layer is probably related to aeolian processes and the gradual drying out of the material.

Lower layers of much greater hardness, probably corresponding to the facies C silts of site AFD23, were not sampled.

2.3.3 Site AFD131

Two sections, one 1.00 m deep (AFD131-I) and the other 1.10 m (AFD131-P), located 2 m apart in the riverbank zone of the palaeochannel, were analyzed at this site. Palaeolithic camp remains were recorded in layers forming the upper part of these sections; there was no evidence of cut anthropogenic features (whether postholes or hearth remains). The area may have been denuded to a greater extent than in the case of sites AFD23 or AFD24 but, alternatively, it could have seen occupation of some kind in the rainy season in a zone situated away from the river and floodplains; the latter interpretation derives from an archaeozoological study of the animal bone remains (see Chapter 3) and the range of raw materials used to make stone tools found at the site (see Chapter 4), both of which can be seen as an indication of activity during the rainy season. Consequently, the stratification from this location complements observations from sites AFD23 and AFD24, providing data on sedimentation conditions in the riverbank zone of the channel naturally predating occupation. The gradual filling of the channel is a process visible in the magnetic imaging [*Fig. 2.13*]. A sample taken from these deposits, at a depth of 0.50 m, was dated to 63.8 ± 4.3 ka (Lub-6552, OSL-MG-CAM).

Section AFD131-I is comprised of silty sands. Towards the top there is a drop in the percentage of the predominant sand fraction (65.37–48.79%) and an increase in silt content (35.57–49.38%) [*Fig. 2.14* top]. The roof layer is an exception, silt constituting here 49.38% compared to 48.79% sand. The clay content is low and does not exceed 2% in any of the samples. The Md and Mz values are in the range of 3.50–4.04 and 3.82–4.38, respectively. Standard deviation is in the range of 1.46–1.72, which indicates poor sorting of the material. However, in the case of skewness (Sk_I), values are in the range of 0.40–0.35 (positively skewed distribution). Similar to the values of other indicators, the K_G values also decrease towards the roof layer, from 1.26 (leptokurtic distribution to a depth of 0.80 m) to 1.11–1.07 (mesokurtic).

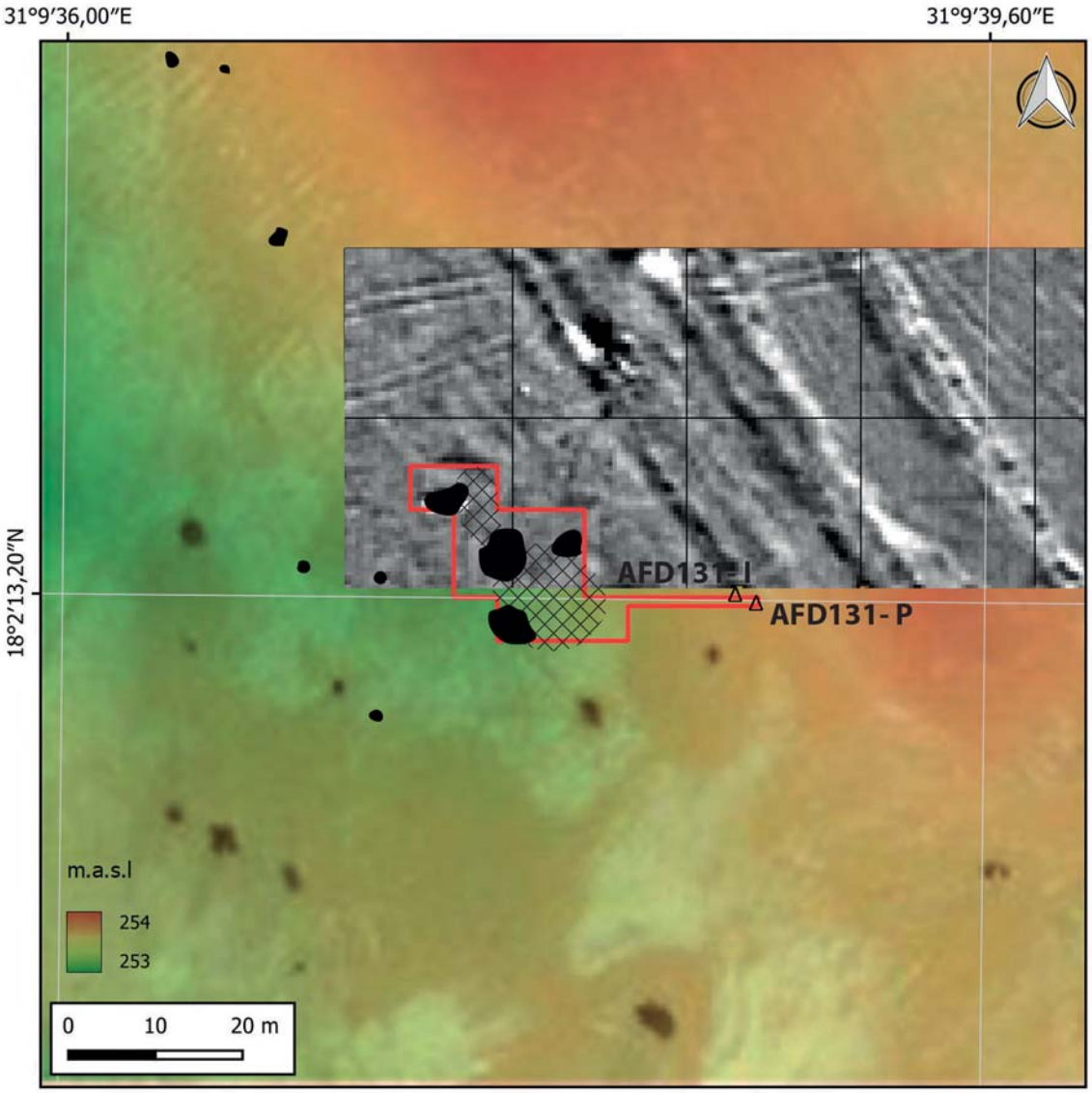

Fig. 2.13. Location of sections examined at site AFD131, superimposed on magnetic imaging of the area and location of archaeological artifacts on the surface, black-line hatching for the stone artifacts and solid black for bone remains

This section is located within an accumulation of fluvial sands. These are sediments deposited by a low-flow stream with a tendency to increase flow energy as indicated by the values of lithodynamic indices. The sediment is poorly sorted, the Mz and Md values indicate that it is fairly homogeneous, while the flattening of the distribution (leptokurtic and mesokurtic) suggests a successive decrease in the flow energy. In the roof layer part, the change of dominant fraction from sandy to silty documents a decrease in flow velocity and/or an increase in the percentage of aeolian material. Analysis of the granulometry of the sediment and the lithodynamic indices indicates that site AFD131 was located in the former riverbank zone of a palaeochannel with low flows, showing a slight growing tendency from the mean. Episodically increased flow energy is also suggested by the jump in magnetic readings of samples taken from a depth of 0.30–0.40 m.

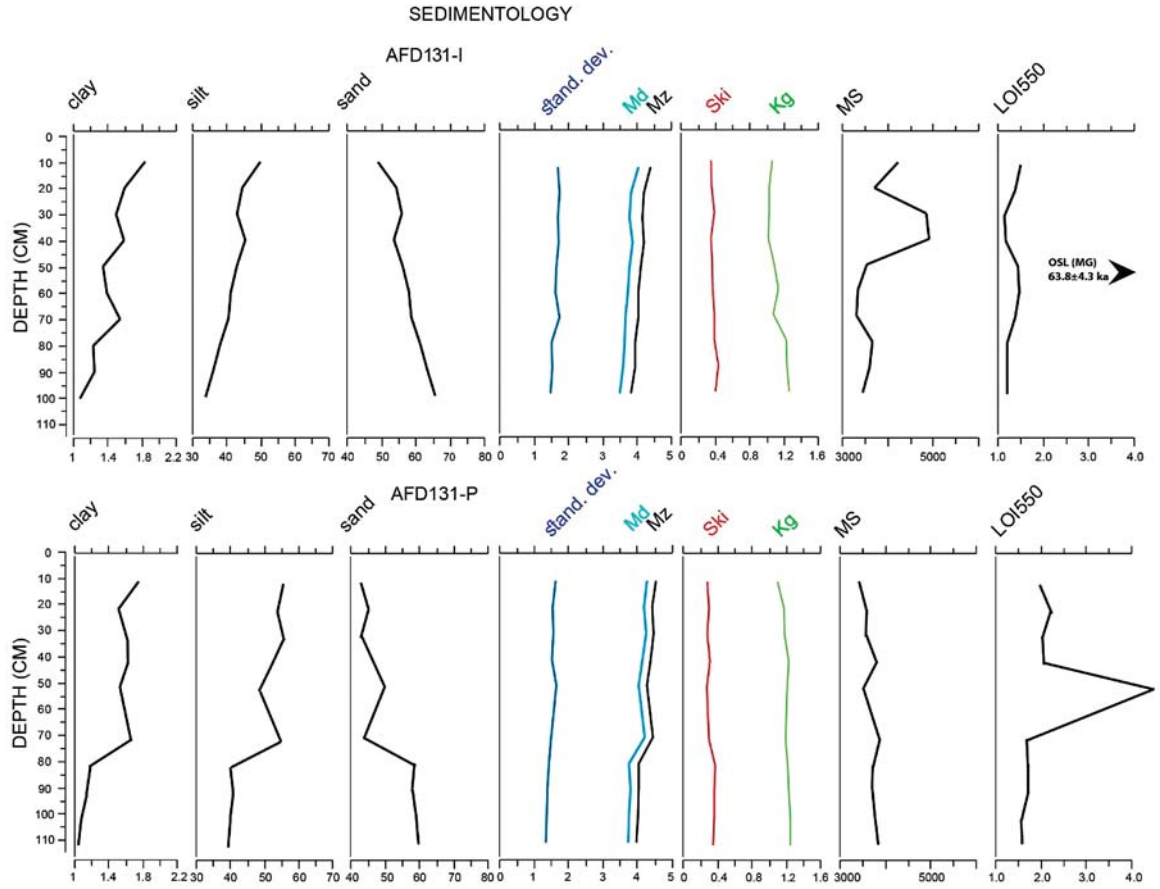

Fig. 2.14. AFD131-I (top) and AFD-P (bottom) sections: comparison of granulometry (clay-silt-sand), lithodynamic indices (standard deviation, Md, Mz, Sk_I, K_G), magnetic susceptibility (MS) and content of organic fractions (LOI550). See Appendix 2.A1 for an explanation of units on the horizontal scale

As for section AFD131-P, it is similarly structured of silts and sands [*Fig. 2.14* bottom]. However, there is a clear difference in the silt-to-sand percentage compared to the previous section. Up to a depth of 0.80 m, the dominant fraction in the range of 59.98–42.94% is constituted by sands, while the silt content is in the range of 38.98–40.08%. This sand-to-silt ratio is not reversed, dust in the 54.58–52.05% range continuing to be the dominant fraction looking towards the roof layer, while the sand content drops to 49.97–43.10%. The Mz and Md values also increase towards the roof layer, reaching 3.71–4.24 and 3.95–4.50, respectively. Standard deviation grows significantly to 1.33–1.62. Skewness values, in turn, decrease to 0.38–0.28. Similarly, kurtosis values towards the roof layer drop to 1.24–1.09.

The AFD131-P section is also located within an accumulation of fluvial sands. However, it seems to record a higher flow energy (sands are the dominant fraction in the lower part). The Mz and Md values indicate a successive decrease in flow velocity. The sediment is poorly sorted, indicating a variation in the flow rate. Sk_I values indicate a very positive flattening of the distribution, which also documents a successive drop in flow energy with a tendency for the average value to decrease. A leptokurtic and, in the upper part, mesokurtic kurtosis of the distribution also confirms a general tendency towards a decrease in energy and low dynamics of flow changes recorded in the section. Episodic drying and the presence of vegetation cover is suggested by a clear peak of increased organic matter content in a sample from a depth of 0.50 m.

2.3.4 Riverbank zone of a palaeochannel: exposures PG1, PG2 and PG3

Another location important for determining the nature of the layers filling the river palaeochannels was the zone between sites AFD125 and AFD122. Magnetic imaging revealed a strong layer differentiation [*Fig. 2.15*]. A sedimentological analysis was carried out on exposures in three key zones, namely: PG1 – furthermost to the south, including relatively homogeneous silt filling a palaeochannel; PG2 – the most varied zone in terms of magnetic susceptibility; and PG3, located in aeolian sands, which turned out to be the oldest element. OSL-MG-CAM dating of samples from PG2 and PG3 showed that the depression (an east–west channel trough) proceeded to be filled from the north, the process starting at the beginning of MIS3 (66.0 ± 7.0 ka: Lub-6550; 58.4 ± 5.7 ka: Lub-6549); fluvial silts accumulated somewhat later (43.8 ± 4.9 ka: Lub-6551).

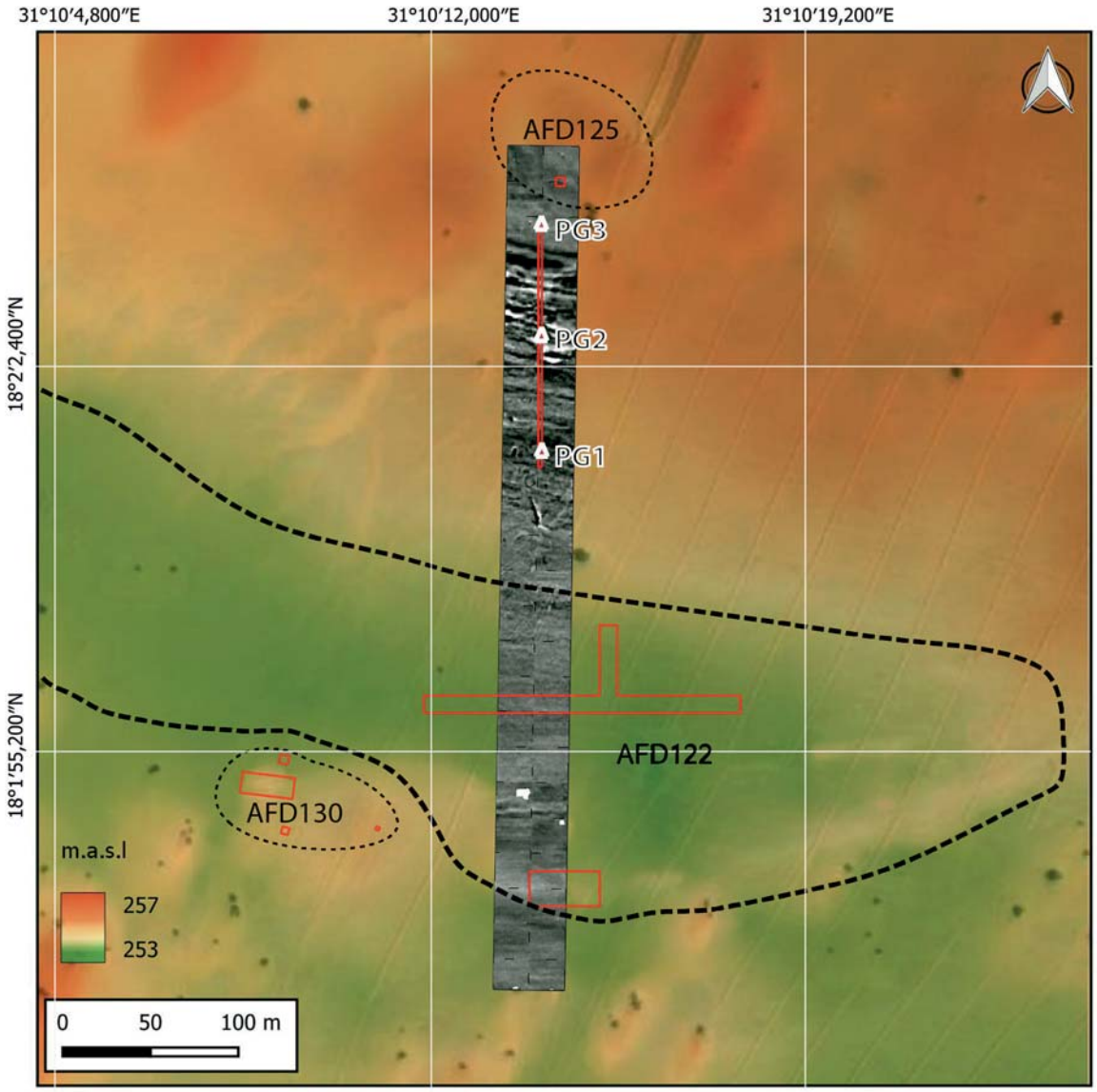

Fig. 2.15. Location of exposures PG1, PG2, and PG3 (marked with a red contour line), examined in the riverbank zone of a palaeochannel indicated on a map augmented with superimposed magnetometric imaging

The three analyzed soil exposures were aligned with one another, forming a line approximately 15 m long [see *Fig. 2.15*]. The dominant fraction in PG1 [*Fig. 2.16* bottom] is silt, the content of which, towards the roof layer, increases to 77.80–81.50%, while the content of sands simultaneously drops (to 18.04–14.21%). The clay content fluctuates between 3.5 and 4.5%. The Mz and Md values increase toward the roof layer, to 5.21–5.50 and 5.38–5.69, respectively. The standard deviation is in the range of 1.84–1.55. Skewness values are at a similar level of 0.13–0.16, with a higher value of 0.24 being recorded only at a depth of 0.40 m. KG values are in the

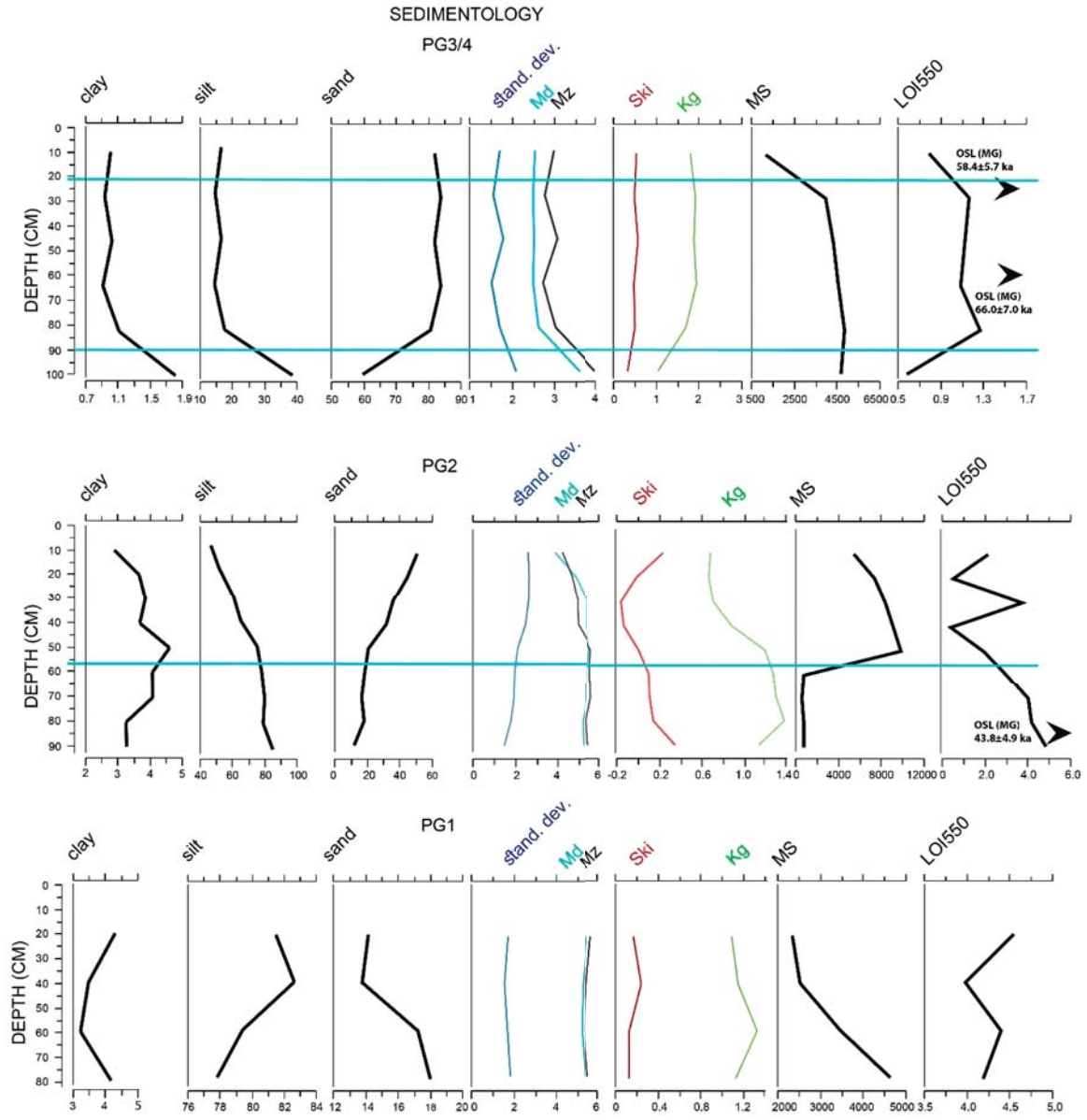

Fig. 2.16. Exposures PG1 (bottom), PG2 (central), PG3 (top): comparison of granulometry (clay-silt-sand), dynamic indices (standard deviation, Md, Mz, Sk_I, K_G), magnetic susceptibility (MS) and the content of organic fractions (LOI550). Blue lines represent stratigraphy recorded macroscopically in the exposure. See Appendix 2.A1 for an explanation of units on the horizontal scale

range of 1.33–1.09. Silt is dominant also in exposure PG2 [*Fig. 2.16* center]; its content gradually decreases towards the roof layer (85.23–51.80%), while the content of sand increases significantly (11.50–44.55%). In the roof layer part, however, the situation is reversed with sands constituting at 50.80% the dominant fraction in relation to 46.33% of silt. The clay content ranges from 4.5% to less than 3% in the roof layer part. The Mz and Md values decrease towards the roof layer, trending 5.49–3.81 and 5.38–4.16, respectively. Standard deviation is calculated in the range of 1.84–1.55. Skewness values generally drop in the direction of the roof layer where they fall in the range of 0.34 to -0.11 but increase to 0.22 in the roof layer itself. K_G values in the range of 1.38–0.68 also show a drop towards the roof layer. Last but not least, exposure PG3 comprises sands [*Fig. 2.16* top], the content of which grows to 59.43–83.98% towards the roof layer. Although the silt content in the roof layer itself amounts to 38.76%, it clearly diminishes to 18.21–15.12% towards the roof layer. The clay content is marginal, exceeding 1% (1.8%) only in the basement. The Mz and Md values drop off towards the roof layer, reaching 5.49–3.81 and 5.38–4.16, respectively. Standard deviation ranges from 2.06 to 1.50. Skewness values increasing towards the roof layer fall within the range of 0.31–0.55. K_G values also increase in the range of 1.03–1.91 towards the roof layer.

The discussed three exposures are located in different zones of a fossil palaeochannel. The northernmost exposure (PG3/4) displays sedimentation of (aeolian) sand with fairly uniform graining and even indications of magnetic susceptibility. The sand percentage is lower only in the bottom of the exposure (sample at a depth of 1.00 m). The PG2 exposure shows a dynamic change in sedimentation, one which is particularly clearly visible in the MS indices for samples from a depth of 0.60 m and 0.40 m. The percentage of organic substances also indicates different characteristics of sediments from the lower and upper parts of the exposure. Similarly, granulometric observation found grain size to be relatively uniform in samples from below 0.60 m, and increasingly more permeated with sand above this level. However, the PG1 exposure shows the most evenly occurring sedimentation process, dominated by silts with successively decreasing MS indices towards the roof layer.

2.3.5 Site AFD113

The fishbone remains from site AFD113 made it an extremely important site from an archaeological point of view (see Chapter 3). Magnetic prospection alongside the western side of the explored trenches indicated that this was in fact the bed of a fossil channel at least seasonally exploited in Palaeolithic times to catch fish, most likely when a falling water level made the use of additional accessories (such as nets) for the purpose redundant.

Samples from a trench section at the site [*Figs 2.3, 2.17*] were expected to provide a characteristic of sediment accumulating in such an environment. The section was 0.75 m deep, displaying a silt/mud structure, this being the dominant fraction (70–88%) [*Fig. 2.18*]. Down to a depth of 0.65 m below the modern surface, the deposits were clearly sandy (11.72–19.05% sand), but with the sandy fraction significantly dropping to 3.96–1.06% within the first 0.15 m in favor of clay, which grew in the range of 10–14%. In the roof layer, clay content dropped to 7.96%, while the sand content increased significantly to almost 10%. Md and Mz values are in the range of

3.50–4.04 and 3.82–4.38, respectively. Standard deviation is in the range of 1.46–1.72, which indicates poor sorting of the material. However, in the case of skewness (Sk_I), the values towards the roof layer demonstrated very positively skewed distribution (0.40–0.35). Similarly, in the case of K_G, values decreased towards the roof layer, going from 1.26–1.14 (leptokurtic distribution) at a depth of 0.50 m to 1.08–1.02 (mesokurtic distribution).

The AFD113 section stands out from all the other exposures in that it has the highest MS values (especially in the upper part of the section), which should be interpreted as a direct indication of a wet environment. Although in samples from a depth of 0.70–0.60 m the sand content is relatively the highest, silts clearly dominate above this level, episodically supplemented with fine gravel (sample depth of 0.30 m).

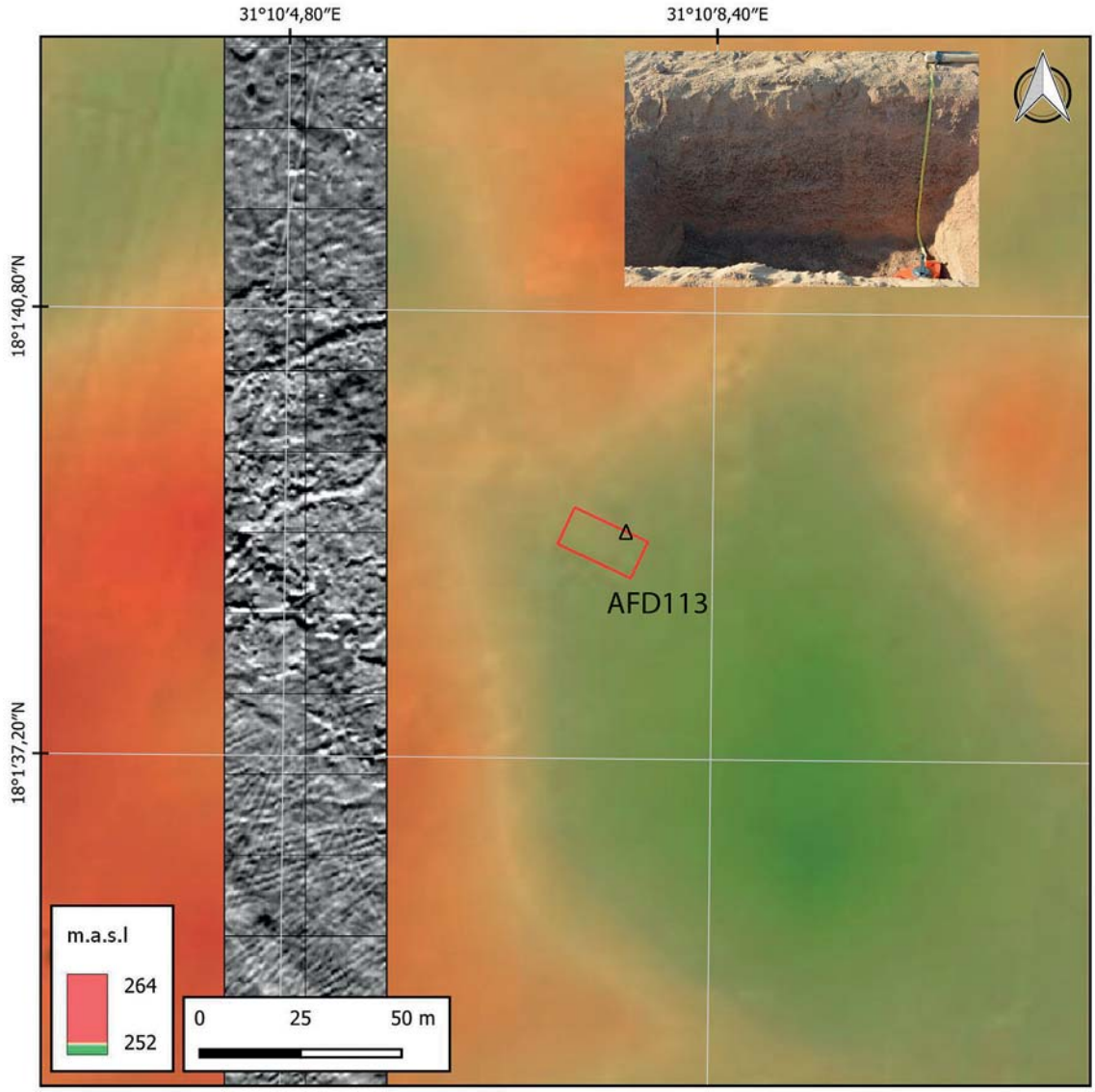

Fig. 2.17. Location of the examined trench section at site AFD113 (trench marked with a red contour line); inset, view of the section

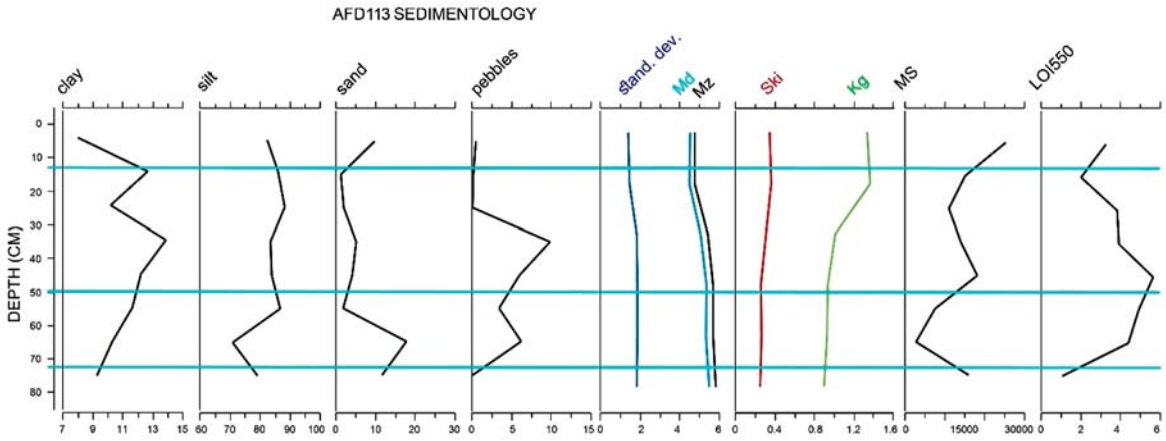

Fig. 2.18. AFD113 section: comparison of granulometry of clay-silt-sand-pebbles, lithodynamic indices (standard deviation, Md, Mz, Sk_I, K_G), magnetic susceptibility (MS) and organic fraction content (LOI550). Blue lines represent stratigraphy recorded macroscopically in the trench.
See Appendix 2.A1 for an explanation of units on the horizontal scale

2.3.6 Modern well and ditch exposures

In 2017, sediments located at a significant depth could be sampled in exposures related to earthworks (wells, ditches) linked to the establishment of farms in the Affad Basin. One such location was a well located in the eastern part of the investigated area [*Fig. 2.19*], while another was a ditch surrounding one of the industrial farms in the western sector of the area.

In the well, working in difficult conditions, the excavators documented a section 7.60 m deep. The sedimentary sequence records a cyclical increase and decrease in the river's energy, which can be phased. In the lowest part, down to a depth of 6.00 m below the ground surface (that is, approximately 246.7 m asl), the changes observed in the rise and fall of the river's energy were rather brief and cyclical. Given the thickness of alternating silts and fluvial sands, it seems that these periods were clearly shorter than those recorded in the higher parts of the section. At a depth of 6 m, a layer with distinct pseudomorphoses around plant roots and macroremains was observed. Similar horizons were recorded at depths of 5.10 m and 4.30 m. They document episodes of changes in the environment enabling vegetation growth, that is, the stabilization of rather small flows. The presence of sandy pseudomorphoses is evidence of successive drying. This is probably a record of periods with clearly lower humidity and proportionately more frequent and intensive aeolian processes (the sand percentage in these horizons is clearly higher). A marked change was observed in the most recent of these layers. Silts (down to a depth of 2.00 m) predominate in a significantly thick formation, which means long-term low-energy flows (a pluvial in the initial period of MIS3?). An OSL date of 61.2 ± 6.1 ka (Lub-6554) was obtained for this formation at a depth of 2.20 m. Another layer lying at a depth of 1.40 m below the surface was again characterized by a higher sand content, with a simultaneous decrease in the MS value and the content of organic fractions. Above this, there is once again a deposit analogous to sediments of low-energy flows. Although this sequence documents a return to cyclical changes in flows, as mentioned above, these periods had become longer and less dynamic than those reflected at the bottom of

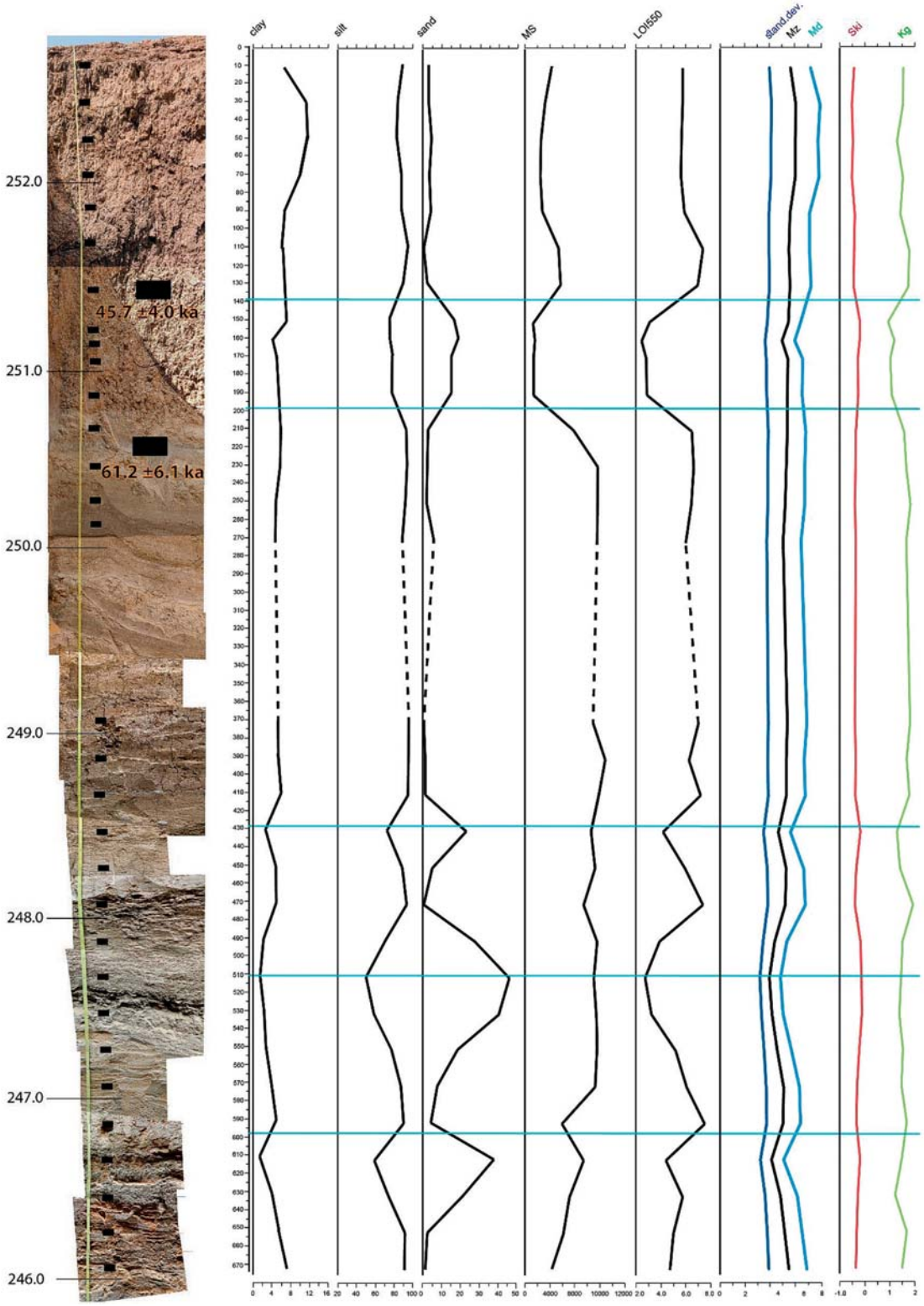

Fig. 2.19. Well section with marked sampling points, absolute altitude and OSL-MG-CAM dating: comparison of granulometry of clay-silt-sand, magnetic susceptibility (MS), organic fraction content (LOI550) and lithodynamic indices (standard deviation, Mz, Md, Sk_I, K_G). Blue lines represent stratigraphy recorded macroscopically in the well excavation. See Appendix 2.A1 for an explanation of units on the horizontal scale

the section. From these layers an OSL date of 45.7 ± 4.0 ka (Lub-6553) was obtained at a depth of 1.35 m below the present surface. Both the dating and the nature of the layers at a depth of 4 m below the modern surface (that is, approximately 249 m asl) suggest their identification with the facies A–D layers from site AFD23 [see below, *Fig. 2.26*].

A cut several hundred meters long, about 8–10 m wide and 1.20–1.50 m deep, was dug in preparation for a future irrigation channel. The exposure thus revealed was 1.50 m deep [*Fig. 2.20*; for the location see *Fig. 2.2*], not counting a roof layer about 0.30 m thick, largely degraded during the construction of the irrigation channel. Two phases were observed in this exposure, namely, one of heightened and another of lowered flow energy. The basement layer, made of fine-grained silts with carbonate precipitates, is a record of a low-energy environment. Towards the roof layer, the sand content increases, indicating a general increase in the energy of the stream. In this deposit, the presence of pseudomorphoses around plant roots was recorded. Following this high-energy phase was one characterized by significantly lower energy. Closing the sedimentary sequence is a layer of silty sands that may indicate a renewed increase in energy but also the growing influence of aeolian processes. Sediments are sorted poorly and very poorly, which can be interpreted as recording a fairly dynamic environment with considerable variability in transport energy. It would have been in all likelihood a phase of sediment formation in a zone periodically flooded with river swells. These sediments correspond to the facies D–E sequence from site AFD23, reflecting environmental changes in Palaeolithic times and afterwards. However, no record of early Holocene stratification (that is, corresponding to facies F at site AFD23) was observed here.

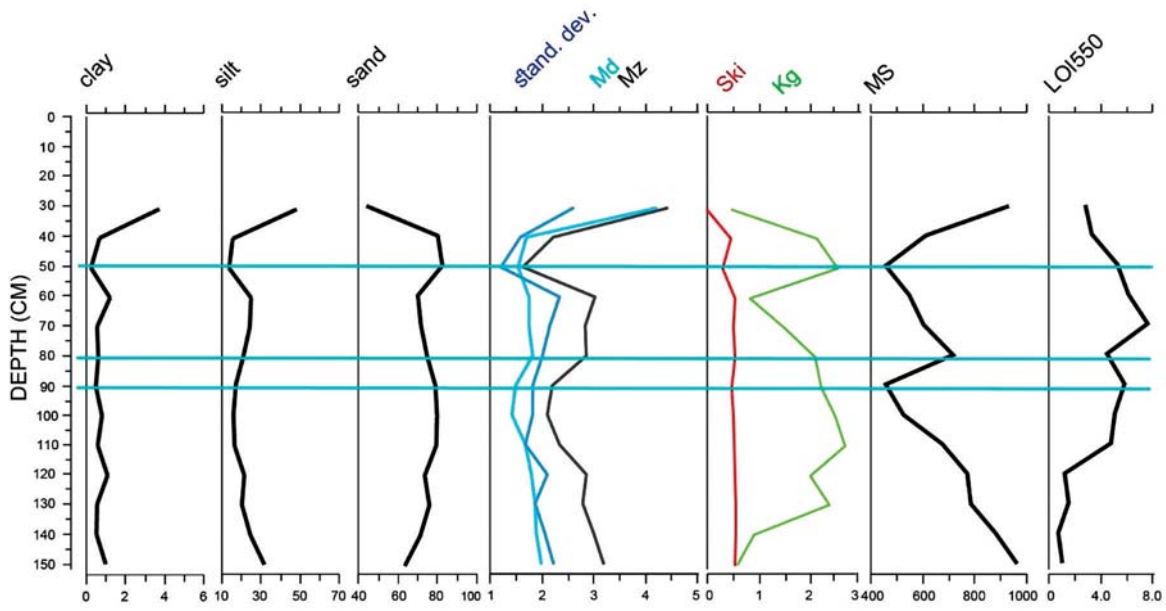

Fig. 2.20. Ditch exposure: comparison of granulometry (clay-silt-sand), lithodynamic indices (standard deviation, Md, Mz, Sk_I, K_G), magnetic susceptibility (MS) and content of organic fractions (LOI550) of the samples taken. See Appendix 2.A1 for an explanation of units on the horizontal scale

2.3.7 Upper plain remnants: exposures GT20, GT21, GT22 and GT24

Exposures GT20, GT21, GT22, GT24 were all made up of gravel material, which set considerable limits on any macroscopic observation of sediment variability—hence the full photographic documentation of sediments with different characteristics making up the individual exposures, and the sampling program for OSL and AMS^{14}C dating.

GT20 was located within an existing anthropogenic exposure, namely a (higher terrace) gravel pit made with bulldozer. It was deepened to 1.20 m [*Fig. 2.21*]. The basement, which is one of the five layers that were identified, is made up of a layer of calcareous sands at least 0.20 m thick, strongly cemented with a calcareous binding agent. Above this, there is a layer of sands (0.60 m), in

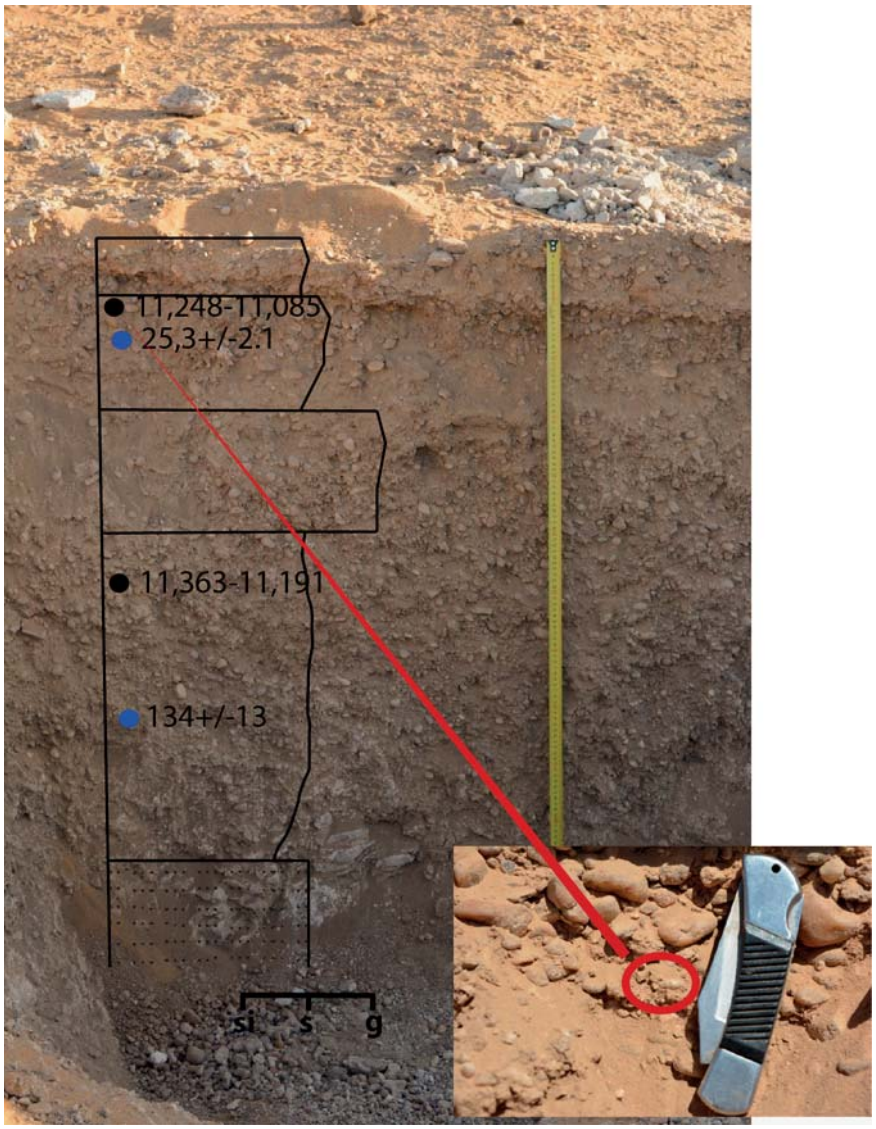

Fig. 2.21. Exposure GT20: stratigraphic-granulometric sketch superimposed on a photo of the examined section. Dots indicate sampling points: blue – OSL; black – AMS^{14}C. Dating is given in ka. Inset, malacofauna (depth 0.12 m below the surface)

some places silty at the basement level, cemented with calcium carbonate. The next layer (0.20 m) consists of medium-sandy gravel with dispersed single gravels, both medium and coarse. The second layer (from the top) (0.20 m) is composed mainly of fine gravel, enriched with medium gravel, with a sandy-dusty filling. The roof layer section (0.10 m) is made of fine gravel, containing a sandy fraction probably of aeolian origin.

The sediment sequence documented in the exposure is a record of alternating high and low sedimentation energy. Two samples were taken for OSL dating. The first, from a depth of 0.82–0.86 m, indicated an age of 134 ± 13 ka (Lub-6545), while the second came from a depth of 0.14–0.18 m and gave a date of 25.3 ± 2.1 ka (Lub-6544). The latter (obtained by the multigrain measurement method and averaged result) is not trustworthy due to the small depth from which the sample was taken and a very probable contamination with grains from later periods (Osypiński et al. 2021). All that can be said on these grounds is that in the period from about 134 ka to the channel indentation stage, probably at the turn of MIS5 and MIS4, there was a gradual increase in flow energy and sedimentation. The fine material present in the basement level indicates a low-energy environment. Carbonate cementations suggest periodically dry or semi-dry conditions. A significant change in environmental conditions was recorded towards the roof layer. The successively growing share of the coarse fraction documents an increase in the flow energy resulting from climatic changes in the Nile basin.

Malacofaunal remains [see *Fig. 2.21* inset photo], found at depths of 0.60 m and 0.12 m, were dated respectively to 11,363–11,191 cal.BP (9413–9241 BC 93.9%) and 11,248–11,085 cal.BP (9298–9135 BC 91.5%), which means that at the turn of the Pleistocene and Holocene further changes of environmental conditions were taking place, although this zone was elevated a few meters above the then flood plain. The remains belonged to the *Gulella* genus, very small air-breathing land snails, terrestrial pulmonate gastropod mollusks in the Streptaxidae family. Their habitat are leaf-litter and underlogs in the coastal forests. Therefore, their presence cannot be a determinant indicating the chronology of the formation of these layers.

Starting from the basement level, the next exposure **GT21** [*Fig. 2.22*] is made up of sands (0.30 m) and dispersed gravel. Overlying this is a layer of small gravel and sandy fill (0.20 m), followed by a layer (0.25 m) of fine gravel with a sandy-silty fill. The roof layer (0.25 m) is made up of sandy gravel of different granularity. There is a thin layer (3 cm) of aeolian sand on the surface.

This sediment sequence is a record of successively growing flow energy. The lamination of finer material is related to periods of lower flow. Gravel of different fractions (the thickest material) in the roof layer can be correlated to a phase of clearly higher flows than before.

Two OSL dates from this section require comment. While the date 92.1 ± 7.9 ka (Lub-6547) obtained for a sample taken at a depth of 0.68 m seems to reflect the chronology of layer formation, the date 51.5 ± 4.8 ka (Lub-6546) for a sample taken at a depth of 0.34 m seems to duplicate the contamination with quartz grains seen in the Lub-6544 sample from exposure GT20.

The sequence in **GT22** [*Fig. 2.23*] begins with sandy silt sediments with numerous carbonate cementations, 0.45 m thick, in the lowermost part. The roof layer (<10 cm) is made up of medium-sized gravel with dispersed coarse gravel. Being located just 10 m away from GT21, GT22 presents similar sedimentation processes reflecting significantly higher levels of environmental energy. Carbonate concretions in the lower sections of the exposure suggest dry or semi-dry conditions, while the roof layer, composed of a gravel fraction, testifies to an increase in environmental energy.

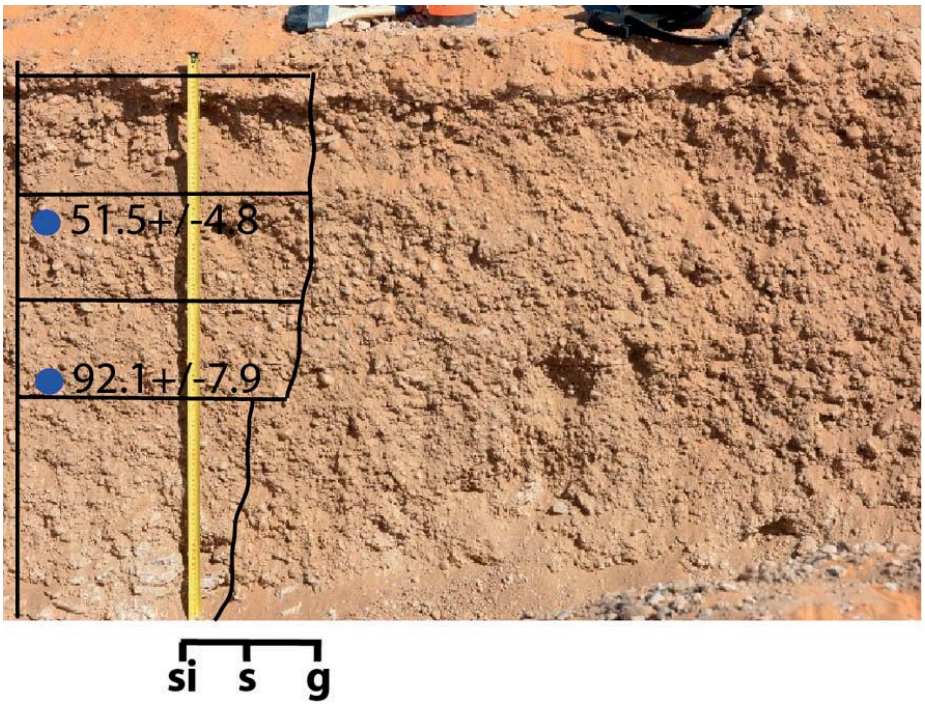

Fig. 2.22. Exposure GT21: stratigraphic-granulometric sketch superimposed on a photo of the examined section. Blue dot indicates OSL sampling point. Dating given in ka

Fig. 2.23. Exposure GT22: stratigraphic-granulometric sketch superimposed on a photo of the examined section

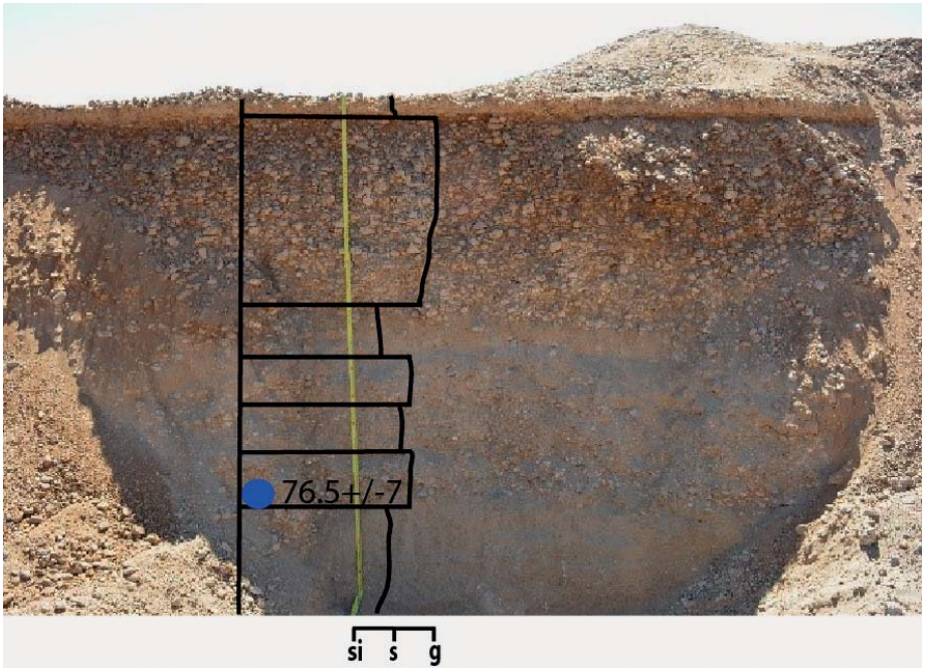

Fig. 2.24. Exposure GT24: stratigraphic-granulometric sketch superimposed on a photo of the examined section. Blue dot indicates OSL sampling point. Dating given in ka

Finally, the sedimentary sequence in exposure GT24 [*Fig. 2.24*] starts at the bottom with silty sands, 0.40 m thick, followed by a layer (0.20 m) of medium gravel with lenticular inserts of sandy fine gravel. The next layer (0.15 m) is composed of fine sandy gravel with a clearly more compact grain structure. Covering this is a layer of fine gravel with dispersed medium-sized gravel. Above these, there are silty sands with single examples of small gravel. The roof layer section is made of a layer (0.80 m) of medium and coarse gravel with visible carbonate cementations.

Changes in sediment granulometry towards the roof layer, meaning a clearly higher content of coarse fractions, indicate a growing trend in the river's energy. Although the alternating layers of finer material testify to episodes of lower flow, the entire section shows a marked increase in the river's energy, which apparently started just as the MIS5 was drawing to an end, as indicated by the date 76.5 ± 7.0 ka (Lub-6548).

2.4 LATE PLEISTOCENE SEDIMENTATION IN THE AFFAD BASIN IN LIGHT OF CURRENT RESEARCH

For many decades researchers have been interested in the evolution of the Nile valley in the Late Quaternary period (especially at the turn of the Pleistocene and Holocene). Early studies focused on identifying the major stages of aggradation (sedimentation) and incision (erosion) of the longest river in Africa, relating these findings to broader climatic changes taking place in northeastern Africa (e.g., Wendorf et al. 1976; 1992; Adamson et al. 1980; Butzer 1980).

Current research highlights the need for generating precise models of river system dynamics in response to long- and short-term climatic change and assessing the impact of environmental changes on past human populations exploiting the river's resources (e.g., Woodward et al. 2007; Williams 2009; 2019; Williams et al. 2010; 2015; Vermeersch and Van Neer 2015). In one of the latest studies on the late Pleistocene of the Sudanese section of the Nile Valley, Martin A.J. Williams (2019) presented a general overview of the chronology of environmental changes based on new OSL datings of sediments. These have revealed phases of a wetter climate in the Late Pleistocene at 55–50 ka and 38–30 ka. The late Pleistocene alluvial record from the Desert Nile is characterized by repeated aggradations and incision, but is fragmentary and not well dated. Optical ages obtained from late Pleistocene Nile alluvium (Williams et al. 2010) indicate that the Nile was migrating laterally and actively aggrading at 83 ± 24 ka, 32 ± 8 ka and 20.7 ± 0.2 ka. The recurrent phases of late Pleistocene channel incision along the main Nile channel would have converted previously swampy flood plains into well-drained alluvial terraces more suitable for sustained or seasonal prehistoric occupation.

One of the most recognized radical turns towards wetter conditions in northern Africa ~15,000 years ago is recorded in the Nile's hydrological, aeolian and sedimentological data (Williams et al. 2006; Williams 2009). Rising water levels in the Victoria and Alberta lakes starting from ~16.25 ka swelled the water supply feeding the White Nile in the 16th millennium BP. This sudden return to a summer monsoon system marked the beginning of a period that lasted, with minor breaks, until ~5000 years ago (Woodward et al. 2007; Williams et al. 2010).

The Affad Basin is the effect of sedimentation of varied origin and generally presents an almost even surface today, approximately 7 m above the modern flood plain. From the north it is bordered by the eroding Mesozoic Nubian sandstone plain (Whiteman 1971), and from the south by the currently cultivated floodplain. Sediments related to the earliest aggradations of the Nile were recorded only in the northern part of the basin and appeared in the form of much higher (up to 261 m asl) outliers made up of layers of coarse-grained material (mainly gravel and quartz pebbles) noted in exposures GT20, GT21, GT24, and possibly GT4 and GT9 [see *Figs 2.2, 2.25*]. Similar layers were also present on the opposite side of the river valley and were interpreted by the Combined Prehistoric Expedition (CPE) team (de Heinzelin 1968a) as elements of the Goshabi Formation, corresponding to sedimentation from the Middle Palaeolithic settlement in this part of the Nile Valley. Williams et al. (2010) attempted a radiocarbon dating of these sediments (malacological samples from CPE research), obtaining an indication beyond the range of the radiocarbon method. At the same time, radiocarbon dating of malacological remains from Affad (exposure GT20), clustering around 10 ka (Poz-90148: 9740 ± 50 BP; Poz-90152: 9850 ± 50 BP), gave an indication of environmental changes much later than the formative period in this area. This early stage of aggradation is currently dated to MIS5 based on OSL dates from the gravel formations in GT20, GT21 and GT24 (Lub-6545: 134 ± 13 ka; Lub-6547: 92.1 ± 7.9 ka; Lub-6548: 76.5 ± 7.0 ka). The MIS5 was drawing to a close when the incision of the river channel probably took place.

The earliest sediments from the next phase are the aeolian sands recorded at the northern edge of the new river channel and OSL-dated to the end of MIS4 (Lub-6549: 58.4 ± 5.7 ka; Lub-6550: 66.0 ± 7.0 ka). A similar dating has been indicated by deposits underlying the silt layers both in the modern well exposure, at a depth of approximately 250 m asl (Lub-6554: 61.2 ± 6.1 ka), and

in GT11, this at 253 m asl (Lub-5657: 60.11 ± 8.70 ka), showing the dynamics of new terrace formation. Sedimentation in MIS3 contributed to the burying of various features of area topography associated with a past riparian environment that included channels and wetlands, recorded in both the archaeological trenches and other exposures. Assuming landscape of this kind, sites AFD23 and AFD24 would have been located on slightly higher ground near the edges of the channel (or channel system), surrounded by wetlands [*Figs 2.25, 2.26*]. The other camps would have probably been located in similar topographical circumstances. However, the location of sites with remains of fish (AFD113) or clams (AFD134), to the exclusion of practically all other faunal remains, calls for a slightly different interpretation. In these cases, based on observations of the archaeological context, it should be assumed that the sites were either flooded (cyclically) or lay on the beds of periodic water channels.

Evidence of a wetland environment was observed in many of the strictly geological exposures in the form of micro-layered, manganese-saturated silts with numerous ferrous precipitates around ancient plant root systems (rhizocreation), silts and fine-grained fluvial sands. The contours of the banks of palaeochannels were also evident in magnetic imaging and DEM modelling of the area [*Figs 2.25, 2.27* on page 80, see also *Fig. 2.2*].

The remains of prehistoric settlement at site AFD23, at least that purportedly from primary contexts, were associated with layers of clayey silts and sands, which illustrate the changes in the riparian environment over several millennia during MIS4/MIS3 (Osypińska et al. 2020). Silts (sedimentation unit 23.C.1) exposed at the base of the stratigraphic sequence in GT11 (area of a former relief depression located west of the encampment), found to be hard and saturated with calcium precipitates, are now dated to 60.11 ± 8.70 ka (Lub-5657), overriding the early OSL dates obtained by the Project, which referred to 21.1 ± 2.32 ka (UJK-OSL-36) (Osypiński et al. 2021). A similar date (63.8 ± 4.3 ka: Lub-6552) was obtained also from the layer preceding the MSA settlement at the next site, AFD131 located a kilometer to the northeast, which reflects the broader context of the formation of layers in the Affad Basin.

Despite the fact that the deepest cut-features of the settlement at site AFD23 intersected the roof layer sections of segmentation unit 23.C.1, the original layer constituting the direct substratum for the Palaeolithic settlement comprised sands and silt, respectively, 23.D.1 and 23.D.1b. During their deposition, that is, from 57.83 ± 9.69 ka (Lub-5656), ever more dry conditions favored further aeolian accumulation in the riverbank zones, as well as in the channels of an increasingly transient river (Osypiński et al. 2016).

Dates close to 52 ka (previously erroneously 15.9 ± 1.75 ka: UJK-OSL-35) obtained for the sandy sediment 23.D.1 (56.8 ± 4.8 ka: Lub-6431; 50.02 ± 5.58 ka: LO18 FMMc.3), as well as the TL dating of silt overheated by human agency at site AFD23 (46.4 ± 4 ka: Lub-6432), are directly related to settlement at the site, and indicate two notable changes: a reactivation of the channel system on the one hand and a flooding of marshy areas in a seasonal cycle on the other. The elevated bank of a channel (or backwater), surrounded by a seasonally flooded area, created a perfect habitat for many species of animals and plants and undoubtedly attracted settlement. Very similar dates were obtained by the TL method for the overheated silt substratum permeated with bivalve fragments at site AFD134 (56.1 ± 6.8 ka: Lub-6433), which is partly confirmed by the results of radiocarbon dating of the shells themselves, going beyond the range of the method itself (>48ka: Poz-102024).

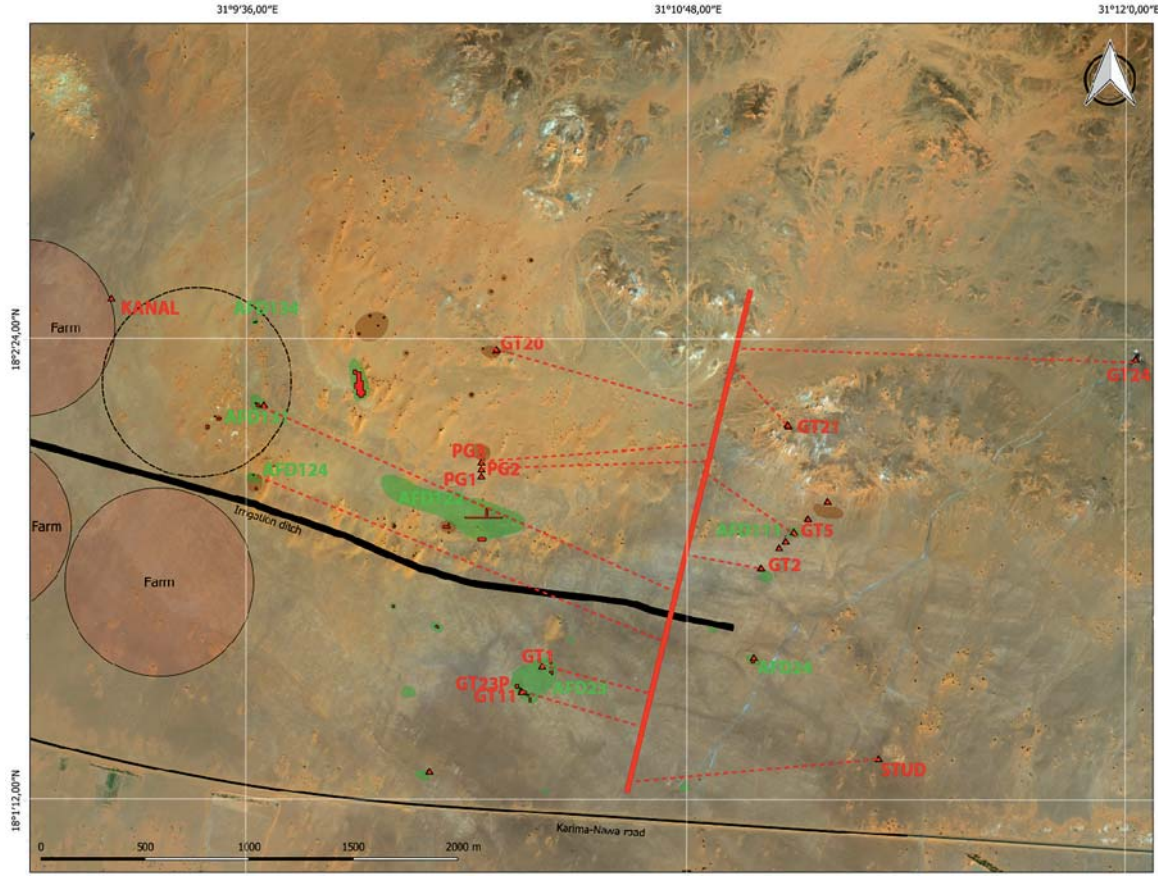

Fig. 2.25. Location of examined geological test pits (GT) ands areas covered by magnetic prospection. Background: compiled satellite image (ESRI 2019) and DEM

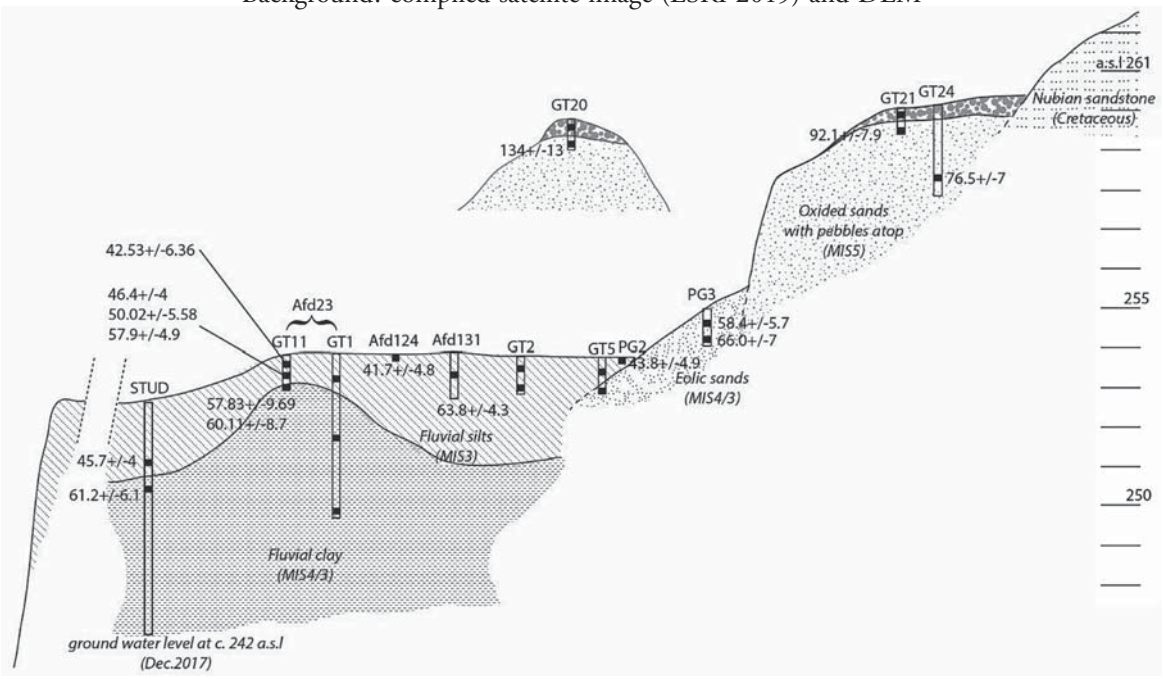

Fig. 2.26. Tentative reconstruction of sedimentation in the Late Pleistocene based on summary results of geological research by the PalaeoAffad Project in the Affad Basin

In light of this evidence, the dates obtained by the ESR method for animal teeth from sites AFD23 and AFD24 require comment. Although they were expected to correlate with the age indicated by the OSL dating, they point in fact towards a much earlier period of MIS4, or even MIS5 (depending on the methodology; Osypiński et al. 2021). Should these dates be taken as an indication of when these animals died and their bodily remains were deposited, it would have to be assumed that the animal bones discovered at archaeological sites in the Affad Basin came from much older contexts and were accidentally redeposited. This is, in the authors' considered opinion, entirely unlikely in view of the documented distribution of bones that were not dated with ESR, which evince clear patterns of original deposition alongside the lithic assemblages. Thus, the authors are inclined to view these anomalous dating results as possibly an indication of a different and not yet fully recognized life cycle of elements, specifically uranium, in this particular landscape.

Another alluvial layer recorded in the relief depression west of the campsite at AFD23 (sedimentation unit 23.E.1), which sealed off some of the cut features, was dated to 42.53 ± 6.36 ka (Lub-5658) (previously 15.3 ± 1.68 ka: UJK- OSL-34) and marked a period of increasingly higher river levels with the intensification of monsoon rains in the upper reaches of the Nile (Williams 2019: 38–30 ka wet period). Analogous layers were also noted in the modern ditch exposure, while a similar OSL date was obtained for the sediment in which the remains of aurochs were found at site AFD124 (41.7 ± 4.8 ka: Lub-6434). This is evident proof of continued Palaeolithic settlement in the area under investigation.

A much later sediment, the youngest in the area under research, comprised a dark red layer of gravel (sedimentation unit 23.F.1) filling a slight relief depression to the west of the Late Pleistocene campsite at AFD23. The gravel contained single stone artifacts, both of an origin identical to the Palaeolithic settlement phase and to early Holocene traditions—all in a secondary context. This stratification was associated with increased humidity and denudation in the early and middle Holocene; it probably corresponds to the fluvial stage recorded in Revel et al. 2010, during which a significant amount of iron-rich elements were delivered from the upper course of the Blue Nile. The periodic nature of local flooding in the early Holocene is also suggested by the fact that most of the settlements from this last period were located on sandy or gravel elevations (Osypińska and Osypiński 2015).

The next, namely middle and late Holocene stages of landscape formation in the Affad Basin, are probably correlated with the migration of the river channel southwards to its present location and the separation of the late Pleistocene zone from the river accumulation system. The Tergis area, west of Affad, shows signs of intense denudation in this period, with sands and gravel being washed away to the south, into the river channel that was significantly lower at that time. In the site zone around Affad, however, this denudation spared considerable areas of former sedimentation, cutting only through the roof sections of layers containing the remains of late Pleistocene settlement.

Based on accumulated evidence generated in the most recent legs of the PalaeoAffad project, which differs significantly from what the authors have already published (see Osypiński, Osypińska, and Gautier 2011; Osypiński et al. 2016), it is now believed that human groups exploited the area in question before it was ultimately cut off from the Nile river system. It was merely by chance that exposure A/34 analyzed in 2003 hit on the spot of a former relief depression lying west of the late Pleistocene campsite which was later filled with another series of alluvia (sedimentation unit 23.E.1). At the time (before 2013), the researchers read the data as two levels of Palaeolithic stratification containing artifacts—one on the surface and the other in the subsurface strata,

separated by a sediment 0.20 m thick and devoid of artifacts—initially interpreted as two settlement horizons. In the wake of the most recent findings, there is most certainly only one occupation horizon at Affad 23 and this is associated with the surface of sandy sediments 23.D.1 and 23.D.1b. Artifacts found on the surface of younger deposits (e.g., 23.E.1–3 silts or 23.F.1 red Holocene gravel) had migrated there due to the denudation of higher-lying parts of the site. Coinciding with this is a radical revision of the chronology based on a new series of dates superseding the flawed results obtained earlier in the Kielce laboratory (Kalicki and Olszak 2016; revised in Osypiński et al. 2021).

APPENDICES

2.A1: Report on granulometric analyses (Soil Laboratory, Department of Physical Geography of the Institute of Geography and Regional Development, University of Wrocław), and organic content and magnetic susceptibility (laboratory of the Czech Research Institute in Prague) of sediment samples from Affad
2.A2: Preliminary results of the magnetic survey, Affad Basin 2016–2017
2.A3: OSL and TL Dating Laboratory Lublin report
2.A4. Oxford Luminescence Dating Laboratory report
2.A5. ESR Dating Report Williamstown Laboratory
2.A6. Report on measurement work and data processing for DEM creation

Appendix 2.A1

Report on granulometric analyses (Soil Laboratory, Department of Physical Geography of the Institute of Geography and Regional Development, University of Wrocław), and organic content and magnetic susceptibility (laboratory of the Czech Research Institute in Prague)

Jerzy Raczyk PhD and Krzysztof Rękas MA
University of Wrocław; Institute of Geography and Regional Development
Assoc. Prof. Mgr. Lenka Lisá PhD
Institute of Geology, Czech Academy of Sciences, Rozvojová 269, CZ-165 00 Prague 6 – Lysolaje

The granulometry of the sediments was determined by laser diffraction using a Malvern Mastersizer 2000 device. Organic content was determined by the roasting method. Magnetic susceptibility was tested in a laboratory at the Czech Research Institute in Prague. The measurement was made on a KLY3–Kappabridge device manufactured in the Czech Republic ("AGICO" Advanced Geoscience Instruments Co., Brno, Czech Republic).

Elemental laser method (with preparation)

Preparation: Sediments were separated into individual fractions using the Udden (1914) grain size classification method as modified by Chester K. Wentworth (1922) and Urszula Urbaniak-Biernacka (1975). Samples were prepared by grinding in a mortar; a sample of 0.3 g was then placed in a beaker, and 50 ml with the addition of 3 ml of 30% H_2O_2 was boiled off until dry

(removing organic material); then 2 ml of 10% HCl was added and boiled off until dry (removing carbonates and residual undecomposed H_2O_2). The next step was to add 10 ml of 10% Calgon (sodium hexametaphosphate), boil it for 10 minutes and leave it until the next day (sample dispersion); the resulting suspension was transferred in its entirety to a measuring beaker with a capacity of 800 ml and 700 ml of H_2O was added. The samples underwent sonication (to break up the aggregates) for 5 minutes (power of 20 units, pump speed of 2,100). After this time, the mineral particles remaining in the suspension were measured one last time.

Results: In the tables below, fraction limits are given in micrometers [μm]. A division of 1 [phi] was used.

The sampling depth is given in meters [m].

Percentage [% V] for each fraction

Exposure AFD/GT23P

Depth/fraction	0.1	0.2	0.3	0.4	0.5	0.6	0.7	0.8	0.9	1.0	1.1	1.2
0.010–0.015	0.00	0.00	0.00	0.00	0.00	0.00	0.00	0.00	0.00	0.00	0.00	0.00
0.015–0.031	0.00	0.00	0.00	0.00	0.00	0.00	0.00	0.00	0.00	0.00	0.00	0.00
0.031–0.061	0.00	0.00	0.00	0.00	0.00	0.00	0.00	0.00	0.00	0.00	0.00	0.00
0.061–0.122	0.00	0.00	0.00	0.00	0.00	0.00	0.00	0.00	0.00	0.00	0.00	0.00
0.122–0.244	0.00	0.00	0.00	0.00	0.00	0.00	0.00	0.00	0.00	0.00	0.00	0.00
0.244–0.488	0.00	0.00	0.00	0.00	0.00	0.00	0.00	0.00	0.00	0.00	0.00	0.00
0.488–0.977	1.07	1.21	1.05	1.06	1.13	1.25	1.43	1.28	1.46	1.32	1.53	1.29
0.977–1.953	3.62	4.24	3.19	3.27	3.83	3.92	4.74	5.12	6.07	5.49	6.56	5.00
1.953–3.906	7.35	9.01	7.16	7.51	8.71	8.54	10.78	11.68	14.05	12.91	15.16	11.45
3.906–7.813	9.75	12.81	10.47	11.16	12.36	12.19	15.09	15.69	19.57	18.43	20.49	16.29
7.813–15.625	15.01	20.24	17.78	17.53	19.27	18.64	18.36	17.54	20.30	19.60	20.41	19.62
15.625–31.250	22.68	28.83	29.72	28.42	28.02	27.52	24.49	20.07	17.28	17.31	16.08	19.64
31.250–62.500	16.38	17.49	22.59	22.82	19.37	20.67	19.98	19.03	14.14	15.90	12.74	16.80
62.500–125.000	5.40	3.82	4.96	5.39	4.60	5.08	5.09	8.83	6.61	8.29	6.53	8.96
125.000–250.000	7.56	1.45	1.36	1.01	1.19	0.75	0.04	0.75	0.51	0.74	0.49	0.96
250.000–500.000	8.89	1.40	1.58	1.56	1.37	1.29	0.00	0.00	0.00	0.00	0.00	0.00
500.000–1000.000	2.26	0.13	0.14	0.26	0.13	0.15	0.00	0.00	0.00	0.00	0.00	0.00
1000–2000	0.00	0.00	0.00	0.00	0.00	0.00	0.00	0.00	0.00	0.00	0.00	0.00
Total	100%	100%	100%	100%	100%	100%	100%	100%	100%	100%	100%	100%

Exposure AFD/GT24

Depth/fraction	0.1	0.2	0.3	0.4	0.5
0.010–0.015	0.00	0.00	0.00	0.00	0.00
0.015–0.031	0.00	0.00	0.00	0.00	0.00
0.031–0.061	0.00	0.00	0.00	0.00	0.00
0.061–0.122	0.00	0.00	0.00	0.00	0.00
0.122–0.244	0.00	0.00	0.00	0.00	0.00
0.244–0.488	0.00	0.00	0.00	0.00	0.00
0.488–0.977	0.548	0.571	0.96	1.15	1.16
0.977–1.953	1.495	1.678	3.40	4.04	3.99
1.953–3.906	2.927	3.21	6.59	8.02	7.95
3.906–7.813	5.104	5.106	8.82	10.64	10.64
7.813–15.625	7.141	6.759	11.54	13.50	13.38
15.625–31.250	15.843	14.946	18.98	19.99	19.81
31.250–62.500	36.029	35.185	27.77	24.89	25.31
62.500–125.000	26.232	27.050	16.78	13.43	3.08
125.000–250.000	3.301	4.110	3.08	2.54	2.31
250.000–500.000	1.238	1.187	1.80	1.60	1.69
500.000–1000.000	0.144	0.200	0.28	0.20	0.15
1000–2000	0.00	0.00	0.00	0.00	0.00
Total	100%	100%	100%	100%	100%

Exposure AFD131/I

Depth/fraction	0.1	0.2	0.3	0.4	0.5	0.6	0.7	0.8	0.9	1.0
0.010–0.015	0.00	0.00	0.00	0.00	0.00	0.00	0.00	0.00	0.00	0.00
0.015–0.031	0.00	0.00	0.00	0.00	0.00	0.00	0.00	0.00	0.00	0.00
0.031–0.061	0.00	0.00	0.00	0.00	0.00	0.00	0.00	0.00	0.00	0.00
0.061–0.122	0.00	0.00	0.00	0.00	0.00	0.00	0.00	0.00	0.00	0.00
0.122–0.244	0.00	0.00	0.00	0.00	0.00	0.00	0.00	0.00	0.00	0.00
0.244–0.488	0.00	0.00	0.00	0.00	0.00	0.00	0.00	0.00	0.00	0.00
0.488–0.977	0.39	0.30	0.28	0.30	0.25	0.26	0.28	0.22	0.23	0.17
0.977–1.953	1.44	1.29	1.21	1.28	1.09	1.13	1.26	0.99	1.01	0.90
1.953–3.906	3.14	2.83	2.79	2.78	2.49	2.45	2.75	2.09	2.13	1.85
3.906–7.813	4.78	4.42	4.37	4.34	3.95	3.65	4.01	3.09	3.28	2.79
7.813–15.625	8.23	7.86	7.56	7.98	6.96	6.22	6.87	5.55	6.04	5.33
15.625–31.250	12.59	11.82	11.48	12.42	11.18	10.51	10.75	9.07	8.59	8.27
31.250–62.500	20.64	17.32	16.62	17.54	18.10	18.01	15.65	18.00	15.61	15.33
62.500–125.000	30.45	29.10	29.96	28.75	30.71	31.57	29.33	35.04	35.75	34.96
125.000–250.000	16.34	21.40	23.18	21.25	22.47	23.13	24.28	24.17	25.98	27.61
250.000–500.000	1.98	3.66	2.56	3.35	2.80	3.06	4.82	1.77	1.38	2.80
500.000–1000.000	0.01	0.00	0.00	0.00	0.00	0.00	0.00	0.00	0.00	0.00
1000–2000	0.00	0.00	0.00	0.00	0.00	0.00	0.00	0.00	0.00	0.00
Total	100%	100%	100%	100%	100%	100%	100%	100%	100%	100%

Exposure AFD131/P

Depth/fraction	0.1	0.2	0.3	0.4	0.5	0.6	0.7	0.8	0.9	1.0	1.1
0.010–0.015	0.00	0.00	0.00	0.00	0.00	0.00	0.00	0.00	0.00	0.00	0.00
0.015–0.031	0.00	0.00	0.00	0.00	0.00	0.00	0.00	0.00	0.00	0.00	0.00
0.031–0.061	0.00	0.00	0.00	0.00	0.00	0.00	0.00	0.00	0.00	0.00	0.00
0.061–0.122	0.00	0.00	0.00	0.00	0.00	0.00	0.00	0.00	0.00	0.00	0.00
0.122–0.244	0.00	0.00	0.00	0.00	0.00	0.00	0.00	0.00	0.00	0.00	0.00
0.244–0.488	0.00	0.00	0.00	0.00	0.00	0.00	0.00	0.00	0.00	0.00	0.00
0.488–0.977	0.39	0.36	0.39	0.40	0.30	0.40	0.24	0.23	0.22	0.22	1.53
0.977–1.953	1.34	1.15	1.21	1.21	1.22	1.25	0.94	0.90	0.85	0.82	6.56
1.953–3.906	2.88	2.44	2.58	2.47	2.57	2.47	1.87	1.80	1.70	1.61	15.16
3.906–7.813	4.65	4.07	4.29	4.00	4.04	3.97	2.84	2.74	2.64	2.49	20.49
7.813–15.625	8.76	7.45	7.61	6.79	6.80	7.27	5.57	5.38	5.26	5.07	20.41
15.625–31.250	14.75	13.47	14.28	12.53	12.00	13.83	9.84	9.84	9.32	9.18	16.08
31.250–62.500	24.14	26.04	26.70	26.27	23.10	27.04	19.78	21.04	20.72	20.63	12.74
62.500–125.000	28.50	30.99	29.56	32.04	30.16	31.05	36.43	37.10	37.81	37.83	6.53
125.000–250.000	12.23	12.18	11.11	12.64	15.49	11.50	21.84	20.58	21.05	21.58	0.49
250.000–500.000	2.15	1.72	2.00	1.53	3.95	1.07	0.65	0.38	0.42	0.57	0.00
500.000–1000.000	0.23	0.14	0.28	0.12	0.37	0.15	0.00	0.00	0.00	0.00	0.00
1000–2000	0.00	0.00	0.00	0.00	0.00	0.00	0.00	0.00	0.00	0.00	0.00
Total	100%	100%	100%	100%	100%	100%	100%	100%	100%	100%	100%

Exposure PG1

Depth/fraction	0.2	0.4	0.6	0.8
0.010–0.015	0.00	0.00	0.00	0.00
0.015–0.031	0.00	0.00	0.00	0.00
0.031–0.061	0.00	0.00	0.00	0.00
0.061–0.122	0.00	0.00	0.00	0.00
0.122–0.244	0.00	0.00	0.00	0.00
0.244–0.488	0.00	0.00	0.00	0.00
0.488–0.977	1.02	0.92	0.83	0.95
0.977–1.953	3.27	2.55	2.40	3.21
1.953–3.906	6.79	5.28	5.14	6.72
3.906–7.813	10.09	8.01	7.55	9.53
7.813–15.625	16.79	14.73	13.86	15.34
15.625–31.250	25.22	27.17	26.63	23.92
31.250–62.500	22.61	27.48	26.26	22.28
62.500–125.000	9.39	10.64	10.21	10.82
125.000–250.000	2.22	1.57	3.47	4.31
250.000–500.000	2.34	1.58	3.28	2.72
500.000–1000.000	0.26	0.07	0.36	0.19
1000–2000	0.00	0.00	0.00	0.00
Total	100%	100%	100%	100%

Exposure PG2

Depth/fraction	0.1	0.2	0.3	0.4	0.5	0.6	0.7	0.8	0.9
0.010–0.015	0.00	0.00	0.00	0.00	0.00	0.00	0.00	0.00	0.00
0.015–0.031	0.00	0.00	0.00	0.00	0.00	0.00	0.00	0.00	0.00
0.031–0.061	0.00	0.00	0.00	0.00	0.00	0.00	0.00	0.00	0.00
0.061–0.122	0.00	0.00	0.00	0.00	0.00	0.00	0.00	0.00	0.00
0.122–0.244	0.00	0.00	0.00	0.00	0.00	0.00	0.00	0.00	0.00
0.244–0.488	0.00	0.00	0.00	0.00	0.00	0.00	0.00	0.00	0.00
0.488–0.977	0.52	0.70	0.74	0.74	1.09	0.97	0.99	0.91	0.94
0.977–1.953	2.35	2.95	3.11	2.92	3.49	3.08	3.09	2.33	2.33
1.953–3.906	5.56	6.74	7.09	6.36	6.98	6.41	6.45	4.87	4.77
3.906–7.813	8.92	10.42	11.12	9.97	10.74	9.43	9.46	7.83	7.52
7.813–15.625	12.86	14.23	16.37	16.22	16.92	14.79	14.97	13.07	12.96
15.625–31.250	12.18	12.90	16.35	18.81	21.48	23.57	24.64	24.56	27.06
31.250–62.500	6.81	7.52	9.67	13.66	19.23	23.98	24.53	28.89	32.93
62.500–125.000	5.00	5.35	5.10	7.30	8.30	9.18	8.28	10.72	11.45
125.000–250.000	17.21	14.65	11.06	9.09	4.04	2.79	2.33	1.84	0.05
250.000–500.000	24.14	21.98	16.26	12.63	6.75	5.03	4.66	4.48	0.00
500.000–1000.000	4.44	2.58	3.14	2.28	0.98	0.77	0.60	0.50	0.00
1000–2000	0.00	0.00	0.00	0.00	0.00	0.00	0.00	0.00	0.00
Total	100%	100%	100%	100%	100%	100%	100%	100%	100%

Exposure PG3/4

Depth/fraction	0.1	0.3	0.5	0.6	0.8	1.0
0.010–0.015	0.00	0.00	0.00	0.00	0.00	0.00
0.015–0.031	0.00	0.00	0.00	0.00	0.00	0.00
0.031–0.061	0.00	0.00	0.00	0.00	0.00	0.00
0.061–0.122	0.00	0.00	0.00	0.00	0.00	0.00
0.122–0.244	0.00	0.00	0.00	0.00	0.00	0.00
0.244–0.488	0.00	0.00	0.00	0.00	0.00	0.00
0.488–0.977	0.13	0.12	0.13	0.09	0.14	0.32
0.977–1.953	0.87	0.81	0.89	0.81	0.96	1.49
1.953–3.906	1.99	1,91	2,13	1,94	2.21	3.42
3.906–7.813	3.11	3.02	3.50	3.08	3.31	5.39
7.813–15.625	4.12	4.05	4.68	3.99	4.04	7.13
15.625–31.250	4.68	4.29	5.58	3.98	4.18	8.39
31.250–62.500	3.32	2.12	2.18	2,14	4,49	14.42
62.500–125.000	14.15	13.71	13.27	13.75	16.98	22.12
125.000–250.000	39.25	40.42	39.75	40.85	37.64	22.10
250.000–500.000	27.15	28.20	27.58	28.22	24.85	13.82
500.000–1000.000	1.24	1.35	1.32	1.17	1.21	1.39
1000–2000	0.00	0.00	0.00	0.00	0.00	0.00
Total	100%	100%	100%	100%	100%	100%

Exposure AFD113

Depth/fraction	0.05	0.15	0.25	0.35	0.45	0.55	0.65	0.75
0.010–0.015	0.00	0.00	0.00	0.00	0.00	0.00	0.00	0.00
0.015–0.031	0.00	0.00	0.00	0.00	0.00	0.00	0.00	0.00
0.031–0.061	0.00	0.00	0.00	0.00	0.00	0.00	0.00	0.00
0.061–0.122	0.00	0.00	0.00	0.00	0.00	0.00	0.00	0.00
0.122–0.244	0.00	0.00	0.00	0.00	0.00	0.00	0.00	0.00
0.244–0.488	0.00	0.00	0.00	0.00	0.00	0.01	0.00	0.00
0.488–0.977	0.98	1.36	1.26	1.39	1.28	1.37	0.94	0.91
0.977–1.953	2.39	3.84	3.07	4.08	3.61	3.43	2.99	2.59
1.953–3.906	4.59	7.51	5.84	8.50	7.38	6.86	6.37	5.77
3.906–7.813	7.24	11.79	9.22	13.49	11.56	11.17	9.26	8.67
7.813–15.625	14.89	21.84	20.25	20.21	19.14	21.00	12.82	13.83
15.625–31.250	29.41	32.12	34.78	27.80	29.21	32.37	20.73	26.58
31.250–62.500	30.71	20.48	23.85	21.83	23.86	21.97	27.84	29.93
62.500–125.000	9.76	1.06	1.72	2.70	3.96	1.82	15.99	11.29
125.000–250.000	0.02	0.00	0.00	0.00	0.00	0.00	2.01	0.42
250.000–500.000	0.00	0.00	0.00	0.00	0.00	0.00	0.91	0.00
500.000–1000.000	0.00	0.00	0.00	0.00	0.00	0.00	0.14	0.00
1000–2000	0.00	0.00	0.00	0.00	0.00	0.00	0.00	0.00
Total	100%	100%	100%	100%	100%	100%	100%	100%

Exposure WELL (0.9 to 2.9)

Depth/fraction	0.9	1.1	1.3	1.5	1.7	1.9	2.1	2.3	2.4	2.5	2.7	2.9
0.010–0.015	0.00	0.00	0.00	0.00	0.00	0.00	0.00	0.00	0.00	0.00	0.00	0.00
0.015–0.031	0.00	0.00	0.00	0.00	0.00	0.00	0.00	0.00	0.00	0.00	0.00	0.00
0.031–0.061	0.00	0.00	0.00	0.00	0.00	0.00	0.00	0.00	0.00	0.00	0.00	0.00
0.061–0.122	0.00	0.00	0.00	0.00	0.00	0.00	0.00	0.00	0.00	0.00	0.00	0.00
0.122–0.244	0.00	0.00	0.00	0.00	0.00	0.00	0.00	0.00	0.00	0.00	0.00	0.00
0.244–0.488	0.00	0.00	0.01	0.00	0.00	0.00	0.00	0.00	0.00	0.00	0.00	0.01
0.488–0.977	1.57	2.34	2.41	1.92	1.63	1.52	1.63	1.29	0.92	1.12	1.24	1.64
0.977–1.953	5.32	9.28	8.94	8.36	5.19	4.74	5.07	5.47	2.90	4.14	4.42	4.45
1.953–3.906	11.47	19.29	17.82	18.67	11.28	9.65	10.65	11.20	6.13	9.59	9.01	8.78
3.906–7.813	18.48	24.55	21.53	24.64	17.76	17.00	18.83	14.21	9.99	14.97	13.35	13.59
7.813–15.625	26.56	22.47	20.04	23.22	24.16	29.89	29.97	13.84	15.09	17.63	18.23	23.79
15.625–31.250	23.85	13.50	15.48	14.04	23.56	28.13	25.15	15.04	19.97	16.97	18.59	29.51
31.250–62.500	10.25	5.85	9.62	6.02	12.69	8.88	6.68	22.51	26.43	20.66	20.16	15.82
62.500–125.000	1.59	1.76	3.05	2.29	2.48	0.19	0.21	14.60	16.81	13.53	13.14	2.41
125.000–250.000	0.57	0.82	0.83	0.52	0.92	0.00	1.46	1.65	1.75	1.38	1.74	0.02
250.000–500.000	0.35	0.13	0.28	0.33	0.34	0.00	0.34	0.20	0.00	0.00	0.13	0.00
500.000–1000.000	0.00	0.00	0.00	0.00	0.00	0.00	0.00	0.00	0.00	0.00	0.00	0.00
1000–2000	0.00	0.00	0.00	0.00	0.00	0.00	0.00	0.00	0.00	0.00	0.00	0.00
Total	100%	100%	100%	100%	100%	100%	100%	100%	100%	100%	100%	100%

Exposure WELL (3.1 to 6.1)

Depth/fraction	3.1	3.3	3.5	4.5	4.7	4.9	5.1	5.3	5.5	5.7	5.9	6.1
0.010–0.015	0.00	0.00	0.00	0.00	0.00	0.00	0.00	0.00	0.00	0.00	0.00	0.00
0.015–0.031	0.00	0.00	0.00	0.00	0.00	0.00	0.00	0.00	0.00	0.00	0.00	0.00
0.031–0.061	0.00	0.00	0.00	0.00	0.00	0.00	0.00	0.00	0.00	0.00	0.00	0.00
0.061–0.122	0.00	0.00	0.00	0.00	0.00	0.00	0.00	0.00	0.00	0.00	0.00	0.00
0.122–0.244	0.00	0.00	0.00	0.00	0.00	0.00	0.00	0.00	0.00	0.00	0.00	0.00
0.244–0.488	0.00	0.00	0.01	0.00	0.00	0.07	0.00	0.00	0.00	0.00	0.00	0.01
0.488–0.977	1.41	1.32	1.16	1.43	1.33	1.59	0.69	1.26	1.33	0.61	0.41	0.47
0.977–1.953	4.01	3.71	3.19	4.21	3.93	3.96	2.18	3.84	3.87	1.78	1.21	1.43
1.953–3.906	7.86	7.08	6.29	8.31	8.17	7.46	4.66	8.21	7.29	3.73	2.53	3.08
3.906–7.813	12.78	12.18	10.11	13.90	12.50	12.59	8.05	13.51	11.87	6.35	4.19	5.34
7.813–15.625	24.39	26.49	21.27	27.72	23.56	25.80	12.28	21.04	27.22	9.07	6.44	7.98
15.625–31.250	31.15	32.44	31.22	32.11	32.85	32.67	18.97	26.55	34.81	17.08	12.08	13.40
31.250–62.500	16.62	15.18	21.53	12.23	16.97	15.25	30.24	20.88	13.61	33.84	27.01	28.13
62.500–125.000	1.78	1.60	5.20	0.09	0.70	0.61	21.02	4.71	0.01	24.89	32.46	29.67
125.000–250.000	0.00	0.00	0.04	0.00	0.00	0.00	1.91	0.00	0.00	2.65	13.52	9.03
250.000–500.000	0.00	0.00	0.00	0.00	0.00	0.00	0.00	0.00	0.00	0.00	0.14	1.44
500.000–1000.000	0.00	0.00	0.00	0.00	0.00	0.00	0.00	0.00	0.00	0.00	0.00	0.04
1000–2000	0.00	0.00	0.00	0.00	0.00	0.00	0.00	0.00	0.00	0.00	0.00	0.00
Total	100%	100%	100%	100%	100%	100%	100%	100%	100%	100%	100%	100%

Exposure WELL (6.3 to 7.5)

Depth/fraction	6.3	6.5	6.7	6.9	7.1	7.3	7.5
0.010–0.015	0.00	0.00	0.00	0.00	0.00	0.00	0.00
0.015–0.031	0.00	0.00	0.00	0.00	0.00	0.00	0.00
0.031–0.061	0.00	0.00	0.00	0.00	0.00	0.00	0.00
0.061–0.122	0.00	0.00	0.00	0.00	0.00	0.00	0.00
0.122–0.244	0.00	0.00	0.00	0.00	0.00	0.00	0.00
0.244–0.488	0.00	0.00	0.00	0.00	0.00	0.00	0.00
0.488–0.977	0.81	1.08	1.23	0.43	0.92	1.38	1.70
0.977–1.953	2.11	3.07	3.28	1.11	2.67	3.71	5.14
1.953–3.906	4.50	6.51	6.22	2.54	5.24	7.11	9.95
3.906–7.813	7.07	10.77	9.99	4.83	9.08	10.79	14.74
7.813–15.625	11.21	18.54	20.22	7.67	18.13	20.90	23.36
15.625–31.250	22.97	28.12	31.84	14.88	24.97	32.77	28.96
31.250–62.500	33.01	24.83	23.39	30.85	18.23	21.40	15.46
62.500–125.000	17.29	7.05	3.83	28.37	8.33	1.95	0.70
125.000–250.000	1.04	0.03	0.00	7.97	8.04	0.00	0.00
250.000–500.000	0.00	0.00	0.00	1.30	4.34	0.00	0.00
500.000–1000.000	0.00	0.00	0.00	0.04	0.05	0.00	0.00
1000–2000	0.00	0.00	0.00	0.00	0.00	0.00	0.00
Total	100%	100%	100%	100%	100%	100%	100%

Exposure DITCH (0.3 to 1.5)

Depth/fraction	0.3	0.4	0.5	0.6	0.7	0.8	0.9	1.0	1.1	1.2	1.3	1.4	1.5
0.010–0.015	0.00	0.00	0.00	0.00	0.00	0.00	0.00	0.00	0.00	0.00	0.00	0.00	0.00
0.015–0.031	0.00	0.00	0.00	0.00	0.00	0.00	0.00	0.00	0.00	0.00	0.00	0.00	0.00
0.031–0.061	0.00	0.00	0.00	0.00	0.00	0.00	0.00	0.00	0.00	0.00	0.00	0.00	0.00
0.061–0.122	0.00	0.00	0.00	0.00	0.00	0.00	0.00	0.00	0.00	0.00	0.00	0.00	0.00
0.122–0.244	0.00	0.00	0.00	0.00	0.00	0.00	0.00	0.00	0.00	0.00	0.00	0.00	0.00
0.244–0.488	0.00	0.00	0.00	0.00	0.00	0.0	0.00	0.00	0.00	0.00	0.00	0.00	0.00
0.488–0.977	0.69	0.13	0.04	0.19	0.10	0.13	0.07	0.11	0.05	0.15	0.09	0.07	0.15
0.977–1.953	3.38	0.91	0.58	1.38	0.82	0.87	0.78	1.06	0.90	1.31	0.83	0.82	1.20
1.953–3.906	8.30	2.16	1.36	3.92	2.14	2.40	2.02	2.57	2.40	3.67	2.47	2.68	3.59
3.906–7.813	12.57	3.14	2.78	6.69	4.87	5.03	3.69	3.66	3.77	5.39	4.83	5.55	6.59
7.813–15.625	12.88	2.81	3.62	6.53	7.58	6.13	4.37	3.58	3.70	4.67	5.26	6.71	8.71
15.625–31.250	7.98	2.51	2.58	3.87	5.91	4.06	3.28	2.70	2.90	3.64	3.90	5.31	7.76
31.250–62.500	6.22	4.39	2.87	3.58	3.21	2.84	2.99	2.94	3.22	3.81	3.23	3.98	4.76
62.500–125.000	6.25	2.69	0.30	1.16	0.41	0.42	0.55	0.28	0.21	0.74	0.32	0.38	0.51
125.000–250.000	15.25	22.85	17.22	17.44	19.53	24.83	15.04	12.58	21.32	22.95	28.68	24.61	21.10
250.000–500.000	22.33	48.43	54.19	42.26	41.88	46.39	46.26	48.67	53.53	44.88	46.82	45.43	40.29
500.000–1000.000	4.16	9.98	14.47	12.97	12.85	6.91	20.12	21.80	8.00	8.79	3.57	4.46	5.34
1000–2000	0.00	0.00	0.00	0.00	0.71	0.00	0.84	0.04	0.00	0.00	0.00	0.00	0.00
Total	100%	100%	100%	100%	100%	100%	100%	100%	100%	100%	100%	100%	100%

Other samples

Depth/fraction	GT21 0.7	AFD130 G1	AFD130 G2
0.010–0.015	0.00	0.00	0.00
0.015–0.031	0.00	0.00	0.00
0.031–0.061	0.00	0.00	0.00
0.061–0.122	0.00	0.00	0.00
0.122–0.244	0.00	0.00	0.00
0.244–0.488	0.00	0.00	0.00
0.488–0.977	0.52	0.24	0.24
0.977–1.953	1.86	1.17	1.11
1.953–3.906	4.64	2.90	2.83
3.906–7.813	8.36	4.80	4.90
7.813–15.625	16.25	7.60	8.48
15.625–31.250	21.47	10.61	11.82
31.250–62.500	12.64	8.85	9.19
62.500–125.000	5.47	11.57	14.80
125.000–250.000	12.25	25.76	27.39
250.000–500.000	13.97	22.10	17.17
500.000–1000.000	2.56	4.39	2.07
1000–2000	0.00	0.00	0.00
Total	100%	100%	100%

Statistical parameters of the particle size distribution (for the results of the laser method)

Exposure AFD/GT23/P (0.1 to 1.2)

Depth	0.1	0.2	0.3	0.4	0.5	0.6	0.7	0.8	0.9	1.0	1.1	1.2
μm	388.833	75.504	79.396	78.710	75.854	73.549	62.977	79.920	72.015	78.989	71.966	82.632
mm	0.389	0.076	0.079	0.079	0.076	0.074	0.063	0.080	0.072	0.079	0.072	0.083
φ5	1.363	3.727	3.655	3.667	3.721	3.765	3.989	3.645	3.796	3.662	3.797	3.597
μm	170.687	39.856	45.322	46.029	42.343	43.481	40.573	48.168	39.552	45.387	37.742	47.605
mm	0.171	0.040	0.045	0.046	0.042	0.043	0.041	0.048	0.040	0.045	0.038	0.048
φ16	2.551	4.649	4.464	4.441	4.562	4.523	4.623	4.376	4.660	4.462	4.728	4.393
μm	58.673	30.686	35.598	36.050	32.619	33.674	31.350	35.241	26.616	31.157	24.389	33.346
mm	0.059	0.031	0.036	0.036	0.033	0.034	0.031	0.035	0.027	0.031	0.024	0.033
φ25	4.091	5.026	4.812	4.794	4.938	4.892	4.995	4.827	5.232	5.004	5.358	4.906
μm	23.626	16.917	20.346	20.160	17.710	18.166	15.428	14.884	10.494	11.799	9.580	13.808
mm	0.024	0.017	0.020	0.020	0.018	0.018	0.015	0.015	0.010	0.012	0.010	0.014
φ50	5.403	5.885	5.619	5.632	5.819	5.783	6.018	6.070	6.574	6.405	6.706	6.178
μm	9.393	7.211	9.180	8.652	7.429	7.475	5.736	5.361	4.451	4.835	4.162	5.429
mm	0.009	0.007	0.009	0.009	0.007	0.007	0.006	0.005	0.004	0.005	0.004	0.005
φ75	6.734	7.116	6.767	6.853	7.073	7.064	7.446	7.543	7.812	7.692	7.909	7.525
μm	5.275	4.309	5.449	5.187	4.518	4.519	3.720	3.526	3.092	3.311	2.931	3.585
mm	0.005	0.004	0.005	0.005	0.005	0.005	0.004	0.004	0.003	0.003	0.003	0.004
φ84	7.567	7.858	7.520	7.591	7.790	7.790	8.070	8.148	8.337	8.239	8.414	8.124
μm	2.027	1.862	2.154	2.125	1.962	1.916	1.741	1.721	1.594	1.673	1.547	1.734
mm	0.002	0.002	0.002	0.002	0.002	0.002	0.002	0.002	0.002	0.002	0.002	0.002
φ95	8.946	9.069	8.859	8.878	8.993	9.028	9.166	9.183	9.293	9.223	9.336	9.172
Md	5.403	5.885	5.619	5.632	5.819	5.783	6.018	6.070	6.574	6.405	6.706	6.178
Mz	5.174	6.131	5.868	5.888	6.057	6.032	6.237	6.198	6.524	6.368	6.616	6.232
Standard deviation	2.403	1.612	1.553	1.577	1.606	1.614	1.646	1.782	1.752	1.787	1.761	1.777
Sk_I	-0.102	0.211	0.244	0.245	0.212	0.231	0.203	0.113	-0.026	-0.008	-0.062	0.058
K_G	1,176	1.048	1.091	1.037	1.012	0.993	0.866	0.835	0.873	0.848	0.890	0.872

Exposure AFD24

Depth	0.01	0.1	0.2	0.3	0.4	0.5
μm	122.664	128.673	126.985	116.282	113.959	103.894
mm	0.123	0.129	0.127	0.116	0.114	0.104
φ5	3.027	2.958	2.977	3.104	3.133	3.267
μm	84.321	87.309	74.162	66.254	66.133	61.306
mm	0.084	0.087	0.074	0.066	0.066	0.061
φ16	3.568	3.518	3.753	3.916	3.918	4.028
μm	69.706	71.913	57.721	50.484	50.708	46.805
mm	0.070	0.072	0.058	0.050	0.051	0.047
φ25	3.843	3.798	4.115	4.308	4.302	4.417
μm	44.707	45.855	30.995	25.056	25.380	22.788
mm	0.045	0.046	0.031	0.025	0.025	0.023
φ50	4.483	4.447	5.012	5.319	5.300	5.456
μm	24.206	24.591	11.009	8.353	8.404	7.488
mm	0.024	0.025	0.011	0.008	0.008	0.007
φ75	5.368	5.346	6.505	6.903	6.895	7.061
μm	14.124	13.878	5.919	4.749	4.785	4.368
mm	0.014	0.014	0.006	0.005	0.005	0.004
φ84	6.146	6.171	7.400	7.718	8.707	7.839
μm	3.928	3.607	2.123	1.910	1.919	1.838
mm	0.004	0.004	0.002	0.002	0.002	0.002
φ95	7.992	8.115	8.880	9.032	9.025	9.088
Md	4.483	4.447	5.012	5.319	5.300	5.456
Mz	4.732	4.712	5.388	5.651	5.642	5.774
Standard deviation	1.397	1.445	1.806	1.849	1.840	1.835
Sk_I	0.352	0.361	0.310	0.257	0.268	0.249
K_G	1.333	1.365	1.012	0.936	0.931	0.902

Exposure AFD131/I

Depth	0.1	0.2	0.3	0.4	0.5	0.6	0.7	0.8	0.9	1.0
μm	198.538	231.575	220.668	227.426	222.073	224.672	247.672	211.540	209.606	226.047
mm	0.199	0.232	0.221	0.227	0.222	0.225	0.248	0.212	0.210	0.226
φ5	2.333	2.110	2.180	2.137	2.171	2.152	2.013	2.241	2.254	2.145
μm	132.849	156.293	156.016	154.532	154.993	157.192	168.988	153.386	155.460	165.222
mm	0.133	0.156	0.156	0.155	0.155	0.157	0.169	0.153	0.155	0.165
φ16	2.912	2.678	2.680	2.694	2.690	2.669	2.565	2.705	2.685	2.598
μm	106.720	125.195	127.001	123.873	125.749	128.170	136.550	127.279	130.409	137.873
mm	0.107	0.125	0.127	0.124	0.126	0.128	0.137	0.127	0.130	0.138
φ25	3.228	2.998	2.977	3.013	2.991	2.964	2.872	2.974	2.939	2.859
μm	60.605	70.223	73.200	68.787	73.042	75.989	79.046	79.825	83.723	88.204
mm	0.061	0.070	0.073	0.069	0.073	0.076	0.079	0.080	0.084	0.088
φ50	4.044	3.832	3.772	3.862	3.775	3.718	3.661	3.647	3.578	3.503
μm	23.670	25.861	26.935	25.312	29.782	32.554	29.628	38.757	39.698	33.045
mm	0.024	0.026	0.027	0.025	0.030	0.033	0.030	0.039	0.040	0.044
φ75	5.401	5.273	5.214	5.304	5.069	4.941	5.077	4.689	4.655	4.505
μm	13.637	14.888	15.401	14.925	17.153	18.695	16.620	22.092	20.699	24.211
mm	0.014	0.015	0.015	0.015	0.017	0.019	0.017	0.022	0.021	0.024
φ84	6.196	6.070	6.021	6.066	5.865	5.741	5.911	5.500	5.594	5.368
μm	3.930	4.364	4.475	4.415	4.971	5.016	4.501	5.934	5.761	6.773
mm	0.004	0.004	0.004	0.004	0.005	0.005	0.005	0.006	0.006	0.007
φ95	7.991	7.840	7.804	7.823	7.652	7.639	7.796	7.397	7.439	7.206
Md	4.044	3.832	3.772	3.862	3.775	3.718	3.661	3.647	3.578	3.503
Mz	4.384	4.193	4.158	4.207	4.110	4.043	4.046	3.951	3.953	3.823
Standard deviation	1.678	1.716	1.687	1.705	1.624	1.599	1.713	1.480	1.513	1.459
Sk_I	0.353	0.359	0.390	0.350	0.366	0.373	0.387	0.390	0.438	0.405
K_G	1.067	1.032	1.030	1.017	1.081	1.137	1.075	1.232	1.238	1.260

Exposure AFD131/P

Depth	0.1	0.2	0.3	0.4	0.5	0.7	0.8	0.9	1.0	1.1
μm	190.380	181.384	182.845	179.768	235.116	170.274	194.734	188.173	189.713	193.008
mm	0.190	0.181	0.183	0.180	0.235	0.170	0.195	0.188	0.190	0.193
φ5	2.393	2.463	2.451	2.476	2.089	2.554	2.360	2.410	2.398	2.373
μm	119.846	118.221	115.497	119.297	139.666	113.970	142.799	138.503	139.749	141.656
mm	0.120	0.118	0.115	0.119	0.140	0.114	0.143	0.139	0.140	0.142
φ16	3.061	3.080	3.114	3.067	2.840	3.133	2.808	2.852	2.839	2.820
μm	94.727	94.992	92.025	96.421	109.456	92.047	119.168	115.741	117.001	118.493
mm	0.095	0.095	0.092	0.096	0.109	0.092	0.119	0.116	0.117	0.118
φ25	3.400	3.396	3.442	3.375	3.192	3.441	3.069	3.111	3.095	3.077
μm	52.833	56.134	53.511	57.887	62.461	54.771	75.565	73.776	75.321	76.336
mm	0.053	0.056	0.054	0.058	0.062	0.055	0.076	0.074	0.075	0.076
φ50	4.242	4.155	4.224	4.111	4.001	4.190	3.726	3.761	3.731	3.711
μm	22.570	26.634	25.373	28.351	28.699	26.556	37.554	37.895	39.639	40.653
mm	0.023	0.027	0.025	0.028	0.029	0.027	0.038	0.038	0.040	0.041
φ75	5.469	5.231	5.301	5.140	5.123	5.235	4.735	4.722	4.657	4.620
μm	13.768	16.220	15.547	17.041	16.956	16.347	22.422	23.234	24.283	25.272
mm	0.014	0.016	0.016	0.017	0.017	0.016	0.022	0.023	0.024	0.025
φ84	6.183	5.946	6.007	5.875	5.882	5.935	5.479	5.428	5.364	5.306
μm	4.207	4.859	4.599	4.737	4.696	4.716	6.528	6.814	7.186	7.583
mm	0.004	0.005	0.005	0.005	0.005	0.005	0.007	0.007	0.007	0.008
φ95	7.893	7.685	7.764	7.722	7.734	7.728	7.259	7.197	7.121	7.043
Md	4.242	4.155	4.224	4.111	4.001	4.190	3.726	3.761	3.731	3.711
Mz	4.495	4.394	4.448	4.351	4.241	4.420	4.004	4.013	3.978	3.946
Standard deviation	1.614	1.508	1.528	1.497	1.616	1.484	1.410	1.369	1.347	1.329
Sk_I	0.285	0.301	0.283	0.317	0.280	0.306	0.377	0.365	0.365	0.355
K_G	1.089	1.167	1.172	1.217	1.198	1.182	1.205	1.218	1.239	1.240

Exposure PG1

Depth	0.2	0.4	0.6	0.8
μm	121.216	99.179	188.947	168.629
mm	0.121	0.099	0.189	0.169
φ5	3.044	3.334	2.404	2.568
μm	58.117	58.210	65.826	68.337
mm	0.058	0.058	0.066	0.068
φ16	4.105	4.103	3.925	3.871
μm	43.112	45.395	48.902	48.524
mm	0.043	0.045	0.049	0.049
φ25	4.536	4.461	4.354	4.365
μm	22.157	25.723	26.998	24.067
mm	0.022	0.026	0.027	0.024
φ50	5.496	5.281	5.211	5.377
μm	9.505	12.232	13.010	10.047
mm	0.010	0.012	0.013	0.010
φ75	6.717	6.353	6.264	6.637
μm	5.671	7.406	7.854	5.830
mm	0.006	0.007	0.008	0.006
φ84	7.462	7.077	6.992	7.422
μm	2.145	2.488	2.590	2.179
mm	0.002	0.002	0.003	0.002
φ95	8.865	8.651	8.593	8.842
Md	5.496	5.281	5.211	5.377
Mz	5.688	5.487	5.376	5.557
Standard deviation	1.721	1.549	1.704	1.838
Sk_I	0.164	0.238	0.127	0.128
K_G	1.094	1.152	1.328	1.132

Exposure PG2

Depth	0.1	0.2	0.3	0.4	0.5	0.6	0.7	0.8	0.9
μm	488.096	450.171	450.452	416.218	326.364	280.770	260.632	249.227	78.423
mm	0.488	0.450	0.450	0.416	0.326	0.281	0.261	0.249	0.078
φ5	1.035	1.151	1.151	1.265	1.615	1.833	1.940	2.004	3.673
μm	345.713	320.169	286.261	235.681	78.487	67.285	62.168	65.774	55.603
mm	0.346	0.320	0.286	0.236	0.078	0.067	0.062	0.066	0.056
φ16	1.532	1.643	1.805	2.085	3.671	3.894	4.008	3.926	4.169
μm	274.576	246.594	192.099	111.431	50.725	48.969	46.319	50.796	45.669
mm	0.275	0.247	0.192	0.111	0.051	0.049	0.046	0.051	0.046
φ25	1.865	2.020	2.380	3.166	4.301	4.352	4.432	4.299	4.453
μm	71.145	36.356	24.889	25.688	22.293	25.129	24.520	28.789	27.884
mm	0.071	0.036	0.025	0.026	0.022	0.025	0.025	0.029	0.028
φ50	3.813	4.782	5.328	5.283	5.487	5.315	5.350	5.118	5.164
μm	12.010	9.737	9.007	10.007	8.917	10.358	10.298	13.181	13.539
mm	0.012	0.010	0.009	0.010	0.009	0.010	0.010	0.013	0.014
φ75	6.380	6.682	6.795	6.643	6.809	6.593	6.601	6.245	6.207
μm	7.155	5.864	5.557	6.152	5.405	6.045	6.003	7.845	8.072
mm	0.007	0.006	0.006	0.006	0.005	0.006	0.006	0.008	0.008
φ84	7.127	7.414	7.491	7.345	7.531	7.370	7.380	6.994	6.953
μm	2.678	2.331	2.258	2.341	2.060	2.224	2.214	2.636	2.636
mm	0.003	0.002	0.002	0.002	0.002	0.002	0.002	0.003	0.003
φ95	8.545	8.745	8.791	8.739	8.923	8.813	8.819	8.567	8.567
Md	3.813	4.782	5.328	5.283	5.487	5.315	5.350	5.118	5.164
Mz	4.157	4.613	4.875	4.904	5.563	5.526	5.579	5.346	5.429
Standard deviation	2.536	2.593	2.579	2.447	2.072	1.927	1.885	1.761	1.438
Sk_I	0.222	-0.022	-0.166	-0.146	0.000	0.092	0.106	0.137	0.338
K_G	0.682	0.667	0.709	0.881	1.194	1.276	1.300	1.382	1.144

Exposure PG3/4

Depth	0.1	0.3	0.5	0.6	0.8	1.0
μm	416.685	421.192	419.122	416.883	411.631	384.237
mm	0.417	0.421	0.419	0.417	0.412	0.384
φ5	1.263	1.247	1.255	1.262	1.281	1.380
μm	312.987	317.630	314.944	315.668	304.332	243.243
mm	0.313	0.318	0.315	0.316	0.304	0.243
φ16	1.676	1.655	1.667	1.664	1.716	2.040
μm	264.705	269.451	266.771	268.448	254.887	181.482
mm	0.265	0.269	0.267	0.268	0.255	0.181
φ25	1.918	1.892	1.906	1.897	1.972	2.462
μm	176.319	181.683	178.933	182.039	164.941	85.382
mm	0.176	0.182	0.179	0.182	0.165	0.085
φ50	2.504	2.461	2.483	2.458	2.600	3.550
μm	100.178	108.962	103.612	109.888	88.683	28.815
mm	0.100	0.109	0.104	0.110	0.089	0.029
φ75	3.319	3.198	3.271	3.186	3.495	5.117
μm	38.414	57.483	31.858	62.276	38.776	13.290
mm	0.038	0.057	0.032	0.062	0.039	0.013
φ84	4.702	4.121	4.972	4.005	4.689	6.234
μm	6.255	6.551	5.810	6.497	5.693	3.764
mm	0.006	0.007	0.006	0.006	0.006	0.004
φ95	7.321	7.254	7.427	7.266	7.457	8.054
Md	2.504	2.461	2.483	2.458	2.600	3.550
Mz	2.961	2.745	3.041	2.709	3.002	3.941
Standard deviation	1.674	1.527	1.762	1.495	1.679	2.060
Sk_I	0.522	0.471	0.554	0.462	0.489	0.315
K_G	1.771	1.885	1.854	1.909	1.662	1.030

Exposure AFD113

Depth	0.05	0.15	0.25	0.35	0.45	0.55	0.65	0.75
μm	74.985	49.978	52.867	55.467	59.367	52.652	106.560	81.173
mm	0.075	0.050	0.053	0.055	0.059	0.053	0.107	0.081
φ5	3.737	4.323	4.241	4.172	4.074	4.247	3.230	3.623
μm	52.467	35.587	38.290	38.684	41.347	37.365	68.167	55.284
mm	0.052	0.036	0.038	0.039	0.041	0.037	0.068	0.055
φ16	4.252	4.813	4.707	4.692	4.596	4.742	3.875	4.177
μm	42.716	28.970	31.609	30.904	33.296	30.454	53.543	44.527
mm	0.043	0.029	0.032	0.031	0.033	0.030	0.054	0.045
φ25	4.549	5.109	4.984	5.016	4.909	5.037	4.223	4.489
μm	25.747	17.026	19.564	16.679	18.824	18.055	28.721	26.009
mm	0.026	0.017	0.020	0.017	0.019	0.018	0.029	0.026
φ50	5.279	5.876	5.676	5.906	5.731	5.791	5.122	5.265
μm	13.063	7.988	10.111	7.021	8.254	8.612	10.842	11.767
mm	0.013	0.008	0.010	0.007	0.008	0.009	0.011	0.012
φ75	6.258	6.968	6.628	7.154	6.921	6.859	6.527	6.409
μm	8.258	4.919	6.343	4.425	5.057	5.343	6.123	6.814
mm	0.008	0.005	0.006	0.004	0.005	0.005	0.006	0.007
φ84	6.920	7.667	7.301	7.820	7.628	7.548	7.352	7.197
μm	2.600	1.906	2.157	1.851	1.981	2.005	2.264	2.446
mm	0.003	0.002	0.002	0.002	0.002	0.002	0.002	0.002
φ95	8.587	9.035	8.857	9.077	8.980	8.962	8.787	8.675
Md	5.279	5.876	5.676	5.906	5.731	5.791	5.122	5.265
Mz	5.484	6.119	5.894	6.139	5.985	6.027	5.449	5.546
Standard deviation	1.402	1.428	1.348	1.525	1.501	1.416	1.711	1.521
Sk_I	0.297	0.298	0.316	0.259	0.288	0.299	0.301	0.315
K_G	1.163	1.039	1.150	0.940	0.999	1.060	0.988	1.079

Exposure WELL (0.9 to 2.5)

Depth	0.9	1.1	1.3	1.5	1.7	1.9	2.1	2.3	2.4	2.5
μm	47.506	44.041	57.202	47.239	55.329	37.350	38.453	97.732	99.788	94.061
mm	0.048	0.044	0.057	0.047	0.055	0.037	0.038	0.098	0.100	0.094
φ5	4.396	4.505	4.128	4.404	4.176	4.743	4.701	3.355	3.325	3.410
μm	27.721	20.087	27.824	20.867	31.728	25.189	24.121	63.392	67.104	60.259
mm	0.028	0.020	0.028	0.021	0.032	0.025	0.024	0.063	0.067	0.060
φ16	5.173	5.638	5.168	5.583	4.978	5.311	5.374	3.980	3.897	4.053
μm	21.070	14.068	18.499	14.678	23.689	20.236	19.074	48.561	52.860	45.042
mm	0.021	0.014	0.018	0.015	0.024	0.020	0.019	0.049	0.053	0.045
φ25	5.569	6.151	5.756	6.090	5.400	5.627	5.712	4.364	4.242	4.473
μm	11.217	6.713	7.635	7.082	11.903	11.954	10.997	19.265	26.825	17.347
mm	0.011	0.007	0.008	0.007	0.012	0.012	0.011	0.019	0.027	0.017
φ50	6.478	7.219	7.033	7.142	6.393	6.386	6.507	5.698	5.220	5.849
μm	5.203	3.252	3.390	3.455	5.283	5.980	5.447	5.549	10.113	6.388
mm	0.005	0.003	0.003	0.003	0.005	0.006	0.005	0.006	0.010	0.006
φ75	7.586	8.264	8.204	8.177	7.564	7.386	7.520	7.494	6.628	7.290
μm	3.480	2.363	2.415	2.519	3.520	3.927	3.645	3.522	6.173	4.159
mm	0.003	0.002	0.002	0.003	0.004	0.004	0.004	0.004	0.006	0.004
φ84	8.167	8.725	8.694	8.633	8.150	7.992	8.100	8.149	7.340	7.910
μm	1.639	1.299	1.297	1.392	1.640	1.713	1.649	1.670	2.311	1.900
mm	0.002	0.001	0.001	0.001	0.002	0.002	0.002	0.002	0.002	0.002
φ95	9.253	9.588	9.591	9.489	9.252	9.189	9.244	9.226	8.757	9.040
Md	6.478	7.219	7.033	7.142	6.393	6.386	6.507	5.698	5.220	5.849
Mz	6.606	7.194	6.965	7.119	6.507	6.563	6.660	5.942	5.486	5.937
Standard deviation	1.484	1.542	1.709	1.533	1.562	1.344	1.370	1.932	1.684	1.817
Sk_I	0.135	-0.046	-0.061	-0.050	0.117	0.229	0.187	0.189	0.267	0.101
K_G	0.987	0.986	0.915	0.999	0.961	1.036	1.030	0.769	0.933	0.819

Exposure WELL (2.7 to 5.3)

Depth	2.7	2.9	3.1	3.3	3.5	4.5	4.7	4.9	5.1	5.3
μm	96.685	51.361	49.630	47.900	63.377	40.567	46.323	44.863	104.579	61.550
mm	0.097	0.051	0.050	0.048	0.063	0.041	0.046	0.045	0.105	0.062
φ5	3.371	4.283	4.333	4.384	3.980	4.624	4.432	4.478	3.257	4.022
μm	60.362	33.302	33.315	31.919	41.256	28.313	32.555	31.135	73.619	40.802
mm	0.060	0.033	0.033	0.032	0.041	0.028	0.033	0.031	0.074	0.041
φ16	4.050	4.908	4.908	4.969	4.599	5.142	4.941	5.005	3.764	4.615
μm	44.583	26.283	26.628	25.627	32.591	23.053	26.511	25.261	59.694	31.743
mm	0.045	0.026	0.027	0.026	0.033	0.023	0.027	0.025	0.060	0.032
φ25	4.487	5.250	5.231	5.286	4.939	5.439	5.237	5.307	4.066	4.977
μm	17.923	14.812	15.467	15.377	18.789	13.939	15.805	15.148	33.996	16.577
mm	0.018	0.015	0.015	0.015	0.019	0.014	0.016	0.015	0.034	0.017
φ50	5.802	6.077	6.015	6.023	5.734	6.165	5.983	6.045	4.878	5.915
μm	6.828	6.757	7.480	8.028	9.416	7.017	7.506	7.610	13.562	7.240
mm	0.007	0.007	0.007	0.008	0.009	0.007	0.008	0.008	0.014	0.007
φ75	7.194	7.209	7.063	6.961	6.731	7.155	7.058	7.038	6.204	7.110
μm	4.241	4.195	4.691	5.173	5.956	4.463	4.632	4.795	8.041	4.614
mm	0.004	0.004	0.005	0.005	0.006	0.004	0.005	0.005	0.008	0.005
φ84	7.881	7.897	7.736	7.595	7.391	7.808	7.754	7.704	6.958	7.760
μm	1.822	1.729	1.856	1.947	2.139	1.816	1.895	1.807	2.825	1.930
mm	0.002	0.002	0.002	0.002	0.002	0.002	0.002	0.002	0.003	0.002
φ95	9.100	9.176	9.074	9.005	8.869	9.105	9.044	9.112	8.468	9.017
Md	5.802	6.077	6.015	6.023	5.734	6.165	5.983	6.045	4.878	5.915
Mz	5.911	6.294	6.219	6.196	5.908	6.372	6.226	6.251	5.200	6.097
Standard deviation	1.826	1.489	1.425	1.356	1.439	1.345	1.402	1.377	1.588	1.543
Sk_I	0.118	0.242	0.254	0.244	0.235	0.273	0.293	0.277	0.340	0.208
K_G	0.867	1.023	1.061	1.131	1.119	1.070	1.038	1.097	0.999	0.960

Exposure WELL (5.5 to 7.5)

Depth	5.5	5.7	5.9	6.1	6.3	6.5	6.7	6.9	7.1	7.3	7.5
μm	41.319	110.660	168.919	160.854	94.742	68.964	58.783	155.686	236.481	52.459	45.792
mm	0.041	0.111	0.169	0.161	0.095	0.069	0.059	0.156	0.236	0.052	0.046
φ5	4.597	3.176	2.566	2.636	3.400	3.858	4.088	2.683	2.080	4.253	4.449
μm	29.467	79.461	117.508	105.836	66.153	46.271	40.616	100.562	89.070	37.002	31.385
mm	0.029	0.079	0.118	0.106	0.066	0.046	0.041	0.101	0089	0.037	0.031
φ16	5.085	3.654	3.089	3.240	3.918	4.434	4.662	3.314	3.489	4.756	4.994
μm	24.277	65.664	95.494	85.379	53.837	36.725	32.802	80.908	50.446	30.164	25.021
mm	0.024	0.066	0.095	0.085	0.054	0.037	0.033	0.081	0.0050	0.030	0.025
φ25	5.364	3.929	3.388	3.550	4.215	4.767	4.930	3.628	4.309	5.051	4.231
μm	15.155	40.660	57.722	50.935	32.184	20.439	19.326	48.953	23.059	17.995	13.824
mm	0.015	0.041	0.058	0.051	0.032	0.020	0.019	0.049	0.023	0.018	0.014
φ50	6.044	4.620	4.115	4.295	4.958	5.613	5.693	4.352	5.439	5.796	6.177
μm	8.011	19.049	29.017	23.609	15.129	9.232	9.496	24.837	10.793	8.583	5.952
mm	0.008	0.0019	0.029	0.024	0.015	0.009	0.009	0.025	0.011	0.009	0.006
φ75	6.964	5.714	5.107	5.405	6.047	6.759	6.718	5.331	6.534	6.864	7.392
μm	5.067	10.501	17.283	13.086	8.796	5.751	5.924	14.963	6.997	5.191	3.733
mm	0.005	0.011	0.017	0.013	0.009	0.006	0.006	0.015	0.007	0.005	0.004
φ84	7.625	6.573	5.855	6.256	6.829	7.442	7.399	6.062	7.159	7.590	8.065
μm	1.908	3.301	4.626	3.923	2.828	2.199	2.093	4.611	2.442	1.932	1.624
mm	0.002	0.003	0.005	0.004	0.003	0.002	0.002	0.005	0.002	0.002	0.002
φ95	9.034	8.243	7.756	7.994	8.466	8.829	8.900	7.761	8.678	9.016	9.266
Md	6.044	4.620	4.115	4.295	4.958	5.613	5.693	4.352	5.439	5.796	6.177
Mz	6.251	4.949	4.353	4.597	5.235	5.829	5.905	4.576	5.362	6.047	6.412
Standard deviation	1.307	1.498	1.478	1.566	1.495	1.505	1.423	1.456	1.917	1.430	1.498
Sk_I	0.296	0.384	0.331	0.340	0.335	0.255	0.281	0.293	-0.040	0.309	0.256
K_G	1.137	1.163	1.238	1.184	1.134	1.023	1.103	1.221	1.215	1.077	0.953

Exposure DITCH (0.3 to 1.0)

Depth	0.3	0.4	0.5	0.6	0.7	0.8	0.9	1.0
μm	481.748	560.232	619.311	613.660	654.998	527.856	726.774	701.447
mm	0.482	0.560	0.619	0.614	0.655	0.528	0.727	0.701
φ5	1.054	0.836	0.691	0.704	0.610	0.922	0.460	0.512
μm	336.360	449.742	487.373	471.115	473.804	416.243	546.240	548.873
mm	0.336	0.450	0.487	0.471	0.474	0.416	0.546	0.549
φ16	1.572	1.153	1.037	1.086	1.078	1.265	0.872	0.865
μm	261.228	393.780	427.896	403.866	401.222	363.308	468.629	477.517
mm	0.261	0.394	0.428	0.404	0.401	0.363	0.469	0.478
φ25	1.937	1.345	1.225	1.308	1.318	1.461	1.093	1.066
μm	50.083	282.642	318.351	274.316	273.449	261.690	329.285	343.842
mm	0.050	0.283	0.318	0.274	0.273	0.262	0.329	0.344
φ50	4.320	1.823	1.651	1.866	1.871	1.934	1.603	1.540
μm	7.839	177.143	223.869	48.888	124.063	158.823	208.211	225.554
mm	0.008	0.177	0.224	0.049	0.124	0.159	0.208	0.226
φ75	6.995	2.497	2.159	4.354	3.011	2.655	2.264	2.148
μm	4.869	61.981	168.483	11.326	16.376	19.298	46.114	52.431
mm	0.005	0.062	0.168	0.011	0.016	0.019	0.046	0.052
φ84	7.582	4.012	2.569	6.464	5.932	5.695	4.439	4.253
μm	2.173	5.885	8.203	3.660	5.492	5.101	6.041	5.030
mm	0.002	0.006	0.008	0.004	0.005	0.005	0.006	0.005
φ95	8.846	7.409	6.930	8.094	7.508	7.615	7.371	7.635
Md	4.320	1.823	1.651	1.866	1.871	1.934	1.603	1.540
Mz	4.525	2.329	1.753	3.139	2.960	2.965	2.305	2.220
Standard deviation	2.708	1.711	1.328	2.464	2.259	2.122	1.939	1.926
Sk_I	0,131	0.615	0.445	0.698	0.654	0.698	0.630	0.656
K_G	0.631	2.337	2.736	0.994	1.670	2.298	2.420	2.698

Exposure DITCH (1.1 to 1.5)

Depth	1.1	1.2	1.3	1.4	1.5
μm	540.272	556.662	476.510	491.574	505.772
mm	0.540	0.557	0.477	0.492	0.506
φ5	0.888	0.845	1.069	1.025	0.983
μm	432.469	431.286	380.624	389.654	392.547
mm	0.432	0.431	0.381	0.390	0.393
φ16	1.209	1.213	1.394	1.360	1.349
μm	382.601	373.339	336.326	342.197	339.392
mm	0.383	0.373	0.336	0.342	0.339
φ25	1.386	1.421	1.572	1.547	1.559
μm	287.779	263.952	251.160	249.634	232.406
mm	0.288	0.264	0.251	0.250	0.232
φ50	1.797	1.922	1.993	2.002	2.105
μm	199.149	147.667	163.777	59.558	23.341
mm	0.199	0.148	0.164	0.060	0.023
φ75	2.328	2.760	2.610	4.070	5.421
μm	48.568	18.259	24.378	15.924	11.235
mm	0.049	0.018	0.024	0.016	0.011
φ84	4.364	5.775	5.358	5.973	6.476
μm	5.400	3.833	5.103	4.853	3.944
mm	0.005	0.004	0.005	0.005	0.004
φ95	7.533	8.027	7.614	7.687	7.986
Md	1.797	1.922	1.993	2.002	2.105
Mz	2.457	2.970	2.915	3.112	3.310
Standard deviation	1.795	2.229	1.983	2.163	2.343
Sk_I	0.677	0.695	0.708	0.714	0.692
K_G	2.891	2.200	2.584	1.082	0.743

Sieve method, content of organic matter and magnetic susceptibility

Mass in grams (g)

Exposure AFD/GT23/P (0.1 to 0.7)

Depth/fraction	0.1	0.2	0.3	0.4	0.5	0.6	0.7
<1 mm	117.73	71.82	81.29	92.59	85.33	73.57	89.04
1–2 mm	10.92	0.09	0.24	0.11	0.31	0.15	0.02
2–4mm	7.91	0.20	0.57	0.18	0.46	0.94	0.14
>4 mm	4.61	0.46	0.90	3.96	4.92	2.10	2.00
Total mass (g)	141.17	72.57	83.00	96.84	91.02	76.76	91.20
$CaCO_3$ (%)	8.60	6.53	6.60	5.76	3.84	4.61	4.22
Organic matter (%)	1.08	4.22	4.06	4.59	4.82	2.49	5.74
MS sample weight (g)	39.16	35.83	45.08	46.04	49.58	39.18	45.64
Total MS [10^-6*SI]	3346	8682	10292	10012	9382	7352	7052
Mass specific MS [10^-9*m^3.kg^-1]	854.44	2423.11	2283.05	2174.63	1892.30	1876.47	1545.14

Exposure AFD/GT23/P (0.8 to 1.2)

Depth/fraction	0.8	0.9	1.0	1.1	1.2
<1 mm	69.97	85.37	66.15	68.09	73.58
1–2 mm	0.17	0.05	0.00	0.00	0.05
2–4mm	0.50	0.00	0.58	0.26	0.00
>4 mm	2.54	2.06	1.17	7.97	0.12
Total mass (g)	73.18	87.48	67.90	**76.32**	**73.75**
$CaCO_3$ (%)	6.60	2.46	3.84	4.45	3.07
Organic matter (%)	3.61	13.59	4.08	4.16	3.28
MS sample weight (g)	42.99	42.97	41.07	41.62	48.33
Total MS [10^-6*SI]	5982	6382	6832	6642	7792
Mass specific MS [10^-9*m^3.kg^-1]	1391.49	1485.22	1663.50	1595.87	1612.25

Exposure AFD/GT24

Depth/fraction	0.01	0.1	0.2	0.3	0.4	0.5
<1 mm	28.41	67.30	48.14	36.13	46.76	51.54
1–2 mm	0.07	0.09	0.00	0.00	0.00	0.00
2–4mm	0.62	0.11	0.00	1.55	0.14	0.65
>4 mm	0.00	0.00	0.20	0.47	0.00	0.00
Total mass (g)	29.10	67.50	48.34	38.15	46.90	52.19
$CaCO_3$ (%)	12.98	15.89	17.58	11.44	10.67	18.43
Organic matter (%)	4.07	3.69	0.07	2.10	2.66	3.55
MS sample weight (g)	15.08	28.25	46.54	31.45	34.26	41.76
Total MS [10^-6*SI]	2056	3794	6382	7692	8212	8367
Mass specific MS [10^-9*m^3.kg^-1]	1363.40	1343.01	1371.29	2445.79	2396.96	2003.59

Exposure AFD131/I

Depth/fraction	0.1	0.2	0.3	0.4	0.5	0.6	0.7	0.8	0.9	1.0
$CaCO_3$ (%)	1.60	1.76	1.12	0.96	1.72	0.84	0.92	0.80	0.96	1.32
Organic matter (%)	1.47	1.33	1.09	1.14	1.40	1.42	1.35	1.16	1.17	1.17
MS sample weight (g)	20	20	20	20	20	20	20	20	20	20
Total MS [10^-6*SI]	4216.4	3696.4	4836.4	4886.4	3521.4	3326.4	3291.4	3651.4	3581.4	3431.4
Mass specific MS [10^-9*m^3.kg^-1]	2108.2	1848.2	2418.2	2443.2	1760.7	1663.2	1645.7	1825.7	1790.7	1715.7

Exposure AFD131/P

Depth/fraction	0.1	0.2	0.3	0.4	0.5	0.7	0.8	0.9	1.0	1.1
$CaCO_3$ (%)	8.38	6.87	5.35	3.75	3.67	3.83	1.64	2.40	1.52	1.00
Organic matter (%)	1.98	2.19	2.02	2.05	4.48	1.67	1.70	1.70	1.55	1.56
MS sample weight (g)	20	20	20	20	20	20	20	20	20	20
Total MS [10^-6*SI]	3396.4	3571.4	3556.4	3796.4	3496.4	3856.4	3711.4	3686.4	3746.4	3836.4
Mass specific MS [10^-9*m^3.kg^-1]	1698.2	1785.7	1778.2	1898.2	1748.2	1928.2	1855.7	1843.2	1873.2	1918.2

Exposure PG1

Depth/fraction	0.2	0.4	0.6	0.8
$CaCO_3$ (%)	2.63	1.28	1.36	1.08
Organic matter (%)	4.55	3.97	4.39	4.18
MS sample weight (g)	20	20	20	20
Total MS [10^-6*SI]	2339.4	2525.4	3457.4	4621.4
Mass specific MS [10^-9*m^3.kg^-1]	1169.7	1262.7	1728.7	2310.7

Exposure PG3/4

Depth/fraction	0.1	0.3	0.5	0.6	0.8	1.0
$CaCO_3$ (%)	0.92	0.88	0.92	0.96	3.67	7.66
Organic matter (%)	0.79	1.16	1.12	1.08	1.26	0.58
MS sample weight (g)	20	20	20	20	20	20
Total MS [10^-6*SI]	1115.4	3961.4	4336.4	4586.4	4836.4	4671.4
Mass specific MS [10^-9*m^3.kg^-1]	557.7	1980.7	2168.2	2293.2	2418.2	2335.7

Exposure PG2

Depth/fraction	0.1	0.2	0.3	0.4	0.5	0.6	0.7	0.8	0.9	1.1
$CaCO_3$ (%)	2.87	12.53	14.53	14.37	29.50	15.93	9.74	4.31	3.71	1.00
Organic matter (%)	2.09	0.54	3.63	0.42	1.90	2.96	3.91	4.08	4.74	1.56
MS sample weight (g)	20	20	20	20	20	20	20	20	20	20
Total MS [10^-6*SI]	5416.4	7411.4	8346.4	9121.4	9866.4	671.4	538.4	658.4	698.4	3836.4
Mass specific MS [10^-9*m^3.kg^-1]	2708.2	3705.7	4173.2	4560.7	4933.2	335.7	269.2	329.2	349.2	1918.2

Exposure AFD113

Depth/fraction	0.05	0.15	0.25	0.35	0.45	0.55	0.65	0.75
<1 mm	72.35	72.15	78.49	66.15	59.47	61.17	69.01	50.91
1–2 mm	0.02	0.02	0.10	2.04	0.21	0.00	0.09	0.00
2–4mm	0.06	0.03	0.00	4.17	2.02	0.31	3.60	0.00
>4 mm	0.26	0.00	0.00	3.57	1.88	1.88	1.12	0.00
Total mass (g)	72.69	72.20	78.59	75.93	63.58	63.36	73.82	50.91
$CaCO_3$ (%)	5.07	10.60	7.91	5.30	6.37	13.13	7.14	9.60
Organic matter (%)	41.21	31.62	21.17	36.9	43.86	20.17	19.49	50.36
MS sample weight (g)	25292	14852	10712	13872	17892	7322	2522	15772
Total MS [10^-6*SI]	6137.35	4697.03	5059.99	3759.35	4079.34	3630.14	1295.99	3131.85
Mass specific MS [10^-9*m^3.kg^-1]	854.44	2423.11	2283.05	2174.63	1892.30	1876.47	1545.14	1545.14

Exposure WELL (0.9 to 2.3)

Depth/fraction	0.9	1.1	1.3	1.5	1.7	1.9	2.1	2.3
$CaCO_3$ (%)	0.09	0.12	0.73	1.72	5.43	0.86	0.38	16.13
Organic matter (%)	5.71	5.71	5.62	5.60	5.58	7.34	6.93	3.12
MS sample weight (g)	20	20	20	20	20	20	20	20
Total MS [10^-6*SI]	4371.4	3226.4	2556.4	2497.4	2805.4	5416.4	5776.4	1325.4
Mass specific MS [10^-9*m^3.kg^-1]	2185.7	1613.2	1278.2	1248.7	1402.7	2708.2	2888.2	662.7

Exposure WELL (2.4 to 4.5)

Depth/fraction	2.4	2.5	2.7	2.9	3.1	3.3	3.5	4.5
$CaCO_3$ (%)	2.42	3.63	0.76	1.10	2.95	0.48	2.63	1.68
Organic matter (%)	2.45	2.84	2.86	6.47	6.61	6.40	5.97	6.97
MS sample weight (g)	20	20	20	20	20	20	20	20
Total MS [10^-6*SI]	1677.4	1449.4	1395.4	7806.4	11661.4	11611.4	11531.4	10911.4
Mass specific MS [10^-9*m^3.kg^-1]	838.7	724.7	697.7	3903.2	5830.7	5805.7	5765.7	5455.7

Exposure WELL (4.7 to 5.9)

Depth/fraction	4.7	4.9	5.1	5.3	5.5	5.7	5.9
$CaCO_3$ (%)	1.28	0.14	3.25	0.00	0.00	0.00	0.00
Organic matter (%)	6.21	7.14	4.17	5.89	7.35	3.91	2.75
MS sample weight (g)	20	20	20	20	20	20	20
Total MS [10^-6*SI]	12811,4	11741,4	10551.4	11271.4	9351.4	11511.4	10991.4
Mass specific MS [10^-9*m^3.kg^-1]	6405.7	5870.7	5275.7	5635.7	4675.7	5755.7	5495.7

Exposure WELL (6.1 to 7.5)

Depth/fraction	6.1	6.3	6.5	6.7	6.9	7.1	7.3	7.5
$CaCO_3$ (%)	0.00	2.48	0.00	0.68	0.44	2.95	0.32	0.18
Organic matter (%)	3.25	5.16	6.05	7.49	4.37	5.73	4.98	4.72
MS sample weight (g)	20	20	20	20	20	20	20	20
Total MS [10^-6*SI]	11411.4	11611.1	11201.4	5971.4	9441.4	7111.4	6151.4	4286.4
Mass specific MS [10^-9*m^3.kg^-1]	5705.7	5805.7	5600.7	2985.7	4720.7	3555.7	3075.7	2143.2

Exposure DITCH (0.3 to 0.9)

Depth/fraction	0.3	0.4	0.5	0.6	0.7	0.8	0.9
$CaCO_3$ (%)	0.56	0.00	0.00	0.00	0.00	0.00	0.00
Organic matter (%)	1.16	1.43	0.65	0.98	0.77	0.76	0.73
MS sample weight (g)	20	20	20	20	20	20	20
Total MS [10^-6*SI]	931.4	609.4	452.4	546.4	600.4	715.4	454.4
Mass specific MS [10^-9*m^3.kg^-1]	465.7	304.7	226.2	273.2	300.2	357.7	227.2

Exposure DITCH (1.0 to 1.6)

Depth/fraction	1.0	1.1	1.2	1.3	1.4	1.6
$CaCO_3$ (%)	0.78	0.76	1.04	0.72	0.80	5.91
Organic matter (%)	0.58	0.72	1.03	1.11	1.00	3.74
MS sample weight (g)	20	20	20	20	20	20
Total MS [10^-6*SI]	522.4	673.4	772.4	783.4	881.4	961.4
Mass specific MS [10^-9*m^3.kg^-1]	261.2	336.7	386.2	391.95	440.7	480.7

Other samples

Depth/fraction	GT21 0.7m	AFD130 G1	AFD130 G2
<1 mm	62.62	33.58	49.66
1–2 mm	0.15	0.02	0.09
2–4mm	1.05	0.00	0.00
>4 mm	0.85	0.00	0.00
Total mass (g)	64.67	33.60	49.75
$CaCO_3$ (%)	18.04	n.w.	n.w.
Organic matter (%)	48.56	32.78	47.55
MS sample weight (g)	1420	3532	5987
Total MS [10^-6*SI]	292.42	1077.49	1259.10
Mass specific MS [10^-9*m^3.kg^-1]	854.44	2423.11	2283.05

APPENDIX 2.A2

PRELIMINARY RESULTS OF THE MAGNETIC SURVEY, AFFAD BASIN 2016–2017

Robert Ryndziewicz MA and Krzysztof Kiersnowski MA
Institute of Archaeology and Ethnology, Polish Academy of Sciences

Site: Affad Basin, Southern Dongola Reach, Sudan
Date: 3–12 December 2016, 3–10 December 2017
Method: Magnetic survey
Instrument: Geoscan Research FM256 fluxgate gradiometer
Resolution and survey details: 8 measurements per 1 m^2 (0.25 × 0.5 m), parallel and zigzag mode, 20 × 20 m grid, log zero drift
Area surveyed: 6.84 ha in four areas 160 × 100 m (area A) and 480 × 40 m (area B), 40 × 500 m (area C) and 360 × 40 m (area D)
Software: Geoplot 3.0, Surfer 8.0
Surveyors: Krzysztof Kiersnowski MA and Robert Ryndziewicz MA (Institute of Archaeology and Ethnology, Polish Academy of Sciences)
Scientific supervisor: Tomasz Herbich MA (Institute of Archaeology and Ethnology, Polish Academy of Sciences)
Project: "Levallois Tradition Epigones in the Middle Nile" PALAEOAFFAD PROJECT – SUDAN directed by Marta Osypińska PhD (Institute of Archaeology and Ethnology, Polish Academy of Sciences)

Results: Magnetic maps showing changes of the intensity of the Earth's magnetic field in four selected areas of the Affad Basin [see above, *Fig. 2.3*]. The survey in the 2017 season constituted the second stage of noninvasive investigations started in 2016.

Dual lines (set about 2 m apart), crossing two of the areas in random directions, correspond to modern car tracks, some of them visible on the site surface. High amplitude, dipole anomalies probably reflect modern metal trash. In theory, none of the anomalies influencing the magnetic field presented in the results are at a depth exceeding one meter.

Magnetic map of the southern part of the site (area A: 160×100 m) [*Fig. 2.27*].

Interpretation: Two regular, linear anomalies, parallel (set about 40 m apart), cross the area SE–NW with a homogenous structure in between. They reflect with a high degree of probability a phase of the river palaeochannel. Distinctive spot-shaped anomalies (about -3/+3 nT) in the southern part of the mapped area may reflect hearths or combustion features of some kind. Regular, rectangular anomalies, visible in the northeastern part of the map indicate the location of archaeological trenches.

Magnetic map of the northern part of the site (area B: 480×40 m) [*Fig. 2.28*].

Interpretation: Changes of the intensity of the magnetic field revealing different phases of the river palaeochannel. The first, low-amplitude discontinuity is visible on the one-hundredth meter of the investigated area. Another large, relatively high amplitude (up to -20/+20 nT), multi-phase diversion can be seen as black-and-white stripes, located between the 320th–420th meter of the area.

Magnetic map of area C located in the northwestern part of the site (40×500 m) [*Fig. 2.30*]**.**

Interpretation: Series of regular, parallel, linear anomalies crossing the area in a general SE–NW direction are observed over most of the surveyed area; they reflect different phases of the river palaeochannel. Three of them, visible as sharp lines, were traced roughly between the 20 m and the 80 m mark. More anomalies can be observed between the 210 m and the 320 m mark. A relatively dense series of high-amplitude anomalies recorded in this area resembles the discontinuity recorded in 2016 in area B, most probably reflecting the same phase of the palaeochannel. A large, oval-shaped anomaly, recorded between the 355 m and the 390 m mark, might reflect part of an anthropogenic structure of unknown function and date.

Magnetic map of area D located in the southwestern part of the site (360×40 m), in the vicinity of area A investigated in 2016 [*Fig. 2.29*]**.**

Interpretation: Parallel, very low amplitude anomalies on the 0–60th m and the 270th–320th m, crossing the area in a SE–NW direction, reflecting with high probability one of the phases of the river palaeochannel. Anomalies of different type and higher amplitude, visible between the 80th–200th m and the 300th–360th m of the investigated area, reflecting probably water erosion rills, not visible on the ground surface.

Conclusions: The survey recorded anomalies caused by the presence of palaeochannels of the Nile and other water activity in the past. In effect, it was possible to trace changes of soil structure. The application of the magnetic method to the study of this site has been demonstrated to be highly effective and has given positive results. The collected data shall be studied in comparison with data from geomorphological, topographical, satellite imagery studies, etc. to produce the final report.

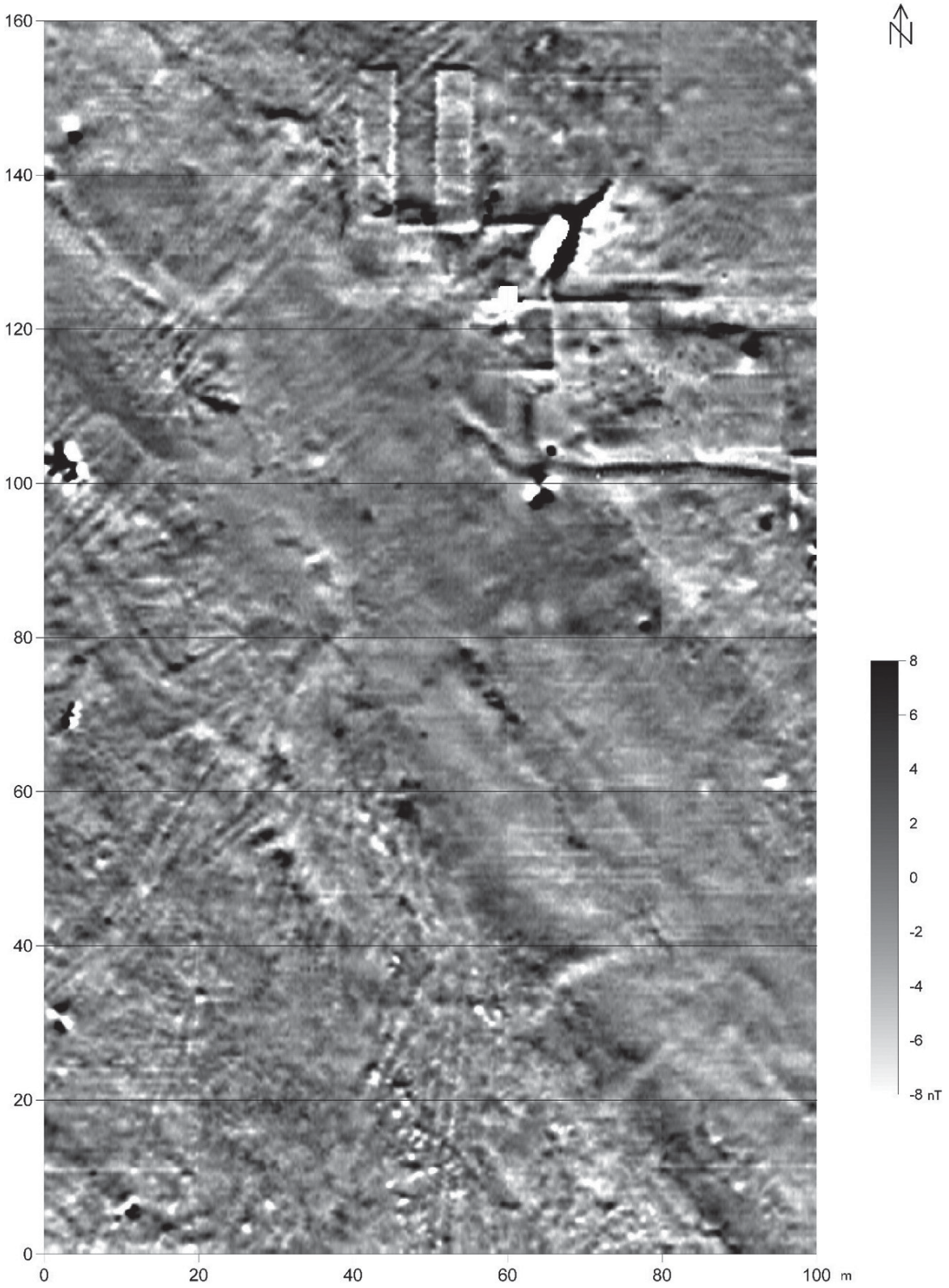

Fig. 2.27. Affad Basin, Southern Dongola Reach, Sudan, magnetic map of the southern part of the site (area A: 160 × 100 m). Fluxgate gradiometer Geoscan Research FM 256. Sampling grid 0.25 × 0.5 m, interpolated to 0.25 × 0.25 m. Dynamics -10/+10 nT

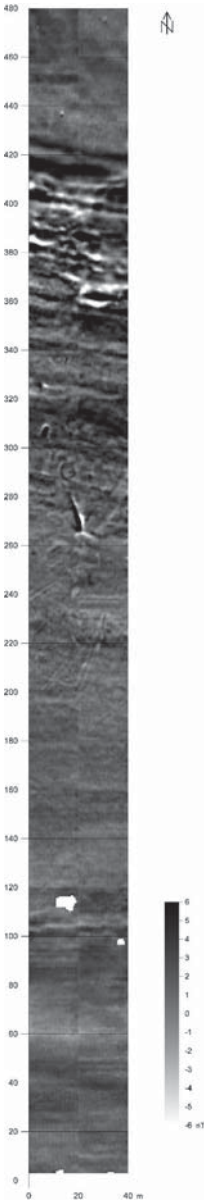

Fig. 2.28. Affad Basin, Southern Dongola Reach, Sudan, magnetic map of the northern part of the site (area B: 480 × 40 m). Fluxgate gradiometer Geoscan Research FM 256. Sampling grid 0.25 × 0.5 m, interpolated to 0.25 × 0.25 m. Dynamics -4/+8 nT. Note: images 2.28, 2.29, and 2.30 are not to scale

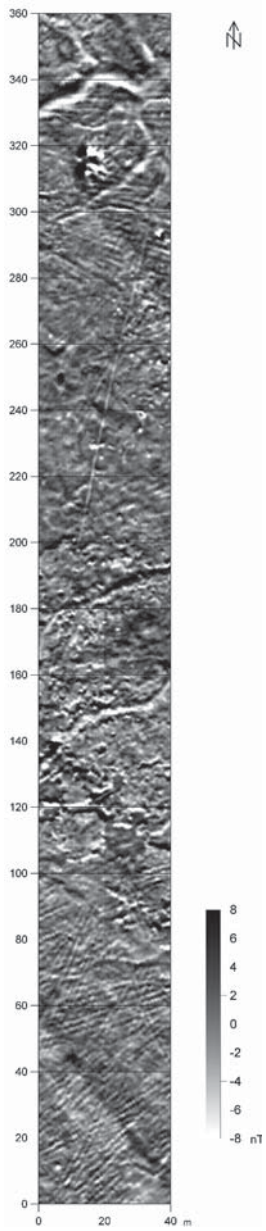

Fig. 2.29. Affad Basin, Southern Dongola Reach, Sudan, magnetic map of area D located in the southwestern part of the site (360 × 40 m), in the vicinity of area A investigated in 2016. Fluxgate gradiometer Geoscan Research FM 256. Sampling grid 0.25 × 0.5 m, interpolated to 0.25 × 0.25 m. Dynamics -8/+8 nT

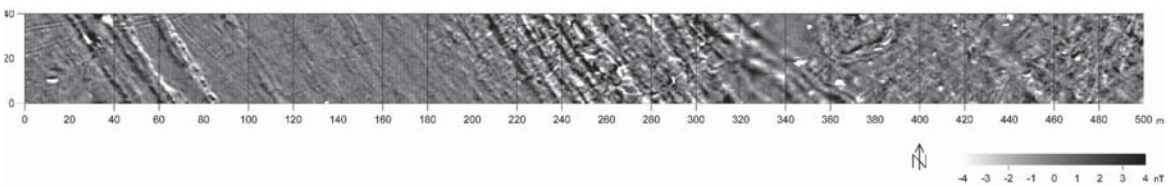

Fig. 2.30. Affad Basin, Southern Dongola Reach, Sudan, magnetic map of area C located in the northwestern part of the site (40 × 500 m). Fluxgate gradiometer Geoscan Research FM 256. Sampling grid 0.25 × 0.5 m, interpolated to 0.25 × 0.25 m. Dynamics -4/+4 nT

Appendix 2.A3

Report of the Laboratory of the Faculty of Earth Sciences and Spatial Management, Maria Curie-Sklodowska University in Lublin (OSL multi-grain, TL)

Karol Standzikowski
Faculty of Earth Sciences and Spatial Management, Maria Curie-Sklodowska University, Lublin

Samples of 600–800 g were dried in the laboratory, put into Marinelli beakers, and placed in a protective chamber of a three-channel gamma-ray spectrometer of the MAZAR-01 type (produced by Polon IZOT Warszawa). Concentrations of Ra, Th, K isotopes were measured. Each sample was analyzed from 40 to 100 times in the spectrometer, and each measurement lasted 2000 s. The concentrations of ^{226}Ra, ^{228}Th, ^{40}K were converted into dose rates—*alpha* (dα), *beta* (dβ) and *gamma* (dγ)—using the conversion factors of Adamiec and Aitken (1998). Average values were calculated for the 45–63 μm grain size. The cosmic radiation dose (D_c) to the sampling site was calculated according to the Prescott and Hutton (1994) method. Dose rate (D_r) is a sum of doses from *alpha*, *beta*, *gamma* and cosmic radiation. Moisture content of 5.8 and 10% was adopted for sample 6431, and measured moisture values 'as found' for all other samples.

Each multigrain sample was sieved to obtain the 45–63 μm grain size fraction [*Fig. 2.31*]. Grain fractions were treated with 10% HCl and 30% H_2O_2; after each phase of the treatment, grains were washed with distilled water several times. Samples were not etched with hydrofluoric acid (HF), nor were the feldspars separated from the quartz (a polymer sample was analyzed). For loess, sand-loess sediments, even riverine ones from Poland and Ukraine, such preparation gives 80% efficiency when it comes to the correlation of luminescence dates with stratigraphic interpretation (e.g., Fedorowicz et al. 2018; Łanczont et al. 2015).

The OSL measurement cycles and recording of decay curves were performed using the RISO TL/OSL DA–20 reader. For OSL measurements the reader was equipped with the U340 filter, and a sample was stimulated by blue LEDs (470 nm) delivering ~60 mW/cm^2 at the sample. During the measurement, the sample was irradiated using the beta ^{90}Sr/^{90}Y source. In the case of the OSL method, an equivalent dose (D_e) was determined using the SAR procedure (Murray and Wintle 2000) and a statistical model averaging the single-aliquot measurement results (CAM). The OSL SAR protocol used in measurements consisted of the following steps: 1) Give dose (d_i); 2) Pre-heat at 260°C for 10 sec; 3) Optically stimulate for 100 sec at 125°C; 4) Give test dose (d_t); 5) Heat to 220°C for 0 sec; 6) Optically stimulate for 100 sec at 125°C; 7) Return to step 1.

Sample preparation for the thermoluminescence method (TL) was the same as for the OSL method. SAR-TL measuring cycles (Hong et al. 2006) and curve recording were carried out with the RISO TL/OSL DA-20 reader. For SAR-TL measurements, the reader was equipped with a U340 filter. Measurements were carried out in a nitrogen atmosphere. The annual dose was set as the sum of the internal and external dose. The internal dose is the sum of doses of *alpha*, *beta* and *gamma* radiation inside the sample. The external dose is derived from the sediment surrounding the sample (burnt sediment) and is the sum of doses obtained from *beta* and *gamma* radiation.

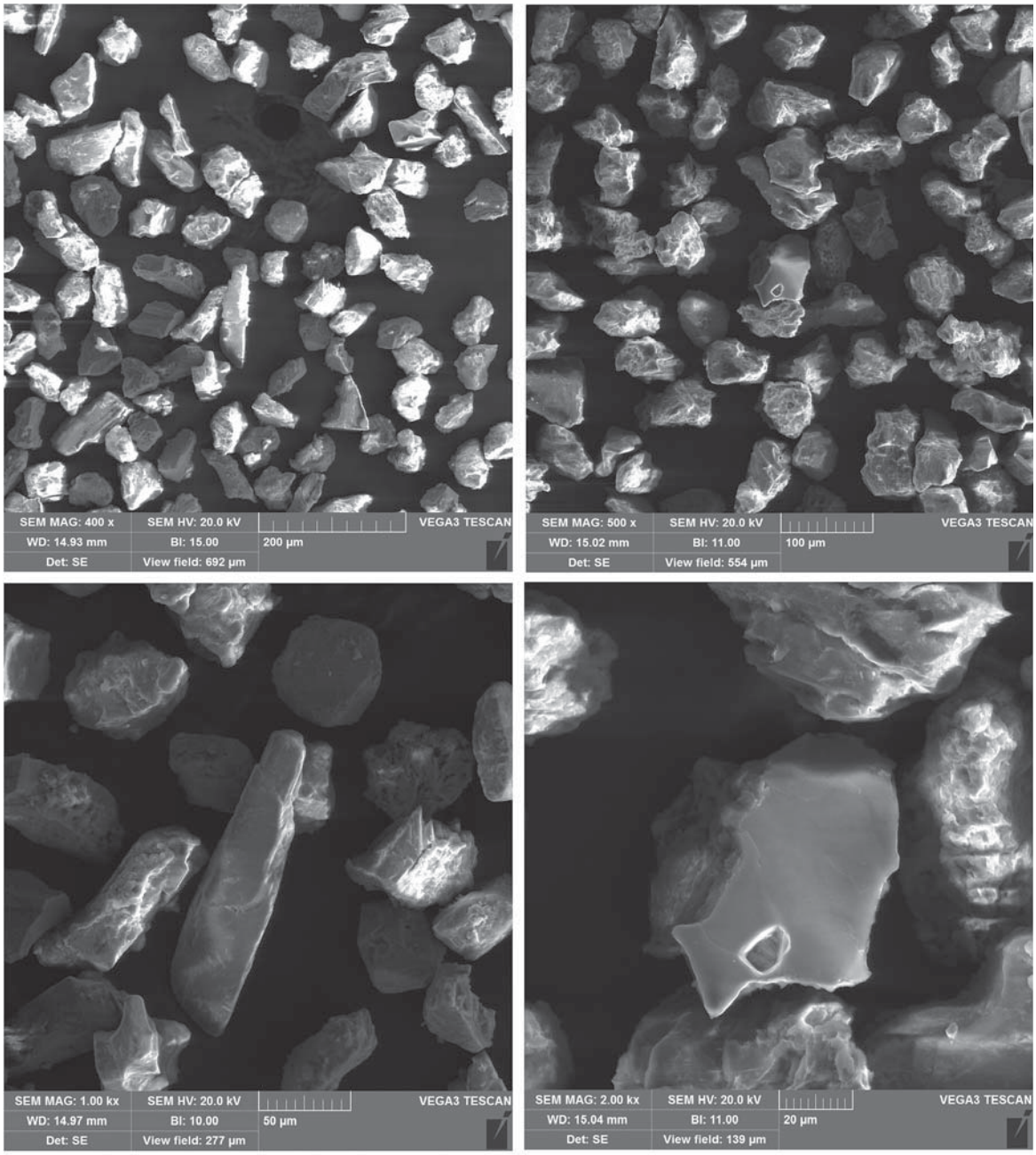

Fig. 2.31. SEM microphoto of a silt-sized multigrain surface after treatment with HCl under different magnifications

Table 2.1. OSL and TL age results for samples analyzed in the Lublin laboratory. For the OSL results: 45–63 μm grain size, aliquots *n*=5 (except sample Lub-6431, where *n*=14); overdispersion (Dis), sample moisture measured "as found" (M) with a control sample (Lub-6431) recalculated additionally by 10% (in bold)

Sample ID (depth)	Lab ID	^{40}K [Bq/kg]	^{226}Ra [Bq/kg]	^{228}Th [Bq/kg]	M [%]	Dc [Gy/ka]	DR [Gy/ka]	DE [Gy]	Dis [%]	OSL age (ka)
AFD23 2013/3 (0.70 m)	Lub-5656	249.77 ± 19.98	7.53 ± 0.70	16.15 ± 1.41	5.4	0.15	1.58 ± 0.23	91.37 ± 2.84	8.26	57.83 ± 9.69
AFD23 2013/4 (0.85 m)	Lub-5657	224.69 ± 23.77	5.9 ± 0.53	17.43 ± 1.48	5.7	0.15	1.48 ± 0.21	88.96 ± 2.57	7.57	60.11 ± 8.70
AFD23 2013/5 (0.25 m)	Lub-5658	288.06 ± 29.65	6.45 ± 0.59	22.59 ± 1.92	4.8	0.17	1.84 ± 0.27	78.26 ± 2.20	12.99	42.53 ± 6.36
AFD23 2013/6 (0.25 m)	Lub-5659	261.53 ± 21.18	10.08 ± 0.95	16.61 ± 1.48	5.1	0.17	1.71 ± 0.26	92.26 ± 2.72	5.76	53.95 ± 8.36
AFD23 2017/1 (0.50 m)	Lub-6431	318 ± 9	7.46 ± 0.78	24.97 ± 1.06	5.8/**10.0**	0.16/**0.19**	1.86 ± 0.15 /**1.84 ± 0.15**	105.68 ± 2.76	6.03	56.8 ± 4.8 /**57.9 ± 4.9**
AFD124 2017/2 (0.20 m)	Lub-6434	248 ± 6	11.08 ± 1.04	10.06 ± 0.82	7.0	0.17	1.43 ± 0.16	59.55 ± 1.49	2.88	41.7 ± 4.8
GT20/1 (0.16 m)	Lub-6544	303 ± 8	12.52 ± 1.23	25.81 ± 0.75	6.4	0.18	1.96 ± 0.15	49.66 ± 1.29	23.13	25.3 ± 2.1
GT20/2 (0.84 m)	Lub-6545	243 ± 7	12.05 ± 1.11	16.24 ± 0.71	7.5	0.15	1.54 ± 0.14	206.65 ± 5.68	5.29	134 ± 13
GT21/1 (0.34 m)	Lub-6546	299 ± 8	11.58 ± 1.02	25.64 ± 0.90	6.0	0.17	1.91 ± 0.17	98.38 ± 2.35	3.70	51.5 ± 4.8
GT21/2 (0.68 m)	Lub-6547	251 ± 7	12.40 ± 1.02	16.31 ± 0.97	4.7	0.16	1.58 ± 0.13	145.48 ± 3.75	7.56	92.1 ± 7.9
GT24/1 (1.58 m)	Lub-6548	220 ± 6	9.29 ± 0.92	15.20 ± 0.76	5.4	0.14	1.37 ± 0.12	104.75 ± 2.77	13.25	76.5 ± 7.0
PG3_1 (0.25 m)	Lub-6549	232 ± 6	8.39 ± 0.78	8.63 ± 0.65	7.2	0.17	1.28 ± 0.12	74.70 ± 1.92	3.45	58.4 ± 5.7
PG3_2 (0.55 m)	Lub-6550	218 ± 6	9.81 ± 0.88	8.81 ± 0.77	6.3	0.16	1.26 ± 0.13	83.13 ± 2.21	5.14	66.0 ± 7.0
PG2 (0.85 m)	Lub-6551	187 ± 6	9.63 ± 0.92	11.54 ± 0.77	6.5	0.15	1.21 ± 0.13	52.93 ± 1.44	3.36	43.8 ± 4.9
AFD131 (0.50 m)	Lub-6552	342 ± 9	17.97 ± 1.57	15.48 ± 0.88	5.2	0.16	1.99 ± 0.16	126.97 ± 3.49	5.94	63.8 ± 4.3
STUD1 (2.15 m)	Lub-6553	319 ± 9	13.98 ± 1.27	25.46 ± 1.24	5.1	0.13	1.98 ± 0.16	90.48 ± 2.79	4.98	45.7 ± 4.0
STUD2 (3 00 m)	Lub-6554	244 ± 8	17.11 ± 1.13	15.67 ± 1.00	5.8	0.11	1.46 ± 0.14	89.33 ± 2.28	8.94	61.2 ± 6.1
TL AFD23/1+2 (0.95 m)	Lub-6432 Smpl	189 ± 7	14.23 ± 1.49	16.38 ± 0.87	2.7	0.15	1.34 ± 0.16	3.27 ± 0.26	151.56 ± 9.85	4.75	46.4 ± 4.0
	Ext	313 ± 6	17.98 ± 1.75	23.26 ± 0.96	4.5	0.15	1.93 ± 0.18			
TL AFD134 (0.10 m)	Lub-6433 Smpl	235 ± 8	23.90 ± 2.27	26.49 ± 1.05	4.3	0.18	1.97 ± 0.20	110.50 ± 7.17	1.61	56.1 ± 6.8

APPENDIX 2.A4

REPORT OF THE SCHOOL OF GEOGRAPHY AND THE ENVIRONMENT, UNIVERSITY OF OXFORD (OSL MULTI-GRAIN, SINGLE-GRAIN)

Sallie Burrough, PhD
School of Geography and the Environment, University of Oxford

OSL sample preparation was carried out under subdued red light (600 nm) conditions at the Oxford Luminescence Dating Laboratory. The outer light contaminated material was removed and later sub-sampled for dosimetry. Quartz grains used to determine equivalent doses (D_e) were isolated from the remaining sediment bulk using 37% HCl and 30% H_2O_2 to remove carbonates and organics respectively. The 90–125 and 180–212 μm fraction was separated by wet-sieving. Density separation using sodium polytungstate was used to separate non-quartz minerals (<2.62 and >2.7 gcm^{-3}). The sample was then treated with 40% HF for 50 minutes to remove the α-irradiated outer surface and any remaining feldspars. This was followed by a 24-hour HCl wash to remove fluorides and then back-sieved using a 125/180 μm sieve mesh. Grains were then mounted on to either i) aluminium discs using a 2 mm diameter mask (90–125 μm) and silicon oil spray for multigrain analysis, or ii) into an array of a hundred 300-μm holes in the surface of an aluminium disc for single grain analysis (180–212 μm).

Equivalent dose (D_e) determination

Following multi-grain preheat plateau and range-finder tests (n=11) that revealed a significant degree of overdispersion (~50%) in the D_e distribution, the sample was dated using 1600 individual quartz grain D_e measurements from which there was a yield of 101 grains with a useable signal. The D_e for each grain was measured using single-aliquot regenerative-dose (SAR) protocol (Murray and Wintle 2000; 2003). The distribution of D_e measurements from single-grain analyses is advantageous primarily because it provides a D_e distribution that allows a much clearer assessment of depositional and/or post-depositional processes, critical for informing the choice of age model used to produce the final age.

OSL measurement conditions and rejection criteria

A TL-DA-15 reader with an EM19235QA photomultiplier fitted with two 3 mm thick U-340 filters was used. Laboratory radiation doses were given through exposure to a $^{90}Sr/^{90}Y$ beta source calibrated for each grain position within a single disc. Preheats (PH1 = 240°C, 10 seconds and PH2 = 220°C, 0 seconds) were chosen following preheat plateau tests that indicated relatively little systematic dependency on preheat. OSL measurements were made using a focused 532 nm laser for 1 second of stimulation with data recorded in 60 channels. Luminescence signals were integrated using the first three channels (0.06s) to maximise fast component dominance and minimise any possible unstable medium component contamination. Instrumental noise was measured using a background subtraction of the last 20 channels (0.4s) of the OSL decay. Sensitivity corrections were monitored using recycled laboratory dose responses and potential feldspar contamination was measured using IR-OSL depletion ratios (Duller 2003). In both cases aliquots

were rejected if these ratios lay outside 30% of unity (Murray and Wintle 2000) Flake with average recycling and IR depletion ratios being 1.09 and 1.02 respectively. Additionally, grains were also rejected if the test dose signal (Tn) was dim (less than 3 times instrumental background). Thermal transfer was monitored by measuring the OSL response of each quartz grain to a 'zero dose' irradiation, expressed as a percentage of the natural signal. Grains were rejected for potential transfer of charge during SAR if this measurement exceeded 5% of the natural signal. We assumed a 2.5% uncertainty for measurement reproducibility (Thomsen, Murray, and Bøtter-Jensen 2005). A dose recovery test (DRT) at the expected D_e value (determined using the initial range finder test) was undertaken for 200 grains (yielding 15 useable signals) and an average recovery ratio of 0.9 ± 0.3.

Table 2.2. Multigrain and single-grain OSL dating results of samples analysed in the Oxford laboratory. Age model calculations were carried out in R (Burow 2019)

Sample lab ID	**SUD1 = L018**					
Laboratory	**Oxford**					
Method[1]	**SG SAR**		**SG SAR**		**MG SAR**	**MG SAR**
Age model used[2]	**MAM4**	**FMMc1**	**FMMc2**	**FMMc3**	**CAM**	**MAM**
n (grains/aliquots)			74		11	11
AGE (ka)	**6.28**	**5.98**	**12.91**	**50.02**	**45.17**	**21.53**
error (ka)	0.70	0.66	2.05	5.58	7.97	3.57
[1] **SG = Single Grain; MG = Multigrain; SAR = Single Aliquot Regeneration** [2] **MAM = Minimum Age Model; FMM = Finite Mixture Model; CAM = Central Age Model**						
D_e (Gy)	8.98 ± 0.61	8.43 ± 0.58	18.46 ± 2.45	71.54 ± 4.92	66.34 ± 10.06	31.62 ± 4.40
Proportion of grains in FMM components		46%	18%	36%		
Overdispersion (%)				97.4 ± 8.94		50.1 ± 12.5
Grain size (μm)	180–212				90–125	
Measured concentrations (± 10% standard fractional error)						
Method	ICP-MS					
K %	0.873					
Th (ppm)	3.910					
U (ppm) / Ra (ppm)	50.1 ± 12.5					
Depth (m)	0.50 ± 0.1					
Cosmic dose rate (μ Gy/ka)	0.190 ± 0.040					
Moisture (water/wet sediment)	50.1 ± 12.5					
Total dose rate (Gy/ka)	1.43					
error (% error)	0.13 (8.78%)					

Dose rate (D')

The dose rate for OSL age calculation was determined using Inductively Coupled Plasma Mass Spectrometry (ICP-MS) to measure isotope concentrations (^{232}Th, ^{238}U and ^{40}K) Flake within the sample. Conversion to external beta and gamma components (to account for grain-size, HF etching and moisture content) used the dose-rate conversion and beta attenuation factors of Guerin et al. (Guérin, Mercier, and Adamiec 2011; Guérin et al. 2012) and Mejdahl (1979), assuming radioactive equilibrium in the ^{238}U and ^{232}Th series. Sample moisture contents during burial were estimated at 10 ± 5 % and cosmic-ray dose was calculated according to Prescott and Hutton (1994).

Results

Less than 1% of grains yielded an OSL signal but these were reasonably bright with a good signal to noise ratio even where the D_e was small [*Fig. 2.32*]. A total of 74 OSL signals from individual grains was accepted with D_e's that ranged from 4 ± 1 Gy to 128 ± 44 Gy. The D_e distribution exhibited a high level of overdispersion (97 ± 9 %) Flake with a strong positive skew [*Figs 2.33, 2.34*].

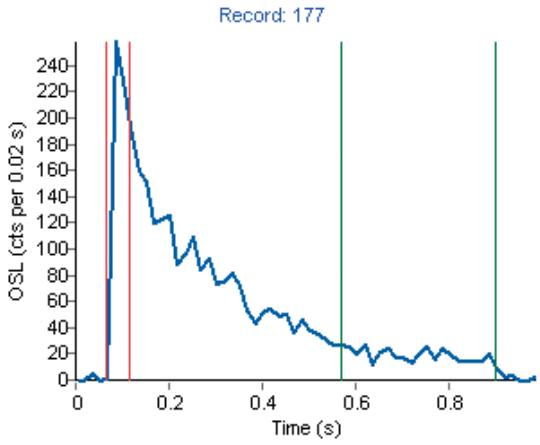

Fig. 2.32. Typical OSL characteristics of a single quartz grain natural signal

Age calculation

The broad distribution of D_e's seen fully in the single grain data is likely due to one of two factors: i) incomplete bleaching of the sediment during transport prior to deposition, with some grains yielding anomalously large D_e's due to the presence of a partly-bleached residual dose from a previous deposition cycle; or ii) post-deposition mixing of grains by biological processes introducing anomalously young material into an older deposit. Based on these two scenarios, the final age estimates were calculated using single grain data and the MAM4 (4 component minimum age model) (Arnold et al. 2009; Burow 2019) and Finite Mixture Model (FMM) respectively. The optimal FMM fit was determined using the maximum log likelihood (llik) and the Bayes Information Criterion (BIC) (Galbraith and Green 1990; Roberts et al. 2000; Dietze et al. 2016).

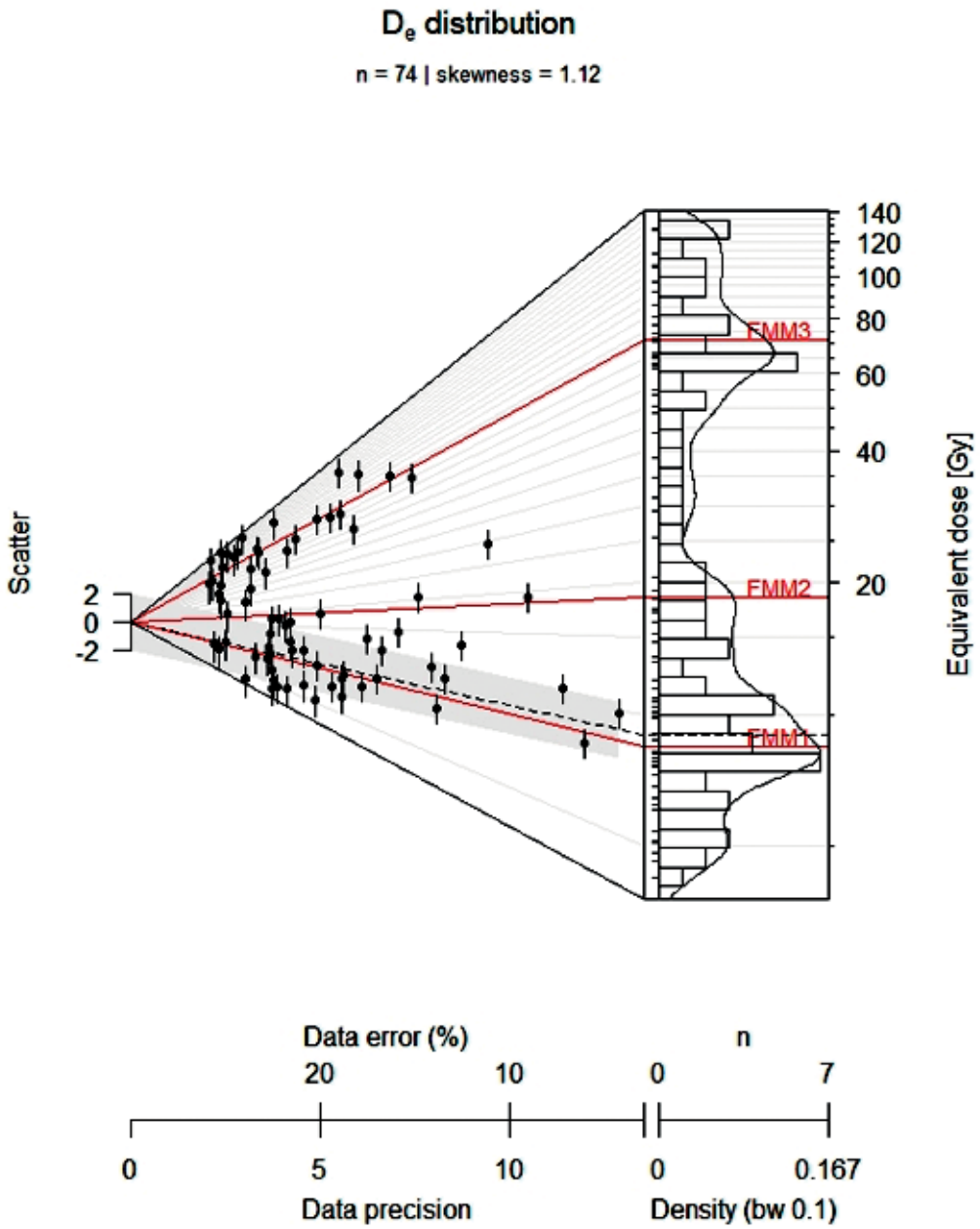

Fig. 2.33. Abanico plot showing single grain D_e distributions. Shaded bar shows 2 sigma range of the D_e estimate using the MAM4 age model. Red lines show the three possible D_e components identified by the Finite Mixture Model

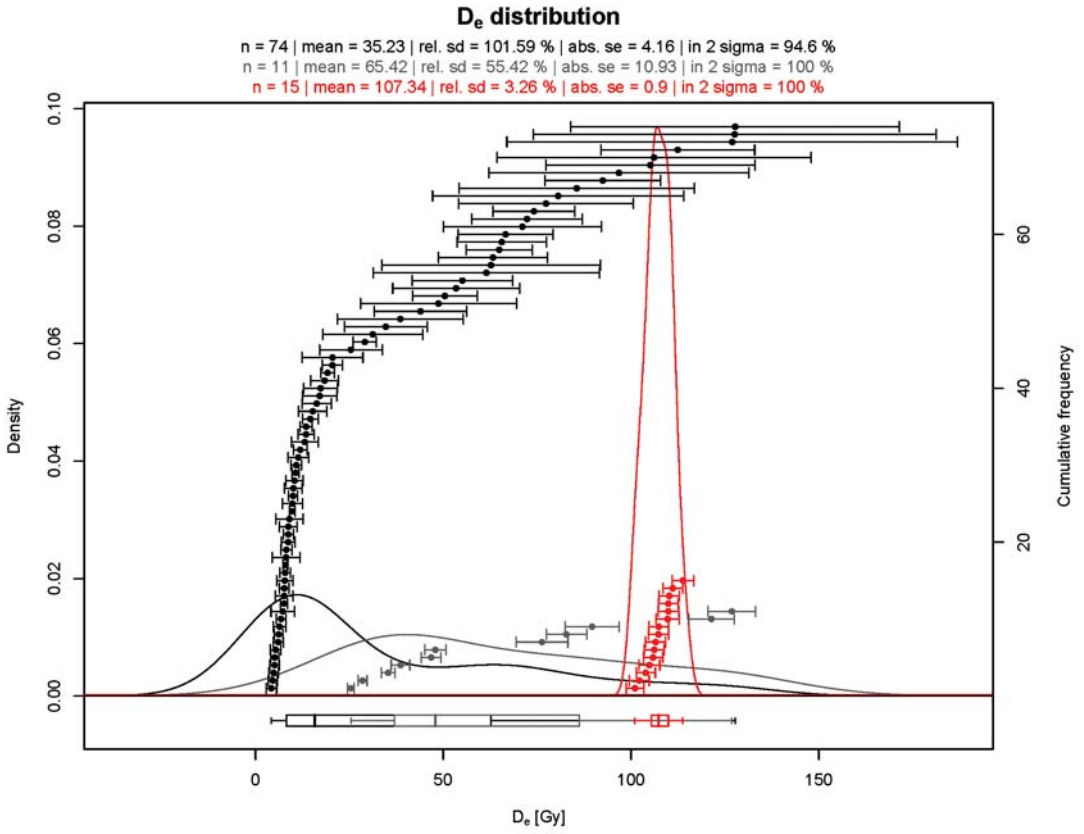

Fig. 2.34. Plot of measured D_e (SAR, multi-grain) in samples analysed in Oxford and Lublin (red). Black = single grain (180–210 μm); grey = multigrain (90–125 μm); red = multigrain (45–63 μm). Plot shows the increasing influence of large D_e's as the averaging effect increases with decreasing grain-size and increasing number of grains per aliquot

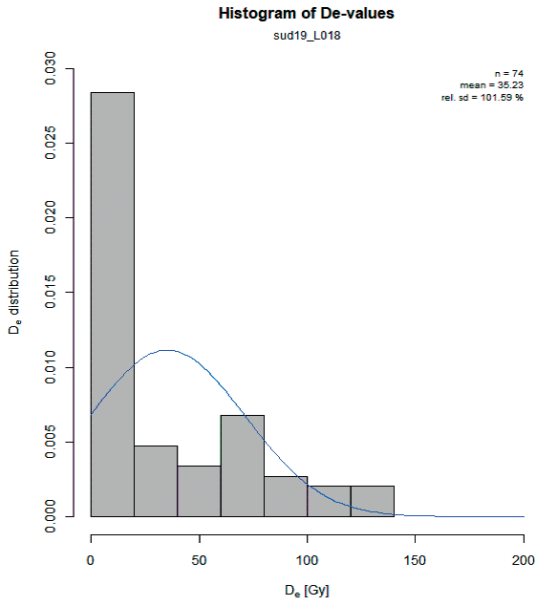

Fig. 2.35. Histogram of D_e values obtained by the Oxford laboratory (single-grain method)

APPENDIX 2.A5

REPORT OF THE DEPARTMENT OF CHEMISTRY, WILLIAMS COLLEGE (ELECTRO SPIN RESONANCE – ESR)

Anne Skinner, PhD
Department of Chemistry, Williams College, Williamstown, MA, USA

Like OSL, ESR measures radiation damage accumulated over millennia. To determine age, one must measure the rate of damage internal to the sample and that from the surrounding environment. The greatest uncertainty in ESR dating arises from uncertainty in the environmental dose (Skinner 2015). Teeth can be reworked within a site and also into a site from another location. When the environmental dose is considerably higher than the internal dose, this uncertainty is maximized. For the Affad 23 samples, the internal dose is comparable to the external; this is less true for the Affad 24 samples.

While both ESR and OSL ages derive from the same physical phenomenon, there are differences. OSL looks at quartz in sand. Recent efforts have suggested that ESR can also detect radiation damage in quartz, but teeth are the most widely used samples. The relevant material in teeth is hydroxyapatite. Also, external dose rates for OSL include a beta radiation contribution from the sediment. Beta radiation penetrates approximately 2 mm. The enamel in teeth for ESR dating is covered by >2 mm of dentine or cementum and so the external dose rate is simply gamma radiation from the sediment plus cosmic radiation.

Samples

'ET23': Affad sample 2012/B/98. Lechwe molar (bovid). Two subsamples prepared.
'ET24': Affad sample 2013/M/37. Fragment of hippo molar. Two subsamples prepared.
'ET36': Affad Sample AFD24/97, sample 2. *Bovidae* molar. Five subsamples prepared. One subsample differs significantly from the others, possibly because there are fewer points on the growth curve. The effect of this subsample on the average age of that tooth is statistically insignificant.
'ET37': Affad Sample AFD24/97, sample 1. Two small *Bovidae* teeth in jaw fragment. One subsample from each tooth. Bone analyzed as contributing to the external dose.

Results

As noted, ESR dating is based on the accumulation of radiation damage over time. As a result, one of the important factors is the amount of radioactivity in the tooth itself, almost always due to the presence of uranium. Uranium can accumulate in the tooth over time in different ways. The EU (Early Uptake) model assumes the present concentration of uranium was taken up at the time of burial or shortly thereafter. The LU (Linear Uptake) model assumes that uranium has been entering the tooth consistently during burial. The age of the tooth depends on the model. The precise model can in principle be determined by combining ESR analysis with U-series (equilibration of U and Th) ages. That is not possible here due to the small size of the samples. When the uranium concentration is low, the difference in ages can be small. For these teeth, the results do depend on the model. This is considered in the discussion section.

For ET23 and ET24, the external dose was calculated from radioisotope concentrations determined at Oxford, plus 150 mGy/ka of cosmic irradiation. The situation is more complicated for ET36 and ET37. Two sediment samples were analyzed by neutron activation at McMaster University, and again 150 mGy/ka of cosmic irradiation added. For ET37, this has been reduced to reflect the presence of bone, which has a lower dose. The bone contribution is estimated at 2% by volume. This does not actually change the ages. However, in ESR dating one has to consider that the modern sediment dose may not reflect depositional history. EU ages for ET36 and ET37 were recalculated assuming 10%, 20% and 30% change in D_{ext} both increasing and decreasing. At 30% change, the EU ages change by 15–20%. Thus increasing D_{ext} by 30% would bring these two samples within $\pm 2\sigma$ of the Affad 23 ages. But there is no reason to do this. The [U] content of dentines in the second set is internally consistent and significantly different from the first two. That alone suggests that they have a different history, remembering that the sites are approximately 1 km apart.

Discussion

The LU model is most often used in ESR dating, although there is no reason to presume that it is valid for this site. In fact, given that the site may have been dry for much of its history, U-uptake make have been minimal, and the EU model is more plausible. The conclusions differ little for most of the samples, so for convenience the discussion will focus on EU results.

ESR age uncertainties in *Table 2.3* represent 1σ. Broadly speaking, the OSL ages range from roughly 45 ka to almost 60 ka, with one at 92 ka. The average EU result for the first set of samples is 89 ± 8 ka, older but not completely inconsistent with the OSL, considering uncertainties. ET36 in the second set of samples again overlaps with the first set at 2σ. However, ET37 exceeds any comparison, barely overlapping with ET36 at the 2σ level. There is no immediate explanation for the greater [U] concentration in the Affad 23 dentines, but as noted this throws doubt on the same origin for ET23/24 and ET36.

The teeth are still clearly older than both the initial and remeasured OSL ages. It is quite possible that the discrepancy with the remeasured OSL ages is due to reworking of the teeth, either vertically or horizontally. Alternatively, again as noted, the OSL samples may not reflect the original time of deposition but be affected by windblown or other turbation effects.

Conclusions

The ESR ages for ET23 and ET24 are roughly consistent with the OSL ages if one assumes the Early Uptake (EU) model. The ages of the second set of samples, ET36 and ET37, are older than the first set. Although ET36 is close to ET24 in age, the difference in [U] content in the dentine suggests that it has a different history. It could be that Affad 23 and Affad 24 teeth were deposited at different times or that they were reworked from different parts of the site. A useful rule of thumb is that one should have three teeth from a site with congruent ages before saying definitively that the site age has been determined. Unfortunately, we are always limited by the samples that are available. At any rate, these results provide a preliminary estimate of the time during which this area was settled, an estimate that agrees with the ages of other MSA sites in Africa.

Table 2.3. ESR results for Affad teeth. [U] concentrations determined by NAA. D_{int} is the internal dose rate assuming LU model, showing that it is small compared to the external dose rate, D_{ext}. Ages are somewhat model-dependent

Sample	Cat. No.		AD (Gy)	$[U]_{en}$ ppm	$[U]_{den1}$ ppm	$[U]_{den2}$ ppm	D_{int} (EU) (mGy/ka)	D_{int} (LU) (mGy/ka)	D_{ext} (mGy/ka)	Age (ka) EU	Age (ka) LU
ET23en1	2015SUD01		129.9	0.70	13.24	14.01	982	480	680	78	112
		±	13.3	0.02	0.02	0.02	22	10	70	9	13
ET23en2	2015SUD01		137.6	0.70	13.24	13.22	846	410	680	90	126
		±	4.1	0.02	0.02	0.02	28	13	70	6	9
ET24en1	2015SUD02		109.3	0.96	13.11	6.17	580	276	680	87	114
		±	5.1	0.02	0.02	0.02	19	9	70	7	10
ET24en2	2015SUD02		156.4	2.35	13.11	6.17	820	445	680	98	139
		±	4.6	0.02	0.02	0.02	33	17	70	7	11
ET36en1	2018SUD01		160.9	0.50	4.58	7.95	483	215	889	117	145
		±	5.0	0.02	0.02	0.02	14	8	70	8	3
ET36en1A	2018SUD01		160.9	0.50	4.58	7.95	483	215	889	113	141
		±	5.0	0.02	0.02	0.02	14	8	70	7	10
ET36en2	2018SUD01		131.6	0.62	8.64	8.64	618	192	889	87	111
		±	5.0	0.02	0.02	0.02	16	7	70	6	8
ET36en4	2018SUD01		170.2	0.74	8.61	4.58	539	252	889	112	143
		±	4.7	0.02	0.02	0.02	14	6	70	7	10
ET36en5	2018SUD01		178.4	0.62	8.64	8.61	657	311	889	115	149
		±	10.1	0.02	0.02	0.02	18	9	70	9	12
ET36 Avg.										**109**	**137**
		±								**8**	**9**
ET36 Avg. c/o en2		±								**114** **8**	**144** **8**
ET37en1	2018SUD02		168.0	0.19	4.70	4.55	362	147	884	135	160
		±	4.0	0.02	0.02	0.02	9	3	70	8	11
ET37en2	2018SUD02		159.7	0.08	4.70	4.55	304	124	884	134	156
		±	4.0	0.02	0.02	0.02	7	3	70	9	11

APPENDIX 2.A6

REPORT ON MEASUREMENTS AND DATA PROCESSING FOR DEM CREATION

Paweł Wiktorowicz
Institute of Archaeology and Ethnology, Polish Academy of Sciences

Previous to the PaleoAffad Project, mapping and measurements carried out during excavations or field surveys in the Southern Dongola Reach (SDRS) in Sudan were based on methods generally recognized as standard and classic in the practice of archaeology (e.g., Hodder and Orton 1976; Barker 1993). The location of individual archaeological sites was established by recording geographic coordinates with standard GPS receivers (a wide range of Garmin tourist GPS receivers). The standard adopted by the SDRS survey (before 2000) were N and E coordinates in the hddd ° mm 'ss.s" format in the WGS-84 frame of reference, with absolute altitudes given in meters above sea level (Żurawski 2003). At the beginning of the 21st century (even after the Selective Availability mechanism was turned off in May 2000), these values were often corrected when the same location was measured again several months or years later (e.g., Osypińska and Osypiński 2016). The greatest discrepancies were recorded in absolute height measurements, the differences sometimes reaching even a dozen meters (sic!).

A further problem with positioning sites using GPS receivers was the plotting of this data onto maps available at that time. Today's commonly used digital maps were not available 20 years ago. In fact, the Google Earth platform only made its services available for free after Google bought it from Keyhole Inc. in 2004 (https://pl.wikipedia.org/wiki/Google_Earth). However, it must be admitted that in version 5.0 (from 2009), the database of shared satellite images (from NASA and Landsat 7 sources) permitted use of archival images available at that time, sometimes reaching as far back as the end of the 20th century.

Initially, therefore, armed only with maps of Sudan printed in the second half of the 20th century and aerial photographs obtained by Bogdan Żurawski from the Sudan Survey Department, topograpers created multi-scale maps with the locations of discovered archaeological sites almost from scratch. Initially, the Fugawi ver.3 (2000) application was used to calibrate aerial photos using the orthorectification method. As presented in the 2003 publication, these maps used scales of 1:30,000 and 1:75,000.

However, the GPS method was not used for the exploration of individual sites due to low signal quality and specifications of receivers at disposal at the time. Measurements within the research areas (excavations/trenches, zones) continued to be made using traditional techniques (tape measures, poles, as well as optical levels and theodolites), occasionally only applying first-generation electronic total stations (Żurawski 2003: 67).

The implementation of the "Epigones of Levallois traditions …" grant project in 2012 marked the beginning of a new phase using state-of-the-art devices and measurement techniques in archaeological exploration. Professional experience gained in Poland in the course of a long-term salvage research program made it possible to apply electronic total stations on a large scale (in this case, the GTS-229 laser device manufactured by Topcon). This made it possible to take measurements in three planes within the device's range of operation, i.e., within a maximum radius of approximately 2000 m (according to the device's specifications; in fact, this range turned out to be significantly smaller, that is, approximately 200 m).

The collected data was then processed using WinKalk and MikroMap software by Coder. It was possible not only to take precise measurements, but also to mark out local geodetic grids of the areas under investigation. The maps based up to then on two-dimensional aerial or satellite images (of a much lower resolution) were supplemented with a precise image of the surface relief. While undoubtedly the use of an electronic total station had many advantages, its basic limitation was the long-term involvement of a two-man team of surveyors, which, given the logistical difficulties of conducting research in Sudan, usually meant a choice between conducting strictly archaeological research and measurement work. Nevertheless, thanks to this technique, it proved possible to present the first high-resolution hypsometric maps of site AFD23 and its surroundings (Osypiński et al. 2016: Fig. 2). It also became much easier to map the precise location of individual finds (both stone and bone artifacts, as well as cut features), and to carry out spatial analyses within the spaces explored.

The limitation resulting from a separate team having to be delegated to do the measuring work triggered a search for alternative solutions. DEM (Digital Elevation Model) analyses were of interest in this respect, because they enabled a study of spatial relationships of individual locations from different epochs (Pleistocene campsites and killing sites, as well as Holocene settlements and burial grounds) in relation to ancient and modern landscape forms in the area. RTK (Real Time Kinematic) GPS technology met expectations in this regard. In 2016, having joined the "TPI EDU" Polish education support program and the "Topcon University Educational Partnership Program", the Project commenced using the EPP Topcon GNSS HiPer V kit and Topcon's Magnet Field software.

In 2016, the Affad research team was equipped with an effective new tool for acquiring and recording spatial data. The measurement kit consisted of two RTK GPS signal receivers operating in the Base-Rover system. Due to the lack of a network of terrestrial reference signal transmitters (which operate in Europe), the Project was limited to this set, using the results of the first GPS RTK measurements for arbitrarily selected elements of the space (benchmarks) as permanent reference points. Measurements started with the determination of the position of the first reference point, over which the base receiver was mounted, using the multiple averaged measurement method. From that point on, all acquired data was related to a large extent to the coordinates of this first spatial point. Measurement accuracy was 1–3 cm in E–N dimensions and 5 cm in absolute height according to the technical specification of the devices. Although the accuracy of mapping the relationships of individual measurements met the team's expectations in terms of relative datum points, the precision of absolute measurements was still burdened with an inaccuracy of several meters. This was shown by the example of measurements of two zones, namely, one near site AFD23 and another about 10 km to the east of site AFD69. In both cases, the difference in the absolute height of most of the surfaces in the DEM was about 3 m. Corrections could be made only by linking these two zones with an additional measurement grid and combining the two models. This demonstrates the scale of precision of these key first measurements.

Use of RTK GPS kit while conducting research at Affad (2017–2021)

The area where the measurement work was carried out was located near the town of Affad (Sudan), more precisely in a square area approximately 3 km to the side. Its boundaries were the

Nawa–Karima road in the south and the sandstone plateau—the edge of the former Nile terraces—in the north. The use of the RTK GPS kit enabled the mapping of this relatively large area in the course of three field seasons and provided the necessary mapping context for the complex of Pleistocene and early Holocene archaeological sites. The second area (1.3 km by 1.3 km) to be measured independently applying a similar procedure was the location of site AFG69 lying 10 km to the east. The RTK (base-rover) measurement method based on a radio connection made it possible to perform measurements with the use of a set within a radius of up to 3 km from the base device. This reduced to a minimum the necessity of troublesome adjustments of the measuring device.

The stage of field measurements began with a determination of the basic reference point, a permanent benchmark in the form of a stabilized stone. The internal GPS receiver of the base unit was used to establish the coordinates and the absolute height of the marked reference point on the stone surface (averaged several times). The measurement was made in the WGS84 system. This measurement later became the basis for a local measurement grid and a network of several auxiliary benchmarks. The Magnet Field software of the FC-236 controller, which together with the second Hiper V GPS antenna served as a mobile kit (rover device), made it possible to convert the global WGS84 coordinates to the form of a local Sudan datum called Adindan (EPSG20136) (Mohammed and Mohammed 2013). This is a rectangular plane coordinate system based on the Clark ellipsoid and using a meter grid. This solution greatly facilitates fieldwork, which is why the Adindan datum was used for all field measurements in subsequent works. It should also be noted that modern GIS software can automatically convert cartographic material available on the Internet, such as satellite photos or digitized topographic maps, which have reference data referring to virtually any local reference system. This makes it possible to implement the acquired field data almost immediately on various underlay maps available on the Internet (Google Earth, Esri, Bing, etc.).

After establishing a reference benchmark network, a detailed situational and altitude map of the designated area was created. The work began with setting the base over the selected benchmark, and then, after entering the appropriate coordinates and establishing a radio base-rover connection, a series of measurements of elevation points in relation to the local system of base benchmarks was taken based on the initial point from the GPS measurement. Rows of stakes were measured along north–south lines. Due to the relatively large area to be mapped, the distances between individual measurements, both in terms of the lines and the distance between the lines, were set at 50 m. In the Magnet Field software, it was possible to obtain on the controller screen virtual lines with a north–south orientation, at a distance of a 50-m module. This, and the visible distance from the last measured point made it possible to control the measurement of stakes in the field. In areas of more diverse topography, the measuring points were adequately concentrated. Systematic measurements taken over three seasons generated sufficient data to create an accurate contour map and, on its basis, a digital elevation model (DEM).

The Topcon GNSS set was also used for staking out excavation trenches, marking areas for geophysical prospection and a systematic planigraphy of archaeological artifacts. Trenches were staked out in places where there was a concentration of archaeological material. The cut-off points were saved in the device's memory. The range of geological exposures (GT) was determined by a similar method. After entering the data into the computer, it was possible to create collective

maps of research excavations, as well as to overlay them on contour maps or DEMs. The measurement capabilities of the RTK set were used also for the magnetic prospection. The boundaries of the investigated areas were delineated before starting the magnetometer measurements. Then, after obtaining survey results in raster format, simple georeferences were inputted in the geodetic software and placed on map visualizations in GIS software.

Another important application tested in the field was a detailed planigraphy of archaeological finds. Typically, numerous finds are present on the modern surface at sites in the Affad Basin as a result of sediment erosion. A precise planigraphy of artifacts divided by category (e.g., different chronology, raw materials, etc.) could be used for later detailed study analyses. While the planigraphy was being performed, the FC-232 controller software enabled the separation of individual categories of finds on an ongoing basis using assigned unique codes. Due to the large radio communication range of the base-rover kit, it was possible to perform the planigraphy over a relatively large area.

At the office stage, the collected data was processed using specialist computer programs. The result was a whole series of thematic maps and analyses created using GIS software. The basic geodetic software used at this stage was MikroMap software by Coder. Software used for GIS analyses included QGIS and SAGA GIS, as well as Internet imagery sources such as Google Maps, Esri, and Bing. Publicly available DEM data were also used, such as the NASA SRTM mission (https://pl.wikipedia.org/wiki/Shuttle_Radar_Topography_Mission) and data resources provided by the Japanese Space Agency JAXA (https://www.eorc.jaxa.jp/ALOS/en/aw3d30/data/index.htm).

After completing field measurements, a list of all of the measurement points was exported first as a .txt file downloaded from the device's memory. At this stage, the points were reclassified and categorized, breaking them down into individual measurement groups. The "contour lines" module in MikroMap software was used to generate a situational and altitude base map of the studied area based on the reclassified measurement data. All the excavations and geological exposures were additionally marked on this base map. It also served as the basis for the preparation of maps (large-scale: 1:1000, 1:500) of individual archaeological sites.

One of the most important tasks for which the use the measurement data was planned was to create an accurate digital terrain model on their basis and to capture the buried topography, including remains of palaeochannels of the Nile. A DEM created in this way would allow for better imaging of environmental conditions for the period of prehistoric settlement.

Work on generating a local DEM was commenced using the SAGA GIS program. After reading the point clouds from field measurements with the use of interpolating algorithms (tool: gridding/nearest neighbor), a model of the grid of points with one square meter cells was created. Next, the resulting point cloud was exported to an .sgrd file. This file format is editable in most GIS programs. On this basis, a DEM raster was created using the QGIS program of the area measured at Affad. Subsequently, various types of visualizations of the area of interest were generated, combining satellite images available on the Internet with the aid of various tools in the QGIS software (including: DEM shading, dynamic hypsometry with a quantile color scale). The DEM visualization undergoing the shading process turned out to be particularly useful, applied using the transparency scale to the raster generated also on the basis of the DEM, with an assigned hypsometric color scale. The DEM model, after a detailed analysis, revealed the outlines of a

paleochannel of the Nile along which Palaeolithic campsites were located. The level of detail of the obtained model also allowed one to use it for the development of individual sites in larger scales.

Since all the data obtained in the field were saved within one mapping datum (Adindan), it was possible to place on various map underlays both the archaeological excavation grid, as well as data obtained from the planigraphy of artifacts, for which advanced GIS software symbolization was employed.

It should be emphasized that both in field and office work, the use of the RTK and DEM techniques is a significant step forward compared to previous solutions. In field measurements, the quantity and quality of data obtained with a relatively low expenditure of effort is a major advantage. It is also very important that the entire set may be operated by one person. In turn, taking into account the availability of more and more online sources of cartographic materials and improved GIS software that can be combined with field data, it is sometimes the only method to create good map images for use in later spatial analyses in archaeology. This is especially important in African projects, where access to good-quality local mapping resources is often difficult and sometimes impossible. In addition to Affad, the GNSS RTK kit has also been used in other IAE PAN research projects in Egypt's Western Desert, namely at the Bargat el Shab site, or in Poland, where, however, free access to the TPI_NETpro reference network under an agreement to support educational institutions allows one to work with a single GPS antenna kit plus controller, with no need for a base-rover kit.

CHAPTER 3

LATE PLEISTOCENE FAUNA IN THE MIDDLE NILE VALLEY: ARCHAEOZOOLOGICAL ANALYSIS

The current state of knowledge regarding fauna living during the late Pleistocene in the central part of the Nile Valley is still fragmentary and limited to random and often accidental finds (Bate 1951; Gautier 1968; 1987; Peters 1989a; 1992; Chaix et al. 2000; Gautier et al. 2012). The complex of archaeological sites at Affad with its numerous and homogeneous animal bone remains and established chronology turned out to be an invaluable source of information on the ancient environment, as well as, and perhaps above all, on the hunting strategies of Middle Stone Age hunters.

Ten sites in the Affad complex yielded rich collections of animal remains: AFD23, AFD24, AFD110, AFD111, AFD113, AFD120, AFD122, AFD124, AFD131 and AFD134 [*Table 3.1*]. Of these, AFD23 and AFD124 offered the greatest scientific potential, albeit for different reasons: site AFD 23 because of the partly preserved horizontal and vertical relations, and AFD124 (and partly AFD131 as well) because the finds there proved to be important in terms of not only the archaeology of the region but also the general zoological, palaeontological and archaeozoological knowledge, despite being, to a significant degree, recorded on the surface or at a shallow depth. The multidisciplinary project launched in 2013 helped to assess in full the environmental data contextualizing everyday life and adopted hunting strategies of Palaeolithic human groups. In 2016, the first comprehensive list of faunal data from the excavations in the Affad Basin was published, building upon the preliminary results of an archaeozoological analysis of a small collection from the surface that had benefitted so much at the beginning from the experience of Achilles Gautier (Osypiński, Osypińska, and Gautier 2011).

It merits explaining at this point that mineralized animal remains are still the chief source for understanding the environmental context of the functioning of the human community in Affad approximately 50 kya. Despite efforts in this direction, no direct sources on the flora of the Affad Basin during the Pleistocene era have been forthcoming: the destruction of plant remains in the alluvial soils of the Nile is of such a degree that no macroremains have been recorded so far; nor has it been possible to conduct palynological studies or phytolith analysis. However, an indirect picture of the Middle Stone Age environmental context in the Middle Nile Valley comes from studying the biotope of the animal species recorded at Affad.

Table 3.1. The faunal collection from methodically explored MSA sites in the Affad Basin in numbers (not counting malacofauna and chance finds from the surface)

Sites	AFD23	AFD24	AFD110	AFD111	AFD113	AFD120	AFD122	AFD124	AFD131	TOTAL
Excavation	4280	417	1197	438	2170			1461	4066	14,029
Planigraphy						11	10			21
										14,050

3.1 STATE OF PRESERVATION OF OSTEOLOGICAL MATERIAL

The state of preservation of Late-Pleistocene remains from Affad is the result of deposition conditions—a marshy environment, saturated with iron and manganese compounds (Osypińska and Osypiński 2016). A series of chemical processes have left the animal bones from Affad discolored a dark grey or dark brown, mineralized to a significant degree and considerably harder that non-mineralized bones (for example, modern bones from the surface) [*Fig. 3.1*]. This made them more resistant to mechanical erosion, to which they were subjected while lying on the modern surface. These bones looked very different from the Holocene-age material from Affad. What the two sets of bones had in common was an advanced disintegration of organic components, namely, collagen, which made them fragile and susceptible to mechanical damage. Observations of faunal taphonomy in Pleistocene and Holocene assemblages suggest that, at least for the Southern Dongola Reach, the state of preservation of the bones may constitute a crucial chronological marker distinguishing the assemblages. Further research and taphonomic analysis will clarify to what extent this observation may be generalized.

Laboratory tests revealed the lack of collagen and organic substances in the late Pleistocene remains, facilitating their radiocarbon dating. However, minimal amounts of mineral (carbonate) substances (0.1% N; 2.8% C; 0.04 mg C) question the validity of the dating (T. Goslar, FUAM Radiocarbon Laboratory, personal communication). As for the chemical composition of Pleistocene teeth subjected to isotopic analyses (Osypińska et al. 2021: Fig. 4), bioapatite recrystallisation is not present in the enamel (compare with Dal Sasso et al. 2018).

The remains were colored dark shades of brown or grey, while the dentine kept its grey or beige color. Bones from subsurface contexts often had gypsum or calcium carbonate precipitated on them. It proved possible to remove them with acetic acid (revealing traces of bone taphonomy in individual cases). Regardless of the advanced state of mineralization, the condition of the bone material from Affad allowed taxonomic and anatomical identification, not to mention assemblage dating, of a surprisingly high percentage of finds (NISP=31%), compared to the standard rate of approximately 10% [*Table 3.2*]. Considering this, the animal remains from the Pleistocene sites at Affad are assessed among the exceptionally well preserved collections from this age.

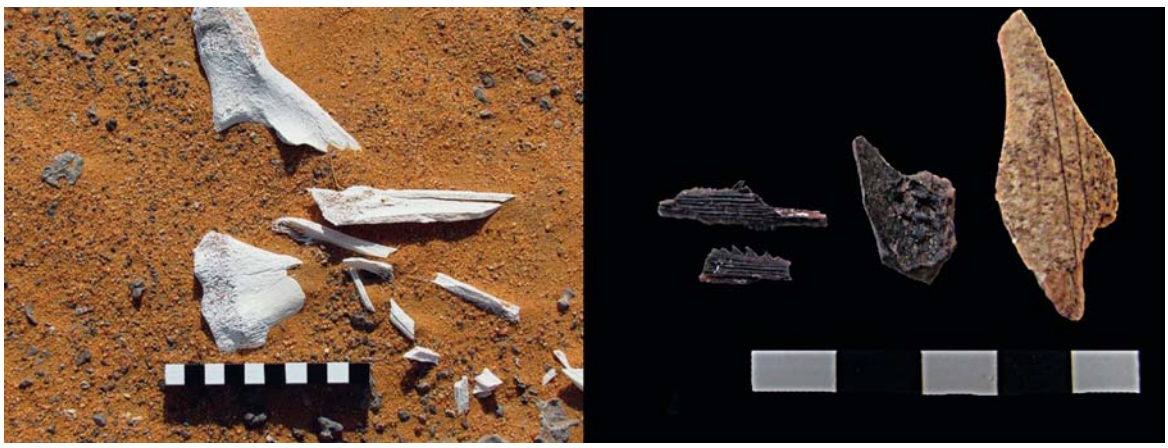

Fig. 3.1. State of preservation of animal bones found on the modern surface: left, modern remains; right, prehistoric material – bones of Pleistocene age are dark in color, those of Holocene age yellowish

Table 3.2. Frequency and proportion of identified and unidentified archaeozoological remains. Total number of faunal (vertebrate) remains recorded at MSA sites at Affad

Remains	*n*	%
Determined	4305	31
Undetermined	9745	69
Total	14,050	100

3.2 METHODS OF ANALYSIS

At Affad, animal bone remains were collected from the surface and from excavations at Late Pleistocene sites (dry-sieved on a 2 mm mesh). They were recorded in context with archaeological artifacts, namely stone tools and sometimes traces of hearths. Faunal material was recorded using horizontal positioning, which made it possible to determine location in a geomorphological context as well as in relation to other archaeological relics.

Data collection included a taxonomic and anatomical identification of faunal remains, as well as osteometric measurements of mineralized bones and teeth. Bone identification was based on comparative collections and literature (Walker 1985; Plug 2014). Osteometric studies were performed based on standardized procedures (von den Driesch 1976). Detailed identification was carried out in facilities both in Poland and Belgium (Institut royal des Sciences naturelles de Belgique, Palaeontological Research Unit, Ghent University), as well as on the basis of published data (Peters 1986; 1989a; Van Neer 1989). Remains not identified precisely to species owing to the state of preservation were classified into groups with varying degrees of taxonomic identification. There were nine groups in total, namely: megafauna (MF); large-sized ruminant (LSR); large-sized mammal (LSM); middle-sized ruminant (MSR); middle-sized mammal (MSM); small-sized ruminant (SSR); small-sized mammal (SSM); rodent (R); and mammal (M). Insofar as it was possible, the age and sex of the animals were determined. The archaeological context was also taken into account, individually for each investigated site.

In the case of the collection of animal bones from the best investigated site AFD23, the anatomical distribution of the most frequently occurring species (*Kobus* sp., *Ourebia ourebi*, *Madoqua saltiana*, *Hippopotamus amphibius*, as well as *Chlorocebus aethiops*) was studied. Three of these—kob antelope, hippopotamus and grivet monkey—were assessed in terms of frequency of skeletal elements from parts of the carcass attractive for consumption (after Lasota-Moskalewska 2008):

- H (head) – *cranium, dentes, maxilla, mandibula, processus cornuales*
- B (body) – *vertebrae, costae*
- PPAL (proximal part of the anterior limb) – *scapula, humerus, radius, ulna*
- DPAL (distal part of the anterior limb) – *ossa carpi, ossa metacarpalia* I-V
- PPPL (proximal part of the posterior limb) – *pelvis, femur, patella, tibia*
- DPPL (distal part of the posterior limb) – *calcaneus, talus, ossa tarsi, ossa metatarsalia* I-V
- D (digits) – *phalanx proximalis, phalanx media, phalanx distalis*

Given that kob antelope remains were the most numerous at site AFD23, they were analyzed separately by sector (northern, southern and southwestern).

The collections of osteological sources were also subjected to a taphonomic assessment in terms of damage resulting from environmental factors at the time of deposition and throughout the post-deposition period until the moment of discovery. Observations of damage concerned both the biostratinomic and diagenetic stages.

Fish remains were identified by Wim Van Neer and Veerle Linseele from the Institut royal des Sciences naturelles de Belgique in Brussels. As in the case of the other remains, the species and anatomy were identified, as well as the size of the fish from which a given bone had come. The size was expressed as a standard length (SL), i.e., from the snout to the base of the tail.

Hunting strategies and dietary variation constituted a separate aspect of the archaeozoological analysis at Affad, in keeping with the current trend in research on early societies in southern and eastern Africa. Preliminary assumptions, based on ethnographic observations among others, suggest a preference for the optimal hunting haul (characterized by the highest energy benefit obtained with the lowest expenditure of time and effort), supplemented with the less valuable or riskier elements only when the ecosystem is upset (due to natural as well as cultural factors, i.e., a drastic demographic increase; Kaplan and Hill 1992; Bird and O'Connell 2006; Lupo 2007; Clark and Kandel 2013). Larger herbivores provide more energy resources and, in primitive societies, they are preferred to small animals (Broughton and Grayson 1993; Kelly 1995; Lupo and Schmitt 2005; Lupo 2007). Theories concerning Middle Stone Age hunting in Africa have assumed, among others, that a growing interest over time in small animals and food-gathering reflects a trend towards dietary variation in groups with a demographic growth tendency (Marean et al. 2000; Lombard and Clark 2008; Lombard 2012; Clark and Kandel 2013). At the same time, factors influencing such changes should be taken into account, that is, "opportunities", skills or available hunting tools. A useful method in tracking such trends, applied so far mainly in the south of the African continent, is analyzing a group's exploitation and preference for hunted animals of a certain size category present in archaeological collections (Thompson 2010; Thompson and Henshilwood 2011; Clark and Kandel 2013). In the case of collections of animal remains from site AFD23, such categories were created especially for this site (see above). Given the marginal quantities of reptile and fish, as well as a complete lack of bird and invertebrate remains, this list included only mammals.

3.3 SURFACE COLLECTION FROM THE AFFAD BASIN

Field surveying in and around the Affad Basin in 2012–2015 resulted in the identification of 24 sites with distinctive mineralized bone material occurring in conjunction with stone products representing the Levallois production tradition. These were: AFD20, AFD23, AFD24, AFD84, AFD85, AFD99, AFD100, AFD102, AFD103, AFD105, AFD108, AFD110, AFD111, AFD112, AFD113, AFD114, AFD120, AFD122, AFD123, NFB8, NFB9, NFB10, RKB10, RKB11 (Osypińska and Osypiński 2015; several of these were later excavated; see below, sections 3.4.1–3.4.10). This surface collection of 1074 osteological remains [*Table 3.3*] was treated separately from the excavated material. It included skeletal elements of mammals of an unidentified species, sorted into eight general taxonomic groups (the ninth being fish).

The most numerous group of mammal remains came from the largest land animals in Africa: the elephant and the hippopotamus. It must be emphasized, however, that these figures only

reflect the state of preservation of the remains and the degree to which they could be recognized. For instance, elephant skeletal elements were recorded at only one site—AFD105—where they comprised the entire collection. Since the remains were accompanied by single stone products, the find was interpreted as a hunting site or a place where natural carrion was processed. In turn, the hippopotamus remains were represented almost exclusively by fragments of teeth and skulls occurring on the surface at several locations.

Several types of antelope were commonly identified among the remains. These included the small oribi, the slightly larger reedbuck and significantly larger kob antelope. The collection was supplemented with single fragments of giraffe bones, as well as skeletal remains of small animals, such as guenon, Nile monitor and crocodile.

Predominant among the skeletal remains of mammals of unidentified taxonomic origin were megafauna or large mammals, followed by middle-sized ruminants/mammals, most probably antelopes.

The collection also included 99 remains of fish from at least five different taxa [see *Table 3.3*]. Most of these were catfish belonging to the Clariidae family. They were found on all but one of

Table 3.3. List of determined and undetermined remains from surface research in the Affad Basin through 2015 (Osypiński et al. 2011: Table 1; Osypińska and Osypiński 2016b: Table 3)

Species	*n*	%
Grivet (*Chlorocebus aethiops*)	1	0.43
African elephant (*Loxodonta africana*)	39	17.10
Hippopotamus (*Hippopotamus amphibius*)	31	13.59
Oribi (*Ourebia ourebi*)	31	13.59
Bohor reedbuck (*Redunca redunca*)	2	0.87
Kob (*Kobus* sp.)	16	7.01
Giraffe (*Giraffa camelopardalis*)	3	1.31
Nile monitor (*Varanus niloticus*)	6	2.63
Clarias	92	40.35
Bagrus	2	0.87
Synodontis	3	1.31
Cuprinidae	1	1.31
Tilapiini	1	1.31
NISP	228	100 / 37.81
Megafauna (MF)	101	26.93
Large-sized ruminant (LSR)	2	0.53
Middle-sized ruminant (MSR)	7	3.07
Small-sized ruminant (SSR)	2	0.53
Large-sized mammal (LSM)	78	20.8
Middle-sized mammal (MSM)	38	10.13
Small-sized mammal (SSM)	30	8.00
Mammal (M)	116	30.93
Fish	1	0.26
Unidentified	375	100 / 62.18
TOTAL	603	100

the sites where fish remains were identified. The two genera known from the Sudanese Nile, namely *Clarias* and *Heterobranchus*, could not be distinguished for lack of diagnostic elements. Most of the Clariidae remains are from very large individuals, around one meter standard length and even larger (up to 110–120 cm SL); the smallest individuals measured 50–60 cm SL. Another catfish that was found at Affad is the *Bagrus*, but it was not possible to determine whether the remains pertain to *Bagrus docmak* or *Bagrus bajad*, which are the two species occurring in the Nile. The two finds are precaudal vertebrae from fish measuring 50–60 cm SL (AFD84) and 80–90 cm SL (AFD113). The third catfish found in Affad represents the genus *Synodontis* and again cannot be identified to species. A skull-roof fragment, found at AFD103, is from a fish measuring 25–30 cm SL, whereas the two fin spines collected at AFD120 fall within the range of body size measured as 25–35 cm SL. The carp family (Cyprinidae) is represented by a single vertebra of a fish measuring 40–50 cm SL; in the Sudanese Nile only *Barbus bynni* and the four *Labeo* species attain such size.

3.4 ANIMAL BONE REMAINS FROM EXCAVATED SITES

Of greatest scientific value were the collections of animal remains from archaeologically excavated sites—a total of 14,050 from nine sites plus malacofauna from one site [see *Table 3.2*]. A selection has been published, namely, the collections from sites AFD23, AFD110 and AFD111 (Osypińska and Osypiński 2016), but given their significance for the environmental and behavioral reconstructions presented in this study, they will be included in the present discussion with modifications resulting from a growing database of sources collected from site AFD23 after 2015. Selected aspects of the research on animal remains, concentrating on auroch remains, have also been presented already in other publications (Osypińska 2018; Osypińska et al. 2021).

3.4.1 Affad 23 (AFD23)

3.4.1.1 Taphonomy and state of preservation

The AFD23 collection of animal remains certainly supports taphonomical studies. Yet, apart from one example of incisions on the vertebra of a kob antelope [*Fig. 3.2*], no evident effect of biostratinomic factors on the state of preservation of the collection was noted. The mineralization of the remains significantly impacted their fragmentation, which made an assessment of the scale of so-called green fractures effectively impossible. A reliable assessment of traces of overheating on the bones was not possible for the same reasons. No traces of post-depositional predator activity were recorded (compare with Lyman 1994).

The quality of taphonomic data is due to the state of preservation of the remains, which was greatly influenced by the marshy environment. The mineralization of the bones indicated quick "burial" under layers of silt from a flooding river. This certainly influenced the observed absence of any visible damage caused by climatic (weathering, cracking) or biological factors (traces of predator activity, mold, fungi, etc.). Bone mineralization was accompanied by penetration of water saturated with mineral compounds. The state of preservation of different sections of anatomically identified

Fig. 3.2. Traces of incisions on the shaft of a thoracic vertebra of a kob antelope from trench 2013/M (AFD23)

remains was found to reflect a greater degree of mineralization of bones of a thin, dense nature, such as the short or thin bones, the density of which is usually lower (Meadow 1980; Brain 1981; Gifford-Gonzalez 1989; Lyman 1994). By comparison, bones characterized by a greater density, that is, thicker, denser in nature (e.g., shafts of long bones), as well as teeth, were mineralized to a lesser degree, thereby undergoing greater degradation. Therefore, long-bone shafts (particularly of larger species) are few compared to the high percentage of heads of such bones. Completely preserved long bones in trench 2012/B [*Fig. 3.3* inset] exemplify this situation. In fact, most of the undetermined fragments come from heavily eroded long-bone shafts. This observation, one of the most important conclusions from the research on the collections from Affad, has implications for animal bone collections with a confirmed high degree of mineralization of the remains.

The good preservation of bones in trench 2012/B enabled a reconstruction of how prehistoric people dealt with an antelope carcass. A cluster of vertebrae and ribs occurred separately from a concentration of skulls and teeth. The next cluster contained only pieces of limbs [see *Fig. 3.3*]. This dispersal indicates stages of the carcass division process. Following skinning and removal of the head, the meat was systematically filleted without detaching the bone or the limbs at the joints. The filleted meat would have been processed further to make the most of it; it could have been dried, for instance. Circumstantial evidence of such a form of treatment of ruminant meat is provided by a series of postholes, which could be interpreted as the remnants of a light wooden structure (see Chapter 5). Similar arrangements of postholes were observed in the southern [*Fig. 3.4*] and southwestern [*Fig. 3.5*] sectors of the site, but it was only in the case of the campsite (southwestern sector) that a cluster of remains was found with similar sections of the limbs and body (which could explain the surplus of these parts of the carcass in a general sense; see below, *Table 3.6*).

Curiously, there is little evidence of tool marks on the bones. The only case, as said earlier, is a series of incisions on the shaft of a thoracic vertebra of an antelope [see *Fig. 3.2*]. Moreover, there is no record of bones being transformed into tools or decoration (awls, tool hafts, pendants etc.). Filleting of meat as a highly probable way of processing carcasses must have corresponded to the arsenal of available tools: a large number of sharp stone flakes with edges no longer than

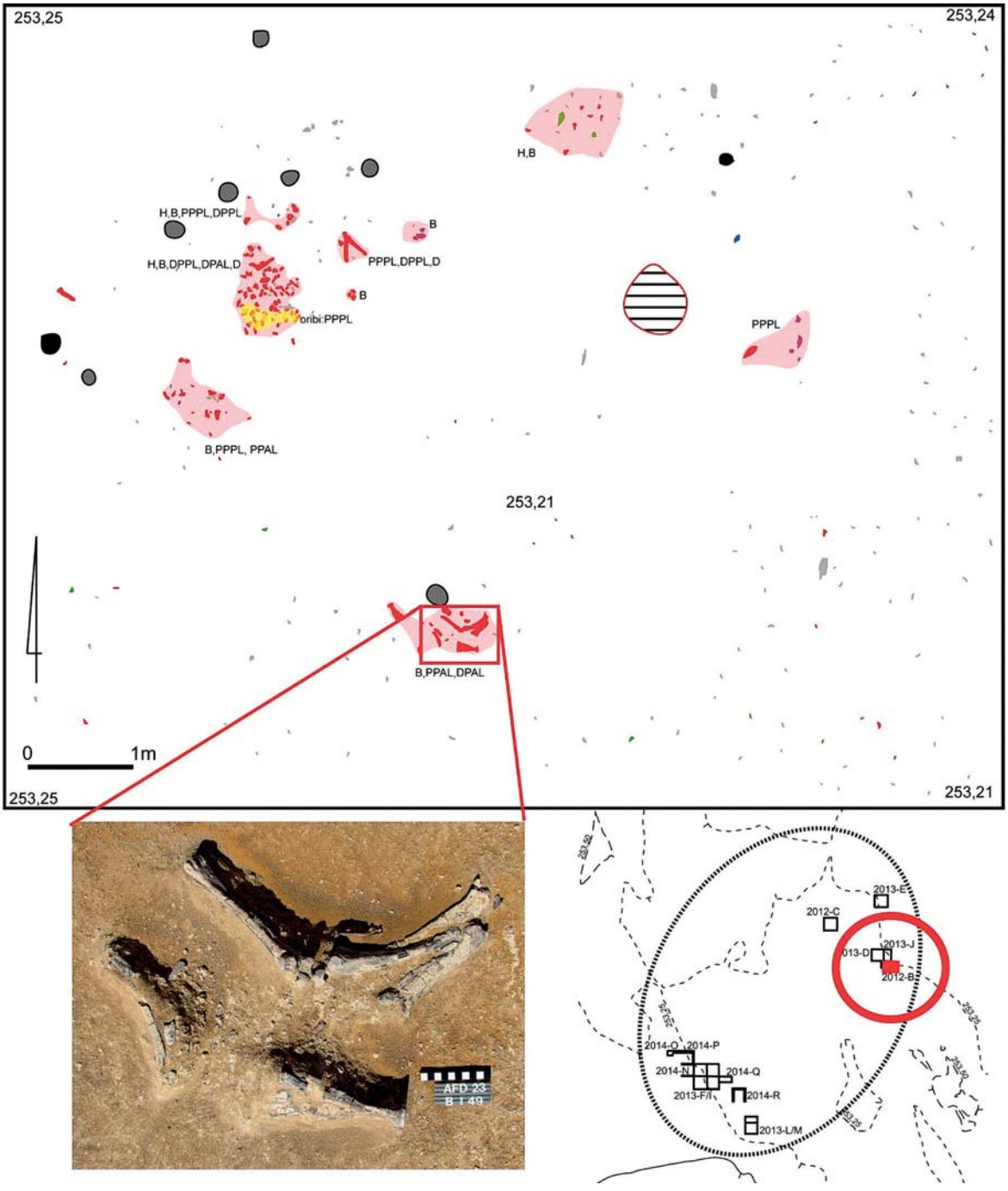

Fig. 3.3. Distribution of animal remains in trench 2012/B (AFD23). Colors signify remains identified to species: red – *Kobus* sp.; yellow – *Ourebia ourebi*; green – *Madoqua saltiana*. For the anatomical labelling of particular bone clusters see § 3.2. Gray/black features indicate the presence of postholes while the circular figure hatched in black in the upper right part of the plan marks a patch of burnt alluvium

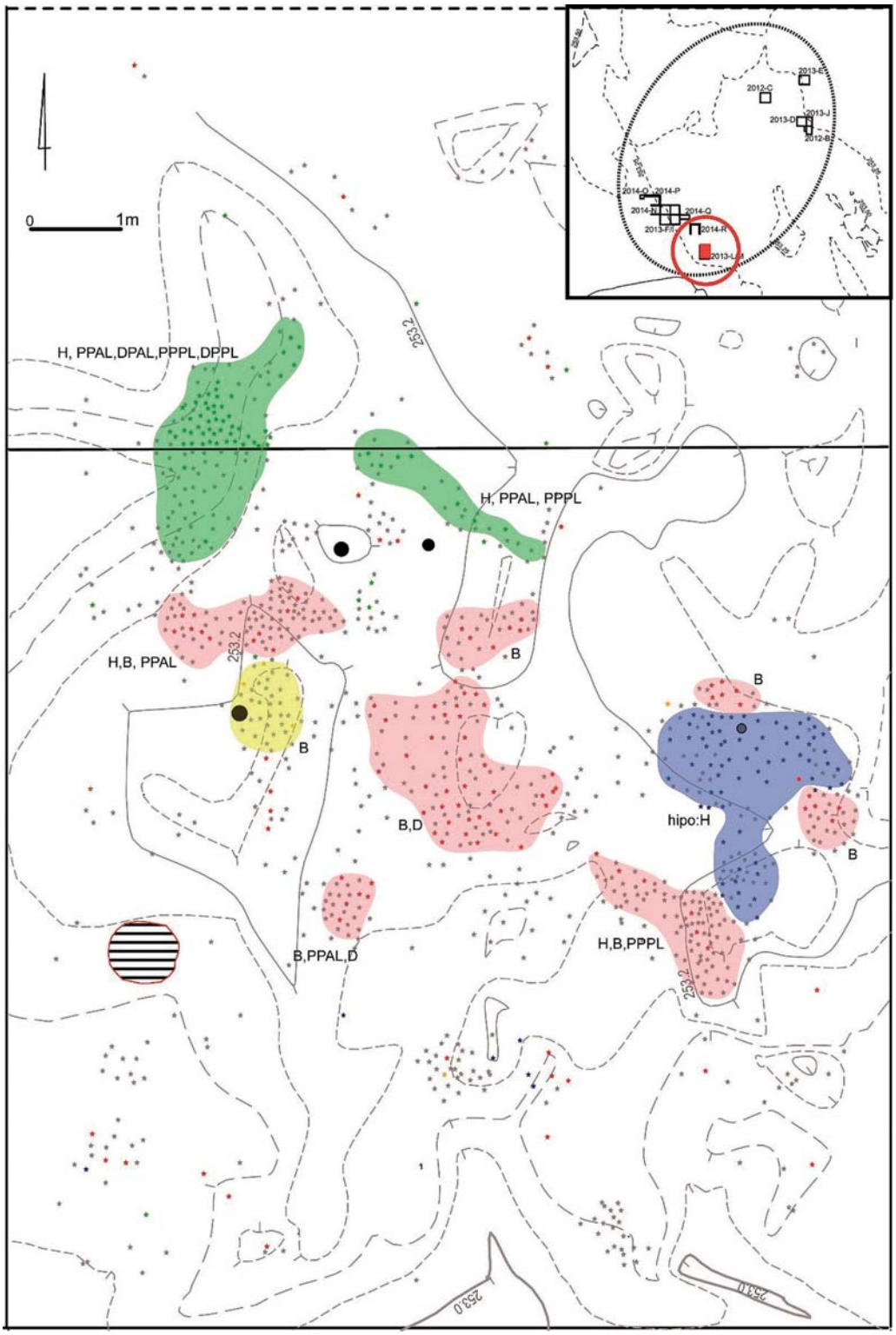

Fig. 3.4. Distribution of animal remains in trenches 2013/L–M (AFD23). Colors signify remains identified to species: red – *Kobus* sp.; yellow – *Ourebia ourebi*; green – *Chlorocebus aethiops*; dark blue – *Hippopotamus amphibius*. For the anatomical labelling of particular bone clusters see § 3.2 in the text. Gray/black features indicate the presence of postholes while the circular figure hatched in black at left marks a patch of burnt alluvium

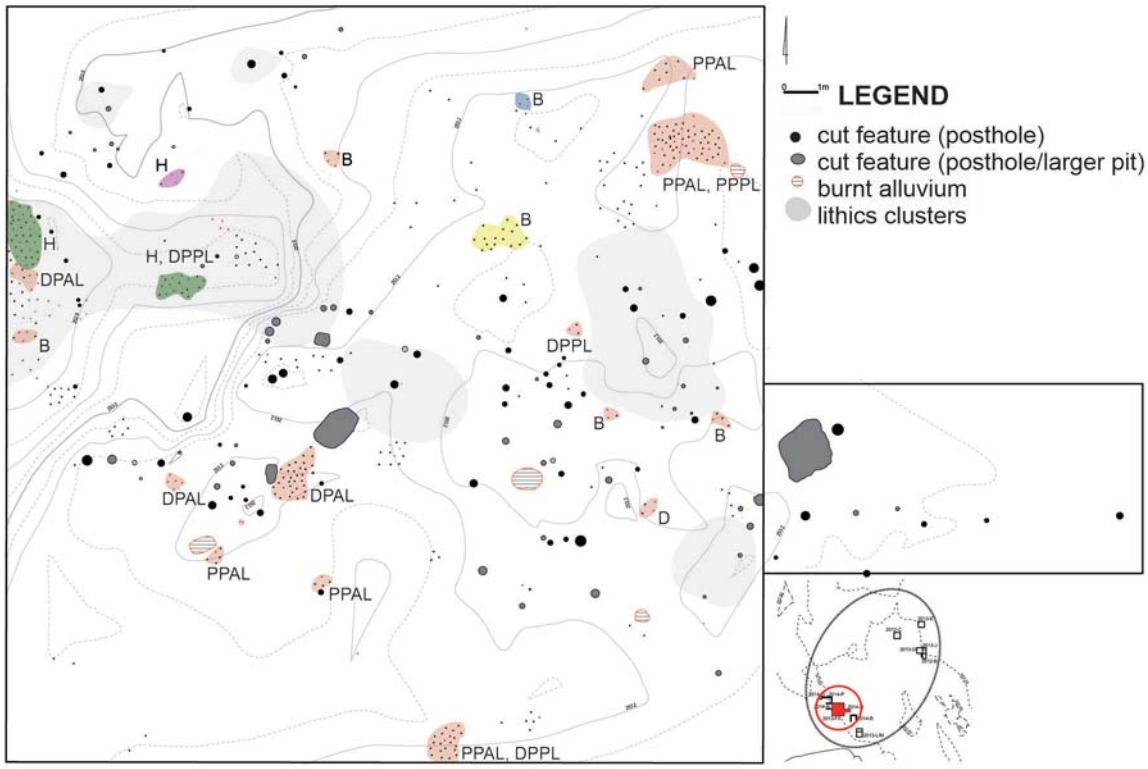

Fig. 3.5. Distribution of animal remains in trenches 2013/F–I, Q (AFD23). Colors signify remains identified to species: red – *Kobus* sp.; yellow – *Gazella dorcas* (*Ourebia ourebi*?); green – *Chlorocebus aethiops*; purple – *Thryonomys swinderianus*; dark blue – *Varanus niloticus*. For the anatomical labelling of particular bone clusters see § 3.2. Gray/black and hatched features indicate the presence of postholes and patches of burnt alluvium

10 cm (usually around 5 cm). Detachment of bones and joints during filleting would have left in most cases some evidence of incisions and crushing of the shafts; none have been recorded in the assemblage, hence the suggestion that they were not detached as a rule (Cain 2006).

3.4.1.2 Species

Excavation at AFD23, the main Pleistocene site in the Affad Basin, yielded altogether 4280 animal bone remains: 252 fragments in the first investigations in 2003, 3870 during the work in 2012–2014, and another 158 in 2016–2018. Of the total number, 23.8% were identified to the type or species level.

Remains of ten species in total were found, mainly representing mammals but also reptiles and fish. Skeletal elements of mammals predominated, among them definitely animals of the Arctiodactyla or even-toed-ungulate order. As many as six species were represented, namely, kob antelope, hippopotamus, oribi, dik-dik, bohor reedbuck and African buffalo [*Table 3.4*]. The species with the greatest frequency of remains was the kob antelope (649 fragments), the second in terms of numbers was the hippopotamus (186 fragments). The third most numerous species from AFD23 was the grivet monkey, a representative of the order of primates (127 fragments). Species represented by significantly lower numbers of remains included: oribi (15 fragments),

Table 3.4. List of determined and undetermined remains from excavations at AFD23 (after Osypiński et al. 2011; Osypińska and Osypiński 2016b: Table 5 updated)

Species	*n*	%
PRIMATES		
Grivet (*Chlorocebus aethiops*)	127	12.4
RODENTIA		
Cane rat (*Thryonomys swinderianus*)	14	1.4
ARTIODACTYLA		
Hippopotamus (*Hippopotamus amphibius*)	186	18.2
Salt's dik-dik (*Madoqua saltiana*)	12	1.2
Oribi (*Ourebia ourebi*)	15	1.5
Bohor reedbuck (*Redunca redunca*)	6	0.5
Kob (*Kobus* sp.)	649	63.7
African buffalo (*Syncerus caffer*)	3	0.3
REPTILIA		
Nile monitor (*Varanus niloticus*)	6	0.6
FISH		
Clariidae	1	0.1
NISP	1019	100/23.7
Megafauna (MF)	73	2.2
Large-sized ruminant (LSR)	24	0.7
Middle-sized ruminant (MSR)	227	7.0
Large-sized mammal (LSM_	115	3.5
Middle-sized mammal (MSM)	339	10.3
Small-sized mammal (SSM)	167	5.1
Unidentified mammals	945	28.8
Subtotal	2336	71.2
Unidentified bones	3281	76.3
TOTAL	4300	100

Table 3.5. Percentage of remains from site AFD23 by mammal-size class (after Osypińska and Osypiński 2016b: Table 8 updated)

Size class		%
I	Small	7.6
II	Small–medium	0.3
III	Large–medium	28.4
IV	Large	3.3
V	Megafauna	6.1

cane rat (14 fragments) and dik-dik (12 fragments). Small assemblages of the remains of a large ruminant were also recorded, probably a buffalo or auroch, as well as a bohor reedbuck. The least numerous remains represented non-mammal species: six fragments of the skeleton of a Nile monitor and single fish bones [see *Table 3.4*]. Neither bones or eggs of birds nor remains of mollusks were recorded.

The main conclusion concerning species distribution over the extensive area of site AFD23 is the evident predominance of remains of kob antelope (*Kobus* sp.), reflected also in the quantity of bones belonging to middle-sized ruminants (class III) [*Table 3.5*].

3.4.1.3 Spatial distribution and anatomical composition

The northeastern sector (trench 2012/B and extensions 2013/D, 2013/J, 2013/K) yielded 892 bone fragments, of which 34% could be identified to species. The list includes just three species of antelope, the kob antelope making up 95% of the remains, and the Nile monitor. Trench 2012/B is also the only excavation so far where animal bones were recorded in undisturbed anatomical position, reflecting deposition of large limb fragments, as well as separate clusters of vertebrae and skull remains. These occurred in the context of a series of postholes, a small hearth and an assemblage of stone artifacts [see *Fig. 3.3*].

Trenches 2013/F–I, located in the southwestern sector of the site (area of the campsite and a relief depression filled with layers contemporary with the campsite), merit attention because of the diversity of species identified in a fairly small assemblage of remains. Of the seven species recorded, the most numerous was the grivet monkey, followed by middle-sized antelopes (kob, reedbuck), and single clusters of small animals (cane rat, Nile monitor) [see *Fig. 3.5*]. The remains of a large mammal (buffalo/auroch?) occurred only in a ground survey to the north and west of trenches 2013/F–I.

Animal remains were most numerous in the southern sector of the site (trenches 2013/L–M). Of the 1064 bones from this area, 26% were identified to species level. In these assemblages there was a predominance of kob antelope (38%) and hippopotamus remains (32%). Moreover, the skeletal elements of grivet monkeys were also fairly numerous (26%), while the remaining species (oribi, buffalo/auroch) were represented by individual bone fragments. Here, the bones were evidently clustered between some postholes and a hearth [*Fig. 3.4*].

On the northwestern fringes of the site (trenches 2016/O, S–W), scattered animal remains were observed. Many of them were preserved in large fragments, with very well visible morphological features allowing taxonomical and anatomical identification. Kob antelope remains predominated: 31 fragments of skeletons along with 68 fragments most probably from this species (middle-sized ruminant). Single fragments of a grivet monkey pelvis were recorded, as well as 13 skeletal fragments of an animal of the Bovinae sub-family (large ruminant). One should keep in mind that the only place where remains of a large ruminant (buffalo or auroch) had been recorded was the survey between the trenches of the southwestern (2013/F–I) and northwestern (2016/O, S–W) sectors. The remaining 45 mammal remains could not be determined to species.

Considering the anatomical composition of remains from the explored contexts of site AFD 23, the most numerously represented species, the kob antelope, reveals mostly body fragments (category B, 30%; *Table 3.6*]. Category H bone fragments (skull and teeth) was also present in number (18%), perfectly corresponding to modern data for a model ruminant skeleton. However,

Table 3.6. Anatomical composition of the remains of the most numerously represented (in a general sense) species at AFD23. Values of modelled ruminant skeleton (mrs) after Lasota-Moskalewska 2008

Anatomical category	Kob			Hippopotamus		Grivet	
	n	%	% mrs	*n*	%	*n*	%
H	110	18.4	**20**	78	88.63	51	50.49
B	179	30.0	**43**	9	10.22	8	7.92
PPAL	107	18.0	**5**	–		20	19.80
DPAL	58	9.7	**8**	–		–	
PPPL	64	10.7	**3**	–		14	13.86
DPPL	43	7.2	**7**	–		8	7.92
D	36	6.0	**14**	–		–	

the percentage of remains from the proximal part of the pectoral girdle was relatively high (almost four times higher than in the model skeleton). In turn, the percentage of digit elements (category D) was significantly smaller, only 6%. The northeastern sector of the site (trench 2012/B) revealed evidence of the deposition of complete limbs (proximal and distal parts together). The other clusters of remains reflected separate deposition of sections of the carcass with a higher (proximal part of the pectoral girdle, ribs, vertebrae) and lower (head section, lower parts of the limbs and digital elements) degree of attractiveness for consumption. The northwestern parts of the site (trenches 2016/O, S–W) were dominated by limb bone fragments, particularly the long bones. Single fragments of ribs or head were noted occasionally. However, no dense clusters were recorded, while the remains were dispersed. A similar phenomenon was observed in the southwestern sector of the site (trenches 2013/F–I). The number of kob antelope fragments of little attractiveness for consumption, such as head or digits, was marginal in the encampment area. Such elements were recorded in the southern sector of the site (trenches 2013/L–M), creating the impression of separate clusters rather than scattered remains.

Regarding hippopotamus remains, almost all of the identified fragments represented a mandible, found in a cluster in the southern sector of the site (trench 2013/M) [see *Table 3.6*]. Just a few pieces of a category B (body) element were recorded on the surface in other sectors of the site. More than half of the identified grivet monkey bones represent the head section (category H; see *Table 3.6*]. Limbs or digits were either not represented or comprised significantly lower proportions than the proximal part of the limbs, suggesting the post-consumption nature of the collection. In the case of the cane rat, mainly head fragments were found in a small isolated cluster in the southwestern sector of the site (trench 2013/I).

An assessment of the age of animals from site AFD23 revealed few remains of morphologically immature kob antelopes (4.37%); these came primarily from the northern sector of the site. No remains of very young animals were recorded; all were individuals of a subadult age, that is, they would have been almost the size of adult animals. Among the remains of animals of other species, a small number of bones of young oribi antelopes occurred (five bones dispersed all over the site) and a large mammal (buffalo or auroch, two bones between the southwestern and northwestern sectors of the site). The hippopotamus mandible from the southern sector of the site also came from a young individual.

3.4.2 Affad 24 (AFD24)

The faunal material discovered at site AFD 24 came from both the surface and the explored basement layers, 417 fragments of heavily mineralized pieces of animal skeletons, forming no visible clusters [*Table 3.7*]. The material was well preserved, analogously to the collection from AFD23. Many bones displayed sufficiently well preserved osteometric and morphologically diagnostic features to permit identification to species.

The collection from AFD24 was clearly dominated by mammal remains. Only one fish vertebra and a single fragment of a Nile monitor vertebra were recorded. Remains of middle-sized kob-type antelopes predominated in the collection, the bones yielding an extensive set of osteometric data [see below, *Table 3.20*]. The second large group comprised skeletons and teeth of a large *Bos* / auroch-type. Other species identified at AFD24 were represented by a significantly smaller number of remains. These comprised giraffe, oribi, reedbuck, the greater kudu, bushpig and hippopotamus [see *Table 3.7*]. Of interest is the fact that all the taxa recorded at this site represented the same order, namely even-toed ungulates.

Table 3.7. Taxonomic composition of remains from site AFD24 coming from both excavation and field survey

Species	*n*	%
ARTIODACTYLA		
Bushpig (*Potamochoerus larvatus*)	1	1.8
Hippopotamus (*Hippopotamus amphibius*)	2	3.5
Greater kudu (*Tragelaphus strepsiceros*)	1	1.8
Oribi (*Ourebia ourebi*)	8	14.3
Bohor reedbuck (*Redunca redunca*)	3	5.3
Kob (*Kobus* sp.)	21	37.5
Giraffe (*Giraffa camelopardalis*)	8	14.3
Auroch (*Bos primigenius*)	10	17.8
REPTILIA		
Nile monitor (*Varanus niloticus*)	1	1.8
FISH		
Clariidae	1	1.8
NISP	56	100 / 13.3
Megafauna (MF)	0	–
Large-sized ruminant (LSR)	241	65.8
Middle-sized ruminant (MSR)	56	15.3
Large-sized mammal (LSM)	0	–
Middle-sized mammal (MSM)	0	–
Small-sized mammal (SSM)	0	–
Mammal (M)	69	18.8
Unidentified mammal	366	100 / 86.7
TOTAL	422	100

The anatomical composition of remains from site AFD 24 represented all elements of the skeleton and teeth [*Table 3.8*].

Table 3.8. Anatomical composition of remains from site AFD24 (from excavation)

Anatomical category	Kob	Auroch	Giraffe	Oribi	Reedbuck	*n*	%
H	1	4	3	1	–	51	50.49
B	2	2	2	2	–	8	7.92
PPAL	2	–	–	4	1	20	19.80
DPAL	1	–	1	–	–	–	
PPPL	2	–	1	–	–	14	13.86
DPPL	7	2	–	–	2	8	7.92
D	5	2	1	1	–	–	

3.4.3 Affad 110 (AFD110)

Exploration at the site AFD110 revealed the remains of probably a single individual representing the Bovinae sub-family, genus either *Bos* or *Syncerus* [*Table 3.9*]. The poor state of preservation of the remains, as well as the lack of distinctive features, made a positive species identification impossible. The remains were initially suggested to be those of an African buffalo, but given later discoveries—unambiguously indicating the presence of aurochs in the ecosystem of the Affad Basin from the Late Pleistocene—this identification should probably be revised. Recorded among the remains were fragments of long bones (radius, tibia) with the shafts incompletely grown to the epiphysis. An assessment of the remains indicated an individual of subadult age. Skeletal fragments, including numerous fragments of vertebrae, ribs, and flat bones, were dispersed over a small area and originally lay in a layer corresponding to the sandy silts of facies 23.D.1 from site AFD23. This deposit (110.2 and 110.3) lay directly on clayey silt (110.1, corresponding to the floor of pluvial silts), while an insignificant relief depression was filled with more sand (110.4) [*Fig. 3.6*].

Table 3.9. List of determined and undetermined remains from site AFD110 (after Osypińska and Osypiński 2016b: Table 4 updated)

Species		*n*	%
Bos sp. / *Syncerus* sp.		106	
	NISP	106	8.85
Bovinae		89	
Large-sized mammal		615	
Mammal		387	
Unidentified bones		1091	91.15
	TOTAL	1197	100

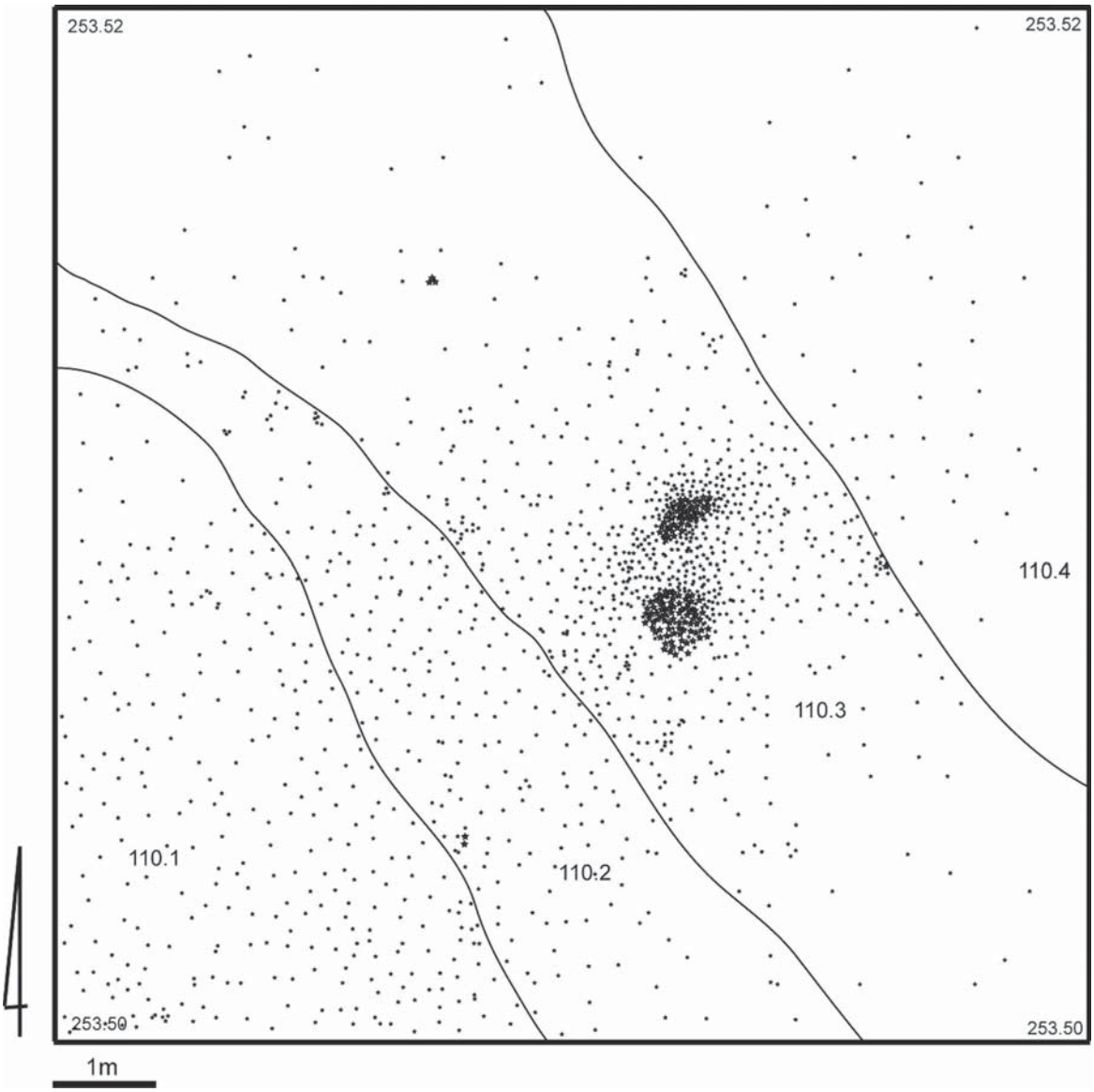

Fig. 3.6. Distribution of bone remains in explored deposits at site AFD110

3.4.4 Affad 111 (AFD111)

The total assemblage of mammal, reptile and fish remains from site AFD111 amounts to 438 in number. The bones were mineralized in a manner typical of Pleistocene assemblages at Affad and characterized by significant fragmentation. However, the composition of fauna from this site proved to be fairly atypical for the Affad Basin [*Table 3.10*]. It was the only Pleistocene site in which animals from the Suinae sub-family, a species of wild boar (*Potamochoerus larvatus*), or the common warthog (*Phacochoerus africanus*) were represented.

Another unique animal identified among the remains discovered at site AFD 111 was the Nile crocodile (*Crocodylus niloticus*). All fragments of the crocodile skeleton were found in one location, approximately 50 m from the main site. These were skull fragments exclusively from a very large individual.

Table 3.10. List of determined and undetermined remains from site AFD111 (after Osypińska and Osypiński 2016b: Table 5 updated)

Species	AFD 111a		AFD 111b	
	n	%	*n*	%
African buffalo (*Syncerus caffer*)	5		0	
Grivet (*Chlorocebus* sp.)	3		0	
Suidae (*Phacochoerus* sp./*Potamochoerus* sp.)	1		0	
Hippopotamus (*Hippopotamus amphibius*)	1		0	
Nile monitor (*Varanus niloticus*)	1		8	
Nile crocodile (*Crocodylus niloticus*)	0		142	
Clariidae	1		2	
Cyprinidae	1		0	
Tilapiini	1		0	
NISP	14	5.78	144	73.46
Megafauna	16		0	
Large-sized ruminant (LSR)	7		0	
Middle-sized ruminant (MSR)	99		0	
Small-sized ruminant (SSR)	2		0	
Large-sized mammal (LSM)	49		0	
Middle-sized mammal (MSM)	25		0	
Small-sized mammal (SSM)	2		0	
Mammal (M)	28		0	
Reptile (R)	0		48	
Unidentified bones	228			
TOTAL	242			

3.4.5 Affad 120 (AFD120)

Surface planigraphic research at site AFD120 recorded several hundred mineralized animal remains. However, the overwhelming majority was preserved as very small non-diagnostic fragments. Only 11 animal remains presented well-preserved diagnostic and osteometric features [*Table 3.11*]. The collection appears to comprise strictly mammal bone elements. No fish or reptile bones were recorded. Generally, the list is dominated by large animals. However, skeletal elements of a middle-sized ruminant constituted a significantly smaller part of the assemblage.

Apart from the predominant ruminant remains at site AFD120, a single bone (humerus) of a predator was found, namely that of an African wild dog (*Lycaon pictus*).

3.4.6 Affad 122 (AFD122)

At site AFD122 animal bone fragments were dispersed over a wide area. The overwhelming majority presented no diagnostic features. All of the bones were mineralized in a manner characteristic of Pleistocene material from Affad. Three species were identified among the remains: two mammals and a reptile [*Table 3.12*]. The member of the *Reptilia* class was a Nile crocodile

Table 3.11. Taxonomic, anatomical and osteometric data of the animal remains from site AFD120

Species	Bone	Comment/osteometry (mm)
Auroch (*Bos primigenius*)	I phalanx	Bd-40.25
Auroch (*Bos primigenius*)	Talus	GLI-95.72; Glm-83.04; Bd-65.81
Auroch (*Bos primigenius*)	Scapula	GLP-84; SLC-68.02
Auroch (*Bos primigenius*)	Os metatarsi III	Bd-31.32
Large-sized ruminant (LSR)	Vertebrae Th	
Large-sized ruminant (LSR)	Vertebrae Th	
Large-sized ruminant (LSR)	Atlas	
Large-sized ruminant (LSR)	Vertebrae	
Large-sized ruminant (LSR)	Os tarsi	
Kob (*Kobus* sp.)	Humerus	
African wild dog (*Lycaon pictus*)	Humerus	

Table 3.12. Taxonomic, anatomical and osteometric data for animal remains from site AFD122

Species	Anatomical part	Comment/osteometry (mm)
Nile crocodile (*Crocodylus niloticus*)	3 teeth	
African elephant (*Loxodonta africana*)	tooth	
Large-sized ruminant (LSR)	4 teeth	
Mammal (M)	2 long bone fragments	

(*Crocodylus niloticus*): three complete teeth of a large individual. The mammals were also represented by teeth: a large fragment of a cheek tooth of an elephant (*Loxodonta africana*) and four fragments of pre-molar and molar teeth from a large ruminant, probably an auroch. Fragments of long-bone shafts can probably be assigned to the same size category of mammals.

3.4.7 Affad 124 (AFD124)

The finds from site AFD124 were of fundamental significance for reconstructing fauna exploitation by MSA communities in the Affad Basin, but also for extending current knowledge of paleozoology, mammalogy and archeozoology. Similar to site AFD110 (see above), animal remains occurred here in clearly defined isolated clusters with few lithic artifacts in context. Taking into account site topography, the sand dunes in the immediate vicinity and the fact that the bones were lying in layers of silt, it seems likely that dune migration was responsible for the early protection and the relatively recent exposure of bones originally lying in Pleistocene alluvial soils. This hypothesis is supported by the state of preservation of many of the osteological elements from the site.

Seven clear concentrations of bones representing a large ruminant were distinguished during a preliminary analysis of the finds. Four of the clusters followed an E–W alignment, at a distance of approximately 5–10 m from one another. They were densely concentrated within a diameter

of about 1–2 m. A further three clusters were found several meters to the north. Between the concentrations, single lithic artifacts, as well as loose bone and teeth fragments were found.

All of the animal remains from site AFD124 were mineralized in a manner typical of Pleistocene material. They were dark in color, from grey to the predominant black and dark grey. Only teeth fragments were a light color, beige and white.

Cluster B1 was the largest concentration, one which additionally comprised the largest big bone fragments at the site. In addition to being the most eastward concentration of bone, cluster B1 was found in the immediate vicinity of a large dune. Closer analysis indicated that all of the recorded elements came from the horncore, which could even be reconstructed owing to how well preserved these remains were [*Fig. 3.7* inset]. The morphological features of the horncore

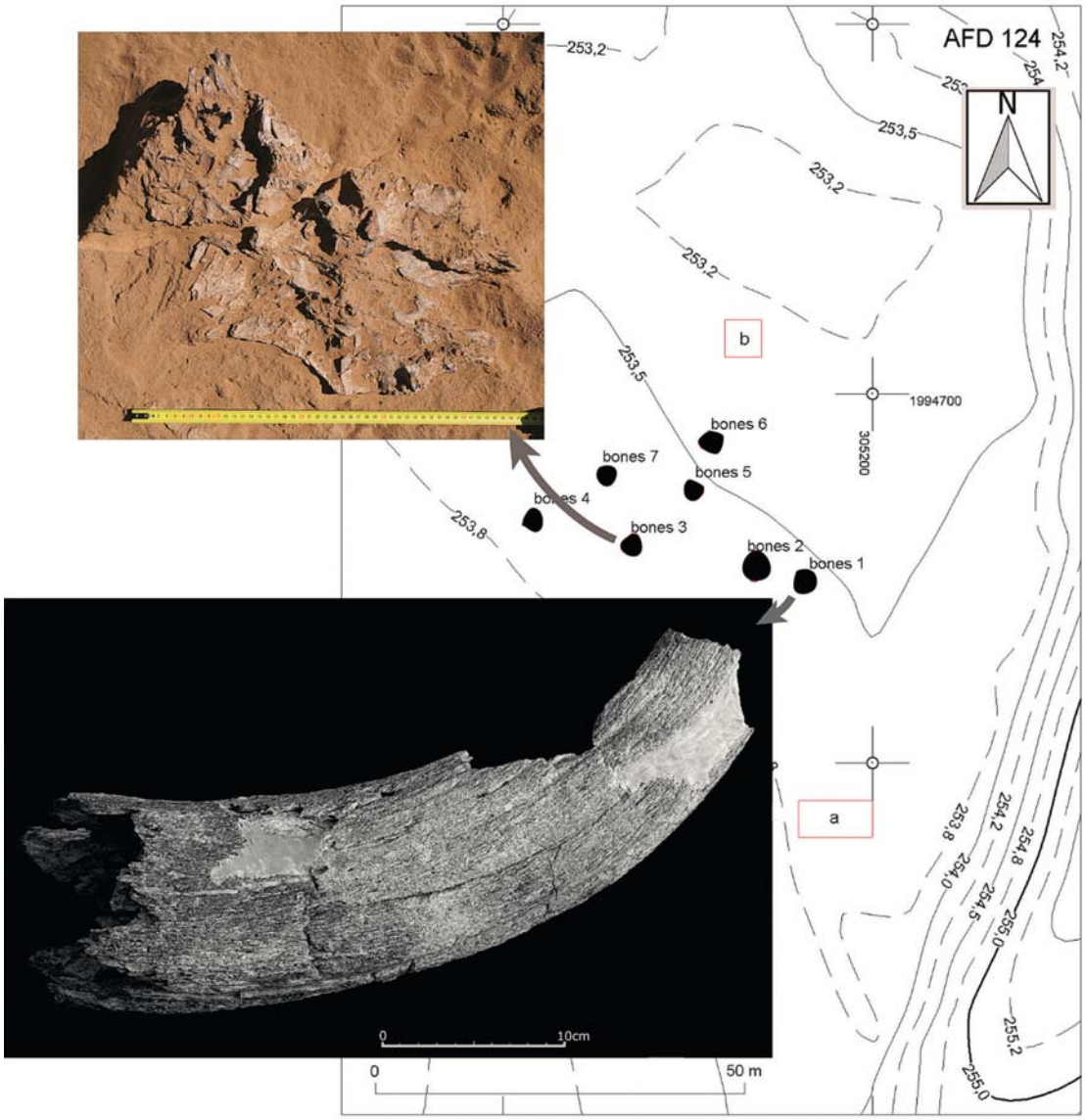

Fig. 3.7. Location of clusters of skeletal remains at site AFD124; insets, state of preservation of the frontal bone of an auroch (top) and a reconstructed auroch horncore (bottom)

identified it as belonging to an African auroch (*Bos primigenius opistonomus/africanus*). The diameter of the horncore at the base was approximately 48 cm.

Cluster B2, which was approximately 1.50 m in diameter, was found around 5 m west of B1. Most of the remains comprised very small fragments, devoid of morphological features permitting anatomical and taxonomic identification. However, a more thorough assessment of this assemblage indicated that all of the recognizable fragments came from the skull of a large mammal. Two fragments of molar teeth of a large ruminant, an auroch in all probability, were also found in the concentration.

Lying alongside B1 and approximately 7–8 m west of cluster B2, cluster B3 constituted a discovery of fundamental significance for the archaeozoological research carried out at Affad. It was no greater than 1 m in diameter. Just below the surface of this sediment was a large fragment of the skull of a large-sized ruminant resting on its frontal bone. The find was cleaned with great difficulty, revealing the morphological features of the skull: frontal bone (*os frontale*), fragmentary occipital bone (*os occipitale*), facial bone (*ossa faciei*) including the nasal bone (*os nasale*), and the upper jaw (*maxilla*) [see *Fig. 3.7* inset]. It belonged to an auroch (*Bos primigenius*). The approximate diameter of the preserved horncores was assessed at about 40 cm.

Cluster B4 was located approximately 10 m west of B3. It was relatively small (a few dozen centimeters), but the several dozen skeletal fragments, comprising small pieces of the flat bones of a large mammal, were dispersed. Among these fragments was a very well preserved P1 tooth of a large ruminant, most probably an auroch.

Clusters B5 and B6 were relatively small in size, comprising several dozen fragments of large mammal bones. Their state of preservation did not allow identification of these fragments in terms of taxonomy or anatomy.

Cluster B7 differed from the others in several respects. It was located distinctly north of the 'line' formed by the other concentrations. Twenty fragments of a humerus or other long bones of a large ruminant, along with a fragment of what was most probably the skull of a large mammal, were recorded in a clear concentration about 1 m in diameter. The bones were in very good condition, a complete distal head of a humerus being even sufficiently well preserved to be measured [*Table 3.13*].

Table 3.13. Taxonomic, anatomical and osteometric data for animal remains from site AFD124

Species	Anatomical part	Comment/osteometry (mm)
Auroch (*Bos primigenius*)	106 horncore fragments	
	Numerous fragments of a single skull	*os frontale, os nasale, os lacrimale*
	20 tooth fragments	
	20 humerus fragments	Bd-105.08
Large-sized ruminant (LSR)	45 long bone fragments	
Kob (*Kobus* sp.)	Scapula fragment	
	Mandibula fragment	
Middle-sized ruminant (MSR)	5 vertebra fragments	
TOTAL	198	

3.4.8 AFFAD 131 (AFD131)

Site AFD131 was one of the most extensive Pleistocene sites investigated by the Project. The concentration of osteological material coincided with a cluster of lithics. All diagnostic osteological elements in the neighborhood were mapped. Altogether 4066 animal remains, representing various taxa, were recorded, but their poor preservation and heavy fragmentation made identification to the level of type or species impossible [*Table 3.14*].

Table 3.14. Taxonomic, anatomical and osteometric data for animal remains from site AFD131

Species	Anatomical part	Comment/osteometry (mm)
Hippopotamus (*Hipopotamus amphibius*)	teeth	
Elephant (*Loxodonta africana*)	2 tooth fragments	
Giraffe (*Giraffa camelopardalis*)	2 scapula fragments	
Auroch (*Bos primigenius*)	calcaneus, humerus, talus, femur, teeth P3 o. metatarsi III	 37.02/16.15 Bd-31.32
Hartebeest (*Alcelaphus buselaphus*)	4 tooth fragments	
Kob (*Kobus* sp.)	2 teeth	
Plains zebra (*Equus quagga*)	4 teeth	
Spotted hyena (*Crocuta crocuta*)	1	
Crested porcupine (*Hystrix cristata*)	3 teeth; 1 mandibula fragment	
Catfish (*Siluriformes* sp.)	7	
Fish (*Pisces*)	36	
Large-sized ruminant (LSR)	3 pelvis, costae, vertebrae 541 long bone fragments	
Middle-sized ruminant (MSR)	2 mandibulae 15 teeth 2 metapodia, burnt 1 scapula 3 humeri 8 vertebrae 3 skull fragments 56 bone fragments	
Middle-sized mammal (MSM)	49	
Small-sized ruminant (SSR)	1 tooth fragment	
Small-sized mammal (SSM)	12	
Mammal (M)	3303	
Unidentified	763	
TOTAL	4066	

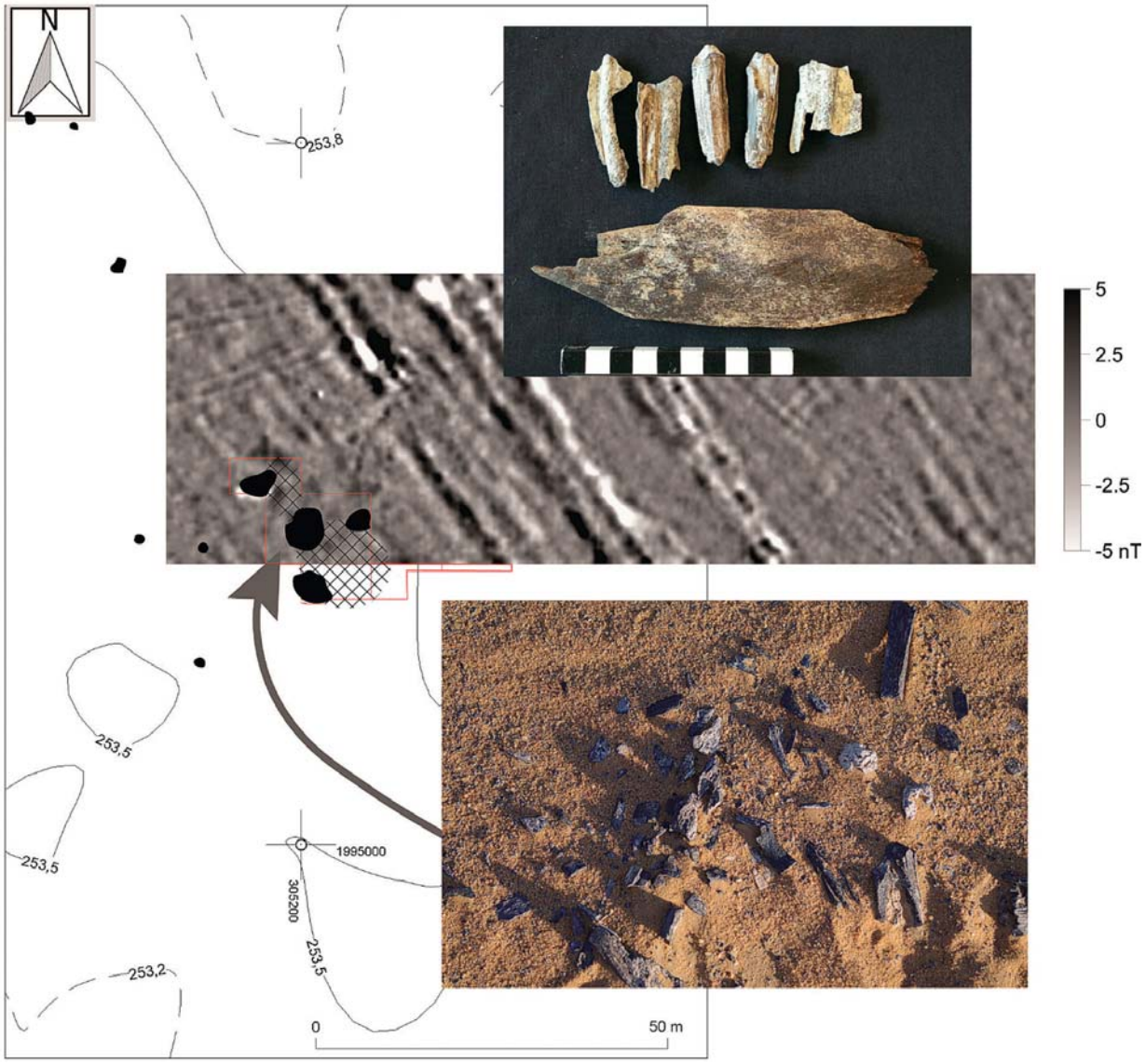

Fig. 3.8. Location of animal remains at site AFD131 (solid black on the plan). Inset photos: state of preservation of animal remains

A distinct and dense concentration of osteological remains and lithic artifacts was located in the western part of the site. It was approximately 1.50 m in diameter [*Fig. 3.8*]. Almost all of the skeletal elements recorded in this location came from a large ruminant, comprising ribs along with the thoracic and lumbar vertebrae. A few bone fragments of a middle-sized ruminant were also recorded, as well as fish vertebrae. At a distance of a few to several dozen meters to the north of the cluster were molar and premolar teeth of an auroch, single bones of middle-sized and small ruminants (kob, hartebeest), as well as the teeth of a zebra. More than a dozen teeth and fragments of a porcupine mandible were found about 10 m to the south. Fairly large skeletal fragments of a hippopotamus lay on the western fringes of the site, while parts of an elephant skeleton were located on the eastern fringes. A hyena bone was also found on the edges of the site (northwestern part).

3.4.9 Affad 113 (AFD113)

Affad 113 was one of three sites in the Affad Basin where nothing but fish remains were found (the other two were AFD84 and AFD112; see above, section 3.3). Two tangential trenches (A and B) with the combined dimensions of 20 × 10 m yielded bone material from a surface layer reaching 10 cm below the ground surface [*Fig. 3.9*]. The collection of lithic sources from the site (see § 4.3.6) consisted of flakes of a kind typically used to make MSA tools, presumed to be evidence of tool repair on the spot. The absence of microlithic elements in this assemblage made an early Holocene chronology untenable. The zone was situated on the bed of a seasonally active palaeochannel (see Chapter 2).

Fig. 3.9. State of preservation of fish remains from AFD113, including Clariidae

Linseele identified 1300 of the bone fragments from trench B as Clariidae, all of them likely to be of the genus Clarias. In addition, two remains of *Bagrus* were recorded; the other bones could not be identified [*Table 3.15*]. *Clarias* and *Bagrus* are both catfish, the first being an open-water taxon, the second a shallow-water one. The remains were likely displaced by river action and their composition is much affected by differential preservation. Nevertheless, the very pronounced predominance of one taxon indicates anthropogenic deposition. Most of the Clariidae bones belong to individuals with reconstructed standard lengths (length from the tip of the snout to the start of the tail) between 70 and 100 cm. Although in part the bones of small individuals are likely to have been completely destroyed, their large size suggests fishing at the beginning of the yearly summer floods. For a short period, spawning adult Clariidae can then be found in concentrations, making them easy prey, to be caught with very simple techniques, even by hand.

The large number of remains at AFD113 indicates possible repeated use of the location as a fishing ground. As yet, no patterns have been detected in the skeletal element distribution that could reveal how the fish were processed.

Table 3.15. Fish remains from AFD113 (V. Linseele). Not included 28 skeletal elements of Clariidae and one precaudal vertebra from the species *Bagrus* sp., 80–90 SL, recorded in the 2015 field survey

Skeletal elements	SL estimated	*Clarias gariepinus*	*Clarias* sp.	Clariidae	Bagrus	Siluriformes	Unidentified
Neurocranium	70–80			4			
	80–90			8			
	90–100			11			
	100–110			1			
	n/o			476			
Other head elements**	40–50			1			
	60–70			11	1		
	70–80	1		48			
	80–90			36			
	90–100	1		29			
	100–110			6			
	110–120			1			
	n/o			102			
Precaudal vertebrae	20–30			1			
	40–50			1			
	50–60			1			
	60–70			12			
	70–80			57			
	80–90			93			
	90–100			44			
	100–110			6			
	110–120			2			
	n/o			32			
Caudal vertebrae + hypural	60–70			1			
	80–90			1			
	90–100			1			
	100–110			1			
	n/o			257			
Cleithrum, coracoid, pectoral spine	20–30				1		
	60–70		1	2			
	70–80		2	10			
	80–90		1	3			
	90–100			5			
	n/o		2	25		4	
Pelvis	90–100			1			
TOTAL		2	6	1290	2	4	866
				2170			

* – including: mesethmoid, suborbitale, supraorbitale, jugale, lateral ethmoid, posttemporale, anterior process of dermethmoid, dermethmoid; ** – including: operculum, epihyale, vomer, premaxillare, quadratum, dentale, ceratohyale, glossohyale, urohyale, hyomandibulare, articulare, parasphenoid, apparatus weberianus, palatinum

3.4.10 Affad 134 (AFD134)

The most northward location in the investigated area, recorded as a separate archaeological site, comprised an irregular oval of overheated alluvium, about 5 × 3 m in size, with a large amount of Nile oyster shells (*Etheria elliptica*), also bearing evidence of high temperatures [*Fig. 3.10*]. Extrapolated from the weight of the shells from the explored space, the mass overallof this assemblage would be approximately 40 kg. Initially identified with early-Holocene gathering activity, the shells were dated by two independent methods: TL (Lub-6433: 56.1 ± 6.8 ka) of the overheated alluvium, as well as AMS ^{14}C (Poz-102024: >48 ka, which is already beyond the range of the method), indicating clearly a relationship with the late Pleistocene time horizon. While some of the smaller specimens were preserved closed, most were open and broken [see *Fig. 3.10* inset].

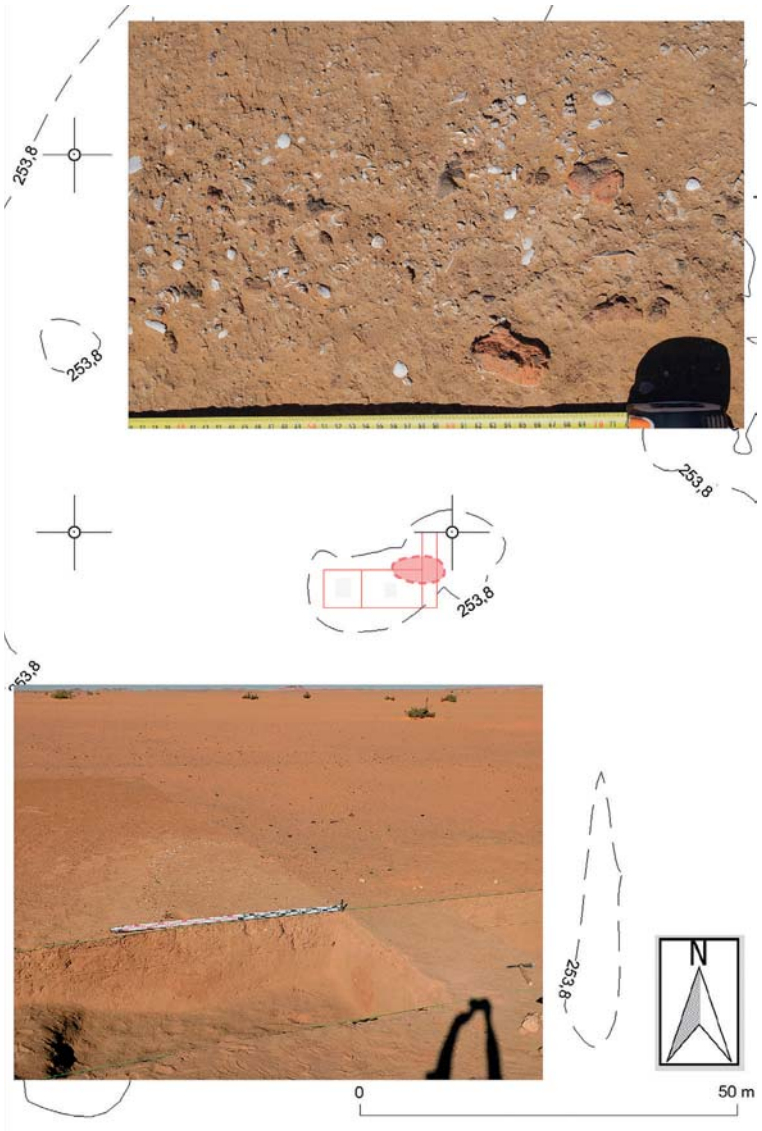

Fig. 3.10. Zone of heavily overheated alluvium with a large amount of shells (marked in pink) during exploration; inset photos, close-up top view of the cluster at top and general view of the location of the find at bottom

A preliminary analysis of the size and species composition of the oysters did not provide evidence of intentional selection by a human group or groups. The authors are inclined to think that this location, being the bed of a periodically dry channel, comprised the habitat of a mussel (Bivalvia) colony (Van Damme and Van Bocxlaer 2009) and that the burning attested here was either a wildfire or anthropogenic in nature. Although natural savannah fires constitute an inseparable element of the renewal cycle of the plant cover, they are usually short-lived (Kingdon et al. 2013/I: 58). The intensity with which the fire impacted the alluvium at AFD 134 must have been significantly greater, resulting in the clayey floor being scorched to a depth of 15–20 cm. This suggests intentional activity on the part of human groups supplementing their diet with clams. Sites of this kind from the MSA have not been discovered so far in African territory. However, there is evidence in the Levant of mussel collection from the Middle Palaeolithic and regular use for making ornaments from the Upper Palaeolithic (Bar-Yosef Mayer 2005). In Europe, shells of marine mollusks have been used as food for around 400,000 years, while around 30,000 years ago they were also used for decorative and symbolic purposes. They were distributed great distances with this purpose in mind. The best-known examples of clam consumption are linked to Upper Palaeolithic cave sites, as well as open sites with large shell middens from the Mesolithic on (Bailey and Milner 2008). The supplementation of human diet with the meat of mollusks, mainly mussels (Bivalvia) was and still is a common phenomenon, also in modern Africa. In periods of meat scarcity, freshwater clams constitute an important and eagerly exploited element in the diet, being a good substitute for the meat of vertebrates.

3.5 LATE PLEISTOCENE ANIMAL SPECIES FROM AFFAD: A BEHAVIORAL APPROACH

A behavioral analysis of the late Pleistocene animal species discovered at different sites in the Affad Basin, when considered holistically, draws a picture of the environment exploited by the MSA human communities from Affad. The presentation in this section, encompassing a total of 19 species, follows a generally accepted order in systematic animal taxonomy. It starts with the grivet monkey (§ 3.5.1) and cane rat (§ 3.5.2), and continues with the African wild dog (§ 3.5.3), spotted hyena (§ 3.5.4), plains zebra (§ 3.5.5), bushpig (§ 3.5.6), hippopotamus (§ 3.5.7), Nubian giraffe (§ 3.5.8), African buffalo (§ 3.5.9), auroch (§ 3.5.10), greater kudu (§ 3.5.11), dik-dik (§ 3.5.12), oribi (§ 3.5.13), bohor reedbuck (§ 3.5.14), kob antelope (§ 3.5.15), waterbuck (§ 3.5.16), hartebeest (§ 3.5.17), only to end with the Nile monitor (§ 3.5.18) and fish from the catfish family (§ 3.5.19). The elephant has not been included here.

3.5.1 Grivet (*Chlorocebus aethiops*)

Remains of small Savannah monkeys of the *Chlorocebus* type, altogether 127 bone fragments, were identified in two sectors at AFD23: southern (trench 2013/L–M) and southwestern (trench 2013/I, encampment area) [***Fig. 3.11***; ***Table 3.16***]. Identification to the species level was not successful. Even so, two of the six species of this type—*Chlorocebus aethiops* and *Chlorocebus*

Fig. 3.11. State of preservation of *Chlorocebus* remains from site AFD23

Table 3.16. Osteometric measurements of *Chlorocebus* bones from AFD23

Anatomical part	Osteometry (mm)
Humerus	Bd-15.46; 13.16
	Bd-12.30; BT-11.59

tantalus—currently live in a similar habitat in the Upper Nile basin. They differ only slightly in terms of coloring and were in fact classified until recently as varieties of one species (*Chlorocebus aethiops*).

Chlorocebus aethiops currently inhabits extensive areas of sub-Saharan Africa and is one of the most common species of monkey (Wolfheim 1983; Nowak 1999; Kingdon et al. 2013/II: 264). Individuals reach a body length of 100–130 cm (males being slightly larger than females), with a weight ranging from 4 to 8 kg. They live in groups of around 20 individuals, inhabiting the savannah, parkland forests, riparian forests, and even orchards. Their presence is conditioned by the proximity of permanent sources of drinking water, as well as the presence of large trees in which they sleep (all data concerning their behavior after Kingdon et al. 2013/II: 264). While they prefer forests and savannah woodland, they often focus on areas of open savannah.

Grivets are omnivorous and live in ecosystems in which the annual precipitation ranges between 350 mm and 3000 mm. Their average range is 24.5 ha and they can cover around 700 m daily. During the day grivets spend 27% of their time looking for food. They feed intensively in the evening. Up to 57% of their time grivets spend in high trees where they sleep. Most of their food is from trees (56%), with other sources being herbaceous plants (33.5%), bushes (4.1%) and grasses (3.7%). The main component of their diet comprises fruit and seeds (50.6%), leaves (18.7%) and flowers (17.6%). Apart from this, grivets eat insects and tree bark. It has been observed that they most often eat the fruit of *Maytenus undata*, *Ficus* sp., *Acacia* sp., *Zizyphus* sp., and *Opuntia* sp., as well as the leaves and flowers of *Trifolium ruepellianum* and the fruit of *S. Guineese*. They also frequently eat termites. Generally, approximately a third of their food is obtained on the ground and two-thirds in the trees.

3.5.2 Cane rat (*Thryonomys swinderianus*)

Single fragments of the skeleton of a large rodent, a cane rat, were identified in layers related to Late-Pleistocene occupation in AFD23 trench 2013/I (encampment). These were pieces of a mandible with teeth [*Fig. 3.12*], along with well-preserved skull fragments, incisors and molar teeth.

Cane rats occur south of the Sahara and are currently an animal farmed for food in several equatorial countries. In their natural state, these creatures reach a length from 35 to 60 cm and weigh up to 10 kg (Macdonald 1984). They most often inhabit marshy areas with reeds, floodlands and savannah with tall grasses and brush (Kingdon et al. 2013/III: 688).

Fig. 3.12. Mandible of a cane rat (*Thryonomys swinderianus*) from AFD23

3.5.3 African wild dog (*Lycaon pictus*)

The African wild dog, a humerus bone of which was discovered at site AFD120, is one of the large predator mammal species from the Canidae family, considered to be a relic line of canids living throughout most of the African continent in the past.

African wild dogs inhabit various environments from short-grass plains, through semi-desert, bushy savannahs, woodlands, right up to upland forest. They often hunt middle-sized antelope. While the average weight of the animals they hunt is most often about 50 kg, they have been known to hunt prey weighing up to 200 kg (Kingdon et al. 2013/V: 50). Many of the species which the African wild dog preyed on have been recorded at Affad, namely the Greater kudu, Hartebeest, Bohor reedbuck, African buffalo, Suidae, as well as small antelopes such as the dik-dik.

3.5.4 Spotted hyena (*Crocuta crocuta*)

Hyena remains have been recorded only on the edges of site AFD131.

Currently, it is a species which inhabits very diverse environments, namely semi-desert, savannah and open forest. It is not found in deserts and rainforests. In the best habitats, populations of spotted hyenas predominate among other predators, forming clans. Although hyenas are able to survive long periods without water, they are dependent on access to watering holes. Incidents are known of a clan being dispersed following the drying out of a source within the pack's range (Kingdon et al. 2013/V: 272).

3.5.5 Plains zebra (*Equus quagga*)

Zebra remains in the form of complete and fragmentarily preserved teeth were recorded at only one site, namely AFD131.

Plains zebra inhabit grassy savannah, woodland savannah, as well as parkland forests. They are not to be found in rainforests or desert. Water is a basic requirement because plains zebra will not venture further than 12 km from a watering hole. They feed on grasses, which comprise 90% of their diet. Research conducted at Kruger National Park (South Africa) has indicated that plains zebra eat 50 species of grass and eight species of herbaceous plants. However, a certain selectivity was also observed and a clear predominance (40%) in the zebras' diet of grasses of the Panicum type, regardless of the time of year. Other grass species liked by plains zebra are *Themeda triandra*, *Cynodon dactylon*, *Eragrostis superba* (Kingdon et al. 2013/V: 428), although availability is the chief factor determining choice. In the Serengeti, the plains zebra is instrumental in opening up grazing land to other species. This particularity may be of great significance for research on fauna in Pleistocene Affad. Plains zebra are pioneers of land grazing. They are the first to move into areas overgrown with tall grass, focusing on the upper layers. This is possible because unlike ruminants, they use their upper and lower incisors rather than their tongues to tear off the grass. In this way, they clear access to low grasses for other species, such as gnu, antelopes and, in the case of Affad, probably also aurochs. In the dry season, plains zebra will eat the fibrous stems of grass avoided by other animals. The low quality of such forage is compensated by the large amounts

consumed, this because equids are able to eat far more than ruminants owing to a different digestive system.

Migrations of plains zebra are correlated with seasonal availability of water. In the rainy season the animals migrate to drier grazing lands, while during the dry season they will concentrate near permanent fluvial troughs. One example may be their presence in South Sudan, in the area of the Sudd swamps. During the rainy season, the zebra keep to higher-lying, drier areas, while in the dry season, following the drying out of plant cover and periodical bush fires, they are content to approach the river, grazing on thick, freshly grown, swamp grasses. Plains zebra are not territorial animals. Their seasonally changing habitats are located in different areas, depending on the topographical circumstances. In the Serengeti, this comprises 400–600 km^2, in the Ngorongoro crater 80–250 km^2, which is the actual crater surface. The daily movement of a herd of zebra is estimated to be around 25–30 km (Kingdon et al. 2013/V: 428). Currently, plains zebra are inclined to graze with other herbivores, especially gnu, the strategy being based on inter-species social attraction and inter-species facilitation (Kingdon et al. 2013/V: 428). The co-occurrence of plains zebra and giraffes is more incidental and there is no scientific evidence that this is based on similar relations to those in the case of ruminants.

3.5.6 Bushpig (*Potamochoerus larvatus*)

Single bushpig remains were discovered at sites AFD24 and AFD111, hence the species can hardly be considered as commonly occurring in late Pleistocene Affad.

The bushpig is behaviorally linked to dense plant cover providing abundant food and located near water. It most commonly inhabits a floodplain forest and riverbank scrub. Frequent rolling in mud, air circulation and access to damp locations ensure body thermoregulation in its case. Bushpigs are mainly nocturnal and generally feed from dusk to midnight, as well as in the morning. They are omnivorous, eating both the above- and below-ground parts of plants (rhizomes, bulbs, roots, fruit, fungi, leaves). Bushpigs are continually on the move while feeding, stopping only when they discover larger amounts of food (Kingdon et al. 2013/VI: 31).

3.5.7 Hippopotamus (*Hippopotamus amphibius*)

Identified remains of hippopotamus skeletons from site AFD23 counted 186 bone fragments [*Fig. 3.13*]. They were found in a single large concentration in the southern part of the site (trench 2013/M). The rest of the bones classified as megafauna come mostly from the same place, and are most likely also hippopotamus. Single remains were also noted in the animal bone collections from sites AFD120 and AFD24.

Although the hippopotamus is one of the largest mammals, it is the only species of African megafauna adapted to living in the aquatic-terrestrial environment of rivers and lakes. Its dimensions reach 4 m in length and 1.50 m in height. Males weigh from 1000 to 2000 kg, females are slightly smaller (up to 1700 kg). Water is a basic feature of a hippopotamus habitat, allowing both full immersion and access to large amounts of food. Hippopotamuses also need water for thermoregulation. In order to satisfy their nutritional needs, these animals sometimes travel long

Fig. 3.13. Bone fragments (teeth) of a hippopotamus from AFD23

distances on land. However, they spend most of the day in the water or on riverside beaches (Kingdon et al. 2013/VI: 68).

As hippopotamuses feed mainly on grass, their occurrence depends on the availability of meadow pastures. Studies show that the following grasses consistently prevail in the hippo diet: *Bothriochloa* sp., *Bracharia decumbens*, *Chloris gayana*, *Cynodon dactylon*, *Heteropogon contortus*, *Hyparrhenia flipendula*, *Sporobolus pyrimidials* and *Themeda triandra*. Dicotyledons are eaten randomly because they intertwine with grass. In extreme situations, hippos also feed on tree shoots and their fruit, e.g., the sausage tree *Kigelia pinnata*. By contrast, aquatic vegetation is usually rare in their diet (Kingdon et al. 2013/VI: 68). Large populations of hippopotamuses have a serious impact on the environment and the ecosystem, in which they can play an important role. Their intensive, non-selective grazing in one place causes a decrease in the number of combustible plant parts, suppressing the risk of cyclical grass fires and allowing shrubs and bush to spread. This consequently limits meadows and grazing areas, resulting in hippos withdrawing from grazing in a given location. Over time, however, the absence of these large grass eaters causes dry grasses and shrubs to increase in volume, stocking up thus on combustible material. In the longer term, this leads to open fires and the burning of shrubs and trees, and therefore the reappearance of grasslands and an increase in the population of hippopotamuses in a given place.

Hippopotamuses also have a significant impact on the landscape as their paths can alter the flow pattern of water. They also maintain deep channels through reed beds allowing water to move more freely and providing access to watering sites for other animals. In swampy and flood-plain areas, the paths of hippos lead to the formation of new canal systems. Hippos defecate in water, thus greatly fertilizing rivers and lakes. This is a major factor in supporting the development of a fish population (Kingdon et al. 2013/VI: 68).

3.5.8 Nubian giraffe (*Giraffa camelopardalis*)

Remains of Nubian Giraffes, identified as large fragments of limb bones, were recorded at two sites, namely AFD24 and AFD131.

Giraffes are among the largest ruminants: 450–600 cm high at the withers, females weighing 540–1180 kg and males 1800–1930 kg. Giraffes are associated with the presence of acacia savannas, *Commiphora* and *Combretum*. They do not inhabit rain forests or open savannahs. Studies have shown that although South Sudan's giraffes avoided the constantly flooded Sudd swamps, they were widespread in the floodplain all year round. Interestingly, at the peak of the flood season, only a few individuals stayed in the dry parkland forests. However, the giraffes' seasonal preference for the quite highly flooded areas located near swamps has been observed (Kingdon et al. 2013/VI: 96–110). Observations have also shown that floodplains, especially large ones abundantly covered with termite mounds, which rise like islands above the floodwaters, attract giraffes. While low temperatures, combined with rainfall and wind, are capable of killing giraffes, these animals are very tolerant of high temperatures, even exceeding 40°C. In East Africa, giraffes disperse during the rainy season, while in the dry season they gather close to rivers.

3.5.9 African buffalo (*Syncerus caffer*)

Single bone fragments of a large ruminant, most likely an African buffalo, were identified both in the southern sector of site AFD23 (trench 2013/M), and the southwestern one (survey 2014/P, as well as on the surface in 2003, although early on in the project it was not clear whether the remains were from buffalo or auroch; Osypiński, Osypińska, and Gautier 2011: 186). Similar objections have been raised with regard to the remains from site AFD110.

As one of the most dangerous animals in Africa, buffaloes reach 140 cm in height at the withers, with males weighing up to 600 kg (subspecies *Syncerus caffer brachyceros*, present in the upper Nile river basin). Although these animals favor a woodland savannah with constant access to sources of water, they are able to inhabit a wide variety of environments, apart from dry ones. They live in large herds, with their only natural predator (other than humans) being lions. To protect themselves from lions, buffaloes take refuge in dense thickets, positioning themselves with their 'unsecured' hindquarters towards trees and shrubs and forming a phalanx of dangerous horns (Kingdon et al. 2013/VI: 124–136).

3.5.10 Auroch (*Bos primigenius*)

A total of about 500 remains, clearly identified as those of aurochs (*Bos primigenius*), or identified as such with a high degree of probability, were found at Affad. The anatomical composition of the remains [*Table 3.17*] was mainly influenced by taphonomic processes, which determined to a large extent the state of preservation of long, short and variously shaped bones.

Recent discoveries in Ethiopia and Tunisia have rekindled the debate on the origin of cattle in Africa, which had surrounded the initial discoveries of the 1960s, 1970s and 1980s (Martínez-Navarro et al. 2007; 2014). Until recently, it was widely accepted that aurochs originated from

Table 3.17. Anatomical composition of auroch bone remains from sites in the Affad Basin (LSR – Large-Sized Ruminant)

Bone	AFD24		AFD124		AFD131	
	Auroch	LSR (probably auroch)	Auroch	LSR (probably auroch)	Auroch	LSR (probably auroch)
Cranium	2		numerous			
Processus cornuales		2	106			
Dentes	11		20	4	48	
Maxilla						
Mandibula		1			26	
Vertebrae		15				217
Costae		4			4	232
Scapula					1	2
Humerus			20			
Radius	2					
Ulna						
O. carpi						
O. metacarpi	1					
Pelvis		2				
Femur		1			1	
Patella						
Tibia						
Talus					1	
Calcaneus					1	
O. tarsi						
O. metatarsi						
Ph. proximalis					1	2
Ph. media	1					
Ph. distalis						
Long bone fragment	1	93				17

the *Bos acutifrons* species and lived in Asia approximately 2 million years ago (van Vuure 2005). From there, they were believed to have spread to Asia, Europe, and eventually also to Africa. This generally accepted picture of species evolution was complicated by the discovery a few years ago of the oldest known remains of aurochs at the Wadi Sarrat site in Tunisia (Martínez-Navarro et al. 2014). These finds have been dated to 700,000 years ago. The oldest evidence from Europe are the remains discovered in Italy, 500,000–600,000 years old, found at one of the oldest known Acheulean sites in Europe (Martínez-Navarro et al. 2014). Until recently, paleontologists have failed to give due consideration to the role of Pliocene and early-Pleistocene forms of large ruminants from Africa in the evolution of the *Bos* genus. The animals in question are from the Pelorovis group that evolved from the early Pliocene *Simatherium*; they are known in palaeontology as the Oldovai buffalo after their place of discovery (Martínez-Navarro et al. 2007). New verification

studies on the remains of early Bovidae from Ethiopia indicate that there were in fact two separate lines of the Bovinae subfamily, namely, one belonging to the *Syncerus* genus (buffalo) and the other to animals of the *Bos* genus, which includes not only aurochs and modern domesticated cattle, but also a number of varieties such as the gayal, banteng, kouprey and gaur.

The current evolutionary model of the *Bos* genus, proposed on the grounds of morphometric data from Ethiopian and Eritrean finds, points to central and eastern Africa, not Asia, as its source of origin (Martínez-Navarro et al. 2007). However, the noticeable absence of Pleistocene auroch remains in Africa, apart from the narrow Mediterranean zone and the Egyptian section of the Nile Valley, constituted a major weakness of the new theory. Evidence of this species occurring beyond this range would serve as an important argument in favor of the idea that the *Bos* genus evolved in the central–eastern part of Africa and migrated through North Africa to Europe and then on to Asia. The older concepts, based on the dispersal of finds—Late Pleistocene palaeontological and archaeological sites with remains of aurochs were concentrated mainly in central Egypt, and in the Dakhlah and Fayum oases in the Western desert (Linseele 2004)—assumed that aurochs had come to Africa in the Pleistocene via Gibraltar and inhabited mainly the Mediterranean coast, from Morocco to the lower part of the Nile Valley. Only episodically, in periods of more favorable climatic and ecological conditions, did their range extend to cover also areas of northern Africa, the northern part of the Sahara, and in the east, the Nile valley up to the first Nile cataract. Until recently, the southernmost Pleistocene site where the remains of aurochs were discovered was Erg Tibodaine in southern Algeria (after Linseele 2004). In Sudan, the only site from which auroch remains have been reported is Kashm el-Ghirba in the Atbara region, dated to the turn of the Pleistocene and Holocene (Peters 1989a). In light of these data, the Affad finds are therefore an important contribution to the discussion about the range of aurochs in Africa at the close of the Pleistocene. They are currently the southernmost evidence of the presence of aurochs in Pleistocene Africa (Osypińska et al. 2021).

While there is a wealth of literature on European aurochs: their evolution, history, behavior and morphology, which is based not only on recent multidisciplinary analyses of organic artifacts of Pleistocene and Holocene aurochs (e.g., Noe-Nygaard, Price, and Hede 2005), but also on a rich historical literature (Bogolubski after Lasota-Moskalewska 2005), the same cannot be said of the auroch in Africa. The specific morphological nature of African aurochs has already been discussed (Gautier 1988; Peters et al. 1994; Linseele 2004), but issues related to behavior, habitat and diet have not been the subject of in-depth studies so far. This is due to both a relatively sparse and scattered set of paleontological and archaeozoological sources from Africa and the specific nature of the preservation of these organic remains. The extremely hot and dry environment in which faunal relics are usually deposited is not conducive to the preservation of organic bone components necessary in modern chemical and biological analyses. Knowledge of the living environment and diet of African aurochs, especially important in the context of the community life of Pleistocene human groups and their hunting model, is therefore mainly based on European parallels. According to the current state of knowledge, European aurochs lived in parkland forests, deciduous forests with a denser forest stand, forest steppes and steppes, demonstrating a very high adaptability. Access to water is emphasized as the main condition for aurochs to occupy a given biotope. The diet of European aurochs was essentially based on young tree shoots, leaves, flowers and grass. The great diversity and similarity to a bison diet has also been stressed, this currently

including about 370 plant species (Lasota-Moskalewska 2005). The current narrative in discussions concerning the biotope and diet of European and often African aurochs is that in the Late Pleistocene and Holocene they inhabited mainly forests (Noe-Nyygaard, Price, and Hede 2005), parkland forests or areas of wet riparian forests (Peters 1989a; Linseele 2004).

However, considering the data from Affad, but also new zoological research, there are grounds for determining the range of the Arican animals not as a simple transposition of the habitat, diet and behavior of European aurochs. Kaye E. Reed (1998) conducted an extensive analysis of bovid distribution across African habitats and concluded that ecological adaptations were more reliable indicators of environment than taxonomic affiliation. One element of the environment that determines the presence of aurochs—as various authors have emphasized—is easy and permanent access to water. This is clearly confirmed by the observations from Affad, where the sites are located close to the floodplains of the main course of the Nile. The list of species occurring together with the auroch at sites in Affad seems to suggest a slightly different biotope from the parkland forest commonly accepted as the habitat of African aurochs. The presence of the plains zebra, giraffe, buffalo and porcupine testifies to a slightly more open environment, namely a woodland savannah, savannah, or bright Miombo-type woodland with large tracts of grassy meadows, but also the presence of acacia trees and *Commiphora myrrha*. All the species identified in Affad are heavily dependent on permanent, year-round access to nearby water. This element of the behavior of aurochs is also emphasized by researchers studying this species in Europe.

Osteometric data indicate that the Pleistocene aurochs discovered at Affad correspond in size to Pleistocene aurochs known from the lower reaches of the Nile (e.g., Wadi Halfa [*Table 3.18*]).

Table 3.18. Osteometric measurements of auroch remains from Affad compared with data from other sites in the Nile valley

Bone		Affad (mm)	Wadi Halfa (mm)	Hierakonpolis (mm)	Kom Ombo (mm)
M3 and M2	L	37.02; 30.31			32.7; 23.0
	B	16.15; 14.0			19.2; 17.0
Scapula	GLP	84.2; 84.2; 58.9	82.4		77.5; 64.7; 69.5; 65.9
	SLC	64.1; 68.0; 51.1	–		80; 59.2; 70
Humerus	Bd	105.08	121; 128		98; 100; 91.7
Calcaneum	GL	175.92	193		
Talus	GLI	91.00; 95.72	95; 92.8; 88.5; 84.8; 84.6; 84.2; 84.0; 80.0	93; 85	–
	GLm	86.30; 83.04	87; 83.9; 77.3; 78.8; 77.8; 77.9; 78.3; 73	81; 77	
	Bd	62.71; 65.81	–60.5; 59.3; 53.5; 55.0; 51.0; –53	65; –	
O. metacarpi	Bd	28.91 31.32 63.55			30; 31.1; 30.2; 32.5
O. metatarsi	Bd	31.23			26.7; 29.4; 33.0
I phalanx	Glpe	–+ 97mm	75.2		66.6
		40.25	–(38)		30.4

However, they are clearly larger than the Holocene animals. The process of diminishing body proportions in Africa is a universal phenomenon described in the literature (Linseele 2004). Data from Affad fits this trend well, considering the horncores discovered at AFD124. Their circumference at the base indicates that these were animals with very large, massive horns, their size comparable to the largest known examples for the European populations (Lasota-Moskalewska 2005).

3.5.11 Greater kudu (*Tragelaphus strepsiceros*)

Remains of this antelope, mainly characteristic horncore fragments, were discovered at site AFD24.

The greater kudu is a large antelope with clearly expressed sexual dimorphism. Its height at the withers ranges from 100 to 150 cm, and its body weight is 120–315 kg. The horns are found only in males and can reach a length of up to 120 cm. It can inhabit diverse environments, from savannah with an average rainfall of just 200 mm to deciduous forests with an average rainfall of up to 1000 mm. Kudu are especially common in areas and valleys with green, succulent brushwood, especially where they have access to the succulent leaves of Spekboom (*Portulacaria afra*). The kudu does not inhabit dense "closed forests" and treeless savannas, preferring instead a parkland forest with dense shrub vegetation. Males in particular concentrate in floodplain forests, wandering along water courses. Only in the dry season do herds of females transfer their foraging to the riverside zone. Kudu have a very varied diet of nearly 150 plant species (Kingdon et al. 2013/VI: 439). However, the leaves of woody plants, including the thorny mimosa (*Acacia* sp.) are a basic component of their diet.

3.5.12 Dik-dik (*Madoqua saltiana*)

Single fragments of the skeleton of the smallest African antelope were identified in the northeastern (trench 2012/B) and southwestern (2013/I) sectors of site AFD23.

The dik-dik is only 37 cm high at the withers and weighs up to 4 kg. These animals live in dry and dense shrubbery on the savannah where *Aloe* and *Sansevieria* are found. They feed on grasses and leaves or flowers knocked down by larger herbivores (such as elephants, antelopes or monkeys). They live alone or in small groups (Kingdon et al. 2013/VI: 323).

3.5.13 Oribi (*Ourebia ourebi*)

The oribi is the second most numerous antelope present in the collection from site AFD23 and at other locations in the Affad Basin [see ***Tables 3.3, 3.4***]. Scattered remains were recorded in the northeastern sector of AFD23 (trench 2012/B with extension 2013/D), the southwestern one (trenches 2013/I and 2014/N and 2014/O), as well as in the southern one (trench 2013/M) [***Table 3.19***].

This antelope reaches 60 cm in height at the withers and weighs from 14 to 20 kg. It is the largest of the "small" antelopes. Male horns measure an average of 10 cm in length (Stuart and Stuart 2006; Kingdon et al. 2013/VI: 406). The oribi live alone, in pairs or in small harem groups.

Table 3.19. Osteometric measurements of Oribi (*Ourebia ourebi*) remains from sites in the Affad Basin

Bone	Osteometry (mm)
Horncore – male	A-P. diameter base 25.3; TR. Diameter base 18.5
Horncore – female	A-P. diameter base 13.6; TR. Diameter base 10.5
Humerus	Bd-27.0
Radius	Bp-25.5
O. metacarpi	Bd-18.8
Talus	GLm-26.8

The oribi prefer flat or gently sloping meadows and parkland forests where seasonal fires maintain good grass pastures. The oribi occurs in areas where the average annual rainfall is between 500 and 2000 mm. The presence of the oribi is also conditioned by access to sources of drinking water (including dew), especially in areas where rainfall is scarce or occurs irregularly throughout the year. The ecosystems inhabited by the oribi vary from forests through tree savannah, open grasslands to wet riverside savannah and floodplains. Within each of these habitats, the oribi favors open microhabitats: pastures with short and middle-sized grasses with good visibility, but also shrubs that provide shelter. The largest populations of oribi are found in most tropical grasslands, where the average annual rainfall exceeds 1100 mm. Large oribi populations are also found in open floodplains. The oribi prefer the company of large, selective herbivores: plains zebra, wildebeest, hippopotamus, African buffalo, topi, Thompson's gazelle, and hartebeest, whose role is to keep pastures open to short grasses and help the oribi to avoid predators. However, oribi numbers dwindle wherever populations of large herbivores are in decline, thereby lessening the quality and availability of good pastures.

3.5.14 Bohor reedbuck (*Redunca redunca*)

Single skeletal fragments of the bohor reedbuck antelope were recorded in the southwestern (trench 2013/I with surveys 2014/N, O) and southern sectors (2013/M) of site AFD23. Reedbuck remains were also recorded at site AFD24.

Sexual dimorphism is clearly defined in reedbucks: males are larger, reaching 70–90 cm in height at the withers and 45–65 kg in weight, while the corresponding figures for females are 65–80 cm and 35–55 kg, respectively. These antelopes live both alone and in large herds.

Reedbucks inhabit mainly forests and floodplain grasslands. The most characteristic feature of the reedbuck's adaptation strategy is how it has adjusted to radical seasonal changes in its habitat, namely pastures with high-water levels during the flood-prone rainy season and dry, burnt vegetation in the dry season. Although the bohor reedbuck is heavily dependent on access to water, when choosing habitats, it favors vast floodplains and open floodplain grasslands, where access to water in the dry season may be severely limited. The bohor reedbuck's seasonal migrations from burned, overgrazed or waterless areas are local and typically only involve shifting of herds towards the water. In winter, during the dry season, these animals gather closer to water and fresh grass (Mammals of Africa, vol. VI: 431).

3.5.15 Kob antelope (*Kobus* sp.)

This is the most numerous antelope group in all of the explored sectors of site AFD23 as well as beyond the site [*Fig. 3.14*; see *Tables 3.3, 3.4*]. Identification to the species level was not usually possible for lack of diagnostic elements (relatively complete dentition). It can be presumed that this group includes more than one species (Osypiński, Osypińska, and Gautier 2011: 185–186). Osteometric measurements were supported by the state of preservation of the bones [*Table 3.20*].

In modern times, the kob antelope species known from the upper Nile basin are the *Kobus kob*, *Kobus megaceros* and *Kobus ellipsiprymnus*. Sexual dimorphism is clearly marked by color and the presence of large, spiral horns only in males (Stuart and Stuart 2006). The antelope live in harem groups, the young are born during the rainy season and become independent from their mothers at the age of 6–8 months (Estes 1974; Walther 1990; Falchetti and Mostacci 1993; Nowak 1999). During the rainy season the animals are spread over vast areas, but in the dry season they gather in larger groups around sources of water. Another very characteristic feature is the highly territorial nature of kob antelopes.

Fig. 3.14. State of preservation of kob antelope remains (*Kobus* sp.) from site AFD23

Table 3.20. Osteometric measurements of kob antelope bones from AFD23 (in mm). Measurements of material from the excavation in 2003 marked with an asterisk

Bone	Osteometry (mm)
Scapula	GLP-36.43; SLC-20.95 SLC-24.73; 33.08
Humerus	Bd-42.84; 41.07; 39.8* Bd-42.30; BT-38.73
Radius	GL-190; Bd-39.24; Bp-45.78 Bd-32.11; 37.65; 32.02; 31.5*; 34.2* Bp-42.92; 42.48; 39.40; 33.0*
O. metacarpi	GL-185.0; Bp-32.99; Bd-35.65 Bd-35.48 Bp-28.2*; 29.0*
Tibia	Bd-36.83; Bd-36.64; 36.37; 35.81; 34.46
Talus	GLI-42.38; GLm-37.89; Bd-22.46 GLl-42.2*; GLm-38.8*; Bd-24.6* GLl-40.89; GLm-43.6; Bd-25.33 GLl-38.51; GLm-37.54; Bd-22.09 GLl-38.3*; GLm-35.8*; Bd-21.7* GLl-37.63; GLm-36.78; Bd-22.18 GLI-36.12; GLm-35.09; Bd-21.21 Bd-22.29
Patella	GL-39.97
Centrotarsale	GB-25.64
Calcaneus	GL-85.44; 85.44
O. metatarsi III+IV	Bd-37.08; 28.12; 27.0*
O. metatarsi III	Bd-12.08; 11.62
Phalanx proximalis	GL-51.13; GLpe-49.95; Bp-16.29; SD-12.02; Bd-13.66 GL-48.83; Bp-16.72; SD-12.0; Bd-14.6; GL-47.88; Glpe-45.19; SD-11.65; Bd-13.24; Bp-17.7*; 16.57; 15.0*; 14.10 Bd-14.0; 13.42; 12.88; 12.38
Phalanx media	GL-30.77; Bp-16.85; SD-12.55; Bd-11.96 GL-28.0*; Bp-15.0*; Bd-12.0* GL-27.73; Glpe-26.26; Bp-14.71; SD-11.77; Bd-11.03 GL-26.96; Bp-14.26; SD-11.80; Bd-13.04 GL-26.01; Bp-11.43; Bd-9.76; SD-8.32 GL-25.3*; Bp-13.6*; Bd-11.0* Bp-14.71; SD-11.77; Bd-11.03 Bp-13.77
Phalanx distalis	DLS-43.71; 42.40 DLS-43.71 DLS-42.61; Ld-38.31 DLS-42.4 DLS-42.27; Ld-36.49 DLS-41.83; Ld-36.75 DLS-41.49; Ld-39.75 DLS-41.41; Ld-38.83; MBS-9.46 DLS-40.59; Ld-33.59; MBS-10.20 DLS-40*; Ld-35* DLS-39.0*; Ld-31.4* DLS-38.4*; Ld-31.6* DLS-37.7*; Ld-30.8* DLS-37.54 DLS-37.20; Ld-30.62 DLS-37.2*; Ld-30.6* DLS-34.5*; Ld-29.0*

The habitat inhabited by kobs is limited to areas of open and woodland savannah that have year-round access to water. They gladly inhabit riparian grasslands, floodplains, and large grassy clearings in parkland forests. It is believed that they favor a combination of forest cover and, at the same time, good visibility, that is, the edges of woodland areas, bush and forest. Research shows that the habitat favored by kobs is conditioned by a combination of the presence of other herbivores, seasonal fires, and a sufficiently high level of water. Such a set of factors creates the right conditions for the emergence of kob grasslands and habitats. It is even believed that this antelope species evolved to exploit and maintain floodplain grasslands. It has also been noted that the daily routine movement of kob antelopes along permanent routes determines the herd's attachment to permanent short-term grazing sites, while long-term fluctuations in the size of the population cause the development or decline of specific sites.

Males with a high degree of territoriality prefer to choose open areas near geographic discontinuities, namely gorges, slopes or other topographic obstacles. It has been observed that during their daily migrations between grazing land and water, it was in these places that the herds stopped even for several hours in order to gather more animals together and thus reduce the risk of a predator ambush (Kingdon et al. 2013/VI: 437–468). Females prefer areas of high visibility, recently burned, with access to young, short grass. Kob regularly visit mineral licks, access to which also affects the choice of a given habitat.

3.5.16 Waterbuck (*Kobus ellipsiprymnus*)

The inability to clearly identify to species most of the kob antelope remains makes it possible that some of the "alarmingly large" fragments could have come either from male kobs or from a species of waterbuck, which is still found in habitats corresponding to what Pleistocene Affad would have looked like, like the Dinder National Park in Sudan. It is a very water-dependent species that occurs in parkland forests and shrub savannah, in areas where the annual average rainfall is within the range of 400–1600 mm and temperatures range between 13°C and 37°C, which is optimal for waterbucks. The largest populations of waterbuck can be found in areas featuring lakes or well-watered valleys with an abundance of good quality grassland (Kingdon et al. 2013/VI: 461). A waterbuck's range is always limited by the need to stay in close proximity to a permanent water source during the dry season. In the rainy season, female herds are more scattered over a large area. Interestingly, the waterbuck's diet and behavior vary with the latitude and climate. For example, in western Uganda, the waterbuck has not been found in open grassland. Their preferred habitats are grasslands with a moderate level of tree density, near a lake where there are no lions. Male preferences regarding habitat change with age: from parkland forest, through dense bush and open bush, to open grasslands. In other areas, such as the Dinder National Park, the waterbuck favors predominantly riparian forests [*Fig. 3.15* bottom right].

3.5.17 Hartebeest (*Alcelaphus buselaphus*)

A small number of hartebeest remains were recorded at site AFD131.

This is a large antelope weighing from 75 to 200 kg and reaching a height of 110–150 cm at the withers. Hartebeests form large herds of up to 300 individuals. Although hartebeest cows inhabit grasslands, they will shy away from the vast grassy plains, preferring instead areas on the forest fringe or clearings in parkland forests. The occurrence of hartebeests is strictly dependent on access to drinking water and access to suitable grazing lands, which must have an abundance of medium and long grasses. Excessively large populations of, for example, wildebeest in Kenya caused the disappearance of hartebeests. However, in a situation when torrential rains caused the grass to grow back to a longer level, the wildebeest disappeared and the number of hartebeests abruptly increased (Kingdon et al. 2013/VI: 510).

3.5.18 Nile monitor (*Varanus niloticus*)

Nile monitor remains, represented only by vertebrae, were present in both the northeastern (trench 2012/B) and the southwestern (trench 2013/F) sectors of site AFD23. It was the only reptile species found at this site.

This animal reaches a significant size—up to 170 cm in length—and inhabits the banks of larger rivers practically in all of Africa, including the Nile. It feeds on small game and carrion.

3.5.19 Fish from the catfish family (Clariidae)

Archaeoichthyological analyses of the material from the Pleistocene sites at Affad indicate the predominance of remains of fish from the Clariidae family, suggesting a possible specialization in catching fish from this group. Clearly identified "concentrations" of fish remains were in fact distinguished as separate sites (AFD84 and AFD113). Apart from these, fish remains were recorded in minimal numbers at other sites (AFD23, AFD24, AFD131) [see ***Table 3.3***].

The data seem to suggest that fish may have been harvested by humans seasonally and occasionally. The choice of catfish could be related to the behavior of this ichthyologic group, part of which is that many species that normally live in open waters spawn in the shallows. It is then that these fish, often growing to large sizes, become relatively easy prey. Such hunting techniques, taking advantage of the seasonal availability of fish, are reported from MSA communities in various regions of Africa, such as the Congo (van Reybrouck 2016).

The finding of oyster shell concentrations with traces of overheating, recorded at AFD134, also points, in the authors' opinion, to an occasional exploitation of aquatic fauna resources, possibly related to seasonal availability. The fish and clam harvesting techniques at Affad can be classified as part of gathering rather than hunting/fishing.

Whether fish or mollusk, these concentrations bear witness to a wide variety of adaptation strategies presented by humans exploring the various ecological niches in the Affad Basin in Late Pleistocene times.

3.6 ECOSYSTEM: BIOCENOSIS AND BIOTOPE

The behavioral and environmental data concerning animals, the remains of which have been discovered at the archaeological sites in Affad, record a wide range of environmental features essential to the sustaining of these species in the Affad Basin about 50,000 years ago.

Judging by the behavioral data, it seems that we are dealing with two main groups of animals inhabiting two similar, although slightly different biotopes. One is an ecosystem directly related to rivers, namely floodplains, reed beds, riparian grasslands, riverside thickets and riparian forests. Animals inhabiting this biotope comprise the hippopotamus, kob antelope, cane rat, oribi, reedbuck, crocodile, Nile monitor and, of course, fish and bivalves. The other ecosystem clearly attested by the faunal remains functioned in close proximity to permanent sources of water, but was drier: areas of woodland savannah, open grassland spaces, parkland forests with the presence of large trees, but also specific species of both trees and grasses. Access to expanses of good grazing land, rich in a variety of grass species, is crucial here. The species inhabiting such a biotope comprised: buffalo, giraffe, hyena, plains zebra, porcupine, wild pig, greater kudu and, most likely, the now extinct auroch. Species making good of both habitats are also present among the remains from Affad: African buffalo, grivet monkey and elephant.

From the viewpoint of the environmental requirements of animal species known from Affad, the Affad Basin area approximately 50,000 BP lay within the range of a climatic zone with annual rainfall ranging from about 300 mm to about 2000 mm and temperatures from 15°C to 40°C. It was an area rich in grass species (high, medium and low) kept at bay by seasonal fires. Acacia (*Acacia* sp.) and *Panicum* grasses were surely found here in large numbers. The area had to be topographically diverse, with natural mineral licks and waterholes.

Taking into account all of the habitats of the Pleistocene animals from Affad, along with other environmental and climatic indications, Affad is proposed to have lain within the range of the so-called "Northern savannah" representing currently two biotic zones: the slightly drier Sudan Savannah Biotic Zone (SSBZ) and the more humid Guinea Savannah Biotic Zone (GSBZ) (Happold and Lock 2013). The latter zone in particular has the features essential to almost all of the animal species recorded at Affad. The GSBZ comprises areas directly north of the rainforests. These vast areas, called a "savannah derivative" or "forest-savannah mosaic", surround the rainforest biotic zone. They constitute a mix of forest and savannah habitats, often with sharp boundaries resulting in a complete change in plant species composition over a distance of about 100 m. Today, the GSBZ stretches from the edge of the rainforest in western Africa to northern Uganda in the east. East of the Nile, in Uganda, this zone is characterized by extensive parkland forests known as "tall grass–low tree savannahs". Typical trees in this zone include, for example, *Daniella oliveri*. In Uganda, one may also find the shea nut tree and tree species such as *Terminalia* and *Combretum*. The average annual rainfall in the GSBZ is 800–1500 mm, while the rainy season lasts 7–8 months (March–October), sometimes with a short dry season in July and August. Typical vegetation in this zone consists of open forests with very rich, dense and tall grasses, which reach a height of 2–3 m at the end of the rainy season. As the dry grass season passes, the grasses die off and thereby provide the fuel for the intense annual fires typical of this zone. These fires reduce the amount of dry vegetation and stimulate the growth of new grass, which is attractive food for many herbivores. Most of the trees reach a height of 10–20 m. They have thick fire-resistant bark

and specific mechanisms that protect germinating plants. The GSBZ is divided into northern and southern zones described by the occurrence of different tree species. A point to emphasize is that the GSBZ is characterized by instability, with its borders undoubtedly changing significantly over past millennia.

The SSBZ stretches from the Atlantic Ocean to the Ethiopian highlands and northern Uganda. The temperatures in this zone are 24–28°C, with annual rainfall in the range of 500–800 mm. The rainy season lasts 4–6 months (from May to October). It is considered primarily as a transition zone between the Sahel and the GSBZ. Today, the eastern part of the SSBZ runs from the Cameroon Highlands to the western lowlands of Ethiopia. In the north it forms a strip of dry meadows and acacia savannahs, while in the south it takes the form of a forest-savannah mosaic. The SSBZ is characterized by the coexistence of trees and grasses. The dominant trees are *Combretaceae*, *Caesalpinioidae* and acacia, which is also important for this ecosystem. It is a region where there are also trees such as the baobab, shea or the Locust-bean tree. The dominant grasses are Andropogoneae (especially Andropogon and Hyparrhenia, and Loudetia and Aristida in the floodplain areas. Today, SSBZ areas are intensively used mainly as grazing land for cattle (sic!).

Fig. 3.15. Dinder National Park landscape analogies (dry season): a – clumps of tall grasses growing on the banks of the Dinder River channel; b – sandy riverbeds by the main river channel; c – drying pools on the floodplains; d – woodland savannah surrounding the floodplain

With regard to the contemporary range of biotic zones, Affad is located in the Sahara Arid Biotic Zone (Happold and Lock 2013), while the range of potential ecosystems postulated for this area during the Pleistocene, that is, the Sudan/Guinea Savannah Biotic Zones is from 2000 km to 3000 km further to the south. This illustrates the range of climatic and ecological changes in the area over approximately 50,000 years. While simple translations of the realities of contemporary biotic zones into palaeo-environmental reconstructions are something to beware off, there is a great likelihood that the environment of late Pleistocene Affad resembled the contemporary savannah zones described above, even keeping in mind the undoubted specificity of the topography, geological base and circulation of air masses in the region under discussion [*Fig. 3.15*].

3.7 FOLLOWING THE GAME: MIDDLE STONE AGE HUNTING BEHAVIOR IN THE AFFAD BASIN

Modelling environmental exploration strategies, especially hunting and game acquisition practiced by the Pleistocene communities around 50,000 BP is possible based on archaeozoological data from the Affad Basin. The research involved frequency analyses of individual animal species and classes represented in the material. Evidence of hunting specialization and preferences for animals of certain size classes was observed at particular sites. The prime objective was to search out any regularities that could suggest a conscious choice by MSA groups of hunting models already known from ethnographic analogies.

Similar studies of hunting models undertaken much earlier in South Africa (e.g., Clark and Kandel 2013) had assumed that the MSA communities preferred game with the highest positive correlation coefficient of energy gains relative to costs incurred for its acquisition. Ethnographic and empirical studies have confirmed this idea, showing that in the hunting ranking of preference, animals with greater body weight but less dangerous nature are usually preferred. Such creatures have a clearly higher rank than smaller animals.

The present study used the same methods previously employed in South Africa, namely a simplified classification of fauna from archaeological sites, grouped into several size classes, modified to adapt to the size classes of East African animals. The size classification of individual species was based on data from Gagnon and Chew (2000) and Kingdon et al. (2013). The table was restricted to mammals. Five age classes were distinguished arbitrarily based on the vital weight of individual species recorded at the Pleistocene sites at Affad [*Table 3.21*]. One of the important advantages of the method of classifying species by size is the possibility of using in the analyses remains identified at lower taxonomic levels, namely genus, family or order. For the study, four sites were selected with a sufficiently large sample of remains of diverse fauna occurring in context with numerous lithic artifacts, namely AFD23, AFD24, AFD111 and AFD131.

Surprisingly, the two models of hunting preferences that emerged were clearly different. The first model was characterized by a preference for animals of class III, namely medium–large, that is, weighing 60–400 kg. However, the percentage of remains of class II (11–59 kg) and class I (2–10 kg) animals, that is, small animals, on one hand, and megafauna, mainly class V hippopotamus (>1500 kg), on the other hand, turned out to be relatively high. The second model

Table 3.21. Size classes of animals from late Pleistocene sites in the Affad Basin

Size class		Approximate weight (kg)	Examples
I	Small	2–10	grivet, dik-dik, cane rat
II	Small–medium	11–59	wild dog, hyena, bushpig, porcupine, oribi
III	Medium–large	60–499	equid, kudu, hartebeest, kob, waterbuck
IV	Large	500–1500	giraffe, auroch, buffalo
V	Megafauna	>1500	hippopotamus, elephant

Table 3.22. Percentages and proportion of animal remains of various size classes in material from MSA sites at Affad

Size class	Weight range	AFD 23 (NISP=1901)		AFD 111 (NISP=340)		AFD 24 (NISP=353)		AFD 131 (NISP=771)	
I	Small (2–10 kg)	8.3%	158	2.6%	9	0.5%	2	5.57%	43
II	Small–medium (11–59 kg)	9.5%	182	42.3%	144	2.5%	9	2.2%	17
III	Medium–large (60–499 kg)	67.9%	1291	39.0%	132	22.6%	80	19.7%	152
IV	Large (500–1500 kg)	0.5%	11	15.8%	54	73.6%	260	72.1%	556
V	Megafauna (>1500 kg)	13.6%	259	0.3%	1	0.5%	2	0.4%	3

revealed a very clear predominance of animals from class IV, that is, large animals weighing in the range of 500–1500 kg, with little interest in animals from other size classes [*Table 3.22*].

One could also observe another division, based on environmental factors. As described in the previous section (§ 3.6), mammals in the Affad Basin inhabited two slightly different biotopes: a wetter one, strongly associated with water, backwaters, riparian thickets and floodplain forests (kob/waterbuck, hippopotamus, cane rat, oribi, bushpig, crocodile, fish, Nile monitor), and one with a more open environment, that is, a woodland savannah, extensive grasslands, parkland forest with large trees and acacia (zebra, giraffe, hartebeest, elephant, African buffalo, greater kudu, hyena, dik-dik, grivet).

A similar, dichotomous view of hunting preferences was observed by a team studying MSA and LSA (Late Stone Age) hunting models in South Africa (Clark and Kandel 2013). Two models were also observed there. One was "flattened/broad", covering both small mammals and the largest and dangerous ones. The other one was much more "specialised", targeting African buffaloes (*Syncerus caffer* and *Pelorovis antiquus*) and eland antelopes (*Taurotragus oryx*). At Affad, aurochs (*Bos primigenius*) would have been the analogous "hunting preference", along with African buffaloes (*Syncerus caffer*) and occasionally giraffes (*Giraffa camelopardalis*). The factors suggested to have an impact on an alternate functioning of hunting preference models, according to the South Africa study, were climatic, behavioral, cognitive and economic.

Hunting models determined for the MSA and LSA predicted that animals of first choice were those with the most favorable energy gains ratio relative to costs incurred in tracking, pursuit and the risk of confrontation. Only in the event of a decrease in the availability of animals of first choice would hunters extend their list of game species to include animals of lower categories: on the one hand, the small animals down to the smallest, and on the other, the large animals, including the most dangerous ones. Ethnographic and empirical studies have shown that in individual hunting the rank of the prey is closely related to the animal's body size. Thus, large animals are generally higher in the hunting ranking preference than smaller animals. Accordingly, an increased interest in the species of small animals may indicate an increase in the range and variety of one's diet.

An alternative approach to the presence of large and aggressive animals in the hunting model treats them as an indicator of high-level hunting abilities, and thus also the cognitive abilities of a given human group. Should we adopt a completely rational interpretation, however, then the assumption is that aggressive animals, such as buffaloes, should have a relatively low position in the ranking preference. This is because hunting dangerous animals can potentially pose a greater risk and therefore will come at a higher cost in relation to the benefits. Hence the small number of large predators, for instance, present in the osteological material.

Hypotheses linking changes of the hunting model in the MSA to climatic changes and the availability of large ungulates—highest ranked according to the preference models—affected by environmental changes have also been proposed (Clark and Kandel 2013). It has been observed that large and very large ungulates occur more frequently in interglacial/interfluvial periods, MIS 5 and 3, than in MIS 6 and 4. Given that larger ungulates occupy more open environments, this may indicate that differences in the presence of the largest ruminants are associated with changes in their availability to hunters.

Demographic factors can also be considered, although it is of course extremely difficult to identify possible demographic changes in the Pleistocene communities in Africa. It is a possibility, however, that a widening range of environmental exploration observed from MIS 6 to MIS 4 could be associated with pressure caused by a growing population or the existing human groups drawing nearer to one another.

In cognitive terms, a non-linear adaptation of innovative technologies and behaviors is a characteristic of the MSA. While the level of hunting skills of late Pleistocene communities is not in question at present, it is not explicitly accepted that a greater presence of large or dangerous animals in the hunting model signifies growing cognitive abilities of the hunters. Neither has it been demonstrated satisfactorily that technological tool differentiation (MSA versus LSA) could have made a difference with regard to the hunting model adopted. The Affad discoveries have contributed significantly to this disussion, showing a correlation of different factors that had previously been considered either separately or not at all. The Late Pleistocene Affad sites, representing both hunting models typical of the MSA, are located in a limited, relatively small area of the Affad Basin. Their high cognitive value is also influenced by their nature, that is, open-air instead of closed cave sites. The narrow chronological frame is important as well. Geomorphological studies correlated with OSL dating indicate that the Affad Basin formed and was settled by humans over a relatively short period of time, between 55,000 and 45,000 years ago. Therefore, the timespan is not hundreds of millennia but a few or several thousand years.

From the point of view of the present authors, there is no indication in the literature dealing with the issue of hunting models in the Pleistocene that the research does not concern sedentary communities and that the faunal remains discovered by archaeologists do not, in a simple way, reflect the year-round diet and generally the hunting model chosen by a given group. Although the Affad research supports the idea of a high level of behavioral flexibility of the late Pleistocene people, for whom the main factor shaping the diet, but also the selection of raw materials, would have been the availability of these resources, whether a given group of animals or a specific stone raw material. The hypothesis proferred on the basis of the Affad finds, slightly different from the one discussed above, is that the diversity of hunting strategies among MSA communities and the exploration of fauna in different (although similar) environments can be explained by a seasonal differentiation of environmental exploitation. The "broad/flattened" model, with a large share of middle-sized and small animals, but also with the presence of megafauna, may, in the case of the Affad microregion, reflect the exploitation of a closed and wet environment, namely riparian forest and floodplain bush. This zone, and activities related to its exploitation by humans, may have been possible mainly and maybe only in the dry season.

Data from lithic analyses also support the hypothesis of the exploitation of the floodplain, mainly in the dry season. Acquiring and functional testing of large nodules of chert lying in the watercourse beds was possible only at low water level, precisely what would be expected during the dry season. Workshops for the pre-processing of blocks of chert (at site AFD23, for example) were located on elevations of the terrain, in the vicinity of watercourses and together with the remains of fauna typical of the floodplains, illustrating at the same time a "broad" hunting model.

The second hunting model identified at Affad would correspond to the exploitation of the environment during the rainy season, away from the flood zone, which was then inaccessible and dangerous. Human groups could move at this time to higher-lying arid areas, a more open area of woodland savannah inhabited by large ruminants—aurochs, giraffes, zebras and antelopes. This type of strategy, reflecting the choice of a more specialized hunting model targeting large ungulates, is observed at sites AFD24, AFD131, but also indirectly at AFD124, AFD110 and AFD120. This hypothesis is supported not only by archaeozoological data, indicating the dominance of fauna from more open environments, grassland-savannah and woodland savannah. The topographic data also seem to provide arguments in favor of this line of reasoning, because these sites were located north of the zone of sites with floodplain fauna, towards the uplands and the foothills of the Mesozoic inselbergs. A characteristic feature of lithic products at these last sites (i.e., AFD124, AFD131, AFD120) is the lack or low share of chert as a raw material for tool production. At sites with a dominant proportion of large ruminant remains (mainly aurochs), ferruginous sandstone was definitely preferred as the raw material, being easy to obtain on a plateau about 4 km away.

The concept of seasonal diversification of animal protein harvesting strategies is further supported by the few sites with solely fish remains (e.g., AFD113). Interestingly, archaeo-ichthyologic analyses seem to indicate intentional selection of fish of a certain size from the catfish family. The fish remains from the sites at Affad belonged to mature animals. Their catching was most likely related to the behavior of fish from the *Siluriformes* order and their spawning period in the shallows in the rainy season. Species identified in the Affad basin usually spawn in shallow bodies of water in the floodplains (Van Neer, Augustynen, and Linkowski 1993; Van Neer, Paulissen, and Vermeersch

2000; Van Neer 2004). Apart from typically shallow-water species, two species (*Bagrus* sp. and *Synodontis* sp.), associated with deeper parts of the river's main course, were also identified. Their presence has not yet found analogies in the Pleistocene collections. Perhaps they were available in the deeper branches of the channel system of the then Nile. Were this to be the case, it would mean that the fish could also be caught outside of the spawning season. The role of small fish, usually present in shallow floodplains or drying ponds, is unclear as no remains have been reported in surface (hand-gathered) collections.

Interestingly, there are no fish in the material from the AFD23 site (most probably inhabited during the dry season), except for one bone—possibly a randomly deposited item (a significant cluster of fish remains labelled as AFD84 was located a hundred meters to the north of the AFD23 limits). Fish remains were more numerous at the hypothetical "summer" sites related to the rainy season, that is, in the model with a predominance of large ruminants (AFD131, AFD120).

An important element in these considerations is the observation that the animals of first choice, regardless of the biotope or season, were the less-skittish ruminants: kobs in the dry season and aurochs in the rainy season, so much preferred in the "summer" hunting model that they practically eliminated other species of hunting interest. This indicates a kind of hunting specialization and, importantly, the high availability of these animals in the ecosystem of that time.

The hunting specialization focused on aurochs that has been observed in Affad is all the more important because it can be considered as the first step towards further adaptation strategies, meaning the willingness to "control" herds and to follow them, which is sometimes postulated in considerations regarding adaptation strategies of early Holocene communities (Wendorf 1968; Close 1984).

Even so, hypotheses concerning the seasonality of hunting strategies, their diversity and the exploitation of various ecosystems cannot be put forward without making some reservations. It is a very attractive concept that assumes that the sites at Affad illustrate, to some extent, the year-round adaptation strategies of people in MIS3, based on seasonality, allowing them to exploit various zones and methods of acquiring available animals, depending on the season. However, from a much broader chronological perspective, possibly spanning tens of thousands of years, it is plausible that differentiated models of fauna exploitation would have rather reflected climate and environmental changes and the necessity to adapt, as has been suggested with regard to southern Africa.

3.8 RECAPITULATION

A holistic consideration of environmental adaptation strategies by MSA communities in the Middle Nile Valley is one of the most important results of the archaeozoological studies of the community site complex at Affad representing a technological and behavioral model typical of the MSA. In turn, the discovery of auroch remains has broadened considerably knowledge of the range of this species in the late Pleistocene in northeastern Africa. They have provided new arguments in the palaeontological discussion on the origin of the *Bos* genus in Africa, as well as in the discourse on the origin of the presence of cattle in the early Holocene in eastern Africa. Of particular importance is the clear hunting specialization concerning these large ruminants,

which indirectly indicates their commonness and a significant position among late Pleistocene fauna. The Affad data also provides important information on hunting patterns. An apparent consistency with what has been observed in South Africa is interesting to consider. In the Nile Valley two hunting models can also be observed, namely broad and specialized. Additionally, at Affad, we can link them with the exploration of slightly different ecological niches. Up to now, no such considerations have been undertaken for northeastern Africa and the Middle Nile Valley. The occurrence of specific factors leads us to propose a new hypothesis on the basis of a binary differentiation of hunting models in the MSA community, enriching it with the aspect of seasonality. Detailed archaeozoological analyses also expand current knowledge of the range of individual mammal species in the Pleistocene. The Affad research shows that over the last 50,000 years there has been a drastic (2000–3000 km) shift to the south of the savannah environments with which the MSA communities in the Nile Valley were closely related.

CHAPTER 4

LATE PLEISTOCENE LITHIC PRODUCTION IN THE AFFAD BASIN

The lithic production from the late Pleistocene horizon in the Affad Basin was studied based on the whole collection of finds, from both legs of the project, including also some material collected from site AFD23 in the early pre-project survey stage (see Chapter 1). The material has been studied in detail for Piotr Osypiński's doctoral dissertation and is presented here *in extenso*, in a manner not common in African prehistoric studies, which includes also refittings and a tentative reconstruction of the *chaîne opératoire* of stone tool-making in the Affad Basin. Based on the results, a case has been made for the stone-tool production materials and processes in this region in the Pleistocene.

The chapter opens with a description and discussion of the lithic material discovered at site AFD23 (§ 4.1). The finds are presented in a sector-by-sector basis (southwestern, southern, northwestern, northern and northestern), marshalling the archaeological stratigraphic data in order to identify patterns of dispersal and propose functional identification of the various artifact clusters, often in relation to concentrations of animal bones (for a discussion of the latter see above, Chapter 3). The presentation follows the same formal scheme in all cases: first a presentation of the general morphological-technological structure of the collection, a discussion of the raw material, followed by a technical description of the different categories—cores, flakes, chunks and, last but least, predetermined products and formal tools. This section also includes a brief presentation of methods of analysis (§ 4.1.2) and raw material structure (§ 4.1.3), which holds for the study as a whole.

The most extensive part concerns the southwestern sector of site AFD23 with material discussed separately for the four clusters of finds: western, southwestern, eastern and southeastern). This material was also subjected to a painstaking refitting of blocks—44 were identified—and the results of this work appears in § 4.1.4.2 and includes mapping of the dispersal of individual fragments pertaining to each block, description of joining fragments, drawings of individual pieces, some photos and in two instances a reconstruction of the *chaîne opératoire*. The detailed presentation supports a discussion of the lithic production at site AFD23 broken down by the sectors (§ 4.2). In effect, suggestions are made concerning the functionality of the different zones.

The same order of presentation of the lithic material (without block refittings) is followed in the section bringing together the results from other sites in the Affad Basin investigated by the Project, either by excavation or field survey, starting with the oldest currently known evidence of settlement in the area (§ 4.3). The discussed sites are (in order): AFD111, AFD131, AFD120 and AFD122, AFD24, and the killing sites AFD110 and AFD124, and fish- and mollusk-gathering sites AFD113 and AFD34. In the case of each of the sites, the presentation ends with a recapitulation of the findings, including evidence of observed use-wear (for a report on use-wear traces see the appended lab report).

The results are discussed comprehensively in the last section (§ 4.4), which is dedicated to a characteristic of traditional MSA strategies for procuring stone tools, postulating an equal measure of copying as well as collecting of earlier products for reuse.

4.1 LITHIC MATERIAL FROM SITE AFD23

The lithic artifacts discussed in this section represent the entire available collection of finds from the Affad 23 (AFD23) site, from the earliest ground survey by the Polish Joint Archaeological Expedition to the Middle Nile Valley conducted in 1999 through the latest grant project dedicated to a study of adaptation strategies of the sub-Saharan societies in the terminal Pleistocene and early Holocene (for a history of research at the Affad 23 site and in the Affad Basin in general see the Introduction).

4.1.1 The lithic finds collection

The first archaeological finds from the site included 11 flakes: one of yellow sandstone and the rest of chert. Five of them had facetted striking platforms. Those of a Middle-Palaeolithic type, accompanying finds of heavily mineralized animal bones, were found to be in relatively good condition. The ground survey in 2003 added 1931 lithic artifacts (initially reported erroneously as 2014 due to a counting error; Osypińska and Osypiński 2003). In view of the possibility to continue studies of this material in Poland, a certain amount determined by weight was selected, taking into account the varied state of preservation of the finds and concentrating on samples promising effective refitting of blocks. Patinated and eroded objects with rounded edges, most of them chunks or initial flakes were rejected [*Fig. 4.1*]. In the end, the collection brought to Poland counted 1283 lithic artifacts (66% of the collection). (The different figure of 1242 artifacts given in Osypiński, Osypińska, and Gautier 2011 resulted from assumptions made at that time concerning certain flakes [so-called unintentional breaks]. The state of preservation and the possibility of refitting artifacts, rather than the nature of the raw material, were crucial when selecting finds for further study.)

The collection was augmented in 2012–2014 by 4521 lithic artifacts, which could now be categorized as coming from either primary or secondary archaeological contexts based on the stratigraphic observations made during this phase of the research (see Chapter 1). Contexts of a secondary nature comprised sediments occurring relatively later than loose silts and sands, recorded in various sectors of the site and contemporary with settlement (category 2 contexts). They also included silts carried by flooding directly after the settlement episode (category 3 contexts), as well as significantly later sand and gravel units of a Holocene nature, together with modern surface weathering (category 1 context) (for a discussion of sedimentation processes in the area see Chapter 2). In light of the new spatial data, the planigraphy of finds from 2003 was re-examined for evidence of tentative post-depositional relocation [*Fig. 4.2*]. Another shipment of finds was sent to Poland, leaving behind, as before, most of the chunks and initially processed stone nodules [see *Fig. 4.2* top].

The 300 additional lithic artifacts collected in the final stage of the project through 2018 did not counter any of the conclusions formed on the basis of the already studied material. The finds came from the northwestern zone of the site, as well as some sectors of the southwestern zone, along with some additional samples. The collection that was transferred to Poland is now in storage at the Institute of Archaeology and Ethnology of the Polish Academy of Sciences, whereas the finds left in Sudan are stored at the Banganarti Archaeological Station.

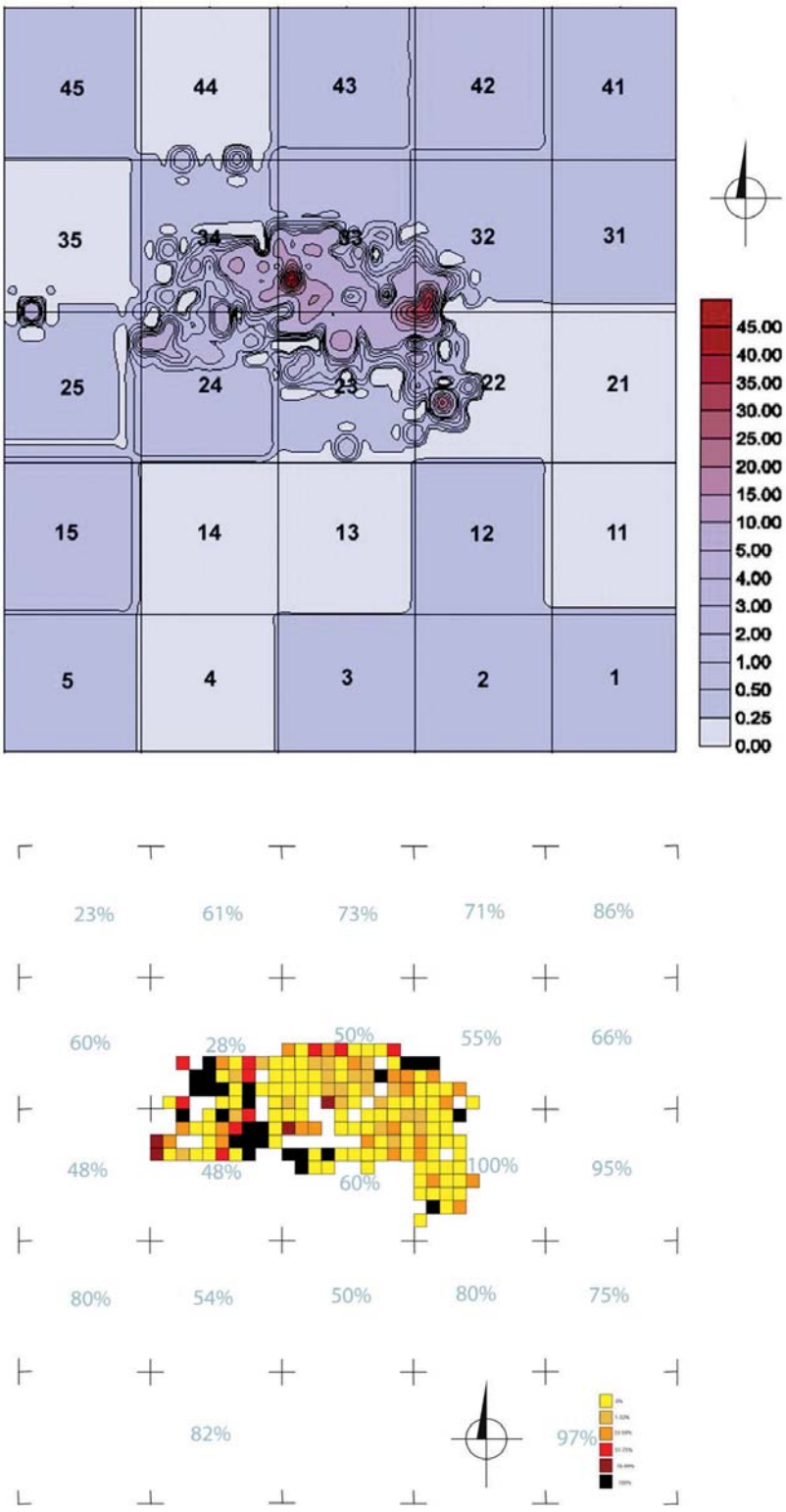

Fig. 4.1. Site AFD23 (2003): top, frequency of lithic artifacts on the surface (investigated area 50 × 50 m within a larger grid of exploratory units referred to by the numbers), proportions per square meter signified by color; bottom, percentage of lithic artifacts not selected for further detailed study; values for the investigated area 50 × 50 m in color, for the exploratory units of the larger grid in numerical form

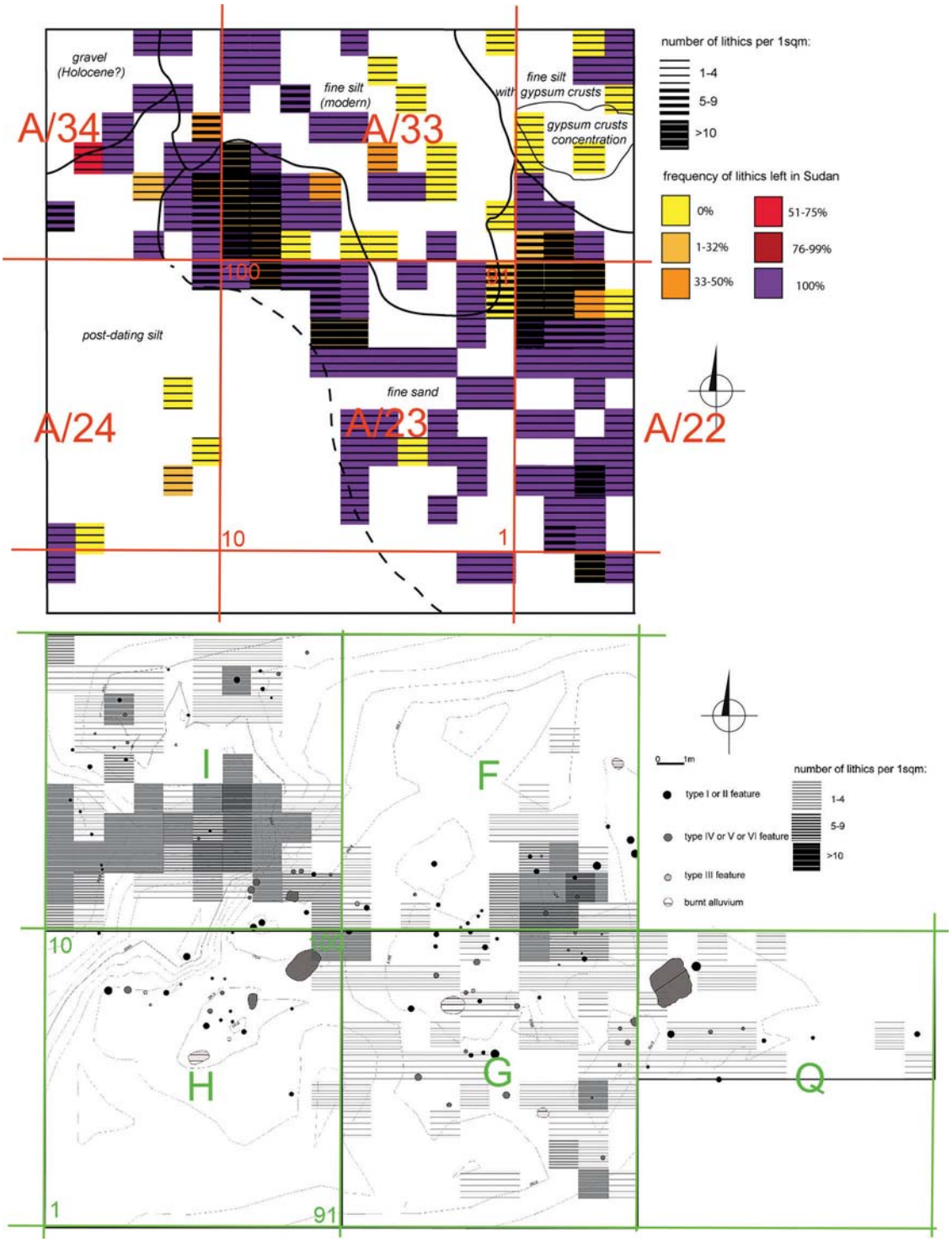

Fig. 4.2. Site AFD23: top, trench 2013/F–I (state of exploration in 2013), frequency of lithic artifacts in the first subsurface level to a depth of 10 cm (investigated area 20 × 20 m), superimposed on a mapping of stratigraphic units and exploration grid from 2003 (marked in red); proportions presented per square meter with the percentage of lithic artifacts not selected for further detailed study marked in color; bottom, trench 2013/F–I and 2014/Q (state of exploration in 2014 with new exploration grid marked in green), frequency of lithic artifacts from primary contexts superimposed on a hypsometric map of the Pleistocene landscape and cut features (explanation of the types of cut features in Chapter 5)

4.1.2 Methods of analysis

Stratigraphy, both vertical and horizontal defined the separate nature of particular batches of lithic material from the AFD23 site. Isolated concentrations of artifacts noted in different parts of the site resulted in a division, in 2016, of the explored area into four sectors, namely northern (trenches 2012/C+2013/E), northeastern (trenches 2012/B+2013/D,J,K), southern (trenches 2013/L-M) and southwestern (trenches 2013/F-I, Q+2014/O-W [see *Fig. 1.8*]. Recording of lithic artifacts within these sectors included an indication of the geomorphological context determining position relative to sediments of Late Pleistocene age (primary or secondary; see *Table 4.1*). In the southwestern sector, where the largest concentration of lithic artifacts was observed, four clusters were distinguished, lying most likely in a primary context (that is, not redeposited as a result of natural factors or constituting a fake clustering of artifacts). A stratigraphic assessment of the find contexts formed the basis for an analysis of functional differentiation of encampment space in terms of deposition of debris from stone-tool production and other associated activities.

The basic classification and graphic presentation of the Affad lithic material follows universally accepted academic principles (Schild 1980; Ginter and Kozłowski 1990; Inizan, Roche, and Tixier 1992; Andrefsky 2005). Calipers were used to measure the parameters of each artifact with an accuracy of 1 mm; length (in the case of flakes measured along the technological axis in similarity to Levallois cores), width of the central section and thickness in the same place. Typical artifacts from each morphological category were also documented in drawing and photography, retaining standards of technical projection and scale. Artifacts were assigned unique numbers and catalogued in a digital database (Microsoft Access®) including all morphometric data.

Raw material identification depended primarily on macroscopic observations, compared with current knowledge on the origins of particular rocks and their usage by prehistoric societies of the Middle Nile Valley (Whiteman 1971; Marks and Mohammed-Ali 1991; Osypiński 2010). The rock raw materials were divided into six major groups as follows: 1) cryptocrystalline chert, 2) translucent flint, 3) mudstone and agate, 4) coarse-grained amorphous quartzitic sandstone, including ferruginous sandstone, 5) crystalline quartz, and 6) other raw materials with a mosaic internal structure (so-called conglomerate, as well as petrified wood). The purpose of this was to explore prehistoric preferences for particular raw materials and the inclination to choose rocks with the most similar properties. Within the most numerous group of chert artifacts, variants were distinguished by color (determined with the aid of color tables included in the Munsell Soil-Color Charts, 2010 edition) and the presence of macroscopic chemical precipitates or inclusions. This was particularly useful for the reconstruction process of certain nodules and for estimating the number of discrete objects. Examination of the state of preservation of the outer surface of nodules subjected to prehistoric processing served to indicate the primary or secondary geological context of the exploited sources.

The technological structure of particular collections of artifacts was presented using a formal division into: 1) cores, 2) flakes and initial flakes, 3) chunks, and 4) final products in the form of tools (retouched or non-retouched) based on the assumption of a predetermined nature of production processes. This division refers to the concept of a *chaîne opératoire* (Leroi-Gourhan 1964), a production cycle assuming a relationship of a technological nature between elements of a lithic assemblage.

The group of cores includes initial forms (including nodules/pre-cores with initial flaking negatives), cores with a legible defined surfaces schema, as well as striking platform preparation, adhering to a concept defined in the literature as Levallois technology (Boëda 1986; 1995), as well as residual cores of a reduced form matching the discoidal schema. Also distinguished were small discoidal cores produced from crude flakes, as well as microlithic single-platform cores; both of these categories match different non-Levallois production schemas.

A range of morphological and metric features determined the composition of the group of initial flakes, as well as chips (flakes no greater than 2 cm in size). A basic criterion adopted for the division of the flakes was the form of the butt: cortical (unprepared, comprising a piece of the original external surface of the nodule), with a plain/unifacial, edged (including the point), or multifaced straight or convex butt (excluding facetted products with the butt formed into a *chapeau-de-gendarme*). The last category were distal flakes/chip fragments. The angle of the butt and the ventral/positive surface were also noted (a feature defined as the flaking angle). Within each flake category, a graphic presentation was made of the metric features (length–width and width–thickness correlation) labelling the raw material as well as find context, in order to indicate relationships between artifacts demonstrating similar technological features (including homogeneity in terms of production), but also to be able to compare flakes from different categories. This procedure resulted from preliminary assumptions regarding the dominant part of flakes from the various categories (meaning with different striking platforms) being related to different phases in the reduction of the nodule. For each flake category (including predetermined artifacts) an assessment was made (as a percentage) of the covering of the dorsal surface with natural surface of the nodule. Thanks to a large sample, a detailed assessment of flake damage (transverse break, longitudinal fractures, overheating or erosion of the edge and surface) permitted the scale of the impact of post-deposition factors on artifacts from assumed primary or secondary contexts to be estimated. Moreover, the size of the sample of chert flakes from the southwestern zone of the site (especially from a primary context) allowed for the identification of a pattern that facilitated a comparative study of many components of the assemblages from the different zones of the site (as well as from other sites).

The group of chunks, meaning products devoid of features of cores and flakes, but bearing traces of having been intentionally split, included foremost fragments of raw materials with a provenance or purpose impossible to establish. On the assumption that they represented production debris not fulfilling morphological or volumetric criteria, only their dimensions and origin from a primary or secondary context were described.

The metric characteristics of the final product group (predetermined flakes and points, as well as retouched forms) were characterized analogically as in the case of flakes. A supplementary outline of these items was presented in the form of detailed description of the relief of negatives on the dorsal surface, details of the butts, along with the form and location of retouching. The distribution of these products in relation to the concentration of other artifacts was also examined. Most of the elements of this group were also documented graphically. Levallois predetermined artifacts were given particular attention, comparing their parameters and state of preservation with the other categories of artifacts. In the case of retouched forms, both the method of retouching and the form of the blank were analyzed. These were generally divided into: 1) denticulate and notched tools, 2) flakes with burin blows, and 3) blanks retouched at their edges at a semi-

abrupt or an abrupt angle (retouch angle close to 90°). The typological determination of tools from Affad referring to Bordes' formal lists has only a reference value in this study. The list of final predetermined forms also includes single bifacial artifacts, as well as backed blade microliths; both of these categories were recorded at the AFD23 site, exclusively in secondary contexts.

Refitting was applied as an alternative, albeit supplementary form of analyzing lithic artifacts from the southwestern sector of site AFD23. This method has a long tradition (Tomaszewski 1986; Cziesla et al. 1990 with further references) and a well-developed range of applications. The basic relationships joining the artifacts being refitted are defined by the term "refitting". The elements were selected on the basis of characteristics of the raw material (color, internal structure, features of the external surface of the nodule) regardless of size or findspot. The results are presented here in narrative and illustrative forms, as well as in tabular format. Once entered in the database, the data of all relevant elements were systematized in tables including the unique number of each artifact, its location, metric and morphological values, as well as additional information (identification of refitting, illustration references). The narrative layer brings a description of characteristic features of the raw material, and a reconstruction of the order of detaching of individual artifacts, thus leading *à rebours* to a separate reconstruction of the knapping process in the case of every nodule thus examined. Each refitted element was mapped and the lines joining detached elements were presented in the form of schemas superimposed on a plan of the horizontal stratigraphy (for several blocks together in order to maintain clarity of illustration). Although the features of the raw materials were documented photographically for most of the refitted nodules, drawings were used to document the refitting of two representative blocks (Nos 22 and 44). These illustrations present successive stages of core knapping in the form of a projection of the refitting sequence. The progress of splitting further artifacts (or negatives of the missing parts) was additionally indicated with different colors.

The results of an analysis of descriptions and reconstructions of the production processes produced for the collection from the southwestern sector of the site—the most promising from the point of view of lithics research—were subsequently used to test the raw material structure and production of final forms in each of the four clusters identified in this zone. Particular attention was placed on the frequency of individual stages of nodule knapping, as well as the distribution of pieces from each of these stages. The resulting plan of the encampment revealed a behavioral significance of the individual clusters of lithic artifacts, based not only on their mutual existence in a single space, but also on their being a correlate of specific production behaviors.

An analysis of the correlations resulting from the refitting study enabled a characteristic of production schemas employed in the production of final/predetermined products. A critical description of these referred to current knowledge regarding potential Levallois production models in the Nile Valley (Guichard and Guichard 1968; Marks 1968a; 1968b; 1968c; 1968d; Van Peer 1991; Bar-Yosef and Van Peer 2009; Schild and Wendorf 2010), as well as general knowledge in this regard (Boëda 1995).

The correlation of metric characteristics of refitted artifacts from particular stages of processing also permitted a verification of conclusions concerning artifacts (mainly flakes) from the first stage of the collective analysis. Taking into account the parameters of nodules processed in Affad, it became possible to present a fuller interpretation of the frequency of particular categories of initial pieces (in the southwestern zone as well as beyond).

A comparison of metric characteristics of final products assembled into refitted blocks also facilitated their assessment in relation to analogous artifacts produced, presumably, outside the Affad encampment. The recorded variances were interpreted in a behavioral perspective, highlighting the homogeneity of the collection in reference to the proposed model of an encampment functioning in the southwestern zone of the site for a restricted time period. This complex model builds on premises resulting from a spatial analysis of lithic artifacts (including refitting), as well as the results of stratigraphic and palaeoenvironmental analyses, as well as examination of remnants of encampment features like hearths, postholes, and pits.

A preference for retouched blanks, which the refitted blocks demonstrated, turned out crucial in interpreting the general relationship between producer and end-user of the stone tools in question. Assumptions concerning the predetermined, instrumental character of each point or Levallois flake were subjected to critical assessment.

The detailed analysis of the collection from the southwestern zone yielded data suitable for examining the morphological and metric characteristics of lithic finds from other zones of the site lying several dozen to several hundred meters away, in an effort to identify elements of a potentially identical technological production tradition, this despite the lack of refitting between the different zones or clusters of the southwestern zone. Based on palaeo-topographical and palaeoenvironmental premises, as well as the occurrence of an identical range of cut and non-cut features in each of the zones, all four zones of site AFD23 are considered as being contemporaneous (within a time window covering MIS3). Consequently, on the assumption that people act in a rational manner, mainly by intentionally selecting artifacts in the production zone for use in other zones, it was possible to take the frequency and parameters of finds from these zones and try to identify tool (or at least blank) preferences in a functional sense. The differences in the way such blanks/byproducts were supplied to the various zones, as well as the completeness of the correlates of the production processes, enabled a functional interpretation of the different zones observed at the AFD23 site, revealing their differentiation with regard to one another.

The collections/assemblages from other MSA sites in the Affad Basin were studied in the context of the finds from site AFD23 in an effort to establish the broader context of the functioning of the Late-Pleistocene community at Affad 23, in terms of both the supply of raw material for stone tools and the production techniques. The mobility range of these communities was tracked by analyzing the frequency of artifacts made of particular stone raw materials. The parameters of selected elements of these external collections (cores, as well as Levallois flakes/points) were also compared to the AFD23 collection in order to display the similarities and differences in the technological traditions of the Late Pleistocene on a microregional scale.

4.1.3 Raw material structure

The range of raw materials identified among the lithic artifacts from Affad included a very coarse-grained raw material provisionally termed as a conglomerate, petrified wood, white quartz, ferruginous sandstone and light-colored quarzitic sandstone, greenish-brown mudstone, dark-brown translucent flint, a striped raw material known as Egyptian flint, and agate [*Fig. 4.3*; *Table 4.1*]. Their share of the collection rarely exceeded 1% (disregarding the effect of statistically insignificant

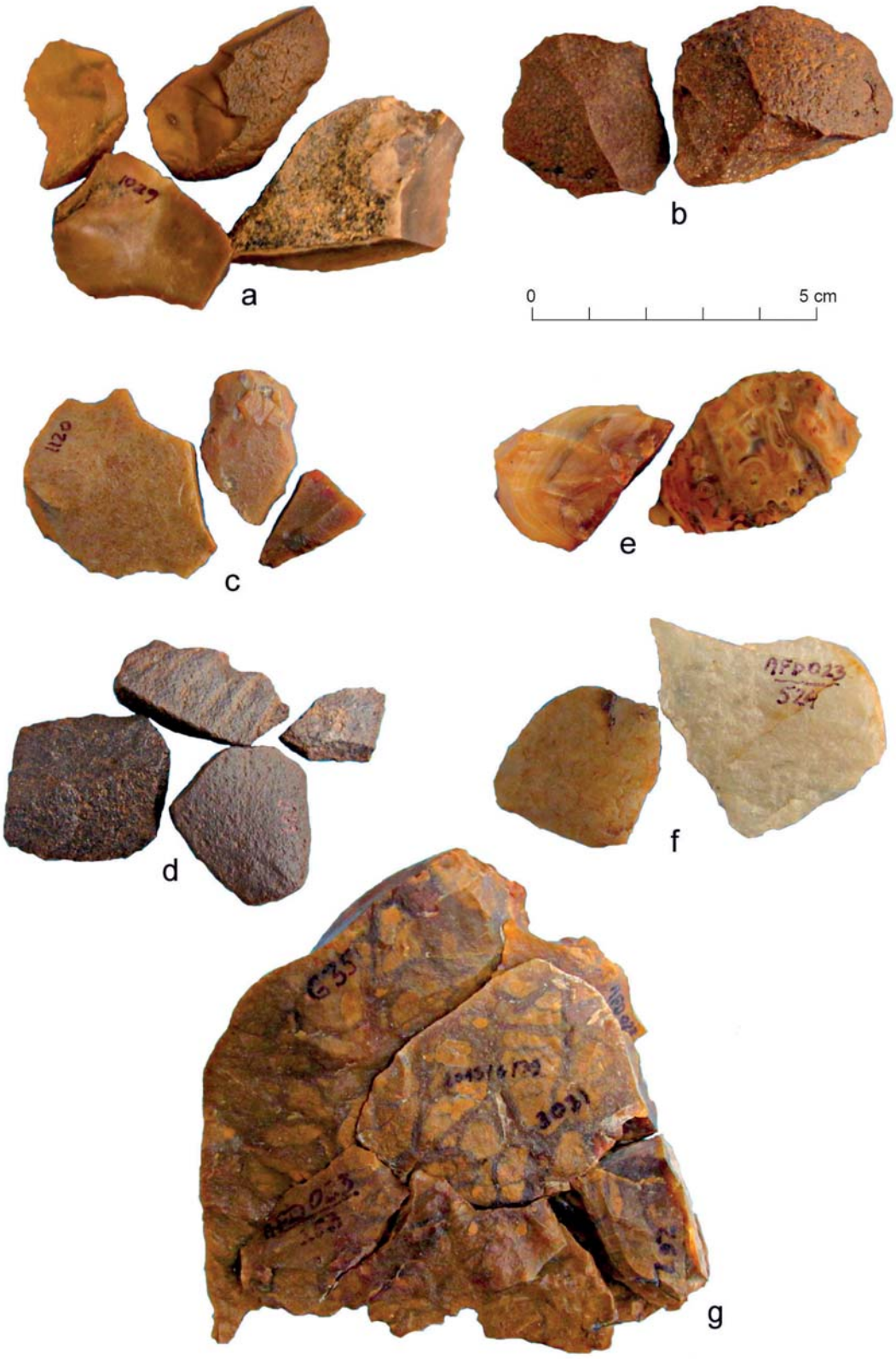

Fig. 4.3. Raw materials rarely used by the MSA knappers from Affad: a – Egyptian flint; b – flint; c – quarzitic sandstone (light variety); d – ferruginous sandstone; e – agate; f – quartz; g – conglomerate (jasper)

samples from certain contexts). At least four artifacts of a very fine-grained raw material (Egyptian flint) represented a microlithic tradition from a much later time (Early Holocene). Chunks of coarse-grained raw material could actually be the remains of stone tools (hammerstones). The remaining raw materials reflect incidental attempts at processing them with flaking methods (especially quartz), or accidental (or possibly intentional) deposition of artifacts not made at the site.

Table 4.1. Raw material structure of lithic artifacts from specific contexts (color-coded) at site AFD23 in stratigraphic breakdown:
1x – site surface without closer indication of loci;
1a – surface contexts in the southwestern sector considered as secondary relative to Late Pleistocene sediments;
1b – surface contexts in the southern sector;
1c – surface contexts in the northeastern sector;
1d – surface contexts in the northern sector;
2a – subsurface contexts of contemporaneous Late-Pleistocene settlement in the southwestern sector;
2b – subsurface contexts of contemporaneous Late-Pleistocene settlement in the southern sector;
3a – subsurface contexts secondary relative to sediments linked to Late-Pleistocene settlement in the southwestern sector;
1/2e – subsurface and surface contexts of contemporaneous Late-Pleistocene settlement in the northwestern sector

Stratigraphy	Chert		Flint, mudstone and agate		Quarzitic sandstone		Ferruginous sandstone		Quartz, quartzite		Conglomerate, petrified wood		Total
	∑	%	∑	%	∑	%	∑	%	∑	%	∑	%	∑
1999 1x	10	90.91	0	–	1	9.09	0	–	0	–	0	–	11
2003 1x	8	100	0	–	0	–	0	–	0	–	0	–	8
2003 1a	383	94.80	5	1.24	4	0.99	4	0.99	4	0.99	4	0.99	404
2003 2a	859	98.63	5	0.58	1	0.11	1	0.11	1	0.11	4	0.46	871
2012– 2014 1x	9	81.82	1	9.09	1	9.09	0	–	0	–	0	–	11
2013–2014 1a	33	97.06	0	–	0	–	1	2.94	0	–	0	–	34
2013–2014 1b	8	100	0	–	0	–	0	–	0	–	0	–	8
2012 1c	65	80.25	8	9.88	0	–	2	2.46	5	6.17	1	1.23	81
2012 1d	1650	87.81	19	1.01	17	0.90	6	0.31	170	9.04	17	0.90	1879
2013–2018 2a	2202	95.08	3	0.13	15	0.65	2	0.09	86	3.71	8	0.35	2316
2013–2014 2b	60	95.24	0	–	0	–	0	–	3	4.76	0	–	63
2013–2014 3a	133	98.51	0	–	0	–	0	–	2	1.49	0	–	135
2016 1/2e	295	96.72	4	1.31	1	0.33	1	0.33	3	0.98	1	0.33	305

The overwhelming majority of lithic artifacts from AFD23 were made of local chert occurring in the form of relatively large nodules transported by the river and bearing traces of erosion. They were dominated by those with rolled and smoothed external surfaces [*Fig. 4.4:b*; *4.6*]. Only a few artifacts possessed a partly preserved cortex and more sculpted external sections [*Fig. 4.4:a*]. This is a matt and opaque raw material, with a very varied internal structure, frequently taking on a mosaic form and including fossils and crystalline inclusions. It displays a wide range of colors from yellow, brown and red to greenish-brown (disregarding the secondary red coloration of overheated artifacts). This frequently facilitated the processing and making of tools from sections of nodules of an exceptionally uniform and fine-grained nature. Those most familiar to the authors are nodules of chert of this kind, shaped as irregular cubes over 30 cm in length, used as building material in the construction of medieval churches in Old Dongola, a medieval site which lies 50 km northwest of Affad [*Fig. 4.5*]. For the region of interest here, this raw material is defined as chert from the Tertiary period with its origin being linked to the Hudi formation (Whiteman 1971: 90). The eponymous site of Hudi Station in Atbara yielded evidence of chert

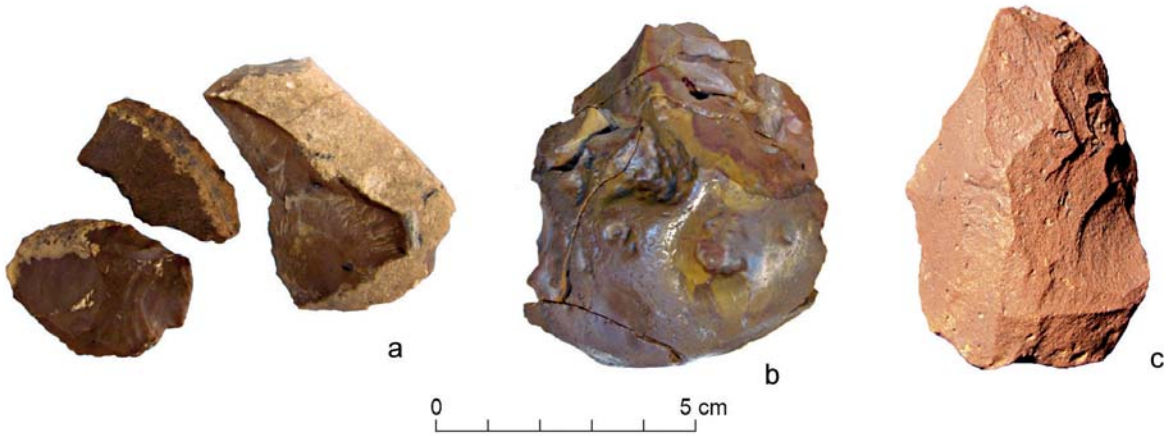

Fig. 4.4. Condition of MSA artifacts from Affad: a – chert flakes with preserved lime cortex; b – natural polishing of outer surfaces; c – erosion of edges and faces

Fig. 4.5. Blocks of chert used in the construction of church buildings in Old Dongola (Kom A)

nodules below layers of volcanic basalt that were dated to the late Tertiary period. The origin of the Hudi cherts is connected with the extensive areas of volcanic activity in the Bayuda desert and the shallow lakes which existed there during the Tertiary period. According to the theory cited by Arthur J. Whiteman (1971, here and further publications), silica containing microorganisms (diatoms) in the form of a gel, which is left in water of a suitable acidity, is transformed into chalcedony and micro-crystalline quartz. Once the lakes dried up and sediment erosion commenced, this led to the formation of spheroidal nodules of chert. The (formerly) active water courses of Wadi Muqaddam and Wadi el-Melik were—besides the Nile itself—the main corridors for the transport of chert to the north, including the zone of the Middle Nile Valley. At the same time, a local origin of chert from today's completely eroded limestone rocks cannot be excluded. The last such remnants of chert-bearing limestone may be nodules of light-colored chert with still well-preserved external surfaces and even a lime/chalk cortex. Premises exist concerning the procuring of raw material of this kind through mining-like activities during the Early Holocene in the environs of the current town of Debba [Al Dabbah] or the Wadi el-Melik outlet in broader view (Osypiński 2010).

A very large number of artifacts from the external sections of nodules, as well as nodules of chert with single barely detached flakes indicate the close proximity of the source of this sort of raw material. Although there is no evidence of mining methods for securing chert nodules at Affad, behavior of this kind has been documented at other Middle Palaeolithic sites, such as Taramsa (Van Peer, Vermeersch, and Paulissen 2010). As a result of digging pits to a depth of 1.50 m, nodules of chert were extracted from layers of gravel forming the terraces of the Nile near Taramsa. However, the simplest method in this case is collecting the nodules from places in seasonally dry riverbeds to which they had been transported by the river current cutting through older sediments elsewhere.

4.1.4 General technological structure

4.1.4.1 Lithic artifacts from the southwestern sector

The inventory of lithic artifacts collected from the main, southwestern sector of site AFD23 is dominated by debris from flake blanks production. They were represented in all the morphological categories of artifacts: cores, initial flakes (sometimes of extended proportions), chunks, relatively few predetermined forms, as well as retouched forms [*Table 4.2*].

Cores

Initial cores of a form impossible to determine in terms of final production (flakes or points) were the most numerous among the finds. This assemblage included primarily nodules with single negatives of detached flakes [*Fig. 4.6*]; however, some specimens demonstrated signs of the surrounding striking platform being formed, e.g., core 754, or one of the surfaces being given a convex shape (by implication, a prospective flaking surface), such as core 519 [*Fig. 4.7*]. The sizes of part of these artifacts did not diverge in a fundamental way from residual forms [*Table 4.3:1*; *Fig. 4.8*]. Therefore, this may be an indication that they were discarded already at an initial stage, precisely because of their small size. At the same time, the largest specimens

Table 4.2. General technological structure of the collection of lithic artifacts from the southwestern sector of site AFD23 transported to Poland following preliminary selection, divided by context: primary / secondary (separated by a backslash)

Group	Description	Raw material			Total
		Chert	Flint, mudstone	Other	
Cores	Initial cores and tested nodules	22/3	–	1/–	26
	Cores for flakes/points	9/3	–	1/–	13
	Final cores	15/4	1/–	1/–	21
	Discoidal cores on flakes	1/2	–	–	3
	Uniplatform microlithic cores	–/1	1/–	–	2
Flakes and chips	Flakes with unprepared butt	420/120	–/1	18/4	563
	Flakes with plain/uniface butt	625/105	1/1	5/3	740
	Flakes with point & edge butts	411/54	–/–	2/3	470
	Flakes with multi-faced prepared butt	482/56	1/1	2/1	543
	Flake fragments	632/96	3/–	6/3	740
Chunks	Chunks	385/83	–/–	80/5	553
Predetermined products and formal tools	Levallois flakes	9/7	1/–	–/1	18
	Points	11/3	1/–	–/–	15
	Flakes/points with denticulate retouch	17/3	–/–	–/–	20
	Flakes with burin scars	6/1	–/–	–/–	7
	Flakes with abrupt retouch	9/8	–/–	–/–	17
	Bifacial forms	–/–	–/–	1/–	1
	Backed tool (Holocene)	–/1	–/1	–/–	2

actually exceeded the size of artifacts from later stages, indicating the upper limit of the size of nodules set aside for further processing.

Initial cores were scattered over the entire investigated area [see below, *Figs 4.19, 4.20*], accounting for the largest clusters of lithic artifacts: eastern, southwestern, western, and in a ground relief depression to the west of the encampment.

Initial forms of cores bearing visible features of predetermined products were represented in a significantly more modest way, but it should be emphasized that these products had not been detached [see *Table 4.3:2*]. Noted here were six cores with uni-direction, a converging pattern for flaking surface preparation [*Fig. 4.10:973, 410, 2412, 2050*], and a centripetal pattern [*Fig. 4.10:1482, 2749, 1046*]. These schemas account for variants in the production of points and Levallois flakes. On these cores there are no visible negatives of faceting the striking platform, although its position is already determined by the preparation (cortex removal and shaping of proper angle for knapping).

Apart from one core in the eastern cluster, the remaining examples of this category occurred in the ground relief depression to the west of the encampment [see below, *Figs 4.19, 4.20*, marked in orange].

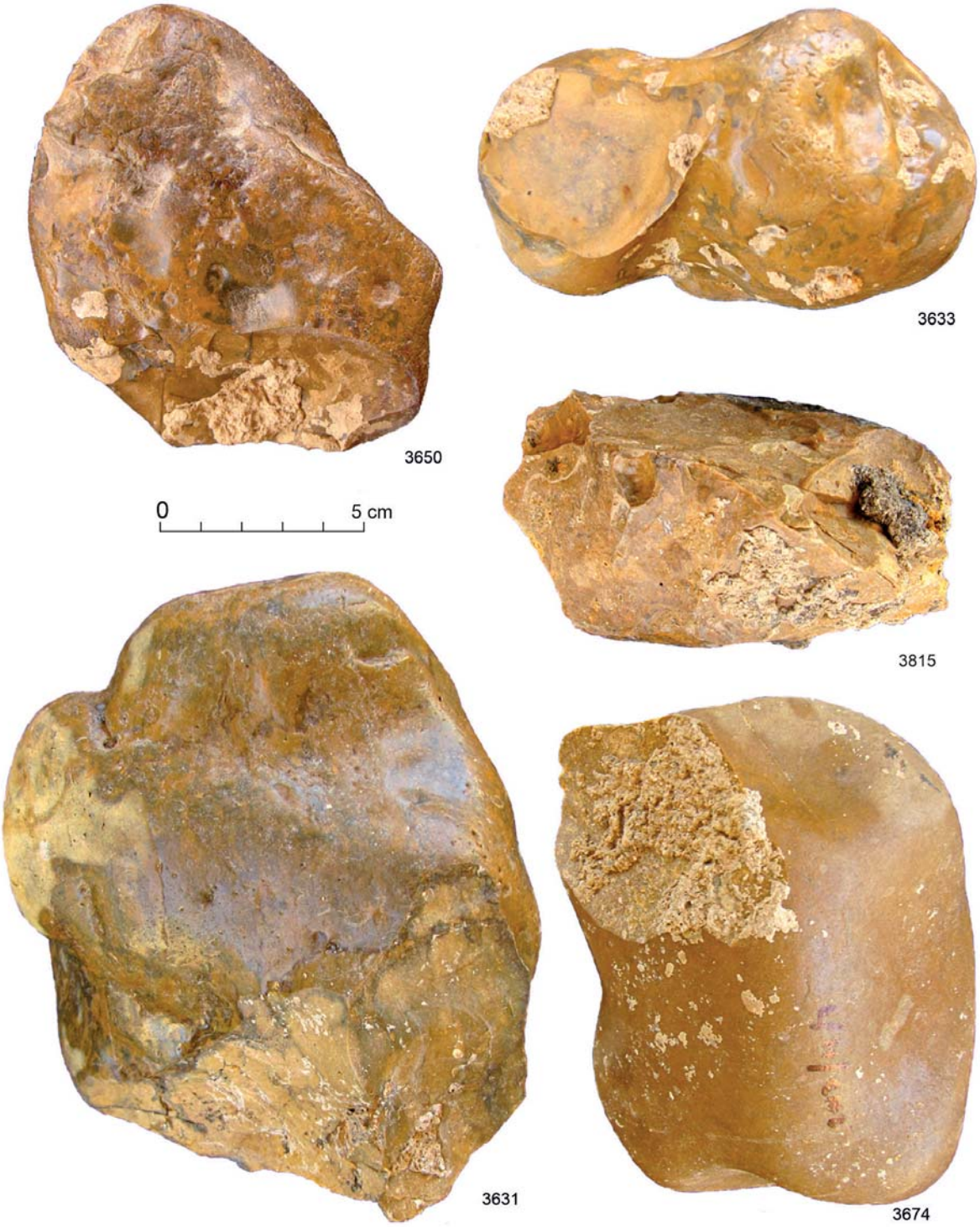

Fig. 4.6. Nodules displaying single negatives made when testing the raw material

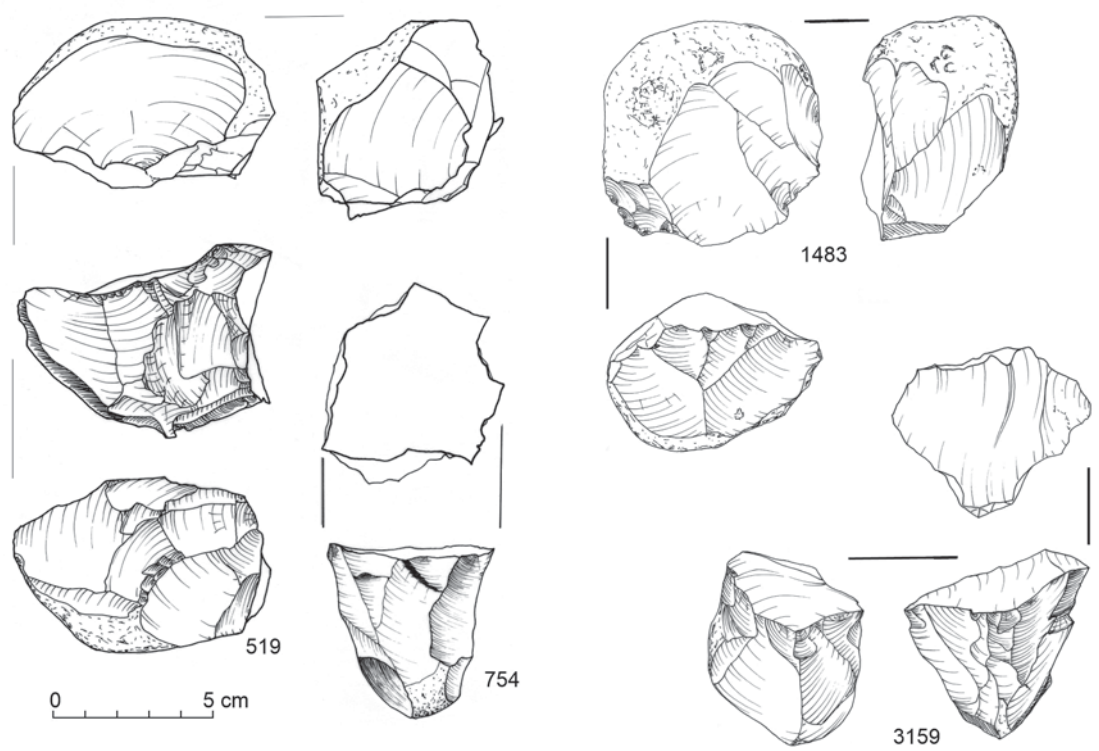

Fig. 4.7. Initially treated cores from site AFD23 (sector SW): 519, 754, 1483, 3159

Residual/final core forms were also noted, most of them remodeled after detaching a predetermined product [*Fig. 4.11*]. Their sizes indicate the lower range of the dimensions of final products (flakes, points), while decidedly larger specimens (such as core 399) could not be further reduced because of the imperfections of the raw material.

Residual cores were scattered over the entire surface of the area under investigation, accompanying other categories of cores within the boundaries of clear clusters [see below, *Figs 4.19, 4.20*, marked in red]. The most numerous occurred in the ground relief depression west of the encampment but also in the eastern cluster.

Both on the site surface and in subsurface contexts (defined as secondary) small residual discoidal cores formed on crude flakes/chunks occurred [see *Table 4.3:3*; see *Fig. 4.9*]. Production of flakes of such small size is undoubtedly linked to a different technological tradition or a different purpose in mind. One of these specimens bore traces of erosion (transportation in gravel formations).

Both examples of discoidal cores on flakes from the surface occurred very close to one another, in Are 24 [see below, *Fig. 4.19*, marked in green]. A third artifact came from a dusty sediment on the opposite side of the ground relief depression west of the encampment.

The last recorded category, all of them from the surface, comprised small, residual single-platform forms identified with microlithic production [see *Fig. 4.9*]. One of these cores was made from a small flint pebble, a raw material seldom used in the Late Pleistocene. Their loci were random [see below, *Fig. 4.19*, marked in purple].

Table 4.3. Dimensions and loci of cores from site AFD23 (sector SW): 1) initial, 2) Levallois, 3) residual/final, 4) discoidal, and 5) microlithic single-platform

Inv. No.	Locus	Context	Dimensions (mm) L/W/Th	Comments	Reference
		1) INITIAL CORES			
70	A/22/88=2013/F/81/I	2a	82/44/40		
219	A/23/74=2013/G/30/I	2a	67/45/21		
519	A/22/37=2013/G/96/I	2a	47/80/53	Block 3	*Fig. 4.7*
754	A/34/test pit	2a	52/54/47		*Fig. 4.7*
956	A/23/71=2013/G/60/I	2a	34/58/49		
1080	A/23/96=2013/F/2/I	2a	54/48/27		
1458	2013/I/34/IIa	2a	100/83/55		
1459	2013/I/34/IIa	2a	82/67/52		
1483	2013/I/33/IIb	2a	73/73/45		*Fig. 4.7*
1806	2013/I/65/Ia	2a	91/80/51	Refitting 1805	See *Table 4.8*
2066	2013/I/3/IIb	2a	70/57/40	Sandstone	
2541	2013/I/91/Ib	2a	60/65/35		
2828	2013/F/73/Ia	2a	100/80/39		
2965	2013/G/88/Ia	2a	53/57/47		
3159	2014/N/91/II	2a	45/41/55		*Fig. 4.7*
3476	2014/Q/NW/I	2a	35/32/12	Eroded	
3562	2013/H/13/Ib	3		Tested nodule	
3574	2013/H/100/Ib	2a		Tested nodule	
3575	2013/H/100/Ib	2a		Tested nodule	
3576	2013/H/100/Ib	2a		Tested nodule	
3631	2013/F/99/Ia	3		Tested nodule	
3632	2013/F/77/Ib	3		Tested nodule	
3354	2013/I/26/II	2a	100/95/64		
3365	2013/I/10-100/Ic	2a	47/48/25		
3407	2013/I/28/II	2a	61/58/25	Refitting 3408	See *Table 4.8*
		2) LEVALLOIS CORES			
410	A/23/83=2013/F/31/I	2a	54/55/36		*Fig. 4.10*
549	A/33/26=2013/F/5/I	1a	38/70/30		
973	A/33/39=2013/I/76/I	1a	63/56/41		*Fig. 4.10*
1046	A/33/30=I/65/I	2a	71/65/41	Block 32	*Fig. 4.10*
1482	2013/I/33/IIb	2a	60/50/27	Quartz	*Fig. 4.10*
1823	2013/I/73/Ib	2a	55/50/23		
1885	2013/I/3/IIb	2a	37/38/14		
1898	2013/I/3/IIb	2a	64/74/28		

Table 4.3. continued

Inv. No.	Locus	Context	Dimensions (mm) L/W/Th	Comments	Reference
1952	2013/I/34/II	2a	73/56/37		
2050	2013/I/73/Ib	2a	55/51/22		*Fig. 4.10*
2412	2013/I/13/IIa	2a	60/46/25		*Fig. 4.10*
2749	2013/F/72-73/Ib	2a	62/54/31		*Fig. 4.10*
3218	2014/P/10/Ia	3	52/47/27		
		3) RESIDUAL/FINAL CORES			
143	A/33/18=2013/I/84/I	2a	47/45/27	Block 7	
399	A/43	1a	83/68/49	Block 8	*Fig. 4.11*
755	A/34/sondage	2a	47/46/33		*Fig. 4.11*
1009	A/32/17=2013/F/94/I	1a	56/46/35		
1044	A/33/30=2013/I/65/I	2a	91/77/41	Block 2	
1048	A/34	2a	67/52/37	Block 22	*Fig. 4.11*
1067	A/32/8=2013/F/83/I	2a	45/45/24		*Fig. 4.11*
1299	2013/I/65/Ia	2a	41/57/14		
1435	2013/I/35/Ib	3	38/39/11		*Fig. 4.11*
1577	2013/I/5/IIb	2a	46/49/16		*Fig. 4.11*
1578	2013/I/5/IIb	2a	51/45/18		*Fig. 4.11*
1579	2013/I/5/IIb	2a	40/48/23		
2031	2013/I/2/IIb	2a	55/40/20		
2032	2013/I/2/IIb	2a	40/43/17		
2672	2013/I/40/Ia	3	41/44/19		
2750	2013/F/72-73/Ib	2a	58/55/24		*Fig. 4.11*
2760	2013/F/72/Ib	2a	77/68/32		
3092	2013/G/82/Ib	2a	57/49/33		
3108	2013/G/10/Ia	2a	49/45/41		
3419	2013/I/NW/II	2a	64/52/35		
3294	2014/P/94/IIb	2a	60/68/24	Ferruginous sandstone	
		4) DISCOIDAL CORES			
486	A/24/87		46/38/16		*Fig. 4.9*
965	A/24/94=2013/I/22/I		38/35/11	Eroded	*Fig. 4.9*
		5) MICROLITHIC SINGLE-PLATFORM CORES			
505	A/25/I	1a	34/36/30		*Fig. 4.9*
895	A/32/I	2a	23/26/18		*Fig. 4.9*

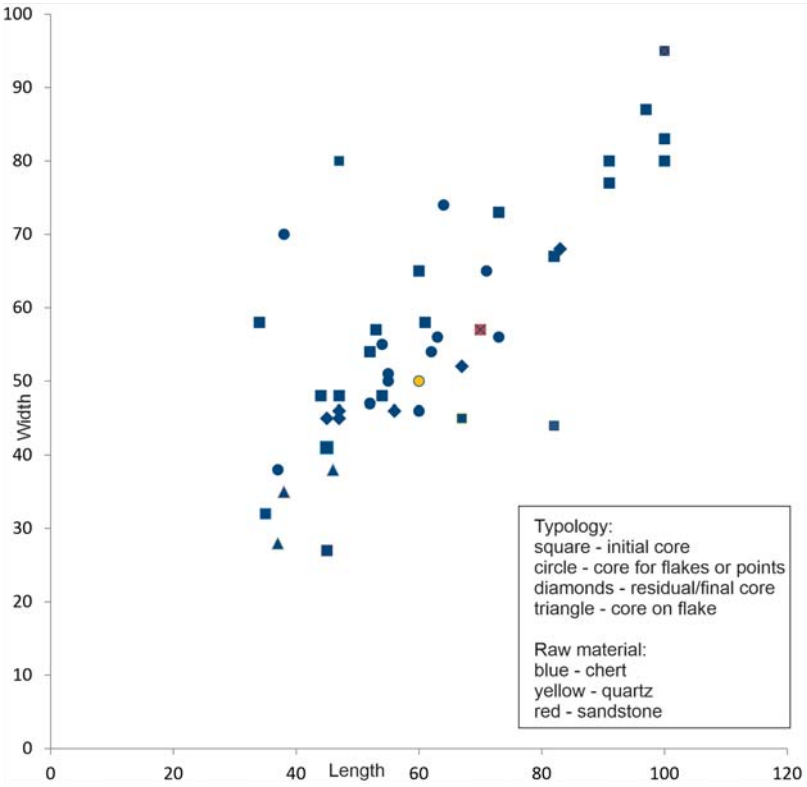

Fig. 4.8. Discoidal cores from site AFD23 (sector SW): length-to-width correlation (mm)

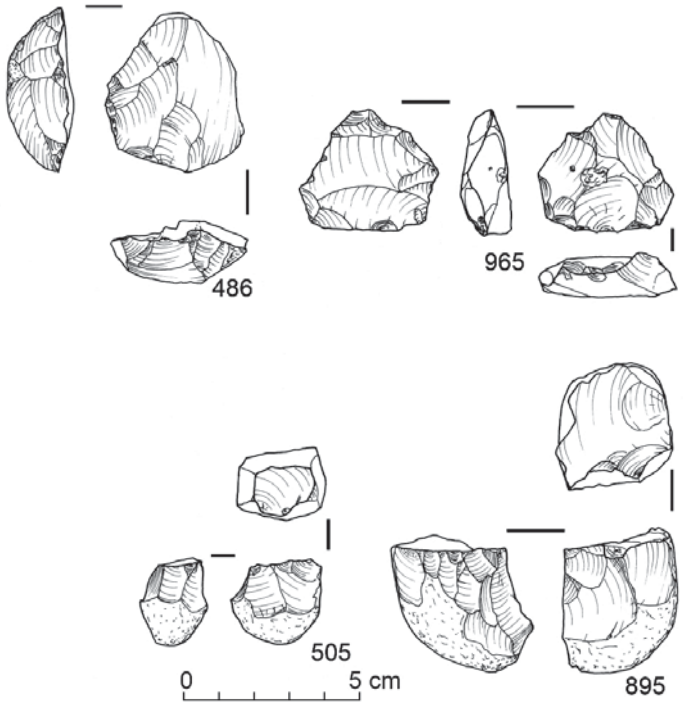

Fig. 4.9. Cores on flakes and microlithic cores from site AFD 23 (sector SW): 486, 505, 895, 965

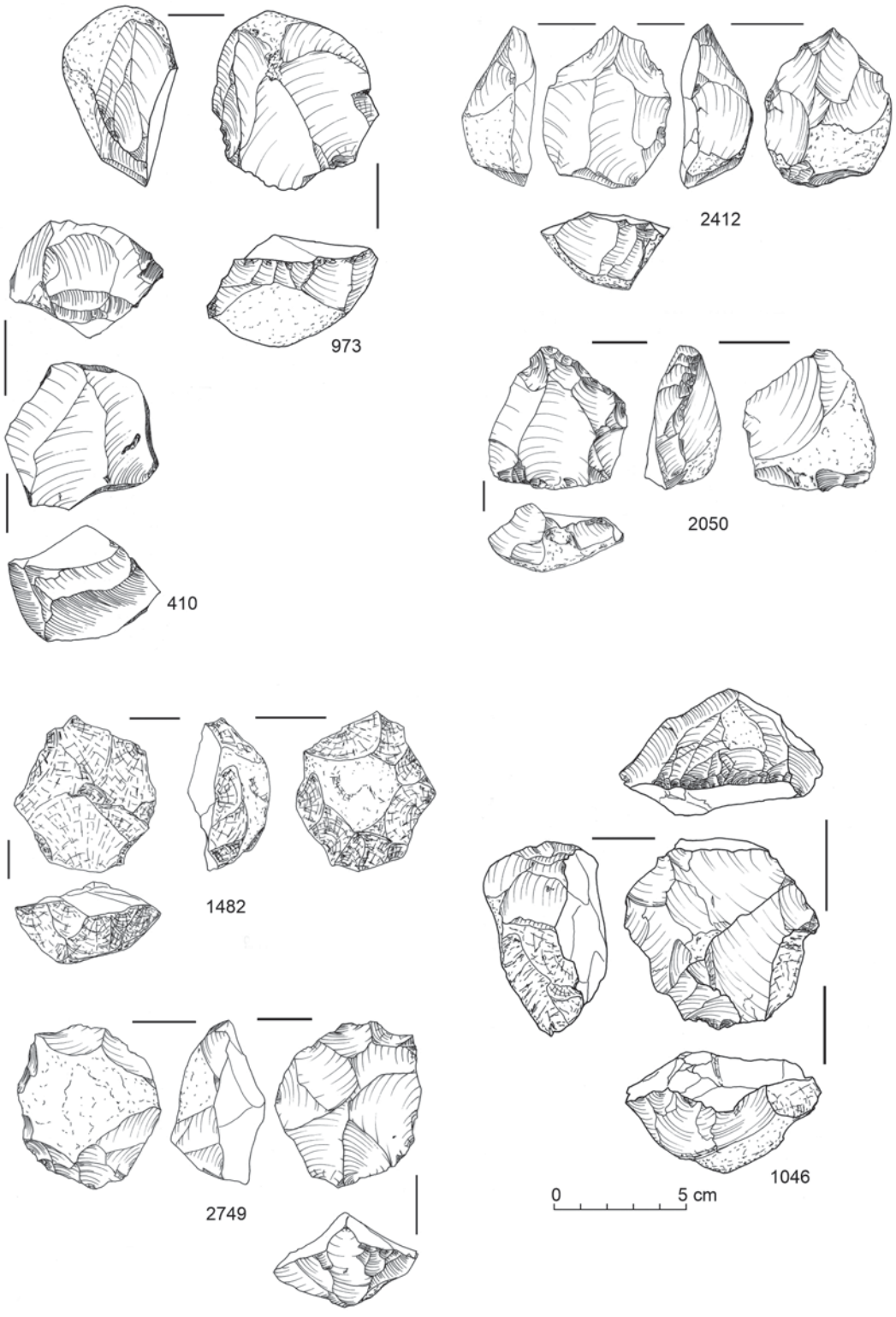

Fig. 4.10. Levallois cores from site AFD23 (sector SW): 410, 973, 1046, 1482, 2050, 2412, 2749

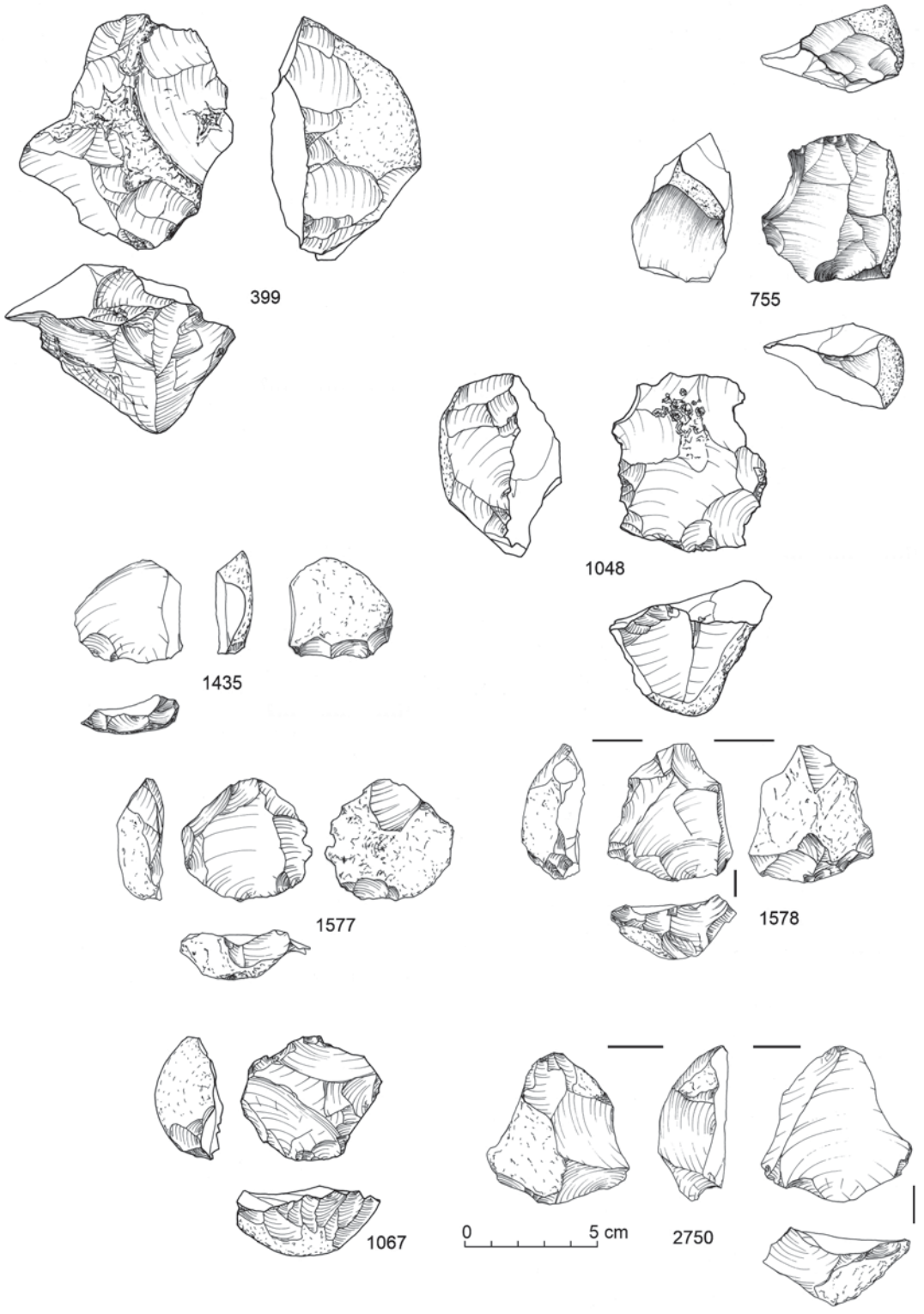

Fig. 4.11. Final cores from site AFD23 (sector SW): 399, 755, 1048, 1067, 1435, 1577, 1578, 2750

Flakes

Preparation flakes or core treatment waste constituted the dominant part of the collection from site AFD23 in the southwestern sector. Several categories could be distinguished in terms of the distinctive morphology of the butt, reflecting the degree of preparation of the nodule at the moment of flake detachment.

Natural/unprepared butt

The first category of flakes had natural butts not worked on in any way. The butt constituted the external section of a nodule. The size of these particular flakes reveals a great degree of irregularity [*Fig. 4.12*]. Most of the flakes with unprepared butts displayed significantly wider proportions or were of equal length. A decidedly small number of flakes had significantly elongated proportions. One flake from a very fine crystalline raw material (Egyptian flint; symbol of a triangle in the graph) displayed parameters similar to a blade. This observation refers to artifacts recorded in primary contexts (symbols in black) as well as secondary ones (symbols in red and green), leading to the assumption that the entire assemblage is of a common provenance. Similar correlations in terms of the thickness and width of the artifacts from both categories of contexts show few deviations [*Table 4.4*].

The majority (almost 70%) of flakes from this category featured on the dorsal sides fragments of the original external surface of the nodule [*Table 4.5*], while compared to the remaining flake categories, the percentage of opening flakes was the highest here (over 30%).

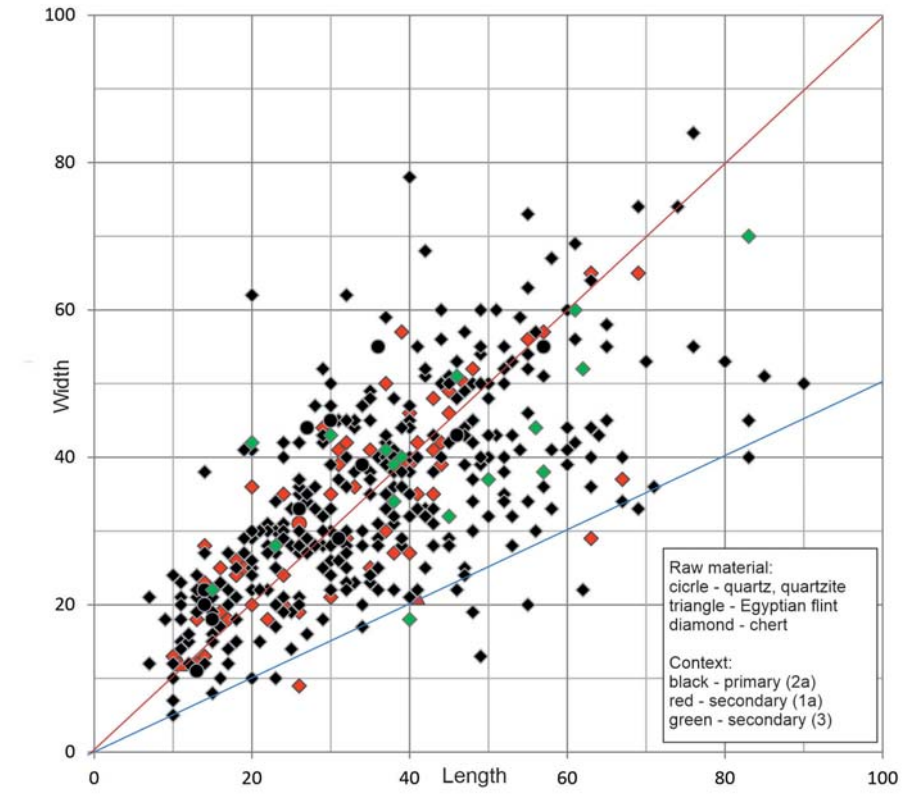

Fig. 4.12. Flakes with natural/unprepared butts from site AFD23 (sector SW): length-to-width correlation (mm). Raw material and context category indicated

Table 4.4. Thickness-to-width (mm) correlation of flakes from primary and secondary contexts from site AFD23 (sector SW). Width presented as a range and, in parentheses, as a median. Values presented against a benchmark from primary contexts in sector SW; higher values in green, lower values in red

Thickness	Unprepared butt		Plain/uniface butt		Point & edge butts		Multi-faced prepared butt	
	Primary context	Secondary context	Primary context	Secondary context	Primary context	Secondary context	Primary context	Secondary context
1	–	–	10–33	–	–	–	–	–
2	14–24	–	7–38 (15)	9–11	9–24 (16)	9–14	11–28 (19)	14–16
3	8–30 (17)	12–24 (13–15)	6–38 (18)	12–28 (16–17)	4–46 (19)	13–29 (18–19)	10–37 (21)	21–24
4	10–33 (23)	20–26 (24)	12–38 (21)	12–28 (16–17)	9–37 (20)	5–25 (15–17)	8–45 (23)	17–23 (21)
5	10–37 (23)	9–43	12–43 (24)	16–48 (20)	10–36 (22)	19–28 (26)	10–41 (22)	20–35 (25–27)
6	17–50 (27–28)	19–43 (23)	13–41 (25)	16–37 (26)	12–39 (25)	16–27 (24)	7–44 (26)	17–33 (23–24)
7	19–39 (28)	18–45 (39)	11–42 (28)	15–40 (25)	17–44 (30)	20–38	18–52 (28)	22–30
8	16–48 (33)	19–40 (32)	15–47 (30)	24–36 (27)	19–49 (31)	28	21–50 (31)	21–37 (27–28)
9	20–57 (38)	23–49 (35)	14–50 (32–33)	23–64 (31–43)	10–37 (28)	30–43	19–52 (31)	30
10	23–62 (39)	33–57 (42)	16–52 (35)	27–47 (33)	26–47 (30)	–	19–46 (35)	26–70 (32)
11	23–59 (37–40)	18–51 (30–35)	23–78 (37)	30	16–51 (37)	22	27–52 (37)	–
12	22–60 (40)	–	22–62 (34)	37–47	32–73 (38)	39–59	27–57 (41)	36–54
13	22–78 (40–42)	34–50 (39)	24–67 (38)	26–59 (44)	18–64 (29)	48	25–62 (45)	34–48 (42)
14	28–55 (44)	38–145 (45)	24–70 (45)	50	36	–	34–58 (46)	–
15	22–56 (39)	28–65	31–65 (40–45)	35–68	41–52	–	35–49	–
16	40–73 (49)	37–41	21–61 (35–40)	40–60	28–64 (44–46)	42	35–48	–
17	28–57 (43–45)	39–60	35–55 (41–44)	40–45	22–55	–	24–53 (44–49)	–
18	35–50 (50)	65	32–63 (43)	–	52	–	38–64	21
19	29–64 (54–55)	–	42–56 (45–47)	30–46	54	–	44	–
20	33–74 (59)	44–56	47–60	49	48	–	67	–
21	–	–	27–64 (38)	50	75	–	43	–
22	45–47	–	47–55	–	73	–	–	–

Table 4.4. continued

Thickness	Unprepared butt		Plain/uniface butt		Point & edge butts		Multi-faced prepared butt	
	Primary context	Secondary context	Primary context	Secondary context	Primary context	Secondary context	Primary context	Secondary context
23	40–84 (67)	50	52	–	–	–	53	–
24	69	–	49–60	–	–	–	–	–
25	53–90 (55)	–	39	–	–	–	67	–
26	53	70	–	36–53	–	–	70	–
28	–	–	62	–	–	–	–	–
30	42	–	–	–	–	–	–	–

Table 4.5. Cortex frequency on flakes with different butts from site AFD23 (sector SW)

Share of cortex	Unprepared butt	Plain/unifacial butt	Point & edge butt	Multi-faced prepared butt	Facetted butt
0%	31.39%	36.45%	47.88%	60.98%	100%
10%	6.38%	11.20%	6.16%	11.17%	0.00%
20%	5.67%	7.83%	5.30%	6.37%	0.00%
30%	3.90%	5.40%	4.03%	3.42%	0.00%
40%	2.48%	2.83%	2.12%	1.67%	0.00%
50%	4.96%	7.42%	5.75%	3.50%	0.00%
60%	3.37%	4.59%	3.18%	3.13%	0.00%
70%	1.95%	3.24%	1.27%	1.28%	0.00%
80%	4.26%	6.34%	5.95%	1.66%	0.00%
90%	5.14%	5.53%	4.88%	2.39%	0.00%
100%	30.50%	9.17%	13.48%	4.79%	0.00%

Table 4.6. Damage to flakes from site AFD23 (sector SW);
in parentheses – number of artifacts from other context categories (1a–2a–3)

Flake damage	Unprepared butt		Plain butt		Point butt		Prepared butt		Facetted butt		Unidentified butt
	∑	%	∑	%	∑	%	∑	%	∑	%	∑
Longitudinal breakage	93 (22-66-5)	16.48	69 (9-60-0)	9.31	54 (9-45-0)	11.46	49 (4-45-0)	9.22	1 (1-0-0)	2.56	45
Transverse breakage	49 (3-41-5)	8.68	73 (5-65-3)	9.85	46 (5-41-0)	9.76	81 (6-75-0)	14.94	19 (5-13-1)	48.71	723
Overheating	9 (3-4-2)	1.59	8 (1-7-0)	1.08	8 (2-6-0)	1.69	11 (1-10-0)	2.02	1 (1-0-0)	2.56	34
Eroded surfaces	2 (2-0-0)	0.35	8 (4-3-1)	1.08	4 (2-2-0)	0.84	9 (3-6-0)	1.66	2 (1-0-1)	5.12	15

The damage to flakes with an unprepared butt [*Table 4.6*] comprised transverse (8%) and longitudinal breakage or fracturing (over 16%, which was the highest among all flakes categories). It should be remembered here that the calculations were made as initial values before refitting the material. Single flakes of the group described here also bore traces of secondary overheating. Natural butt flakes with smoothened edges were only found in secondary contexts of category 1a.

Plain/unifacial butt

Flakes with plain/unifacial butts constitute the second category [*Fig. 4.13*]. None of flakes under study bore any trace of additional treatment of the edge of the butt and dorsal face (ablation). The flaking was invariably close to a right angle. Compared to flakes with unprepared butts, this category tended to display proportions close to achieving a balance between length and width [see *Table 4.4*]. Slightly more flakes with plain butts also had elongated proportions. Moreover, in the case of this group no significant differences were noted in the proportion of flakes from primary and secondary contexts, both in terms of length-width and thickness-width correlations [see *Table 4.4*].

The percentage of flakes with plain butts, which had on their dorsal sides fragments of the natural surface of the nodule, was similar to that for the previous category and reached over 60%. Although the share of opening products was not very high, it reached 10%. The intermediate ranges often reached similar values [see *Table 4.5*].

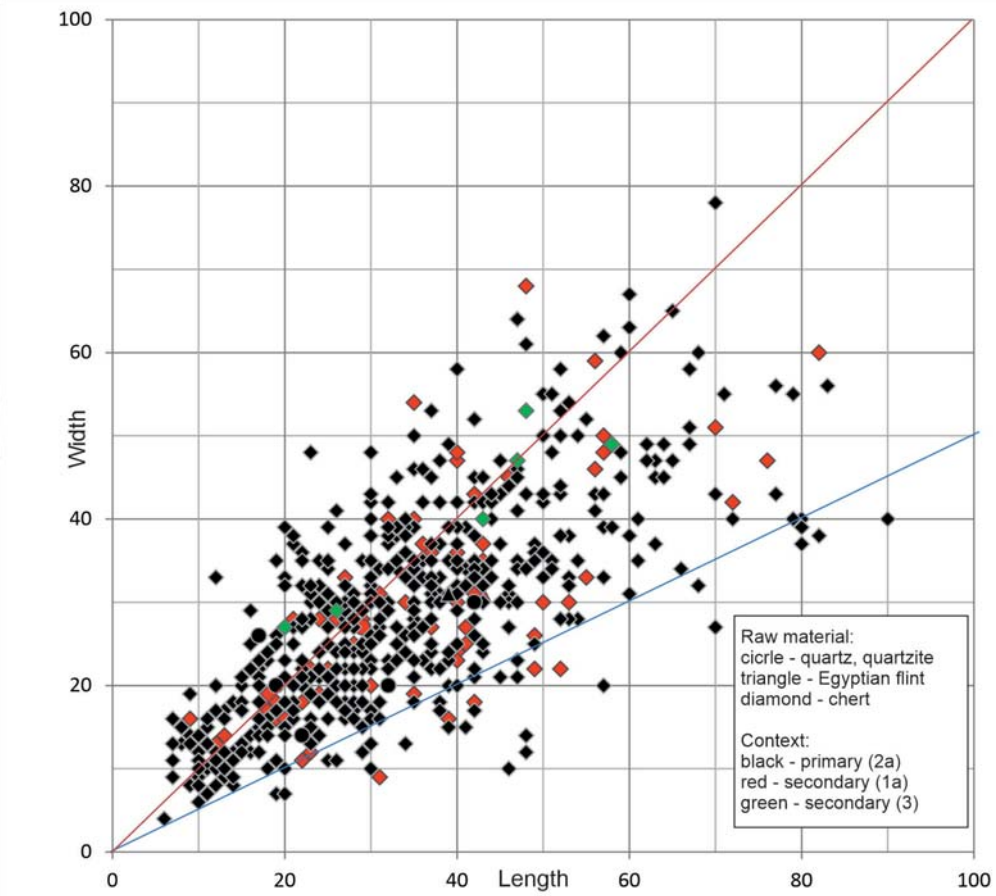

Fig. 4.13. Flakes with plain/unifacial butt from site AFD23 (sector SW): length-to-width correlation (mm)

Damage was also noted on flakes with plain butts [see *Table 4.6*] in the form of transverse (over 9% artifacts) or longitudinal breakage or fracturing (over 9% artifacts). Single flakes in this category also bore traces of overheating and significant smoothening of the edges (the latter most often occurred in secondary contexts of category 1).

Edge and point butts

The third category of flakes, featuring edged and pointed butts, followed the size proportions of flakes with a plain butt [*Fig. 4.14*]. The overwhelming majority were included in a range of products which were of equal or slightly extended length. Significantly fewer flakes with edged or pointed butts, compared to the previous categories, preserved a natural external nodule surface on their dorsal sides [see *Table 4.5*]—just over 50%. Among these, the percentage of opening products was decidedly the highest, reaching over 13%.

The presence of damage was noted on flakes of this category [see *Table 4.6*] in the form of transverse (over 9% artifacts) or longitudinal breakage or fracturing (over 11% artifacts). Single artifacts of this category were burned or significantly more eroded.

Multi-faced butt

The size and proportions of flakes with multi-faced butts were similar to those of flakes with plain butts [*Fig. 4.15*]. Despite the similar sizes, significantly fewer flakes with multi-faced butts displayed on their dorsal sided a natural external nodule surface [see *Table 4.5*]—slightly less than 40% (compared to about 60% of the other categories of preparation flakes). Dominating this category were flakes covered with such a surface to an insignificant degree; indeed, the highest percentages were reached by examples with 10% and 20% coverage.

The presence of damage was noted [see *Table 4.6*] in the form of transverse (over 14%) or longitudinal breakage or fracturing (less than 10% of the examples). Moreover, traces of overheating and significant smoothening of the edges were noted on several artifacts of this category.

Other

The remaining finds not assigned to any of the above-described categories comprised mesial or distal flake fragments. These artifacts were seen as the result of damage in the form of transverse breakage [see *Table 4.6*]. Some of these also bore traces of additional damage in the form of longitudinal fractures, overheating and clear smoothening of the edges.

Chunks

The collection from the southwestern sector of the site included exactly 550 artifacts assigned to the chunks group. Most of these were not selected for further laboratory study because they provided the least amount of information. The size of the largest chunks [*Fig. 4.16*] indicated the lowest range of the size of nodules chosen for processing on the assumption that chunks were the raw material considered by the knappers (that is, fulfilling metric, technological and even non-utilitarian conditions).

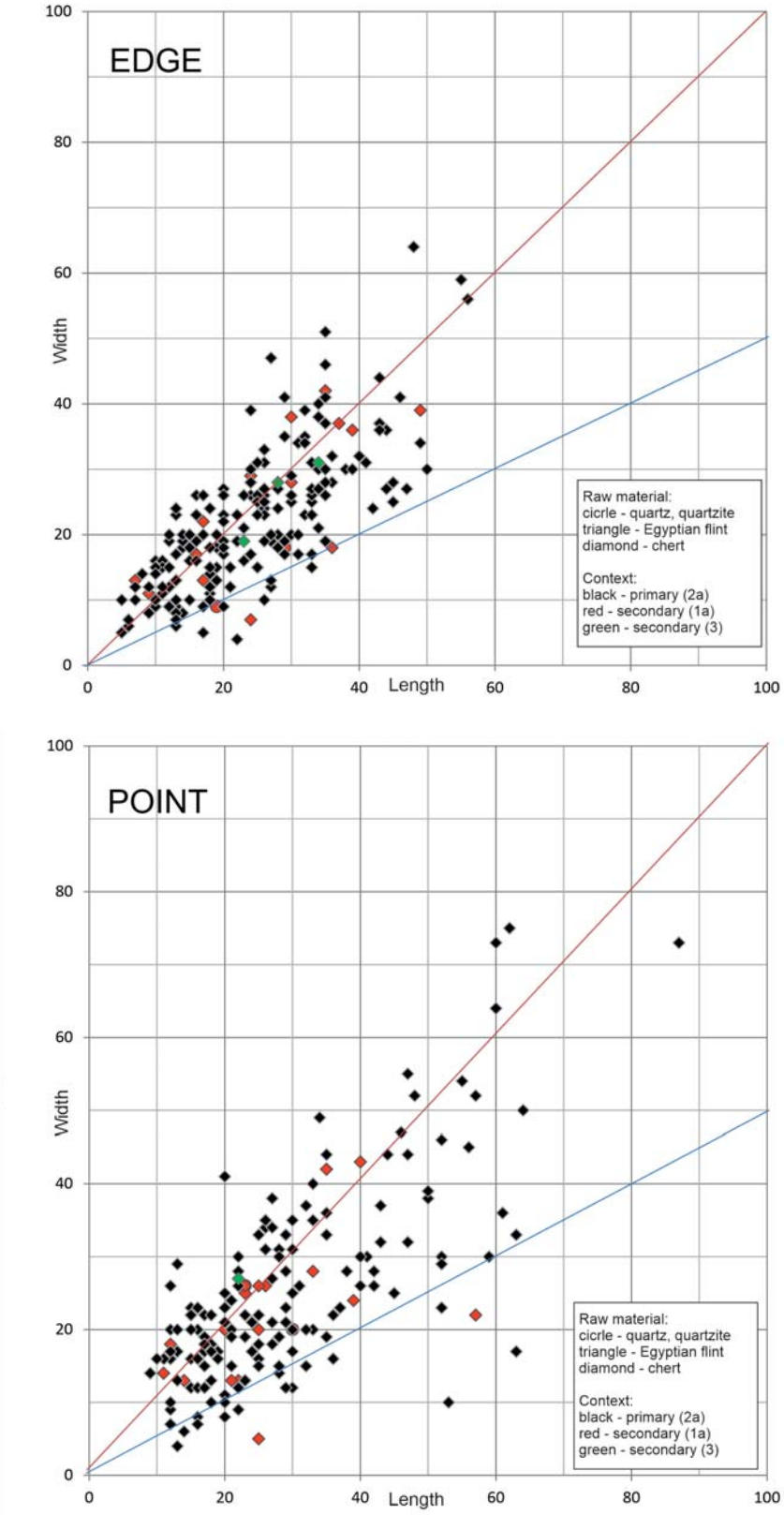

Fig. 4.14. Flakes from site AFD23 (sector SW), top, with edge butt, bottom, with point butt: length-to-width correlation (mm)

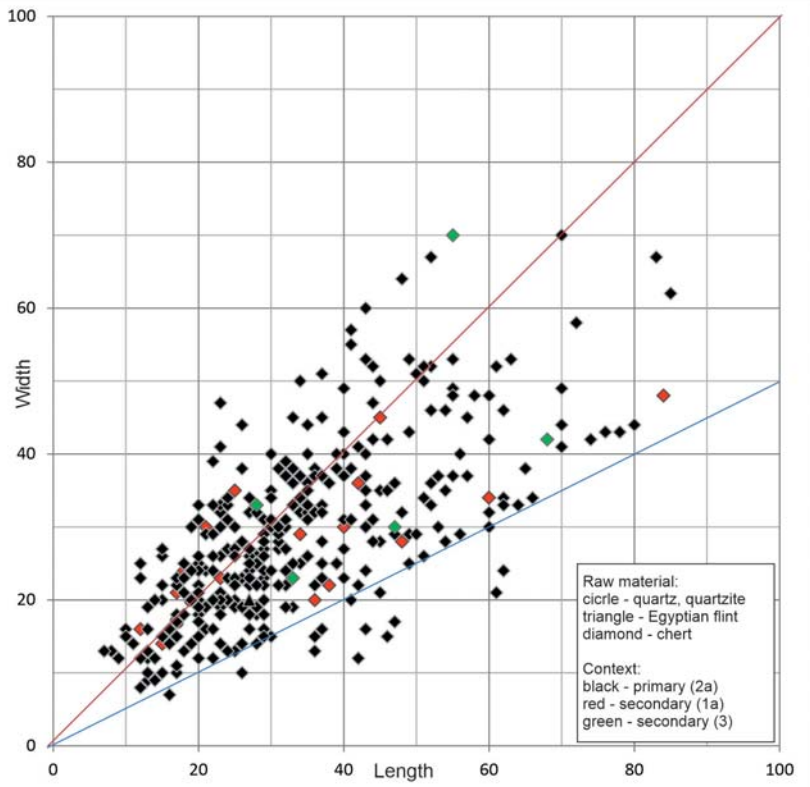

Fig. 4.15. Flakes with multi-faced butt from site AFD23 (sector SW): length-to-width correlation (mm)

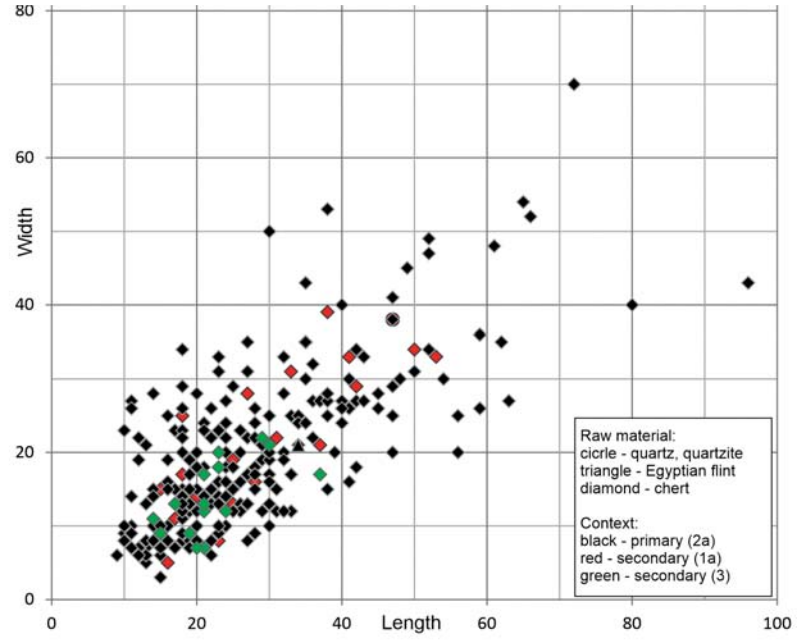

Fig. 4.16. Chunks (two largest measurements) from site AFD23 (sector SW): length-to-width correlation (mm)

Predetermined products and tools

Flakes with facetted butt without macroscopically noticeable traces of use (retouching, smoothening, wear) were among the most numerous artifacts in the predetermined products category. They are characterized by a slightly elongated form [*Fig. 4.17*], as well as sizes exceeding 4 cm in length and 3 cm in width. The largest examples present in the collection in the southwestern sector reached a length of approximately 6 cm and a width of 5 cm. The proportion of points indicated greater slenderness than in the case of flakes.

Flakes and points of this category did not have any natural external nodule surface on the dorsal side [see *Table 4.5*]. This feature points toward the detachment of flakes with a facetted butt from nodules which had already been worked on (cores).

Traces of damage of a similar nature to other categories was also noted on flakes and points with a facetted butt [see *Table 4.6*]. The percentage of transverse breakage significantly exceeded longitudinal fractures/breakage, which is an unusual relationship compared to the other categories of flakes. Relatively more burned flakes were noted in this category compared to the other ones, although one should keep in mind that the sample was small. A number of flakes bore traces of accidental chipping of the edge in the form of irregular series of small negatives [for example, *Fig. 4.18:1012*].

Flakes with a facetted butt were recorded as being spread on the surface over all of the area investigated in 2003. Flakes and points from excavations in 2013–2014 are concentrated in the southeastern section of Are 33 (western cluster), where Levallois cores were also recorded [see *Fig. 4.19*]. Flakes with facetted butt were found only occasionally in the other parts of the site. In terms of stratigraphic relations, although Levallois flakes, or fragments of them, occurred both in primary and secondary contexts in similar quantities, most of the points were recorded in primary contexts.

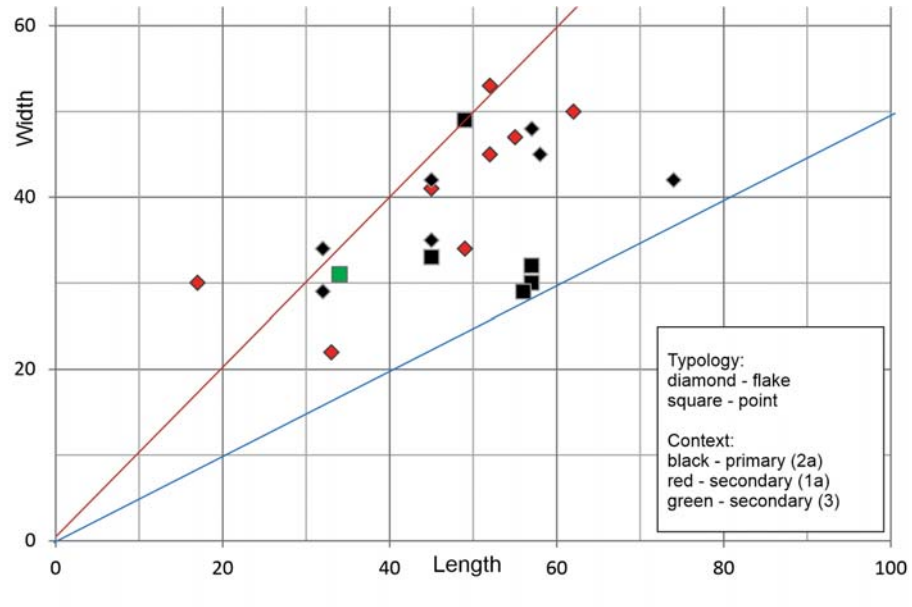

Fig. 4.17. Flakes and points with facetted butts from site AFD23 (sector SW): length-to-width correlation (mm; only complete artifacts considered)

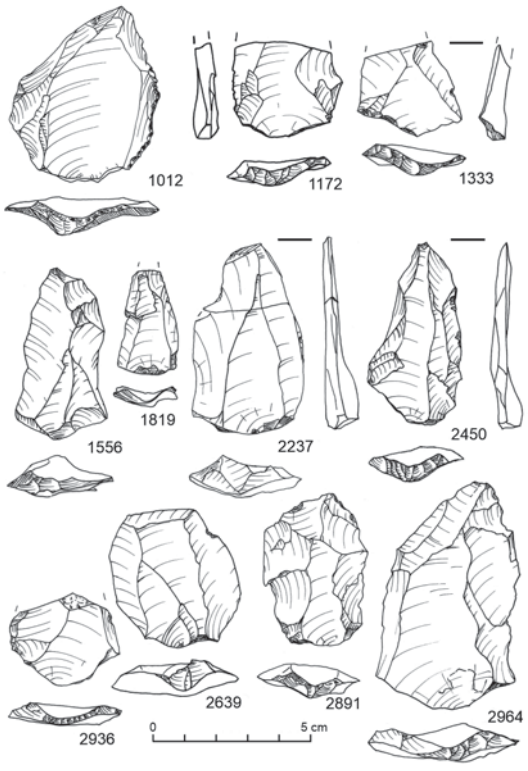

Fig. 4.18. Levallois points and flakes from site AFD23 (sector SW): 1012, 1172, 1333, 1556, 1819, 2237, 2450, 2639, 2891, 2936, 2964

In all cases of Levallois flakes from the southwestern sector, the pattern of negatives on the dorsal side corresponds with the centripetal shaping of the flaking surface. Among the points recorded there was not one case of a Nubian type 1 point, although some examples featured elements of flaking surface shaping from various directions, not excluding the opposite side of the core (e.g., *Fig. 4.18:2964 or 2450*). In the case of some specimens, small negatives are also observed, bearing the greatest protuberance of the inter-negative ridges in the proximal part, which may indicate the application of operations tapering the base of the point (e.g., *Fig. 4.18:2237, 2936, 2450*). However, similar negatives also occur on some flakes (e.g., *Fig. 4.18:2891*).

Flakes with denticulate and notched retouching were recorded as being scattered all over the investigated surface [see *Figs 4.19, 4.20*, labelled with the letter M). Relatively fewer tools of this type occurred in the western cluster, which contained instead the largest number of Levallois flakes and points.

One could probably also include in this group a Levallois flake with two notches on the distal edge [see below, *Figs 4.34, 4.35:95* = Block 22]. These notches supplement the naturally jagged course of this edge, but the edge is not denticulated along its entire length raising doubts as to the intentionality of this retouching. In most cases denticulate retouching covered the longer edge of the artifact for almost its entire length.

Given the fragmentary nature of the preservation of artifacts of this category, it is difficult to determine the blank preferences used in their production. They were also undoubtedly made of flakes covered to a large degree with the natural external surface of the nodule, although one should mention denticulate tools produced from large Levallois flakes [*Fig. 4.21:1832, 3067*]. Meriting attention are Levallois points with denticulate retouching of both convergent edges (Tayac type in a typological (formal) sense, e.g., *Fig. 4.22:3534*).

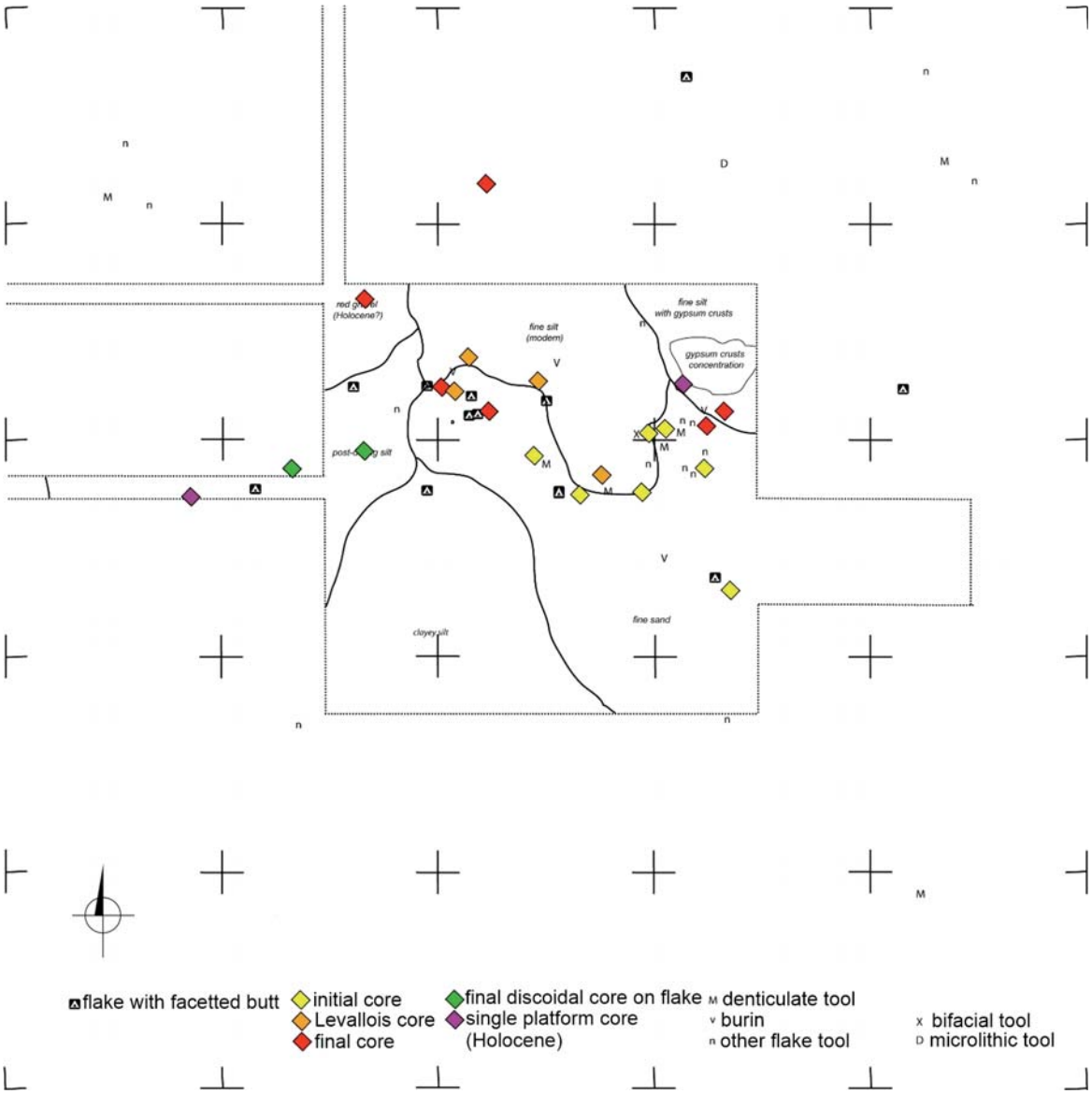

Fig. 4.19. Mapping of selected artifacts on the surface of site AFD23 (sector SW): flakes and points with facetted butt, cores and retouched tools

Flakes with burin scars, burins in a typological (formal) sense, were also found [*Table 4.7*]. Although they occurred mainly in the western cluster with the greatest cluster of Levallois artifacts [see *Fig. 4.19*], they did not make for a distinct concentration.

A characteristic feature of three artifacts was the presence of a burin spall negative/negatives that removed the ridge of the butt and the ventral (positive) surface. No evident blank preferences could be discerned in the small collection of burins, with each artifact representing a different category: chunks, opening flakes, as well Levallois flakes with a facetted butt. An overlapping of burin scars was also noted repeatedly.

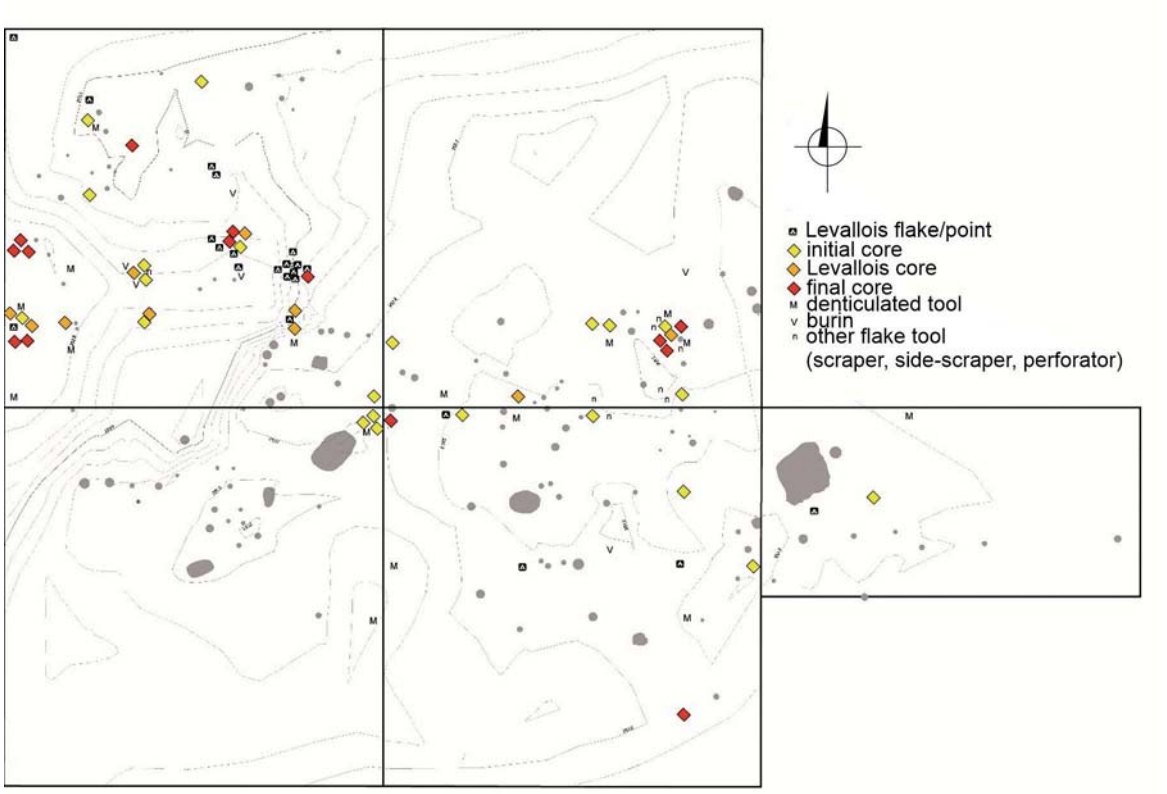

Fig. 4.20. Dispersal of selected lithic artifacts in primary contexts (category 2a) at site AFD23 (sector SW)

The last category of tools connected with Palaeolithic flake production were forms retouched at abrupt or semi-abrupt angles on one or several edges [see *Table 4.7*]. Although they were scattered throughout the investigated area, they formed a small concentration in the eastern cluster where numerous denticulate/notched tools were also found [see *Fig. 4.19*].

Based on the location of the retouch, these artifacts can be divided into a number of typological categories: endscrapers, racloirs/sidescrapers, perforators. Such divisions would suggest an utilitarian function, but there is nothing to suggest it. The intentional character of all of the retouching also constitutes an issue to be resolved.

An individual bifacial artifact found at the site, connected with Late Pleistocene occupation, is made of sandstone with a slightly eroded surface covered with a darkish brown patina. Despite this, the pattern of negatives on its surfaces is legible. Its dimensions were 62/42/25 mm [*Fig. 4.22:327*].The blank for this artifact was a crude flake with a fragment of the positive (ventral) surface still visible. Although the butt was not preserved, the crudeness and general section of this piece indicated that it had been obtained by hard direct percussion. Moreover, because the processing did not achieve a perfect symmetry of both planes, it should be viewed as a semi-processed bifacial by-product (point?). On the positive side of the blank, broad negatives of flat retouching covered the bulbar section (the most protuberant), as well as, fragmentarily, the distal

section. Although the opposite side is completely covered with negatives, a number of them (in the central section) come from the stage of flaking surface formation at the core. Only negatives along the edge (with a more abrupt angle relative to the opposite side) come from a stage of bifacial shaping. This artifact was recorded in the eastern part of the cluster of Palaeolithic artifacts (Ares 33, 32 and 23).

A single fragment of a backed tool, a sickle insert, from Holocene times was picked up from the site surface in 2003 [*Fig. 4.22:539*]. This small tool was made of a raw material known as Egyptian flint, retouching the arched back on a blade, 13 mm wide and 3 mm thick, on the negative/dorsal side. The preserved length of the tool reaches 20 mm and represents more or less half its original size. The edges of the artifact bear clear traces of erosion (smoothening) indicating its transportation in gravel formations and redeposition in a secondary context. A similar state of preservation was displayed by another fragment of a lunate insert made of chert [*Fig. 4.22:2717*]. It was excavated in 2013 in a layer of gravel connected with the Holocene stage of sedimentation at Affad. This specimen was also incomplete (dimensions: 19/10/2).

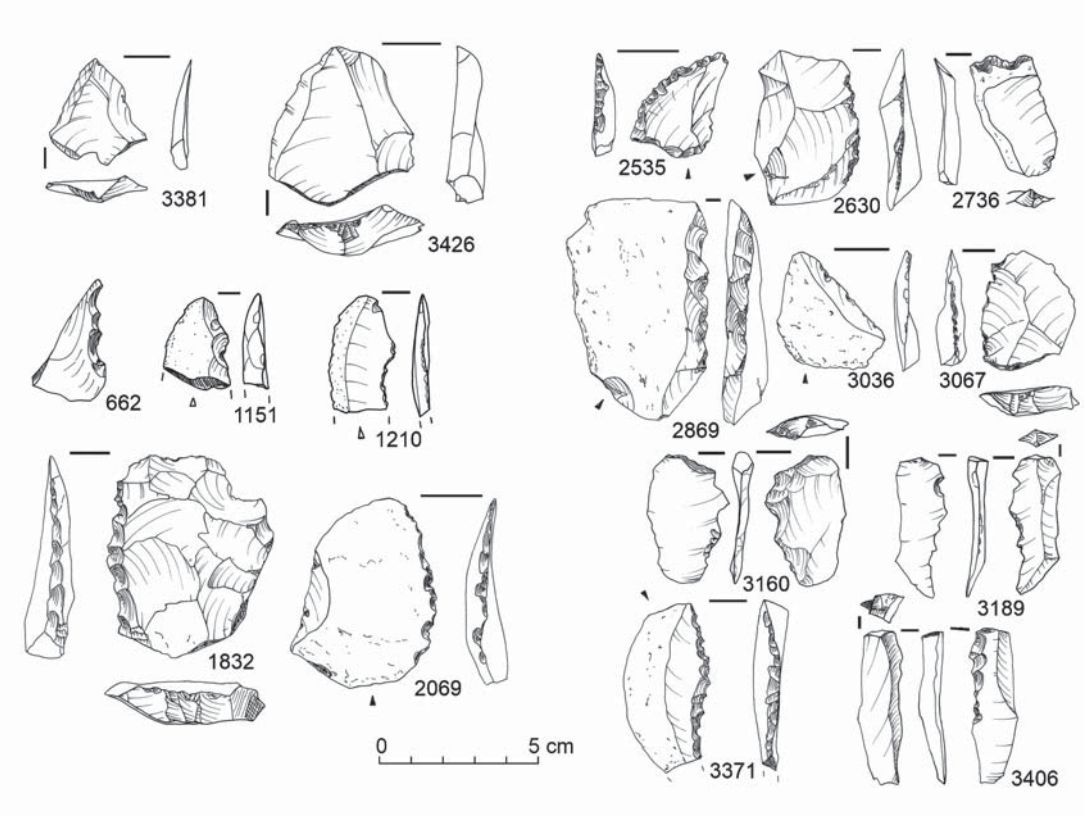

Fig. 4.21. Levallois points and denticulate tools from site AFD23 (sector SW): 662, 1151, 1210, 1832, 2069, 2535, 2630, 2736, 2869, 3036, 3067, 3160, 3189, 3371, 3381, 3406, 3426

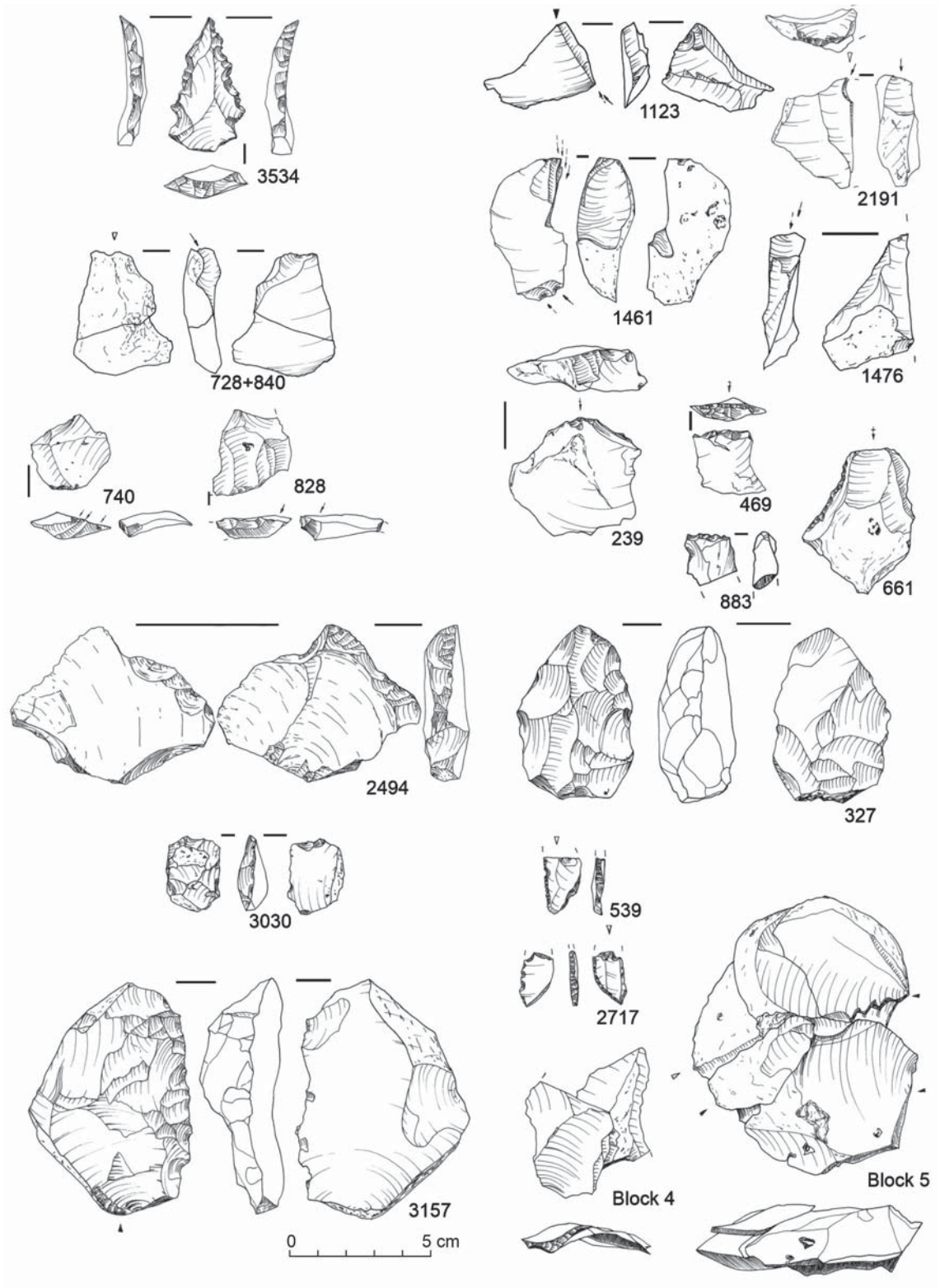

Fig. 4.22. Predetermined products and tools from site AFD23 (sector SW): Tayac point and items with burin blow negative – 728+840, 740, 828, 3534, burins and tools with abrupt retouch – 239, 469, 661, 883, 1123, 1461, 1476, 2191; formal tools with semi-abrupt retouch – 2494, 3030, 3157; preform of bifacial tool?, arch-backed pieces (Early Holocene) and refittings – 327, 539, 2717, refitted Block 4 [dorsal face], refitted Block 5 [dorsal face])

Table 4.7. Flakes from site AFD23 (sector SW): 1) Levallois flakes and points; 2) flakes with denticulate and notched retouching (including one flake from sector NW); 3) flakes with burin scars; 4) flakes with abrupt and semi-abrupt retouching

Inv. No.	Locus	Context	Block/ refitting/ concentration	Dimensions (mm)	Description/raw material	Reference
1) LEVALLOIS FLAKES AND POINTS						
47	A/34/21 =2013/I/55/I	2a		32/29/6	Levallois flake/flint	
93	A/31	1a		17/30/3	Levallois flake/overheated	
155	A/33/18 =2013/I/84/I	2a		(15)/22/6	Levallois flake, fragment	
196	A/33/19 =2013/I/74/I	2a	Block 8 Z-3	(28)/17/6	Levallois flake, fragment	
220	A/34/25 =2013/I/15/I	1a		(25)/35/6	Levallois flake, fragment	
229	A/24/79	1a		27/(19)/5	Levallois flake, fragment (Siret acc.)	
359	A/33/30 =2013/I/65/I	2a	Block 8 Z-3	52/45/9	Levallois flake	
425	A/33/29 =2013/I/75/I	2a		(20)/36/5	Levallois flake, fragment	
521	A/22/37 =2013/G/96/I		Block 10	32/34/6	Plunging Levallois flake	
554	A/33/26 =2013/F/5/I	2a		(35)/50/11	Levallois flake, fragment	
682	A/23/75 =2013/G/20/I	2a	Block 4 Z-1	(41)/32/4	Levallois flake, fragment	
969	A/23/89 =2013/I/71/I	2a	Block 7	33/22/5	Levallois flake	
1012	A/42/59	1a		55/47/7	Levallois flake/post-depositional damage to edges	*Fig. 4.18*
1172	A/24/71 =2013/H/60/I	1a		(31)/34/6	Levallois point, fragment, thinned base	*Fig. 4.18*
1302	2013/I/65/Ia	2a	Block 44	57/48/11	Levallois point	
1333	2013/I/74/Ia	2a		(30)/33/6	Levallois point, fragment	*Fig. 4.18*
1546	2013/I/64/Ia	2a	Block 38	62/50/9	Plunging Levallois flake	
1556	2013/I/64/Ia	2a		56/29/10	Levallois point	*Fig. 4.18*
1819	2013/I/73/Ib	2a		(34)/19/2	Levallois point, fragment	*Fig. 4.18*
1901	2013/I/3/IIb	2a	1898, 1902	57/48/12	Levallois flake	
2237	2013/I/57/Ia	2a	2238+2237	62/35/8	Levallois point, fragment	*Fig. 4.18*
2238	2013/I/57/Ia	2a	2237+2238	See above	Levallois point, fragment	
2383	2013/I/74/Ib	2a		58/45/8	Levallois flake	
2393	2013/I/74/Ib	2a		45/33/4	Levallois point	
2394	2013/I/74/Ib	2a		(21)/29/4	Levallois point, fragment	
2395	2013/I/74/Ib	2a		(24)/27/5	Levallois point, fragment	

Table 4.7. continued

Inv. No.	Locus	Context	Block/ refitting/ concentration	Dimensions (mm)	Description/raw material	Reference
2450	2013/I/55/Ia	2a		57/30/3	Levallois point(?), thinned base	*Fig. 4.18*
2639	2013/I/10/II	2a		45/42/7	Levallois flake	*Fig. 4.18*
2658	2013/I/16/Ia	3		(34)/25/3	Levallois point, fragment/ eolic erosion, post-depositional damage to edge	
2891	2013/F/36/Ia	1a		49/34/7	Levallois flake, base thinning(?)	*Fig. 4.18*
2905	2013/F/60/Ia	1a		45/41/7	Levallois flake/ferruginous sandstone, eolic erosion	
2936	2013/F/98/Ia	1a		(29)/35/4	Levallois point, fragment, base thinning, additional retouch(?)	*Fig. 4.18*
2964	2013/G/46-56/Ia	2a		74/42/9	Levallois point	*Fig. 4.18*
3031	2013/G/85/Ia	2a	Block 25 Z-1	45/35/10	Levallois flake	
3381	2013/dump	3		34/31/3	Levallois point on flake with edge butt	*Fig. 4.21*
3426	2013/I/NW/II	2a		49/49/9	Levallois point	*Fig. 4.21*
3474	2014/Q/NW/I	2a		(38)/40/9	Levallois point, fragment/ flint	
			2) FLAKES WITH DENTICULATE AND NOTCHED RETOUCHING			
95	A/22/100 =2013/F/62/I	2a	Block 22	52/53/12	Levallois flake with two notches retouched in the distal part to the ventral face	*Figs 4.34, 4.35*
315	A/23/73 =2013/G/40/I	2a		(19)/12/5	Flake with denticulate retouch to the ventral face, distal part	
662	A/32/9 =2013/F/73/I	2a		(40)/(21)/9	Flake with denticulate retouch to the dorsal face, distal part	*Fig. 4.21*
805	A/45	1a		44/30/10	Flake with retouched notch	
927	A/23/85 =2013/F/11/I	2a		59/22/7	Flake with edge butt and denticulate retouch	
1151	A/41	1a		(30)/22/7	Flake with denticulate retouch to the dorsal face along one edge, distal part	*Fig. 4.21*
1210	A/1	1a		(37)/21/4	Elongated flake with retouched shallow notch to the dorsal face, distal part (fragment of denticulate tool?)	*Fig. 4.21*
1832	2013/I/12/II	2a		66/53/8	Flake with facetted butt and denticulate retouch to the dorsal face along one edge, partly cortical	*Fig. 4.21*

Table 4.7. continued

Inv. No.	Locus	Context	Block/ refitting/ concentration	Dimensions (mm)	Description/raw material	Reference
2069	2013/I/3/IIb	2a		60/44/10	Flake with plain butt and denticulate retouch, almost fully cortical	*Fig. 4.21*
2535	2013/I/1-5,11-15,21-25/II	2a		35/27/5	Flake with edge butt and denticulate retouch to the dorsal face of arch-shaped distal part, partly cortical	*Fig. 4.21*
2630	2013/I/72/Ib	2a		42/50/8	Flake with plain butt and irregular denticulate retouch (accidental/use retouch?)	*Fig. 4.21*
2736	2013/H/95/II	2a		42/22/5	Flake with prepared butt and denticulate ratouch to the dorsal face in the distal part, partly cortical	*Fig. 4.21*
2869	2013/F/82/Ia	2a		67/44/11	Flake with plain butt and denticulate retouch to the dorsal face, almost fully cortical	*Fig. 4.21*
3036	2013/G/85/Ia	2a		35/36/6	Flake with plain butt and irregular denticulate retouch at one edge (accidental/use retouch?)	*Fig. 4.21*
3067	2013/G/6/Ia	2a		39/32/7	Flake with facetted butt and irregular denticulate retouch to the dorsal face, almost fully cortical (accidental/use retouch?)	*Fig. 4.21*
3160	2014/N/91/II	2a		42/27/4	Flake with prepared/ multiface butt and denticulate retouch to the dorsal face at one edge	*Fig. 4.21*
3189	2014/O/10/IIa	2e		44/16/3	Elongated flake with prepared butt and irregular denticulate retouch to both faces (accidental/ use retouch?)	*Fig. 4.21*
3371	2013/I/1/IIc	2a		49/28/9	Flake with plain butt and denticulate retouch to the dorsal face, partly cortical	*Fig. 4.21*
3406	2013/I/28/II	2a		49/13/7	Elongated flake with unprepared butt and denticulate retouch to the ventral face along one edge	*Fig. 4.21*
3534	2014/Q/50/II	2a		57/32/7	Levallois point with denticulate retouch at both edges	*Fig. 4.22*
3577	2013/H/100/Ib	2a	Remains in Sudan		Flake with denticulate retouch	
3474	2014/Q/NW/I	2a		(38)/40/9	Levallois point, fragment/ flint	

Table 4.7. continued

Inv. No.	Locus	Context	Block/ refitting/ concentration	Dimensions (mm)	Description/raw material	Reference
			3) FLAKES WITH BURIN SCARS			
728	A/33/40 =2013/I/66/I	2a	Block 27	38/31/13	Cortical flake with a burin scar at the proximal part, ventral face	*Fig. 4.22*
740	A/22/50 =2013/G/67/I	2a		(32)/33/10	Flake with multiplicated burin scars in the proximal part (ventral face)	*Fig. 4.22*
828	A/32/18 =2013/F/84/I	2a		(30)/(30)/10	Levallois flake with burin scar in proximal part (ventral face)	*Fig. 4.22*
1123	A/33/35 =2013/F/16/I	1a	Block 22	25/(37)/8	Flake with multiplicated burin scars on the side (surface of longitudinal breakage)	*Fig. 4.22*
1461	2013/I/34/IIa	2a		52/27/18	Chunk with multiplicated burin scars on two opposite parts, partly cortical	*Fig. 4.22*
1476	2013/I/34/IIa	2a		47/(34)/10	Multiface/prepared butt flake broken along its technological axis with multiplicated burin scars on the side (dorsal face)/ overheated	*Fig. 4.22*
2191	2013/I/64/Ia	2a		39/25/10	Flake with multiface/ prepared butt and burin scar on the side (dorsal face), partly cortical	*Fig. 4.22*
			4) FLAKES WITH ABRUPT AND SEMI-ABRUPT RETOUCHING			
15	A/33	1a		36/39/7	Cortical flake with plain butt and abrupt retouch of a side = scraper	
239	A/22/89 =2013/F/71/I	2a		(42)/47/13	Flake with abrupt retouch of side (bulb/butt part), fragment = scraper	*Fig. 4.22*
249	A/22/89 =2013/F/71/I	2a		(18)/22/6	Flake with abrupt retouch of side, fragment = scraper	
469	A/22/98 =2013/F/82/I	2a		22/22/6	Flake fragment with abrupt retouch of side (bulb/butt part) = scraper	*Fig. 4.22*
649	A/32/9 =2013/F/73/I	2a	Block 15	43/50/22	Flake with semi-abrupt retouch on the side = sidescraper	
661	A/32/9 =2013/F/73/I	2a		52/39/7	Flake with abrupt retouch of side (dorsal face), partly cortical = scraper	*Fig. 4.22*
708	A/14	1a		56/34/13	Flake with abrupt retouch of two sides = perforator	

Table 4.7. continued

Inv. No.	Locus	Context	Block/ refitting/ concentration	Dimensions (mm)	Description/raw material	Reference
803	A/45	1a		36/39/12	Flake with abrupt retouch of two sides = perforator	
811	A/45	1a		(17)/29/8	Flake fragment with abrupt retouch of side = scraper	
883	A/34/13 =2013/I/34/I	2a	Block 22	19/18/9	Flake with abrupt retouch of side (dorsal face), distal part = scraper	*Fig. 4.22*
1030	A/12	1a		38/27/8	Flake with plain butt and abrupt retouch of side = scraper	
1131	A/23/81 =2013/F/51/I	2a		45/37/19	Flake with abrupt retouch of side = scraper	
1147	A/41	1a		35/32/8	Flake with abrupt retouch of two sides = perforator/eolic erosion	
1148	A/41	1a		43/39/13	Flake with abrupt retouch of three sides (two convergent) = perforator	
2494	2013/I/27/Ia	3		50/60/12	Flake with multi-faced prepared butt and abrupt retouch of one side (dorsal face) and accidental/use retouch(?) (ventral face) = scraper/ doubly patinated	*Fig. 4.22*
3030	2013/G/70/Ia	2a		20/29/9	Flake with unprepared butt and semi-abrupt retouched side sidescraper, partly cortical/eolic erosion	*Fig. 4.22*
3157	2014/N/40/Ic	2a		82/58/24	Robust flake with unprepared butt and semi-abrupt retouch of one side, partly cortical = sidescraper	*Fig. 4.22*
3572	2013/H/48/Ib	3	Remains in Sudan		Scraper/eolic erosion	

4.1.4.2 Refitting of lithic artifacts

The process of refitting artifacts was based on the collection transferred to Poland in 2003 and a second set deriving from the excavations at AFD23 in 2012–2014. To date, 512 artifacts have been refitted, forming altogether 44 blocks, which are presented in detail below [see *Table 4.8* for a list of refitted pieces in the case of each block]. Some of the smaller assemblages (refittings) were assigned to a single nodule despite no connecting parts. The results of this painstaking process modified the characteristics of the different assemblages from the site, leading to an improved understanding of the functional differentiation between given parts.

Table 4.8. Blocks 1–44: list of refitted pieces for each block

Inv. No.	Locus	Refitting	Dimensions (mm)	Description	Comments	Reference
				BLOCK 1		
656	A/32/9	Z-1	36/30/11	Flake removing a huge part of the striking platform		
38	A/32/20		(20)/30/7	Flake with plain butt, proximal part		
670	A/32/9		(17)/39/5	Distal part of flake		
573	A/22/99		36/23/7	Flake with plain butt		
1281	A/32/29	Z-2	40/30/9	Flake with multiface butt		
911	A/24/93		35/19/5	Flake with plain butt		
1156	A/33/2		36/37/6	Flake with plain butt		
634	A/33/19		13/5/2	Chunk		
				BLOCK 2		*Fig. 4.24*
364	A/33/30	Z-1	56/41/10	Flake with plain butt, partly cortical (70%)		
2619	2013/I/64/Ib		33/25/9	Flake with multiface prepared butt, fully cortical		
27	A/33/10		(44)/40/12	Flake with plain butt, proximal part, partly cortical (20%)		
1802	2013/I/65/Ia		62/75/21	Flake with point butt		
1044	A/33/30		91/77/41	Final core		
				BLOCK 3		
3019	2013/G/95/Ia	Z-1	80/40/10	Flake with plain butt, partly cortical (60%)		
397	A/22/46		26/27/6	Flake with edge butt, partly cortical (5%)		
337	A/22/47		23/16/4	Flake with plain butt		
2966	2013/G/84/Ia		(22)/23/4	Distal part of flake		
1095	A/22/58		16/23/4	Flake with edge butt		
520	A/22/37		23/21/5	Flake with plain butt		
519	A/22/37		47/80/53	Final core		*Fig. 4.7*
				BLOCK 4		*Fig. 4.22*
682	A/23/75	Z-1	(41)/32/4	Flake with facetted butt, proximal part, partly cortical (5%)		
452	A/23/65		(39)/25/6	Flake, distal part, partly cortical (5%)		*Figs 4.22, 4.24*
				BLOCK 5		
1186	A/33/28	Z-1	46/25/6	Flake with edge butt, partly cortical (80%)		

Table 4.8. continued

Inv. No.	Locus	Refitting	Dimensions (mm)	Description	Comments	Reference
400	A/43		56/59/13	Flake with plain butt, partly cortical (5%)		
401	A/43		59/145/14	Flake with unprepared butt, partly cortical (15%)		
402	A/43		48/52/17	Flake with unprepared butt, partly cortical (40%)		
776	A/33/7		56/56/15	Flake with unprepared butt, partly cortical (20%)		
932	A/33/8	Z-2	20/(26)/6	Flake with edge butt, fragment broken along its technological axis		
340	A/23/87		18/(24)/4	Flake, fragment broken along its technological axis, partly cortical (10%)		
				BLOCK 6		
82	A/24/64	Z-1	(40)/27/11	Flake with unprepared butt, proximal fragment, partly cortical (30%)		
1170	A/33/21		(15)/25/6	Flake, distal fragment, partly cortical (30%)		
396	A/22/46	Z-2	40/35/12	Cortical flake with unprepared butt		
117	A/34/34		40/39/17	Flake with unprepared butt, partly cortical (60%)		
398	A/33/45		30/48/13	Flake with edge butt, partly cortical (90%)		
1171	A/33/21	Z-3	(18)/29/5	Flake, distal fragment, partly cortical (60%)		
1225	A/33/15		40/46/10	Flake with unprepared butt, partly cortical (20%)		
344	A/32/30		47/25/10	Flake with unprepared butt, partly cortical (60%)		
1222	A/33/42		43/48/13	Flake with unprepared butt, partly cortical (15%)		
				BLOCK 7		*Fig. 4.24*
941	A/33/8	Z-1	20/31/9	Flake with multi-faced prepared butt, partly cortical (75%)	Rear platform	
1058	A/34		28/31/5	Flake with plain butt, partly cortical (10%)	Flaking surface, from rear side	
322	A/34/32		40/32/8	Flake with plain butt	Flaking surface, from front side	
1154	A/24/88		24/19/6	Flake with plain butt	Flaking surface, from front side	
986	A/33/9		(20)/16/7	Flake with plain butt, proximal fragment	Flaking surface, from front side	

Table 4.8. continued

Inv. No.	Locus	Refitting	Dimensions (mm)	Description	Comments	Reference
969	A/23/89		33/22/5	Flake with multi-faced/ facetted platform	Flaking surface, from front side	
1199	A/23/99		25/34/6	Flake with multi-faced/ prepared butt	Flaking surface, from front side	
936	A/33/8		25/19/7	Flake with unprepared butt	Flaking furface, from side	
2724	2013/I/84/Ia		38/22/12	Side-flake with plain butt, partly cortical (20%)	Flaking surface, from rear side	
143	A/33/18		47/45/27	Final core		
				BLOCK 8		*Fig. 4.26*
1808	2013/I/73/Ib	Z-1	42/24/4	Cortical flake with edge butt	Initial shaping with a front striking platform	
1324	2013/I/74/Ia		24/21/5	Flake with point butt	Faceting?	
186	A/33/19		(19)/23/5	Flake with edge butt, proximal fragment	Faceting?	
2390	2013/I/74/Ib		30/(19)/10	Flake with unprepared butt, fragment broken along its technological axis	Flaking surface from cortical side	
1810	2013/I/73/Ib		35/(23)/10	Flake with unprepared butt, fragment broken along its technological axis		
1782	2013/I/63/Ib	Z-3	(28)/40/12	Flake, distal fragment, partly cortical (60%)	Flaking surface from right side	
619	A/33/19		(21)/20/3	Cortical flake, distal fragment	Rear striking platform	
1050	A/34		48/43/5	Flake with plain butt, partly cortical (45%)	Rear striking platform	
2676	2013/I/72/Ib		27/30/10	Flake with plain butt	Side-blow, shaping rear platform	
1548	2013/I/64/Ia		43/38/9	Flake with unprepared butt	Side-blow, shaping rear platform	
590	A/33/19		70/43/18	Flake with plain butt, partly cortical (70%)	Rear platform	
423	A/33/29		(21)/37/12	Flake with plain butt, proximal fragment, partly cortical (10%)	Flaking surface, from rear platform	
591	A/33/19		(60)/52/8	Flake, mesial fragment		
599	A/33/19		(7)/35/5	Flake, mesial fragment		
1325	2013/I/74/Ia		(16)/30/4	Flake, distal fragment		
1331	2013/I/74/Ia		(21)/21/4	Flake, distal fragment, partly cortical (60%)	Flaking surface, from rear platform	
1508	2013/I/73/Ia		72/40/15	Flake with plain butt, partly cortical (80%)	Right edge of flaking surface, from rear platform	

Table 4.8. continued

Inv. No.	Locus	Refitting	Dimensions (mm)	Description	Comments	Reference
1318	2013/I/74/Ia		38/(20)/9	Flake with multi-faced butt, fragment broken along its technological axis, partly cortical (5%)	Rear platform	
1547	2013/I/64/Ia		72/(58)/14	Flake with multi-faced butt, partly cortical (20%)	Rear platform	
189	A/33/19		37/33/13	Flake with plain butt	Flaking surface, from rear platform	
613	A/33/19		36/27/6	Flake with plain butt	Flaking surface, from rear platform	
1319	2013/I/74/Ia		(25)/32/4	Flake, distal fragment	Flaking surface, from rear platform	
490	A/33/20		(35)/39/8	Flake with plain butt, proximal fragment	Flaking surface, from rear platform	
366	A/33/30		(27)/(16)/4	Flake, distal fragment		
616	A/33/19		(27)/(17)/5	Flake, distal fragment		
191	A/33/19		41/15/5	Flake with plain butt	Flaking surface, from rear platform	
607	A/33/19		18/34/8	Chunk	Flaking surface, from rear platform	
1316	2013/I/74/Ia		36/(30)/13	Flake with unprepared butt, fragment broken along its technological axis	Flaking surface from left side	
428	A/33/29		34/(27)/7	Flake, fragment broken along its technological axis		
603	A/33/19		66/34/9	Flake with plain butt, partly cortical (60%)	Rear platform	
2171	2013/I/64/Ia		(24)/39/5	Flake with multi-faced butt, proximal fragment	Rear platform	
1809	2013/I/73/Ib		(22)/30/3	Flake, mesial fragment		
1323	2013/I/74/Ia		(27)/30/6	Flake, distal fragment		
1313	2013/I/74/Ia		(43)/37/9	Flake with plain butt, proximal fragment	Flaking surface, from rear platform	
187	A/33/19		(20)/18/2	Flake, distal fragment		
601	A/33/19		27/16/4	Flake with plain butt, partly cortical (80%)	Rear platform	
1807	2013/I/73/Ib		(25)/35/9	Flake with plain butt, proximal fragment, partly cortical (70%)	Rear platform	
182	A/33/19		36/27/6	Flake with plain butt	Rear platform	
No data available				Flake, distal fragment	Flaking surface, from rear platform	
1781	2013/I/63/Ib		(48)/19/8	Flake with unprepared butt, proximal fragment, partly cortical (60%)	Flaking surface, from front platform	
2530	2013/I/1-5/II		(38)/32/7	Flake, distal fragment, partly cortical (40%)		

Table 4.8. continued

Inv. No.	Locus	Refitting	Dimensions (mm)	Description	Comments	Reference
384	A/33/30		44/36/11	Cortical flake with edge butt	Front platform	
1317	2013/I/74/Ia		40/20/8	Flake with plain butt, partly cortical (50%)	Front platform	
594	A/33/19		37/25/5	Flake with plain butt, partly cortical (15%)	Front platform	
624	A/33/19		(20)/17/4	Flake, distal fragment	Front platform	
175	A/33/19		61/36/11	Flake with point butt, partly cortical (70%)	Front platform	
2561	2013/I/5/Ib		(19)/35/5	Flake, distal fragment	Flaking surface, from the front platform	
1416	2013/I/64/Ib		63/33/7	Flake with point butt, partly cortical (10%)	Flaking surface, from front platform	
1314	2013/I/74/Ia		(42)/26/9	Flake with plain butt, proximal fragment, partly cortical (20%)	Flaking surface, from front platform	
1321	2013/I/74/Ia		(20)/30/9	Flake, distal fragment		
570	A/22/99		(38)/26/7	Flake, distal fragment, partly cortical (70%)	Flaking surface, from front platform	
1322	2013/I/74/Ia		23/32/3	Flake with plain butt, partly cortical (5%)	Front platform	
1315	2013/I/74/Ia		46/15/6	Flake with multiface prepared butt and burin blow on the side	Flaking surface, from front platform	
26	A/33/10		31/27/3	Flake with multiface/ prepared butt	Flaking surface, from front platform	
185	A/33/19		(20)/30/6	Flake with plain butt, proximal fragment, partly cortical (30%)	Front platform	
359	A/33/30		52/45/9	Flake with multiface prepared butt	Predetermined flake, flaking surface, from front platform	
196	A/33/19		(28)/17/6	Flake with multiface prepared butt, proximal fragment	Flaking surface, from front platform	
146	A/33/18		(28)/34/6	Flake, distal fragment	Flaking surface, from front platform	
933	A/33/8		20/18/6	Chunk	Flaking surface, from front platform	
2060	2013/I/73/Ib		25/30/6	Hinge flake with multiface prepared butt	Flaking surface, from front platform	

Table 4.8. continued

Inv. No.	Locus	Refitting	Dimensions (mm)	Description	Comments	Reference
2690	2013/I/82/Ia		33/45/12	Flake with multiface butt	Flaking surface, from left side	
399	A/43		83/68/49	Final core		*Fig. 4.11*
660	A/32/9	Z-4	22/(12)/5	Flake with plain butt, fragment broken along its technological axis		
474	A/22/98		27/(17)/6	Flake, fragment broken along its technological axis		
				BLOCK 9		
1053	A/34	Z-1	(31)/38/10	Flake, distal fragment, partly cortical (80%)		
2	A/33		43/32/11	Cortical flake with point butt		
365	A/33/30		(49)/39/15	Flake with unprepared butt, proximal fragment, partly cortical (15%)		
1437	2013/I/75/Ia		(19)/21/7	Flake, distal fragment, partly cortical (90%)		
1238	A/15	Z-2	(39)/16/7	Flake with plain butt, proximal fragment		
706	A/14		(35)/23/8	Flake with multi-faced prepared butt, proximal fragment		
				BLOCK 10		
254	A/22/38	Z-1	61/56/20	Flake with unprepared butt, partly cortical (90%)	Flaking surface, from rear platform	
266	A/22/38		30/30/10	Cortical flake with plain butt	Rear platform	
251	A/22/38		52/50/14	Flake with plain butt, partly cortical (10%)	Flaking surface, from rear platform/left side	
637	A/22/28		(20)/31/10	Flake with unprepared butt, proximal fragment	Flaking surface, from rear platform	
3018	2013/G/75-85/Ia		41/33/5	Flake with unprepared butt	Flaking surface, from right side	
1112	A/22/59		46/48/10	Flake with unprepared butt	Flaking surface, from right side	
3116	2013/G/75/Ia		50/43/17	Flake with unprepared butt	Flaking surface, from left side	
255	A/22/38		26/41/8	Flake with plain butt, partly cortical (25%)	Rear platform	
275	A/22/38		16/25/10	Chunk	Rear platform	
261	A/22/38		36/31/11	Flake with unprepared butt, partly cortical (60%)	Rear platform	

Table 4.8. continued

Inv. No.	Locus	Refitting	Dimensions (mm)	Description	Comments	Reference
1145	A/22/27		29/38/14	Flake with unprepared butt	Flaking surface, from left side	
3042	2013/G/85/Ia		37/23/8	Flake with multi-faced prepared butt, partly cortical (90%)	Front platform	
260	A/22/38		23/13/3	Flake with plain butt, partly cortical (5%)	Front platform	
638	A/22/28		27/18/4	Flake with multi-faced prepared butt, partly cortical (15%)	Front platform	
250	A/22/38		70/44/19	Flake with multi-faced butt, partly cortical (5%)	Flaking surface, from front platform, right edge	
636	A/22/28		21/37/7	Flake with plain butt, partly cortical (5%)	Front platform	
3103	2013/G/86-87/Ia		30/40/16	Flake with plain butt, partly cortical (80%)	Front platform	
271	A/22/38		27/28/12	Flake with plain butt, partly cortical (15%)	Front platform	
3045	2013/G/85/Ia		27/25/7	Flake with multi-faced butt, partly cortical (20%)	Front platform	
521	A/22/37		32/34/6	Flake with facetted butt	Predetermined product, hinged	
522	A/22/37		38/30/9	Flake with edge butt, partly cortical (40%)	Reshaping flaking surface, from front platform, right edge	
2760	2013/F/72/Ib		77/68/32	Levallois core, final		
3040	2013/G/85/Ia	Z-2	(20)/27/7	Flake with plain butt, proximal fragment, partly cortical flake (80%)	Initial shaping in front platform zone	
3041	2013/G/85/Ia		31/30/7	Flake with plain butt partly cortical (50%)	Initial shaping in front platform zone	
				BLOCK 11		
4	A/33	Z-1	35/33/11	Flake with point butt, partly cortical (98%)		
513	A/25		(16)/24/3	Flake with unprepared butt, proximal fragment		
324	A/34/32		40/(25)/8	Flake with unprepared butt, fragment broken along its technological axis		
488	A/34/14		50/(26)/8	Flake, fragment broken along its technological axis, partly cortical (30%)		
268	A/22/38		15/16/4	Flake with unprepared butt		

Table 4.8. continued

Inv. No.	Locus	Refitting	Dimensions (mm)	Description	Comments	Reference
				BLOCK 12		*Fig. 4.24*
97	A/22/100	Z-1	33/44/12	Cortical flake with unprepared butt	Flaking surface	
132	A/22/98		27/37/12	Flake with unprepared butt, partly cortical (75%)	Flaking surface	
79	A/23/93		23/28/7	Cortical flake with plain butt	Striking platform shaping	
643	A/32/9		24/39/8	Flake with edge butt, partly cortical (55%)	Striking platform shaping	
1141	A/23/81		(18)/13/4	Flake, distal fragment, partly cortical (10%)	Striking platform shaping	
954	A/23/71		50/42/10	Flake with plain butt, partly cortical (50%)	Striking platform shaping	
1268	A/33/11		26/33/8	Flake with edge butt, partly cortical (80%)	Striking platform shaping	
2973	2013/G/70-60/Ia	Z-2	20/33/9	Flake with plain butt, partly cortical (50%)		
3060	2013/G/100/Ia		25/21/4	Flake with plain butt, partly cortical (30%)		
				BLOCK 13		
561	A/22/99	Z-1	56/25/30	Chunk		
411	A/23/83		56/20/16	Chunk		
				BLOCK 14		*Fig. 4.24*
1308	2013/I/65/Ia	Z-1	58/48/11	Cortical flake with multi-faced prepared butt	Rear striking platform	
2522	2013/I/65/Ib		53/38/7	Flake with plain butt, partly cortical (90%)	Flaking surface, from rear platform	
1290	2013/I/65/Ia		57/39/9	Flake with plain butt, partly cortical (15%)	Flaking surface, from rear platform	
360	A/33/30		50/55/18	Flake with plain butt, partly cortical (90%)	Rear platform, left edge	
1061	A/34		28/20/4	Flake with plain butt, partly cortical (80%)	Flaking surface, from rear platform	
1184	A/33/28		(37)/30/8	Flake, distal fragment, partly cortical (75%)	Flaking surface, from rear platform	
1970	2013/I/65/Ia		40/31/6	Flake with plain butt, partly cortical (20%)	Flaking surface, from rear platform	
836	A/33/50		36/20/6	Flake with multi-faced prepared butt	Flaking surface, from rear platform	
1968	2013/I/65/Ia		52/28/8	Cortical flake with plain butt	Front striking platform	

Table 4.8. continued

Inv. No.	Locus	Refitting	Dimensions (mm)	Description	Comments	Reference
1977	2013/I/65/Ia		34/(22)/5	Flake with edge butt, fragment broken along its technological axis, partly cortical (20%)	Front striking platform	
1978	2013/I/65/Ia		34/(20)/5	Flake with edge butt, fragment broken along its technological axis, partly cortical (20%)		
17	A/33		(35)/27/7	Flake, distal fragment, partly cortical (30%)	Front striking platform	
1295	2013/I/65/Ia		57/45/9	Flake with plain butt, partly cortical (50%)	Flaking surface, from front platform	
425	A/33/29		20/35/6	Flake with multi-faced prepared butt, hinged	Front platform, right edge	
421	A/33/29		47/(44)/9	Flake with point butt, broken along its technological axis, partly cortical (15%)	Front platform	
501	A/33/20		(17)/23/6	Flake, distal fragment	Front platform	
981	A/33/9		53/32/12	Flake with plain butt, partly cortical (5%)	Front platform, left edge	
1982	2013/I/65/Ia		(14)/23/2	Flake with plain butt, proximal fragment	Flaking surface, left part	
1981	2013/I/65/Ia		(19)/15/6	Flake, distal fragment		
493	A/33/20		56/43/10	Flake with plain butt, partly cortical (15%)	Flaking surface, from front platform, left part	
878	A/33/46		57/50/21	Flake with plain butt, partly cortical (30%)	Front platform, right edge	
				BLOCK 15		
2742	2013/F/62/Ib		33/19/7	Flake with multi-faced prepared butt, partly cortical (20%)	Z-1	
104	A/22/100		27/22/8	Flake with plain butt, partly cortical (30%)		
2753	2013/F/72-72/Ib		40/47/10	Flake with unprepared butt, partly cortical (5%)		
826	A/32/18		42/52/16	Flake with unprepared butt, partly cortical (50%)		
343	A/32/30		(49)/54/19	Flake with unprepared butt, proximal fragment, partly cortical (20%)		
649	A/32/9		(43)/50/22	Flake with semi-abrupt retouch of one edge, distal fragment, partly cortical (40%) = sidescraper		

Table 4.8. continued

Inv. No.	Locus	Refitting	Dimensions (mm)	Description	Comments	Reference
752	A/33/40	Z-2	31/(28)/7	Cortical flake with multi-faced prepared butt, fragment broken along its technological axis		
1200	A/23/99		29/(26)/8	Cortical flake with multi-faced prepared butt, fragment broken along its technological axis		
1072	A/33/6		48/61/16	Flake with plain butt, partly cortical (80%)		
459	A/32/19	Z-3	32/34/8	Flake with edge butt, partly cortical (75%)		
240	A/22/89		29/35/13	Flake with plain butt, partly cortical (10%)		
2979	2013/G/58/Ia	Z-4	24/20/4	Flake with multi-faced prepared butt		
1070	A/23/63		41/42/9	Flake with unprepared butt		
308	A/23/61	Z-5	50/42/10	Flake with plain butt, partly cortical (10%)		
335	A/33/1		38/37/11	Flake with plain butt		
3046	2013/G/99/Ia		60/64/16	Flake with point butt, partly cortical (20%)		
94	A/22/100	Z-6	42/52/13	Flake with plain butt		
133	A/22/90		21/24/3	Flake with point butt		
				BLOCK 16		
835	A/33/50	Z-1	50/30/19	Flake with plain butt, partly cortical (30%)		
361	A/33/30		47/34/12	Flake with plain butt, partly cortical (10%)		
				BLOCK 17		
22	A/24/91	Z-1	32/20/7	Flake with plain butt, partly cortical (80%)		
1193	A/24/76		12/13/3	Flake with plain butt		
24	A/24/91		22/14/6	Flake with plain butt, partly cortical (50%)		
543	A/34/12	Z-2	19/20/6	Flake with unprepared butt, partly cortical (10%)		
939	A/33/8		17/14/6	Flake with unprepared butt		
				BLOCK 18		
456	A/33/5	Z-1	72/42/16	Flake with plain butt, partly cortical (40%)		
1076	A/33/6		63/37/11	Flake with plain butt, partly cortical (30%)		

Table 4.8. continued

Inv. No.	Locus	Refitting	Dimensions (mm)	Description	Comments	Reference
1253	A/33/16		56/46/19	Flake with plain butt, partly cortical (50%)		
1257	A/23/86		35/28/7	Flake with plain butt		
787	A/33/7	Z-2	(39)/35/11	Flake with plain butt, proximal fragment		
769	A/23/84		(37)/37/11	Flake, distal fragment, partly cortical (50%)		
152	A/33/18	Z-3	42/26/7	Flake with point butt, partly cortical (40%)		
407	A/43		(38)/32/11	Flake, distal fragment, partly cortical (50%)		
408	A/43		43/28/8	Flake with unprepared butt		
877	A/33/46		45/45/13	Flake with multi-faced prepared butt		
788	A/33/14		53/30/19	Flake with plain butt		
1255	A/33/16	Z-4	39/36/13	Flake with multi-faced prepared butt		
1259	A/23/86		21/15/4	Hinged flake with plain butt		
				BLOCK 19		*Fig. 4.31*
1	A/33	Z-1	52/29/13	Flake with unprepared butt, partly cortical (80%)		
855	A/24		23/16/7	Cortical flake with edge butt		
834	A/33/50		(48)/25/5	Flake, distal fragment, partly cortical (30%)		
1000	A/23/91	Z-2	35/19/5	Flake with edge butt, partly cortical (45%)		
460	A/32/19		50/43/9	Flake with plain butt, partly cortical (25%)		
881	A/22/69	Z-3	(18)/24/5	Flake, distal fragment		
473	A/22/98		44/33/10	Flake with plain butt		
60	A/23/76	Z-4	64/50/16	Flake with point butt, partly cortical (10%)	Flaking surface, from front platform	
742	A/22/50		43/53/11	Flake with plain butt, partly cortical (90%)	Front striking platform, left part	
558	A/22/99		77/43/13	Flake with plain butt, partly cortical	Front striking platform, left part	
1165	A/22/79		22/36/5	Side flake with plain butt	Flaking surface, from front platform	
2063	2013/I/92/Ia		32/37/11	Flake with point butt	Front striking platform, left part	
763	A/23/72		52/47/23	Chunk – flake with unprepared butt	Flaking surface, from rear platform	

Table 4.8. continued

Inv. No.	Locus	Refitting	Dimensions (mm)	Description	Comments	Reference
838	A/24		37/36/26	Flake with plain butt, partly cortical (30%)	Flaking surface, from front platform, right side	
571	A/22/99		45/43/18	Flake with plain butt	Flaking surface, from front platform, right side	
1223	A/22/67		57/52/15	Flake with point butt, cortical (100%)	Rear striking platform	
563	A/22/99		47/55/17	Flake with plain butt, partly cortical (5%)	Flaking surface, from rear platform	
1219	A/22/78		27/35/23	Chunk	Flaking surface, from rear platform	
577	A/22/99		(35)/34/6	Flake, distal fragment	Flaking surface, from front platform	
793	A/45		70/51/13	Side flake with plain butt	Flaking surface, from front platform	
882	A/22/69		(16)/34/9	Flake, distal fragment	Flaking surface, from front platform	
760	A/23/72		(40)/32/15	Flake with plain butt, proximal fragment, partly cortical (30%)	Flaking surface, from front platform	
1096	A/22/58		18/23/7	Flake with plain butt	Rear striking platform	
241	A/22/89		33/23/9	Flake with plain butt, partly cortical	Front striking platform	
1127	A/44		23/(12)/5	Flake with multi-faced prepared butt, fragment broken along its technological axis	Flaking surface, from front platform	
1218	A/22/78		38/(20)/10	Flake with multi-faced prepared butt, fragment broken along its technological axis		
657	A/32/9		40/30/6	Flake with point butt	Flaking surface, from front platform	
559	A/22/99		35/43/18	Chunk – irregular flake	Flaking surface, from rear platform	
906	A/22/80		38/36/10	Flake with multi-faced prepared butt	Flaking surface, from rear platform	
413	A/23/83		28/33/8	Flake with multi-faced prepared butt	Flaking surface, from rear platform	
				BLOCK 20		
177	A/33/19	Z-1	(33)/34/10	Flake with plain butt, proximal fragment, partly cortical flake (80%)		
422	A/33/29		(38)/51/13	Flake, distal fragment, partly cortical (80%)		

Table 4.8. continued

Inv. No.	Locus	Refitting	Dimensions (mm)	Description	Comments	Reference
492	A/33/20	Z-2	60/73/12	Flake with point butt, partly cortical (30%)		
732	A/33/40		48/37/11	Flake with unprepared butt		
975	A/33/39		49/39/12	Flake with edge butt		
974	A/33/39		59/54/12	Flake with multi-faced prepared butt, partly cortical (5%)		
751	A/33/17	Z-3	(21)/(26)/9	Flake with unprepared butt, proximal fragment broken along its technological axis		
983	A/33/9		25/(22)/9	Flake with unprepared butt, fragment broken along its technological axis		
338	A/23/87		(25)/(11)/4	Flake, distal fragment broken along its technological axis		
				BLOCK 21		
159	A/23/54	Z-1	60/41/17	Cortical flake with plain butt		
949	A/23		(33)/28/10	Flake with plain butt, proximal fragment, partly cortical (40%)		
450	A/23/65	Z-2	13/23/6	Cortical flake with multi-faced prepared butt		
3063	2013/G/19/Ia		30/31/9	Flake with multi-faced prepared butt, partly cortical (20%)		
684	A/23/75		24/33/13	Flake with multi-faced prepared butt		
68	A/23/76		25/19/3	Flake, broken along its technological axis, partly cortical (15%)		
1097	A/24/86		(27)/24/7	Flake, distal fragment		
1105	A/34/1		29/(24)/7	Flake with edge butt, broken along its technological axis, partly cortical (90%)		
				BLOCK 22 Block 41 was later refitted with Block 22 and is included here		*Fig. 4.31*
2782	2013/F/72/Ib	Z-1 stage 1	29/(28)/9	Cortical flake with multi-faced prepared butt, broken along its technological axis		
2781	2013/F/72/Ib		29/(24)/9	Cortical flake with multi-faced prepared butt, broken along its technological axis		

Table 4.8. continued

Inv. No.	Locus	Refitting	Dimensions (mm)	Description	Comments	Reference
2783	2013/F/72/Ib		35/(23)/10	Flake with plain butt, broken along its technological axis, partly cortical (90%)		
330	A/33/1		37/53/11	Flake with plain butt, partly cortical (20%)		
709	A/33/24		30/(7)/8	Flake with point butt, broken along its technological axis		
908	A/22/80		28/33/9	Cortical flake with unprepared butt		
106	A/22/100		32/23/6	Flake with unprepared butt, partly cortical (40%)		
138	A/22/90		(34)/30/8	Flake, distal fragment, partly cortical (45%)		
659	A/32/9		48/45/17	Flake with unprepared butt, partly cortical (70%)		
2738	2013/F/62/Ib		50/38/11	Flake with point butt, partly cortical (25%)		
2840	2013/F/61/Ia		34/27/7	Flake with edge butt, partly cortical (30%)		
2780	2013/F/72/Ib		50/(36)/10	Flake with plain butt, fragment broken along its technological axis, partly cortical (20%)		
1123	A/33/35		25/(37)/8	Flake with plain butt, fragment broken along its technological axis; burin scar on breakage face		
994	A/23/91		25/12/5	Chunk		
2779	2013/F/72/Ib		45/(26)/7	Flake with multi-faced prepared butt, fragment broken along its technological axis, artly cortical (50%)		
2784	2013/F/72/Ib		(22)/33/11	Flake, distal fragment, partly cortical (50%)		
1245	A/13		50/50/14	Flake with plain butt, partly cortical (25%)		
103	A/22/100	Z-1 stage 2	(38)/25/17	Flake, distal fragment		
332	A/33/1		(20)/18/12	Chunk – flake with plain butt, proximal fragment		
651	A/32/9		43/28/9	Flake with multi-faced prepared butt, partly cortical (50%)		
1004	A/23/91		55/30/9	Flake with multi-faced prepared butt, partly cortical (15%)		
726	A/33/40		23/33/13	Chunk/overheated		

Table 4.8. continued

Inv. No.	Locus	Refitting	Dimensions (mm)	Description	Comments	Reference
883	A/22/69		19/18/9	Flake with abrupt retouch of one side to dorsal face		
1157	A/33/2		35/31/6	Flake with point butt, broken along its technological axis		
96	A/22/100	Z-1 stage 3	47/35/17	Flake with plain butt, partly cortical (25%)		
108	A/22/100		23/16/4	Flake with plain butt		
124	A/32/10		46/27/5	Flake with plain butt, partly cortical (5%)		
536	A/42		22/19/3	Flake with edge butt		
762	A/23/72		23/19/5	Flake with point butt		
1209	A/24/68		27/23/7	Flake with multi-faced prepared butt		
95	A/22/100	Z-1 stage 4	52/53/12	Levallois flake with retouched notches on one side		
123	A/32/10	Z-1 stage 5	34/30/7	Flake with unprepared butt, partly cortical (15%)		
137	A/22/90		30/23/8	Flake with plain butt, partly cortical		
225	A/33/22		24/24/7	Flake with unprepared butt, partly cortical (50%)		
2835	2013/F/73/Ia	Z-1 stage 6	22/22/6	Flake with unprepared butt		
333	A/33/1		20/22/5	Flake with unprepared butt		
1048	A/34		67/52/37	Final core		
				BLOCK 23		
461	A/32/19	Z-1	39/31/9	Flake with plain butt, partly cortical (95%)		
655	A/32/9		52/52/12	Flake with multi-faced prepared butt, partly cortical (20%)		
237	A/22/89	Z-2	46/53/26	Flake with unprepared butt, partly cortical (50%)		
1013	A/23/5		(24)/28/7	Flake with unprepared butt, proximal fragment		
74	A/22/88		45/51/18	Flake with unprepared butt, partly cortical (50%)		
328	A/33/1		52/55/15	Flake with unprepared butt, partly cortical (30%)		
				BLOCK 24		
719	A/33/25	Z-1	39/(42)/10	Flake with plain butt, fragment fragment broken along its technological axis, partly cortical (80%)		

Table 4.8. continued

Inv. No.	Locus	Refitting	Dimensions (mm)	Description	Comments	Reference
930	A/33/8		(55)/62/12	Cortical flake with plain butt, proximal fragment		
940	A/33/8		(29)/41/6	Cortical flake, distal fragment		
995	A/23/91	Z-2	(30)/20/11	Flake, distal fragment, partly cortical (75%)		
81	A/23/93		52/46/16	Flake with point butt, partly cortical (50%)		
782	A/33/7	Z-3	51/48/20	Flake with point butt, partly cortical (40%)		
150	A/33/18		(33)/45/12	Flake with unprepared butt, proximal fragment, partly cortical (10%)		
1081	A/23/96		(32)/54/11	Flake, distal fragment, partly cortical (50%)		
29	A/33/10	Z-4	38/(24)/8	Flake with unprepared butt, fragment broken along its technological axis, partly cortical (10%)		
697	A/23/97		24/(28)/7	Flake with unprepared butt, fragment broken along its technological axis		
				BLOCK 25		
635	A/22/28	Z-1	85/62/13	Flake with multi-faced prepared butt, partly cortical (20%)		
272	A/22/38		(22)/35/6	Flake with multi-faced prepared butt, proximal fragment		
274	A/22/38		(26)/35/9	Flake, distal fragment, partly cortical (10%)		
270	A/22/38		(37)/24/6	Flake with plain butt, proximal fragment, partly cortical (90%)		
714	A/22/48		(30)/26/10	Flake, distal fragment, partly cortical (90%)		
257	A/22/38		47/28/10	Flake with plain butt		
267	A/22/38		25/29/6	Flake with plain butt		
3031	2013/G/85/Ia		45/35/10	Flake with multi-faced prepared butt		
253	A/22/38		60/30/10	Flake with multi-faced prepared butt, partly cortical (25%)		
258	A/22/38	Z-2	43/37/7	Flake with multi-faced prepared butt, partly cortical (30%)		
3034	2013/G/85/Ia		(36)/29/9	Flake with multi-faced prepared butt, proximal fragment, partly cortical (5%)		

Table 4.8. continued

Inv. No.	Locus	Refitting	Dimensions (mm)	Description	Comments	Reference
?	A/22/			Flake, distal fragment, partly cortical		
1264	A/33/37	Z-3	44/50/14	Flake with unprepared butt, partly cortical (25%)		
3098	2013/G/82/Ib		30/(33)/15	Flake with unprepared butt, fragment broken along its technological axis, partly cortical (20%)		
2178	2013/I/64/Ia	Z-4	30/50/9	Flake with unprepared butt, partly cortical (90%)		
1073	A/33/6		58/67/23	Flake with unprepared butt, partly cortical (75%)		
3096	2013/G/82/Ib	Z-5	55/34/12	Flake with unprepared butt, partly cortical (20%)		
3032	2013/G/85/Ia		(50)/38/11	Flake, distal fragment, partly cortical (80%)		
3109	2013/G/83/Ia	Z-6	(30)/51/12	Flake with unprepared butt, proximal fragment, partly cortical (50%)		
3110	2013/G/83/Ia		(48)/51/12	Flake, distal fragment		
				BLOCK 26		
420	A/33/29	Z-1	43/40/13	Flake with multi-faced prepared butt, partly cortical (60%)		
149	A/33/18		47/35/8	Flake with multi-faced prepared butt		
				BLOCK 27		
870	A/33/49	Z-1	40/47/12	Flake with plain butt, partly cortical (75%)		
541	A/34/12		41/30/11	Chunk – flake, distal fragment		
728	A/33/40	Z-2	(38)/31/13	Cortical flake with burin scar taking off the butt, proximal fragment		
840	A/24		(21)/39/11	Cortical flake. distal fragment		
675	A/23/94	Z-3	(57)/31/9	Cortical flake, mesial fragment		
1168	A/22/79		24/27/10	Chunk – cortical flake, distal fragment		
1069	A/23/63		67/37/16	Cortical flake with unprepared butt		
683	A/23/75		36/25/10	Flake with unprepared butt, broken along its technological axis, partly cortical (50%)		
560	A/22/9		52/35/13	Flake with unprepared butt, partly cortical (25%)		

Table 4.8. continued

Inv. No.	Locus	Refitting	Dimensions (mm)	Description	Comments	Reference
				BLOCK 28		*Fig. 4.39*
696	A/23/97	Z-1	30/(27)/10	Flake with unprepared butt, broken along its technological axis		
713	A/34/9		19/(20)/8	Flake, fragment broken along its technological axis		
1189	A/33/34		28/28/15	Flake with unprepared butt		
412	A/23/83		25/42/15	Chunk		
937	A/33/8		(19)/31/7	Cortical flake, distal fragment		
				BLOCK 29		*Fig. 4.41*
665	A/32/9	Z-1	32/38/8	Cortical flake with plain butt	Rear striking platform	
2869	2013/F/82/Ia		67/44/11	Denticulate tool made of partly cortical flake (90%) Flake with plain butt	Flaking surface, from rear platform	*Fig. 4.21*
2796	2013/F/72/Ib		29/41/11	Cortical flake with edge butt	Rear platform	
673	A/32/9		36/43/23	partly cortical (70%)	Rear platform	
2883	2013/F/82/Ia		26/(26)/12	Flake with edge butt, fragment broken along its technological axis	Rear platform	
2798	2013/F/72/Ib		29/(17)/5	Flake, fragment broken along its technological axis		
565	A/22/99		27/34/7	Flake with point butt, partly cortical (10%)	Rear platform	
642	A/32/9		37/51/12	Flake with multi-faced prepared butt, partly cortical (95%)	Rear platform	
2849	2013/F/71/Ia		35/35/15	Flake with multi-faced prepared butt, partly cortical (20%)	Rear platform	
475	A/22/98		24/42/10	Flake with point butt	Rear platform	
668	A/32/9		20/23/4	Flake with point butt	Rear platform	
2901	2013/F/63/Ib		27/13/5	Flake with edge butt	Rear platform	
2795	2013/F/72/Ib		30/40/8	Flake with multi-faced prepared butt	Rear platform	
35	A/34/38		18/24/4	Cortical flake with unprepared butt	Rear platform	
2794	2013/F/72/Ib		35/34/12	Flake with plain butt, partly cortical (30%)	Rear platform	
1065	A/32/8		28/30/7	Flake with plain butt	Rear platform	
582	A/22/99		28/17/6	Flake with plain butt, partly cortical (25%)	Rear platform	

Table 4.8. continued

Inv. No.	Locus	Refitting	Dimensions (mm)	Description	Comments	Reference
464	A/32/19		18/24/8	Flake with edge butt	Flaking surface, from rear platform	
2746	2013/F/62/Ib		13/19/2	Flake with multi-faced prepared butt	Flaking surface, from rear platform	
581	A/22/99		31/28/6	Flake with plain butt, partly cortical (60%)	Front platform	
517	A/25		24/(15)/3	Flake with point butt, fragment broken along its technological axis	Front platform	
2743	2013/F/62/Ib		(20)/28/4	Flake with plain butt, proximal fragment	Flaking surface, from front platform	
1138	A/23/81		(22)/20/3	Flake, distal fragment, partly cortical (20%)		
2927	2013/F/81/Ia		34/39/5	Flake with plain butt, partly cortical (5%)	Flaking surface, from front platform	
663	A/32/9		33/20/5	Flake with point butt	Front platform	
478	A/22/98		(23)/34/4	Flake with point butt, proximal fragment	Flaking surface, from front platform	
112	A/22/100		(18)/27/2	Flake, distal fragment		
–	–		–	Levallois point from front platform	Not present in the collection	
644	A/32/9		30/32/5	Flake with plain butt	Flaking surface, from front platform	
45	A/24/85		(13)/15/3	Flake with plain butt, proximal fragment	Flaking surface, from front platform	
2900	2013/F/63/Ib		(23)/21/4	Flake, distal fragment		
463	A/32/19		26/28/5	Flake with unprepared butt	Flaking surface, from front platform	
107	A/22/100		28/20/4	Flake with plain butt	Flaking surface, from front platform	
2852	2013/F/71/Ia		27/(19)/6	Flake with multi-faced prepared butt, fragment broken along its technological axis	Flaking surface, from rear platform	
2921	2013/F/86/Ib		31/(15)/4	Flake, fragment broken along its technological axis		
2855	2013/F/71/Ia		23/20/6	Flake with multi-faced prepared butt	Flaking surface, from rear platform	
2749	2013/F/72-73/Ib		62/54/31	Levallois core for flake		*Fig. 4.10*
2851	2013/F/71/Ia	Z-2	21/27/6	Cortical flake with plain butt	Front platform	
588	A/22/99		(11)/16/3	Cortical flake, distal fragment	Front platform	

Table 4.8. continued

Inv. No.	Locus	Refitting	Dimensions (mm)	Description	Comments	Reference
2854	2013/F/71/Ia	Z-3	24/14/3	Flake with plain butt, partly cortical (30%)		
2850	2013/F/71/Ia		30/26/5	Flake with plain butt, partly cortical (50%)		
				BLOCK 30		
566	A/22/99	Z-1	47/20/16	Chunk		
346	A/32/30		22/26/13	Chunk		
121	A/32/10		44/48/19	Chunk		
334	A/33/1		45/27/15	Chunk		
923	A/23/85	Z-2	62/22/15	Flake with unprepared butt, partly cortical (40%)		
1269	A/23/92		57/51/19	Flake with unprepared butt, partly cortical (20%)		
				BLOCK 31		
1026	A/12	Z-1	47/47/12	Flake with multi-faced prepared butt, partly cortical (40%)		
884	A/34/13		48/45/14	Flake with unprepared butt, partly cortical (5%)		
				BLOCK 32		*Fig. 4.43*
2457	2013/I/55/Ia	Z-1	(35)/30/5	Flake with plain butt, proximal fragment, partly cortical (10%)		
2458	2013/I/55/Ia		(32)/24/5	Flake, distal fragment, partly cortical (50%)		
844	A/24		34/30/11	Flake with plain butt, partly cortical (45%)		
383	A/33/30		40/26/15	Chunk		
381	A/33/30		56/40/7	Flake with multi-faced prepared butt, partly cortical (5%)		
1046	A/33/30		71/65/41	Levallois core		*Fig. 4.10*
1100	A/34/11	Z-2	(27)/20/4	Cortical flake with edge butt, proximal fragment		
1195	A/24/76		39/15/7	Flake with plain butt, partly cortical (50%)		
654	A/32/9	Z-3	22/22/3	Flake with plain butt		
164	A/33/32		21/21/4	Flake with multi-faced prepared butt		
645	A/32/9	Z-4	33/23/6	Partly cortical with edge butt		
468	A/22/98		40/49/15	Partly cortical with multi-faced prepared butt		

Table 4.8. continued

Inv. No.	Locus	Refitting	Dimensions (mm)	Description	Comments	Reference
				BLOCK 33		
843	A/24	Z-1	60/(24)/8	Flake with facetted butt, broken along its technological axis, partly cortical fragment (15%)		
982	A/33/9		(44)/(19)/7	Flake with facetted butt, broken along its technological axis, proximal fragment, partly cortical (10%)		
1052	A/34		(20)/(20)/7	Flake, distal fragment, partly cortical (50%)		
890	A/34/8		(24)/34/6	Mesial fragment of flake		
				BLOCK 34		
281	A/34/II	Z-1	42/68/13	Flake with unprepared butt, partly cortical (10%)		
289	A/34/II		34/35/3	Flake with multi-faced prepared butt, partly cortical (5%)		
298	A/34/II		32/22/4	Flake with plain butt, partly cortical (5%)		
284	A/34/II		50/55/20	Flake with plain butt, partly cortical (98%)		
				BLOCK 35		
351	A/34/II	Z-1	80/53/25	Flake with unprepared butt, partly cortical (70%)		
293	A/34/II		38/36/11	Flake with unprepared butt, partly cortical (10%)		
				BLOCK 36		
288	A/34/II	Z-1	43/34/11	Chunk, partly cortical		
287	A/34/II		21/44/11	Cortical flake with unprepared butt		
291	A/34/II		74/74/20	Flake with unprepared butt, partly cortical (60%)		
278	A/34/II		45/50/18	Flake with unprepared butt, partly cortical (20%)		
295	A/34/II		55/46/14	Flake with unprepared butt, partly cortical (30%)		
2161	2013/I/56/Ic		56/30/4	Flake with unprepared butt, partly cortical (20%)		
292	A/34/II		34/47/9	Flake with unprepared butt, partly cortical (5%)		
296	A/34/II	Z-2	32/(28)/12	Flake with unprepared butt, fragment broken along its technological axis		

Table 4.8. continued

Inv. No.	Locus	Refitting	Dimensions (mm)	Description	Comments	Reference
2162	2013/I/56/Ic		28/(17)/8	Flake with unprepared butt, fragment broken along its technological axis		
305	A/34/II		(25)/27/4	Flake, distal fragment		
				BLOCK 37		
3001	2013/G/9-10/Ia	Z-1	30/39/7	Flake with unprepared butt, partly cortical (90%)		
2961	2013/G/9/Ia		44/60/12	Flake with unprepared butt, partly cortical (20%)		
924	A/23/85		52/(25)/10	Flake with unprepared butt, broken along its technological axis, partly cortical (40%)		
922	A/23/85		53/(23)/8	Flake with unprepared butt, broken along its technological axis, partly cortical (70%)		
3005	2013/G/9-10/Ia		(40)/32/10	Flake, distal fragment, partly cortical (50%)		
759	A/23/72	Z-2	(30)/23/5	Flake with unprepared butt, proximal fragment		
1220	A/22/78		33/(19)/7	Flake with unprepared butt, broken along its technological axis		
2221	2013/I/63/Ic	Z-3	39/29/19	Flake with unprepared butt, partly cortical (10%)		
2601	2013/I/65/Ic		40/44/14	Flake with unprepared butt, partly cortical (20%)		
2602	2013/I/65/Ic		27/29/12	Flake with unprepared butt		
				BLOCK 38		*Fig. 4.46*
48	A/34/21	Z-1	30/22/4	Cortical flake with plain butt	Front striking platform	
2003	2013/I/65/Ia		23/32/4	Flake with multi-faced prepared butt	Flaking surface, right side	
2168	2013/I/64/Ia		18/18/2	Flake with edge butt	Flaking surface, right side	
380	A/33/30		20/10/5	Flake with unprepared butt	Flaking surface, right side	
1104	A/34/1		24/24/4	Flake with plain butt, partly cortical (15%)	Front striking platform	
2673	2013/I/44/Ib		60/32/8	Flake with multi-faced prepared butt, partly cortical (10%)	Side-blow, flaking surface, from front platform	
2002	2013/I/65/Ia		(20)/21/4	Flake, distal fragment, partly cortical (20%)	Front striking platform	
2001	2013/I/65/Ia		22/27/3	Flake with point butt, partly cortical (10%)	Front striking platform	

Table 4.8. continued

Inv. No.	Locus	Refitting	Dimensions (mm)	Description	Comments	Reference
2391	2013/I/74/Ib		20/15/3	Flake with multi-faced prepared butt/overheated	Front striking platform	
1106	A/34/1		(19)/17/5	Flake with multi-faced prepared butt, proximal fragment	Flaking surface, from front platform	
1996	2013/I/65/Ia		26/35/4	Flake with point butt	Flaking surface, from front platform	
1546	2013/I/64/Ia		62/50/9	Plunging flake with multi-faced prepared butt	Predetermined product	
1299	2013/I/65/Ia		41/57/14	Final core, formally discoidal		
				BLOCK 39		
1023	A/35	Z-1	(15)/(6)/4	Cortical flake, distal fragment broken along its technological axis		
1020	A/35		36/(12)/8	Flake with point butt, broken along its technological axis, partly cortical (80%)		
				BLOCK 40		
691	A/23/75	Z-1	30/31/8	Flake with point butt, partly cortical (25%)		
1260	A/23/86		35/50/9	Flake with plain butt, partly cortical (15%)		
				BLOCK 41 (see above, Block 22)		
				BLOCK 42		
2263	2013/I/43/Id	Z-1	42/17/3	Flake with plain butt, partly cortical (20%)		
2264	2013/I/43/Id		30/20/4	Flake with edge butt		
2261	2013/I/43/Id		48/14/9	Flake with plain butt, partly cortical (30%)		
2259	2013/I/43/Id		57/20/10	Flake with plain butt, partly cortical		
2260	2013/I/43/Id		30/19/10	Flake with multi-faced prepared butt		
2265	2013/I/43/Id		28/27/5	Flake with edge butt, partly cortical (60%)		
755	A/34/II		47/46/33	Final core with opposite-direction flaking surface treatment		*Fig. 4.11*
2262	2013/I/43/Id	Z-2	(15)/24/7	Flake with plain butt, proximal fragment, partly cortical (70%)		
2258	2013/I/43/Id		(28)/24/7	Flake, distal fragment, partly cortical (70%)		

Table 4.8. continued

Inv. No.	Locus	Refitting	Dimensions (mm)	Description	Comments	Reference
				BLOCK 43		*Fig. 4.48*
1867	2013/I/35/II	Z-1	26/20/4	Flake with plain butt		
1869	2013/I/35/II		25/26/7	Flake with multi-faced prepared butt, partly cortical (20%)		
1870	2013/I/35/II		22/28/4	Flake with plain butt, partly cortical (10%)		
1871	2013/I/35/II		23/48/11	Flake with plain butt, partly cortical (10%)		
1863	2013/I/35/II		44/27/8	Flake with edge butt, partly cortical (60%)	Flaking surface, from rear platform	
1866	2013/I/35/II		40/40/8	Flake with multi-faced prepared butt, partly cortical (30%)	Flaking surface, from rear platform	
1859	2013/I/35/II		29/26/6	Flake with multi-faced prepared butt	Flaking surface, from rear platform	
1955	2013/I/34/II		(27)/32/5	Flake with multi-faced prepared butt, proximal fragment	Flaking surface, from rear platform	
1953	2013/I/34/II		(13)/30/4	Flake with multi-faced prepared butt, proximal fragment	Flaking surface, from front platform	
1952	2013/I/34/II		73/56/37	Levallois core for flake with opposite-direction flaking surface treatment		
				BLOCK 44		*Fig. 4.50, 4.51*
2471	2013/I/55/Ia	Z-1	(44)/52/9	Cortical flake with plain butt, proximal fragment	Flaking surface	
2005	2013/I/65/Ia		(21)/28/3	Flake, distal fragment		
2472	2013/I/55/Ia		53/37/10	Flake with multi-faced prepared butt, partly cortical (20%)	Flaking surface	
2479	2013/I/55/Ia		24/32/7	Flake with plain butt, partly cortical (50%)	Striking platform	
2006	2013/I/65/Ia		28/30/5	Flake with plain butt, partly cortical (20%)	Striking platform	
2473	2013/I/55/Ia		43/43/14	Cortical flake with unprepared butt	Striking platform	
2484	2013/I/55/Ia		(36)/25/8	Flake, distal fragment, partly cortical (10%)	Striking platform	
2478	2013/I/55/Ia		35/26/6	Flake with multi-faced prepared butt, partly cortical (5%)	Striking platform	
2483	2013/I/55/Ia		30/17/3	Flake with plain butt	Striking platform	
2485	2013/I/55/Ia		20/41/3	Flake with edge butt	Flaking surface	
2490	2013/I/55/Ia		(27)/16/3	Cortical flake with plain butt, proximal fragment	Flaking surface	

Table 4.8. continued

Inv. No.	Locus	Refitting	Dimensions (mm)	Description	Comments	Reference
2486	2013/I/55/Ia		(31)/16/3	Cortical flake, distal fragment		
2480	2013/I/55/Ia		37/32/7	Flake with plain butt, partly cortical (30%)	Flaking surface	
2007	2013/I/65/Ia		35/46/3	Flake with edge butt, partly cortical (10%)	Flaking surface	
1443	2013/I/55/Ib		32/30/9	Flake with multi-faced prepared butt	Flaking surface	
2482	2013/I/55/Ia		32/30/5	Flake with point butt, partly cortical (60%)	Striking platform	
2188	2013/I/64/Ia		(14)/25/2	Flake with multi-faced prepared butt, proximal fragment	Striking platform	
2189	2013/I/64/Ia		(14)/25/2	Flake, distal fragment		
2481	2013/I/55/Ia		(15)/45/13	Flake with multi-faced prepared butt, proximal fragment	Flaking surface	
2474	2013/I/55/Ia		(37)/45/13	Flake, distal fragment, partly cortical (20%)		
1454	2013/I/46/Ia		55/(30)/10	Flake with multi-faced prepared butt, fragment broken along its technological axis	Flaking surface	
2475	2013/I/55/Ia		63/(29)/9	Flake with multi-faced prepared butt, fragment broken along its technological axis, partly cortical (5%)		
2187	2013/I/64/Ia		(28)/17/2	Flake with multi-faced prepared butt, proximal fragment	Flaking surface	
2477	2013/I/55/Ia		41/38/9	Flake with multi-faced prepared butt, partly cortical (20%)	Flaking surface	
2187	2013/I/64/Ia		(28)/17/2	Flake with multi-faced prepared butt, proximal fragment	Flaking surface	
2477	2013/I/55/Ia		41/38/9	Flake with multi-faced prepared butt, partly cortical (20%)	Flaking surface	
1302	2013/I/65/Ia		57/48/11	Levallois point	Predetermined product	
1417	2013/I/64/Ib		23/21/3	Flake with multi-faced prepared butt	Striking platform	
2008	2013/I/65/Ia		27/20/6	Flake with plain butt, partly cortical (10%)	Striking platform	
2004	2013/I/65/Ia		43/33/6	Flake with multi-faced prepared butt	Flaking surface	
2009	2013/I/65/Ia		13/23/2	Flake with edge butt	Flaking surface	
973	A/33/39		63/56/41	Levallois core for point		*Fig. 4.10*

BLOCK 1

Description: A nodule of porous chert with dark yellowish-brown coloring (10YR4/4) with internal streaks almost black in color and irregular small yellowish-brown (10YR4/6) or maroon (10YR4/4) marks. Single internal holes. Smoothed external surface (only visible on artifacts which could not be refitted).

Processing: The pieces of the two refittings present an advanced stage of core reduction. Refitting 1 comprised three flakes detached from the surface of the striking platform. Their crudeness and irregularity indicate the action of modelling a proper angle for detaching further flakes forming the relief of the flaking surface. Refitting 2 comprised irregular flakes and a chunk detached from the flaking surface, all three being the result of giving the flaking surface a convex form and terminated at an internal imperfection with hinges. The detachment of chunk 634 most certainly constituted an element of the remodeling of the nodule in order to get rid of an awkward crack. Its detachment preceded a slight correction of the edge of the flaking surface and striking platform (chipping) [see *Table 4.8*]. Non-conjoining pieces include a piece of initial processing (flake partly covered with cortex 744 found 3 m east of the eastern cluster and a similar flake 457 from the eastern cluster), and a residual core.

Dispersal: All the refitted pieces were recorded on the surface in the eastern cluster of the encampment in the southwestern sector, indicating where the processing had taken place [*Fig. 4.23*]. The location of the conjoined chunk in the area of the western cluster could reflect the general direction of post-depositional shifts of the debitage of this block, the other two pieces of refitting 2 also being strung out in a westerly direction in line with the ground relief.

BLOCK 2

Description: Nodule of porous chert with an internal, clearly mosaic structure. Color-varied fractions of different grain size creating irregular patterns. Yellowish-brown was the dominant color (10YR5/6). The external surface was smoothed and cracked in places (on the edges) [*Fig. 4.24*].

Processing: The debris added to core 1044 reflected the detachment of crude flakes from a large nodule, both from the surface of the opposite striking platform (flakes 2619 and 364), and the flaking surface (27, and then 1802). At the same time, the lack of a significant number of flakes with natural external surfaces suggests a preliminary splitting of primary nodules of substantial size. Therefore, insofar as in the case of refitting 1 we are dealing with an almost complete sequence of rough processing of one part of the nodule, the presence of singular non-matching pieces of Levallois core treatment (edge flake 2616, flakes with multifaced butts 1489 and 1490) may constitute the remnants of a methodical processing of the remaining section of the block [see *Table 4.8*].

Dispersal: The refitted pieces of Block 2 were recorded both on the surface in the western cluster, as well as the subsurface layers corresponding to this location. Levallois elements of Block 2 recorded in the subsurface layers of the western cluster (2616), as well as in the ground relief depression 3 m further to the west (1489, 1490) were not conjoined [see *Fig. 4.23*].

BLOCK 3

Description: Nodule of porous chert, olive green-yellowish in color (5Y6/3), with slightly browner sections (10YR5/3) and characteristic veins of a more crystallized material. External surface smoothed and cracked.

Processing: The opening piece of the refitting was a flake with a large share of cortex (3019) detached during the shaping phase from an edge of the flat surface (seemingly intended to be the flaking surface). It is not clear whether at this stage the nodule possessed extensive negatives in the section opposite the two convergent striking platform planes. Other pieces conjoined to core 519 represent a stage of shaping of a convex (flaking?) surface from two opposite sides. These comprise small flakes without traces of diligent preparation of their butts. This nodule was not processed further, hence it is difficult to say whether the worked surface was intended for detaching a larger flake or point [see *Table 4.8*].

Dispersal: All refitted elements of Block 3 occurred in the southeastern cluster or in the immediate vicinity (slightly to the northeast) [see *Fig. 4.23*]. Non-conjoining pieces of the block (that is, flakes 256, 270, 337, 1111) were recorded in the same location.

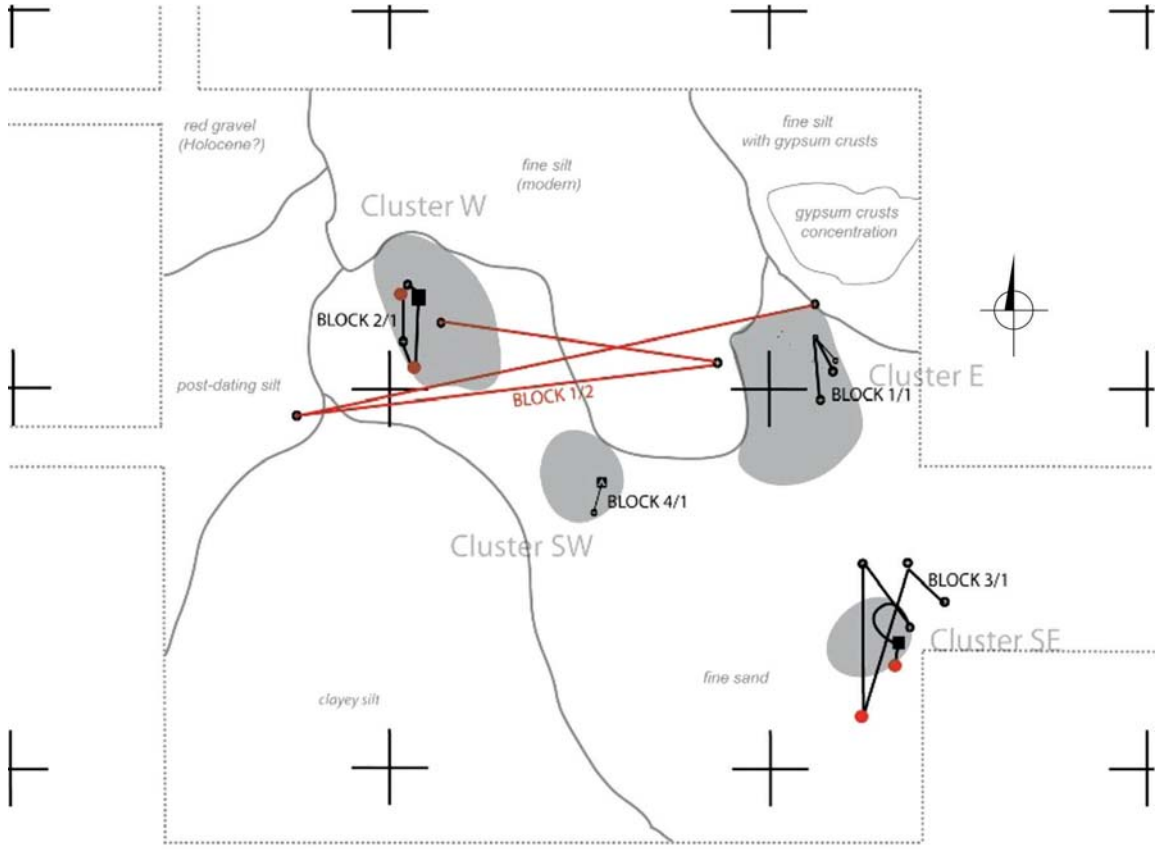

Fig. 4.23. Dispersal of debitage from Blocks 1, 2, 3, and 4, mapped onto a plan of site AFD23 (sector SW, season 2013) with the location of the largest clusters of lithic artifacts

BLOCK 4

Description: Block 4 consists of only two pieces of a characteristic light yellowish-brown (2.5Y6/4) coarse-grained material. On the dorsal face of both artifacts, the primary surface of the nodule is fragmentarily visible while the negatives are covered with a thick dark brown patina.

Processing: Both refitted pieces represent a stage of the final shaping of the relief of the flaking surface. Although one of them has a butt made into a *chapeau-de-gendarme* shape, due to the slenderness of the artifact and its position in the process, it was probably not a final product. The two flakes are fragmentarily preserved and no other pieces of this nodule—neither products of the initial processing nor the residual core—were discovered [see *Table 4.8*].

Dispersal: Despite both flakes being found in the southwestern sector of the site, the fragmentary state of the sequence did not allow this location to be considered as the place where Block 4 was processed [see *Fig. 4.23*].

BLOCK 5

Description: The nodule possessed a characteristic internal mosaic structure, with an orange (7.5YR7/8) matrix, highly porous (even large blisters), and embedded fragments of a much more siliceous material of brown color (7.5YR4/4) on the inside and pink (10YR7/3) on the outside. Original surface of the nodule smoothed and cracked [see *Fig. 4.24*].

Processing: Both pieces of the refitting come from a stage of forming of a flat extensive flaking surface. The original outer surface present on a large number of flakes indicates that the pieces constitute the initial preparation of a nodule. Refitting 1 displays treatment of the surface from two opposite sides of the nodule. No pieces were found in the collection attesting to the further exploitation of this nodule—neither flakes of the prepared striking platforms, nor the core itself [see *Table 4.8*].

Dispersal: The two pieces were recorded on the surface in the eastern part of the western cluster or else they had been transported quite a distance either northwards (refitting 1) or south-eastwards (a flake fragment from refitting 2) [*Fig. 4.25*]. Another flake fragment from this nodule (1235), also discovered on the surface approximately 20 m to the southwest, was not conjoined.

BLOCK 6

Description: Nodule of a mosaic structure, dominated by a fine-grained matrix, brownish-yellow (10YR6/8) in color, or brown (7.5YR4/6) in the subcortical section. Interior containing a section with numerous cavities. External surface of the nodule smoothed and cracked at the edges.

Processing: All of the refitted pieces represent a stage in the formation of the nodule when the original outer surface is removed. Most of the butts on the flakes were also not worked on in any way. Refittings 2 and 3 most probably come from shaping the side surfaces (platforms), thereby describing their general bulkiness. One should note the incompleteness of the refitting and the absence of further pieces of advanced working on the core. Other non-conjoined pieces from the processing of Block 6, such as cortical flake fragment 662 with denticulate retouching, also come from the initial stages of processing [see *Table 4.8*].

Fig. 4.24. Refitted blocks: Block 2 (dorsal face); Block 5 (ventral face); Block 7 (dorsal face); Block 12 (ventral faces; refitting 1); selected elements of Block 14 (ventral face)

Dispersal: The pieces of Block 6 were recorded exclusively on the surface, scattered around the eroded zone north of the eastern cluster and within 10 m of this location [see *Fig. 4.25*]. The flake fragment (662) with denticulate retouching was also discovered within this eastern cluster. Some elements of this block bore traces of secondary overheating (e.g., chunk 808 or a piece of refitting 2, namely flake 117).

BLOCK 7

Description: Nodule of waxy chert, primarily reddish-brown (5YR5/4) in color, with an irregular darker (5YR3/3) streak. External surfaces richly sculpted, smoothed and cracked at the edges [see *Fig. 4.24*].

Processing: The pieces of the refitting constitute an almost complete sequence of core reduction with opposite-directional knapping into the final form [see *Table 4.8*]. The lack of any pieces from earlier stages of the processing indicates that the core was brought to the site in the form into which it was reconstructed, that is, an already-shaped (flake-reduced?) core with one striking platform (which will be termed as the front platform) formed by two large negatives, the opposite (rear) platform merely chipped, as well as a convex flaking surface the relief of which was formed from two directions defining the positions of the platforms. The refitting shows that the processing carried out at the site commenced with the formation of the rear platform (detachment of flake 941). Then, a flat hinged flake (1058) was detached from this platform, also taking off the edge of the flaking surface. The small flake (or series of chips) removing the hinge from the flaking surface was not found. However, five other flakes had already been detached from the front platform. Considering that the platform had additionally been facetted just before the detachment of flake 969, this should be assumed to be the final product. However, this flake was neither retouched nor taken beyond the location of deposition of the other elements. After that, one more hinged flake (1199) was struck from the same side. Another two flakes (936 and another not preserved) were detached from the side of the flaking surface, and a thick ridge flake, the last to be detached, was struck from the rear platform. The residual core (143) still presented the pattern of two opposite platforms and a convex flaking surface.

Dispersal: All of the refitted pieces were discovered on the surface in the southern part of the western cluster or scattered westwards within a distance of 10 m [see *Fig. 4.25*].

BLOCK 8

Description: One of the most characteristic nodules, light yellow (5Y7/4) in color with greyish-olive (10Y5/2) and brown sections (7.5YR5/8). Numerous crystalline inclusions inside it. External surface smoothed and cracked on the edges [*Fig. 4.26*].

Processing: The collection lacks a certain number of flakes from the initial processing of this nodule, detached from a surface defined as a flaking surface in later processing [see *Table 4.8*]. These represented most probably the initial testing of the nodule and where left behind wherever the nodule had been collected. Subsequent processing, still in the initial stages, was carried out in the encampment. It is most likely that a flake completely covered in cortex (1808; refitting 1) comes from the initial phases of preparing a plain butt defined as a front platform (which determines subsequent actions for detaching products with facetted butts from this platform). Another two flakes from refitting 1 came from significantly later phases, linked with the faceting of the

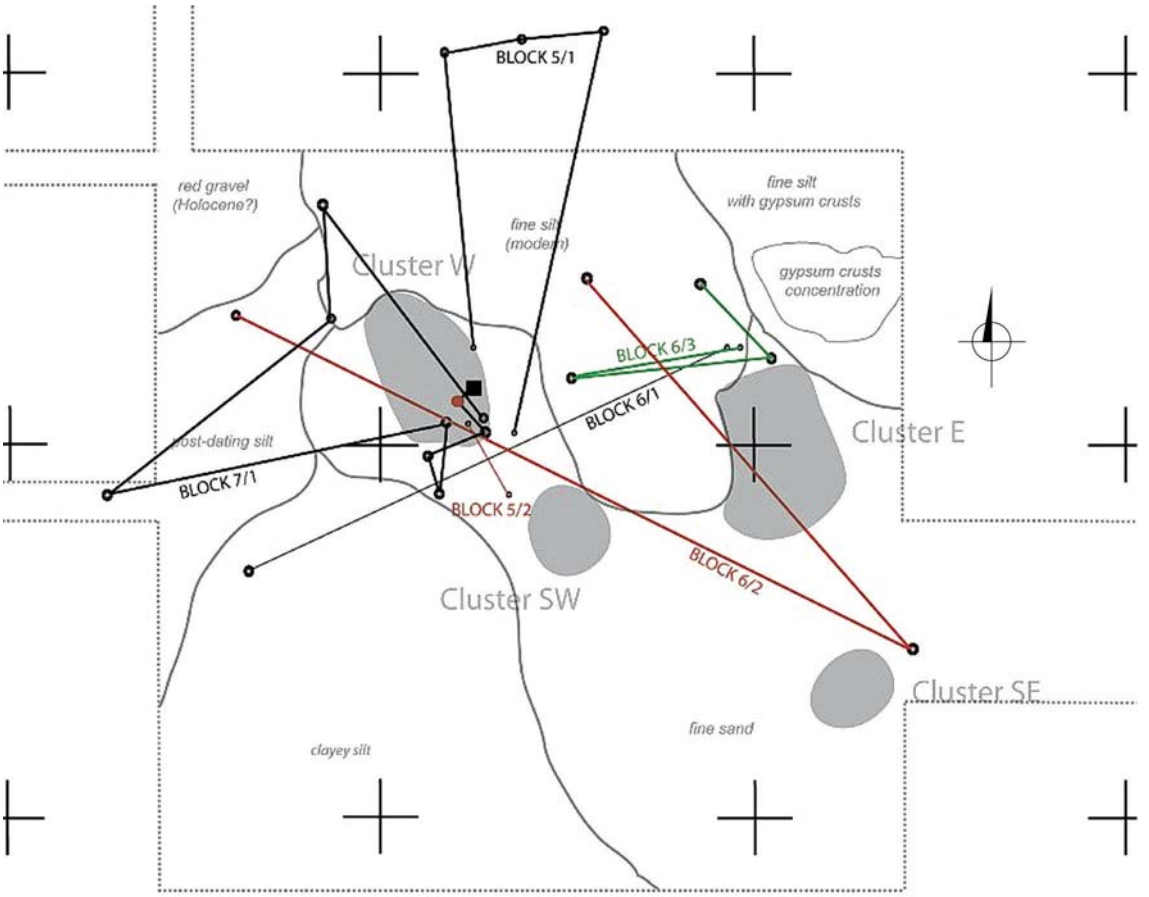

Fig. 4.25. Dispersal of debitage from Blocks 5, 6, and 7 mapped onto a plan of site AFD23 (sector SW, season 2013) with the location of the largest clusters of lithic artifacts

platform. Two flakes (refitting 2) represent the stage preceding that demonstrated by the main refitting (3). Both of these flakes were cracked along the axis of percussion. At the moment of their detachment, the upper section of the nodule had already been divested of its original external surface, although the platform surface was still covered by it.

The commencing piece of the main refitting (3) is a distal fragment of a flake (1782) from the stage of shaping the flaking surface from the right side (most probably identical with the action represented by refitting 2). The next two cortical flakes (619, 1050) start the stage of defining the surface of the rear platform. One of the largest flakes from this stage is missing from the collection, while two lateral flakes (2676, 1548) were detached from its extensive negative, forming the proper angle of the rear platform. Then another crude flake was detached from the rear platform, in line with the direction of detachment of most of the pieces (590). Directly before and after the edge of the platform was formed, two other crude flakes were detached from the previously worked flaking surface (only the second of these is present in the collection, broken into four pieces: 423+591+599+1325), shaping in turn both these surfaces (flaking surface and striking platform). Such a formula was applied consistently until the end of the processing of this section of the nodule. Coarse-crystalline inclusions, which appeared more or less in the middle of the flaking surface with the successive uncovering of this section of the nodule, making the obtaining of large flakes from the greater part of the flaking surface ineffectual.

Fig. 4.26. Block 8, refitted (dorsal face and ventral face)

No evidence was found of a simultaneous working of the flaking surface from both directions (i.e., the front and rear platforms). The front platform, which had until then been shaped only provisionally, started to be worked (opening flake of refitting 1) once the rear platform and the left side of the core was abandoned because of the extensive imperfections (the last flakes from this series: 601, 1807 and 182). Processing commenced with the removal of large elongated flakes from the flaking surface. The only product of this phase preserved in the collection was a broken flake with an edge butt (1781+2530). Then, the striking platform started to be shaped with a series of convergent flakes (384, 1317, 594, 624 and 175). Some pieces from this stage are missing from the collection. A series of flat flakes was subsequently detached from the flaking surface: a distal fragment of one of them was preserved (2561), and another complete one (1416), and once again in order to modify the platform (missing pieces). In processing the front platform—as in the case of the rear one—the detachment of flakes in turn is visible. The next product detached from the right side of the flaking surface was a broken elongated flake (1314+1321), then a distal fragment of another crude product (570). Further correction of the platform (1322) preceded

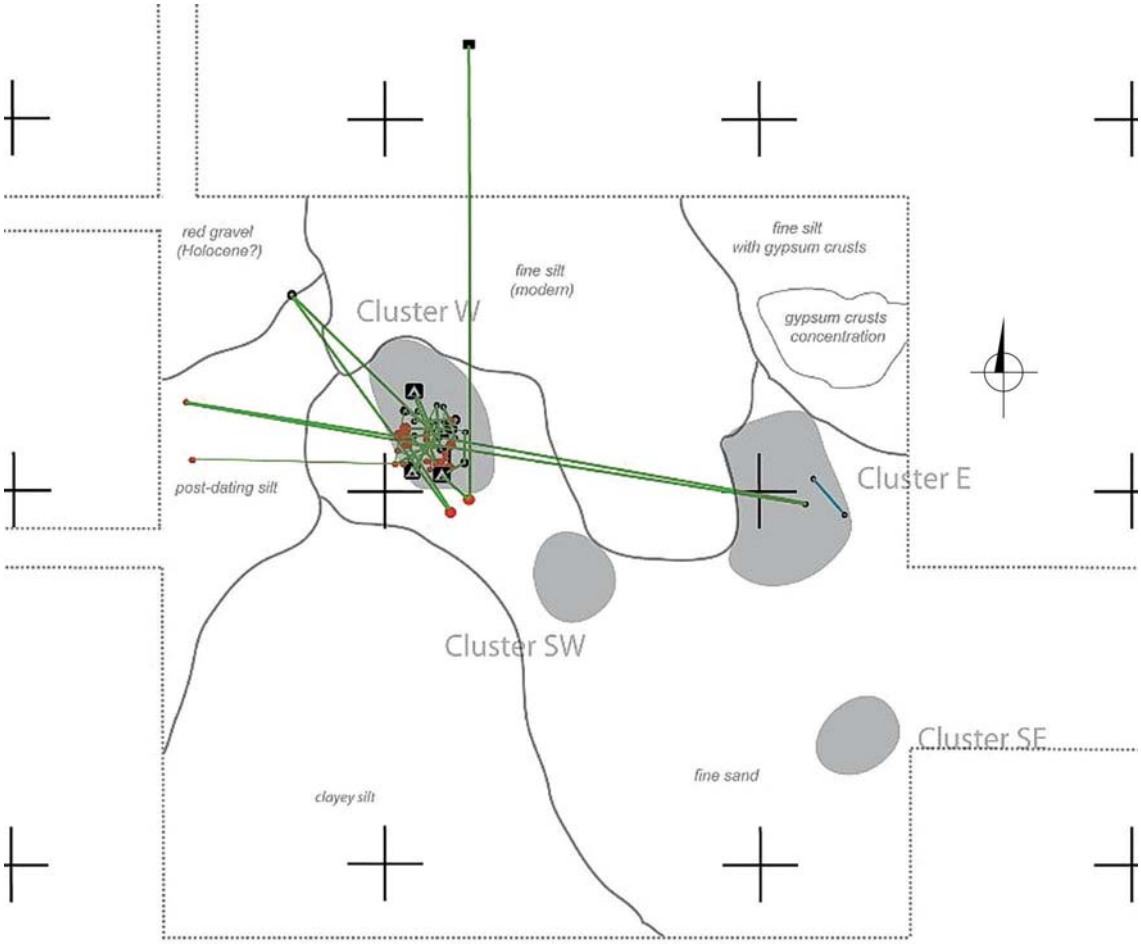

Fig. 4.27. Dispersal of debitage from Block 8 mapped onto a plan of site AFD23 (sector SW, season 2013) with the location of the largest clusters of lithic artifacts

the detachment of two flakes from the right edge of the flaking surface (1315 and 26). Although the first of these bears a later burin scar along one entire edge, the intention behind its formal tool-destination gives rise to reservations (due to its irregularity). The platform was subsequently corrected (185), causing the platform to be shaped into a *chapeau-de-gendarme* type and allowing the first of a series of final/predetermined flakes (359) to be detached. This flake was not retouched. Following its detachment, the platform was once again facetted in order to detach the next product, of which only the proximal part was preserved (196). It was probably at this stage that imperfections in the nodule appeared, causing the breakage of products. Further detached artifacts bear marks of actions aimed at correcting the edge of the platform and the flaking surface (including the distal fragment of flake 146 and chunk 993). The final attempt at detaching a flake with a previously facetted platform ended with obtaining a hinged product (2060). This flake also does not bear any traces of retouching.

The last stage of the processing was probably a failed attempt to remove the crystalline imperfections from the right side of the core. A crude flake terminated with a hinge at a crystalline intrusion, simultaneously revealing further imperfections within the nodule. The residual core, which was still large, was abandoned at this stage, the reason for the reluctance to conduct further processing being the unsuitable properties of the nodule (intrusions).

The unfixed refitting 4 represents two fragments of a flake broken along the axis of percussion, from an advanced stage of the processing.

Dispersal: The overwhelming majority of the pieces from Block 8 occurred on the surface and in the subsurface layers of the southern sectors of the western cluster [*Fig. 4.27*]. Single small pieces were scattered in secondary contexts in a northwesterly direction, replicating the natural slope of the ground. The residual core lay farthest to the north. A single piece (570, distal fragment of a flake with a large crystalline inclusion from inside the nodule) found in the eastern cluster on the site, along with the two pieces of refitting 4 which also occurred in this concentration, constitute a premise for considering a different origin for these artifacts, despite the confusing similarity of the raw material.

BLOCK 9

Description: Nodule of a fine-crystalline raw material of a mosaic structure. Matt sections of a yellowish color (10YR7/6) interwoven with a semi-translucent substance of a darker color (10YR5/4). External surface of the nodule smoothed and cracked in places, with domes of the semi-translucent (more fragile?) material.

Processing: The refitting is severely incomplete and represents a preliminary phase of nodule shaping, most probably the striking platforms, considering the general robust proportions of the artifacts [see *Table 4.8*]. The absence of any pieces from later processing phases suggests that a nodule of clearly good quality was brought to the site already with defined working planes (platform and flaking surface).

Dispersal: The pieces were recorded in the western cluster or were scattered in secondary contexts on the surface, sometimes at a significant distance (refitting 2, approximately 15 m to the southwest) [*Fig. 4.28*].

BLOCK 10

Description: A uniform, waxy material of a mottled nature, predominantly yellow (2.5Y7/6) in color, with fairly large sections that were red (2.5YR5/6) or yellowish-brown (10YR5/8). The interior of the nodule displayed crystalline inclusions, revealed during the processing. External surface smoothed and only broken on some edges.

Processing: The refitting of Block 10 reveals the absence of a preliminary stage of processing of the nodule at the site. Negatives observed on the nodule are evidence of the detachment of at least three large cortical flakes, which were not found in the area under investigation [see *Table 4.8*]. Foremost in this refitting is a crude flake (254), which had already been detached from the preliminarily shaped surface defined as the flaking surface. The next flake (266) present in the collection comes from a platform-shaping stage in the part from which flake 254 had been detached. Subsequent knapping stages show that this was the rear platform. Flakes were next detached to form the convex shape of a flaking surface on the left side of the core (251), the rear platform (637), then struck from the right side (3018, 1112) and again from the left (3116). Several pieces from this phase are missing from the collection. A common feature of the preserved flakes is the lack of butt preparation and their location at the rear part of the core. The detachment of more flakes in the central section of the nodule revealed crystalline inclusions that constituted

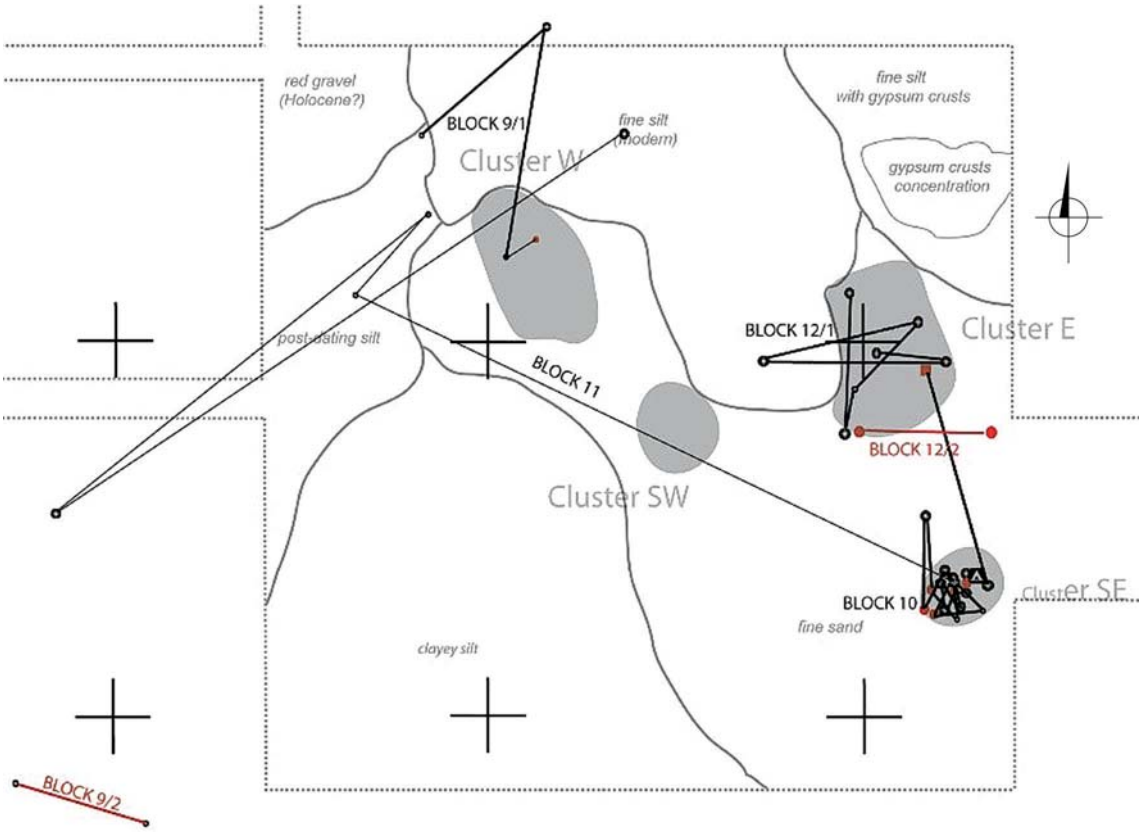

Fig. 4.28. Dispersal of debitage from Blocks 9, 10, 11, and 12 mapped onto a plan of site AFD23 (sector SW, season 2013) with the location of the largest clusters of lithic artifacts

a serious obstacle for shaping the flaking surface. Perhaps with the aim of removing imperfections with another series of flakes, a slightly more precise plane of the rear platform was formed (255, 275, 261). Another flake was detached in this zone (1145), covering with its extent the above-mentioned imperfections which, however, reached slightly deeper.

The knapper then focused on the front part of the core. A series of partly cortical flakes were detached from the surface of the front striking platform (flakes from refitting 2, as well as pieces of refitting 1: 3042, 260, 638). The surface thus formed served to detach several large flakes forming the front part of the flaking surface (including the edge flake 250, as well as others absent from the collection). The next series of detached flakes (3103, 271 and 3045) reflected the intent to give the front platform an appropriate shape with faceting. Flake 521 most probably constituted the final product of the entire process, despite terminating with a hinge not reaching even halfway down the length of the prepared flaking surface and a shallow imperfection in the distal section. This piece underwent no further processing (retouching). Although the detachment of the last edge flake (522) from the front platform could signify an attempt to remodel the core, the processing ceased at this stage. The residual core was abandoned with the two opposite platforms still visible and still large.

Dispersal: Almost all the pieces from the processing of Block 10 were found both on the surface and in the subsurface layers of the southeastern sector [see *Fig. 4.28*]. Only the residual core was found several meters to the north, within the eastern cluster.

Block 11

Description: The nodule is a predominantly dark yellow-brown (10YR3/4) material with a large amount of small brown (7.5YR5/8) inclusions. External surface smoothed and cracked.

Processing: Based on the refitted pieces, the nodule was worked on the spot only in a preliminary way (or simply tested for quality). During this operation, a compact sequence of flakes was detached in the same direction, revealing a fairly smooth surface [see *Table 4.8*].

Dispersal: One flake fragment (268) was recorded on the surface of the southeastern cluster in the southwestern sector of the site, with the remaining pieces of the refitting scattered in secondary contexts in the western sector of the site [see *Fig. 4.28*].

Block 12

Description: Yellowish-brown (10YR5/6) nodule of fine-grained chert with a characteristic black layer of 1 mm in thickness directly under the external surface. External surface currently smoothed and cracked [see *Fig. 4.24*].

Processing: Present in the refitting are pieces from the initial phases of shaping the edge around the concentric flaking surface and the striking platform [see *Table 4.8*]. The first two flakes were detached from the surface of the future flaking surface (unprepared butts in both cases), then the striking platform was shaped. Two small flakes from refitting 2 also come from the initial shaping of one of the surfaces. All of the refitted flakes bore a natural external surface, similar to several other unfitted pieces from the processing of the nodule (71, 740, 109). The lack of artifacts from advanced phases of processing (non-cortical, with multifaced butts) indicates that only preliminary processing was carried out at the encampment. In this context, flake 740 with numerous burin

scars is an isolated example. The location of this artifact also differentiated it from the remaining pieces of Block 12, as well as other burins from the sector of the site.

Dispersal: The pieces occurred exclusively in the eastern cluster or within the closest vicinity [see *Fig. 4.28*].

BLOCK 13

Description: Nodule of chert with mosaic internal structure, interwoven with brown (7.5YR4/6), olive-brown (2.5Y4/3) and dark reddish-brown (2.5YR3/4) zones. Analogous forms of generally fine-crystalline chert were also present in the subcortical pieces of other nodules (e.g., Block 8), as well as marking zones of uncontrolled fracturing of the raw material there. The irregularity of the breakage of pieces making up Block 13 indicates the existence of a series of internal cracks and crystalline imperfections. External surface smoothed and cracked.

Processing: Both refitted pieces are small chunks constituting fragments of a single crude flake [see *Table 4.8*]. The flake is evidence of the nodule being tested already in the area of the encampment. It is possible that no other pieces were found for this refitting because they were too fragmented to be brought to Poland for further study.

Dispersal: The refitted pieces were recorded on the surface within the eastern cluster or in its closest vicinity [*Fig. 4.29*].

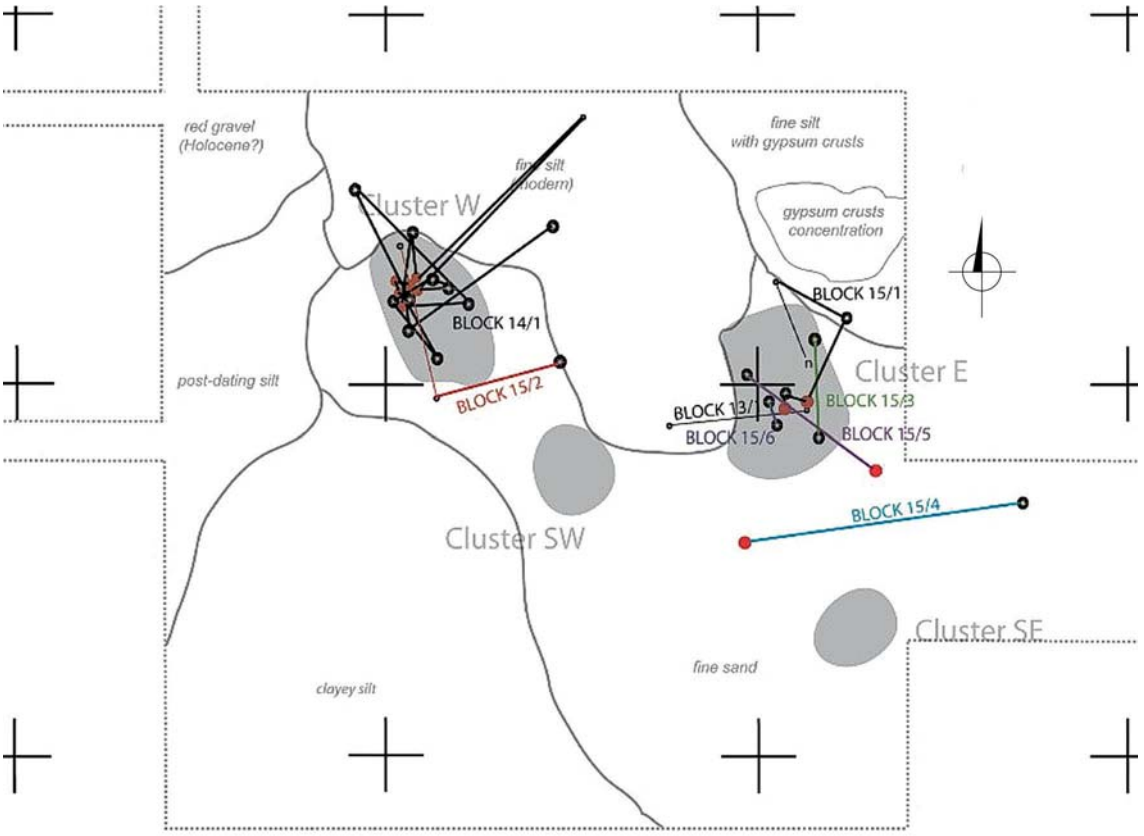

Fig. 4.29. Dispersal of debitage from Blocks 13, 14, and 15 mapped onto a plan of site AFD23 (sector SW, season 2013) with the location of the largest clusters of lithic artifacts

BLOCK 14

Description: Nodule of waxy chert predominantly dark yellowish-brown (10YR4/6) in color with very numerous small spots of lighter colors, as well as visible fossils (shell fragments). Small inclusions are also present: grains of quartz surrounded by chalk. External surface smoothed and cracked [see *Fig. 4.24*].

Processing: The refitted pieces represent a significant part of the debris from preliminary processing. However, considering the negatives of the flakes detached first, which are missing from the collection (detached from the pre-flaking surface), it is to be assumed that the quality of this nodule was tested away from the excavated site [see *Table 4.8*]. Initially, the rear section of the core was worked, shaping alternately the platform surface (flakes 1308, 360) and rear side of the convex flaking surface (2522, 1290 and 1061, 1184, 1970, 836). The knapper then turned his attention to the opposite (front) section of the nodule on which there was already a large negative on the pre-flaking surface (from the testing phase?). This part of the operation commenced with a flake completely covered by the original external surface struck from the striking platform plane (1968) and further flakes (often fractured along the axis of percussion). Only a flake (1982+1981) detached from the (left) side of the flaking surface signifies the next stage of the shaping the flaking surface relief. Another large flake (493), partly removing the left ridge of the flaking surface, as well as flake 878 serving to correct the striking platform, were refitted last.

Pieces of the later stages of processing are missing from this collection, including pieces from the preparation (faceting) stage, final products or residual core. Based on the shape defined by the refitted pieces, the shaped nodule possessed a convex flaking surface ~11 cm in length and ~5 cm in width. The initial parameters of the nodule were ~15 cm in length, ~8 cm in width and ~7 cm in thickness.

Dispersal: The refitted pieces of Block 14 were concentrated in the western cluster, both on the modern surface and in the subsurface layers [see *Fig. 4.29*]. Single pieces were found relocated to the north and northeast, but none in the ground relief depression west of the western cluster.

BLOCK 15

Description: A very characteristic nodule of fine-crystalline chert with an internal mosaic structure and large chalk inclusions, brown (7.5YR4/6) in color. Numerous cracks visible. External surface smoothed and cracked only at the edges.

Processing: All the refittings come from the processing of one nodule and represent the shaping or simply testing of raw material quality [see *Table 4.8*]. A highly non-cohesive structure of the nodule interior and the breakage irregularity of the detached flakes/chunks make it difficult to determine the mutual relationships of particular refittings. However, their dimensions and the lack of a significant number of pieces (which would have been easy to pick out in the collection) suggest only preliminary processing of this nodule within the area of the encampment. It is clear that some pieces of debris were also used, e.g., the distal fragment of a crude flake (649) retouched on one edge quite abruptly, creating a racloir/sidescraper.

Dispersal: The refitted pieces of Block 15 are concentrated around the eastern cluster with only refitting 2 being located in the western cluster [see *Fig. 4.29*]. Either the nodule was processed in two different places, or the pieces of refitting 2 represent another, deceptively similar nodule.

Block 16

Description: Nodule of waxy brown (7.5YR4/6) chert with numerous gas bubbles and internal fractures. External surface smoothed and cracked.

Processing: Only two crude flakes partly covered with the original external surface were refitted. They come from the preliminary stage of forming the core and given the significant incompleteness of the block, it may not be excluded that it constitutes a piece of another block with similar petrographic properties. It was impossible to establish a relationship with any other block examined to date [see *Table 4.8*].

Dispersal: Both of the refitted pieces were recorded in the northern part of the western cluster [*Fig. 4.30*].

Block 17 (petrified wood)

Description: Nodules of petrified wood (trunk fragments) with a visible pattern of mineralized fiber, subjected to processing into fair-sized chunks. The preserved external parts of the one or perhaps several nodules were heavily patinated and smoothed, reflecting the fact they had lain for long periods in geological deposits already in the form of chunks.

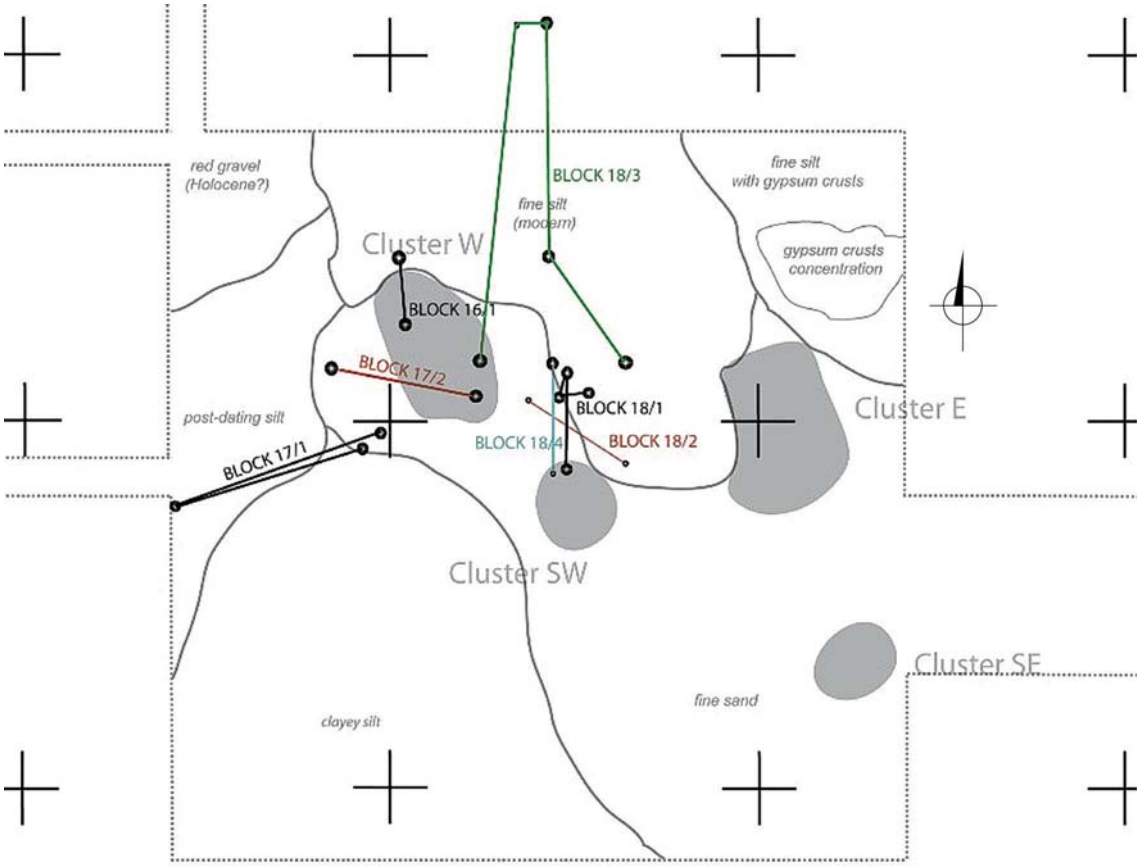

Fig. 4.30. Dispersal of debitage from Blocks 16, 17, and 18 mapped onto a plan of site AFD23 (sector SW, season 2013) with the location of the largest clusters of lithic artifacts

Processing: Although the two refittings differ petrographically (they come from different sections of the nodule or from separate nodules), they represent similar phases of processing. The incompleteness of the refittings indicates that such nodules were only tested for quality at the site [see *Table 4.8*]. No residual or unwanted cores from a preliminary stage of the processing were noted.

Dispersal: The refitted debris occurred on the surface of the southern part of the western cluster and in secondary contexts west of this location. Some flakes (10, 206, 509, 859, 1037, 1062, 1224, 2694) were also scattered in the immediate vicinity of the western cluster. Although two large flakes (36 and 1266) lay on the surface of the eastern cluster, the only flake (3055) representing an advanced phase of processing was recorded in isolation, approximately 5 m south of the southwestern cluster and 5 m west of the southeastern cluster [see *Fig. 4.30*].

BLOCK 18

Description: Nodule of waxy chert, brown (7.5YR4/6) in color, with characteristic, single, round chalk inclusions. External surface smoothed and cracked.

Processing: Despite the lack of direct links between the refittings, the artifacts come probably from the same nodule and represent the shaping of the core [see *Table 4.8*]. Refitting 1 is a series of crude flakes partly covered with the natural external surface (456, 1076, 1253), detached more or less in one direction. They formed an extensive flat (flaking) surface through which they were detached alternately with the pieces shaping the striking platform. The last flake conjoined to the flaking surface (1257) was detached following an action to shorten the core. The newly formed striking platform appears more of less halfway along the previously detached flake (456). Another large flake, broken halfway along its length, probably comes from a similar stage of the working of the flaking surface (refitting 2).

A three-sided working of a platform is observed in refitting 3. First, a flake partly covered with its natural external surface (152 and 407) was detached from the left side of the platform surface, then further pieces from the right side (408, 877). The alternate reduction of the platform and the flaking surface can be seen in refitting 1 and also in refitting 3: a piece was detached from the flaking surface between flake 877 and the last fitted one (788), thereby reducing the length of the striking platform.

The last refitting (4) represents two flakes from a stage of working of the nodule impossible to estimate, although its crudeness suggests, as in other cases, a preliminary stage.

Dispersal: All of the refittings of Block 18 were spread east of the western cluster and, at the same time, north of the southwestern cluster [see *Fig. 4.30*]. Pieces of this nodule which could not be refitted (447, 935, 1254, 1277) were also scattered around this area and come exclusively from the surface.

BLOCK 19

Description: Nodule of waxy chert of an internal mosaic structure, predominantly dark yellowish-brown (10YR4/6) in color. Internal irregular chalk inclusions and empty spaces are clearly visible. External surface smoothed and cracked [*Fig. 4.31*].

Processing: The refittings of Block 19 generally represent two stages of processing: shaping of the core (refittings 4 and 2), and an advanced stage of shaping (remodeling) of the flaking surface

(refitting 5) [see *Table 4.8*]. Although the two stages could not be refitted together, they undoubtedly come from the reduction of the same chert nodule. The nodule, which was processed at the site, already had preliminarily defined planes of the flaking surface and a striking platform, from which large opening flakes were detached. The initial stage of processing at the site is represented by partly cortical flakes from refitting 2, which could not be fitted to the main refitting (4). Refittings 1 and 3 also represent a preliminary stage of the processing, although in this case a different origin could be assumed (refitting 1 due to its different location, and refitting 3 due to the extensive openings inside the nodule not recorded in other artifacts from the block).

In the main refitting (4), a large partly cortical flake (60) was detached first from the flaking surface from the pre-striking platform side. Then the right side of the front striking platform was shaped, detaching a large cortical flake, which was not found during the investigations. Further added flakes (742, 558) served to shape the left side of the front platform. Then, a crude flake was detached from the left side of the flaking surface (1165) and, once again, a flake from the striking platform (2063). After shaping the front of the flaking surface, the kanpper's attention focused on the opposite side of the nodule. A large flake (763) was detached from the flaking surface from the rear side of the pre-striking platform. Further on, the right side of the flaking surface was formed by detaching flakes 838 and 571.

The next step was the detachment of a cortical flake (1223) from the plane of the rear platform, and then two pieces from the flaking surface (563 and 1219) of the platform shaped in this way. It seems that these pieces concluded the stage of shaping the concentric flaking surface and platform in alternate fashion. The next fitted piece represents the shaping of the flaking surface

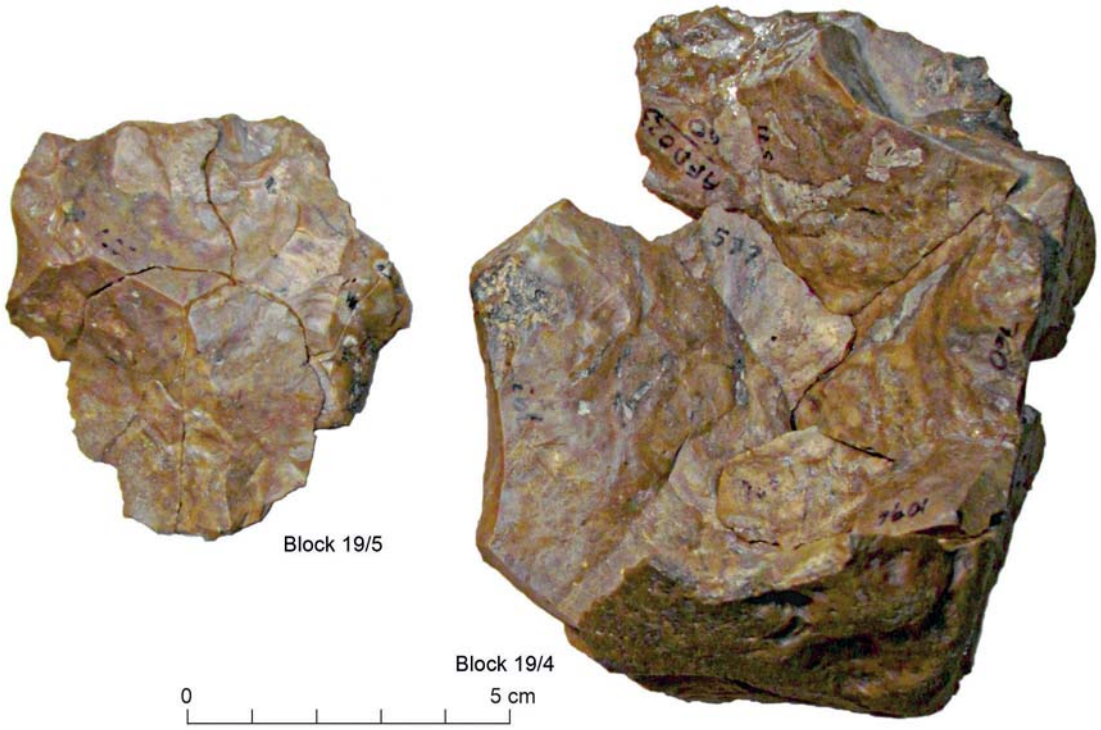

Fig. 4.31. Block 19: refitted elements 4 and 5 (ventral faces)

relief with further negatives of elongated flakes detached exclusively from the front platform side. In the refitting, there is a distal fragment of an elongated flake (577), a large edge flake (793) from the left ridge of the flaking surface, a distal fragment of the next elongated edge flake (882), and the proximal section of an edge flake (760) from the right side of the flaking surface.

Between forming the relief of the flaking surface and the later refitted flakes, there is a gap in refitting 4, perhaps filling refitting 5 (this is supported by an arrangement of some negatives on the side edges of both refittings). Refitting 5 includes a complete series of centripetal remodeling of the flaking surface relief. Of importance here is the absence of any trace of the single directional shaping from the last stage of refitting 4 on the negative/dorsal face of the refitting. Although the reduction stage of a core prepared in this way was conducted away from the area under investigation, the product brought to the site was remodeled there. The first artifact detached in refitting 5 was a flake with a multifaced butt, which broke at the moment of detachment into three fragments (1127, 1218 and 675). It was struck from the direction of the front platform, while the multifacing of the butt could be a remnant of the faceting of the striking platform from a previous stage of reduction. Further flakes were detached from the direction of the rear platform (599, 906, 413).

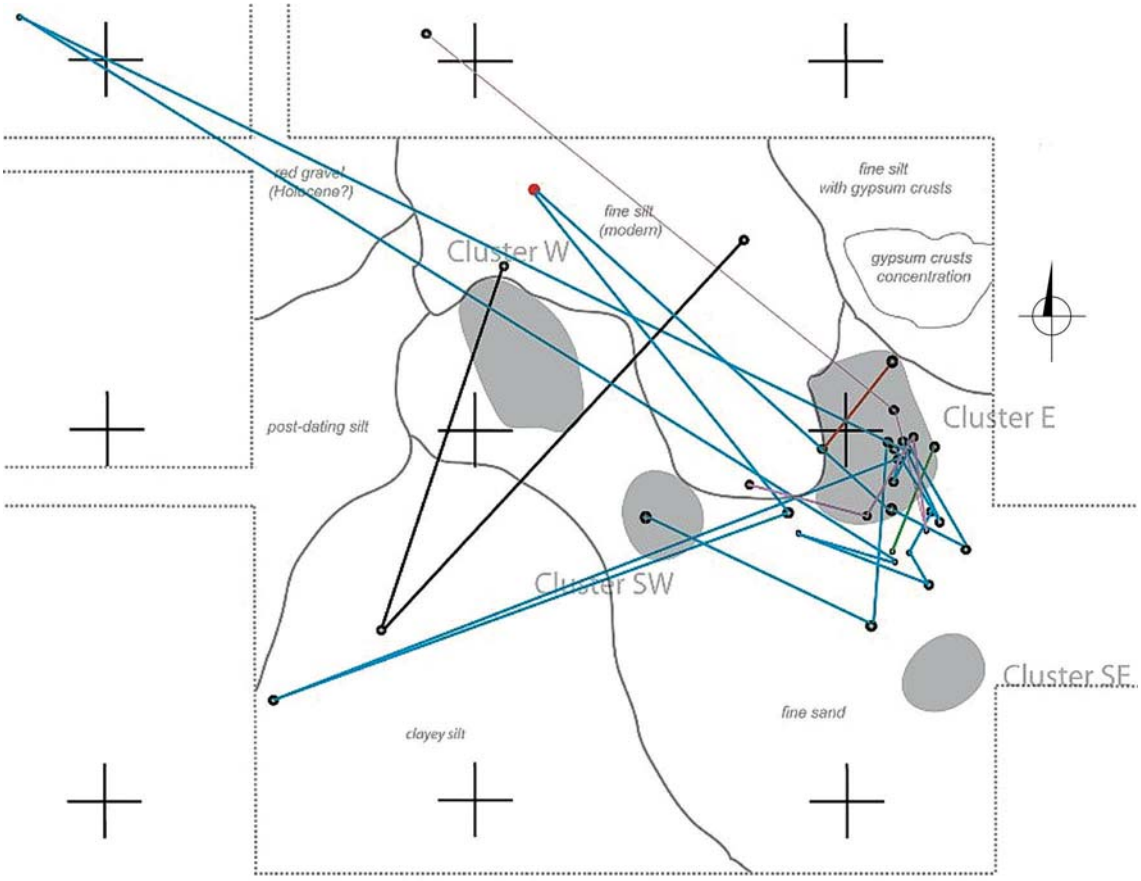

Fig. 4.32. Dispersal of debitage from Block 19 mapped onto a plan of site AFD23 (sector SW, season 2013) with the location of the largest clusters of lithic artifacts

Following remodeling, the core would have had flaking surface dimensions of approximately 6 cm in length and 5 cm in width, with centripetal shaping of the flaking surface relief and two opposite platforms. This piece was not found.

Dispersal: Almost all the pieces making up Block 19 were found on the surface in the eastern cluster and south of it [*Fig. 4.32*]. Single pieces were also relocated to secondary contexts (as well as subsurface layers), often at a significant distance.

BLOCK 20

Description: Nodule of brown (7.5YR5/6) chert with light olive-brown (2.5Y5/6) sections and very characteristic chalk inclusions. Light yellowish-brown (2.5Y6/3) sections with clear boundaries (fossils?) were also visible in places. External layer smoothed and cracked only on the edges. A thin accumulation of a black substance (manganese?) visible directly under the external layer, resembled pieces refitted as Block 12. The two could actually be part of the same nodule despite not having the refittings to prove this.

Processing: The refittings represent incomplete stages of preliminary processing and modelling of the core. No residual core to fit these pieces was located [see *Table 4.8*]. Refittings 1 and 3 are simple refittings of flakes broken into pieces. However, refitting 2 also includes initial flakes (492, 732)

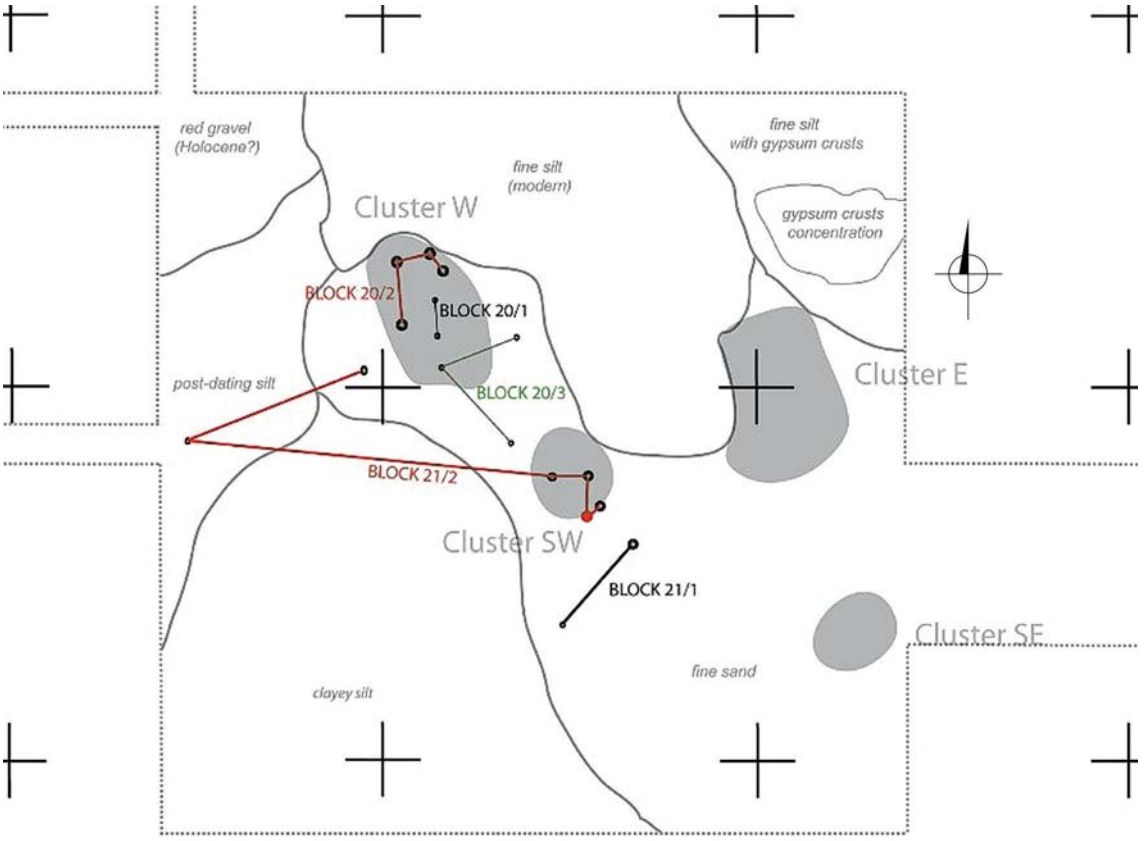

Fig. 4.33. Dispersal of debitage from Blocks 20 and 21 mapped onto a plan of site AFD23 (sector SW, season 2013) with the location of the largest clusters of lithic artifacts

from a large surface (flaking surface?), after which crude flakes were also detached from the surface of the striking platform (absent from the collection), as well as further flakes from the shaping of the flaking surface relief (975 and 974), the lattermost with a multi-faced butt that was shaped right after the detachment of 975. Not fitted are flakes with multifaced butts: 377, 725 and 756, as well as a range or partly cortical flakes, also from subsurface layers (e.g., 1881, 1964). Neither the sequence of core shaping or the actual shape of the core could be reconstructed on this basis.

Dispersal: The refitted pieces were found on the surface in the western cluster (unlike Block 12 which has a similar petrographic character) [*Fig. 4.33*]. Pieces which could not be refitted to this block were concentrated in the western cluster or scattered on the surface in secondary contexts west of it.

BLOCK 21

Description: The pieces of Block 21 demonstrate several similarities to Block 20 but without any chalk inclusions. Predominantly brown (7.5YR4/6) in color with clear brownish-yellow (10YR6/8) sections. External layer smoothed and richly sculpted in places.

Processing: Refitting 1 includes initial cortical flakes shaping an extensive surface (probably the flaking surface) [see *Table 4.8*]. Refitting 2 is a sequence of flakes detached from quite a short plane—probably the striking platform. Their butts are multi-faced (insofar as they are preserved), reflecting simultaneous working of the flaking surface, to which a small cortical flake (450) corresponds.

Dispersal: The refitted pieces of Block 21 are concentrated around the southwestern cluster and are scattered south and west of it [see *Fig. 4.33*].

BLOCK 22

Description: Nodule displaying a slightly mosaic internal structure with mutual intertwining of sections of well-crystallized dark brown (7.5YR4/6) chert, as well as a slightly lighter (7.5YR5/6) porous fraction. External surface smoothed and cracked [*Fig. 4.34*].

Processing: One of a few blocks demonstrating a complete processing sequence, including pieces from the initial working phase, the final product and residual core [see *Table 4.8*]. It is so far the best documented example of the process of knapping stone tools at site AFD23. The collection does not include opening flakes, most probably detached while testing the raw material. Extensive negatives of these are visible on the rear section of the pre-flaking surface, as well as on the surface of the front striking platform.

The initial stage of working the core [*Fig. 4.35*: Phase of reduction I] is represented by a series of flakes with extensive natural external surfaces, detached alternately from the rear platform and flaking surface in its rear zone, as well as from the front platform and the flaking surface in this zone. Therefore, from the very beginning, initial processing covered both ends of the nodule, as if they were independent of one another. Although initial pieces from the working of the core were of the largest dimensions, they did not equal pre-determined product Their butts were plain or natural, while a flake with a multi-faced butt was noted in only one case. The length–width proportions of these flakes were close to equal. The division of these pieces into two size categories was also noticeable: the larger ones from working of the flaking surface and the smaller ones (under 4 cm) detached from the platform plane.

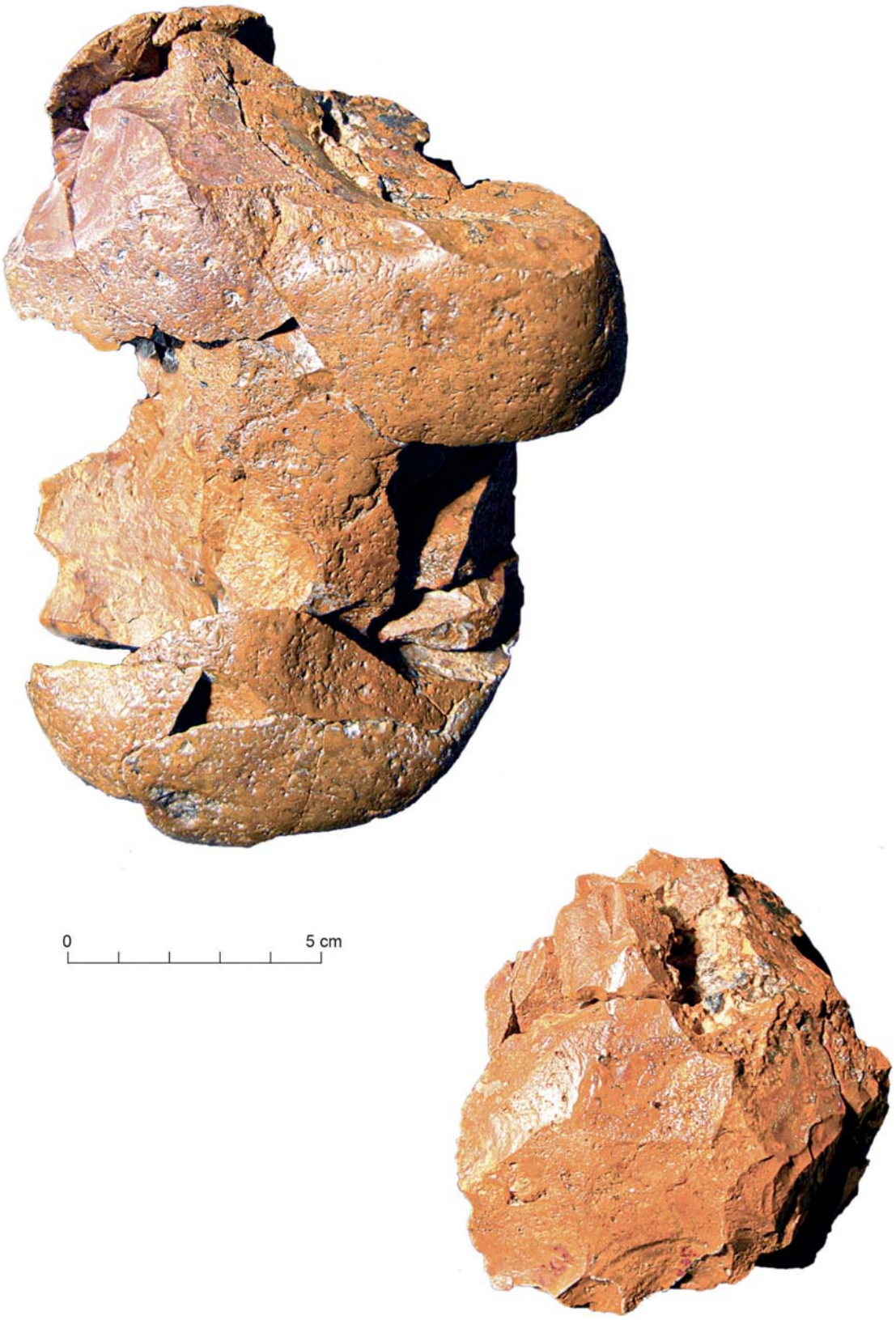

Fig. 4.34. Block 22: top, elements of the block in the initial phase of reduction (I) (dorsal face); bottom, elements of the block in an advanced stage of reduction (IV) (dorsal face)

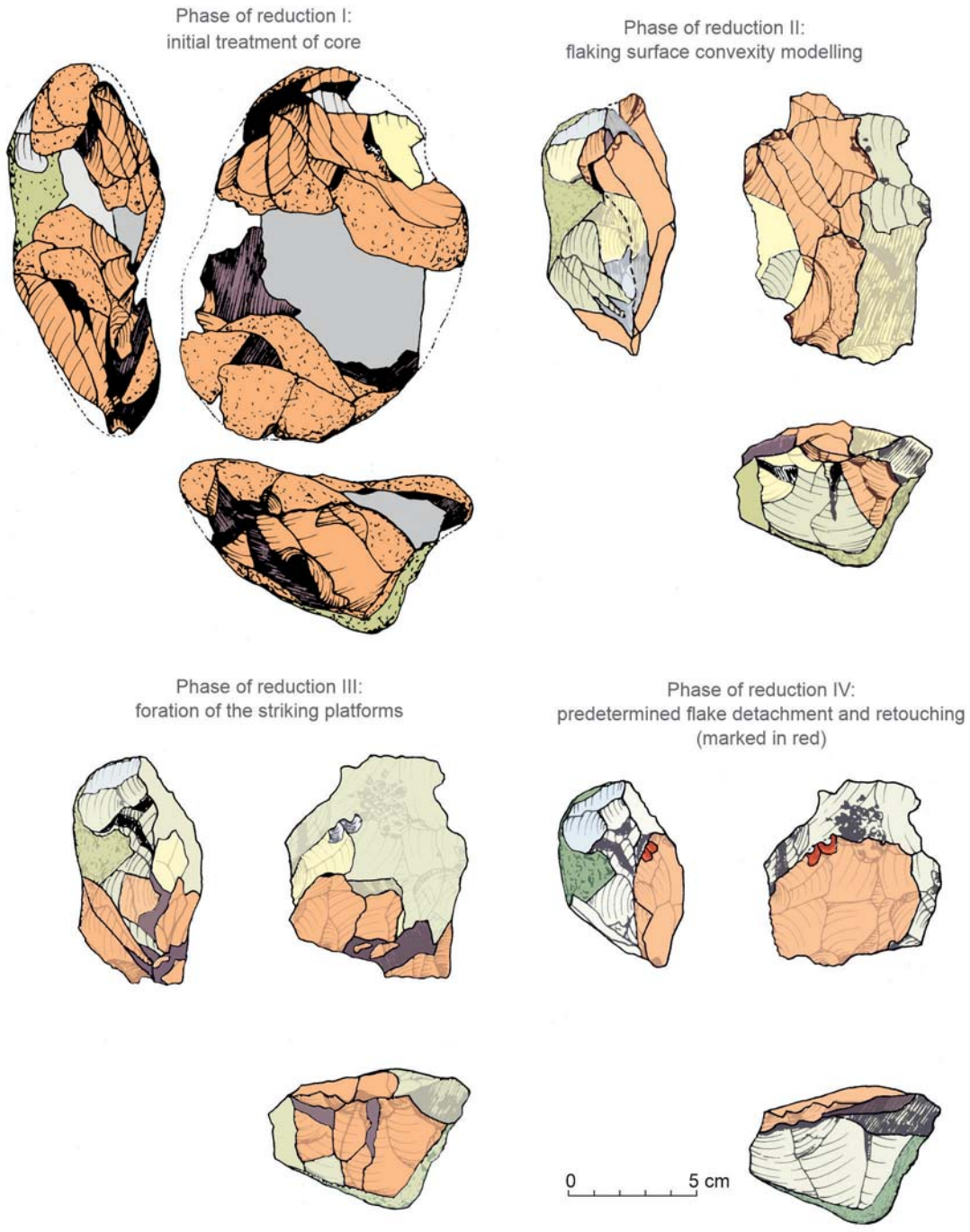

Fig. 4.35 (and opposite page). Block 22: drawing reconstruction of the refitting, phases of reduction I through VI. Color code: green – features (faces) pre-existing current stage of reduction (here, cortex); orange – dorsal faces of products detached in current stage of reduction; purple – ventral faces of these products; yellow – negatives of products detached in current stage of reduction (not found in the collection); blue – faces exposed in subsequent reduction stages

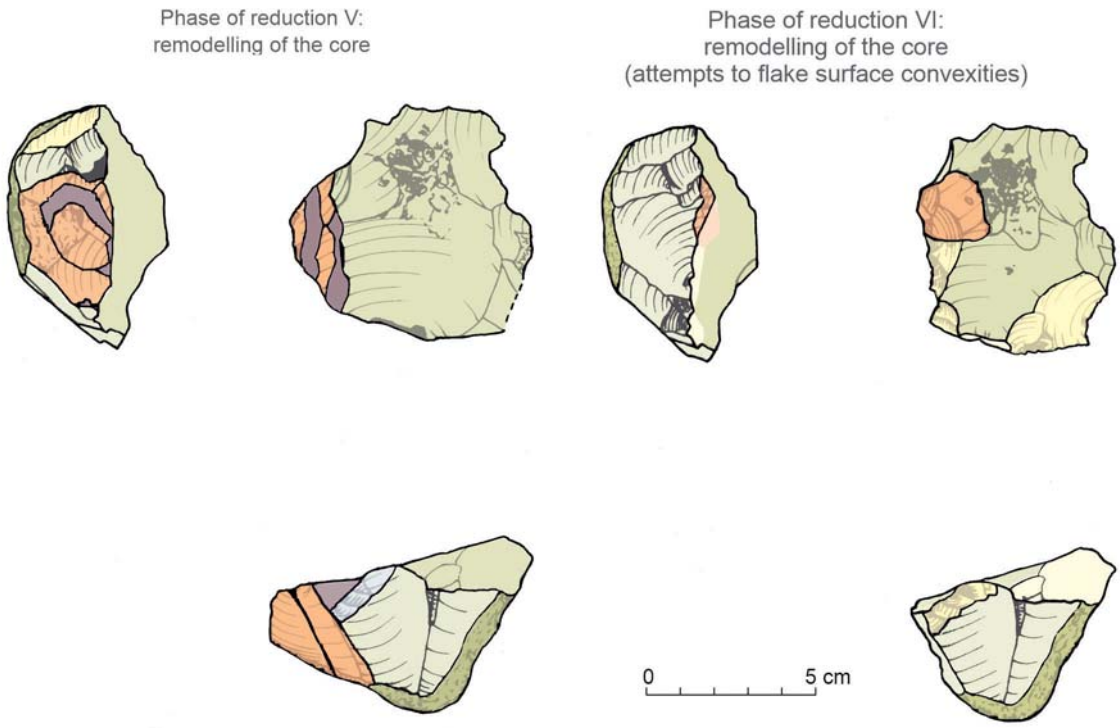

Fig. 4.35 continued

In the next stage, the core was worked (formation of a proper convex shape of the flaking surface) detaching flakes from both the front and the rear of the core, as well as elongated products from opposite sides of the flaking surface [*Fig. 4.35*: Phase of reduction II]. Although the elongated flakes featured both plain and multi-faced butts, their character is typically technical and preparatory.

The knapper then focused his attention on the front section of the core where an almost complete sequence of debitage was recorded, from the shaping of a *chapeau-de-gendarme*-type striking platform, to the detachment of further small products both from the surface of the platform and the front section of the flaking surface [*Fig. 4.35*: Phase of reduction III]. This phase included decidedly less debris than previously, albeit thicker (two slightly more elongated pieces come from correcting the striking platform surface).

A crude Levallois flake detached during a principal stage of reduction had a multi-faced butt of the *chapeau-de-gendarme*-type, as well as being almost of the same size in terms of length–width proportions [*Fig. 4.35*: Phase of reduction IV]. The flake did not cover the entire length of the flaking surface, terminating in the zone of a natural imperfection of the nodule (internal concentration of chalk). Despite this, it exceeded the dimensions of products of debitage from the previous working stage. Its distal edge possessed a naturally jagged line. This feature was additionally supplemented by two intentional notches, giving the edge a strongly denticulate character. This artifact, therefore, belongs to the class of formal denticulate tools, this being an important indication of the production goals of stone knappers working at AFD23.

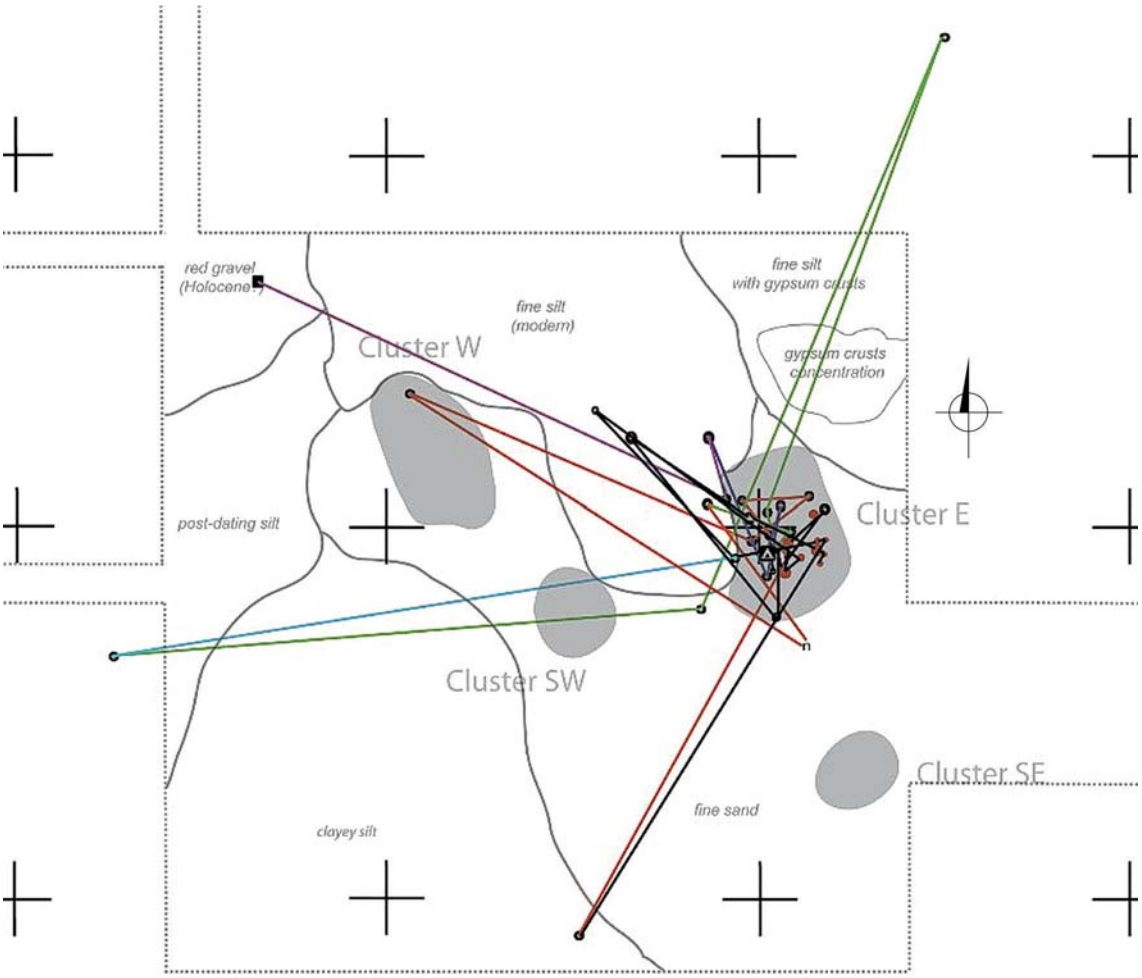

Fig. 4.36. Dispersal of debitage from Block 22 mapped onto a plan of site AFD23 (sector SW, season 2013) with the location of the largest clusters of lithic artifacts

Following the detachment of a predetermined flake, the core underwent a two-stage process of remodeling. First, the course of the side edge of the core was modified by detaching a series of products from the striking platform [*Fig. 4.35*: Phase of reduction V]. The flaking surface took on a more elongated, rectangular shape. Then, the convex shape of the flaking surface started to be formed by detaching products from opposite sides of the striking platform [*Fig. 4.35*: Phase of reduction VI]. The core was abandoned at this stage. The debris of the last phase of reduction (remodeling) displayed small dimensions and plain or multi-faced butts.

Dispersal: The overwhelming majority of pieces making up Block 22 occurred within the eastern cluster, both on the surface and in the subsurface layers [*Fig. 4.36*]. Pieces scattered beyond the eastern cluster lay on the surface, often at a significant distance exceeding 10 m.

Block 23

Description: Nodule of dark brown (7.5YR3/4) color and a range of internal sections which were quite porous and contained gas bubbles. External surface smoothed and cracked.

Processing: Both refittings present an initial working stage of the core. Refitting 2 provides clear evidence of a preliminary shaping of the nodule by detaching a sequence of crude flakes with unprepared butts. The incomplete nature of the refitting suggests that the nodule was moved away from the area where it was first shaped [see *Table 4.8*].

Dispersal: Pieces from both refittings were recorded in the eastern cluster and only on the surface [*Fig. 4.37*].

BLOCK 24

Description: Nodule characterized by very numerous, small, empty spaces resulting in lesser cohesion of the stone. The predominant color is brown (7.5YR4/6). External surface smoothed and cracked. Concentrations of a black material (manganese?) observed directly under the surface.

Processing: The refittings represent incomplete stages of preliminary processing. The refitted artifacts are crude, as a rule, and are covered by large sections of the natural external surfaces [see *Table 4.8*].

Dispersal: These pieces occurred in greatest numbers in a zone east of the western cluster. The nodule may be linked with a temporary notched tool (805), located more than 20 m northeast of the other pieces [see *Fig. 4.37*].

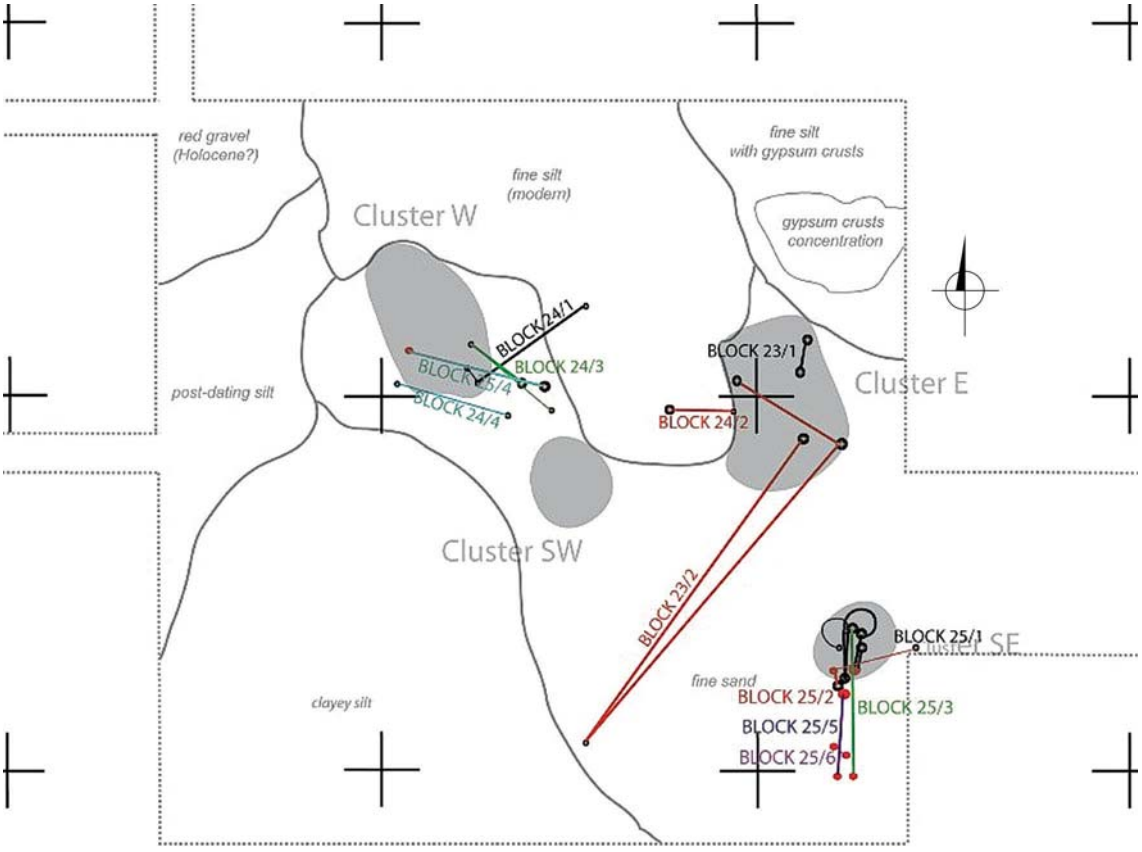

Fig. 4.37. Dispersal of debitage from Blocks 23–25 mapped onto a plan of site AFD23 (sector SW, season 2013) with the location of the largest clusters of lithic artifacts

BLOCK 25

Description: Nodule with a characteristic porous but translucent matrix, brown (10YR4/3) in color, with clearly different fragments of a fine-grained yellowish-brown (10YR5/8) rock apparently 'melted' into it. It it is not jasper, then it could be, due to the lack of a homogeneous interior, a conglomerate.

Processing: The refitted pieces come from preliminary stages of working the nodule (refittings 3, 5, 6), as well as covering an opposite-direction shaping of the convex section of the flaking surface (refittings 1 and 2) [see *Table 4.8*].

Refitting 1 represents a sequence of flakes resulting from the shaping of the flaking surface. Although the first product (635) detached is crude and comes from an initial phase of this stage, its butt demonstrates earlier shaping in the form of several negatives. The next flake, broken into two pieces (272, 274), was detached from the same direction and formed the left side of the flaking surface. Directly before the next phase of shaping the flaking surface, a flake was detached from the platform plane, evening out its whole left side—this piece was not found. The next flake (also broken into two pieces: 270 and 714) formed, in turn, the right side of the flaking surface, and was also detached from the direction of a front platform. It is likely that the next two flakes from the central section of the flaking surface (257 and 267) were detached at the same moment. Directly before the detachment of flake 3031, its butt was facetted with a few small products that are missing from the refitting. Keeping in mind its centripetal location on the flaking surface and the operation of faceting the butt, this product may be acknowledged to be a piece signifying a new phase of precise shaping of the flaking surface relief. This flake did not undergo further processing (retouching). Although it was left in the place of production, it is difficult to justify its interpretation as a final/predetermined product. Directly after this, the last flake (253) present in the refitting was detached from the flaking surface, this time from the side of the rear striking platform. It constitutes evidence of the shaping of the final relief of the core's flaking surface from two opposite directions. Refitting 2 includes two pieces from the working of the flaking surface with multi-faced butts, thus also probably from an advanced stage. The relationship between the two refittings could not be established.

No core matching this blocks was located in the collection, hence it must have been moved away from the site where it was processed.

Dispersal: All of the refitted pieces of Block 25, apart from refitting 4, occurred in the south-eastern cluster, or even south of it [see *Fig. 4.37*]. Owing to the slightly different nature of the raw material in the case of the artifacts making up refitting 4, these pieces could have come from the processing of a different nodule.

BLOCK 26

Description: Nodule of a light shade of brown (10YR6/8) with darker (7.5YR4/6) inclusions. External surface smoothed and cracked.

Processing: Crude flakes from this refitting reflect the stage of shaping a large flat (flaking) surface. Both flakes featured multi-faced butts—the result of detaching flakes from the plane of the striking platform [see *Table 4.8*].

Dispersal: Both flakes occurred on the surface in the western cluster [*Fig. 4.38*]. An unfitted piece of the initial working of this nodule (176) also occurred in this location.

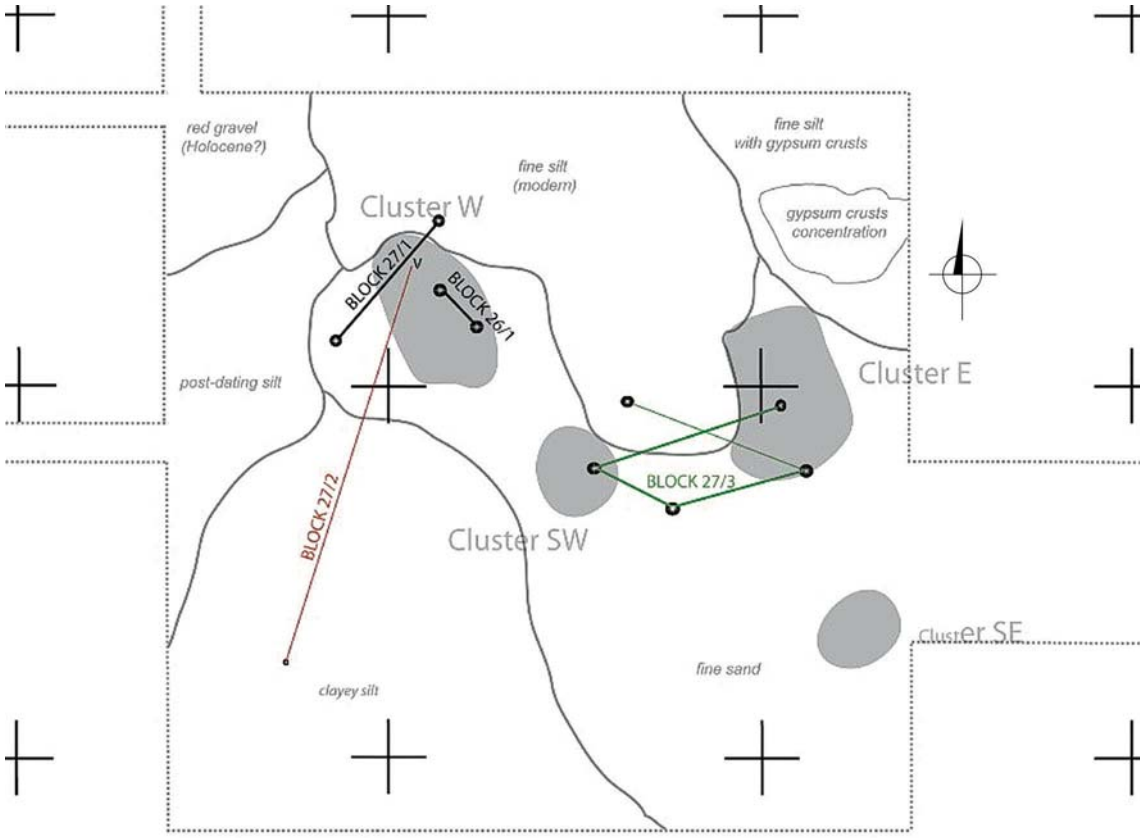

Fig. 4.38. Dispersal of debitage from Blocks 26–27 mapped onto a plan of site AFD23 (sector SW, season 2013) with the location of the largest clusters of lithic artifacts

BLOCK 27

Description: Nodule characterized by a mosaic internal structure, predominantly brown (7.5YR5/8) in color, with numerous inclusions, fractures and gas bubbles. External surface smoothed and cracked.

Processing: All of the refitted pieces represent initial phases of working the flat surfaces (flaking surface and striking platform) [see *Table 4.8*]. Refitting 3 constituted in its entirety products detached without prior preparation of the platform, from the same direction, taking advantage of the natural shape of the nodule. However, refitting 1 comes most probably from the stage of shaping the platform, being decidedly shorter and thicker. The butt of one of the flakes (870) was formed. Of note is the fact that refitting 2 includes two flake fragments (proximal and distal) with a burin scar on the positive/ventral face, which took off the entire butt section. The instrumental use of products of the initial phase of the working is a clue to explaining the lack of any evidence of advanced stages of core reduction in the refittings. It is most likely that the preliminary shaped nodule was relocated outside of the area under investigation.

Dispersal: Each of the refittings occurred in a different zone, all of them on the surface [see *Fig. 4.38*]. Refittings 1 and 2 were generally in secondary contexts around the western cluster, while refitting 3 was both in the southwestern and eastern clusters.

BLOCK 28

Description: Very characteristic raw material differing from other nodules of transparent flint and the large number of fossils. Predominantly olive (5Y5/3) in color. External surface heavily [*Fig. 4.39*].

Processing: This entire refitting is a large, intentionally fragmented flake, resulting from the testing of the quality of the nodule [see *Table 4.8*]. One fragment, resembling a blank for a small core-on-flake, is missing. No pieces of the further processing of a nodule of this kind could be located in the collection.

Dispersal: All the fragments come from the surface, mainly secondary contexts around the western cluster [*Fig. 4.40*].

BLOCK 29

Description: Nodule characterized by a brown-colored (7.5YR4/4) interior with numerous inclusions from the grey (7.5YR5/2) subcortical layers where the rock is both very porous and containing chalk inclusions. External surface smoothed and cracked [*Fig. 4.41*].

Processing: The block does not include any initial flakes detached from the pre-flaking surface from the side of the rear platform; this was done most probably at the stage (and place) of collecting and testing the quality of the raw material [see *Table 4.8*]. Refitting 1 includes cortical flakes detached both from the plane of the rear striking platform (665) and the flaking surface from the side of this platform (2869). The latter large flake, entirely covered with the original outer surface of the nodule, was later preformed into a formal tool through denticulate retouching of one of the longer edges. These operations served to form the proper angles between the simultaneously reduced surfaces of the striking platform and flaking surface. It is likely that flakes from refitting 3, which could not be fitted to any part of the main refitting (2), come from this stage. Another series of flakes had already been detached from the rear platform plane (2796, 673, 2883+2798, 565). Following correction of the flaking angle on the flaking surface, the debris of which was not found in the collection, the rear platform was further reduced (642, 2849, 475, 668, 2901, 2795). Then the surface of the platform on the right side of the core was formed (35, 2794). The last two flakes from the rear platform (1065 and 582) were detached directly before the flakes forming the relief of the flaking surface from the rear platform side (464, 2764), owing to which the final artifact featured a multi-faced butt.

The next working stage commenced with a series of flakes detached from the front platform surface (not added directly to the main refitting 2: 2851 and then 581 and 517). They formed the proper angle for detached flakes forming the right side of the flaking surface (2743+1138, 2927). The next flake from the front platform surface (663) corrected the angle of the front platform. Then, the flaking surface was shaped on the left side (this debris was not preserved), and once again on the right side (488+112). The next piece, missing from the collection, was detached from the middle section of the flaking surface from the side of the front platform and, as its negative shows, had the form of a point. Although its butt was formed by two large negatives, this was not accompanied by more precise faceting. On the negative/dorsal surface, it displayed traces of formation from the same direction (on the right side), as well as several diagonal scars on the left side. Taking the whole of Block 29 into account, this (missing) piece could be designated as a 'final' product.

Fig. 4.39. Block 28, refitted elements (dorsal face)

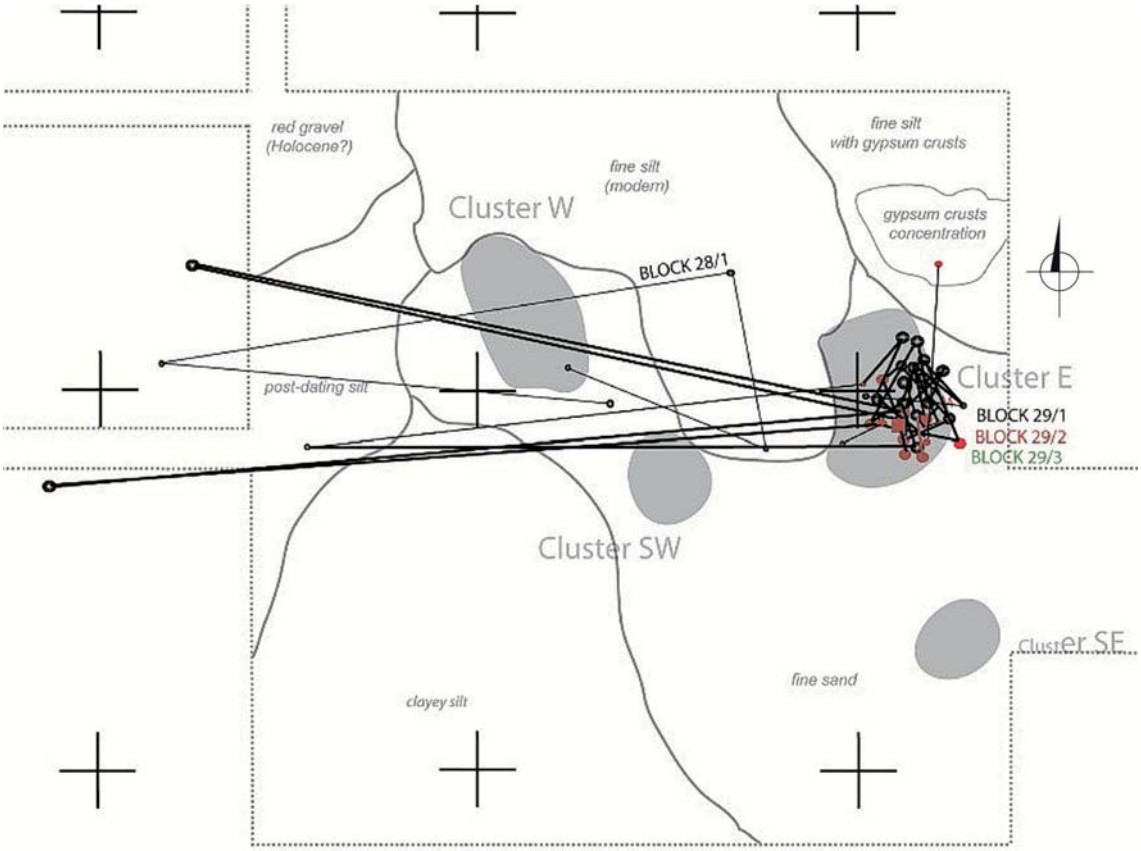

Fig. 4.40. Dispersal of debitage from Blocks 28–29 mapped onto a plan of site AFD23 (sector SW, season 2013) with the location of the largest clusters of lithic artifacts

Fig. 4.41. Block 29, refitted elements; right, denticulate tool made of a cortical flake (dorsal face)

Right after this point was detached, the flaking surface was remodeled from the side of the front platform, first the right side (644), then the left, seemingly removing an edge flake that was too crude (564). The next stage of remodeling of the flaking surface included a series of flakes detached from the right side of the core (136, 45+2900, 463, 107), as well as the rear platform (2852+2921, 2855).

The final stage of shaping the relief around the flaking surface and remodeling the front platform included artifacts absent from the collection. The residual core (2749) was abandoned at the point when it had a shaped convex flaking surface and two opposite platforms.

Dispersal: Almost all of the refitted pieces of Block 29 (including a denticulate tool made from an initial flake and the residual core) occurred on the surface and in the subsurface of the eastern cluster [see *Fig. 4.40*]. Single pieces were relocated (sometimes at a distance of over 20 m) in a westerly direction.

Block 30

Description: Fairly non-cohesive porous chert, brown (7.5YR5/6) in color, with numerous internal fractures causing uncontrolled breakage of detached flakes. External surface smoothed.

Processing: Refitting 1 represents pieces of an artifact fractured into chunks during the initial working, or possibly during the testing of the quality of the raw material [see *Table 4.8*]. Refitting 2 comprises two crude flakes also from the initial working phase with unprepared butts.

Dispersal: Pieces of refitting 1 occurred on the surface in the eastern cluster, whereas elements of refitting 2 came also the surface, spread between the southeastern and eastern clusters [*Fig. 4.42*].

Block 31

Description: Fairly non-cohesive porous chert, brown (7.5YR5/8) in color, including chalk inclusions. Irregular breakage. A black substance (manganese?) in the subsurface layer.

Processing: Refitted flakes come from a stage of shaping the flaking surface from two opposite directions [see *Table 4.8*]. Since the debris is not from the testing of the raw material stage, it follows that even nodules with such a high degree of non-cohesion were subjected to processing.

Dispersal: Both pieces come from the surface, spread 20 m apart, outside of any of the evident clusters [see *Fig. 4.42*].

Block 32

Description: Nodule with a highly cohesive structure, brown (7.5YR4/6) in color. Generally, a fine-crystalline raw material with more porous sections locally. Judging from the number of cores or large flakes with very similar petrographic characteristics, the pieces collected here could represent more than one nodule [*Fig. 4.43*].

Processing: The refittings represent various, incomplete stages of core processing [see *Table 4.8*]. Refitting 1 includes several flakes from the final stage of core shaping, the form of which allow neither the orientation or the final product to be determined. The platform surface was formed on three-fourths of the circumference of the core, while the flaking surface relief in its current state was formed from two opposite directions. A piece of the natural surface of the nodule

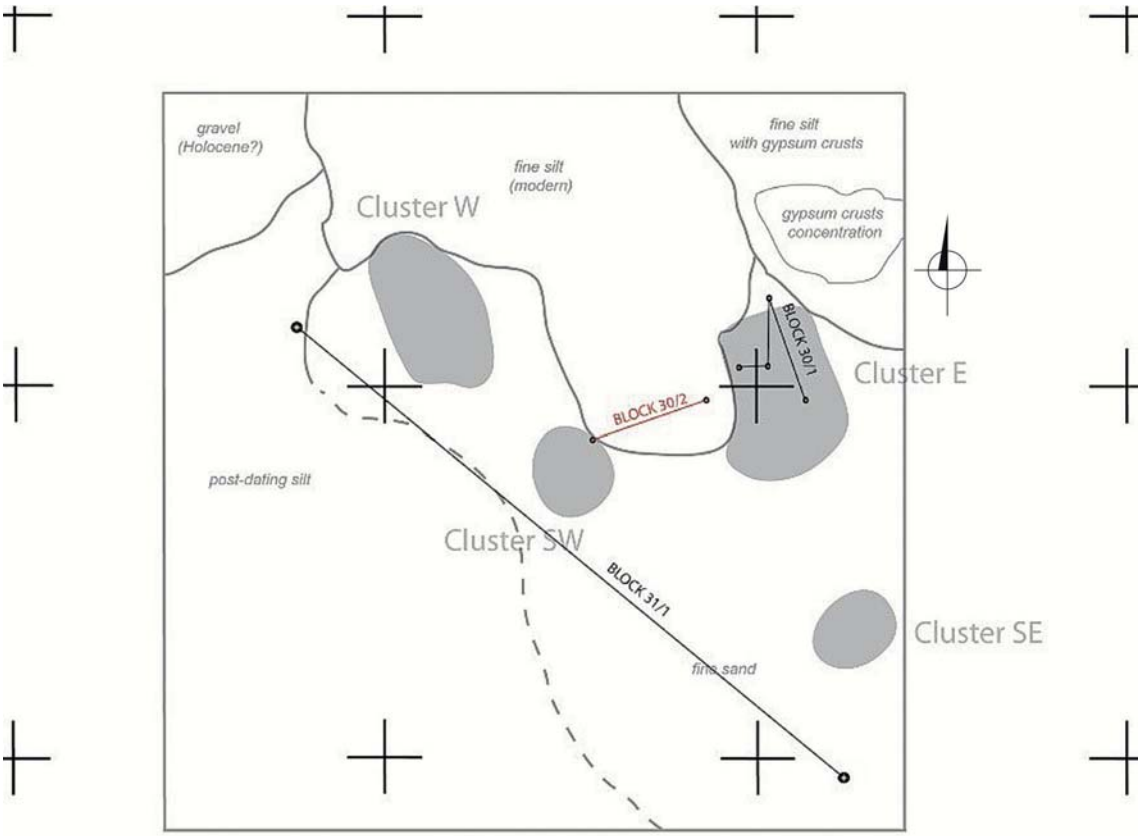

Fig. 4.42. Dispersal of debitage from Blocks 30–31 mapped onto a plan of site AFD23 (sector SW, season 2013) with the location of the largest clusters of lithic artifacts

remains in the middle of the slightly convex flaking surface. On one fragment of the platform, one notes signs of a more precise placing forward of the point of percussion, probably illustrating an operation aimed at faceting the platform for obtaining the intended final product. However, the flake was not detached, the unwillingness to proceed potentially because of an unsuccessful preparation of the edges and flaking angle. The 'faceting' negatives are short and rather too deep, terminating in a hinge as a rule.

Refittings 2 and 3 are simple two-piece joinings. In the case of refitting 3, it is debris from advanced phases of processing (remodeling) with multi-faced butts. Two refittings come from initial working phases.

Dispersal: The dispersal of pieces making up the Block 32 refittings, concentrated around both the western (refittings 1 and 2) and eastern (refittings 3 and 4) clusters [*Fig. 4.44*], constitutes further proof of several nodules of the same kind having been processed at the same time. It should be added that many unrefitted tools and Levallois flakes (e.g., 1172, 469, 980, 1012, 914 and 708) possess very similar petrographic characteristics, indicating a preference for this kind of raw material among the Affad stone knappers. They were scattered all over the entire area under investigation.

Fig. 4.43. Block 32, refitted elements (dorsal face)

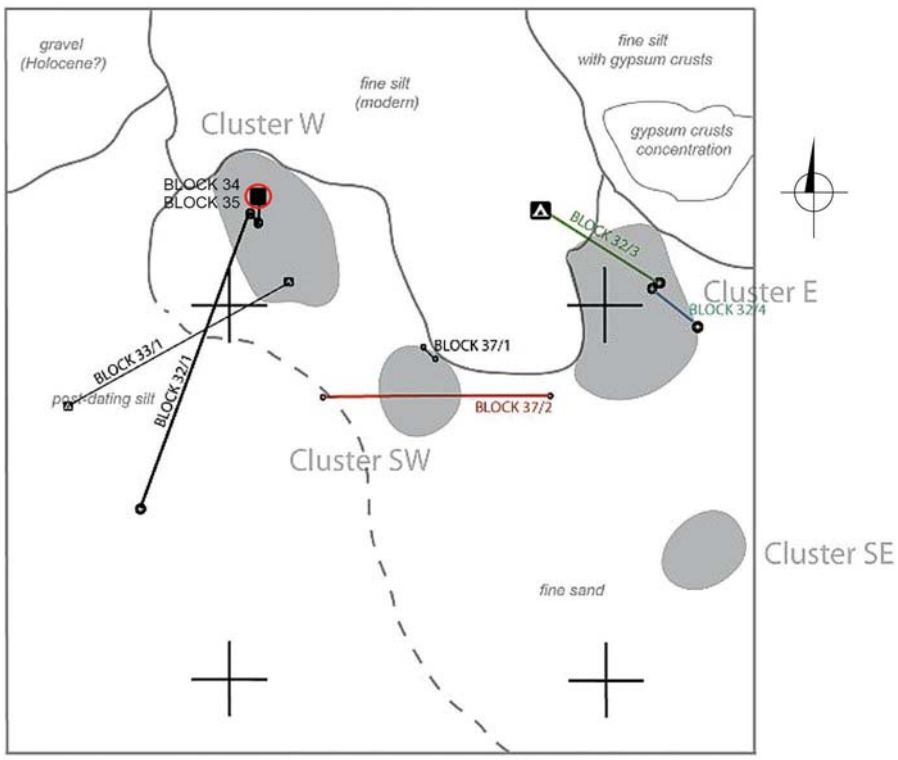

Fig. 4.44. Dispersal of debitage from Blocks 32–35 and 37 mapped onto a plan of site AFD23 (sector SW, season 2013) with the location of the largest clusters of lithic artifacts

BLOCK 33

Description: Chert of brown (7.5YR4/6) color. External surface smoothed. From a petrographic viewpoint, the raw material of this block is very similar to Block 18, but a relationship between the two could not be established by the individual refittings.

Processing: The refitting includes a partly cortical flake broken along the axis of percussion, which displayed a carefully prepared (facetted) butt [see *Table 4.8*]. Following its detachment, another flat and regular artifact was flaked off in the same direction; only a mesial fragment of this has been preserved. Therefore, both detached, fairly large and regular products must have been broken already at the production stage.

Dispersal: The pieces of Block 33 occurred on the surface, scattered to the west of the western cluster [see *Fig. 4.44*].

BLOCK 34

Description: Nodule of porous chert, brown (7.5YR4/6) in color. External surface smoothed and cracked.

Processing: The refitting includes debris from the stage of shaping the nodule. An irregular flake (281) was first detached from the flaking surface, followed by a series of three flakes from the striking [see *Table 4.8*].

Dispersal: The pieces were concentrated over an area of a square meter in subsurface layers [*Fig. 4.44*].

BLOCK 35

Description: Nodule with a mosaic internal structure, brown (7.5YR4/6) in color with manganese permeating the subsurface layer. External surface smoothed and slightly cracked.

Processing: Two pieces from the initial working phase were refitted [see *Table 4.8*].

Dispersal: The pieces were spread over an area of a square meter in subsurface layers [*Fig. 4.44*].

BLOCK 36

Description: Nodule vvery porous with numerous internal gas bubbles, and even larger openings. Predominant color yellowish-brown (10YR5/4). External section smoothed.

Processing: The rrefitting represents debitage from the initial working of the nodule [see *Table 4.8*].

Dispersal: Most of the refitted pieces come from a test pit of 1 m^2 excavated in 2003, to which single artifacts from subsurface layers excavated ten years later were added [*Fig. 4.45*].

BLOCK 37

Description: Nodule comprised of very porous rock, pumice in fact, with a large number of gas bubbles in the interior section. Predominant color light beige (10YR6/3). In the subcortical zone, some 2 cm thick, the rock becomes much more fine-crystalline and yellowish-brown (10YR5/8) in color. External surface smoothed.

Processing: The refittings represent an initial stage of modelling of the nodule [see *Table 4.8*]. The butts of all the refitted pieces are natural/unprepared, although the artifacts themselves

are irregular and thick. The absence of a residual core, or any pieces from an advanced stage of the processing, indicates that the shaped form was relocated outside the site.

Dispersal: Pieces found both on the modern surface and in the subsurface layers around the southwestern cluster, but also in the eastern cluster (refitting 3) [see *Fig. 4.44*].

BLOCK 38

Description: Nodule with an internal mosaic structure, greyish-brown (10YR5/2) in the center and dark yellowish-brown (10YR4/6) in the subcortical section. A fine-crystalline rock, albeit slightly porous. External surface heavily cracked [*Fig. 4.46*].

Processing: An interesting example of core reduction prepared or even utilized outside of the site. Only two flakes from the processing of this nodule (53 and 680) could not be refitted into the block, but it cannot be said whether they come from an earlier phase of reduction [see *Table 4.8*]. The nodule was brought to the site in an already shaped form. The rear platform and flaking surface were completely formed (extensive negatives of products detached from the direction of the rear platform). It also seems that the nodule had already been used as a tool before being brought to the site, because one of the edges is covered with a series of small, irregular negatives

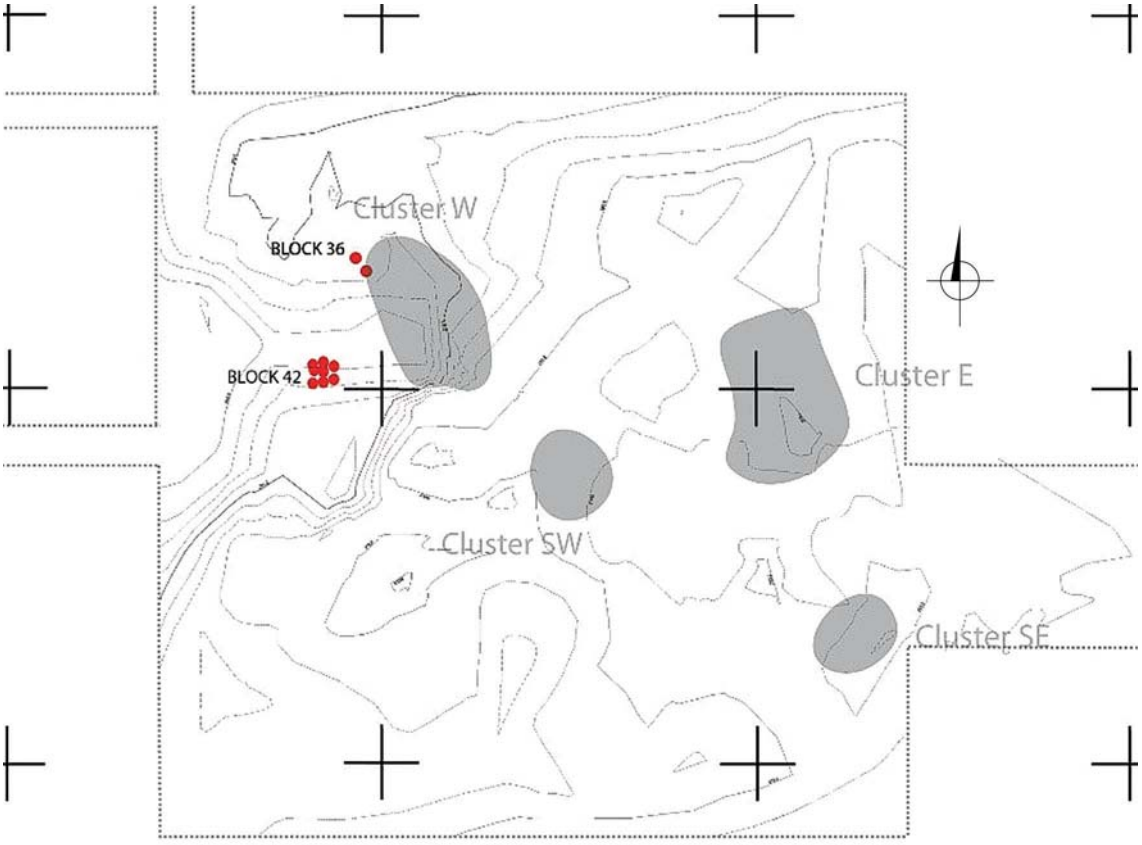

Fig. 4.45. Dispersal of debitage from Blocks 36 and 42 mapped onto a plan of site AFD23 (sector SW, season 2013, plus test pit A/34) with the location of the largest clusters of lithic artifacts, mapped on a reconstruction of the landscape from the time of the MSA settlement

on the flaking surface, which were not meant to correct the surface platform. These negatives resemble *ad hoc* denticulate retouching; in a typological sense, it would have made a crude denticulate racloir on a shaped or utilized core.

The renewed interest in the core appears to have been as a potential source of a Levallois flake or point. Processing started with the formation of a new platform on the opposite side of the older surface, which will be called the front platform. An opening flake (48) was detached, followed by several small cortical flakes forming the surface of the platform on the right side of the core (these products were not found).

After forming the platform, the convex shape of the flaking surface was shaped from the front and on the right side platform (flake series 2003, 2168, 380). The next flake correcting the front platform (1104) preceded the detachment of a large flake from the left side of the flaking surface (2673). Then the flakes forming the flaking surface were detached from the left side of the core, as well as from the direction of the old rear platform (these pieces are also missing from the refitting).

The next stage of the processing was the precise shaping of the front platform. A series of small flakes (2002, 2001, 2391) were detached at this time. This was a requirement for a precise modelling of the relief of the front of the flaking surface (flakes 1106, 1996 and one more which is missing).

Faceting of the platform preceded the detachment of a final product (1546) which, however, presented an overpassing/plunged form; it removed the whole rear section of the core with the platform in its own distal section. Following its detachment, no further steps were taken aimed at repair or using either the flake or the residual core (1299).

Dispersal: All of the refitted pieces lay either on the surface or in subsurface layers of the western cluster [*Fig. 4.47*]. A few were scattered on the surface within 2 m to the west, reflecting the latest stage of landscape erosion. Only a fragment of flake 680, which could not be fitted, and which was most probably from the processing stage of the previous refitting, was found on the surface 10 m to the west.

BLOCK 39

Processing: Both refitted pieces represent one flake broken along the axis of percussion, probably during its detachment [see *Table 4.8*].

Dispersal: Both pieces occurred on the surface at a significant distance from the main concentration of lithic materials in the western cluster [see *Fig. 4.47*].

BLOCK 40

Description: Nodule of a predominantly brown (7.5YR4/6) color with visible yellow (10YR7/6) inclusions. External surface smoothed and cracked. From the point of view of the petrographic characteristics of this raw material, the block resembles closely Blocks 18, 24 and 33; this kind of raw material was obviously preferred by the Affad knappers and hence represents more than one nodule in the collection.

Processing: Both refitted pieces come from an initial stage of shaping the nodule [see *Table 4.8*].

Dispersal: The pieces were surface finds from the southwestern cluster [see *Fig. 4.47*].

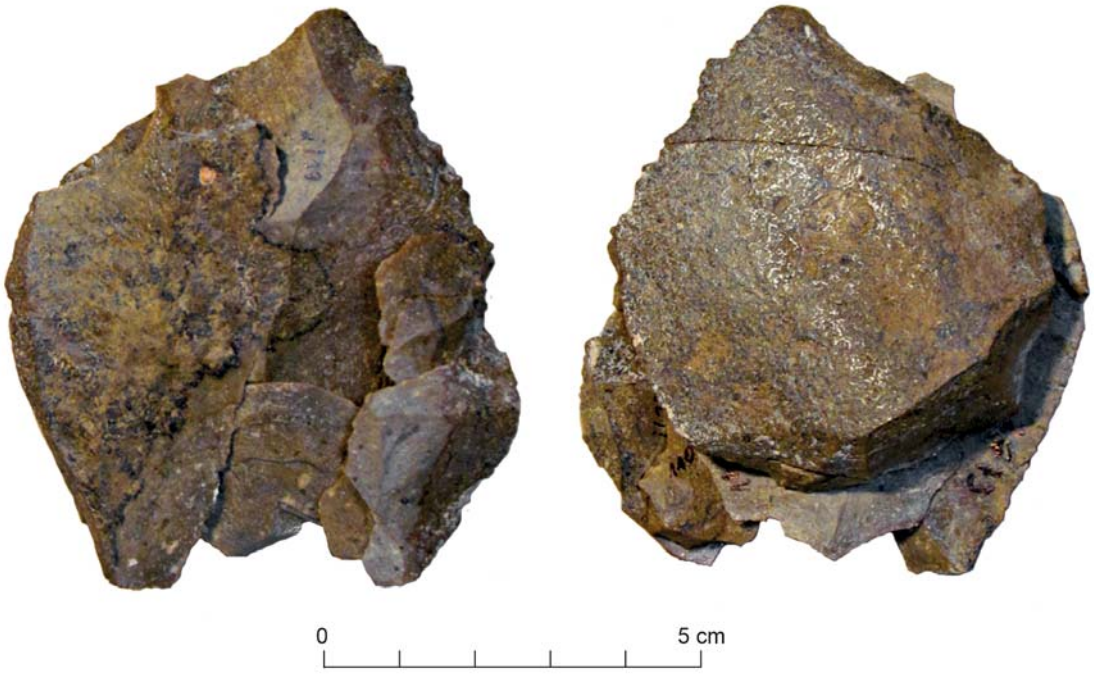

Fig. 4.46. Block 38, refitted elements (from left, dorsal face and ventral face)

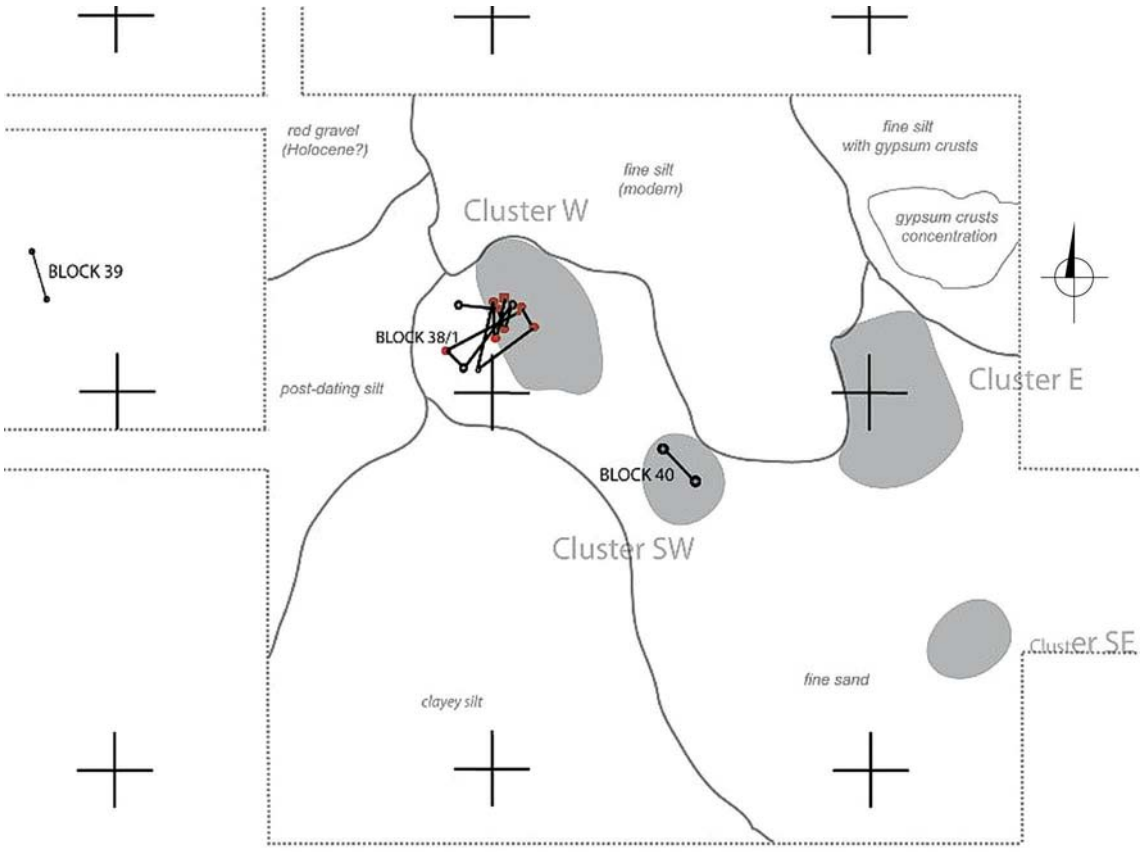

Fig. 4.47. Dispersal of debitage from Blocks 38, 39, and 40 mapped onto a plan of site AFD23 (sector SW, season 2013) with the location of the largest clusters of lithic artifacts

BLOCK 41

The refitting initially designated as Block 41 turned out to be a piece of Block 22 (see above, description of Block 22).

BLOCK 42

Description: Nodule characterized by a yellowish-brown (10YR5/8) color with a large amount of light-colored inclusions in the form of 'veins' or dark-brown spots. External surface smoothed and cracked on the edges.

Processing: The refitted pieces come from an advanced stage of core processing with the flaking surface being shaped in opposite directions. The refitting is incomplete, yielding no information about the preliminary stages [see *Table 4.8*]. Refitting 1 is composed of elongated flakes forming the front platform (2263, 2264). Then a flake, which was also an elongated edge flake (2261), was detached from the left side of the front platform. In the following stage, the next elongated flake (2260) was detached from the same section of the flaking surface, this time from the not-yet-worked rear platform side. The last refitted flake comes from shaping the rear platform (2265). Artifacts detached during the formation of the flaking surface relief, faceting and detachment of the final but unsuccessful product (judging by the very deep and short negative scar) were not found. The residual core was abandoned in a form with two opposite platforms visible.

Refitting 2 consists of two flake fragments that could not be placed precisely in the general chaîne opératoire of this piece.

Dispersal: All of the pieces of the refittings were found in 2013 in a subsurface layer within an area of one square meter [*Fig. 4.45*], while the core was discovered in 2003 within a test pit excavation.

BLOCK 43

Description: Fine-crystalline brown (7.5YR4/4) chert with a slightly lighter subsurface zone. External surface smoothed and cracked [*Fig. 4.48*].

Processing: The refitting of Block 43 contains pieces from the core reduction stage with working of the flaking surface in opposite directions [see *Table 4.8*]. The debitage of the initial working of the front section of the flaking surface is absent from the refitting. The first pieces present comprise a series of flakes correcting the course of the left edge of the core (1867, 1869, 1870, 1871) on the platform surface. Next, it was decided to shape alternately the rear platform and the convex shape of the flaking surface from the side of this platform. Only flakes detached from the flaking surface (1863, 1866, 1859 and 1955) are present in the refitting. Following the formation of the rear section of the flaking surface, the front part of the core was shaped alternately. From this stage comes refitted flake 1954, as well as the proximal fragment of flake 1953, which may have been intended as a final product, but suffered breakage. After its detachment no more attempts were made at remodeling residual core 1952.

Dispersal: All the refitted pieces were found in the subsurface layers of a ground relief depression to the west of the western cluster, in a small space barely 2 m^2 big [*Fig. 4.49*].

Fig. 4.48. Block 43, refitted elements (dorsal face)

BLOCK 44

Description: A very characteristic brown (7.5YR4/4), translucent flint with clear broad matt stripes and porous greyish (10YR5/2) silica. Small chalk inclusions present. External surface smoothed and cracked [*Fig. 4.50*].

Processing: Refittings of Block 44 constitute the only example so far of a complete sequence of preparing a core and detaching a Levallois point. The block was worked on at the site from the beginning to end [see *Table 4.8*]. Processing commenced with the detachment of several flakes from a pre-striking platform surface, which could not be located. Then, an extensive, completely cortical flake was detached from the subsequent flaking surface; this broke into several fragments (2471+2005). Right after this, another flake was detached from the left side of the flaking surface (2472). At the initial stage, the largest flakes of slightly elongated proportions were detached, both with plain and multi-faced butts [*Fig. 4.51*: Phase of reduction I]. The refitting did not include products with natural/unprepared butts from this stage.

The next stage was the formation of the platform surface. The left side (2479, 2006), the right side (2473, 2484), and once again the left side were alternately shaped. The platform was formed by detaching relatively thick flakes with various butts, due to which the product with an edge butt was the thickest. The longest flakes from this stage signify the original length of the butt—approximately 43 mm. The only flake with a natural butt actually came from this stage of processing.

The detachment of flake 2485 opened the phase of shaping the flaking surface [*Fig. 4.51*: Phase of reduction II]. Although this flake formed the left side of the flaking surface, the pieces detached later came from the right side (2490+2486, 2480, 2007). Next, a flake was detached from the middle section of the flaking surface; this was preserved only as a proximal fragment (1443). The right side of the flaking surface was additionally shaped in turns with corrective flakes from the striking platform (2482, 2188+2189). The final relief of the flaking surface was created by flakes from the right side (2481+2474), from the central section (1454+2475), as well as the left side (2187, 2477) of the flaking surface. Most of the flakes detached while shaping the flaking surface relief possessed multi-faced or plain butts, and slightly or clearly elongated proportions. The only product with an edge butt was exceptionally thick. This series also included pieces partly or completely covered with the natural external surface of the nodule.

The faceting of the platform, the debitage of which was not found, preceded the detachment of an irregular Levallois point (1302), unmodified at a later stage [*Fig. 4.51*: Phase of reduction III]. The point displays slightly elongated proportions and dimensions exceeding those of the pieces forming the flaking surface relief. As it was found in the production debris, it was either used directly at the place where it had been made or had been abandoned as a defective product.

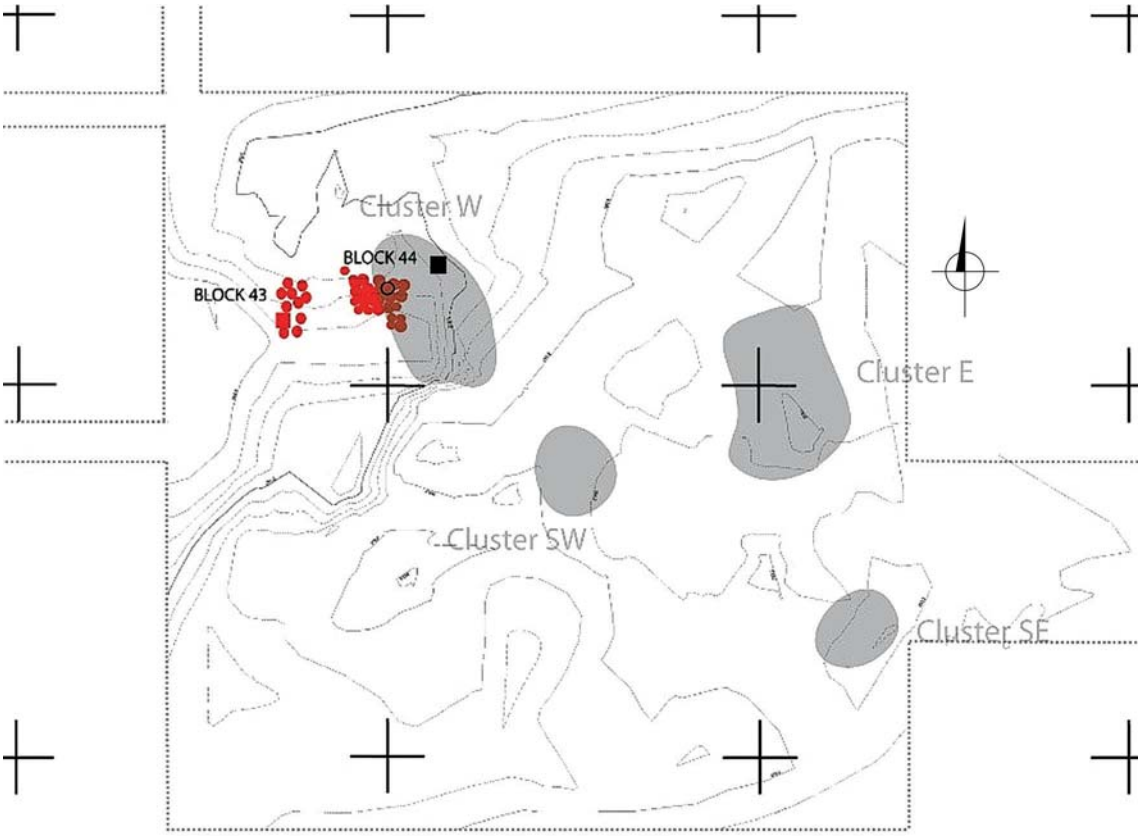

Fig. 4.49. Dispersal of debitage from Blocks 43 and 44 mapped onto a plan of site AFD23 (sector SW, season 2013) with the location of the largest clusters of lithic artifacts, mapped on a reconstruction of the landscape from the time of the MSA settlement

Fig. 4.50. Block 44, refitted elements (dorsal face): top, striking platform and lower side of the core; bottom, advanced phase of core reduction (III)

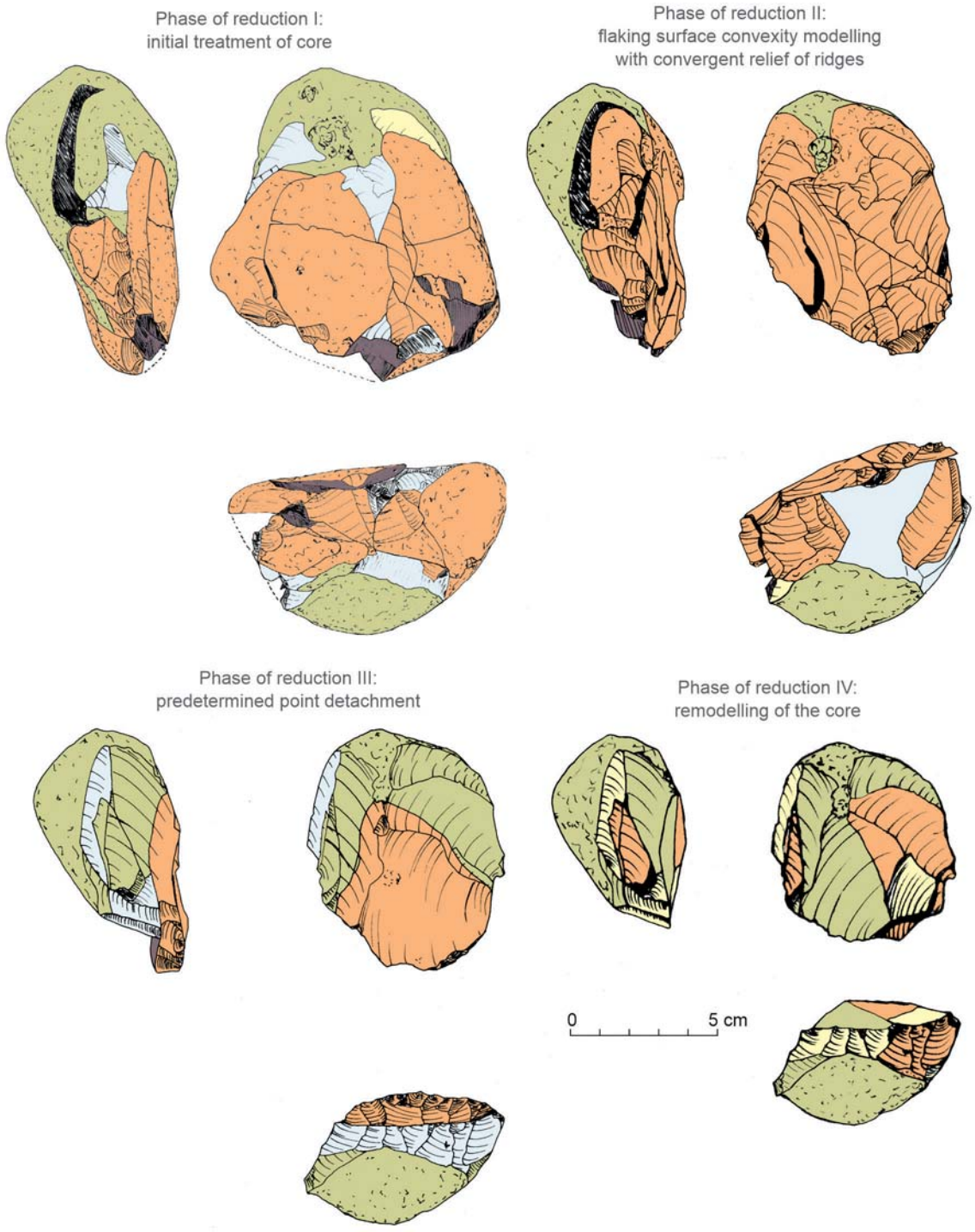

Fig. 4.51. Block 44: drawing reconstruction of the refitting, phases of reduction I through IV. Color code: green – features (faces) pre-existing current stage of reduction (here, cortex); orange – dorsal faces of products detached in current stage of reduction; purple – ventral faces of these products; yellow – negatives of products detached in current stage of reduction (not found in the collection); blue – faces exposed in subsequent reduction stages

Following the detachment of the final product, the core was remodeledby detaching flakes from both the platform surface (1417, 2008) and the flaking surface (2004, 2009) [*Fig. 4.51*: Phase of reduction IV]. However, the residual core (973) does not reveal any evidence of attempts to detach further points. The debitage of core remodeling displayed the smallest size and, once again, the least varied butts. A product with an edge butt was the thickest once again.

Dispersal: All of the refitted pieces of Block 44 occurred in the subsurface layers of the ground relief depression to the west of the western cluster [see *Fig. 4.49*]. Only the residual core was found on the surface already in 2003, a short distance from the other pieces.

4.1.4.3 Southern sector

In terms of the general technological structure of the small collection of lithic artifacts from the southern sector of the site, the dominant form were flake products and retouched denticulate forms. Cores were very few [*Table 4.9*].

Table 4.9. General morphological-technological structure of the collection from site AFD23 (sector S) (number after the backslash refers to artifacts recorded from secondary contexts)

Group	Type	Raw material			Total
		Chert	Flint, mudstone	Other	
Cores	Initial cores and tested nodules	2/0	–	–	2
	Cores for flakes/points	–	–	–	–
	Final cores	–	–	–	–
	Discoidal cores on flakes	0/1	–	–	1
Flakes and chips	Flakes with unprepared butt	11/0	–	1/0	12
	Flakes with plain/uniface butt	15/1	–	–	16
	Flakes with point & edge butts	3/0	–	–	3
	Flakes with multiface prepared butt	11/2	–	–	13
	Flake fragments	8/1	–	2/0	11
Chunks	Chunks	8/1	–	–	9
Predetermined products and formal tools	Levallois flakes	–	–	–	–
	Points	0/1	–	–	1
	Flakes/points with denticulate retouch	2/1	–	–	3

Cores

Two specimens were identified as initial cores preserving no element to indicate the intended predetermined product. In size, they exceeded cores from other sectors of the site [*Table 4.10*]. These forms were found only in the relief depression north of trench 2013/L–M (test trench 2014/R).

A single example of a small discoidal core made from a crude flake was also recorded on the surface of the southern sector of the site (in a secondary context).

Table 4.10. Dimensions and loci of cores from site AFD23 (sector S): 1) initial cores; 2) core from crude flake

Inv. No.	Locus	Context	Dimensions (mm)	Description
1) Initial cores				
3295	2014/R/98/II	2b	137/89/52	Tested nodule
3330	2014/R/93/II	2b	117/106/67	Tested nodule
2) Core from crude flake				
3131	2013/M/25/I	1b	27/41/7	

Flakes

Non-retouched flakes predominated in the collection from the southern sector. The different categories were distinguished by a characteristic form of the butt reflecting the degree of working at the time when a given flake was detached. Six categories were represented.

Natural/unprepared butts

Of the 12 flakes with natural/unprepared butts only one is of quartz and the rest of chert. The length–width proportions are similar: none were elongated and none under 2 cm in length [*Fig. 4.52*; *Table 4.11*]. Flakes with natural butts were characterized by the greatest percentage of the original nodule surface on the negative/dorsal side [*Table 4.12*]. Only three artifacts featured damage in the form of lateral and longitudinal breakage [*Table 4.13*].

Plain/unifacial butt

Flakes with a plain/unifacial butt numbered 16 in all. In terms of size, their length–width dimensions ranged from being equal to twice as long (the parameter of a formal blade). Artifacts less than 2 cm in length occurred in this category [see *Fig. 4.52*; *Table 4.11*]. The percentage of the natural nodule surface on the negative/dorsal side was also substantial [see *Table 4.12*]. Lateral breakage predominated [see *Table 4.13*], while the eroded edges of one of the artifacts reflected post-deposition destruction processes more intense in this case than in the case of other artifacts.

Edge and point butts

The group comprises just three artifacts. The proportions of two complete ones clearly diverged from other flakes in the southern sector, being more like formal blades [see *Fig. 4.52*; *Table 4.11*]. None of them had a significant share of the original nodule surface and the only damage consisted of single lateral breakage [see *Tables 4.12, 4.13*]. Flakes with edge and point butts occurred only in the 2014/R test trench.

Multi-faced butt

The category of flakes demonstrating multiple negative scars is represented by 13 specimens, all made of chert. The majority displayed elongated proportions, but none of these examples was shorter than 2 cm [see *Fig. 4.52*; *Table 4.11*]. Most of them had either an insignificant share or

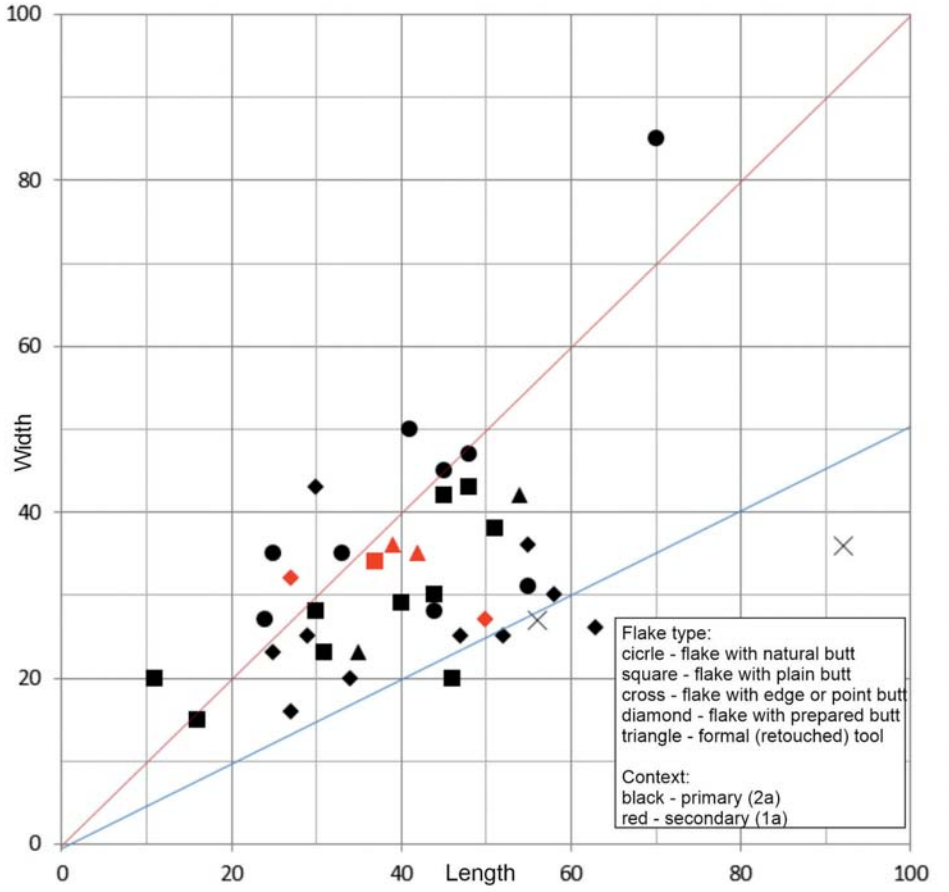

Fig. 4.52. Flakes and tools from site AFD23 (sector S): length-to-width correlation (mm)

no natural nodule surface on the negative/dorsal side, although single examples of products almost of an opening nature with a multi-faced butt were also recorded [see *Table 4.12*]. Contrasting with flakes from the other categories, the most prevalent form of damage in this case was overheating [see *Table 4.13*].

Distal fragments

Most of the distal fragments presented a significant share of the original surface on the negative/dorsal side [see *Table 4.12*], indicating that they should be viewed as supplementing the category of initial flakes. One of these fragments was burnt [see *Table 4.13*].

Chunks

The nine artifacts recognized as chunks are made of chert. The dimensions were small as a rule [*Fig. 4.53*]. None of them bore traces of overheating. The only artifact that came from a secondary context was more eroded than others. All but one chunk came from the 2014/R test trench.

Table 4.11. Thickness-to-width (mm) correlation of flakes from primary and secondary contexts from site AFD23 (sector S). Width presented as a range and a median: red – values lower than the benchmark from primary contexts in sector SW

Thickness	Cortical/unprepared butt		Plain/uniface butt		Point & edge butts		Multi-faced prepared butt	
	CONTEXT							
	Primary	Secondary	Primary	Secondary	Primary	Secondary	Primary	Secondary
1	–	–	–	–	–	–	–	–
2	–	–	15	–	–	–	–	–
3	–	–	17–20	–	–	–	16	–
4	–	–	–	–	18	–	23–42	–
5	–	–	18–28	–	–	–	20–30	27–35
6	–	–	–	–	–	–	30	32
7	20	–	23–29	–	–	–	25	–
8	–	–	–	–	–	–	36	–
9	27–50 (47)	–	30–42	34	–	–	26	–
10	–	–	–	–	–	–	–	–
11	35–45	–	–	–	–	–	43	–
12	–	–	–	–	–	–	–	–
13	28–35	–	–	–	–	–	–	–
14	–	–	–	–	–	–	–	–
15	31	–	43	–	–	–	–	–
16	–	–	38	–	27	–	–	–
17	–	–	–	–	–	–	–	–
23	–	–	–	–	–	–	–	–
24	–	–	–	–	36	–	–	–
28	85	–	–	–	–	–	–	–

Table 4.12. Cortex frequency on flakes with different butts from site AFD23 (sector S)

Share of cortex	Unprepared butt	Plain/ unifacial butt	Point & edge butts	Multi-faced prepared butt	Facetted butt	Distal flake fragments
0%	8.33%	12.50%	33.33%	30.76%	100%	9.09%
10%	16.66%	12.50%	33.33%	30.76%	–	27.27%
20%	–	12.50%	–	15.38%	–	–
30%	–	6.25%	33.33%	7.69%	–	–
40%	8.33%	–	–	7.69%	–	–
50%	8.33%	6.25%	–	–	–	–
60%	–	12.50%	–	–	–	–
70%	16.66%	–	–	–	–	–
80%	16.66%	6.25%	–	–	–	–
90%	–	–	–	7.69%	–	9.09%
100%	25%	31.25%	–	–	–	54.54%

Table 4.13. Damage to flakes from site AFD23 (sector S); in parentheses, number of artifacts from context categories 1b–2b

Flake damage	Unprepared butt		Plain butt		Point butt		Prepared butt		Facetted butt		Unidentified butt
	∑	%	∑	%	∑	%	∑	%	∑	%	∑
Longitudinal breakage	1 (0–1)	8.30%	1 (0–1)	6.25%	0	–	0	–	0	–	2
Transverse breakage	2 (0–2)	16.6%	4 (0–4)	15%	1 (0–1)	33.3%	1 (0–1)	7.69%	0	–	11
Overheating	0	–	0	–	0	–	3 (0–3)	23.07%	0	–	1
Eroded surfaces	0	–	1 (0–1)	6.25%	0	–	0	–	0	–	0

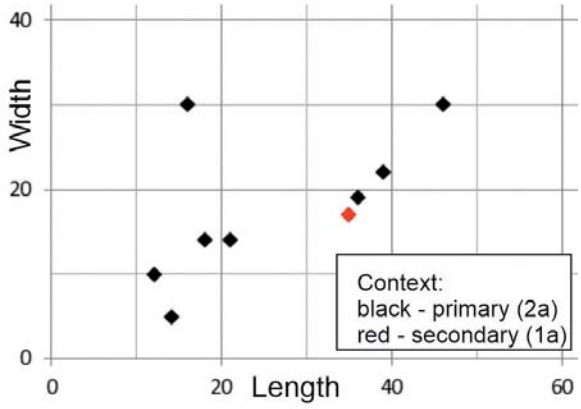

Fig. 4.53. Chunks (two largest measurements) from site AFD23 (sector S): length-to-width correlation (mm)

Predetermined products and formal tools

Tools recorded in the southern zone included one Levallois point (3129) and three denticulate tools from flakes with facetted or multi-faced butts (3126, 3133, 3143), all made of chert [*Fig. 4.54*]. They demonstrated balanced proportions [*Table 4.14*], corresponding in size to the flakes found in this sector. The largest retouched examples reached a length of approximately 5.5 cm and a width of 4 cm. None of the retouched flakes bore any original surface on the negative/dorsal side. Moreover, these forms showed no signs of damage.

The distribution of denticulate tools was like that of a large number of flakes without use-wear marks, occurring strictly in context with the bone remains of grivet monkeys [*Fig. 4.55*]. Single flakes without retouched edges were recorded among the remains of kob antelopes, which was the most popular hunted species. The most numerous burnt artifacts occurred beyond the zones of deposited bone remains, that is, in the 2014/R test trench, which demonstrated other differences as well (i.e., presence of residual cores and chunks).

Table 4.14. Predetermined forms from site AFD23 (sector S)

Inv. No.	Locus	Context	Dimensions (mm)	Description	Comments
3129	2013/M/99/I	1b	39/36/4	Levallois point	*Fig. 4.54*
3126	2013/L/23/Ia	2b	54/42/4	Denticulate tool on flake with multi-faced prepared butt	*Fig. 4.54*
3133	2013/M/30/Ib	2b	35/23/3	Denticulate tool on flake with facetted butt	*Fig. 4.54*
3143	2013/M/60/I	1b	42/35/5	Denticulate tool on flake with multi-faced prepared butt	*Fig. 4.54*

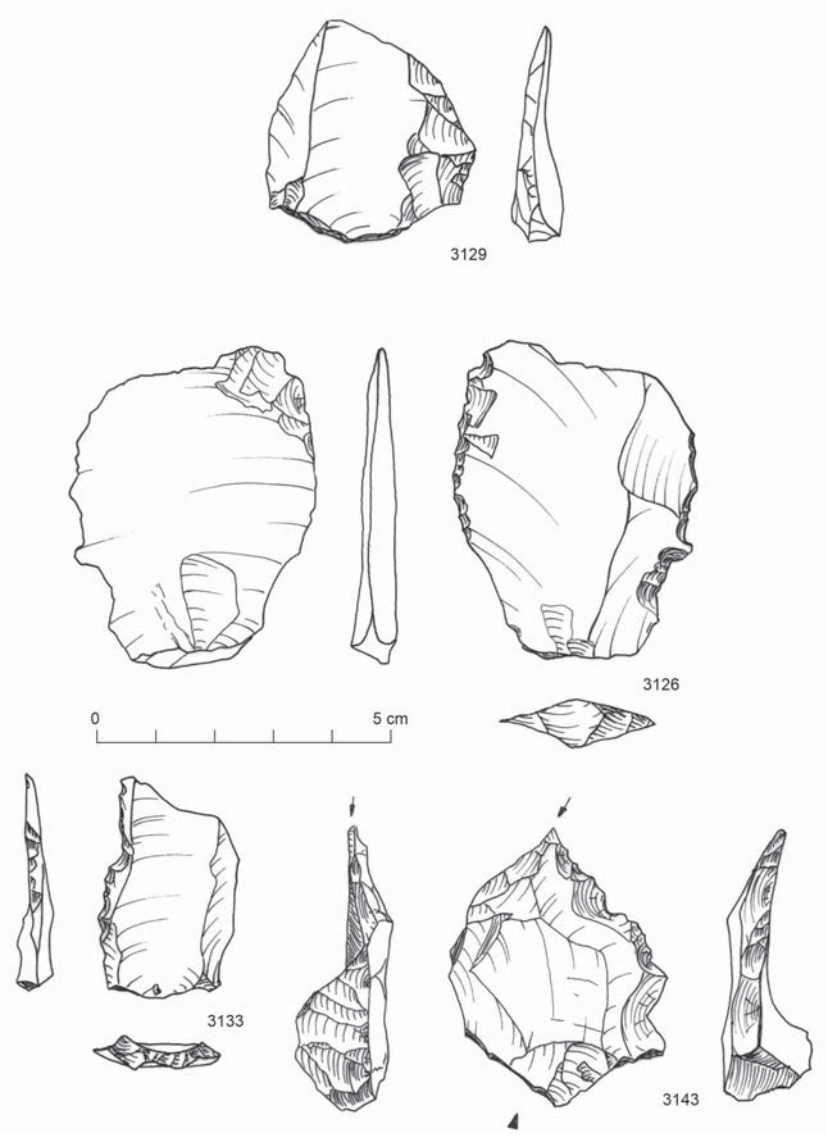

Fig. 4.54. Predetermined products from site AFD23 (sector S): Levallois point – 3129; denticulate tools made of flakes with multi-faced prepared butts – 3126, 3133, 3143

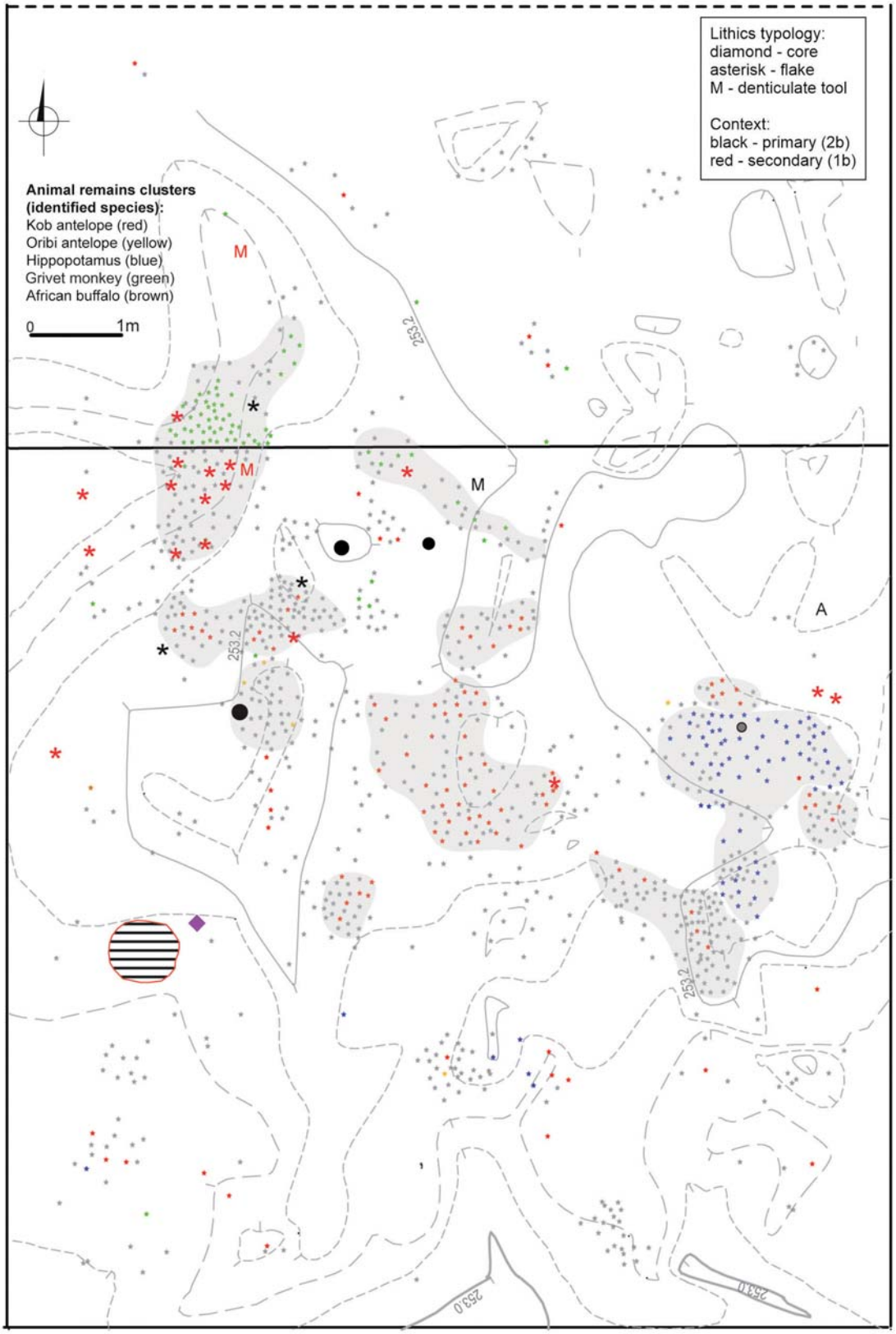

Fig. 4.55. Loci of selected artifacts from site AFD23 (sector S) coded with symbols, juxtaposed with concentrations of animal bone remains and location of cut features

4.1.4.4 Northeastern sector

The general technological structure of the collection of lithic artifacts from the northeastern sector of the site (examined in 2012 and 2013) is characterized by a predominance of flake products, as well as retouched Levallois forms, contrasted with a low presence of cores [*Table 4.15*].

CORES

Cores from this sector included residual and usually eroded forms. Only one (3854) was used for detaching a point during the final phase of reduction, while the remaining specimens reflect simple centripetal flaking surface treatment. Residual cores are slightly smaller than analogous forms from the southwestern zone, resembling more the small cores made from crude flakes [*Table 4.16*].

Cores were scattered throughout trench 2012/B, generally outside the zone of animal bone remains and clustering of postholes, around a small hearth [see below, *Fig. 4.59*].

A single microlithic core was also recorded. It was made of a fine-crystalline raw material (Egyptian flint), and originated most probably from the completely eroded Holocene contexts.

FLAKES

Non-retouched flakes, complete and fragments, representing different butt characteristics, dominate the collection. No elongated forms occurred [*Table 4.17*].

Natural/unprepared butts

Of the ten flakes with natural/unprepared butts two were made of quartz and the rest of chert. The length–width parameters (complete examples) are similar, oscillating around 3–4 cm. Although the length–width correlation of this class does not diverge from the pattern established for the southwestern sector, a significant incompleteness is observed [see *Table 4.17*; *Fig. 4.56*]. The share of the dorsal side covered with the natural nodule surfaces is the most varied in this case [*Table 4.18*]. The most common damage was to the edge and surface of these artifacts [*Table 4.19*].

Plain butt

The 10 flakes in this category were made of flint (two), quartz (one) and chert. They were smaller from the ones with a natural/unprepared butt, reaching dimensions of just 3 cm in length. The two complete examples of flint can be included in the micro-debitage category (less than 2 cm), which generally constituted a significant group in this zone. Although the length–width correltion of these flakes corresponds to the pattern established for the group from the southwestern zone, the absence of large artifacts is visible here [see *Table 4.17*; *Fig. 4.56*]. Some of the flakes bear traces of damage in the form of lateral breakage and the most commonly occurring damage to the edge and surface [see *Table 4.19*].

Edge and point butts

Four flakes from this category were made of chert, one of ferruginous sandstone. Complete examples constitute micro-debitage. In terms of the length–width correlation, these flakes did not diverge from the pattern established for the flakes from the southwestern zone [see *Table 4.17*;

Table 4.15. General morphological-technological structure of the collection from site AFD23 (sector NE)

Group	Type	Raw material			Total
		Chert	Flint, mudstone	Other	
Cores	Initial cores and tested nodules	–	–	–	–
	Cores for flakes/points	–	–	–	–
	Final cores	4	–	–	4
	Discoidal cores on flakes	–	–	–	–
	Uniplatform microlithic cores	–	1	–	1
Flakes and chips	Flakes with unprepared butt	8	–	2	10
	Flakes with plain/uniface butt	7	2	1	10
	Flakes with point & edge butts	3	–	1	4
	Flakes with multi-faced prepared butt	7	1	1	9
	Flake fragments	13	1	1	15
Chunks	Chunks	14	2	1	17
Predetermined products and formal tools	Levallois flakes	6	1	1	8
	Points	–	–	–	–
	Flakes/points with denticulate retouch	3	–	–	3

Table 4.16. Dimensions and loci of cores from site AFD23 (sector NE): 1) residual cores; 2) single-platform core

Inv. No.	Location	Context	Dimensions (mm)	Description	Reference
			1) Residual cores		
3847	2012/B/62/I	1c	45/(25)/20	Discoidal core, fragment, eroded	*Fig. 4:58*
3854	2012/B/54/I	1c	50/47/32	Final core for point	*Fig. 4:58*
3857	2012/B/61/I	1c	40/38/21	Discoidal core, fragment, eroded	
3876	2012/B/85/I	1c	42/31/13	Discoidal core, fragment, eroded	
			2) Single-platform core		
3897	2012/B/58/I	1c	28/31/21	Microlithic prismatic core, eroded	*Fig. 4:58*

Fig. 4.56]. Most of these artifacts were devoid of any natural nodule surface [see *Table 4.18*]. Almost all of them bore damage to the edge or surface, or were broken [see *Table 4.19*].

Multi-faced butt

Flakes with a multi-faced butt were represented by a few specimens from chert, as well as single examples from agate and petrified wood. The flakes were small, 2–3 cm in size, of which the largest was the one made of petrified wood. The length–width correlation demonstrates a very small number of divergences from the pattern for the southwestern group, being slightly smaller than the flakes from that group [see *Table 4.17*; *Fig. 4.56*]. Most of these artifacts presented no natural nodule surface [see *Table 4.18*]. Damage to the flakes of this category was common: most frequently to the edge and lateral breakage [see *Table 4.19*].

Table 4.17. Thickness-to-width (mm) correlation of flakes from primary and secondary contexts from site AFD23 (sectors NE and N). Width presented as a range and, in parentheses, as a median. Values presented against a benchmark from primary contexts in sector SW: higher values in green, lower values in red

Thickness	Unprepared butt		Plain/uniface butt		Point & edge butts		Multi-faced prepared butt	
	Sector		Sector		Sector		Sector	
	NE	N	NE	N	NE	N	NE	N
1	–	9	–	7–15 (9–10)	–	5–19 (9)	–	7–10
2	–	8–16	19–21	7–20 (11)	–	5–21 (12)	10	7–23 (11)
3	16–17	11–22 (17)	11	7–25 (12)	15	7–31 (14)	11-15	8–28 (13)
4	–	7–24 (15)	28	6–32 (16)	–	7–32 (13–14)	18	5–29 (16–17)
5	25	13–31 (24)	26	10–33 (16)	–	10–25 (16)	30	10–39 (17)
6	48	11–34 (25)	37	15–29 (22)	–	13–24 (21)	–	12–34 (20–21)
7	–	18–32 (32)	–	15–37 (21–22)	17	17–22	–	12–38 (25–26)
8	–	20–36	–	15–34 (21)	–	23–38 (27)	–	15–34 (24)
9	39	30–51	–	22–52 (27)	–	23–31	–	8–43 (30–38)
10	36	25	–	22–44 (24)	–	23–35	–	15–28 (25–26)
11	–	–	–	38	–	–	–	26
12	–	–	–	21–45 (34–41)	–	26–30	24	–
13	–	33–39	–	27–48 (37)	–	–	–	–
14	34	–	–	19	–	–	–	60
15	–	–	–	29–34	–	–	–	–
16	–	46	–	32	–	–	–	–
17	–	–	–	–	–	–	–	–
18	–	–	–	–	–	–	–	–
19	–	–	–	45	–	–	–	43–47
20	–	–	–	–	–	–	–	–
21	–	–	–	–	–	–	–	–
22	–	–	–	–	–	–	–	–

Table 4.18. Cortex frequency on flakes with different butts from site AFD23 (sector NE)

Share of cortex	Unprepared butt	Plain/unifacial butt	Point & edge butt	Multi-faced prepared butt	Facetted butt	Distal flake fragments
0%	50%	70%	75%	70%	100%	56.25%
10%	10%	–	25%	30%	–	6.25%
20%	10%	20%	–	–	–	6.25%
30%	–	–	–	–	–	–
40%	10%	–	–	–	–	–
50%	–	–	–	–	–	–
60%	–	–	–	–	–	12.50%
70%	–	–	–	–	–	–
80%	10%	–	–	–	–	–
90%	–	–	–	–	–	6.25%
100%	10%	10%	–	–	–	12.50%

Table 4.19. Damage to flakes from site AFD23 (sector NE)

Flake damage	Unprepared butt		Plain butt		Point butt		Prepared butt		Facetted butt		Unidentified butt
	∑	%	∑	%	∑	%	∑	%	∑	%	∑
Longitudinal breakage	1	10%	0	–	1	25%	1	11.1%	2	20%	1
Transverse breakage	2	20%	2	20%	1	25%	4	44.4%	5	50%	16
Overheating	1	10%	0	–	0	–	2	22.2%	1	10%	3
Eroded surfaces	3	30%	4	40%	3	75%	4	44.4%	5	50%	9

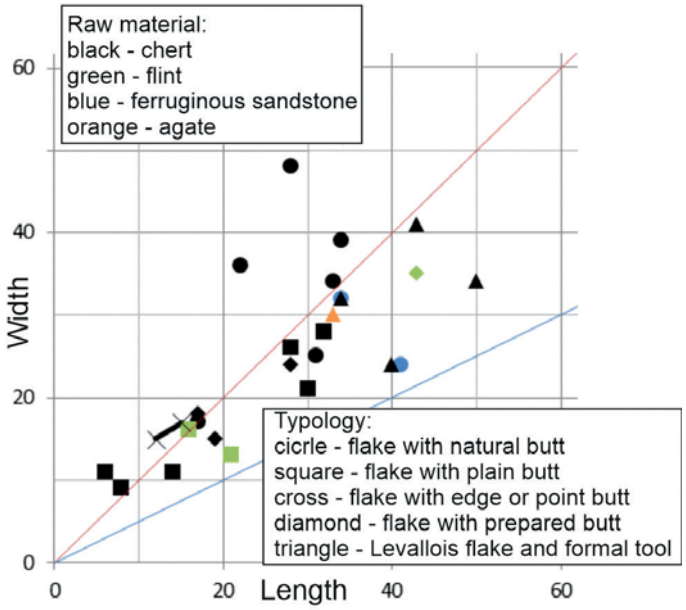

Fig. 4.56. Flakes and tools from site AFD23 (sector NE): length-to-width correlation (mm)

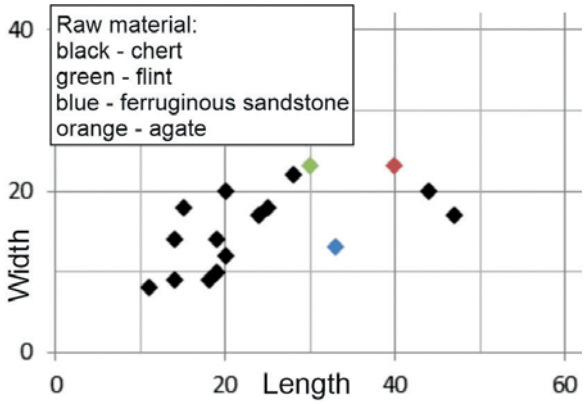

Fig. 4.57. Dimensions of chunks (two largest measurements) from site AFD23 (sector NE): length-to-width correlation (mm)

Distal fragments

Relatively large cortical pieces occurred in this group [see *Table 4.18*]. Eroded edges and surface was the most common form of damage [see *Table 4.19*].

Chunks

The 17 chunks from this sector were for the most part of chert, with single examples of quartz, flint and agate. They were small as a rule [*Fig. 4.57*], sometimes elongated, albeit irregular in form. Four of the chunks bore traces of overheating and up to seven displayed edge and surface damage.

Predetermined products and formal tools

The unretouched Levallois flakes and the other tool forms, made exclusively from Levallois flakes, from the northeastern sector displayed slightly elongated proportions and were approximately 4 cm in size [see *Fig. 4.56*]. Single Levallois flakes were made of agate and ferruginous sandstone, the rest of chert. Only one distal fragment of a Levallois flake (a plunged example bearing a fragment of the opposite platform) from the northeastern sector showed any original nodule surface on the negative/dorsal side, while the complete specimens had absolutely none [see *Table 4.18*]. Most of them also bore traces of erosion of the original surface, the most numerous being damage to the edge (half of the assemblages) and lateral breakage [see *Table 4.19*].

Most of the predetermined products, as well as flakes and even small core forms [*Fig. 4.58*], were found around a small hearth, as well as around a cluster of Kob antelope bones and single posthole remains located slightly more to the south [*Fig. 4.59*]. Although the remaining lithic artifacts from this sector were scattered around the eastern section of trench 2012/B, it is significant that there is a complete lack of such pieces in the zone with the largest concentration of bone remains, which accompanied the remnants of light wooden structures, interpreted most probably as installations for drying meat.

Table 4.20. Predetermined forms from site AFD23 (sector NE)

Inv. No.	Locus	Dimensions (mm)	Description/raw material	Reference
3839	2012/B/I	50/34/10	Plunging Levallois flake	*Fig. 4.58*
3846	2012/B/73/I	(41)/(32)/11	Levallois flake, fragment/overheated	*Fig. 4.58*
3849	2012/B/62/I	(33)/40/7	Plunging Levallois flake, distal fragment/agate	*Fig. 4.58*
3853	2012/B/52/I	(35)/(23)/5	Levallois flake, fragment	*Fig. 4.58*
3873	2012/B/10/I	40/24/5	Denticulate tool on Levallois flake	*Fig. 4.58*
3882	2012/B/30/I	(28)/17/5	Levallois flake, fragment/eroded faces and edges	
3885	2012/B/91/I	(28)/31/3	Levallois flake, fragment/eroded edges	*Fig. 4.58*
3899	2012/B/58/I	43/41/8	Scraper on Levallois flake	*Fig. 4.58*
3907	2012/B/90/I	(18)/16/6	Tool (stem?) on Levallois flake, fragment/eroded faces and edges	*Fig. 4.58*
3916	2012/B/48/I	33/30/9	Levallois flake/ferruginous sandstone, eroded faces and edges	
3917	2012/B/59/I	34/32/4	Levallois flake/eroded edges	*Fig. 4.58*

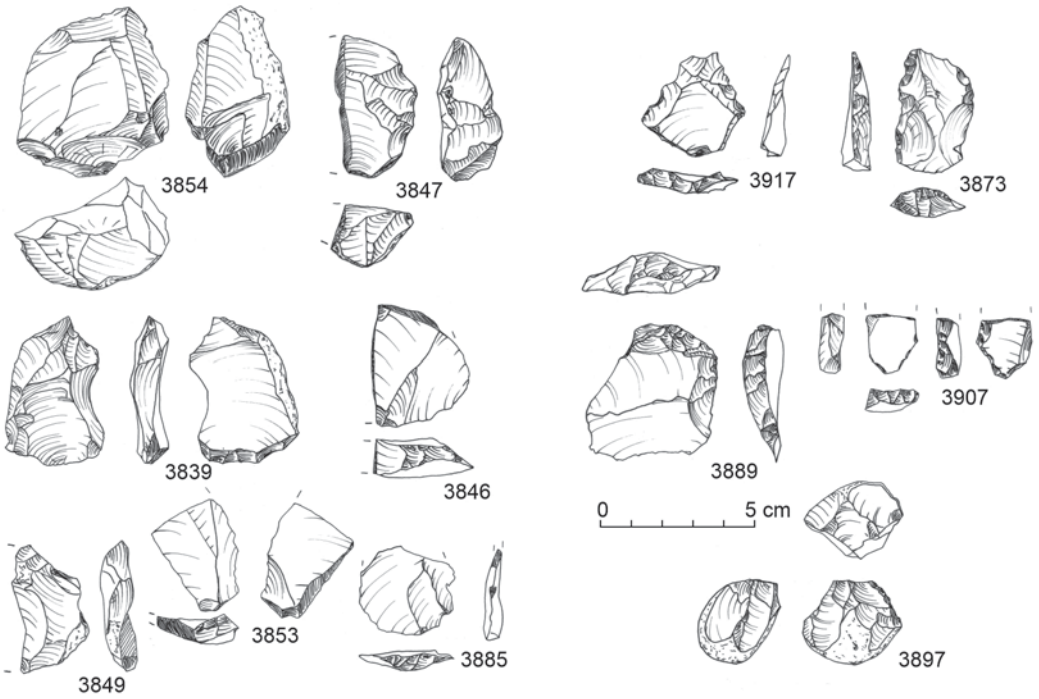

Fig. 4.58. Formal tools from site AFD23 (sector NE): final cores – 3847, 3854; Levallois predetermined products – 3839, 3848, 3849, 3853, 3885; retouched tools – 3817, 3873, 3889, 3907; final microlithic core – 3897

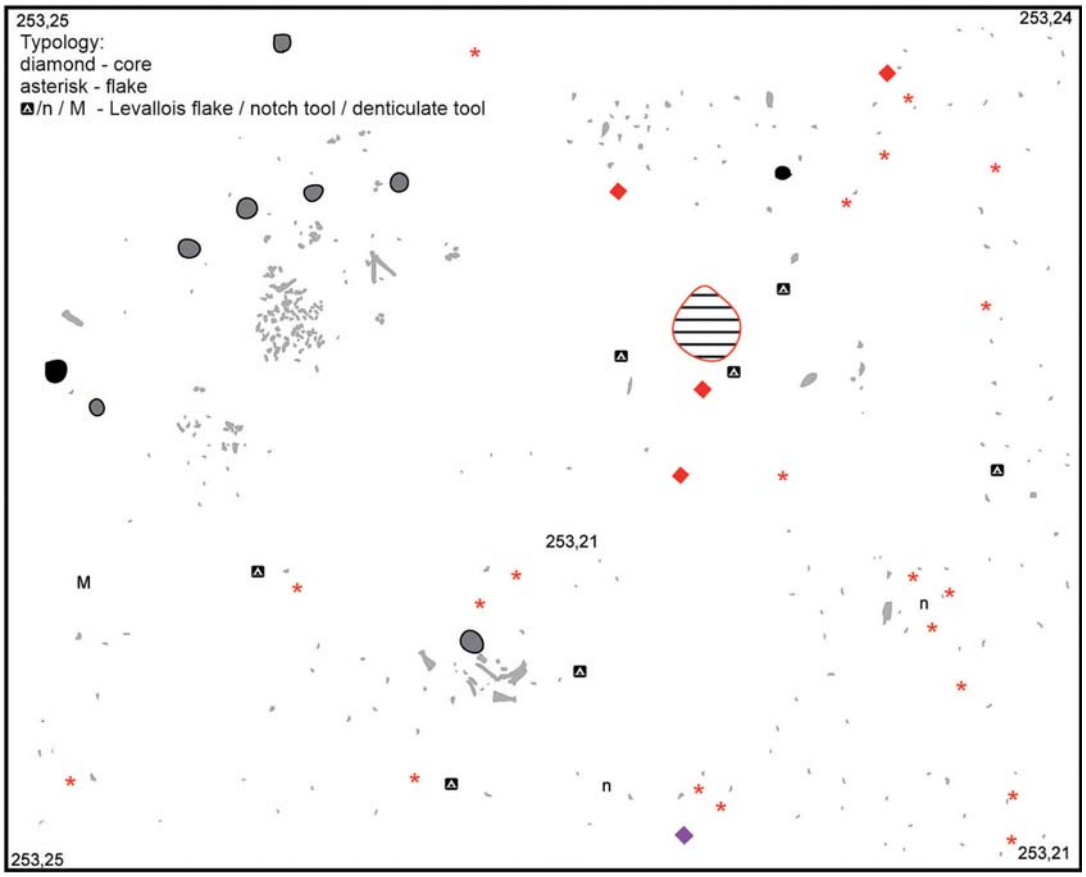

Fig. 4.59. Loci of selected artifacts from site AFD23 (sector NE), coded with symbols, juxtaposed with concentrations of animal bone remains and location of cut features

4.1.4.5 Northern sector

Dominating the technological structure of the collection of lithic artifacts from the northern sector, examined in 2012 and 2013, were flake products, supplemented with a small number of retouched Levallois forms and residual cores [*Table 4.21*].

CORES

Residual and usually eroded forms of cores are represented in the collection from the northern sector. They come from discoidal processing. Only one (4952) bore traces of opposite-platform working of the flaking surface during the final phase of reduction. The rest represents centripetal processing [*Fig. 4.60*]. Residual cores correspond in size with analogous forms from the south-western zone, also with regard to the small cores produced from crude flakes [*Table 4.22*]. Core forms were scattered over the entire area of trench 2012/C [see below, *Fig. 4.66*].

One example of a single-platform microlithic core, most probably from eroded Holocene contexts, was also recorded.

FLAKES

Fragmentary unretouched flakes dominated the collection from the northern sector. These were mostly small forms, representing all six categories of flakes distinguished based on the form of the butt.

Table 4.21. General morphological-technological structure of the collection from site AFD23 (sector N)

Group	Type	Raw material			Total
		Chert	Flint, mudstone	Other	
Cores	Initial cores and tested nodules	–	–	–	–
	Cores for flakes/points	–	–	–	–
	Final cores	4	–	–	4
	Discoidal cores on flakes	–	–	–	–
	Uniplatform microlithic cores	1	–	–	1
Flakes and chips	Flakes with unprepared butt	89	3	17	109
	Flakes with plain/uniface butt	245	3	21	269
	Flakes with point & edge butts	200	1	22	223
	Flakes with multiface prepared butt	219	6	21	246
	Flake fragments	752	5	101	858
Chunks	Chunks	14	2	1	17
Predetermined products and formal tools	Burin spalls	2	–	–	2
	Levallois flakes	7	–	3	10
	Points	1	–	-	1
	Flakes/points with denticulate retouch	11	–	1	12
	Flakes with abrupt retouch	3	–	–	3
	Flakes with a burin blow	1	–	–	1
	Backed tool (Holocene)	1	–	–	1

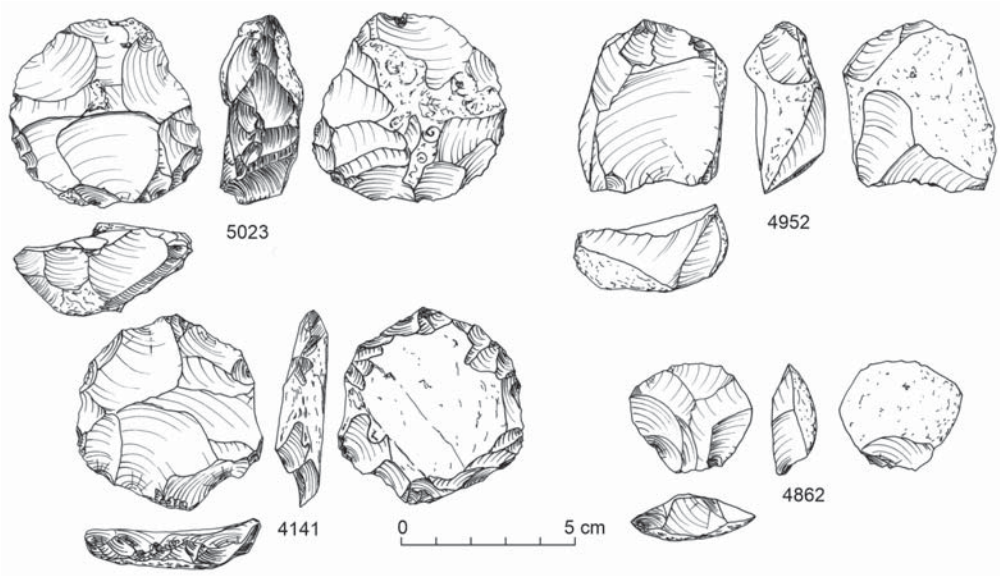

Fig. 4.60. Lithics from site AFD23 (sector N): final cores – 4141, 4862, 4952, 5023

Table 4.22. Dimensions and loci of cores from site AFD23 (sector N): 1) initial cores; 2) microlithic core

Inv. No.	Locus	Context	Dimensions (mm)	Description	Reference
1) Residual cores					
4141	2012/C/51/I	1d	53/56/11	Discoidal core	*Fig. 4.60*
4862	2012/C/36/I	1d	31/34/13	Discoidal core	*Fig. 4.60*
4952	2012/C/46/I	1d	48/42/21	Opposite-direction flaking	*Fig. 4.60*
5023	2012/C/10/I	1d	53/55/23	Discoidal core	*Fig. 4.60*
2) Microlithic core					
4579	2012/C/53/I	1d	30/34/24	Microlithic prismatic core, eroded	

Natural/unprepared butt

Of 109 flakes and proximal parts of flakes just three were made of a fine-crystalline raw material (flint, mudstone), 17 of a variety of quartz, and the rest of chert. The length–width dimensions (complete examples) are generally very similar, ranging 1–4 cm in size [*Fig. 4.61*]. The overall pattern resembles that from the southwestern sector, but in similarity to the northeastern sector there is a negligible number of artifacts thicker than 10 mm and a complete absence of artifacts thicker than 20 mm. The negative/dorsal surface of these flakes are covered by the natural nodule surface to varying degrees, although for the most part they are completely devoid of it (unlike the southwestern and southern sectors of the site) [*Table 4.23*]. Opening flakes clearly constituted a separate and even isolated group. The damage observed on these flakes was of all kinds, the most common being lateral breakage. There is also a very high percentage of burnt artifacts [*Table 4.24*].

Table 4.23. Cortex frequency on flakes with different butts from site AFD23 (sector N)

Share of cortex	Unprepared butt	Plain/unifacial butt	Point & edge butts	Multi-faced prepared butt	Facetted butt	Distal flake fragments
0%	61.47	47.59	52.92	66.67	100	56.65
10%	11.92	8.55	9.42	11.39	–	8.39
20%	5.50	6.69	6.73	5.70	–	5.71
30%	2.75	2.60	2.69	1.22	–	1.75
40%	–	3.35	1.35	3.25	–	1.16
50%	0.92	5.20	4.03	1.62	–	4.78
60%	0.92	3.35	1.79	2.44	–	1.86
70%	–	2.23	2.24	1.62	–	0.93
80%	3.67	2.97	1.34	1.62	–	0.81
90%	–	4.83	3.14	1.22	–	1.63
100%	12.85	12.64	14.35	3.25	–	16.33

Table 4.24. Damage to flakes from site AFD23 (sector N)

Flake damage	Unprepared butt		Plain butt		Point butt		Prepared butt		Facetted butt		Unidentified butt
	∑	%	∑	%	∑	%	∑	%	∑	%	∑
Longitudinal breakage	20	18.34	16	5.94	16	7.17	25	10.16	5	45.45	122
Transverse breakage	27	24.77	59	21.93	39	17.48	87	35.36	6	54.54	858
Overheating	20	18.34	48	17.84	40	17.93	56	22.76	1	9.09	205
Eroded surfaces	5	4.58	9	3.34	12	5.38	28	11.38	3	27.27	53

Plain butt

Three of the 269 flakes with plain butts were of flint, 21 of quartz and the rest of chert. In size, they were similar to flakes with a natural butt; however, a high number of artifacts are smaller than 2 cm [*Fig. 4.61* top]. While the overall length–width correlation of these flakes follows that established for the group from the southwestern sector, there is a noticeable absence of crude flakes, meaning those thicker than 20 mm. Moreover, the most numerous examples, in terms of thickness, up to 10 mm are narrower than an analogous assemblage from the southwestern sector. Almost half of these flakes revealed no natural nodule surface on their negative/dorsal surface, while opening flakes, once again constituting a clearly separate group, were second in terms of frequency [see *Table 4.23*]. Numerous flakes bore traces of damage in the form of (mostly lateral) breakage, or overheating (a form of damage more common in the northern sector) [see *Table 4.24*].

Edge and point butts

Flakes of this category (223 examples in total) were of chert, apart from one flake of flint and 22 of quartz. Most of the complete examples are less than 2 cm in size [*Fig. 4.61* center]. Once again, the general length–width dimensions follow the same pattern already established for the

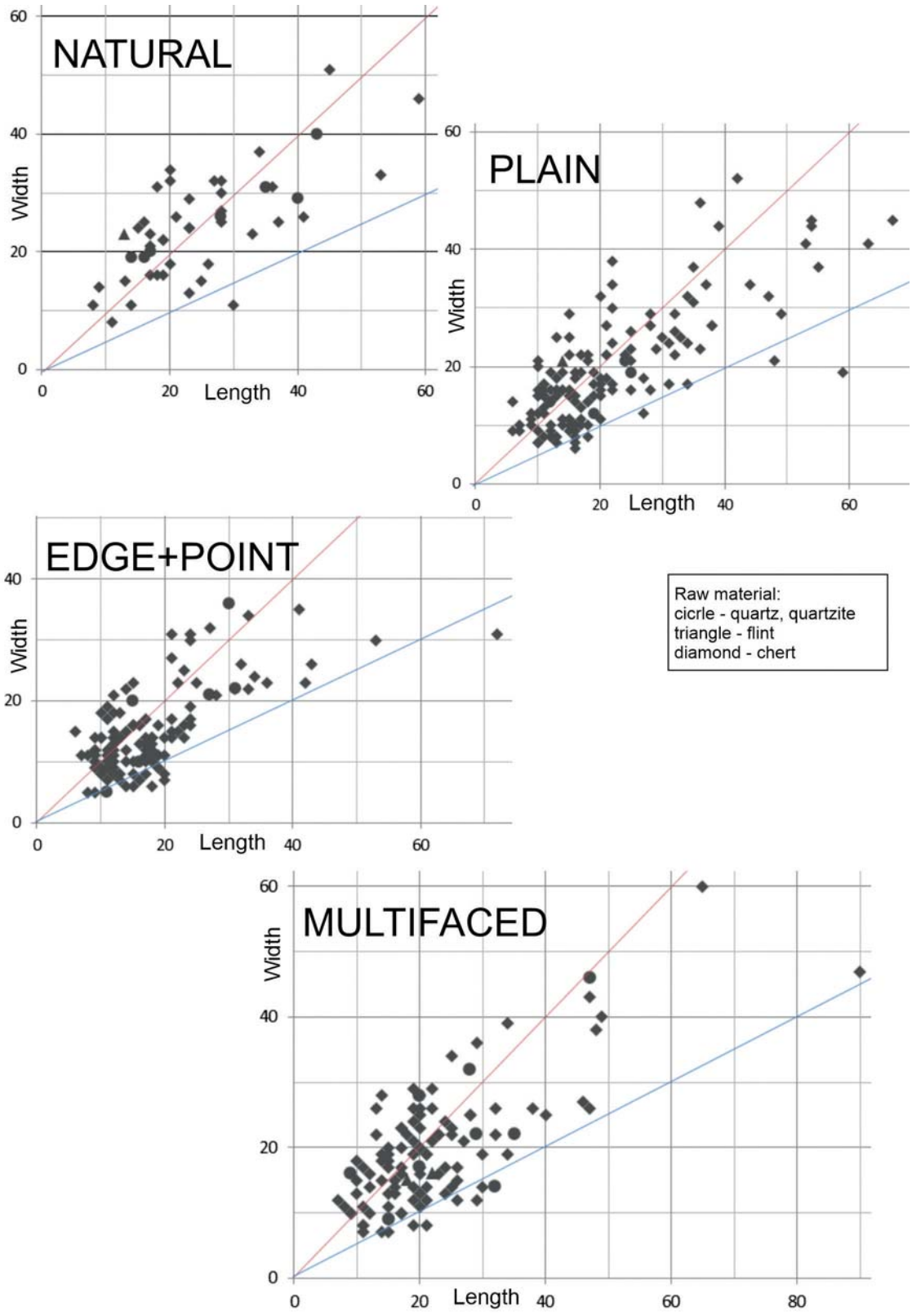

Fig. 4.61. Flakes from site AFD23 (sector N): length-to-width correlation (mm).
From top, with natural butts, with plain butt, with edge and point butts, with multi-faced butt

southwestern sector, with the difference that no specimens thicker than 12 mm occurred here; they were narrower from the most frequent artifacts of each class. More than half had no natural nodule surface to show, while opening flakes once again constituted a clearly separate group [see *Table 4.23*]. The most common form of damage to flakes with an edge butt was overheating and lateral breakage [see *Table 4.24*].

Multi-faced butt

Flakes with a multi-faced butt were represented by 246 examples, of which only six were of flint/agate and 21 of quartz. Once again these were small artifacts, 1–3 cm in size [*Fig. 4.61* bottom]. The length–width correlation shows a slightly lesser width than in the case of the flakes of this category from the southwestern sector. Most specimens had no natural nodule surface on the negative/dorsal side, and opening flakes here formed a definitely smaller group [see *Table 4.23*]. The flakes of this group revealed all kinds of damage, the most common being, once again, overheating and lateral breakage [see *Table 4.24*].

Distal fragments

Most of the distal flake fragments had no original nodule surface on the dorsal side, despite a relatively large presence of cortical pieces [see *Table 4.23*]. Once again, overheating turned out to be a widespread form of damage [see *Table 4.24*].

CHUNKS

Of the 138 artifacts assigned to the chunks group, single specimens came from the processing of quartz, flint and agate. They were small as a rule [*Fig. 4.62*]. Almost half (47%) bore traces of overheating, while just 16% displayed edge and surface damage.

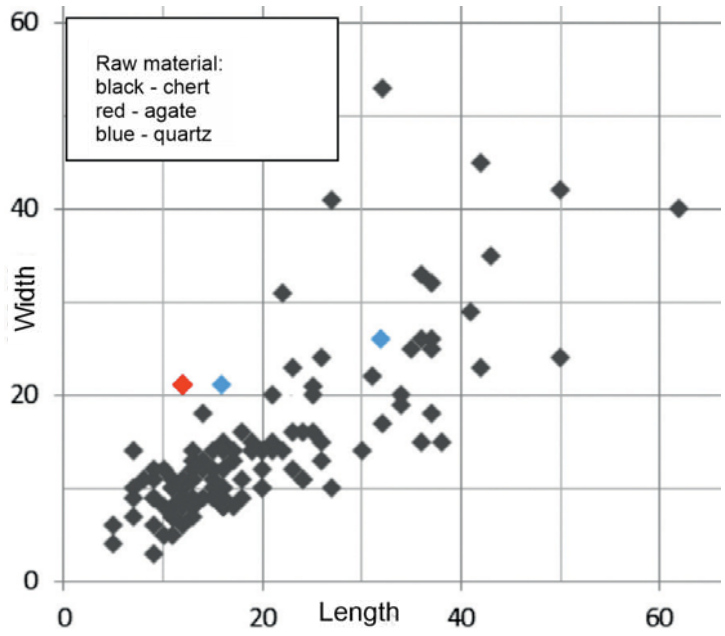

Fig. 4.62. Chunks (two largest measurements) from site AFD23 (sector N): length-to-width correlation (mm)

Debris from tool production/repair

Two burin spalls made of chert were recorded. One of them (5588) comes from the production of a burin on truncation, the other one was detached from an unworked blank [*Table 4.25*; *Fig. 4.64*]. The pieces of debris were found far apart, at the western edge of trench 2012/C.

Table 4.25. Burin spalls from site AFD23 (sector N): loci and dimensions

Inv. No.	Locus	Dimensions (mm)	Reference
5255	2012/C/9/I	12/3/2	*Fig. 4.64*
5588	2012/C/2/I	20/5/4	*Fig. 4.64*

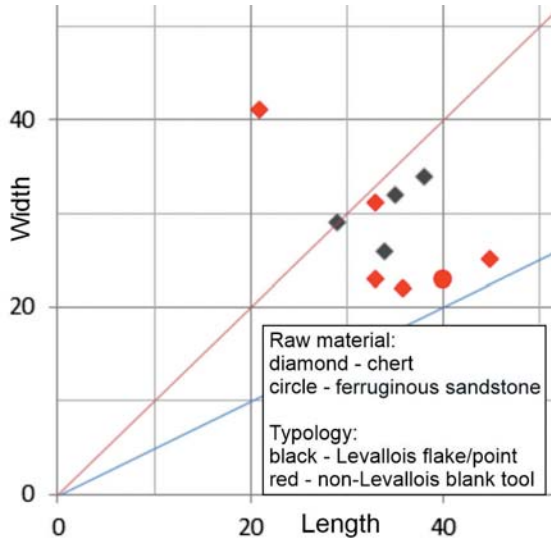

Fig. 4.63. Flakes and points with facetted butt, as well as retouched tools from a non-Levallois blank (marked in red) (only complete artifacts considered) from site AFD23 (sector N): length-to-width correlation (mm)

Predetermined products and formal tools

The unretouched Levallois flakes and other tool forms (some also made from Levallois flakes) from the northern sector displayed slightly elongated proportions and were approximately 3–4 cm in size [*Table. 4.26*; *Fig. 4.63*]. Chert was the major raw material in this group with single Levallois flakes being of quartz and ferruginous sandstone. None of the predetermined Levallois forms displayed any original nodule surface [*Fig. 4.65*; *Table 4.23*]. Most artifacts bore traces of erosion, the most numerous examples of which comprised damage to the edge (half of the assemblage) and lateral breakage. A relatively small percentage was overheated [see *Table 4.24*].

A fragmentary Levallois point (4763). which preserved clear evidence of erosion of the negative/dorsal face, was detached from the core with a convergent uni-directional treatment of the flaking surface [*Fig. 4.65*]. The non-Levallois blank of other retouched forms obviously did not find preference with knappers, even though it met the size requirements [see *Fig. 4.63*]. Opening flakes were retouched just like flakes with multi-faced butt devoid of the original nodule surface. Both ferruginous sandstone (heavily eroded) and quartz were among the raw materials used for tools.

Table 4.26. Predetermined forms from site AFD23 (sector N)

Inv. No.	Locus	Context	Description/raw material	Reference
4003	2012/C/93/I	38/34/9	Levallois flake	
4244	2012/C/54/I	49/(19)/5	Levallois flake, fragment/quartz, broken along technological axis	*Fig. 4.65*
4371	2012/C/63/I	50/(26)/12	Levallois flake, fragment, broken along technological axis	*Fig. 4.65*
4383	2012/C/64/I	(22)/(19)/6	Levallois flake, fragment	*Fig. 4.65*
4409	2012/C/52/I	(30)/32/7	Levallois flake, proximal fragment/quartz, eroded faces and edge	
4471	2012/C/67/I	33/31/12	Sidescraper on flake with unprepared butt, partly cortical (20%)	*Fig. 4.64*
4484	2012/C/27/I	35/32/18	Chunk with retouched notch	
4534	2012/C/18/I	(16)/26/4	Flake, distal fragment with retouched notch	
4652	2012/C/84/I	45/25/8	Flake with multi-faced prepared butt, retouched notch, partly cortical (30%); eroded faces and edges	*Fig. 4.64*
4658	2012/C/84/I	(14)/11/3	Flake, distal fragment with retouched notch, partly cortical (50%)	
4668	2012/C/80/I	21/41/9	Flake with unprepared butt, denticulate retouch, fully cortical	*Fig. 4.64*
4679	2012/C/76/I	(28)/16/4	Flake with denticulate retouch, distal fragment; eroded faces and edges	
4734	2012/C/78/I	(10)/15/3	Flake with denticulate retouch, distal fragment	
4744	2012/C/88/I	39/(36)/9	Levallois flake, fragment, broken along technological axis	*Fig. 4.65*
4763	2012/C/83/I	(29)/29/5	Levallois point, fragment; eroded faces and edges	*Fig. 4.65*
4783	2012/C/20/I	(52)/48/7	Levallois flake, proximal fragment	*Fig. 4.65*
4953	2012/C/46/I	(44)/38/7	Levallois flake, proximal fragment/quartzitic sandstone	*Fig. 4.65*
4954	2012/C/46/I	34/26/11	Flake with denticulate and abrupt retouch	*Fig. 4.64*
5010	2012/C/40/I	40/23/6	Flake with edge butt, denticulate retouch, partly cortical (80%)/ferruginous sandstone, eroded faces and edges	*Fig. 4.64*
5035	2012/C/15/I	(23)/(26)/11	Levallois flake or point, proximal fragment; eroded edges (use-wear?)	*Fig. 4.64*
5240	2012/C/9/I	(27)/27/4	Levallois flake, proximal fragment; overheated	*Fig. 4.65*
5260	2012/C/45/I	36/22/10	Cortical flake with plain butt, semi-abrupt retouch of distal edge; endscraper	*Fig. 4.64*
5261	2012/C/45/I	21/(24)/4	Cortical flake with plain butt, denticulate retouch, proximal frament	*Fig. 4.64*
5392	2012/C/41/I	(25)/18/9	Flake with retouched notch, partly cortical (40%), distal fragment	*Fig. 4.64*
5416	2012/C/8/I	35/(19)/9	Flake with multi-faced butt, burin scar, partly cortical (30%), fragment; overheated	*Fig. 4.64*
5437	2012/C/43/I	33/23/8	Flake with unprepared butt, retouched notch, partly cortical (30%)	*Fig. 4.64*
5470	2012/C/43/I	(17)/(11)/5	Flake with unprepared butt, retouched side, fragment/ quartz; use-wear(?)	
5504	2012/C/6/I	(22)/23/6	Flake with multi-faced butt, retouched notch, fragment; overheated	*Fig. 4.64*
5570	2012/C/16/I	(10)/(6)/2	Microlithic backed tool, fragment; overheated	*Fig. 4.64*
5709	2012/C/23/I	(31)/25/8	Flake with multi-faced butt, retouched side, partly cortical (90%); use-wear(?)	

Fig. 4.64. Retouched tools: notches – 4652, 5392, 5437, 5504; denticulate tools – 4668, 5010, 5261; semi-abrupt retouch – 4471, 4954, 5260; burin – 5416; burin spalls – 5255, 5588; flake with edge impacts (pseudo-burin negatives) – 5035; arch-backed fragment – 5570

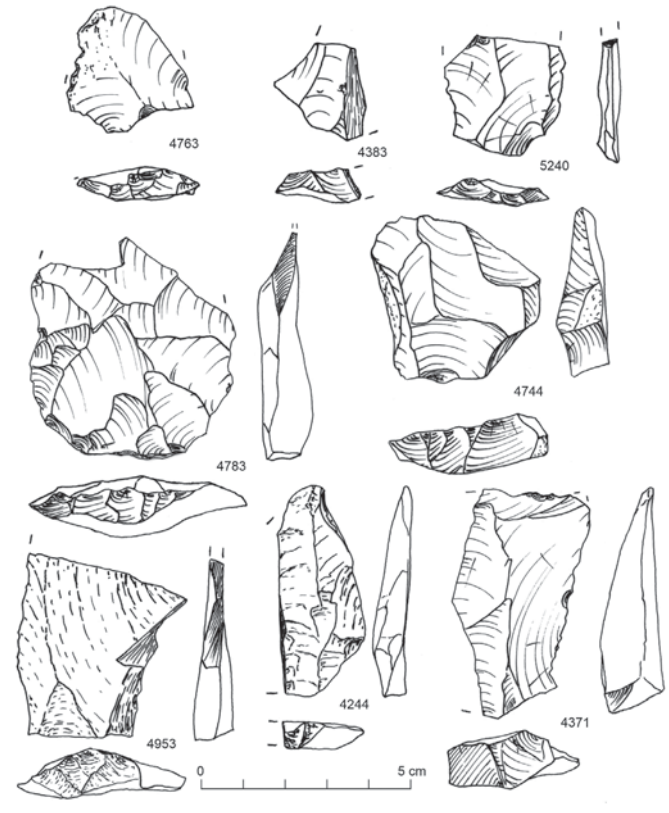

Fig. 4.65. Selected lithic artifacts from site AFD23 (sector N): Levallois predetermined products: point – 4763; flakes – 4953, 4244, 4371, 4383, 4744, 4783, 5240

Notches both on non-Levallois flakes and chunks were the most numerous tool category (seven examples) [*Fig. 4.64:5504, 5437, 5392,* and *4652*]. The flakes were all thick, but none preserved the natural nodule surface in its entirety. One of them bore traces of surface and edge erosion, one was also burnt.

The six denticulate tools, complete or fragmentary, did not exceed 4 cm, like all the other tools of this kind from the site [*Fig. 4.64:5261, 5010, 4668*]. Two were formed from opening flakes.

The edges of just three flakes were covered in quite abrupt retouching [*Fig. 4.64:5260, 4954, 4471*], indicating the probable function of these temporary forms as racloirs, endscrapers and scrapers (the last of these was a tool combined with a denticulate edge).

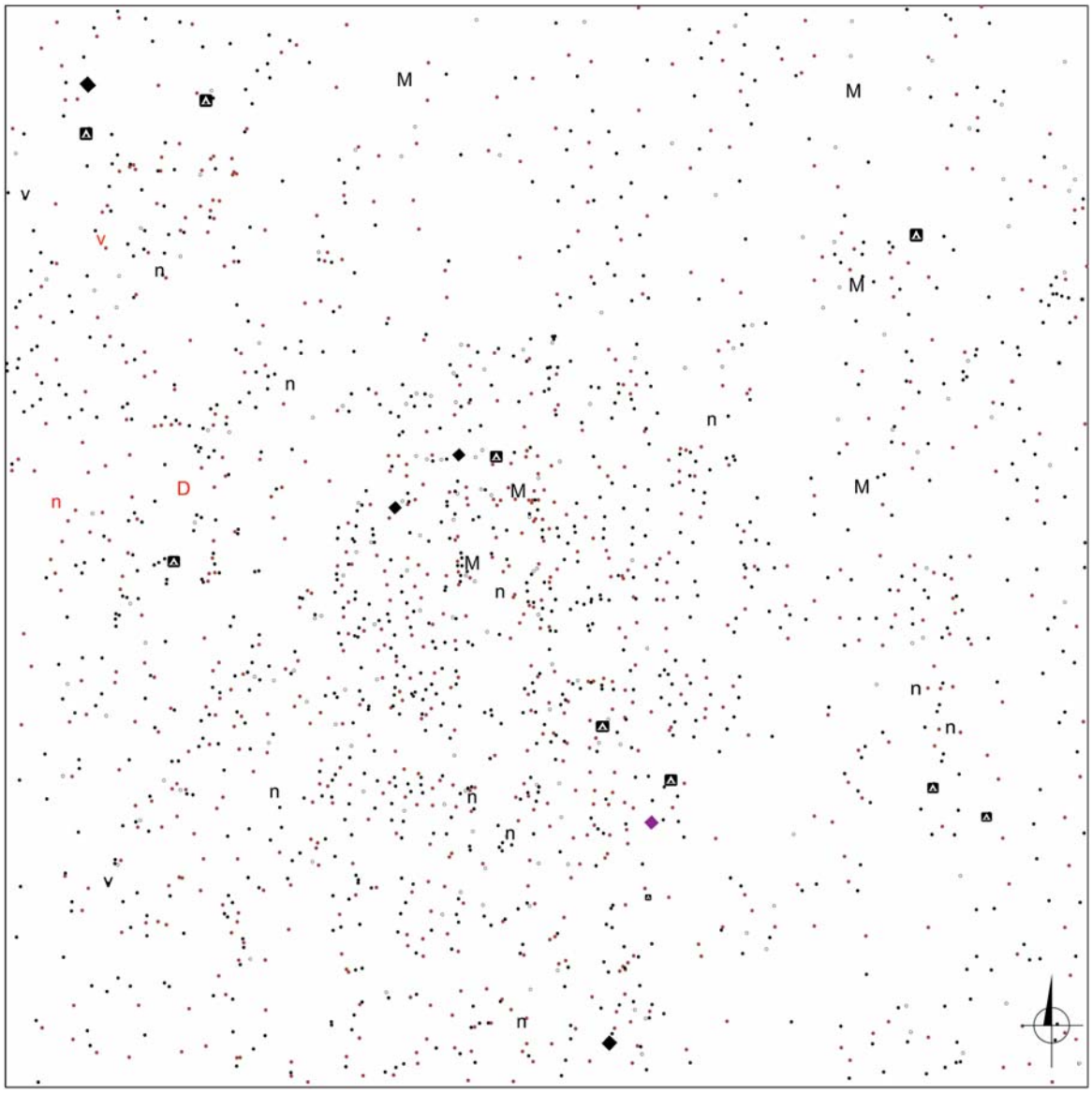

Fig. 4.66. Mapping of selected lithic artifacts from site AFD23 (sector N), coded with symbols: points – debitage, diamonds – cores, black rectangles with white element – Levallois flakes/points, M – denticulated tool, n – notched tools, D – burin, v – abrupt retouched flakes. Overheated artifacts marked in red

Only one flake fragment broken along the axis of percussion bore a burin negative scar [*Fig. 4.64:5416*]. This corresponds to an analogous tool from the southwestern sector of the site, as well as the two burin spalls described above, which were found in the immediate vicinity.

A single fragment of a backed tool was also found in the area of trench 2012/c [*Fig. 4.64:5570*], thus confirming the presence of an Early Holocene settlement, despite the sediments/strata from this period having undergone complete degradation.

Two flakes have on their edges irregular retouching negatives of a seemingly incidental nature.

Tool forms were scattered all over the investigated area, revealing no spatial relationships that could have functional overtones [*Fig. 4.66*].

4.1.4.6 Northwestern sector

The collection of lithic artifacts from the northwestern sector of the site consists of the assemblage from sector O (examined in 2014) and sectors S,T,U,W (examined in 2016). The general technological structure is again characterized by a predominance of flake products, as well as cores from different processing stages, contrasted with a fairly small proportion of final forms [*Table 4.27*]. The percentage of tools is notably lower, and evident forms of denticulate/notched tools are clearly missing from this sector.

Table 4.27. General morphological-technological structure of the collection from site AFD23 (sector NW) (number after the backslash refers to artifacts recorded from secondary contexts)

Group	Description/Type	Raw material			Total
		Chert	Flint, mudstone	Other	
Cores	Initial cores and tested nodules	5/0	–	–	5
	Cores for flakes/points	0/7	–	–	7
	Final cores	–	–	–	–
	Discoidal cores on flakes	1/0	–	–	1
Flakes and chips	Flakes with unprepared butt	54/29	–	1/0	84
	Flakes with plain/uniface butt	31/14	1/3	–	49
	Flakes with point & edge butts	27/7	–	–	34
	Flakes with multiface prepared butt	27/10	0/1	1/0	39
	Flake fragments	21/13	–	2/1	37
Chunks	Chunks	17/26	–	0/1	44
Predetermined products and formal tools	Levallois flakes	0/4	–	–	4
	Points	1/0	–	–	1
	Flakes/points with denticulate retouch	–	–	–	–

Cores

Initial or tested nodules form a group for which the method of further reduction cannot be established. Added to this group is a pseudo-prismatic core (6035) and an after-core (754) suggesting the conscious or incidental application of a schema other than the Levallois method. Another large nodule presented just one flake negative, made no doubt to test the quality of the raw material. Nodule 5822 is the largest piece of its kind discovered to date at AFD23.

Table 4.28. Dimensions and loci of cores from site AFD23 (sector NW): 1) initial cores; 2) Levallois cores; 3) discoidal core

Inv. No.	Locus	Context	Dimensions (mm)	Description	Reference
			1) Initial cores		
3196	2014/O/60/III	2 e	97/87/41		
5822	2016/S/50/IV	2 e	194/120/88	95% cortical	
6035	2016/U/W/III	2 e	63/65/52	Pseudo-single platform	*Fig. 4.67*
6036	2016/U/W/III	2 e	68/52/43		*Fig. 4.67*
6037	2016/U/W/III	2 e	87/67/34		
			2) Levallois cores		
5919	2016/U/78/I	1 e	56/57/21	Centripetal in last phase	
5938	2016/U/88/I	1 e	41/51/22	Centripetal in last phase, eroded	
5939	2016/U/88/I	1 e	54/44/22	Centripetal in last phase	
5953	2016/U/W/I	1 e	38/37/28	Opposite platform in last phase, eroded	
6064	2016/W/87/I	1 e	35/38/17	Opposite platform, final	
6078	2016/W/I	1 e	53/45/16	Nubian II(?)	*Fig. 4.67*
6079	2016/W/I	1 e	51/54/22	Final	
			3) Discoidal core		
3191	2014/O/30/IIa	2 e	37/38/12		

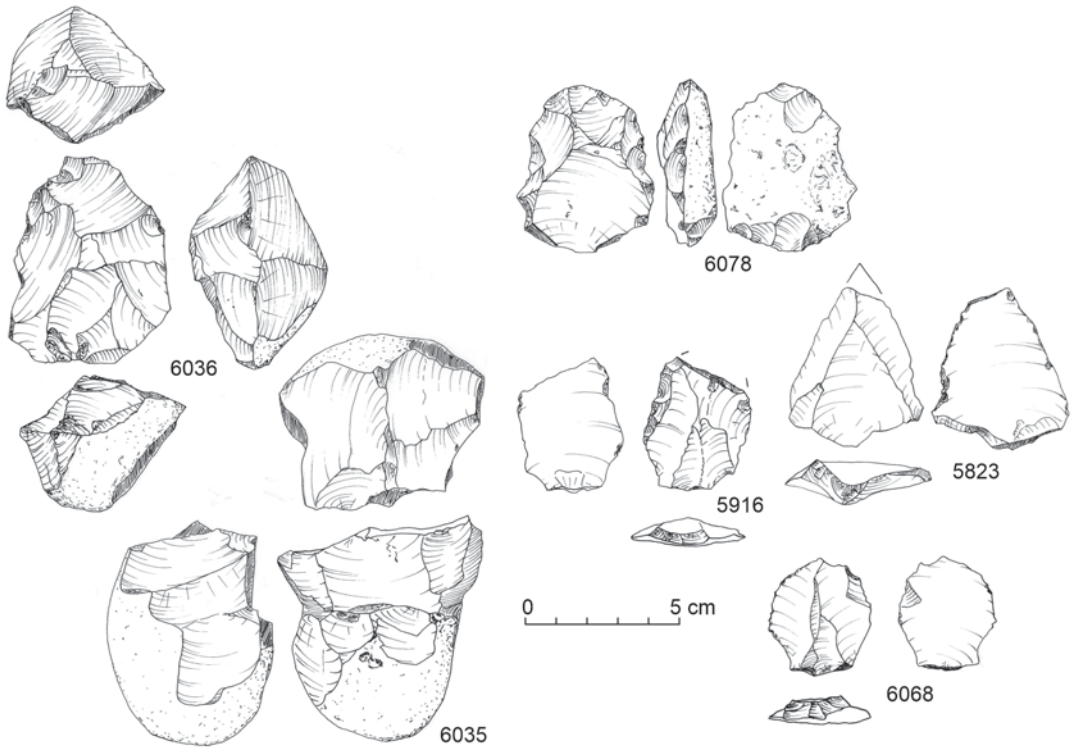

Fig. 4.67. Levallois core and tools from site AFD23 (sector NW): 5823, 5916, 6035, 6036, 6068, 6078

Among cores with established method of reduction, seven intensively exploited Levallois (flake) forms were noted. In one case (6078) premises exist—in the form of negatives forming the distal section of the flaking surface—to assign it to the Nubian II schema [*Table 4.28*; *Fig. 4.67*]. The flaking surfaces of the remaining cores were, during the final phase of reduction, formed in line with the centripetal or opposite-platform schema. All of these cores were recorded on the surface.

A small discoidal core made from a crude flake (3191) came from a subsurface layer.

Flakes

Flakes from the northeastern sector represented all six categories distinguished in this study.

Natural/unprepared butt

Of 84 flakes with natural/unprepared butts only one was made of petrified wood; the rest were of chert. This group displayed generally similar length–width parameters, rarely taking on elongated forms. Flakes less than 2 cm in size did not occur here [*Fig. 4.68*]. Examples slightly larger than those found in the southwestern sector (area of the encampment) were also noted. The dorsal/negative sides of these flakes were covered with the natural nodule surfaces in the largest percentage [*Table 4.29*]. Several artifacts bore traces of damage in the form of lateral (the most common) and longitudinal breakage; two were burnt and one, heavily patinated on the surface, probably came from outside the site [*Table 4.30*].

Plain butt

Four of the 49 flakes with plain butts were of very fine-grained flint, the rest of common chert. In terms of size, their length–width correlation ranged between being equal to being twice as long (these are parameters of a formal blade). Flakes are slightly larger compared to the group from the southwestern sector [*Table 4.31*, values marked in green]. The negative/dorsal side displayed varying degrees of natural nodule surfaces [see *Table 4.29*]. Lateral breakage was the predominant form of damage [see *Table 4.30*], while almost 10% were burnt.

Table 4.29. Cortex frequency on flakes with different butts from site AFD23 (sector NW)

Share of cortex	Unprepared butt	Plain/unifacial butt	Point & edge butts	Multi-faced prepared butt	Facetted butt	Distal flake fragments
0%	13.25%	17.02%	8.82%	37.84%	100%	32.35%
10%	8.43%	8.51%	8.82%	18.92%	–	5.88%
20%	6.02%	10.64%	–	13.51%	–	2.94%
30%	3.61%	4.26%	8.82%	5.41%	–	–
40%	–	4.26%	–	–	–	–
50%	6.02%	10.64%	5.88%	2.70%	–	8.82%
60%	3.61%	8.51%	11.76%	8.11%	–	8.82%
70%	3.61%	6.38%	2.94%	–	–	8.82%
80%	6.02%	10.64%	8.82%	2.70%	–	–
90%	6.02%	4.26%	11.76%	–	–	–
100%	43.37%	14.89%	32.35%	10.81%	–	32.35%

Edge and point butts

The 34 artifacts from this category corresponded in size to flakes of this kind from the southwestern sector. The original nodule surface dominated on almost a third of the specimens [see *Table 4.29*]. The only damage noted is lateral and longitudinal breakage [see *Table 4.30*].

Table 4.30. Damage to flakes from site AFD23 (sector NW)

Flake damage	Unprepared butt		Plain butt		Point butt		Prepared butt		Facetted butt		Unidentified butt
	∑	%	∑	%	∑	%	∑	%	∑	%	∑
Longitudinal breakage	6	7.23	5	11.11	2	5.88	1	2.70	0	–	0
Transverse breakage	7	8.43	8	17.78	4	11.76	5	13.51	3	60.0	34
Overheating	2	2.41	4	8.89	0	–	3	8.11	0	–	5
Eroded surfaces	1	1.20	0	–	0	–	0	–	1	20.0	2

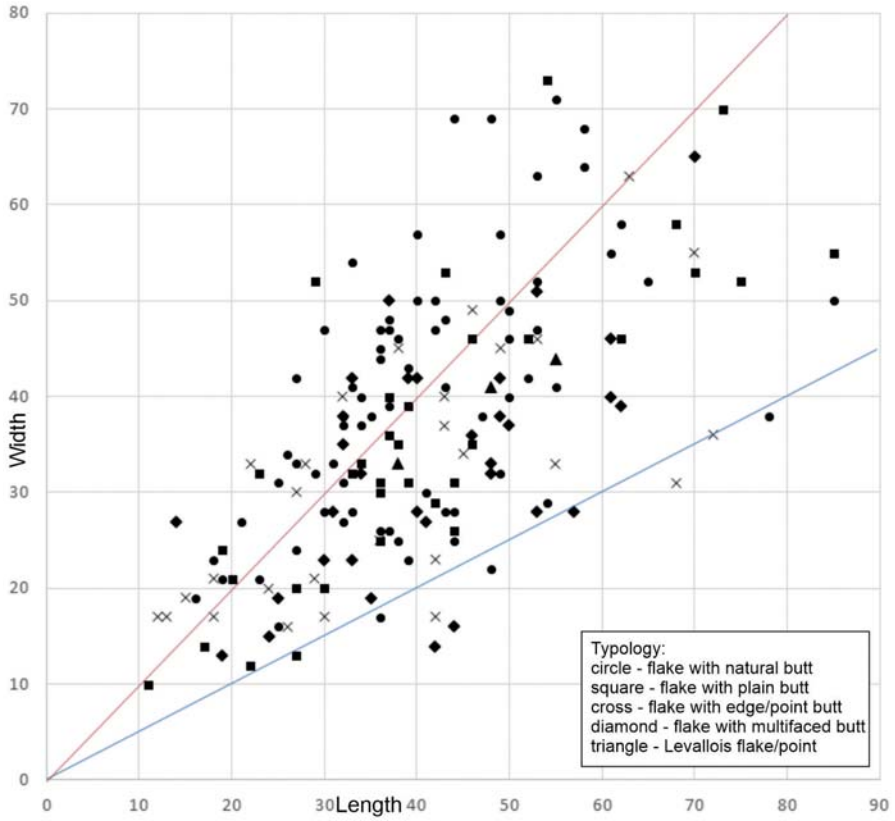

Fig. 4.68. Flakes and tools from site AFD23 (sector NW): length-to-width correlation (mm)

Multi-faced butts

Flakes with a butt formed from many negatives were represented by 37 specimens of chert, and one each of flint and of quartz. In terms of size, again they corresponded to analogous artifacts from the southwestern sector. Most of these flakes had little or no natural nodule surface left on the negative/dorsal side, but cases of opening products with a multi-faced butt were also recorded [see *Table 4.29*]. The most common form of damage was lateral breakage, but overheating is also worth noting [see *Table 4.30*].

Distal fragments

More than half of the distal fragments featured significant patches of the original nodule surface on the negative/dorsal side, indicating that they should be considered as supplementary for the initial treatment flakes [see *Table 4.29*]. Several of these fragments were burnt, while two heavily patinated specimens must have come from outside the workshop site [see *Table 4.30*].

Table 4.31. Thickness-to-width (mm) correlation of flakes from primary and secondary contexts from site AFD23 (sector NW). Width presented as a range and a median. Values presented against a benchmark from primary contexts in sector SW: higher values in green, lower values in red

Thickness	Unprepared butt		Plain/uniface butt		Point & edge butts		Multi-faced prepared butt	
	CONTEXT							
	Primary	Secondary	Primary	Secondary	Primary	Secondary	Primary	Secondary
1	–	–	10	–	–	–	–	13
2	–	–	–	24	17	–	–	–
3	–	–	12–20	–	17	16	16	–
4	19	–	13–33 (17)	–	17–33 (23)	–	19	–
5	–	–	32	–	19–21 (20)	–	–	27
6	16–34	21	–	–	17	–	14–39 (23)	15
7	23–44 (24)	17–27 (24)	–	57	–	–	19–42 (42)	–
8	25–42 (30)	28–47	20–32	–	30–45 (40)	–	32–38	–
9	32–33	40–41	29	39	33	–	27–51 (43)	–
10	22–57 (30)	26–47 (41)	30–40	–	–	34	37	35–38
11	21–47 (40)	–	25	35	40	–	33–50	–
12	28–50 (42)	41–50	26–53	31	37–45	–	28–42 (32)	–
13	28–42 (31)	64	46	35–52	31–36	33	28–40	28–42
14	58–71 (69)	69	–	–	–	–	–	–
15	36–54	–	46	–	46	–	23–46	–
16	50	41–52 (47)	36–53	–	–	49–63	–	–
17	38–49 (48)	–	–	–	23	–	–	–
18	63	43	55	–	–	–	–	–
19	68	39	–	70	–	–	–	–
20	52–55	48	–	–	–	–	–	–
22	–	–	–	–	–	55	–	65
25	–	–	–	73	–	–	–	–
32	–	–	52	46	–	–	–	–

Chunks

Chunks from the northwestern sector, 43 artifacts in all, were of chert. They were small as a rule, but specimens of quite significant dimensions also occurred [*Fig. 4.69*]. Of these, 12 displayed traces of overheating and seven edge and surface damage (whereby eight were refitted as one larger cracked nodule).

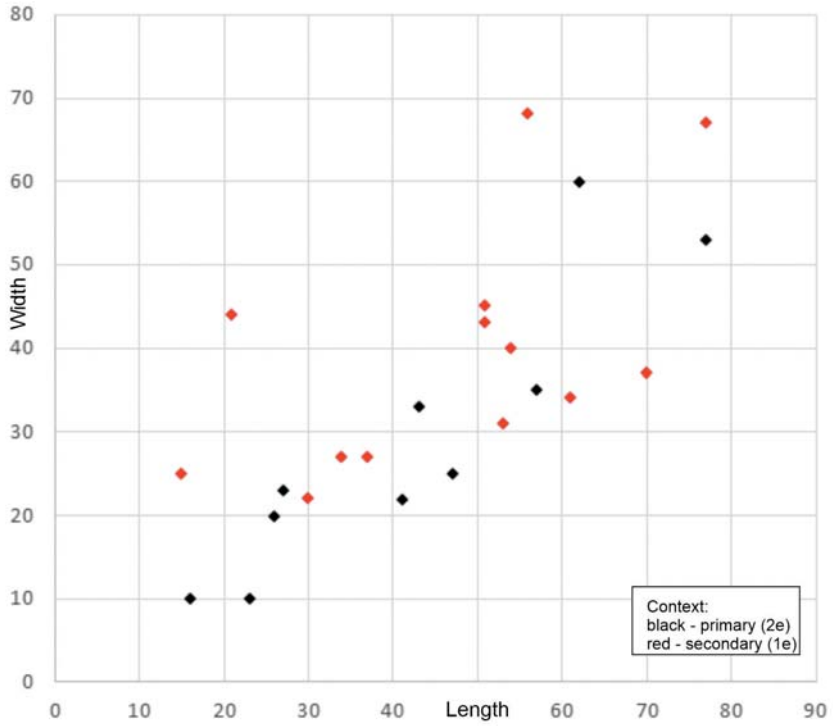

Fig. 4.69. Chunks (two largest measurements) from site AFD23 (sector NW): length-to-width correlation (mm)

Predetermined products and formal tools

Tool forms from the northwestern zone included a single damaged Levallois point (5823), as well as four flakes with facetted butt, all made of chert, with one bearing traces of significantly more intense patination, hence undoubtedly from outside the local workshop [*Table 4.32*]. The Levallois point demonstrated balanced proportions and was in line with corresponding flakes from other areas of the site [*Fig. 4.68*, triangle]. None of the predetermined Levallois products from this sector had any original nodule surface showing on the negative/dorsal side. No damage could be observed apart from surface erosion (patina) and broken tips.

Facetted-butt flakes in the northwestern sector of the site, like a large number of flakes without macroscopic traces of tool use, demonstrate a slight concurrence with antelope bone remains [*Fig. 4.70*]. A cluster of chert pieces showing testing and initial working was noted in trench U [*Fig. 4.70*, cluster marked in grey].

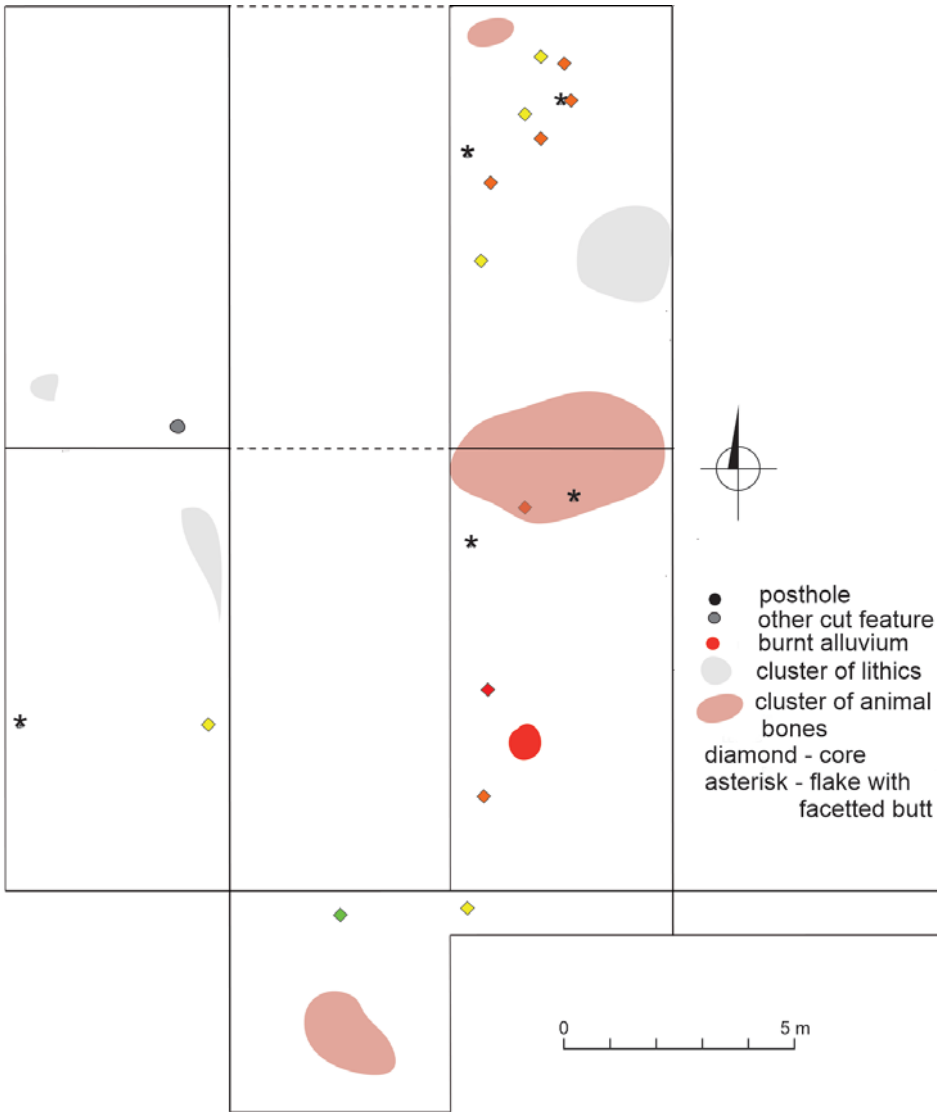

Fig. 4.70. Loci of selected artifacts from site AFD23 (sector NW), coded with symbols, juxtaposed with clusters of antelope bone remains and overheated alluvium. Core types coded in color: Levallois cores – red; initial cores – yellow; discoidal core on flake – green

Table 4.32. Predetermined forms from site AFD23 (sector NW)

Inv. No.	Locus	Context	Dimensions (mm)	Description	Reference
5920	2016/U/78/I	1 e	48/41/5	Levallois flake	
5916	2016/U/66/I	1 e	(44)/33/7	Levallois flake with retouch	*Fig. 4.67*
6068	2016/W/88/I	1 e	38/33/8	Levallois flake with use-retouch	*Fig. 4.67*
5823	2016/S/36/IV	2 e	(53)/44/9	Levallois point with broken tip	*Fig. 4.67*
6080	2016/W/W/I	1 e	(38)/40/9	Levallois flake, fragment (proximal)	

4.2 CHARACTERIZING THE LITHIC PRODUCTION AT SITE AFD 23

The stone-processing tradition at the Affad 23 site is described largely based on observations resulting from the refitting of blocks from the southwestern sector of the site, supplemented with morphometric data on artifacts coming from this sector and other sectors of the site. The schema of processing revealed by the refitted blocks led to a reconstruction of characteristic features of this production. The four concentrations of finds recorded forming the southwestern sector—western, southwestern, eastern and southeastern—are discussed separately, leading up to an overall summary of findings for this part of the site. A discussion of the other sectors (northern, northeastern, southern and southwestern) follows, filling out the picture of the lithic production at the site.

4.2.1 Lithic production in the southwestern sector

Observation of the landscape and contextual evidence from the southwestern sector of the site favors the assumption that we are dealing with a site, an encampment, with clearly defined zones for different stages of the lithic production process, from the testing of nodule quality, through preliminary formation and advanced processing (production of tools). An analysis of refittings revealed that at least some of them, especially Blocks 7, 8, 32, 37, 42, 43 and 44 from the western cluster, which gave an almost complete record of processing (including a residual core), were concentrated in spaces from 2 to 8 m^2 in area. This indicates the small scale of post-depositional shifts. If so, the fact that separate refittings from Blocks 8, 27 and 32 were found in the eastern cluster could indicate that processing of these blocks took place in different parts of the site. However, it is also tenable (and more likely, in fact) that the deceptively similar raw material gave the impression of one block, while in fact these were separate nodules.

4.2.1.1 Western cluster

Judging by the dispersal of the refitted pieces from this cluster [*Table 4.33*] and the reconstructed landscape, which revealed a small relief depression in the western part of trench 2013/I, this part of the southwestern sector appears to have been a place of advanced stone processing. Tool production took place at the edge of the depression, which served both as a dump for debris from the stone processing and a place for storage (selection?) of unprocessed nodules of raw material [see *Fig. 4.6*].

Considered in relative terms, the refitted elements illustrate the greatest scattering of initial pieces from the processing. Their analysis facilitated a closer examination of the processing schemas applied to obtain a final/predetermined form, whether a Levallois flake or a point. No other schema for elaborating a tool blank (discoidal, spheroidal or prismatic-blade) was confirmed. Non-Levallois methods are naturally discernible at all stages of knapping, especially in the initial phases of testing the quality of a nodule. However, insofar it is conducted consistently and to the end, processing with faceting of the striking platform and control of convexity of the flaking surface always turned out be the real aim of the complex processes applied to the shaping of the nodules from Affad.

Table 4.33. List of refitted blocks from the western cluster of site AFD23 (sector SW)

Block	Refitting (description)	Refitted fragments	Location	Initial treatment	Core shaping	Predetermined product detachment	Core reshaping	Final core
2	Z-1 – 3 m²	5	Western cluster	x	–	–	–	x
7	Z-1 – 5 m² & dispersed	10	Western cluster and west	–	x	x	x	x
8	Z-1 – 2 m²	3	Western cluster	x	–	x	–	–
	Z-2 – 2 m²	3	Western cluster	x	–	–	–	–
	Z-3 – 8 m² & dispersed	57	Western cluster, everywhere	x	x	x	x	x
	Z-4 dispersed	2	Eastern cluster	–	x	–	–	–
9	Z-1 dispersed	4	Western cluster and north	x	–	–	–	–
	Z-2 dispersed	2	Everywhere	–	x	–	–	–
14	Z-1 – 5 m² & dispersed	21	Western cluster and north	–	x	–	–	–
16	Z-1 dispersed	2	Western cluster	x	–	–	–	–
17	Z-1 dispersed	3	Southwest of western cluster	x	–	–	–	–
	Z-2 dispersed	2	Western cluster and to west	x	–	–	–	–
20	Z-1 dispersed	2	Western cluster	–	x	–	–	–
	Z-2 – 4 m²	4	Western cluster	–	x	–	–	–
	Z-3 dispersed	3	Western cluster and to south	–	x	–	–	–
26	Z-1 dispersed	2	Western cluster	–	x	–	–	–
27	Z-1 dispersed	2	North and west of western cluster	x	x	–	–	–
	Z-2 dispersed	2	Western cluster and south	x	–	–	–	–
	Z-3 dispersed	5	Between eastern and southeastern clusters	x	–	–	–	–
32	Z-1 – 2 m² & dispersed	6	Western cluster and south	–	x	–	–	x
	Z-2 dispersed	2	Southwest of western cluster	–	–	–	x?	–
	Z-3 dispersed	2	Eastern cluster	–	x	–	–	–
	Z-4 dispersed	2	Eastern cluster	–	x	–	–	–
33	Z-1 dispersed	4	West of western cluster	–	x	–	–	–
34	Z-1 – 1 m²	4	Test 2003 (southwest of western cluster)	–	x	–	–	–
35	Z-1 – 1 m²	2	Test 2003 (southwest of western cluster)	–	x	–	–	–

Table 4.33. continued

Block	Refitting (description)	Refitted fragments	Location	Initial treatment	Core shaping	Predetermined product detachment	Core reshaping	Final core
36	Z-1 – 1 m^2	7	Test 2003 & Western cluster	x	–	–	–	–
	Z-2 – 1 m^2	3		x	–	–	–	–
38	Z-1 – 3 m^2 & dispersed	13	Western cluster and west	–	x	x	–	x
42	Z-1 – 1 m^2	7	West of western cluster	–	x	–	–	x
	Z-2 – 1 m^2	2		–	x	–	–	
43	Z-1 – 2 m^2	11	West of western cluster	x	x	x	–	x
44	Z-1 – 3 m^2 & dispersed	30	Western cluster and west	x	x	x	x	x

The refittings demonstrated two main production schemas for Levallois blanks, both flakes and points. The differences between them are based on the uni-directional formation of the flaking surface relief in the case of points and its opposite-directional mode in the case of flake production. As already mentioned, there are no known cases of the application of the so-called Nubian I (opposite-directional) method to make points in the collections from Affad. The presence of non-fitted pointed flakes [see *Fig. 4.18:1556, 2450*] must be emphasized, however, as well as the core forms corresponding to them [see *Figs 4.10:2050, 2412; 4.11:1578*]. Although we do not find, therefore, confirmation of the application of such methods of shaping points among the refitted pieces, at Affad such items are undoubtedly part of an assemblage of used (and dumped) lithic artifacts. Defining them as Nubian methods is, however, a purely formal idea (Guichard and Guichard 1968; Van Peer 1991; Usik et al. 2013).

Opposite-platform schemas, represented by the refittings of Blocks 2, 7, 8, 14, 38, 42 and 43, are applied usually to commence the shaping of the rear section of the core. Most frequently, a rectangular core with a convex flaking surface is formed, which is indicated by the flake-like character of the final products (not refitted examples, see *Fig. 4.18:2639, 2891, 2964*; retouched, see *Fig. 4.21:1832*). The final flakes or their fragments that were refitted seem to have lost their value for the knappers of retouched tools, perhaps because of their instructional or defective nature (for example, a flake detached from Block 38 or a flake that broke already at the stage of being detached from Block 8). It should be kept in mind, however, that the absence of products filling formal and size requirements is due to their being carried off from the area of the 'workshop', or even the encampment, understandably because they were ready to be used.

The uni-directional schema of working the core is observed in the assemblages of Blocks 9, 33 and 44. Indeed, the last of these contributed the most information for reconstructing the complete processing schema. In the case of Block 44, a triangular point was intended from the start, hence the convergent negatives were formed only from one direction. An analogous core, but without fitted flakes from the initial shaping, was found nearby [see *Fig. 4.7:1483*]. The detached product was crude and not very regular, but it was typologically a classic Levallois point [see *Fig. 4.35*:

phase of reduction IV]. In similarity to flakes found among the debris of their production, one should not dismiss either the instructional nature of this artifact or its significant defectiveness.

Most of the refitted blocks represent a preferential schema, including a remodeling of the nodule after detaching a flake/point. The only deviation is Block 8 where three flakes with facetted butts were detached before the remodeling operation. It should be emphasized, however, that all three flakes were found in the debris and had already been broken, most probably at the production stage.

The sizes of the assembled pieces allowed some features of the flake assemblage to be identified [see *Figs 4.12–4.15, 4.17*]. The initial flakes, or simple testing of the raw material [*Fig. 4.71*, marked in black] are not at all the largest in the assemblage, despite pieces smaller than 40 mm not occurring among them. Although natural (unprepared) butts did indeed predominate among the initial products, single elements with multi-faced butts were also present. Pieces shaping the form of the core (marked in blue) include both the largest and the smallest forms. The discrete division into products larger and smaller than 40 mm indicates foremost a division into pieces from the shaping of either the flaking surface or the striking platforms. In the case of the latter category, while flakes with prepared butts predominated, products with natural butts occurred more frequently among the larger flakes (corresponding to the initial stage of working cores still largely covered with the cortex). In the case of flakes from an advanced stage of shaping the flaking surface relief and striking platforms (marked in green), we may observe a majority of small pieces with multi-faced butts corresponding to the phase of final preparation of the platforms

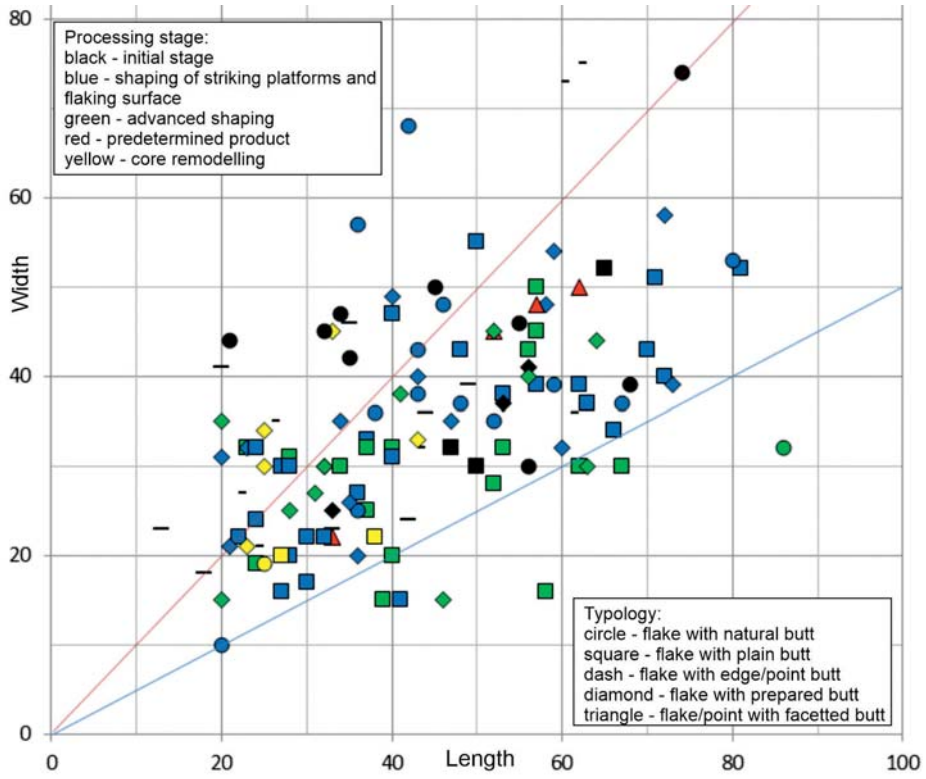

Fig. 4.71. Refitted flakes from site AFD23 (sector SW western cluster): length-to-width correlation (mm). Color coded processing stage and flake types

(*chapeau-de-gendarme*). Most of the most elongated flakes (fulfilling the metric criteria for 'blades') came from the flaking-surface shaping stage. This group was also dominated by products with plain butts (similar to the group of flakes of elongated proportions from the previous phase of shaping the flaking surface). This is extremely important evidence in the context of the frequently cited presence of 'blades' in MSA assemblages.

The dimensions of predetermined products (complete examples, marked in red), apart from one significantly smaller specimen, were concentrated around 60 mm length and 50 mm width, meaning a little more than the remaining Levallois flakes and points (outside the refittings; see *Fig. 4.17*). Therefore, artifacts from this group from the western cluster, found among production debris, were thicker.

Pieces of the last category coming from the core remodeling phase (marked in yellow) differ in the smallest of dimensions and the predominance of multi-faced butts. None of the reconstructed blocks, preserving pieces detached after knapping the first predetermined product, provided any evidence of a successful detachment of another Levallois flake or point. Therefore, the core remodeling operations should be viewed rather as initial operations, with a variety of reasons behind the reluctance to process the pieces further, for instance, the inappropriate properties of the raw material as in the case of Block 8.

4.2.1.2 Southwestern cluster

The southwestern cluster of lithic artifacts, approximately 3 m in diameter, was located roughly 3 m southeast of the edge of the relief depression, scattered among numerous and varied cut features (pits, postholes). Refitted blocks 37 and 4, which represent the raw material testing stage and initial shaping of nodules, even had pieces as far away as in the neighboring western cluster. However, the remaining blocks (4, 18 and 21) signified an advanced processing of Levallois cores, without any evidence of initial working on the spot. Moreover, the cores shaped as a result of these operations were not discovered. Therefore, the pieces found in the southwestern cluster reflect a consistent supply of nodules of proper quality and size, subsequently relocated outside the campsite. Sometimes already shaped nodules with the features of Levallois cores underwent further processing, something exemplified by Block 4, that is, two refitted flakes which had been detached from a core with a platform shaped by many small negatives [see *Fig. 4.22*: Block 4].

The refitted flakes [*Fig. 4.72; Table 4.34*] showed several parallels with artifacts from the western cluster. Flakes with natural butts (generally assigned to the initial stages of processing) were once again the thickest, while the 40 mm size range was observed once again for debitage from the core shaping stage, dividing larger flakes with plain butts from the smaller flakes composed of mainly debitage with multi-faced butts.

None of the pieces from the cluster demonstrated the application of opposite-direction processing schemas or, in other words, other advanced stages of core preparation. Neither was there any evidence of detaching predetermined products. Even the proximal fragment of a flake with a facetted butt from Block 4 comes from the initial stages of core shaping. Moreover, the fact that a butt of the *chapeau-de-gendarme* type had already been shaped at this stage corresponds to a schema of processing also observed in the Block 33 assemblage from the western cluster and could have had an exclusively instructional character.

Table 4.34. List of refitted blocks from the southwestern cluster of site AFD23 (sector SW)

Block	Refitting (description)	Refitted fragments	Location	Initial treatment	Core shaping	Predetermined product detachment	Core reshaping	Final core
4	Z-1 – 2 m²	2	Southwestern cluster	–	x	–	–	–
18	Z-1 – 3 m² & dispersed	4	Southwestern cluster and north	–	x	–	–	–
	Z-2 dispersed	2	North of southwestern cluster	–	x	–	–	–
	Z-3 dispersed	5	North of southwestern cluster	–	x	–	–	–
	Z-4 dispersed	2	North of southwestern cluster	–	x	–	–	–
21	Z-1 dispersed	2	South of southwestern cluster	x	–	–	–	–
	Z-2 – 3 m² & dispersed	6	Southwestern cluster and west	–	x	–	–	–
37	Z-1 – 2 m²	5	Southwestern cluster	x	–	–	–	–
	Z-2 dispersed	2	Western cluster	x	–	–	–	–
	Z-3 dispersed	3	Around southwestern cluster	x	–	–	–	–
40	Z-1 dispersed	2	Southwestern cluster	x	–	–	–	–

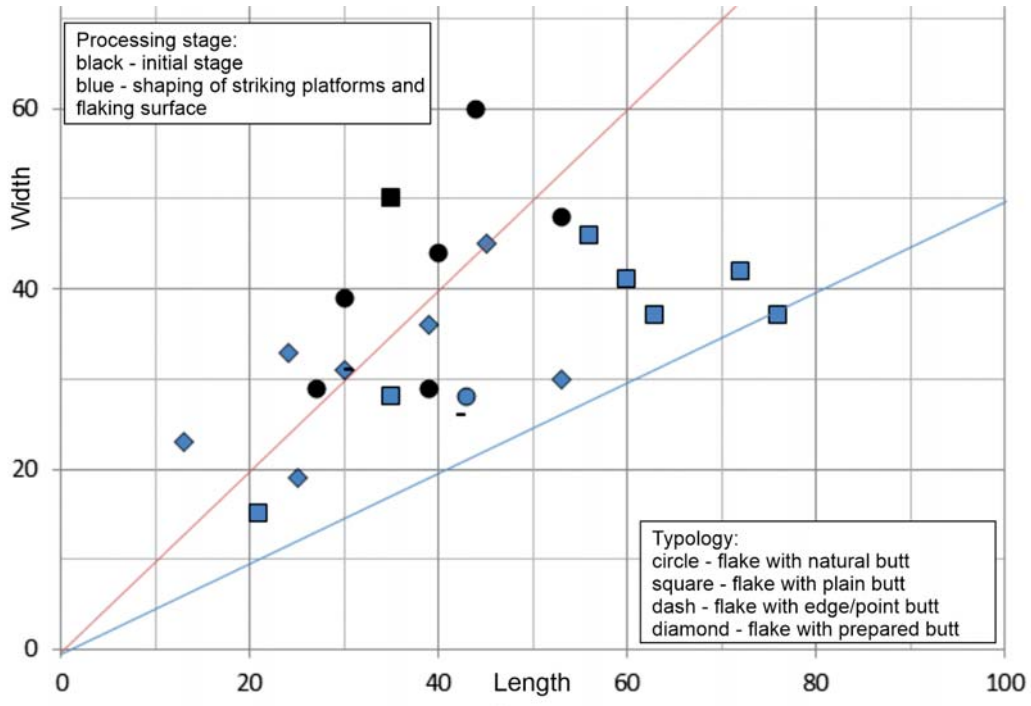

Fig. 4.72. Flakes from site AFD23 (sector SW southwestern cluster): length-to-width correlation (mm). Color coded processing stage and flake types

4.2.1.3 Eastern cluster

Another clearly separate cluster of lithic artifacts lay approximately 7 m east of the western and southwestern clusters. It covered a flat area of slightly rectangular outline, about 4 m by 3 m. The straight course of the eastern border of the cluster may be interpreted as reflecting a physical barrier existing at the time when the artifacts were deposited. It could have been a natural barrier, but given the presence of postholes in this area (and directly in the area of the eastern cluster), one should not exclude the existence of low walls limiting the area of chert processing and deposition of sharp debris.

Most of the refittings of blocks from the eastern cluster (12, 13, 15, 23, 30) represented stages of raw material testing and initial working of nodules later relocated from the investigated area [*Table 4.35*]. The assemblage also included debitage from previously processed nodules (Blocks 1, 19) and nodules processed from beginning to end on the spot, including deposition of a residual core.

The refittings of Blocks 19, 22 and 29 brought additional important data on chert processing at the site. All three blocks represented an opposite-direction schema of working the core, similar to the rectangular flaking surface at the initial stage; the remodeling of the core followed a centripetal schema. Perhaps the divergence from a "bipolar" schema of core shaping was the result of smaller dimensions. The absence of predetermined products from Blocks 19 and 22—most probably of elongated proportions, bearing scars on the negative/dorsal side reflecting centripetal modelling of the flaking surface relief—is a crucial observation. In turn, the Levallois flake from Block 22 did not cover the entire space of the shaped flaking surface but terminated at an imperfection in the raw material.

Reused cores (remodeled following detachment of a flake) had two opposite platforms as well as a rectangular flaking surface exceeding 6 cm in length and 5 cm in width. Cores of this size must have still constituted valuable material for people camping in Affad during the Late Pleistocene. The remaining cores from Affad, defined as 'residual' cores, also oscillated around such dimensions, while the overwhelming majority, namely 'initial cores', exceeded these limits [see *Fig. 4.8*].

The material also provided crucial data concerning production aims. Two of the artifacts—a Levallois flake from Block 22 and a large flake from the initial working of Block 29—underwent denticulate retouching along their longer edges. Taking into account the predominance of denticulate retouching in the lithic inventory from the southwestern sector at Affad 23, the refitting evidence confirms both the use and the production of denticulate tools in the area of the campsite.

An analysis of the metric proportions of the flakes from the refittings [*Fig. 4.73*] reveals slight differences with regard to the results for the western cluster. None of the artifacts are very elongated, despite the presence of such pieces in the refitting of Block 22, for example. This is due to the high degree of fragmentation. Therefore, the largest and at the same time the thickest flakes reflect testing and initial working of the raw material (marked respectively in black and blue). Once again the division into artifacts larger and smaller than 40 mm is marked. There is an evident disproportion between large pieces of debitage from initial working and the smaller pieces from final core shaping (marked in green).

The only final product (marked in red) comes from Block 22. It did not cover the entire prepared flaking surface because of the imperfections of the raw material. Thus, its dimensions

should not be perceived as typical of final products of the Affad knapper(s). Undoubtedly, however, predetermined products constitute some of the largest flakes.

Flakes from the core remodeling stage (marked in yellow) are almost completely within the range of products smaller than 40 mm.

Table 4.35. List of refitted blocks from the eastern cluster of site AFD23 (sector SW)

Block	Refitting (description)	Refitted fragmets	Locus	Initial treatment	Core shaping	Predetermined product detachment	Core reshaping	Final core
1	Z-1 – 3 m²	4	Eastern cluster	–	x	–	–	–
	Z-2 dispersed	4	West of eastern cluster	–	x	–	x?	–
12	Z-1 dispersed	7	Eastern cluster	x	–	–	–	–
	Z-2 dispersed	2	Eastern cluster	x	–	–	–	–
13	Z-1 dispersed	2	Eastern cluster	x	–	–	–	–
15	Z-1 – 2 m² & dispersed	6	Eastern cluster and northeast	x	–	–	–	–
	Z-2 dispersed	3	Western cluster	x	–	–	–	–
	Z-3 dispersed	2	Eastern cluster	x	–	–	–	–
	Z-4 dispersed	2	South of eastern cluster	x	–	–	–	–
	Z-5 dispersed	2	Eastern cluster	x	–	–	–	–
	Z-6 – 2 m²	2	Eastern cluster	x	–	–	–	–
19	Z-1 dispersed	3	Everywhere	–	x	–	–	–
	Z-2 dispersed	2	Eastern cluster	–	x	–	–	–
	Z-3 dispersed	2	Eastern cluster	–	x	–	–	–
	Z-4 – 1 m² & dispersed	17	Eastern cluster and west and south	–	x	–	–	–
	Z-5 dispersed	6	Eastern cluster and northwest	–	–	–	x	–
22	Z-1 – 8 m² & dispersed	37	Eastern cluster, everywhere	x	x	x	x	x
23	Z-1 dispersed	2	Eastern cluster	x	–	–	–	–
	Z-2 dispersed	4	Eastern cluster	x	–	–	–	–
29	Z-1 – 8 m² & dispersed	38	Eastern cluster and north and west	x	x	–	x	x
	Z-2 – 1 m²	2	Eastern cluster	–	x	–	–	–
	Z-3 – 1 m²	2	Eastern cluster	x	–	–	–	–
30	Z-1 dispersed	4	Eastern cluster	x	–	–	–	–
	Z-2 dispersed	2	West of eastern cluster	x	–	–	–	–

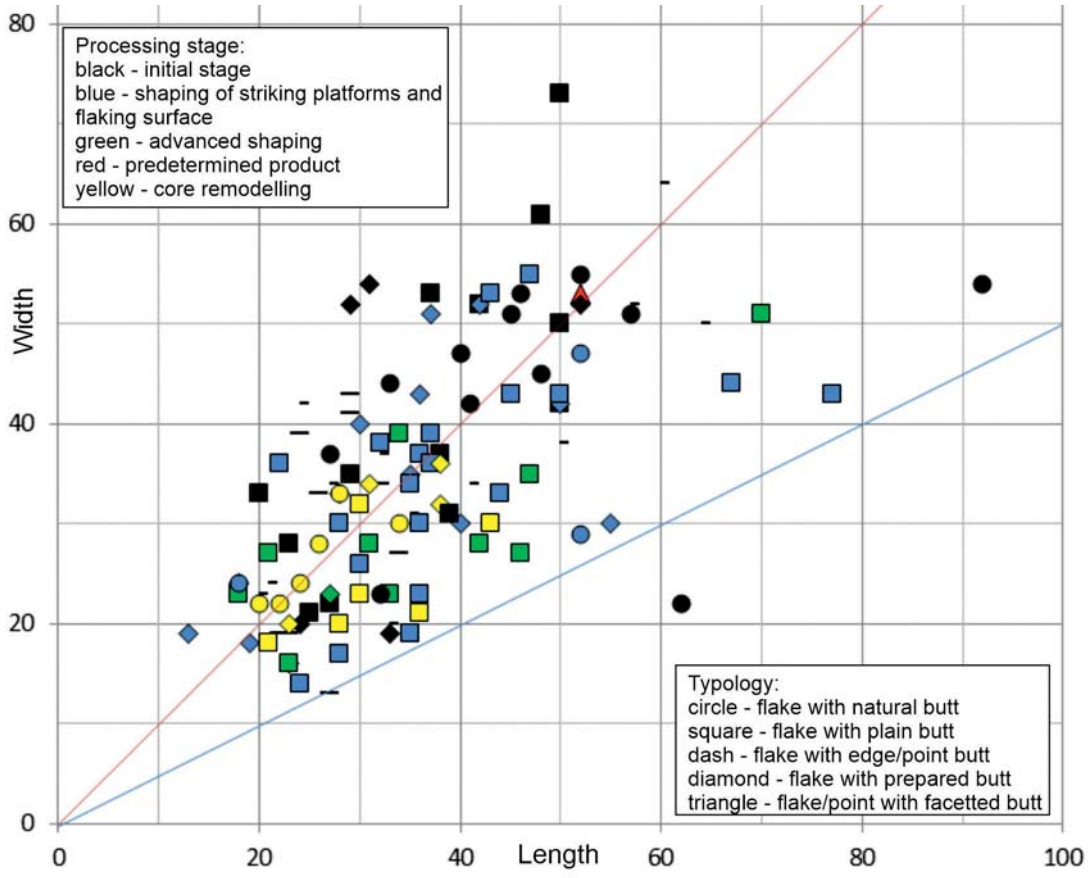

Fig. 4.73. Refitted flakes from site AFD23 (sector SW eastern cluster): length-to-width correlation (mm). Color coded processing stage and flake types

4.2.1.4 Southeastern cluster

The southeastern cluster covered a small flat area separated from the eastern cluster, approximately 4 m to the south of it and 2–3 m in diameter. Cut features of various shape and size, as well as remains of hearths, were located in the immediate vicinity of the cluster, thereby resembling the location of the southwestern cluster.

The three blocks refitted from this cluster are almost complete in terms of their processing [*Table 4.36*]. Only in the case of Block 25 is the core missing which, following the detachment of a predetermined flake and remodeling in line with the opposite-direction schema, possessed dimensions of the flaking surface exceeding 6 cm in length and 3.5 cm in width. The predetermined product had not been retouched and was abandoned in the place of its production, in similarity to the unsuccessful hinged flake from Block 10. This corresponds to analogous behavior from the adjacent clusters, interpreted as the remains of instructional nodule processing. Another feature of Block 25 was the distribution of initial pieces in a southerly direction (apart from refitting 4 which is an exception), suggesting testing of the quality of the collected nodules over a significantly wider area, as well as the processing of only selected pieces within the vicinity of wooden structures and hearths.

Table 4.36. List of refitted blocks from the southeastern cluster of site AFD23 (sector SW)

Block	Refitting (description)	Refitted fragments	Locus	Initial treatment	Core shaping	Predetermined product detachment	Core reshaping	Final core
3	Z-1 – 10 m²	7	Southeastern cluster	x	x	–	–	x
10	Z-1 – 4 m² & dispersed	22	Southeastern cluster and north	–	x	x	x	x
	Z-2 – 1 m²	2	Southeastern cluster	–	x	–	–	–
25	Z-1 – 3 m²	9	Southeastern cluster	x	x	x	x	–
	Z-2 dispersed	3	Southeastern cluster	–	x	–	–	–
	Z-3 dispersed	2	South of southeastern cluster	x	–	–	–	–
	Z-4 dispersed	2	Western cluster	x	–	–	–	–
	Z-5 dispersed	2	South of southeastern cluster	x	–	–	–	–
	Z-6 – 1 m²	2	South of southeastern cluster	x	–	–	–	–

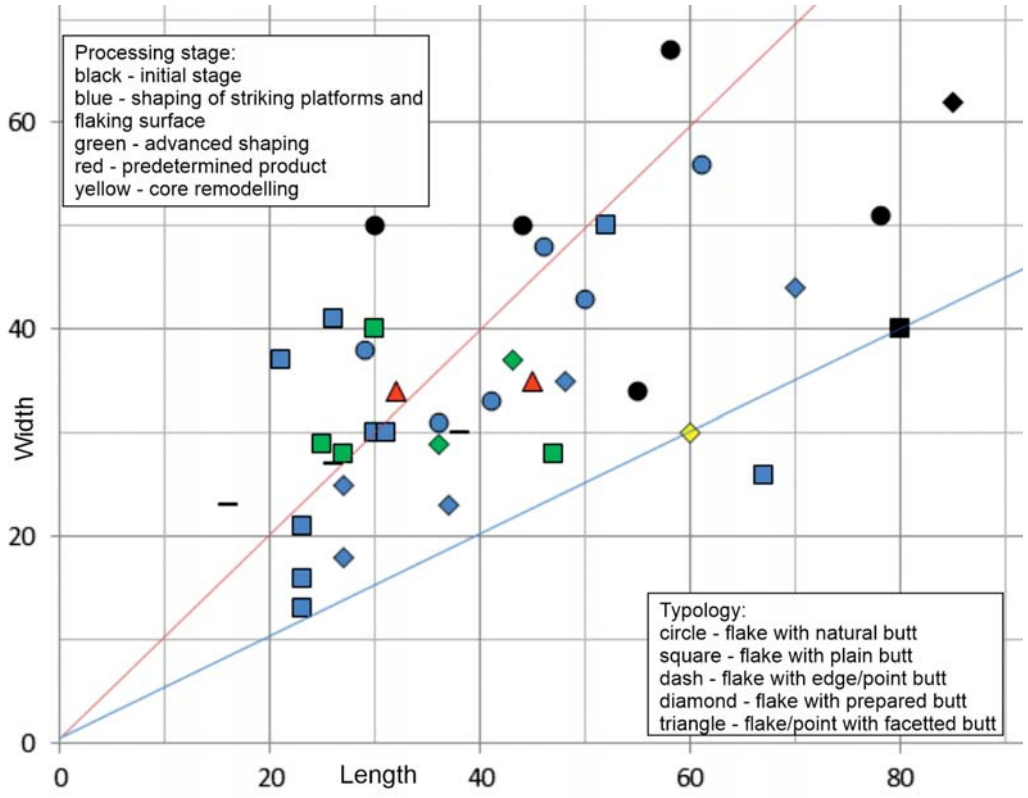

Fig. 4.74. Refitted flakes from site AFD23 (sector SW southeastern cluster): length-to-width correlation (mm). Color coded processing stage and flake types

In turn, Block 3 shows working of a nodule which was not, however, destined for further processing. The dimensions of the shaped core significantly exceed the established (and by implication, optimal) size of relocated forms and the quality of the nodules may also be described as good. It is a riddle, therefore, why such a large nodule was left behind [see *Fig. 4.7:519*].

Refittings from the southeastern cluster provided evidence of processing stone in line with a schema, which was opposite-directional, preferential and meant to detach flakes, not points. The produced cores possessed a flaking surface of rectangular outline analogous to nodules known from the adjacent clusters.

The assembled flakes from the southeastern cluster also correspond in metrical terms to the collections from adjacent clusters. The debitage of initial working/testing of the raw material [*Fig. 4.74*, marked in black] had dimensions exceeding 5 cm and constituted usually the largest pieces in the refittings. Among flakes from core treatment there was a visible division into pieces larger and smaller than 40 mm, which generally corresponds to products detached from flaking surfaces and striking platforms. In turn, most of the debitage from advanced working (marked in green) included flakes less than 40–50 mm in size. Predetermined products were short and thick, which mostly reflected their 'defectiveness' (a hinge in the case of a flake from Block 10).

4.2.1.5 Southwestern sector in summary

The much greater preponderance of refittings indicating relocation of shaped nodules outside the encampment over those representing the complete process of flake/point production attests to the supply character of the southwestern sector at the Affad 23 site. It would have been an area where the stone raw material, mainly chert in the form of relatively large nodules (larger than 60 mm in length, 50 mm in width and 40 mm in thickness), was delivered. This observation is confirmed by the preponderance of initial forms of cores in a general sense [see *Table 4.2*], and their numerous presence (and therefore abandonment) indicating a significant surplus of raw material in this location. Of course, a number of such left behind/abandoned initial cores may have been consciously rejected because of their somewhat low quality or unsatisfactory dimensions. However, some of the refittings (e.g., Block 3) show that relatively large nodules of good quality were also left behind.

The significant number of pieces of initial working of the cores scattered all over the site is proof that there were no set places for performing these operations (at least in the area under investigation). It is to be assumed that the raw material was tested either at the location where the nodules were found, in the direct vicinity of the area under investigation or, incidentally, just anywhere because the entire zone directly constituted a resource base for such an area. The immediate suggestion is that nodules were organized spontaneously and over a long period of time.

The refittings have also demonstrated the size and character of the initial debitage. In each of the analyzed clusters, flakes from this processing stage were thick and on the whole larger than 40 mm, by which flakes with natural and plain butts dominated. However, since flakes with natural and plain butts do not seem to be in the majority [see *Figs 4.12, 4.13*], it should be assumed that the remaining activities related to stone processing and usage balanced out the proportion of smaller pieces of debris, thus distorting the model formed on the basis of the refittings.

The repertoire of lithic products used by the human groups settled in Affad in the Late Pleistocene can be reconstructed to an extent thanks to the data on core processing and the making of final products gleaned from the block refittings. The predominant schema revealed by both partial and almost complete refittings is the opposite-directional one, designed to shape a rectangular flaking surface on the cores. In most cases, "bipolarity" was a way of achieving a convex shape. At the same time, as areas of the side edges of the flaking surface were most often the places where the most elongated flakes had been detached, the idea of achieving the greatest convexity is actually visible in the center of the flaking surface. "Bipolarity" was usually applied progressively rather than simultaneously. One side of the core (e.g., the rear) was shaped first before starting on the section opposite it. In fact, this schema resembles centripetal shaping of the flaking surface, albeit only from two opposite directions. The entire process of knapping the core and preparing a *chapeau-de-gendarme* striking platform served to detach one predetermined product, after which the core underwent remodeling to secure once again a convex shape in the center of the flaking surface. The detached product in the refittings, occupying almost the entire shaped flaking surface, should possess a rectangular outline and dimensions of approximately 60 mm by 50 mm, which corresponds to the dimensions of a large number of flakes found in this sector of the site [see ***Fig. 4.17***]. This method corresponds to a schema considered as preferential in comparison with that which is recurrent, where several products are detached from a flaking surface shaped only once. Although the refittings from Affad have revealed just one case of a recurrent schema (Block 8), given the defectiveness of the predetermined artifacts (breakage at the detachment stages, as well as shortening caused by imperfections in the raw material), one must take into account the exceptionality (or simply the randomness) of this record and, perhaps, the instructional aspect of this entire process.

The second schema used at Affad for securing a final product was a uni-directional shaping of triangular points with facetted butts. Typologically, they correspond to the classic Levallois point. Meager evidence for the use of this method comes from the refitting of Block 44, as well as several other cores which have so far proved impossible to fit with the remaining artifacts. Although this method was undoubtedly not employed as often as the previously described schema for producing flakes, the presence of points of this type is evident in the material [see ***Figs 4.18, 4.21***].

The third schema, resembling the production of so-called Nubian points, called for the shaping of an elongated flaking surface with its convexity running centripetally along its entire length. The shaping of the relief of the flaking surface was conducted both from the side of the front striking platform and the side edges (probably Block 29, albeit without the presence of a predetermined product) which is visible in several products outside the refitted blocks [see ***Fig. 4.18:1556, 2450***]. The presence of cores corresponding to such a schema [see ***Figs 4.10:2050, 2412, 4.11:1578, 2750***], with working of a triangular flaking surface, as well as a point shaped convergent with the side opposite the front platform, may reflect the production on site of points diverging from the classic Levallois point.

Examples of artifacts (mainly cores) suggesting the use of other processing schemas, e.g., striking platform surrounding the flaking surface [see ***Fig. 4.7:754, 3159***] or discoidal [see ***Fig. 4.10:1482, 2749***], should be treated with reserve as a result of the initial or residual character of these artifacts. The fact that the range of skills of those carrying out the selection and processing of chert at Affad facilitated the creation of such shapes does not mean that these were the predominant

schemas in their technological traditions. As there were certainly no pieces from blade blanks (e.g., backed blades), its manufacture from single-platform prismatic cores has no rational basis. All pieces corresponding to bladette technological traditions [see *Figs 4.9:505, 895, 4.22:539, 2717*] lay in secondary contexts of the campsite from around 50,000 years ago and are undoubtedly related with the later episodes of settlement of the Affad Basin.

The complete processing of certain nodules was carried out within the campsite, most probably for instructional/training purposes. The presence of many refittings including final products (a Levallois flake or point) attests to this, despite this product usually diverging in thickness from the standards set by the remaining artifacts (apart from refittings) of this kind. Similar assumptions concerning the instructional role of a very early operation for preparing a *chapeau-de-gendarme*-type platform may also be applied to the interpretation of Blocks 4 and 33, as well as to several cases of thinning the base of the flakes not comprising, however, pieces set aside for hafting [see *Fig. 4.22:728+840, 740, 828*].

The predominant way of shaping retouched tools was by forming denticulate edges on one or two convergent edges of the blank. The choice of blank was not only limited to Levallois flakes/points, although the refittings do not confirm the use of others methods (e.g., discoidal) in its intentional production. The example of the Block 29 refitting indicates the *ad hoc* use of very numerous pieces of debris from the initial working of Levallois cores. Similar observations may be made regarding the *ad hoc* retouching of debris from the knapping of Block 8—a scraper and a burin. A Levallois flake from Block 22, if its defective character (shortened due to an imperfection in the raw material) is accepted, may also be included in the category of '*ad hoc*' blank for a tool.

Much less numerous were scraping tools, namely scrapers/endscrapers and side-scrapers. The only example of a large racloir [see *Fig. 4.22:3157*] made from a crude flake detached from a core with discoidal features, and therefore, by implication, once again the initial stage of working the core.

It seems that the operation to produce burins was applied with two independent aims in mind. The first intention was to manufacture a burin (in a typological sense) from an *ad hoc* flake or simply chunk blank [see *Fig. 4.22:1123, 1461, 1476, 2191*]. The second intention, however, was to model the proximal section of the blank, most probably with the aim of hafting it [see *Fig. 4.22:728+840, 740, 828*]. In such cases, the burin spalls removed most of the convexity, meaning the ridge of the butt and positive surface of the blank. In the case of the records from Affad, as we do not possess examples of complete tools of this type, this observation is circumstantial in nature despite the presence of examples of thinning of proximal sections and a different method [see *Fig. 4.18:1172, 1333, 2450, 2639, 2891, 2936*]. In all of these cases, the internegative ridges were removed in the proximal sections and this applied both to points and flakes. The issue of the form of use or simply the intentionality of the burin blows and objects with thinning of the base remain in the sphere of hypotheses, despite the extended interest of researchers of Middle-Palaeolithic North Africa in the issue of point hafting (Scerri 2013 with further literature).

The discovery of fragments of Levallois points in the area under investigation, which were impossible to fit in with any refitting, indicates operations to repair instruments of which stone tools were a part. These elements were, however, scattered all over the area, not even indicating in the immediate vicinity the location where such repairs could have been carried out.

4.2.2 Lithic artifacts from other sectors of the site

The lithic artifacts from the other archaeologically investigated zones of the Affad 23 site were of a different nature, the difference expectedly deriving from their diverse functions, as well as from a different state of preservation of the original Late-Pleistocene sediments. Just on its own, site AFD23 was already seen as a section of the Affad Basin with the test area providing, therefore, a record of lithic collections with a similar chronology, albeit different due to the proportion of particular categories of artifacts.

4.2.2.1 Southern sector

The southern zone is very likely to have been a part of the AFD23 settlement system, which included the encampment (Southwestern sector or zone) as a separate site situated approximately 50 m northwest of it. Admittedly, no direct evidence of a relationship has been found—no refittings joining fragments from the two zones, for example—but the morphometric features of lithic artifacts from the southern zone [see *Fig. 4.52, Table 4.11*] match the 'pattern' evidenced for the collection from the southwestern zone (see above). Substantiating this are other matching categories of finds: archaeozoological remains (same animal species identified) and anthropic features like postholes and a hearth.

Nothing in the collection from the southern zone suggests a post-production assemblage. There are no refittings to speak of and a negligible differentiation of the raw material, which translates into the number of different nodules, indicating that we are dealing with individual fragments from many independent processes of debitage. This selection—insofar as the rationality of actions by humans living in the Affad region for thousands of years is assumed—should reflect the morphological and metric features of actual tools used by these people, that is, artifacts with a utilitarian function. The two initial cores that were found in this sector should be seen rather as demarcating the zone inside the main campsite where nodules were tested and underwent initial processing—that is because they were discovered in a ground relief depression (test trench 2014/R) dividing the southern sector from the southwestern one.

Unretouched flakes from the southern sector correspond to processing schemas characteristic of Levallois methods, reconstructed on the basis of refittings from the southwestern sector (see above). Looking at the data, one notes the gap between debitage greater than 40–50 mm and smaller fragments [see *Fig. 4.52*]. Predominating among the larger debris are fragments from initial core shaping, with the most elongated pieces featuring edge or multi-faced butts, most probably coming from the side edges of the flaking surface at the stage when they were given a convex shape only in the center. Formal tools (apart from one Levallois point) were made from flakes with facetted or multi-faced butts, without any natural cortex surface preserved. Retouched flakes, which were from 35 to 55 mm in length and from 23 to 42 mm in width, are clustered more or less around the center of the graph for all flakes (including unretouched ones) from the southern sector [see *Fig. 4.52*]. Therefore, both slightly smaller and slightly larger retouched flakes were brought to this area. Moreover, the irregular character of denticulate retouching on flakes from this sector [see *Fig. 4.54:3126, 3133, 3143*], rather than an intended feature, could very well be the effect of intensive use of these tools. Indeed, the only example of a point with

a facetted butt [see *Fig. 4.54:3129*] falls within the lower size range of analogous artifacts from the southwestern sector. Even so, it bears marks of unidirectional shaping of the flaking surface relief, supplementing the small negatives on one side. Also visible on this point are small negatives in the proximal section, interpreted as a way of thinning the base for hafting.

The distribution of flakes and denticulate tools, considered in relation to deposits of animal bone remains in trench 2013/L–M [see *Fig. 4.55*], displays a clear concentration around some monkey remains, found on a spot corresponding to an insignificant ground relief depression. Single lithic artifacts were found among the other clusters of antelope or hippopotamus bone remains. No apparent contextual relationship existed between the deposited artifacts and the few postholes and hearths (not counting a single core made from a crude flake, which however may not be connected with the campsite episode).

4.2.2.2 Northwestern sector

Lithic artifacts from the peripheral northwestern sector appear to be related to the central campsite (southwestern sector), which is situated a dozen or so meters to the south, in much the same way as those from the southern sector. The raw material characteristic and the large number of artifacts match the findings for artifacts from original contexts in the northwestern sector. The scattering, relatively broad, does not display any specific spatial relationship with other find categories, that is, clusters of antelope bone and hearth remnants [see *Fig. 4.70*]. A cluster of cores and initial pre-cores is to be noted [see *Fig. 4.67*]. Taking into account the relatively high proportion of flakes from early stages of the processing (even greater than in the southwestern sector), and the low percentage of predetermined forms [see, e.g., *Fig. 4.67:5823, 6068*], it is probable that the location here was used mainly for testing raw material quality and initial treatment of cores. At the same time, the large concentration of antelope bones suggests that carcasses of hunted animals were also processed here. Therefore, the area supplements the southwestern sector of the site in these two aspects to a much greater degree than the other sectors of Affad 23.

4.2.2.3 Northern sector

The northern sector was situated almost 200 m away from the sectors described above, making it difficult to justify a mutually functional connection between them. However, the absolute age of the sediments yielding artifacts in the northern sector argues in favor of the collection of lithic artifats being considered as one with the remains examined in the southwestern sector. It is currently assumed that this area was occupied by a people using a similar technology and adaptation strategy, albeit representing different episodes of Late Pleistocene settlement in this part of the Affad Basin.

The degree of erosion of the artifacts from this sector is a distinctive feature: the percentage of overheated artifacts of every morphological category is much greater here, as is the extent of lateral breakage and damage to the edges. One may surmise that a significant part of this destruction comes from the post-despositional stage.

Despite the presence of lithic artifacts from every technological category (cores, initial products and final products), the assemblage here is not a correlate of behavior determining the character of the southwestern sector vel central campsite. The morphological and metric features indicate

a convergence of production intent and methods, but only a negligible number of pieces from the initial working stage, greater than 40 mm and covered by the cortex for the most part, was recorded. Nor was there any evidence to be seen of raw material testing or an initial core. Single opening flakes formed a clearly separate group (meaning flakes with intermediate states of cortical coverage in dramatically smaller percentages; see *Table 4.23*) and may have been introduced from outside as a potential blank for retouched forms. Securing blanks for tools explains also the diversity of raw materials.

The knapping process as reconstructed here (without refitting any of the artifacts) is nothing like what was established for the southwestern sector. The core forms were determined to be residual owing to their size or the convexity of the flaking surface (actually its lack, which did not augur well for working it further without remodeling). One of the cores [see *Fig. 4.60:5023*] was made from chert of a yellowish color, with a chalk cortex including numerous fossils; no other example of this exceptional raw material was found at Affad 23. One must therefore assume that core forms (apart from opening flakes) were also brought to the location already in a shaped form, although only a part of them underwent any further operations aimed at securing a tool blank. The modest assemblage of cores from the northern sector includes examples both with a centripetally shaped flaking surface and shaped from two opposite directions [see *Fig. 4.60:4952*]. The latter type corresponds to forms that came from the campsite in the southwestern sector, albeit of significantly reduced size.

The parameters of the recorded cores correspond to the dimensions of the processing debris, most of which was smaller than 40 mm. Here, the percentage of breakage of elongated flakes was comparable to that recorded for the assemblage from the southwestern sector [see *Table 4.24* and *4.6*]. Damage of this type occurs significantly more often when a flake is being detached than as a result of post-depositional processes, thus suggesting that cores were processed in both areas. However, in the case of the northern sector, the detached artifacts were definitely fewer and thinner.

The size range of items with facetted butts is puzzling here. Insofar as complete artifacts [see *Fig. 4.63*] correspond more or less to the parameters of the cores and the debris does not generally exceed 40 mm, the fragmentarily preserved Levallois flakes and points [see *Fig. 4.65*] do not exceed this margin and correspond to analogous artifacts from the southwestern sector [see *Fig. 4.17*]. Again, the potentiality that they were brought in as blanks for tools is high. Arguing in favor of this idea is notched/denticulate tool 3990 made from the distal fragment of such a large flake. Repairs of hunting tools (spears, knives) cannot be excluded in this case, replacing damaged points [see *Fig. 4.64:5035*] made elsewhere, for example, a place like the southwestern sector with free access to large nodules of raw material.

Denticulate, notched and scraping tools dominated the assemblage of retouched tools from this sector [see *Fig. 4.64*]. Of importance is the fact that only the notched forms were created from a blank, the volume of which corresponded to stone working processes in this sector. The others were made from blanks gathered from beyond the investigated space (opening or Levallois flakes, often from differentiated raw materials). Moreover, the notched forms were not made exclusively from flakes with facetted butts (similar to the southwestern sector). The collection also contained a single example of a burin from a thick fragment of a partly cortical flake, and two small burin spalls [see *Fig. 4.64:5416, 5255, 558*], which could have been intentional, even as they reflected damage to lithic tools.

The question is, therefore, whether the assemblage from the northern sector could be considered as at all representing Levallois stone tool manufacturing methods, a riddle made all the more difficult for lack of refittings. Trace evidence of a microlithic tradition [see *Fig. 4.64:5570*] does not make this collection Holocene in date. However, core processing with simple discoidal methods was obviously practiced here, even if the opening products were Levallois cores of reduced dimensions. The need for blanks to produce larger-sized tools was satisfied by collecting artifacts from contemporary 'supply' sites and the preference for such tool blanks is evident in the assemblages from both the southwestern and southern sectors. The collection from the northern sector appears to reflect a situation in which tools of a determined kind were in demand but without the skills to make them. Both the stratigraphic data (analogous dated sediments) and free access to the location from which the lithic artifacts were gathered confirm the contemporaneity of the collections from the northern and southwestern sectors. Differences are to be explained by behavioral or functional factors. Although the skills for simple discoidal processing and manufacturing provisional denticulate, notched and scraping tools were certainly widespread among most members of the group, the ability to select the right raw material and manufacture large Levallois flakes and points was most probably assigned to specific individuals and passed on in specific conditions that we have no means even to surmise.

4.2.2.4 Northeastern sector

The northeastern sector yielded well-preserved animal bone remains along with accompanying postholes and a hearth; hence it was functionally similar to the southern sector, most probably constituting a support area for the campsite in the southwestern sector where carcasses of small and middle-sized animals were butchered and meat dried. However, the relationship to the northern sector is not as clear as in the case of the southern sectors, despite the surprising similarity in their mutual settings.

A small group of cores or their fragments constitute correlates of centripetal schemas during the last stage of reduction or, in a single case, the manufacture of an irregular point with unidirectional working of the flaking surface [see *Fig. 4.58*]. These objects must have been brought in from outside, not with the intention of reducing them further but rather because of their shape and size (some of them are only core fragments). Accidental deposition is a possibility not to be excluded, but the absence of similar clusters beyond an area of approximately 1 are, as well as the perfect state of preservation of undisplaced bone remains contradicts this idea.

In similarity to the southern zone, flakes/points were not produced in this particular sector, while only tool artifacts gathered from the immediate vicinity were used. A look at flakes and retouched forms from the northeastern sector reveals a range of similarities in terms of size with the collections from the northern and southern sectors. Therefore, regardless of the manufacturing skills or other factors (such as lack of time), artifacts most similar to Levallois flakes were preferred, no smaller than 30–40 mm. In the case of the northeastern sector, this hypothesis is confirmed by a high percentage of forms with facetted butts (19.5%).

The poor state of preservation of the tools from the northeastern sector excludes an effective wear analysis and the morphology of the retouching is ambiguous [see *Fig. 4.58*], making a functional identification difficult at best. Only by drawing an analogy with the southern sector, as well

as the contexts in which antelope remains occurred in the vicinity, one may suspect that their basic purpose was to dismember the carcasses of hunted animals. In this context, it is tempting to interpret a fragment of a tool abruptly retouched in the proximal section on both side edges [see *Fig. 4.58:3907*] as the tang of a point. This would, however, be the only example of this manner of preparing the point for hafting in the entire collection from AFD23.

Single artifacts of undeniable microlithic origin—in this case a residual form of a single-platform core [see *Fig. 4.58:3897*]—are present here as elsewhere at AFD23. A similar origin of other artifacts cannot be excluded, although it is not possible to establish the share such pieces could have in the collection. Their presence may be explained by a high percentage of small flakes, smaller than 20 mm.

4.3 LITHIC PRODUCTION AT OTHER STONE AGE SITES IN THE AFFAD BASIN

Archaeological lithic sources were also collected in the course of an extensive field survey of the Affad Basin conducted since 1999. Administratively, the survey covered the *mantiqas* (districts) of Affad (=al-Affat) in the central and eastern sections and Tergis in the western section [*Fig. 4.75*]. The analysis of these collections brings us closer to a broader context of the use of stone raw materials by Late-Pleistocene and Early-Holocene societies in the Affad Basin.

The administrative division reflects two different geomorphological contexts in which Pleistocene sites can be found. In the case of the sites at Affad, these are originally preserved sediments from the Late Pleistocene, while at Tergis all the recorded Palaeolithic artifacts occurred in sands and gravels of a probably later origin. The latter were demarcated by an area of intense erosion of the original alluvium due to their close location to the present river bed of Holocene origin and the transportation of material (sands, gravels) from the north towards the river.

4.3.1 Oldest evidence of settlement in the Affad Basin

The oldest sites in the area of the Affad Basin were recorded the north of the maximum extent of Late-Pleistocene sediments, in a zone of erosion of significantly older (Mesozoic) Nubian sandstone formations. Two locations (AFD115 and AFD118) provided assemblages of almond-shaped handaxes of various size, made of ferruginous sandstone (Osypińska and Osypiński 2015: Fig. 12). This raw material is currently available throughout the area, constituting one of the basic geological elements of the Southern Dongola Reach. The handaxes must have been brought to the site ready-made because there are no other artifacts made of sandstone among the recorded finds. The probable workshops from the earliest stages of settlement in this area should perhaps be sought even further to the north, on the edge of the Mesozoic plain, isolated fragments of which are visible in the landscape in the form of inselbergs (Jebel Abkor, Jebel Umm Nuqqara). Collections of large flakes made of ferruginous sandstone, as well as handaxes are known from a number of sites located on the edges of the inselbergers by the SDRS team (e.g., NUQ4-8; Żurawski 2003: 290). These sites have also yielded large-sized Levallois artifacts (Osypiński 2003: Pls MTC I/4:c, MTC II/6).

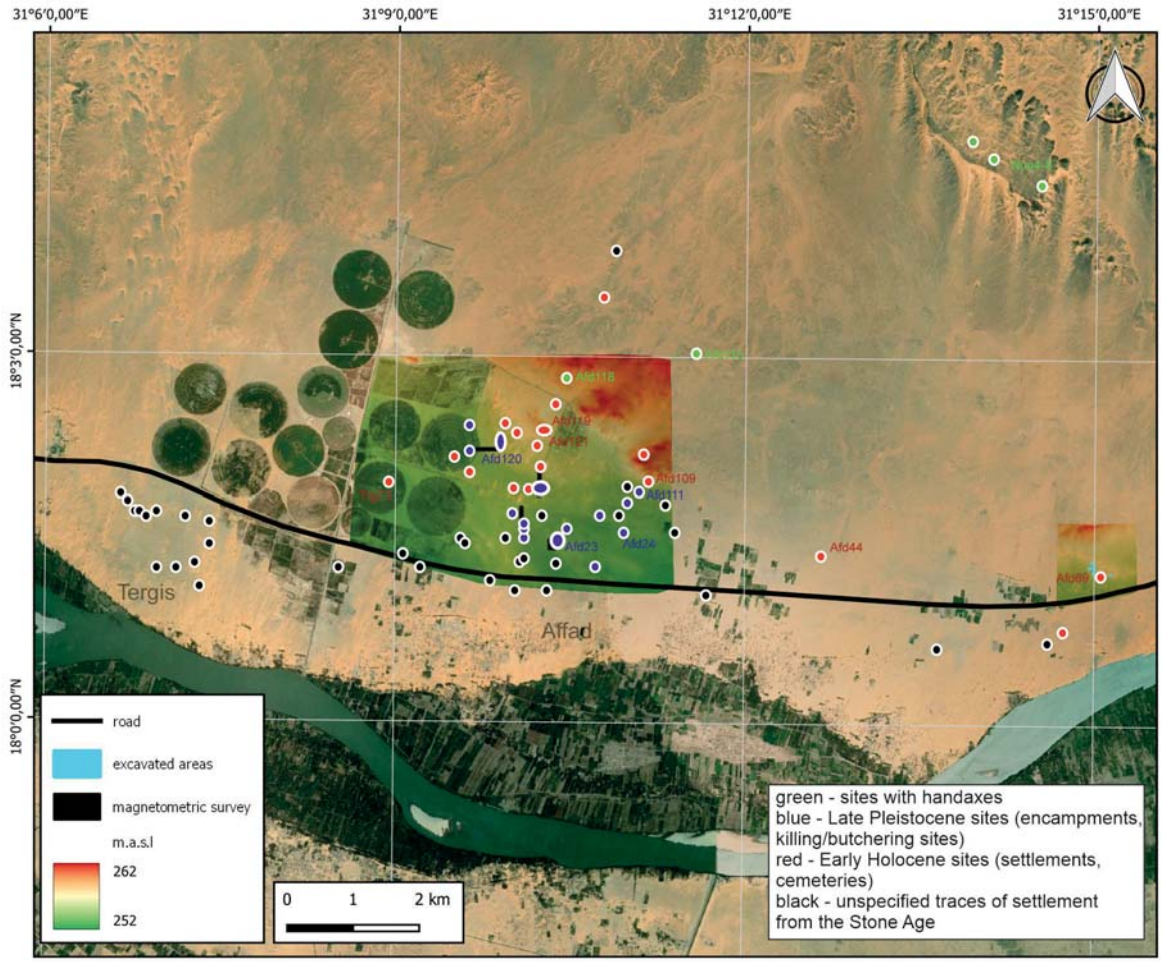

Fig. 4.75. Extent of surface research within the Affad Basin

Single, clearly older artifacts of ferruginous sandstone were also found at sites with later chronology. One of these is the only bifacial artifact (or blank) recorded from the surface at Affad 23 [see *Fig. 4.22:327*]. Another example is a handaxe of the Micoque type from site AFD121 (Osypińska and Osypiński 2015: Fig. 12:c), found among Early Holocene artifacts, and two bifacial points from AFD108 (Osypińska and Osypiński 2015: Fig. 9:a, Osypiński 2012: Fig. 2:a). In the lattermost case, the entire assemblage could have been redeposited during the stripping of the site under road construction in 2009; the gravel sediment, in which the artifacts had been deposited, was disturbed at the time.

Raw materials found in the inventories of Late-Pleistocene sites in the Affad Basin include two 'exotic' and simultaneously easily recognizable kinds: a light yellow chert containing numerous fossils, a chalk cortex, and a silicified sandstone of pink color, the shade resulting from the absorption of derivatives of iron [*Fig. 4.76*]. The chert is of particular interest because the cortex suggests availability from primary geological contexts not presently indicated on modern geological maps of this region. It was processed in the Southern Dongola Reach both in the Late Pleistocene and in the Early Holocene, which is proved by single finds of bladelet artifacts at many

SDRS sites, as well as refittings from the el-Multaga 3 site, thanks to which it was possible to differentiate three different methods of its processing (Osypiński 2014; Osypiński "Summary of the studies on lithic assemblage of prehistoric site el-Multaga 3, Dongola Reach" – manuscript).

In the area of the Affad basin, artifacts made of light chert were recorded on the surface of sites: Tergis 52/ TRG52 (initial treatment Levallois flake); TRG72 (Levallois flake and Type II Nubian core; Osypińska and Osypiński 2015: Fig. 4:c); TRG78 (residual discoidal core; Osypińska and Osypiński 2015: Fig. 5:c); TRG82 (initial Levallois flake fragment); AFD12 (cortical flake); AFD16 (two fragments of partly cortical flakes, of which retouched on its positive/ventral side; Osypińska and Osypiński 2015: Fig. 8:b); AFD20 (fragment of Levallois flake); AFD23 (sector N: Levallois core, as well as a Tayac-type point without a precise location; Osypińska and Osypiński 2015: Fig. 2:d); AFD24 (initial flake fragment, as well as fragment of a microlithic bladelet); AFD62 (partly cortical initial Levallois flake); AFD90 (fragment of a Levallois flake); AFD99 (two initial flakes, small residual cores and a scraper; Osypińska and Osypiński 2015: Fig. 7:a); AFD109 (denticulate tools from a small flake with a plain butt); AFD111 (seven initial flakes); AFD118 (notched tools from a Levallois blank) [*Fig. 4.77*]. Excavation in the southern sector of AFD122 uncovered a larger cluster of flakes made from this raw material indicating processing of nodules (see below). The few artifacts made of light-colored chert recorded at the other locations in Affad were very often pieces of debitage. Obviously, if Late Pleistocene hunters-gatherers were picking up such flakes, then they must have had access to abandoned workshop sites from an earlier time, which were situated away from Affad in all likelihood, hence the claim that the Late Pleistocene groups from this area must have roamed beyond it.

Single artifacts of the silicified pink sandstone have been recorded at the following sites: TRG52 (initial flake fragment from a discoidal core, and a plunged Levallois flake); TRG71 (fragment of a Levallois flake with denticulate retouching); TRG72 (residual Levallois core); TRG79 (fragment of an unifacial point with retouched tang; Osypiński 2003: Pl. MTCII/4e); TRG80 (fragment of a denticulate tool with thinned bulb section; Osypińska and Osypiński 2015: Fig. 6:c); TRG82 (flake with denticulate retouching on two edges); TRG85 (Levallois flake with denticulate retouching); AFD12 (two fragments of denticulate tools; Osypińska and Osypiński 2015: Fig. 7:f); AFD99 (Levallois flake); AFD111 (three flake fragments, one Levallois flake, one denticulate tool, as well as a nodule of the raw material; in the case of this last assemblage, artifacts of this raw material constituted just 0.3% of the finds from a trench 10×10 m in size). Characteristically, no artifacts of pink sandstone were recorded either in the rich collection from AFD23 or from the surface of the other sites around it, but they were present in a much more heavily eroded zone of the *mantiqa* of Tergis. While it cannot be said that raw material of this type was secured from only one zone, none of the artifacts found up to now bear any traces of having been rolled around in gravel formations. It means that nodules were secured from a primary geological context occurring in slab form, one akin to ferruginous sandstone referred to as the Nubian Formation but not as common. The dispersal of artifact finds (mostly tools) also supports the notion of repeated use of this particular raw material. The available data do not indicate use of this raw material during the Early Holocene.

The morphology of the artifacts collected from locations around AFD23 generally falls within the range of the denticulate tool technology reconstructed from the refitting analysis. The size of predetermined Levallois flakes and points places them in the category of 40–60 mm length and

Fig. 4.76. Typical stone raw material used by Late Pleistocene communities in the Affad Basin: A – light-colored chert with cortex; B – pink quarzitic sandstone

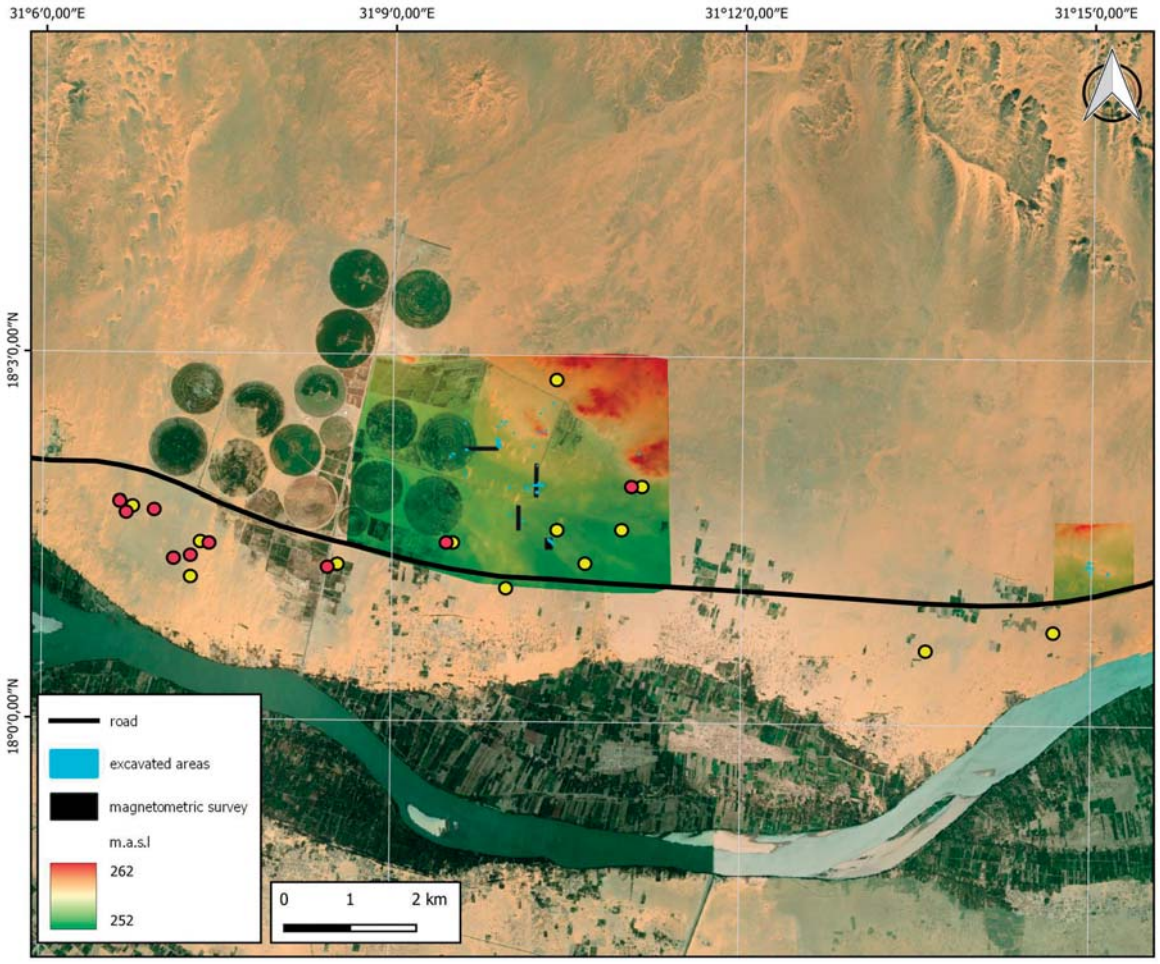

Fig. 4.77. Location of Late Pleistocene sites with lithic artifacts made from specific stone raw materials: yellow – light-colored chert with lime cortex; red – pink quarzitic sandstone

30–50 mm width [*Fig. 4.78*], with the smallest artifacts being of agate occurring in the form of small pebbles, and the markedly larger flakes and points of ferruginous sandstone. The shape and size of discoidal and Levallois cores bears out the technique of reduction to a residual form with a centripetal pattern of negatives on the flaking surface and a diameter of less than 40 mm [*Fig. 4.79*]. No clear traces of chert workshops have been confirmed at the other sites, but given the undulating character of the original Late Pleistocene surface, one must take into account their presence sealed by later sediments. One may state with complete confidence that Affad 23 (south-western sector), Affad 24 and Affad 122 were not the only places where stone raw materials were processed.

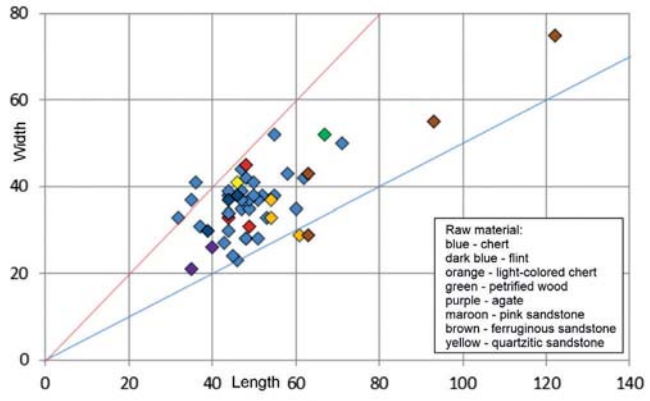

Fig. 4.78. Predetermined Levallois products (complete specimens) from the surface survey in the area of the Affad Basin: length-to-width correlation (mm)

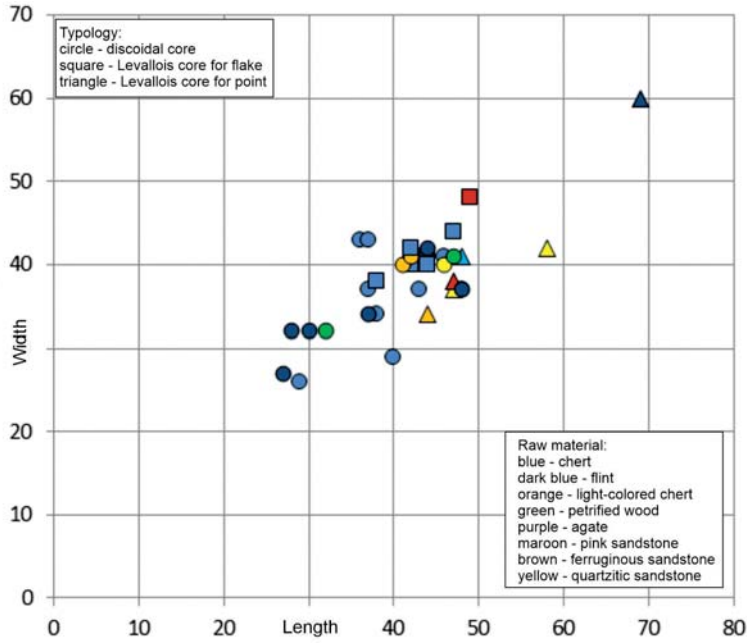

Fig. 4.79. Cores from the surface survey in the area of the Affad Basin: length-to-width correlation (mm)

Among artifacts collected from the surface at other Late-Pleistocene sites in the Affad Basin, points were also found with bases thinned in the manner observed in the collection from Affad 23 where the greatest convexity of inter-negative ridges was removed (Osypińska and Osypiński 2015: Fig. 3). A feature observed only among artifacts from Tergis was, however, the preparation of points for hafting in the form of a broad tang (Osypiński 2003: Pl. MTCII/4e; Osypińska and Osypiński 2015: Fig. 6:c). Both of these artifacts were made of silicified sandstone. Denticulate tools were the most common form of retouched tool from the surface collections, often manufactured from elongated Levallois flakes (Osypińska and Osypiński 2015: Fig. 6). Perforators were recorded in trace quantities (Osypińska and Osypiński 2015: Fig. 7:c,d), while burins were not found at all.

4.3.2 Site Affad 111 (AFD111)

Site AFD111 was discovered while collecting geomorphological data on the edges of the Late Pleistocene terraces in 2013. The terraces turned out to be the remnants of an ancient plain with loose fragments of the Nubian sandstone formation, covered by fluvial deposits of an older aggradation (MIS5?) and aeolian sands. The site was located within a sediment of poorly sorted fluvial deposits accumulated above aeolian sands (see GT5 exposure). Regular excavations in 2014 documented zones A (10×10 m trench) and B (5×1 m trench) [*Fig. 4.80*].

OSL dating of a sandy silt (UJK-OSL-38) sediment from the GT5 exposure corresponding to the location of site AFD111), as well as of underlying dune sand (UJK-OSL-39), indicated a date analogous to site AFD23 (with the reservation that the Kielce laboratory datings show only a minimum age; for a discussion of this issue see above, page 12). The current assumption is that the lithic artifacts and animal bone remains from AFD111 are generally from the same chronological horizon as the assemblages from AFD23, that is, MIS3. However, the aeolian sands recorded at a depth of 50 cm most probably correspond with deposits laid down in MIS4 (analogous to PG3:58-66 ka).

The site was marked by a clear cluster of artifacts made of ferruginous sandstone (overall, just 12% of the 2177 artifacts were of another raw material; see below, *Table 4.38*), which led to the initial assumption (later revised; see below) that the sandstone outcrops still seen today several hundred meters away from the site would have been a likely source of the raw material used here. This matched in a sense the conclusions reached regarding the raw economy strategies in the southwestern sector of AFD23, where chert predominated in the inventory of lithic artifacts with objects made of other raw materials barely exceeding 10% (see *Table 4.1*).

Some lithic artifacts were recorded deeper than the sandy layer of approximately 50 cm in thickness. Neither postholes or hearth remains were observed. Given the 'scattering' of artifacts on a large scale, relocation as a result of natural processes (e.g., bioturbation) is suspected. Hence, the spatial relationships of artifacts were not examined.

The collection of stone artifacts from site AFD111 includes cores, processing debris and retouched forms [*Table 4.37*; *Figs 4.82, 4.83*]. Supplementing it is a microlithic component made of both chert and flint, which represents a significantly later Early Holocene settlement located about 100 m to the northeast, presumably at the edge of the ancient terraces and at an elevation of approximately 5 m (site AFD109).

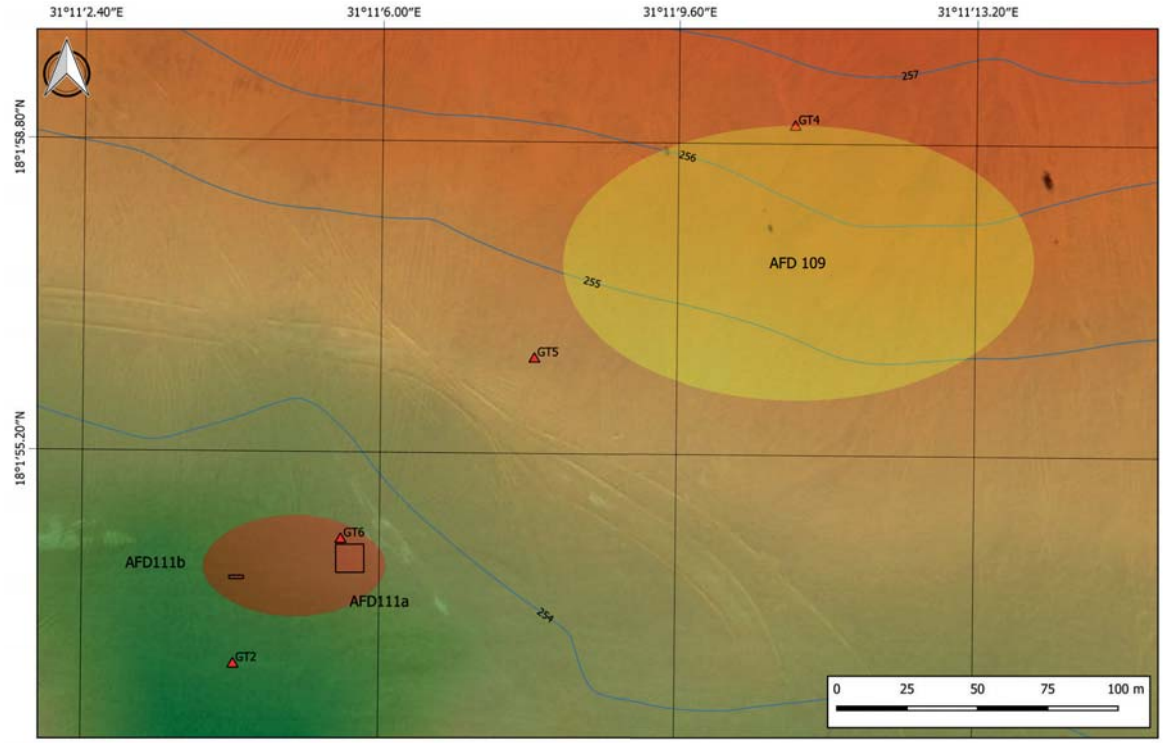

Fig. 4.80. Site AFD111: location of trenches A and B in relation to the edge of the ancient river terraces; extent of Early Holocene site AFD109 marked in yellow

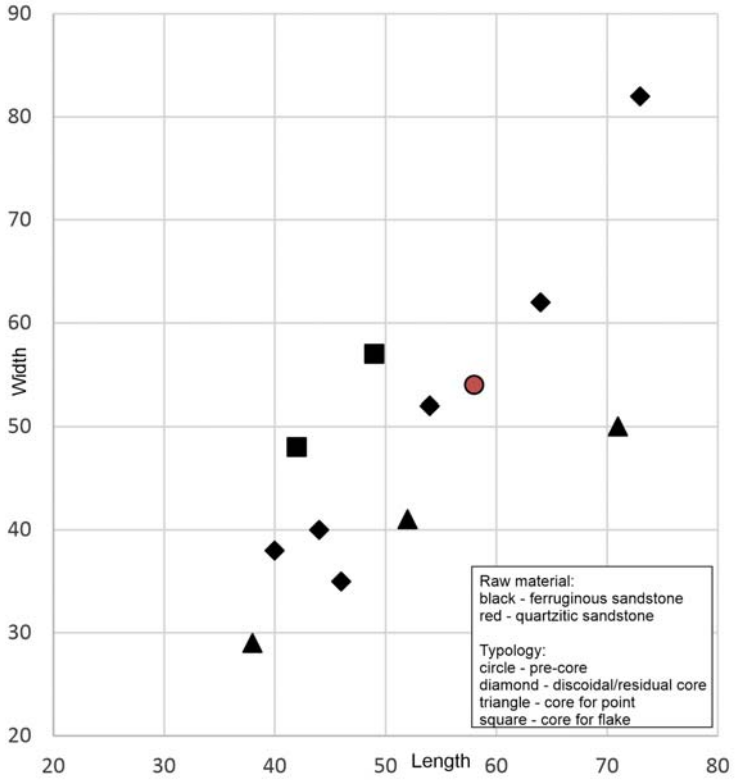

Fig. 4.81. Cores from site AFD111: length-to-width correlation (mm)

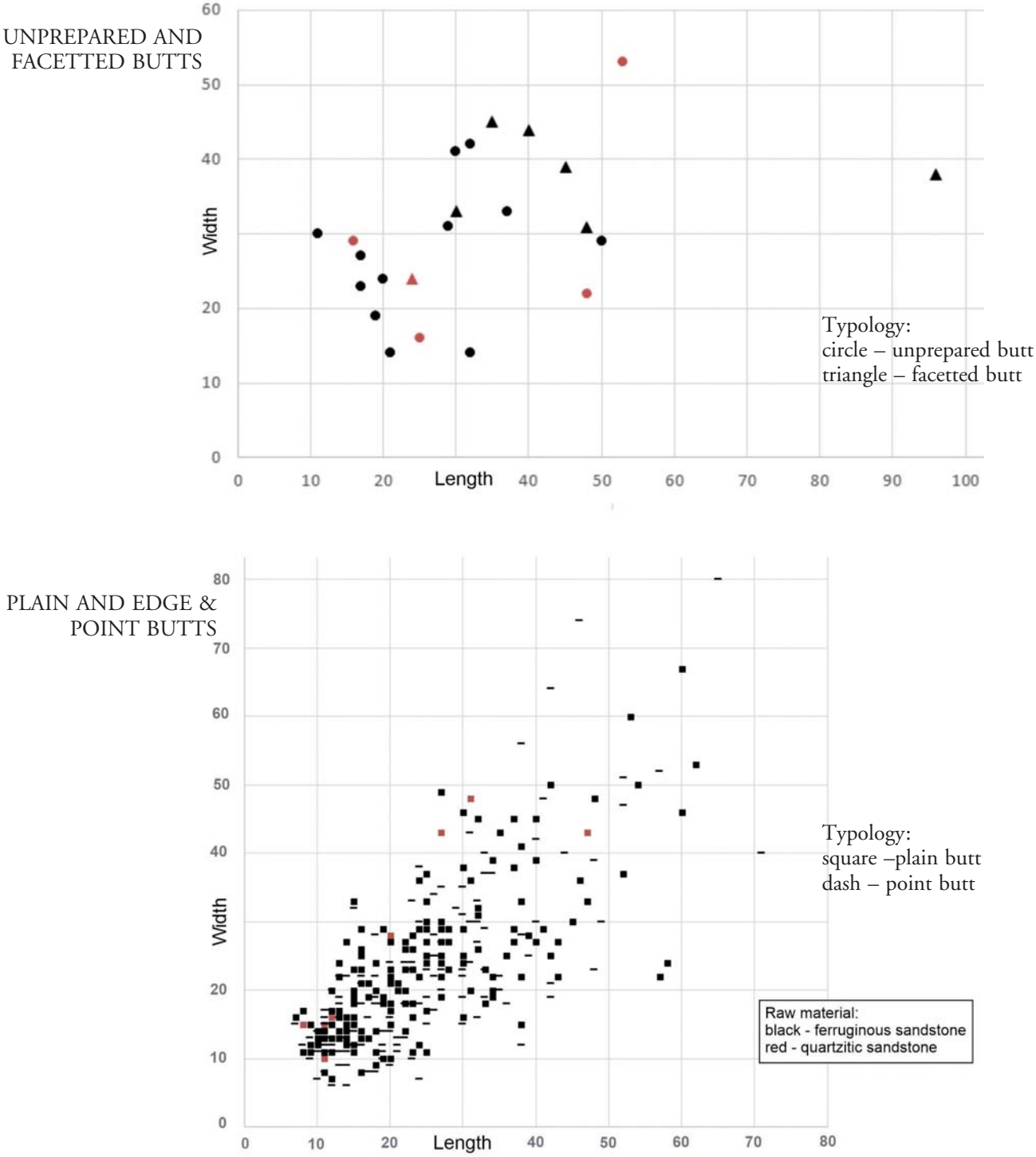

Fig. 4.82A. Flakes from site AFD111: length-to-width correlation (mm).
Top, with unprepared and facetted butts; bottom, with plain and edge & point butts.

Table 4.37. General morphological–technological structure of the collection from site AFD111

Group	Type	Raw material			Total
		Ferruginous sandstone	Quarzitic sandstone	Other	
Cores	Initial cores and tested nodules	–	1	–	1
	Cores for flakes/points	3	–	–	3
	Final cores	6	–	1	7
	Discoidal cores on flakes	2	–	–	2
	Uniplatform microlithic cores	–	–	4	4
Flakes and chips	Flakes with unprepared butt	18	4	3	25
	Flakes with plain/uniface butt	271	12	5	288
	Flakes with point & edge butts	200	7	4	211
	Flakes with multi-faced prepared butt	625	29	4	658
	Flake fragments	759	29	3	791
Chunks	Chunks	20	–	4	24
Predetermined products and formal tools	Levallois flakes	7	2	5	14
	Points	–	–	–	0
	Flakes/points with denticulate retouch	7	1	4	12
	Flakes with burin blow	–	–	–	0
	Flakes with abrupt retouch	2	–	3	5
	Bifacial forms	1	–	–	1
	Backed tool (Holocene)	–	–	4	4

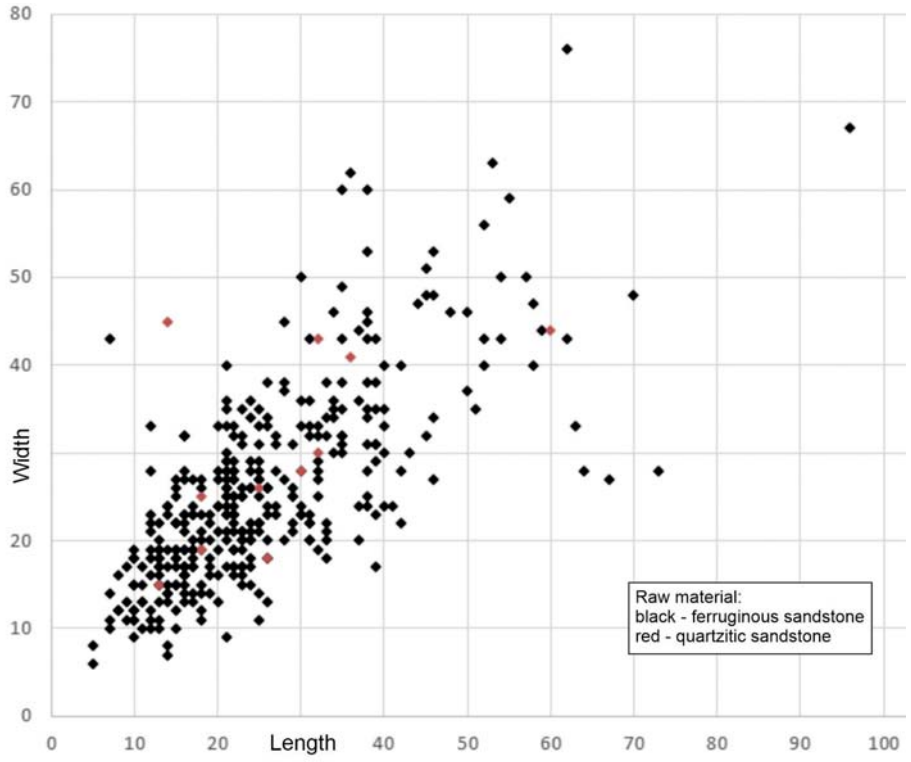

Fig. 4.82B. Flakes with multi-faced butts from site AFD111: length-to-width correlation (mm)

Table 4.38. Raw material structure of the collection from site AFD111

Chert		Flint, mudstone, agate		Quarzitic sandstone		Ferruginous sandstone		Quartz		Conglomerate, petrified wood		
n	%	*n*	%	*n*	%	*n*	%	*n*	%	*n*	%	Total
149	6.84	15	0.69	85	3.90	1921	88.24	4	0.18	2	0.09	2177

Table 4.39. Cores from AFD111: dimensions and loci

Inv. No.	Locus	Context	Dimensions (mm)	Description/raw material	Reference
1623	A/31/Ia	11	58/54/35	Pre-core/quarzitic sandstone, eroded	
247	A/36/Ia	11	38/29/13	Core for point/ferruginous sandstone, eroded	
1621	A/74/Ia	11	71/50/20	Nubian II core/ferruginous sandstone, eroded	*Fig. 4.83*
1800	A/75/Ia	11	52/41/19	Nubian II core/ferruginous sandstone, eroded	*Fig. 4.83*
471	A/76/Ia	11	44/40/19	Discoidal/ferruginous sandstone	
1560	A/97/III	16	40/38/12	Discoidal/ferruginous sandstone	
458	A/6/Ia	11	47/46/10	Discoidal/jasper	
1627	A/96/III	16	54/52/32	Discoidal/ferruginous sandstone	*Fig. 4.83*
742	A/19/Ia	11	73/82/34	Discoidal/ferruginous sandstone	
1885	A/62/Ia	11	64/62/23	Discoidal/ferruginous sandstone, eroded	*Fig. 4.83*
1805	A/86/I	10	46/35/21	Discoidal/ferruginous sandstone, eroded	*Fig. 4.83*
541	A/25/Ia	11	49/57/2	Core on flake/ferruginous sandstone, eroded	
1204	A/93/II	11	42/48/11	Core on flake/ferruginous sandstone, eroded	*Fig. 4.83*
226	A/55/Ia	11	26/22/18	Changed orientation/chert, eroded	
1611	A/39/Ia	11	22/32/20	Single platform/chert, eroded	
739	A/48/Ia	11	35/17/23	Changed orientation/chert, eroded, burnt	
1253	A/17/Ia	11	30/42/28	Single platform/chert, eroded	

Cores

The most numerous group is made up of relatively small (compared to the size of certain flakes) discoidal forms, undoubtedly residual in terms of the stage of reduction [*Figs 4.83:1627, 1800, 1805*]. Commenting on this phenomenon, Andrzej Wiśniewski (personal comment, 2017) points out that discoidal cores are present alongside Levallois ones in many Middle-Palaeolithic assemblages, apparently playing (rather the products of these cores than the cores themselves) a part in butchering practice at least as often as predetermined tools. Wiśniewski also thinks that the presence of discoidal methods may be a sign of a slightly longer stay with optimal access to raw material. While one can hardly disagree with the view that artifacts both with facetted butts and other types (by implication non-Levallois) can be present among the tools (in a functional, not formal sense), one would be hard put to prove (with refittings?) that given flakes were actually the product of processing with the discoidal method rather than the effect of initial stages of Levallois reduction. Refittings of blocks of chert from site AFD23 (see above) display a full spectrum of flake forms resulting from the shaping of Levallois cores, with many having been transformed

into denticulate tools. These refittings have also shown that many cores in the last stage of reduction took on a different shape from that observed at the beginning, whether because the knapper had changed and the new one professed different skills, or because a different knapping strategy had to be embraced once the remodeling of the core anew with a suitably convex flaking surface and the formation of a *chapeau-de-gendarme* platform was no longer possible. Therefore, the presence of a predominant number of small discoidal cores could testify to the intensity of reduction processes right down to residual forms. Contrary to Wiśniewski's suggestion, it signifies limited access to suitable raw material rather than a longer stay in a place satisfying a toolmaker's needs for suitable nodules. In this interpretation, the assemblage of sandstone cores from AFD111 indicates distance from the sandstone outcrops at the edge of the plateau rather than permanent access to the raw material source. It could have been caused by the low quality of these particular pieces of rock available near the loci.

The only core identified as a residual core, manufactured from a pink variety of quarzitic sandstone, and was not different in terms of size. In turn, forms with an evident Levallois schema of reduction possessed slightly elongated proportions [*Fig. 4.83:1621, 1800, 1805*]. The two cores made from large flakes [including *Fig. 4.83:1204*] are of medium size, which also confirms the supposition concerning the final dimensions of other core forms. The group of microlithic cores (both with single platforms and with changed orientation), all made exclusively of a fine-grained raw material, is a component of the Early-Holocene assemblage.

The two cores defined as Nubian variant II (Guichard and Guichard 1968), representing specimens of similar size, were recorded barely a meter apart [*Fig. 4.83:1621*]. However, in the case of AFD111, where both horizontal and vertical relocation of the lithic artifacts (and animal bone remains) is highly probable, this need not be proof of a mutual spatial relationship. Mapping of the current position of the artifacts revealed no clear clusters despite a fairly limited scatter area. One should also note traces of edge and surface erosion on a significant part of the collection (including cores with a visibly Nubian schema of reduction).

Flakes

Given their predominance in this assemblage (1114 specimens), flakes made of ferruginous sandstone, presenting defined butt features, were analyzed from the viewpoint of their morphological and metric features (flakes made of other varieties of quarzitic sandstone demonstrate matching values and characteristics; see *Fig. 4.82*; *Table 4.42*). There were also several flakes of chert (including five Levallois flakes and several denticulate forms—significantly more than in the case of the Holocene artifacts; see *Fig. 4.83:1607, 1609, 2063*). These were produced undoubtedly outside of AFD111, but the fact that they were deposited at the site most certainly during the Pleistocene indicates an ongoing supplementation of the local collection with pieces collected on the way. Similar evidence was also recorded in assemblages typical of the workshops in the southwestern sector of AFD23 (see above, § 4.2). Therefore, the analysis of further assemblages is crucial—also bearing the hallmarks of workshop (predominance of one raw material; presence of correlates of all stages of reduction)—in order to show the context and to attain a better understanding of the adaptation strategies of MSA groups in the microregion of the Affad Basin.

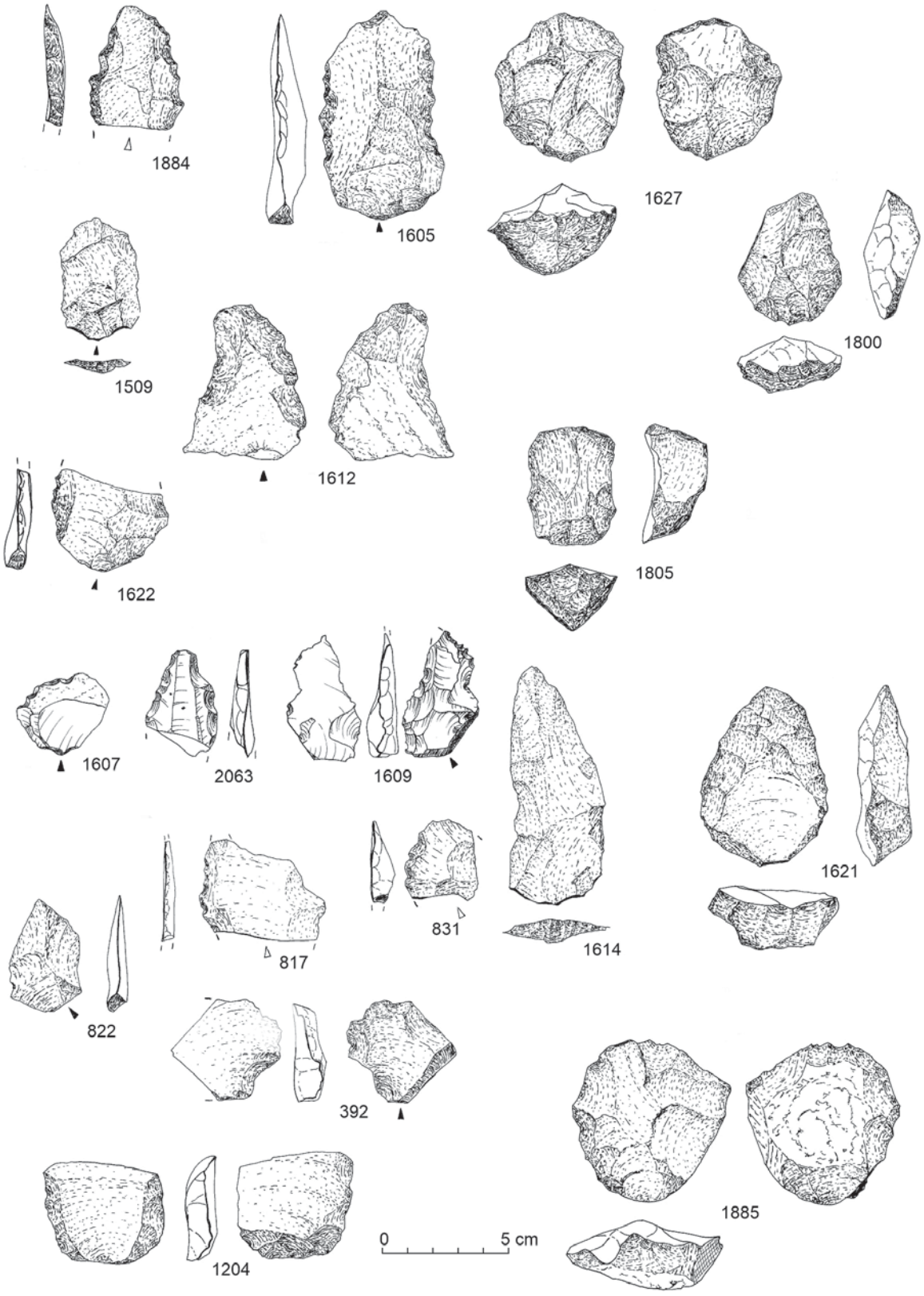
1884
1605
1627
1509
1800
1612
1622
1805
1607
2063
1609
1621
831
817
1614
822
392
1885
1204
0
5 cm

Fig. 4.83. Formal tools from site AFD111: denticulate tools – quarzitic sandstone: 1884, ferruginous sandstone: 392, 817, 822, 831, 1605, chert: 1607, 1609, 2063; Levallois flake – ferruginous sandstone: 1509, 1622; elongated Levallois flake – ferruginous sandstone: 1614; flake with semi-abrupt retouch on both dorsal and ventral faces – ferruginous sandstone: 1612; final forms of flake cores – ferruginous sandstone: 1627, 1800, 1805; core on flake – ferruginous sandstone: 1204; Nubian core – ferruginous sandstone: 1621; Levallois core – ferruginous sandstone: 1885

Natural/unprepared butt

Only 18 sandstone flakes in this assemblage had butts not prepared in any way. This unusually low proportion may be explained by the specific nature of the raw material, usually secured from thick layers of sandstone and hence showing relatively less frequently (compared to chert) an eroded/external surface. This view is also supported by the unusually low proportion of natural surface negatives in every category of flakes [*Table 4.40*]. The greatest number of such surfaces was actually recorded in flakes with natural/unprepared butts (although one should keep in mind the small sample).

Flakes with unprepared butts make up two groups, one smaller than 30 mm and the other bigger [*Fig. 4.82A*]. Observations resulting from the refitting of lithic artifacts from the workshop site AFD23 suggest that the smaller flakes could have come from the working of a core striking platform, while the larger flakes were from a flaking surface following the Levallois schema. A simple comparison with predetermined flakes with facetted butts confirms this hypothesis [see *Fig. 4.82A*]. However, the borderline in the case of the AFD111 sandstone collection is set slightly lower than for AFD23 artifacts made of chert (at about 40 mm for the latter), which would suggest smaller dimensions of the striking platform (less thickness but perhaps simply smaller dimensions of the cores) from AFD111.

The sandstone flakes with natural butts bore the most extensive traces of erosion of the edge (and surface) of all flake categories, although their small sample should be taken into account.

Edge butt

Flakes with plain, edge (or simply point and even multifaced butts) [*Fig. 4.82:A,B*] reflect this size relationship in a slightly different manner. Specimens not exceeding 30 mm are definitely more numerous and create a clear cluster, while the larger flakes present a strongly scattered cloud. This suggests that insofar as the formation of large flakes is characterized by a certain randomness related to initial core working for example, these small artifacts reflect a high degree of control on the part of the knapper, who was intent on producing items of such dimensions and similar proportions. We are dealing here naturally with flakes constituting debris, regardless of whether this was a Levallois, discoidal or bifacial schema. Flakes less than 30 mm in length (irrespective of the form of the butt) also bear less traces of erosion (≈43%) than the larger ones (≈53%).

An analysis of the metric data reveals the duality of the collection, but without refittings it is difficult to decide whether this is all workshop debris or a combination of on-the-spot production and pieces collected somewhere on the way. In the first scenario, the diversity in terms of size will correspond to the dynamic process of reduction of a nodule reaching original dimensions of over 100 mm (the largest pieces in the collection), even though the most frequently used

Table 4.40. Cortex frequency on flakes with different butts, made of ferruginous sandstone, from site AFD111

Share of cortex	Unprepared butt	Plain/ unifacial butt	Point & edge butts	Multi-faced prepared butt	Facetted butt	Distal flake fragments
0%	55.56%	90.04%	87.50%	93.76%	100%	92.49%
10%	11.11%	2.58%	5.00%	2.56%	–	2.24%
20%	11.11%	2.95%	1.00%	1.44%	–	1.84%
30%	–	0.74%	–	0.32%	–	0.66%
40%	5.56%	–	1.00%	0.48%	–	0.26%
50%	11.11%	0.37%	1.50%	0.32%	–	0.26%
60%	–	1.48%	–	0.16%	–	0.40%
70%	–	–	1.00%	0.16%	–	0.26%
80%	–	0.74%	1.50%	0.16%	–	0.26%
90%	5.56%		0	0.16%	–	0.26%
100%	–	1.11%	1.50%	0.48%	–	1.05%

Table 4.41. Damage to flakes made of ferruginous sandstone from site AFD111

Flake damage	Unprepared butt		Plain butt		Point butt		Prepared butt		Facetted butt		Unidentified butt
	∑	%	∑	%	∑	%	∑	%	∑	%	∑
Longitudinal breakage	1	5.56	13	4.80	4	2.00	31	4.96	0	–	0
Transverse breakage	5	27.78	75	27.68	25	12.50	240	38.40	2	25.00	759
Overheating	0	–	0	–	0	–	0	–	0	–	0
Eroded surface	11	61.11	103	38.01	92	45.00	339	54.24	1	12.50	318

technique was shaping small flakes not exceeding 30–35 mm. In the second scenario, the small debris represented knapping at the location while a significant number of the large artifacts would have been brought in from outside, the local workshop being incapable of guaranteeing flakes (functional tool blanks) of such parameters. Taking into account the high degree of erosion of all the flakes (regardless of size), a scenario merging the two models appears to be the most likely one.

A comment on the breakage of sandstone flakes is in order here. Insofar as the overwhelming majority of longitudinal breakage (fractures) occurred while detaching the artifact (Siret accident), lateral breakage could have occurred at any stage: manufacturing, usage, deposition and post-deposition. The clear superiority of lateral breakage over longitudinal one (several times over) stands in clear opposition to chert flake damage as recorded on finds from the workshop in the southwestern sector of AFD23 where damage of both kinds was recorded in much the same proportions [see above, *Table 4.6*]. It is most probably due to the characteristics of the raw material (sandstone is significantly less dense, more coarse-grained and thereby more susceptible to fracturing).

Table 4.42. Thickness-to-width (mm) correlation of flakes made of ferruginous sandstone from site AFD111. Width presented as a range and, in parentheses, as a median (in cases of more than two artifacts)

Thickness	Unprepared butt	Plain/uniface butt	Point & edge butt	Multi-faced prepared butt
1	–	11–17 (12)	6– 20 (11)	6–16 (10)
2	–	7–22 (13)	7–22 (13)	8–22 (15)
3	24–27	8–27 (17)	8–28 (18)	9–28 (17)
4	21–23	10–29 (22)	11–37 (18)	9–38 (20)
5	14–30	8–50 (21)	16–44 (24)	11–45 (22)
6	14–24 (19)	11–43 (26)	11–38 (25)	12–64 (20)
7	20	17–48 (27)	19–45 (24)	5–60 (24)
8	24–31	20–48 (30)	25–51 (33)	18–67 (31)
9	–	27–62 (29)	29–56 (37)	18–62 (34)
10	–	19–53 (36)	23–35	20–56 (36)
11	–	25–46	12–28	22–60 (42)
12	41–42	30–36 (36)	48–74	30–53 (43)
13	33–57	33–55 (45)	32–40	28–65 (36)
14	29	60	30–64	28–33
15	–	25	–	28
16	–	29–67	47	–
18	–	–	52	63
22	–	50	–	–
24	–	–	80	–

A comparison with the collection from the southwestern sector of AFD23 also reveals that longitudinal fractures (Siret accident) occurred while processing sandstone three times less often (up to 5%) than in the case of chert (up to 16%), which stands in opposition to the general view regarding sandstone as a coarse-grained raw material, namely one more susceptible to this kind of damage (Inizan, Roche, and Tixier 1992).

Chunks

A total of 20 artifacts made of ferruginous sandstone could be assigned to the chunks group. The dimensions of the largest chunks [*Fig. 4.85*] determine the lower size range of nodules subjected to processing. In other words, chunks comprised nodules even smaller that cores defined as residual cores. Eight of them bore traces of erosion.

Predetermined products and tools

Flakes with facetted butts without macroscopically observable traces of use (retouching, smoothing, wear) are among the most numerous ferruginous-sandstone products in the predetermined tool category. They are characterized by somewhat elongated forms [*Fig. 4.86*], as well as dimensions exceeding 30 mm in length and 25 mm in width; the largest examples reached a length of

80–100 mm and a width of 40–50 mm [e.g., *Fig. 4.84:1893*]. Considering that the largest flakes exceed the dimensions of cores from Affad 111, it has to be accepted that none of the cores in the set represent initial stages of reduction. One can only surmise that the large flakes had to be brought to the site of the AFD111 encampment from outside.

The Levallois flakes from AFD111 had no part of the external nodule surface preserved on their dorsal sides [see *Table 4.40*], meaning that they had been detached as flakes with facetted butts from worked cores, just like chert artifacts found in the southwestern sector of AFD23. The pattern of negative scars on the dorsal side of these flakes corresponds with the centripetal treatment of the flaking surface. No points that could correspond to the two Nubian-type cores in the collection were recorded.

Lateral breakage was observed in two cases. One flake also bore traces of accidental chipping of the edge.

The most common form of tool were flakes (not only with facetted butts!) with denticulate retouching covering one or two opposite edges. In one case [see *Fig. 4.83:1612*], the retouching covered both surfaces, the positive side taking on a flat form while the negative side demonstrated quite an abrupt angle. The tools come in both sandstone and chert, the latter bearing, without exception, traces of intense erosion, hence undoubtedly brought in from outside. One of these tools—an incomplete specimen—features a clearly retouched notch.

The collection includes a small bifacial tool made of sandstone—a small thick handaxe [see *Fig. 4.84:1868*]. The only thing that distinguishes it from a residual discoidal cores of almost the same size is its amygdaloid shape, hence it could very well be an atypical core form. Assuming forms of this kind found a utilitarian/instrumental application during the Late Pleistocene, it seems probable that the artifact from AFD111 was the intended outcome, which would explain the high numbers of small flakes in the collection.

Clearly retouched perforators were also recorded among the sandstone products. One of these had a sting diverging from the morphological axis; typologically, this is a claw [see *Fig. 4.84:1526*]. Tools of this type were not recorded in the collection from the southwestern sector at AFD23.

Typical microlithic forms—small backed blades and truncations, scrapers, perforators and borers—made exclusively of cryptocrystalline raw materials (flint, chert) that are part of this category come from Holocene manufacturing/usage contexts and were recorded exclusively in the top layer (0–10 cm from the surface).

Recapitulation

The AFD111 Pleistocene lithic artifact assemblage cannot be taken as evidence of a workshop applying Levallois methods to process sandstone raw material, even in the vicinity of the outcrop as had been initially assumed based only on the presence of the cores, numerous flakes and predetermined items, as well as the proximity of the edges of the Cretaceous plateau. A simple comparison of the size of certain categories of artifacts leads one to the conclusion that quarzitic sandstone was processed by a technique that called for detaching relatively small flakes and rarely applying facetting of the butt. The largest Levallois flakes were brought into the area of the encampment from outside, just like all the forms made of cryptocrystalline materials (chert, flint). Therefore, only small Levallois flakes (maximum 50 mm in length and 45 mm in width) could have been made in this area: the dimensions of two Nubian cores found at the site correspond to

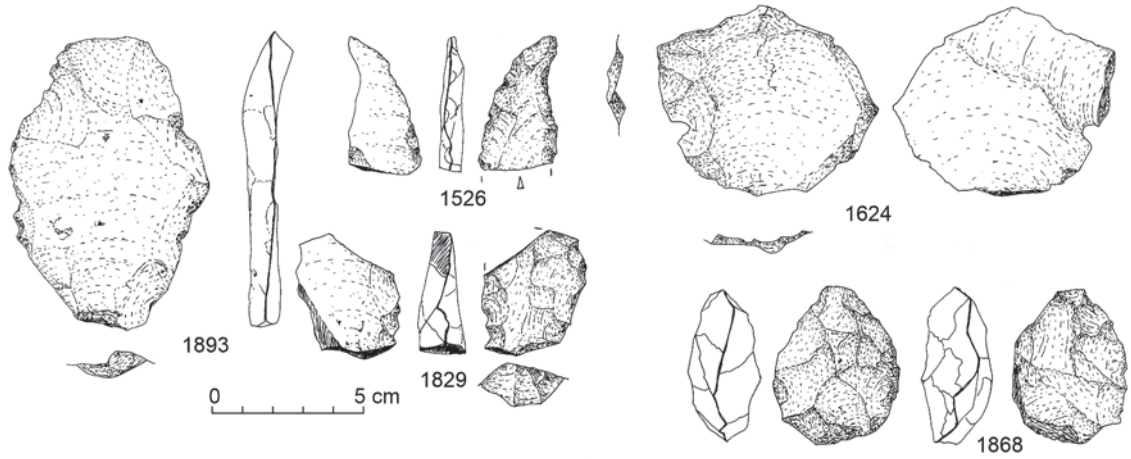

Fig. 4.84. Selected lithic artifacts, made of ferruginous sandstone, from site AFD111: Levallois flake – 1893; "Zinken" – 1526; Levallois flake with bifacial retouch (fragment) – 1829; plunging Levallois flake – 1624; small handaxe – 1868

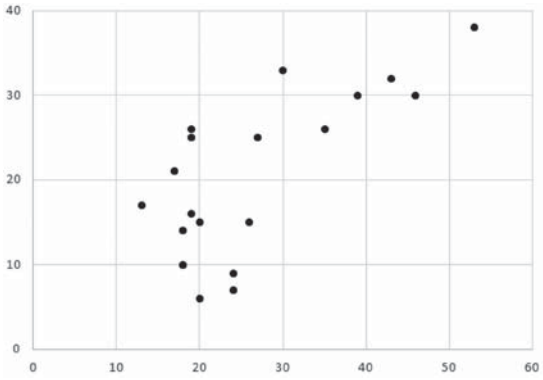

Fig. 4.85. Chunks (two largest measurements) from site AFD111: length-to-width correlation (mm)

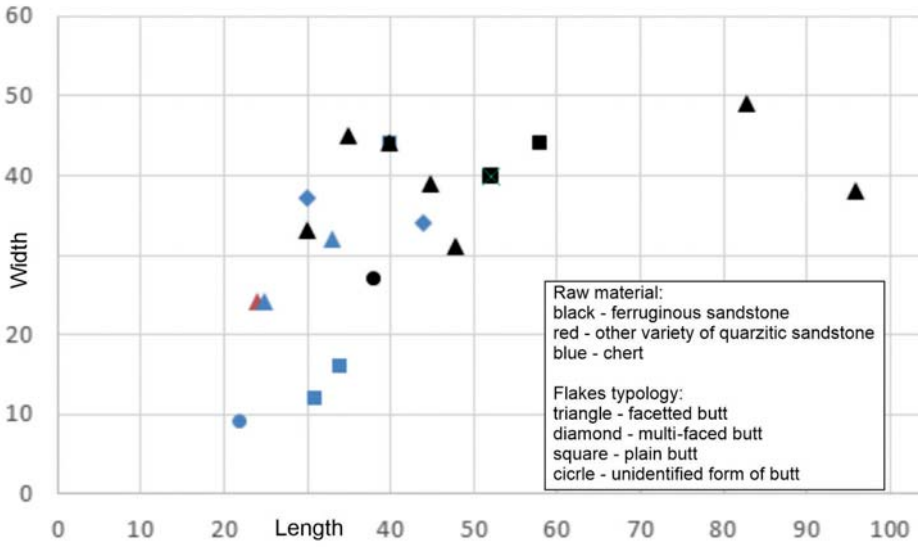

Fig. 4.86. Predetermined flakes or those constituting a blank for retouched tools (only complete specimens considered) from site AFD111

Table 4.43. Levallois flakes and retouched tools from site AFD111

Inv. No.	Locus	Context	Dimensions (mm)	Description/raw material	Reference/ Comment
0019	A/96/V	18	30/33/7	Levallois flake/ferruginous sandstone	
0166	A/87/II	15	(25)/40/7	Levallois flake, fragment/ferruginous sandstone	
0646	A/2/Ia	11	40/44/6	Levallois flake/ferruginous sandstone, eroded	
0900	A/84/Ib	12	45/39/8	Levallois flake/ferruginous sandstone	
0902	A/93/Ib	12	35/45/7	Levallois flake/ferruginous sandstone	
1509	A/96/IV	17	48/31/3	Levallois flake/ferruginous sandstone	*Fig. 4.83*
1614	A/35/Ic	11	96/38/7	Levallois flake/ferruginous sandstone	*Fig. 4.83*
0286	A/36/Ia	11	24/24/5	Levallois flake/quarzitic sandstone, eroded	
1140	A/40/I	10	(28)/28/7	Levallois flake, fragment/quarzitic sandstone	
0227	A/55/Ia	11	(17)/(20)/5	Levallois flake, fragment/chert, eroded	
0421	A/58/Ia	11	25/24/6	Levallois flake/chert, eroded	
0653	A/2/Ia	11	33/32/7	Levallois flake/chert, eroded	
0673	A/34/Ia	11	(27)/36/10	Levallois flake, fragment/chert, eroded	
0980	A/37/Ia	11	(19)/(18)/3	Levallois flake, fragment/chert, eroded	
0392	A/97/II	15	40/44/11	Denticulate tool on plain butt flake/ ferruginous sandstone	*Fig. 4.83*
0831	A/63/Ia	11	(31)/30/8	Denticulate tool, fragment/ferruginous sandstone, eroded	*Fig. 4.83*
1605	A/3m to E	10	83/49/13	Denticulate tool on Levallois flake/ferruginous sandstone, eroded	*Fig. 4.83*
1612	A/89/I	10	58/44/13	Denticulate tool on plain butt flake/ ferruginous sandstone, 60% cortical, eroded	*Fig. 4.83*
1622	A/45/Ia	11	(42)/47/4	Denticulate tool on Levallois flake, fragment/ ferruginous sandstone	*Fig. 4.83*
1829	A/96/Ib	12	(40)/35/13	Denticulate tool on prepared butt flake/ ferruginous sandstone	*Fig. 4.84*
2086	B/69/Ib	32	(38)/50/14	Denticulate tool on prepared butt flake, fragment/ferruginous sandstone, eroded	
1884	A/65/Ib	12	(48)/37/6	Denticulate tool, fragment/quarzitic sandstone	*Fig. 4.83*
0472	A/76/Ia	11	(32)/27/5	Notched tool, fragment/chert, eroded	
1607	A/51/Ia	11	30/37/7	Denticulate tool on prepared butt flake/chert, 5% cortical, eroded	*Fig. 4.83*
1609	A/97/IV	17	44/34/11	Denticulate tool on prepared butt flake/chert, eroded	*Fig. 4.83*
2063	A/65/Ia	11	(40)/28/6	Denticulate tool, fragment/chert, eroded	*Fig. 4.83*
1868	A/95/Ib	12	52/40/23	Small handaxe/ferruginous sandstone	*Fig. 4.84*
1526	A/97/VII	20	(43)/26/7	Perforator, fragment (Zinken)/ferruginous sandstone	*Fig. 4.84*
1818	A/93/I	10	38/27/7	Perforator/ferruginous sandstone, eroded	
0137	A/29/I	10	(12)/20/7	Endscraper, fragment/chert, 5% cortical	Holocene
1613	A/50/Ia	11	(20)/8/4	Perforator, fragment/chert	Holocene
1894	A/8/Ia	11	22/9/4	Borer/chert, eroded	Holocene
1527	A/29/I	10	(25)/9/3	Backed blade, fragment/chert	Holocene
1606	A/49/Ia	11	31/12/3	Use-retouched blade/chert, 5% cortical	Holocene
1608	A/51/Ia	11	(19)/13/3	Truncation, fragment/chert	Holocene
1610	A/39/Ia	11	34/16/4	Backed blade/chert, eroded	Holocene

these flakes (despite the lack of points from a corresponding category). However, this division in terms of size decidedly does not match up with the initial assumption that the workshop was located near a natural sandstone outcrop where large artifacts from initial working should be quite common. It is more likely that the workshop was nowhere near any sandstone source and only small nodules, undoubtedly initially shaped elsewhere, were processed here. It is not possible to determine whether they all came from one outcrop or whether they were also gathered over a larger area. In favor of the second scenario is the presence of artifacts made of various raw materials. However, one may indicate with a high degree of probability that the manufacturing of small discoidal cores (rarely exceeding 70 mm in diameter) most frequently constituted the end outcome of the processing. Analogous artifacts are often viewed as tools from a functional point of view and it is not to be excluded that such was also the intent of the AFD111 knappers.

The matching chronology of all of the sites in the Affad Basin also raises the issue of raw material preferences. Single artifacts made of chert indicate a workshop of the type found in the southwestern sector of AFD23 being on hand in the contemporaneous landscape. However, the group in question preferred to use a significantly more coarse-grained raw material. Late Pleistocene users satisfied their short-term needs most probably with such stone tools, access to outcrops of chert not being necessarily an absolute requirement (as was the case of the significantly later microlithic production). An attractive hypothesis explaining this variation among the sites is the seasonality of the environment with the fluctuating stages of the Nile. Workshops with a predominant sandstone raw material base would have therefore corresponded to summer campsites when ancient river-pebbles containing chert nodules were not available.

4.3.3 Site Affad 131 (AFD131)

The field survey at site AFD131, which was cut short in 2018—barely a year after discovery—by bulldozing to convert the land to agricultural use, covered an area of approximately 200 × 200 m. Methodical exploration was conducted within an established grid of trenches. Distinct concentrations of partly fossilized animal bone and stone artifacts recorded on the surface were excavated archaeologically: the southern half of Are 55, the eastern half of Are 65, all of Are 66, the northern half of Are 76 and the northwestern quadrant of Are 77 [see above, *Fig. 2.13*, area enclosed in red). In addition, a longitudinal section was exposed in the eastern part of the site. Analyses of the geomorphological samples collected from this section contributed data on the general processes of site formation in the Affad Basin (see above, § 2.3.3). The results have indicated the presence of a Pleistocene settlement in the zone on the bank of a river channel formed approximately 65,000 years ago. At the time (probably in MIS3), the area probably still conformed to this description, but it must have already been offset from the very edge of the terrace. Neither should one rule out episodes of elevated river levels and re-inundation of the land. The area of the former channel was most certainly a permanent depression, where elements flushed in from a northeasterly direction accumulated.

A study of the dispersion of Early Holocene artifacts well reflected this phenomenon of secondary relocation. Chert/flint artifacts, most of which are assumed to be from the beginning of the Holocene, were found to be spread fairly evenly over the investigated area, a slightly more intense

concentration occurring in the southwestern section [*Fig. 4.87*; see *Tables 4.44, 4.45*]. This concentration consisted of overheated artifacts and retouched microlithic tools, which occurred elsewhere on site as well, but were much more dispersed. The present location of these particular artifacts may be regarded as an indicator of the erosion of the sediment post-dating the Early Holocene and the direction of flow of the small artifacts in later times. Assuming a likely scenario that erosion-flushing processes were consistent with the slope of the terrain observed today (toward the southwest), the evident concentration of artifacts would indicate a natural redeposition zone of small artifacts. Therefore, the Early Holocene settlement itself must have been located outside the surveyed area, on the slightly higher bank of the former channel (as at site AFD111). These artifacts are generally heavily rolled and patinated, which also indicates advanced erosion processes after initial deposition in an archaeological context. The almost complete absence of pottery (only two small fragments) and bone remains, differing in their state of preservation from mineralized Pleistocene bones, should also be noted. Both these categories of archaeological materials, commonly found at Early Holocene sites, were probably less resistant to erosion than stone artifacts. A mapping of artifacts of agate and quartz, almost certainly not of Pleistocene date, shows a similar chaotic dispersion [see *Fig. 4.87*].

A certain share of Pleistocene artifacts made of chert must be considered as well (e.g., although several denticulate tools were made from a Levallois blank; see *Figs 4.93:3475; 4.97:133, 4575, 7842*), we are unable to distinguish them unless they are typical products.

The case is different with the distribution of quarzitic sandstone artifacts. Here, a linear dispersion pattern is observed, following the course of the palaeochannel, coupled with two discrete clusters of flakes [*Fig. 4.88* top]. This raw material was used to make retouched tools: several denticulate/notched tools associated with Pleistocene production and one Holocene quern fragment

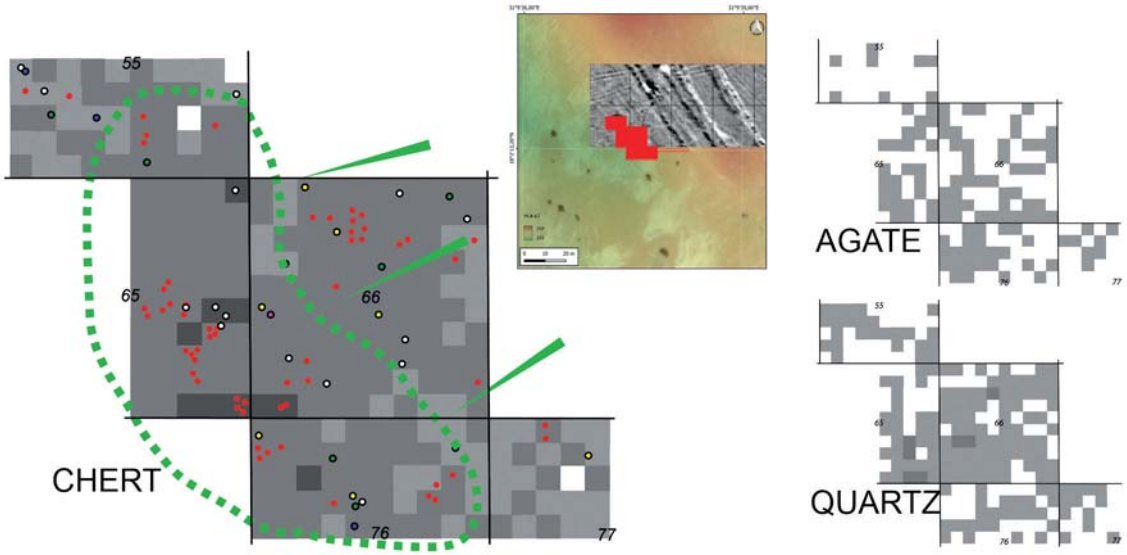

Fig. 4.87. Dispersal of artifacts at site AFD131: top, artifacts made of chert, bottom left, artifacts made of agate; bottom right, artifacts made of quartz. The darker a unit, the greater the number of artifacts. Symbols: red – overheated artifacts; white – Early Holocene backed blade tools; yellow – scrapers; green – perforators/borers; blue – use-wear retouch tools; purple – bifacial tools. Green arrows indicate likely direction of erosion-flushing of small artifacts; green dashed line – probable redeposition zone

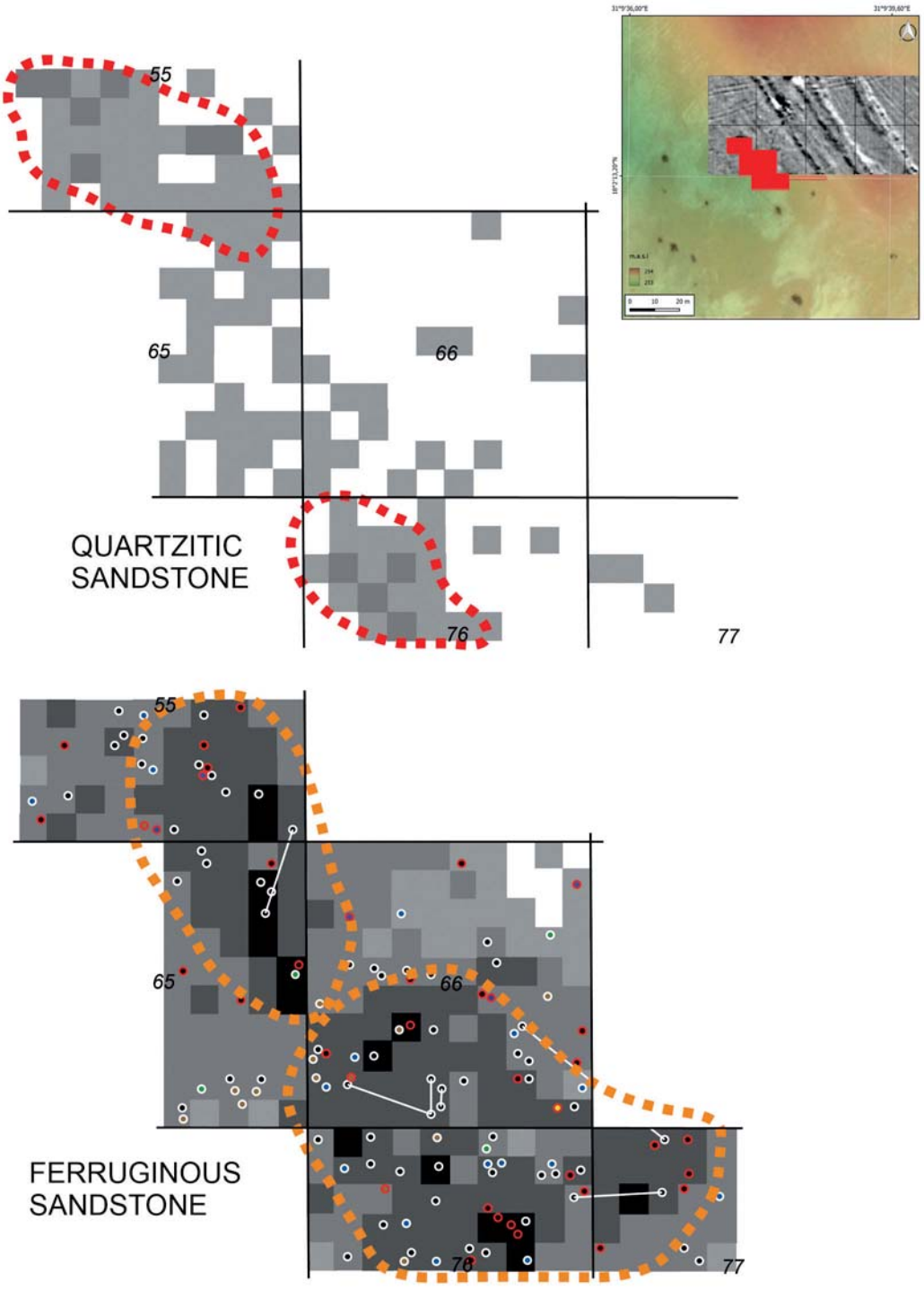

Fig. 4.88. Dispersal of artifacts at site AFD131: top, quarzitic sandstone; bottom, ferruginous sandstone. Symbols: black – ferruginous sandstone, brown – quarzitic sandstone, blue – chert, green – light variety of chert, yellow – quartz; white dashed line – location of tools; red dashed line – location of cores

were recorded. Since quern production required raw material of suitable size to be available on site, one can safely exclude most of the flakes from AFD131 from this kind of production. Interestingly, the clusters of quarzitic sandstone flakes appear on the peripheries of the concentration of ferruginous sandstone products [compare *Fig. 4.88* bottom]. This probably illustrates intentional deposition of processing waste during the Pleistocene settlement episode (rather than natural dispersion due to water flowing in the channel).

Two distinct zones of deposition in distinct concentrations exceeding 100 pieces per square meter [*Fig. 4.88*; black symbols] have been mapped for artifacts made of ferruginous sandstone. No other raw material was observed to show such concentrations. One should add at this point that natural outcrops of this raw material are located about 4 km north of the site. The Pleistocene date of this material is near certain considering that nothing like a bladelet-microlithic component was recorded among the retouched sandstone tools. Their state of preservation distinguishes them from the chert artifacts: they do not have smooth edges in such proportions (only 238 artifacts out of 6026 made of ferruginous sandstone). However, the intensive edge rolling of individual sandstone tools can be explained in two ways: either they were brought to the site in this form from outside (similarly to the double-patina chert denticulate tools), or they had migrated over time within the sediment and were eroded together with the Holocene assemblage. The circumstances of such migrations may have been both natural and anthropogenic (Holocene settlers may have exploited them by deliberately excavating or finding them on the surface). In general, however, the state of preservation of the entire assemblage of sandstone artifacts indicates little erosion, supporting the possibility that the Pleistocene artifacts lie in a relatively unchanged location (unlike the chert microlithic artifacts), although the assemblages are not as legible as in the case of AFD23.

To conclude, the assemblage of artifacts from AFD131 perfectly complements the collection from AFD111, where most of the artifacts were made also of ferruginous sandstone, although at the latter site the degree of displacement of the finds excluded spatial analysis (see above). The proportion of artifacts bearing traces of surface and edge erosion was also much higher there, namely, 884 out of 1921 sandstone artifacts.

Cores

The collection from AFD131 does not record a single example of a pre-core or even one from the initial stage of processing, that is, before the detachment of a predetermined product (save for two examples of small initial forms from large flakes/chunks [*Table 4.46*; *Fig. 4.93:6533*]). The cores were for the most part referred to as Levallois or final Levallois because of the still clear pattern of flaking surface definition and striking platform faceting. Only one core corresponded formally to the Nubian II type (Guichard and Guichard 1968), the others allowing the detachment of flakes rather than points. Yet the cores described as discoidal—recorded in slightly smaller numbers as the collections from AFD23 and even AFD111—may have represented in fact the final form of reduction of a Levallois core or cores used without striking platform faceting from the beginning. The least recognizable specimens were termed residual cores when they took the form of polyhedral chunks. These peculiar core reduction dynamics indicate a pressing deficit of raw material. Almost all of the cores were reduced not only in size but also in form, assuming, of course, that the Palaeolithic knappers from AFD131 had the intention, knowledge and skills to make tools employing Levallois methods.

Table 4.44. General morphological-technological structure of the collection of stone artifacts from site AFD131; microlithic (Early Holocene) artifacts in italics; data on quartz and agate artifacts (100% of Holocene age) not included

Artifact group	Type	Raw material			Total
		Ferruginous sandstone	Quarzitic sandstone	Chert/ flint	
Cores	Initial cores and tested nodules	0	0	0	0
	Cores for flakes/points	1	0	0	1
	Final cores	25	3	5	34
	Discoidal cores on flakes	2	0	0	2
	Uniplatform microlithic cores (Holocene)	0	0	*20*	*20*
Flakes and chips	Flakes with unprepared butt	166	7	4	177
	Flakes with plain/uniface butt	739	35	3	777
	Flakes with point & edge butts	422	30	1	453
	Flakes with multi-faced prepared butt	853	85	5	943
	Flake fragments	3179	74	1240	4493
Chunks	Chunks	546	40	1429	2015
Predetermined products and formal tools	Levallois flakes	63	5	12	80
	Points	1	0	0	1
	Flakes/points with denticulate retouch	10	3	12	25
	Flakes with burin blow	0	0	0	0
	Flakes with abrupt retouch	1	0	7+	5
	Bifacial forms	11	19	–	1
	Backed tool (Holocene)	0	0	*1*	*1*

Table 4.45. Raw material structure of the collection from site AFD131 (number of retouched tools in brackets; microlithic tools in italics)

Chert		Flint, mudstone, agate		Quarzitic sandstone		Ferruginous sandstone		Quartz		Conglomerate, petrified wood		Total
n	%	*n*	%	*n*	%	*n*	%	*n*	%	*n*	%	
2583 [14+*17*]	27.38	176 [0+*6*]	1.86	282 [10]	2.99	6026 [62]	63.89	365 [0+*2*]	3.87	0	–	9432

Cores of a poorer raw material quality appear to be the ones not subjected to further reduction [*Fig. 4.89*]. The cryptocrystalline chert cores are the smallest in the collection. Interestingly, at the beginning of the Holocene, cores of a similar size were considered not suitable for further reduction. Presumably, therefore, if a core was less than 20 mm in diameter, flakes could no longer be separated from it. Of interest also is the fact that sandstone cores with eroded surfaces, which were most probably brought in from outside, were dominated by slightly elongated specimens that were a little less than 50 mm in length. This class includes the only point core (Nubian type) and single cores of quarzitic sandstone and quartzite. As these nodules were not subjected to further reduction, for some reason this size of cores made of coarse-grained rocks constituted the first barrier for Palaeolithic stoneworkers.

Table 4.46. Cores from site AFD131 (excluding residual microlithic forms, single- or multi-platform): dimensions and loci

Inv. No.	Locus	Dimensions (mm)	Description	Reference
2748	65-50-I	57/39/20	Nubian II type core/ferruginous sandstone, eroded	
159	55-62-I	52/43/19	Levallois core/ferruginous sandstone, eroded	
515	55-91-I	56/37/13	Levallois core/ferruginous sandstone	
2934	65-58-I	62/49/16	Levallois core/ferruginous sandstone, eroded	
4285	66-71-I	47/43/11	Levallois core/ferruginous sandstone, eroded	
5556	66-44-I	35/29/11	Levallois core/ferruginous sandstone	*Fig. 4.93*
8320	76-37-I	60/49/19	Levallois core/ferruginous sandstone	
8395	76-38-I	30/26/15	Levallois core/ferruginous sandstone	
8396	76-38-I	48/33/16	Levallois core/ferruginous sandstone	
8524	76-46-I	68/56/26	Levallois core/ferruginous sandstone	
8800	77-03-I	68/68/24	Levallois core/ferruginous sandstone	
8840	77-04-I	40/37/11	Levallois core/ferruginous sandstone	
9006	77-14-I	42/49/21	Levallois core/ferruginous sandstone, eroded	
9358	77-41-I	46/49/23	Levallois core/ferruginous sandstone	
605	55-95-I	37/29/10	Final Levallois core/chert	*Fig. 4.93*
720	55-58-I	33/32/21	Final Levallois core/ferruginous sandstone	
815	55-67-I	44/32/19	Final Levallois core/ferruginous sandstone, eroded	
1017	55-77-I	55/41/20	Final Levallois core/chert	
8243	76-30-I	42/28/9	Final Levallois core/ferruginous sandstone, eroded	
6712	66-99-I	50/47/18	Discoidal core/quartz	
4197	66-64-I	32/39/12	Discoidal core/ferruginous sandstone, eroded	
5320	66-22-I	27/25/13	Discoidal core/chert	
6452	66-80-I	50/44/19	Discoidal core/ferruginous sandstone	*Fig. 4.93*
1849	65-09-I	57/56/32	Final discoidal core/ferruginous sandstone	
2609	65-46-I	38/35/21	Final discoidal core/ferruginous sandstone, eroded	
603	55-95-I	47/45/11	Final discoidal core/quarzitic sandstone	
5319	66-22-I	35/29/14	Final discoidal core/chert	
6085	66-57-I	43/48/26	Final discoidal core/ferruginous sandstone, eroded	
6283	66-70-I	51/48/23	Final discoidal core/ferruginous sandstone	
9213	77-24-I	38/42/19	Finall discoidal core/ferruginous sandstone	
6106	66-57-I	31/36/8	Final discoidal core reused as a scraper/chert	
4630	66-82-I	n/o	Final core/quarzitic sandstone	
5614	66-06-I	48/47/23	Final core/ferruginous sandstone, eroded	
7256	76-23-I	22/30/24	Final core/quarzitic sandstone	
8015	76-20-I	26/20/14	Final core/ferruginous sandstone, eroded	
6533	66-88-I	50/40/15	Initial core on flake/ferruginous sandstone	*Fig. 4.93*
8166	76-27-I	66/38/23	Initial core on chunk/ferruginous sandstone	

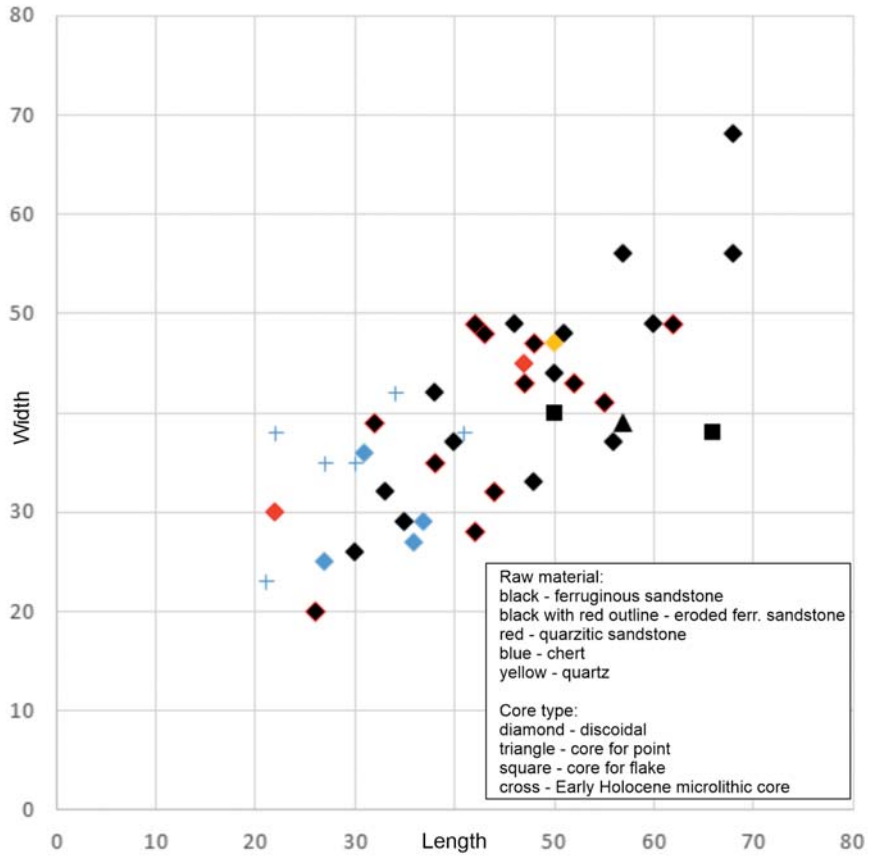

Fig. 4.89. Cores from AFD131: length-to-width correlation (mm)

Flakes and chips

As at AFD111, flakes of ferruginous sandstone and quarzitic sandstone were the prevailing category of lithic finds. Flakes from other raw materials produced during the Pleistocene were also recorded and will be discussed where relevant.

The assemblage is severely fragmented and damaged [*Table 4.48*]. Of a total of 5359 ferruginous sandstone artifacts, as many as 3179 (almost 60%) are small medial or distal fragments (32% in the case of flakes made of other sandstone varieties). The influence of rock material quality on the (presumably) accidental fracturing of artifacts is therefore clearly evident. Ferruginous sandstone nodules were presumably the easiest to obtain, but at the same time they did not offer the same quality as other varieties of rock (assessed by the percentage of flakes cracking). At the same time, retouched forms were fractured to an equally high degree, as attested by the modest assemblages of fragments of denticulate tools. It appears that both issues of raw material quality at the production stage and deposition/post-deposition (e.g., trampling) conditions affected the state of fragmentation of these artifacts.

Artifacts with unprocessed/natural butts were the least numerous among sandstone flakes with a preserved butt, again in semblance of the collection from AFD111, this being the case for both ferruginous sandstone (7.6%) and other varieties of sandstone (4.5%). This corroborates the idea

Table 4.47. Cortex frequency on flakes with different butts, made of ferruginous sandstone, from site AFD131

Share of cortex	Unprepared butt	Plain/ unifacial butt	Point & edge butt	Multi-faced prepared butt	Facetted butt	Distal flake fragments
0%	92.8%	94.6%	95.5%	96.9%	100%	99.6%
10%	1.8%	1.5%	0.7%	0.7%	–	0.1%
20%	0.6%	0.8%	1.4%	0.9%	–	–
30%	0.6%	0.3%	0.2%	0.1%	–	–
40%	–	0.1%	0.2%	0.1%	–	0.1%
50%	1.2%	0.9%	0.5%	0.2%	–	0.1%
60%	–	1.2%	–	0.4%	–	–
70%	1.2%	–	0.2%	0.4%	–	–
80%	0.6%	0.1%	0.2%	0.1%	–	–
90%	–	0.1%	0.2%	–	–	–
100%	1.2%	0.4%	0.9%	0.2%	–	0.1%

Table 4.48. Damage to flakes made of ferruginous sandstone from site AFD131

Flake damage	Unprepared butt		Plain butt		Point butt		Prepared butt		Facetted butt		Unidentified butt
	∑	%	∑	%	∑	%	∑	%	∑	%	∑
Longitudinal breakage	4	2.4	14	1.9	3	0.7	22	2.6	11	14.6	791
Transverse breakage	54	32.5	265	35.8	120	28.4	356	41.7	32	42.7	3179
Overheating	0	–	0	–	0	–	0	–	0	–	0
Eroded surface	4	2.4	44	5.9	26	6.2	66	7.7	8	10.7	73

about the specific nature of raw material extracted from slabs mostly devoid of weathered, by implication external surfaces. Nevertheless, relatively the greatest number of flakes with natural butts bore fragments of naturally weathered surfaces on the dorsal sides [*Table 4.47*].

The size of ferruginous sandstone flakes with unprocessed butts clearly clusters below the 40 mm limit [*Fig. 4.90*; *Table 4.49*]. They clearly differ in this respect from predetermined products (with facetted butts), indicating their true nature as leftovers from the preparation of small-sized cores. This confirms the conclusions formulated with regard to analogous products from AFD111, although no such clear distinction between the two size classes (below and above 30 mm) could be noted here.

Simple size comparisons of the other flake categories (with plain, edge or multi-faced butts) [*Fig. 4.90* bottom] correspond very well with the picture developed for the collection from AFD111. Small, non-bladelet products less than 30 mm in diameter clearly dominated the set. The larger flakes (rarely exceeding 60 mm) must undoubtedly have come from the initial stages of preparing large cores, which the collection from AFD131 does not include. Therefore, as in the case of the assemblage from AFD111, one has to assume that artifacts of this size were brought in from outside for *ad hoc* use as functional tools, even as reductions were made on site to much smaller flake cores, which, incidentally, are present in the collection.

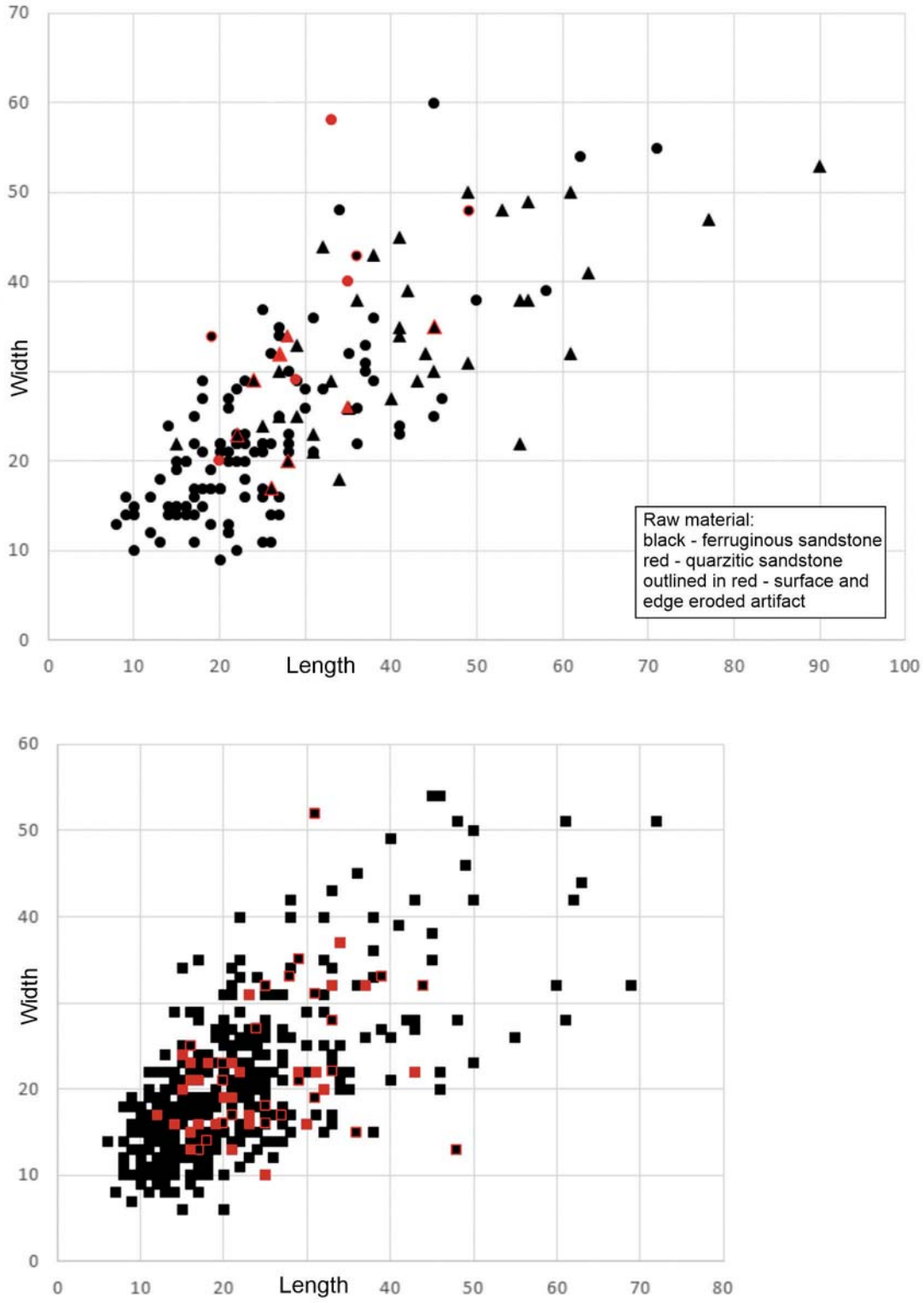

Fig. 4.90. Flakes from site AFD131: length-to-width correlation (mm).
Top, with unprocessed (circles) and facetted (triangles) butts; bottom, with plain butts

Table 4.49. Thickness-to-width (mm) correlation of flakes made of ferruginous sandstone from site AFD131. Width presented as a range and a median (in cases of more than two artifacts)

Thickness	Unprepared butt	Plain/uniface butt	Point & edge butt	Multi-faced prepared butt
1	–	5–19 (11)	6–20 (11)	17–27 (17)
2	11–30 (13)	6–29 (14)	8–27 (14)	8–29 (15)
3	10–26 (15)	7–34 (16)	9–41 (25)	8–41 (17)
4	11–29 (16)	6–42 (18)	10–28 (18)	10–47 (20)
5	10–37 (20)	13–40 (20)	11–35 (19)	12–45 (22)
6	9–41 (23)	11–40 (22)	13–40 (27)	14–47 (26)
7	18–34 (22)	19–40 (23)	18–47 (24)	12–53 (30)
8	21–43 (27)	13–52 (25)	16–41 (29)	17–60 (30)
9	23–32 (26)	9–48 (27)	18–38 (22)	22–47 (31)
10	36–43	22–51 (28)	33–42	26–45 (35)
11	27–50 (29)	19–51 (32)	10–26 (24)	35–57 (43)
12	25–60 (30)	20–40 (32)	37–44	28–46 (38)
13	26–66 (36)	28–42 (28)	34	26–35
14	39–61	39–54 (42)	33	–
15	36–48	17–63 (54)	–	40–64
16	–	42–51	–	58–75
17	48	–	–	30
18	–	–	43	–
19	–	26	38	57
22	–	–	–	–
24	–	–	–	–
25	54	–	–	–
26	–	64	–	–

In general, therefore, the picture of stone products from AFD131 corresponds with that presented for the collection from AFD111. The rich inventory of flakes, which are production waste from the preparation stage of Levallois or discoidal cores, indicates local processing of nodules not exceeding 70 mm in diameter and, at the same time, not smaller than 30 mm. Artifacts of larger sizes were brought to the encampment from outside and should not be directly associated with the range of manufacturing capabilities of the group from AFD131. They were, however, within the range of the group's stone instrument collection, that is, deliberately collected and brought to the encampment presumably with the intention of using them as tools or as semi-processed material, as exemplified by an initial core from a large flake [*Fig. 4.93:6533*].

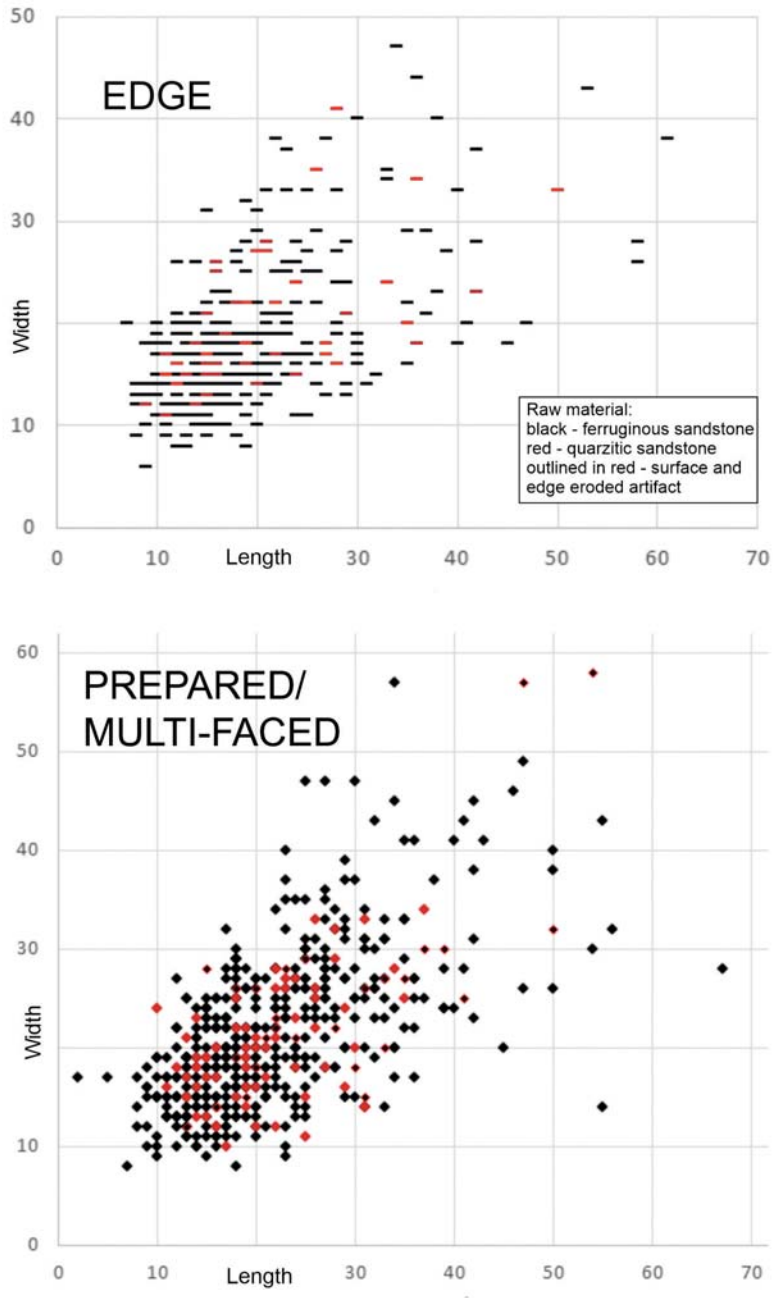

Fig. 4.91. Flakes from site AFD131: length-to-width correlation (mm). Top, with edge butts; bottom, with prepared/multi-faced butts

Chunks

546 ferruginous sandstone artifacts from AFD131 were assigned to the chunks group. The sizes of the largest chunks [*Fig. 4.92*] determined the lower size ranges of nodules subjected to processing, in similarity to the collection from AFD111. In other words, the chunks represented nodules even smaller than cores defined as residual cores.

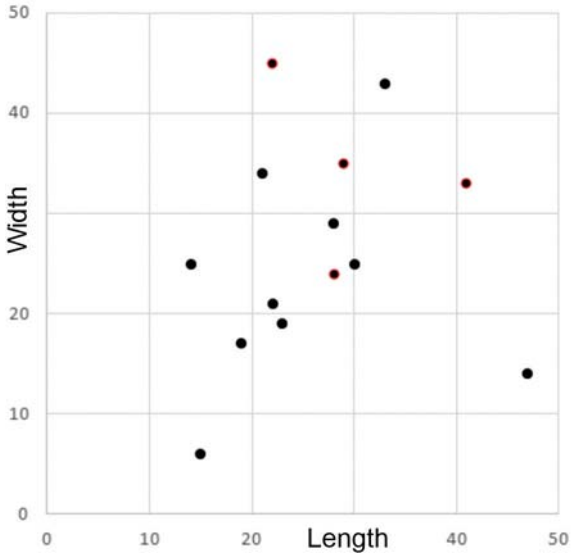

Fig. 4.92. Selected ferruginous sandstone chunks (two largest dimensions) from site AFD131: length-to-width correlation (mm)

PREDETERMINED PRODUCTS AND TOOLS

Flakes with facetted butts, without macroscopically discernible traces of use (retouching, smoothing, burnishing) were among the most numerous products of the predetermined products category made of ferruginous sandstone, same as at AFD111. They were characterized by slightly elongated forms [*Figs 4.93, 4.94*] and sizes exceeding 20 mm in length and 15 mm in width. Signs of intensive erosion on most of the smallest specimens suggest that they were brought in from outside the encampment. The largest predetermined flakes reached a length of 70–110 mm with a width of 40–50 mm [e.g., *Table 4.50*; *Fig. 4.93, 4.94*]. Since the largest flakes exceed the size of cores from AFD131, there are no cores from early stages of reduction of such size in the assemblage. In addition, none of initial flakes reached this size. Therefore, it is presumed that large artifacts were brought in to the encampment, again in analogy with the assemblage from AFD111.

The Levallois flakes from AFD131 did not have any fragments of the natural nodule surface retained on the dorsal side [see *Table 4.47*]. This means that flakes with facetted butts were detached from the processed cores, same as the chert products from the southwestern sector of AFD23. In the case of all Levallois flakes, the pattern of negatives on the dorsal side corresponds to the centripetal variant of flaking surface preparation. No points that could correspond to the presence of Nubian-type cores were recorded.

The damage recorded on retouched forms and flakes with facetted butts [see *Table 4.48*] does not detract from the overall state of preservation of this assemblage. The most common damage comprises transverse fractures, presumably caused by tool use or even by post-depositional factors. Longitudinal fractures were never recorded on retouched forms, which also argues for the occurrence of this type of impact only at the flake production stage. Yet, pronounced surface and edge erosion were recorded on slightly more than 10% of the artifacts in this category, which should

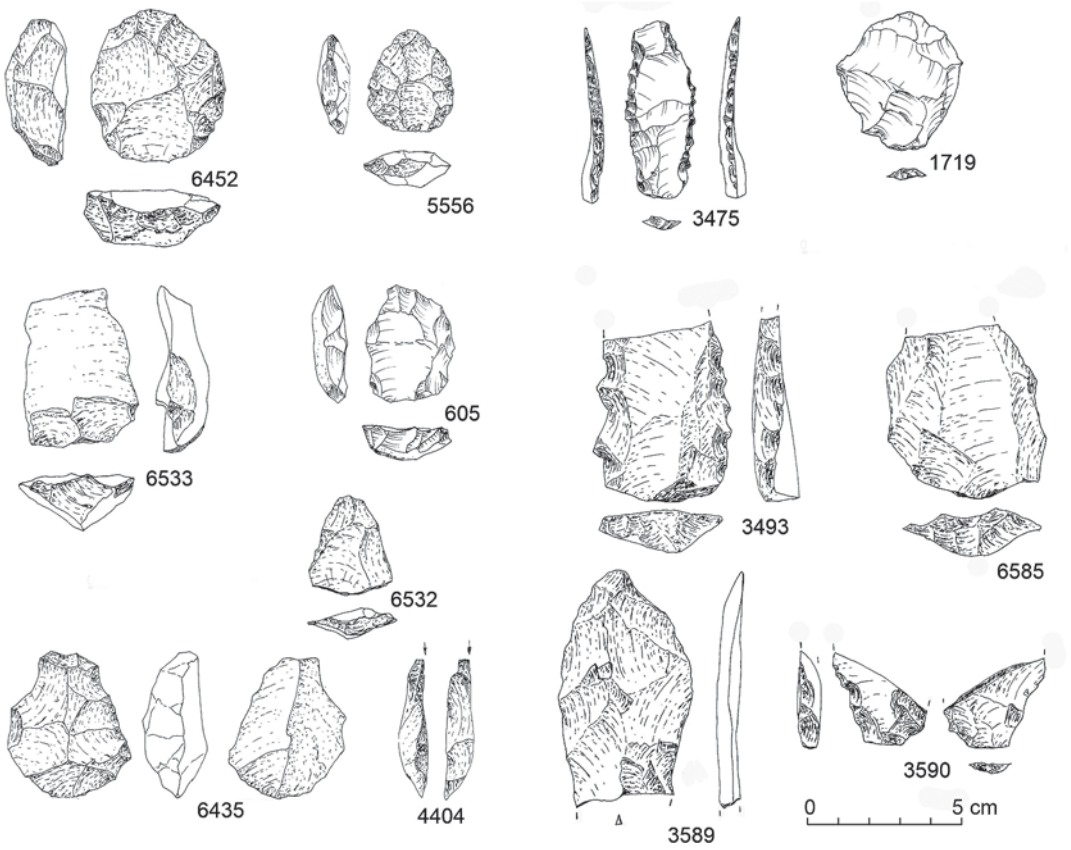

Fig. 4.93. Selected lithic artifacts from site AFD131: Levallois core – ferruginous sandstone: 6452; small Levallois core – ferruginous sandstone: 5556, chert: 605; core on flake – ferruginous sandstone: 6533; core on chunk – ferruginous sandstone: 6435; pseudo-burin spall – ferruginous sandstone: 4404; Levallois flake (and fragment) – chert: 1719, ferruginous sandstone: 6585; Levallois flake with denticulate retouch on both edges – light-colored chert(?): 3475; Levallois flake with retouch on both edges on dorsal face (fragment) – ferruginous sandstone: 3590; elongated Levallois flake (fragment) – ferruginous sandstone: 3589; elongated Levallois flake with denticulate retouch on both edges (fragment) – quartz: 3493; Levallois point – ferruginous sandstone: 6532

be interpreted as an indication that more such artifacts were brought to the encampment. Another example of the reutilization of older Palaeolithic tools is a denticulate tool made of a large chert flake or point, which had already been significantly patinated [*Figs 4.95, 4.97:4575*].

The most popular form of tool was a flake (not only with facetted butt) with denticulate retouching covering one or two opposite edges. These sometimes took the form of Tayac/pseudo-Tayac type points [*Fig. 4.97:6153*, probably also *Fig. 4.97: 91, 3482*]. In one case [*Fig. 4.93:3590*], the retouching covered both faces, taking a flat form on the positive side and the form of semi-abrupt retouching on the negative side. The collection from AFD131, like that from AFD111, includes both sandstone and chert tools of this type. These tools usually have the longest edges of the retouched blanks, which allows some of them to be classified as saws [*Fig. 4.94:353, 7022, 8565*].

No sandstone forms with distinctly retouched perforator or distinct scraping forms of the side-scraper type were recorded.

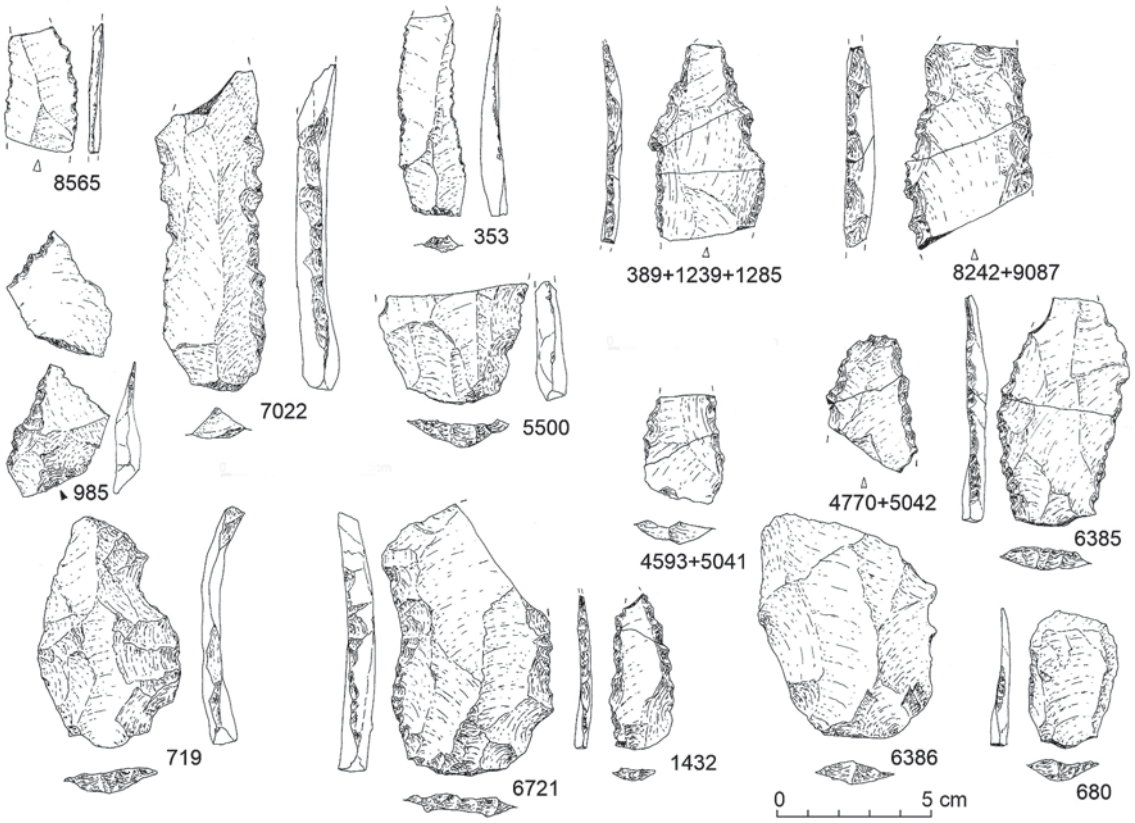

Fig. 4.94. Elongated Levallois flakes with retouched edges, made of feruginous sandstone, from site AFD131: 353, 389+1239+1285, 680, 719, 985, 1432, 4593+5041, 4770+5042, 5500, 6385, 6386, 6721, 7022, 8242+9087, 8565

The presence of a sandstone artifact resembling a burin spall [*Fig. 4.93:4404*] requires comment. Given the absence of burin-type tools in both the AFD131 and AFD111 inventories, the origin of this waste should rather be interpreted as accidental failure (through use?) of a larger flake. Analogous suggestions were also indicated for a similar inventory from AFD23, where burin scars were noted on some initial flakes (e.g., flake 1315 from refitted Block 8).

A component of typical microlithic forms, made exclusively from cryptocrystalline raw materials, includes fine backed pieces, truncated pieces, end-scrapers, perforators and borers. These come from Holocene manufacturing contexts.

Fig. 4.95. Example of reutilisation of a former flake as a blank for a denticulate tool, from site AFD131

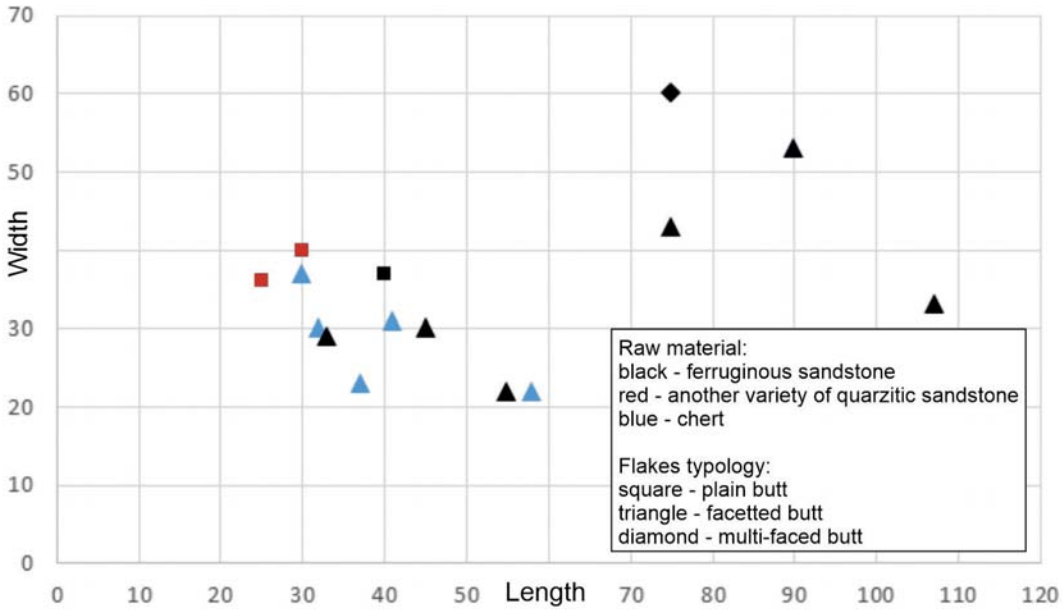

Fig. 4.96. Flakes constituting blanks for tools (only complete products considered) from site AFD131

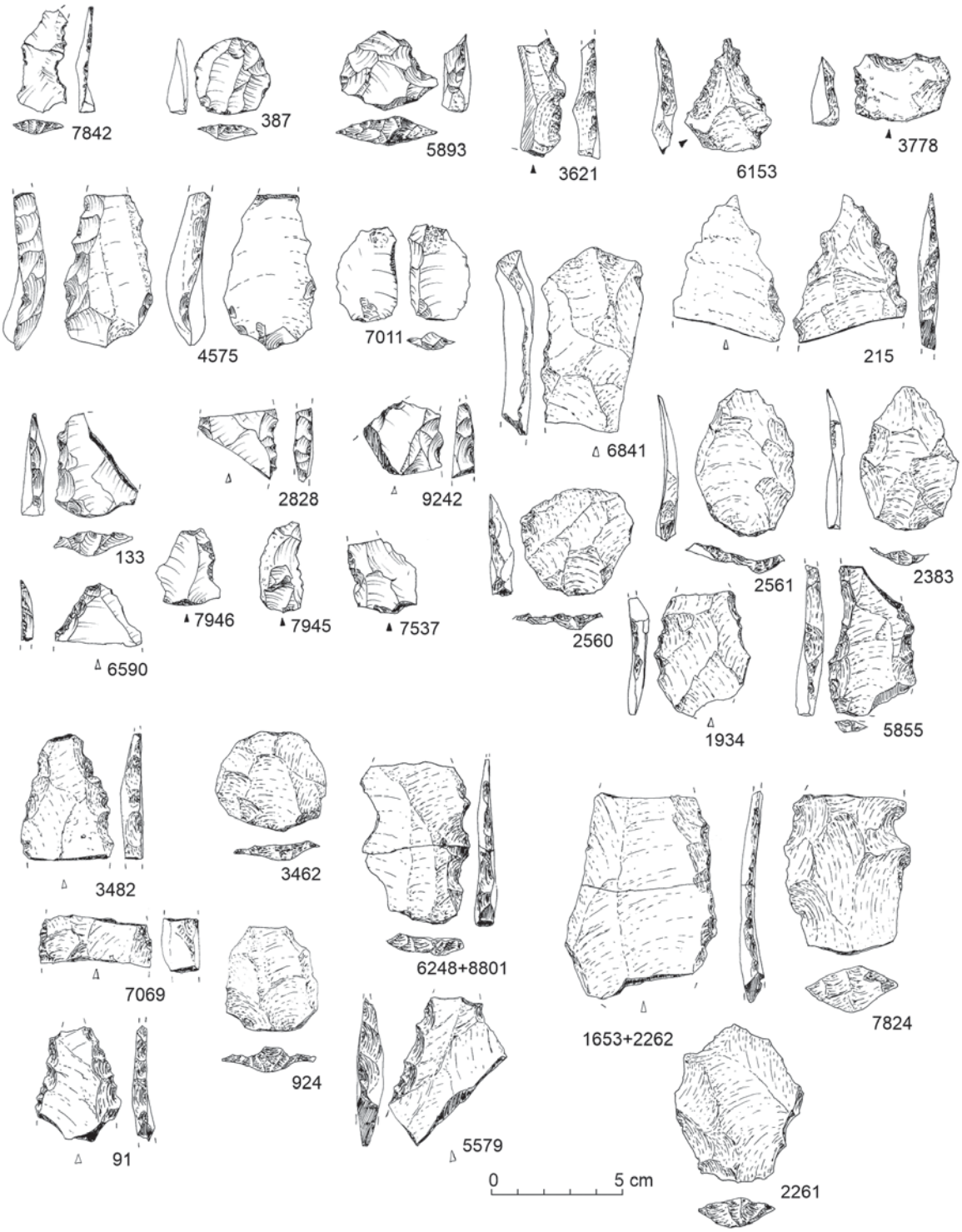

Fig. 4.97. Tools from site AFD131: retouched tools and fragments – chert: 133, 387, 2828, 4575, 5893, 6590, 7011, 7537, 7842, 7945, 7946, 9242; denticulate tools and Levallois flakes – quarzitic sandstone: 3621, 3778, 6153, ferruginous sandstone: 91, 215, 924, 1653+2262, 1934, 2261, 2383, 2560, 2561, 3462, 3482, 5855, 5579, 6248+8801, 6841, 7069, 7824

Table 4.50. Levallois flakes and retouched tools from site AFD131

Inv. No.	Locus	Dimensions (mm)	Description/raw material	Reference
91	55/54/I	(45)/33/5	Denticulate tool, fragment (mesial)/ferruginous sandstone	*Fig. 4.97*
133	55/55/I	41/31/7	Denticulate tool on flake with facetted butt/ chert	*Fig. 4.97*
190	55/63/I	(47)/43/8	Levallois flake, fragment (proximal)/ ferruginous sandstone	
214	55/64/I	–	Levallois flake, fragment (distal)/ferruginous sandstone	
215	55/64/I	(55)/43/8	Denticulate tool, fragment (distal)/ferruginous sandstone	*Fig. 4.97*
257	55/65/I	–	Denticulate tool, fragment (mesial)/ferruginous sandstone	
267	55/65/I	61/32/4	Levallois flake/ferruginous sandstone	
268	55/65/I	34/18/5	Levallois flake/ferruginous sandstone	
308	55/72/I	(7)/7/3	Levallois flake, fragment (proximal)/quarzitic sandstone	
309	55/72/I	35/26/4	Levallois flake/quarzitic sandstone	
353	55/75/I	(67)/20/6	Elongated flake (blade) Flake with prepared butt and use retouch, fragment (proximal)/ ferruginous sandstone	*Fig. 4.96*
387	55/81/I	32/30/8	Scraper(?) on Levallois flake/chert	*Fig. 4.97*
389 +1239 +1285	55/82/I 55/88/I 55/89/I	(35)/30/5	Denticulate tool, fragment (mesial)/ferruginous sandstone; three refitted fragments	*Fig. 4.94*
680	55/57/I	45/30/4	Levallois flake with use-retouch/ferruginous sandstone	*Fig. 4.94*
719	55/58/I	77/47/6	Levallois flake/ferruginous sandstone	*Fig. 4.94*
924	55/76/I	41/35/10	Levallois flake/ferruginous sandstone	*Fig. 4.97*
984	55/77/I	–	Denticulate tool on Levallois flake, fragment/ ferruginous sandstone	
985	55/77/I	40/37/8	Denticulate tool (saw) on flake with plain butt/ ferruginous sandstone	*Fig. 4.94*
1030	55/77/I	28/33/4	Levallois flake/chert	
1167	55/86/I	44/32/6	Levallois flake/ferruginous sandstone	
1202	55/87/I	57/(23)/5	Levallois flake, fragment (Siret)/ferruginous sandstone	
1432	55/96/I	55/22/3	Tayac point on elongated Levallois blank/ ferruginous sandstone	*Fig. 4.97*
1520	55/97/I	38/27/4	Levallois plunging flake/chert	
1653 +2262	55/100/I 65/29/I	(36)/48/5	Denticulate tool, fragment (mesial)/ferruginous sandstone; two refitted fragments	*Fig. 4.97*
1654	55/100/I	63/41/3	Levallois flake/ferruginous sandstone	
1655	55/100/I	51/(30)/5	Levallois flake, fragment (Siret)/ferruginous sandstone	
1719	65/06/I	46/41/4	Levallois flake/chert	*Fig. 4.95*

Table 4.50. continued

Inv. No.	Locus	Dimensions (mm)	Description/raw material	Reference
1726	65/07/I	–	Denticulate tool, fragment (mesial)/ferruginous sandstone	
1727	65/07/I	–	Scraper, fragment(?)/ferruginous sandstone	
1934	65/16/I	(48)/37/5	Denticulate tool, fragment (mesial)/ferruginous sandstone	*Fig. 4.97*
2051	65/19/I	–	Levallois flake/ferruginous sandstone	
2052	65/19/I	–	Denticulate tool, fragment (mesial)/ferruginous sandstone	
2161	65/26/I	28/20/8	Levallois flake/ferruginous sandstone, eroded	
2188	65/27/I	(33)/47/9	Levallois flake, fragment (proximal)/ ferruginous sandstone, eroded	
2261	65/29/I	61/50/12	Levallois flake/ferruginous sandstone	*Fig. 4.97*
2383	65/36/I	55/38/5	Levallois flake/ferruginous sandstone	*Fig. 4.97*
2560	65/40/I	41/45/8	Levallois flake/ferruginous sandstone	*Fig. 4.97*
2561	65/40/I	56/38/5	Levallois flake/ferruginous sandstone	*Fig. 4.97*
2828	65/50/I	(26)/30/7	Denticulate tool, fragment (mesial)/light chert, burnt	*Fig. 4.97*
2969	65/59/I	43/29/8	Levallois flake/ferruginous sandstone	
3103	65/60/I	(19)/30/7	Levallois flake, fragment (proximal)/chert, burnt	
3235	65/70/I	(42)/54/10	Levallois flake, fragment (proximal)/ ferruginous sandstone, eroded	
3282	65/76/I	(22)/26/6	Levallois flake, fragment/quarzitic sandstone, eroded	
3442	65/86/I	41/34/10	Levallois flake/ferruginous sandstone	
3462	65/87/I	38/43/5	Levallois flake/ferruginous sandstone	*Fig. 4.97*
3475	65/87/I	58/22/4	Denticulate tool on elongated Levallois flake/ light chert	*Fig. 4.95*
3482	65/88/I	(50)/34/9	Denticulate tool, fragment (distal)/ferruginous sandstone	*Fig. 4.97*
3493	65/88/I	(58)/45/10	Denticulate tool on elongated Levallois flake, fragment (proximal)/quarzitic sandstone	*Fig. 4.93*
3505	65/89/I	–	Denticulate tool/ferruginous sandstone	
3524	65/89/I	–	Denticulate tool/quarzitic sandstone	
3589	65/96/I	(76)/45/7	Levallois flake, fragment (distal)/quarzitic sandstone	*Fig. 4.93*
3590	65/96/I	(30)/31/7	Denticulate tool (inverse retouch) on Levallois flake, fragment (proximal)/quarzitic sandstone	*Fig. 4.97*
3621	65/98/I	(45)/(15)/9	Denticulate tool on flake with plain butt, fragment (proximal, Siret)/quarzitic sandstone	*Fig. 4.97*
3713	65/100/I	22/23/5	Levallois flake/ferruginous sandstone, eroded	
3778	66/51/I	25/36/11	Denticulate tool on cortical flake with plain butt/quarzitic sandstone	*Fig. 4.97*
3824	66/53/I	29/25/11	Levallois flake/ferruginous sandstone	
4065	66/63/I	25/24/5	Levallois flake/ferruginous sandstone	
4068	66/63/I	53/48/9	Levallois flake/ferruginous sandstone	

Table 4.50. continued

Inv. No.	Locus	Dimensions (mm)	Description/raw material	Reference
4131	66/64/I	(13)/20/5	Denticulate tool, fragment (distal)/quarzitic sandstone	
4174	66/64/I	(20)/29/5	Levallois flake, fragment (proximal)/ ferruginous sandstone	
4175	66/64/I	(27)/24/4	Levallois flake, fragment (proximal)/ ferruginous sandstone	
4232	66/65/I	(23)/17/2	Denticulate tool, fragment (distal)/ferruginous sandstone	
4255	66/65/I	32/28/4	Levallois flake/chert	
4257	66/71/I	–	Denticulate tool, fragment (mesial)	
4286	66/71/I	–	Denticulate tool, fragment (proximal) on flake with plain butt/quarzitic sandstone	
4300	66/71/I	(21)/20/3	Levallois flake, fragment (proximal)/chert	
4347	66/73/I	(21)/23/3	Denticulate tool, fragment (distal)/ferruginous sandstone	
4436	66/74/I	27/30/4	Levallois flake/ferruginous sandstone	
4567	66/81/I	–	Denticulate tool, fragment (distal)/quarzitic sandstone	
4575	66/81/I	(58)/35/11	Denticulate tool on reused flake with edge butt/chert	*Figs 4.95, 4.97*
4593 +5041	66/82/I 66/95/I	(24)/26/7	Denticulate tool on flake with prepared butt/ ferruginous sandstone; refitted fragments	*Fig. 4.94*
4653	66/82/I	(34)/31/5	Levallois flake/light chert, eroded	
4688	66/83/I	–	Levallois flake/chert	
4770 +5042	66/85/I 66/95/I	(25)/25/6	Denticulate tool, fragment (distal)/ferruginous sandstone; refitted fragments	*Fig. 4.94*
4766	66/84/I	22/26/5	Levallois flake/chert	
5045	66/95/I	36/38/13	Levallois flake/ferruginous sandstone	
5144	66/03/I	40/27/8	Levallois flake/ferruginous sandstone	
5146	66/03/I	24/29/7	Levallois flake/ferruginous sandstone, eroded	
5350	66/23/I	31/16/3	Levallois flake/chert	
5430	66/33/I	28/34/7	Levallois flake/quarzitic sandstone	
5500	66/42/I	(40)/50/8	Denticulate tool on Levallois flake, fragment (proximal)/ferruginous sandstone	*Fig. 4.94*
5532	66/43/I	(38)/30/15	Denticulate tool, fragment (distal)/ferruginous sandstone	
5533	66/43/I	(50)/35/13	Notch tool on flake with prepared butt/ ferruginous sandstone	
5579	66/45/I	(57)/45/10	Denticulate tool, fragment (mesial)/ferruginous sandstone	*Fig. 4.97*
5688	66/16/I	(25)/27/9	Levallois flake/ferruginous sandstone	
5855	66/37/I	(60)/35/8	Denticulate tool on Levallois flake, fragment (proximal)/ferruginous sandstone	*Fig. 4.97*
5893	66/39/I	30/37/10	Levallois flake with wide notch/light chert	*Fig. 4.97*
5919	66/46/I	32/44/6	Levallois flake/ferruginous sandstone	

Table 4.50. continued

Inv. No.	Locus	Dimensions (mm)	Description/raw material	Reference
5948	66/47/I	(22)/45/11	Denticulate tool on Levallois flake, fragment (proximal)/ferruginous sandstone	
5984	66/48/I	26/17/6	Levallois flake/ferruginous sandstone, eroded	
6153	66/59/I	30/40/6	Pseudo-Tayac point on flake with plain butt/ quarzitic sandstone	*Fig. 4.97*
6225	66/67/I	(40)/41/7	Levallois flake, fragment (proximal)/ ferruginous sandstone	
6267	66/68/I	(21)/38/8	Denticulate tool, fragment (distal)/chert	
6385	66/78/I	(75)/43/7	Denticulate tool on elongated Levallois flake, fragment (proximal)/ferruginous sandstone	*Fig. 4.94*
6386	66/78/I	75/60/8	Denticulate tool on flake with prepared butt/ ferruginous sandstone	*Fig. 4.94*
6459	66/86/I	(49)/40/20	Flake with semi-abrupt retouch, fragment (distal)/ferruginous sandstone, eroded	
6532	66/88/I	33/29/6	Levallois point	*Fig. 4.97*
6534	66/88/I	(34)/32/4	Levallois flake, fragment (proximal)/ ferruginous sandstone	
6585	66/90/I	(55)/53/14	Levallois flake, fragment (proximal)/ ferruginous sandstone	*Fig. 4.95*
6590	66/90/I	(23)/34/4	Denticulate tool, fragment (distal)/chert	*Fig. 4.97*
6677	66/98/I	(33)/54/9	Levallois flake, fragment (proximal)/ ferruginous sandstone	
6721	66/100/I	90/53/9	Scraper(?)+notch tool on Levallois flake/ ferruginous sandstone	*Fig. 4.94*
6808	76/02/I	43/(24)/3	Levallois flake, fragment (Siret)/ferruginous sandstone	
6841	76/03/I	(73)/(40)/9	Denticulate tool, fragment (distal, Siret)/ ferruginous sandstone	*Fig. 4.97*
7011	76/12/I	37/23/8	Levallois flake with use retouch/chert, burnt	*Fig. 4.97*
7022	76/13/I	(107)/33/10	Denticulate tool on blade with facetted butt/ ferruginous sandstone	*Fig. 4.97*
7069	76/14/I	17/43/15	Denticulate tool (saw), fragment (mesial)/ ferruginous sandstone	*Fig. 4.97*
7231	76/22/I	29/24/4	Levallois flake/light chert	
7304	76/24/I	42/39/13	Levallois flake/ferruginous sandstone	
7453	76/33/I	24/16/9	Denticulate tool/ferruginous sandstone	
7537	76/34/I	(27)/23/5	Denticulate tool, fragment (proximal)/chert	*Fig. 4.97*
7631	76/42/I	–	Denticulate tool, fragment (mesial)/ferruginous sandstone	
7635	76/42/I	56/49/9	Levallois flake/ferruginous sandstone	
7730	76/44/I	–	Denticulate tool on Levallois flake, fragment (proximal)/quarzitic sandstone	
7799	76/06/I	31/23/7	Levallois flake/ferruginous sandstone	
7824	76/07/I	(60)/50/17	Denticulate tool on Levallois flake, fragment (proximal)/ferruginous sandstone	*Fig. 4.97*

Table 4.50. continued

Inv. No.	Locus	Dimensions (mm)	Description/raw material	Reference
7842	76/07/I	42/20/5	Denticulate tool on Levallois flake/light chert	*Fig. 4.97*
7851	76/08/I	35/26/10	Levallois flake/ferruginous sandstone	
7870	76/10/I	29/33/6	Levallois flake/ferruginous sandstone	
7945	76/17/I	35/16/4	Denticulate tool on Levallois flake/chert	*Fig. 4.97*
7946	76/17/I	30/25/5	Notch tool on Levallois flake/chert	*Fig. 4.97*
7961	76/18/I	(28)/34/11	Levallois flake, fragment (proximal)/ ferruginous sandstone	
8141	76/27/I	54/(26)/6	Levallois flake, fragment (Siret)/ferruginous sandstone	
8180	76/28/I	(27)/33/5	Levallois flake, fragment (proximal)/ ferruginous sandstone	
8242 +9087	76/30/I 77/22/I	(35)/35/8	Denticulate tool, fragment (distal)/ferruginous sandstone	*Fig. 4.94*
8523	76/46/I	76/60/21	Scraper on reused discoidal core/ferruginous sandstone	
8565	76/47/I	(42)/23/4	Denticulate tool (saw), fragment (distal)/ ferruginous sandstone	*Fig. 4.94*
8566	76/47/I	(33)/46/7	Levallois flake, fragment (proximal)/ ferruginous sandstone	
8569	76/47/I	(31)/(20)/7	Levallois flake, fragment (proximal, Siret)/ ferruginous sandstone	
8614	76/47/I	27/32/8	Levallois flake/quarzitic sandstone, eroded	
8677	76/48/I	31/21/3	Levallois flake/ferruginous sandstone	
8728	76/50/I	27/25/6	Levallois flake/ferruginous sandstone	
8801 +6248	77/03/I 66/68/I	(30)/40/7	Denticulate tool on levallois flake, fragment (proximal)/ferruginous sandstone; refitted fragments	*Fig. 4.97*
8848	77/04/I	(38)/(38)/7	Levallois flake, fragment (proximal, Siret)/ ferruginous sandstone	
8875	77/05/I	(30)/22/4	Levallois flake, fragment (proximal)/ ferruginous sandstone	
8935	77/12/I	(37)/42/12	Levallois flake, fragment (proximal)/ ferruginous sandstone, eroded	
9007	77/14/I	49/50/8	Levallois flake/ferruginous sandstone	
9038	77/15/I	(33)/33/6	Levallois flake, fragment (proximal)/ ferruginous sandstone	
9045	77/15/I	15/22/3	Levallois flake/ferruginous sandstone	
9105	77/22/I	(14)/24/4	Levallois flake, fragment (proximal)/ ferruginous sandstone	
9155	77/23/I	45/35/9	Levallois flake/ferruginous sandstone, eroded	
9214	77/24/I	49/31/3	Levallois flake/ferruginous sandstone	
9215	77/24/I	(33)/34/4	Levallois flake, fragment (proximal)/ ferruginous sandstone	
9242	77/25/I	(27)/(30)/8	Denticulate tool on flake with prepared butt/ chert	*Fig. 4.97*

4.3.4 Sites Affad 120 (AFD120) and Affad 122 (AFD122)

Two locations situated in the northwestern sector of the area under investigation yielded limited data on the spatial relationship between Pleistocene and later, Holocene, artifacts; these are AFD120 and AFD122, both discovered in 2014 (Osypińska and Osypiński 2015). Numerous animal bone remains and lithic artifacts of various chronologies were scattered over a very wide area. A tool fragment made of a light-colored variety of chert was found to be retouched at the edges in an extraordinarily regular manner (Osypińska and Osypiński 2015: Fig. 10). It would have been done most probably with a metal (copper?) retouching tool and the age of the artifact is no earlier than the Middle Holocene (post-5th millennium BC). However, an earlier phase of occupation is surmised based on the state of preservation of animal bones (analogous to those from AFD23), as well as the presence of numerous lithic artifacts manufactured with Levallois methods. Test excavations did not uncover any artifacts in subsurface layers, hence the dispersal of finds over such a broad area should be explained by deflation and relocation of artifacts most probably in line with the periodic or episodic water flow in depressions left by palaeochannels, which have been mapped as a result of magnetic surveying in this area [see *Figs 4.98* and *4.101*,

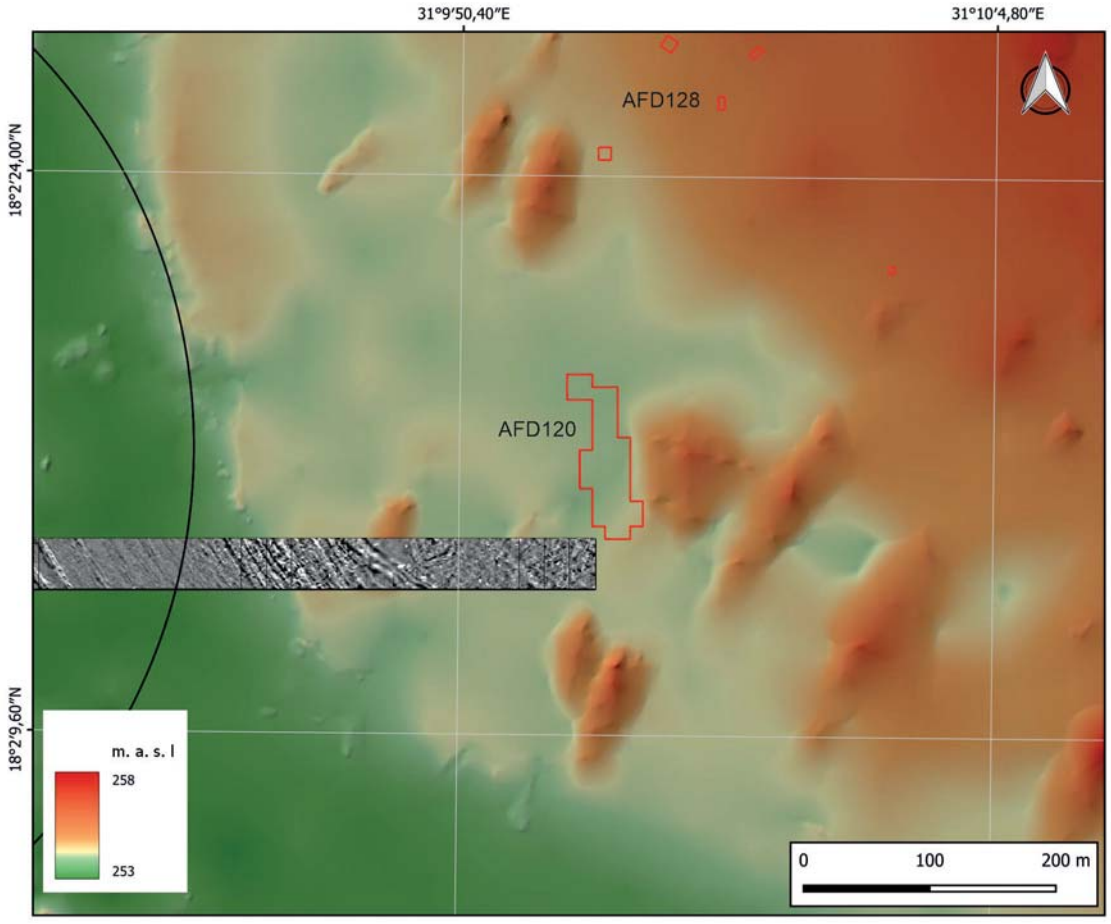

Fig. 4.98. Site AFD120

and above]. The Pleistocene as well as later, Holocene, encampments would have been located beyond the wetland areas. While the collections from AFD120 and AFD122, located within the course of such palaeochannels, have nothing to offer in terms of spatial relationship data at the deposition stage, they are at least evidence of periodic settlement, for example, in dry seasons or during longer lasting dry climate fluctuations.

Site AFD120

At site AFD120, mineralized bone remains (belonging to aurochs among others), as well as distinctive tools manufactured using Levallois methods were scattered in a zone approximately 30 m in width and 140 m in length [see *Fig. 4.98*]. No spatial variation in the occurrence of finds from two different ages was observed, hence the artifacts must be assumed to have been more or less relocated. However, it should be emphasized that neither the lithics nor the mineralized bone remains bear any smoothing of the edges or a thick layer of patina. It is most likely that they had lain sealed in layers of dust and sand until relatively recent times.

The collection from AFD120 was not homogeneous in terms of the raw material, but even so chert prevailed (1145 artifacts). These included products made using flaking methods (related to the MSA), as well as Holocene microlithic perforators, bladelets, and even a fragment of a polished axe [see *Fig. 4.99:907, 730, 1025, 2061*]. The MSA artifacts made of the fine crystalline material were less numerous: 34 pieces (a residual core on flake and retouched tools—a small scraper and a denticulate tool; see *Fig. 4.99:1096, 2037, 2059, 2313, 2517*). Other raw materials were represented: 696 pieces were made of ferruginous sandstone, and 64 objects of different varieties of quarzitic sandstone. Very few were examples made of quartz (27 pieces) and agate (11 pieces), which are so typical of Early Holocene production at sites all over northern Sudan. Moreover, there were just three slightly larger Neolithic artifacts, meaning pieces of grinders and querns, and no fragments of pottery at all, suggesting in effect that the Holocene component was not dominant in this collection. Apparently Holocene communities hardly penetrated the area of the ancient Pleistocene site, possibly inhabiting the settlement at site AFD128 just 100 m to the northeast.

The collection of MSA artifacts from site AFD120 corresponds in raw material preferences, metric data and technologies to other collections from the Affad Basin. However, neither cores (apart from one small example made on a crude flake and reutilized as a scraper) nor large initial flakes (either from chert or sandstone) were found. This type of inventory suggests a hunting camp where stone tools were not produced. The substantial number of lithic artifacts indicates in turn multiple visits to the same place, each time bringing a new collection of *ad hoc* tools made of various raw materials, as well as their usage on many occasions.

Site AFD122

The site appears to have two general zones: the first with a similar degree of degradation of layers containing archaeological material as at AFD120 and the second, the southern zone along the bank of the palaeochannel (AFD122S), where spatial relationships between artifacts seem to be better preserved [*Fig. 4.101*]. The magnetic prospection and supplementary geological surveys revealed the presence here of one of the Nile palaeochannels of a width not exceeding 500 m

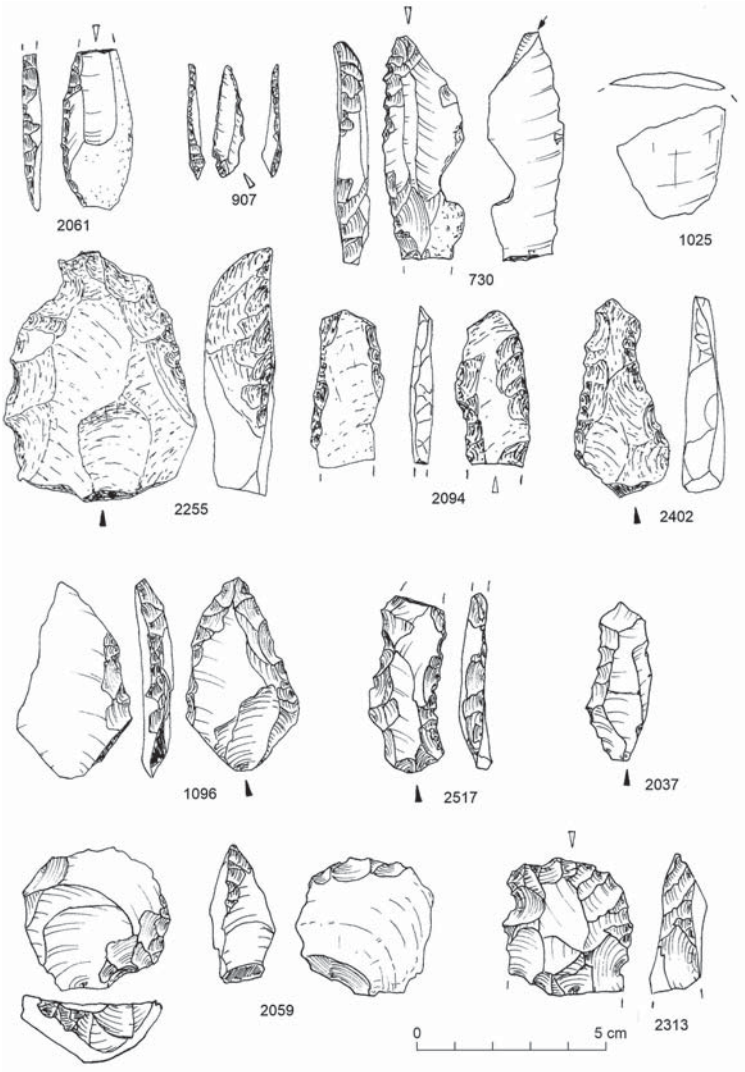

Fig. 4.99. Neolithic formal tools from site AFD120: backed blade – chert: 2061, borer – chert: 907, combined blade tool: denticulate+burin+notched – chert: 730, polished tool fragment – chert: 1025, and Palaeolithic tools: denticulate sidescraper – ferruginous sandstone: 2255, elongated flake with bifacial retouch – chert: 2094, perforator – ferruginus sandstone: 2402, sidescraper – chert: 1096, elongated flakes with denticulate retouch – chert: 2037, 2517, small Levallois core reused as scraper – light-colored chert: 2059, denticulate scraper – chert(?): 2313

from east to west. The channel bed was filled foremost with aeolian sands blown in from the north (yielding two OSL dates: Lub-6550: 66.0±7.0 ka; Lub-6549: 58.4±5.7 ka). Later flooding of the river left layers of silt in the central section of the channel bed (OSL date: Lub-6551: 43.8±4.9 ka). Artifacts related to MSA settlement were observed on the surface of these most recent sediments [*Fig. 4.100*]. The good state of preservation of these pieces (both lithic artifacts and mineralized bone remains) indicate the small scale of relocation in fluvial deposits. At the same time, one should not exclude the possibility that these artifacts could have been deposited as a result of their secondary usage during the Holocene period. Insofar as this is possible and confirmed at other sites in the case of stone tools, it is difficult to justify similar treatment of the subfossil animal bones.

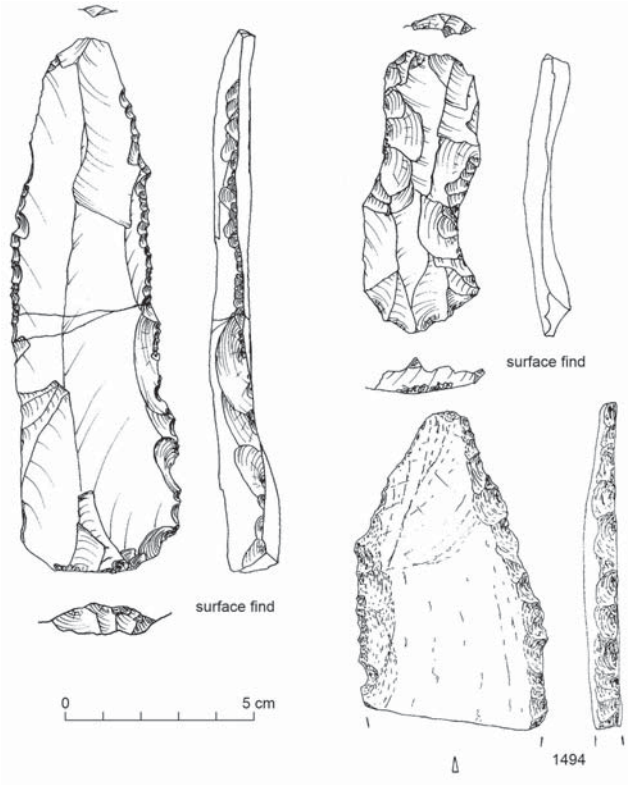

Fig. 4.100. Elongated Levallois flakes with retouched both edges from site AFD122: petrified wood (left) and light-colored chert (top right): unnumbered surface finds, ferruginous sandstone: 1494

Elements of Pleistocene date were evenly dispersed around the central part of the site [AFD122C; see *Fig. 4.102* left). This concerns both bone remains (megafauna, but also large- and middle-sized ruminants, as well as single fish) and lithic artifacts. The situation was different in the southern zone along the bank of the ancient river channel (AFD122S) where a clear concentration of artifacts made of light-colored chert was recorded already in 2014. Refitting of artifacts revealed a pattern of dispersal of broken fragments but also technological refits within a diameter of about 20 m. This indicates the small scale of relocation of layers of deposited artifacts in the marginal zone of the ancient channel. Test excavation uncovered lithic artifacts and a small amount of bones in a sandy layer that was a maximum 15 cm deep.

The remains of Holocene settlement, also scattered all over the surface, revealed discreet concentrations visible thanks to, among other things, an analysis of the dispersal of quern and grinder fragments [see *Fig. 4.102* right]. Although hearth remains, which could be associated with the Holocene episode, were noted, they were not linked to any clusters of ceramic or lithic material around them. Contrary to the picture for the Pleistocene occupation, the small concentrations of Holocene artifacts suggest settlement directly on the bed of a permanently dry channel which remains dry even today, that is, it was already out of range of seasonal Nile flooding. Radiocarbon dating of the nearby remains of burial site AFD130 to the south placed this later settlement, presumed to be contemporary with the occupation of the river channel bed at AFD122, at the end of the 5th millennium BC. The remains of an individual burial discovered within locus AFD122Q [see *Fig. 4.101*] actually constitute a direct reference to AFD130.

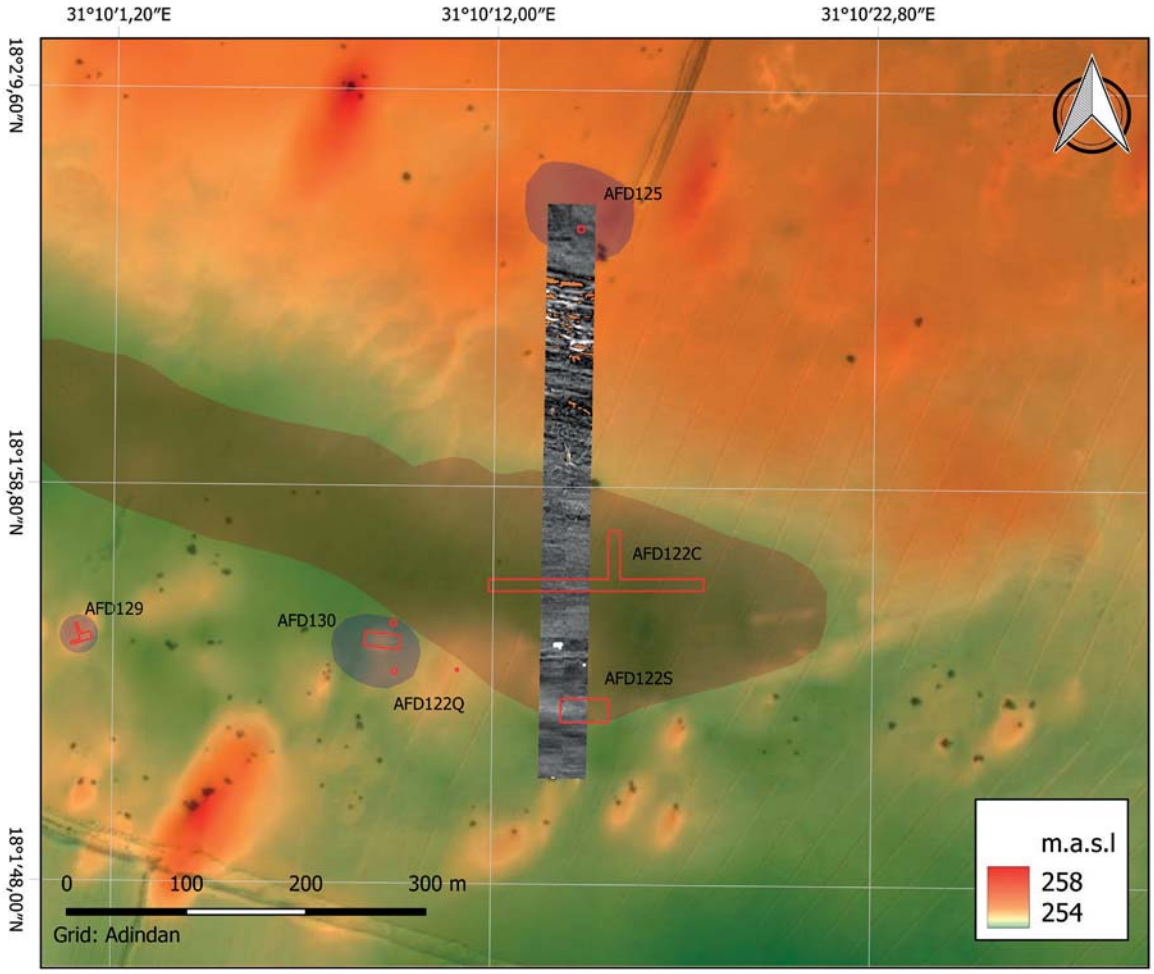

Fig. 4.101. Site AFD122 (extent marked in brown, including magnetic mapping) with Holocene sites AFD125, AFD129 and AFD130 in the vicinity

The collection from the central zone of the site included 121 artifacts made of ferruginous sandstone, including Levallois cores and denticulate tools [*Fig. 4.103:4, 73, 147, 169, 202, 205*], without including the 14 fragments of Holocene querns or grinders. Supplementing this are 16 Levallois flakes made of pink or light-beige quartzite, retouched in a denticulate manner [*Fig. 4.103:245, 256*]. A total of 25 artifacts made of chert and petrified wood represented both Levallois tools and cores [*Fig. 4.103:2, 24, 31, 32, 37, 115, 193, 253*], as well as retouched microlithic bladelets [*Fig. 4.104:5, 79, 346*]. In turn, artifacts made of a light-colored variety of chert comprised 17 exclusively non-microlithic pieces or formally Levallois [*Fig. 4.104:1, 56, 207, 208, 483*]. The only quartz artifact was a spherical hammerstone, while two tools made of agate comprised a small scraper and a wide and irregularly shaped bladelet with two opposing notches resembling an arrowhead [*Fig. 4.104:43, 128*]; both were linked with Holocene technological traditions. Two heavily eroded (thin-walled, undecorated) pottery fragments were found in the zone of concentration of quern fragments.

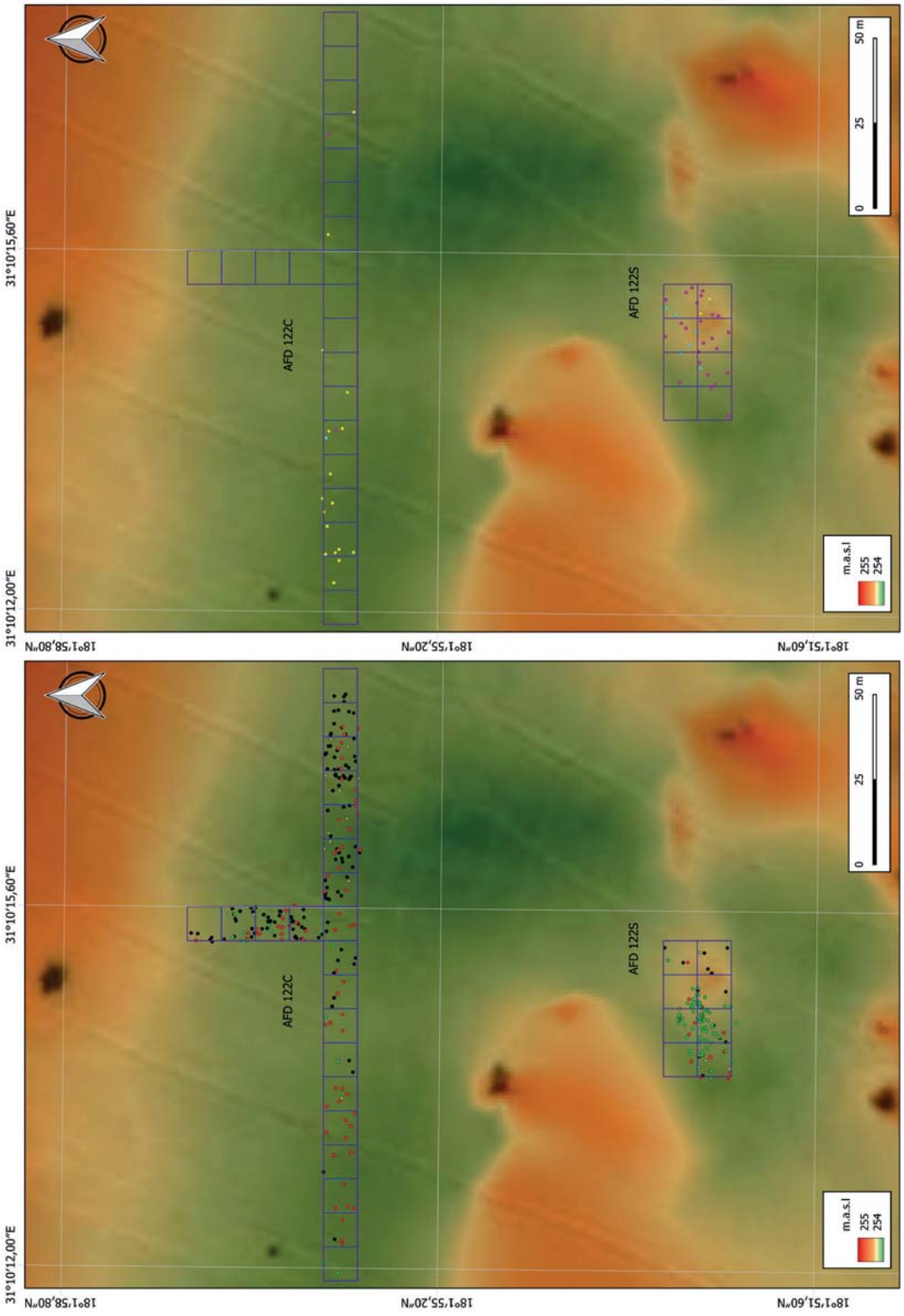

Fig. 4.102. Dispersal of artifacts at site AFD122: left, objects of Pleistocene age; right, objects of Holocene age. Symbols: on the left, black – artifacts made of sandstone, green – artifacts made of light-colored chert, red – mineralized bone; on the right, purple – artifacts made of agate, blue – artifacts made of quartz, yellow – fragments of pottery, querns and grinders (artifacts made of chert not considered)

Fig. 4.103. Tools from site AFD122C: small Levallois cores reused as scrapers – chert(?): 115 and chert: 2, 24; small Levallois point – chert: 31, denticulate tools – chert: 49, 150; denticulate tool with semi-abrupt retouch on the ventral face (fragment) – chert: 96; Levallois flakes (fragments) – chert: 28, 48, 119, 209, quarzitic sandstone: 44; Levallois cores – ferruginous sandstone: 82, 147, 169, 205, light-colored chert: 15, chert: 32, 37, 253; Levallois flakes and denticulate tools – ferruginous sandstone: 4, 27, 50, 51, 62, 73, 125, 136, 161, 202, quarzitic sandstone: 245, 256, petrified wood: 193

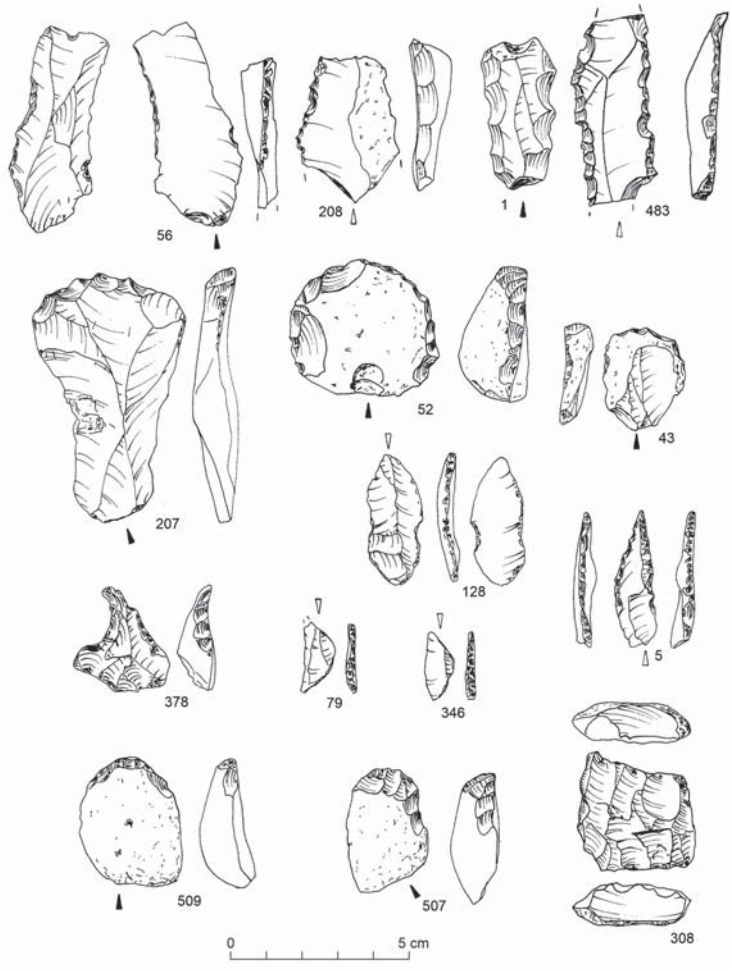

Fig. 4.104. Tools from site AFD122C/S: elongated flakes with denticulate retouch – light-colored chert: 1, 56, 208, 483; Neolithic tools: endscrapers – chert: 52, 207, agate: 43; arrowhead(?) – agate: 128; bent perforator – chert: 378; slender perforator – chert: 5 (Ch), backed lunates – chert: 79, 346; endscrapers – chert: 507, 509; final microlithic core – chert: 308

The collection from AFD122S will be described separately; artifacts from the surface here were supplemented with an assemblage from a test excavation (10 × 10 m in size) located where the greatest concentration of artifacts made of a light-colored variety of chert had been observed [see *Fig. 4.105*]. Both spatial relationship between the artifacts and rock processing technologies were taken into account when studying the refittings of these pieces. One should note that the collection was purely of Pleistocene date, with no formal tools, cores, or debris that could be attributed to Holocene microlithic bladelet production.

The raw material of these artifacts was classified with regard to the key characteristics of the matrix (fine-crystalline, translucent, shades of dark yellow, with internal dark outgrowths resembling veins or sections more matt in appearance) and the presence of a richly sculpted, external lime surface. These nodules originated from limestone units that are not present in the region, but the raw material as such is common at both Pleistocene and Early-Holocene sites, thus suggesting a more or less local origin. The material is sufficiently conspicuous to be easily identified, making technological analyses based on refittings of a smaller collection a viable option. At AFD122, artifacts representing this raw material constitute an internally diverse component that reflects processing of at least several separate blocks.

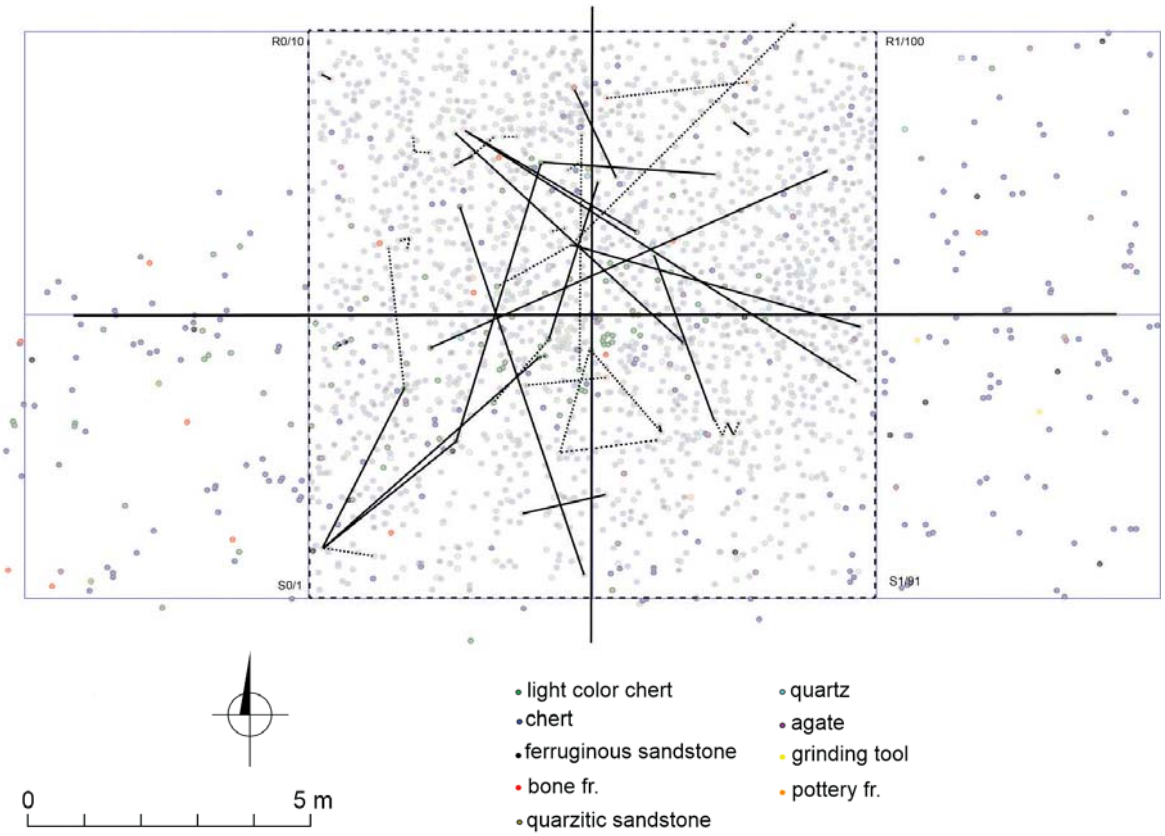

Fig. 4.105. Dispersal of refitted pieces compared to all lithic artifacts at site AFD122S; area 10 × 10 m with an intensive grouping of artifacts excavated and sediment-screened

However, the refitting evidence fails to reveal any testing operations or initial working of the core being conducted here, this despite the identification of over a dozen flakes with external cortical surfaces. The premise is rather that on-site processing concerned nodules initially worked elsewhere. Moreover, cores were not part of the collection made of light-colored chert from AFD122S (apart from a small chunk described below).

The largest nodules processed at the site measure 120 mm and represent a stage of operations linked to preparing the edge of the flaking surface shaped from two opposite striking platforms with elongated flakes [*Fig. 4.106:a*]. Direct parallels are known from AFD23 (e.g., Block 8). In turn, most of the flakes with a cortical surface (both refitted and not fitted) are of smaller dimensions. The width of the flaking surface may be estimated from the refitting of several flakes forming a striking platform [*Fig. 4.106:e, f*], as well as the refitting of products with facetted butts [*Fig. 4.106:b–d*]. It has been determined at approximately 50 mm width and 100 mm length, which once again finds parallels of a metric nature in the refitted blocks from AFD23. The method for obtaining flakes is suggested based on a refitting of several products with facetted butts demonstrating a recurrent schema, but this evidence is doubtful given the size of these artifacts: always shorter than 30 mm, meaning that they stand out from the majority of denticulate tools or

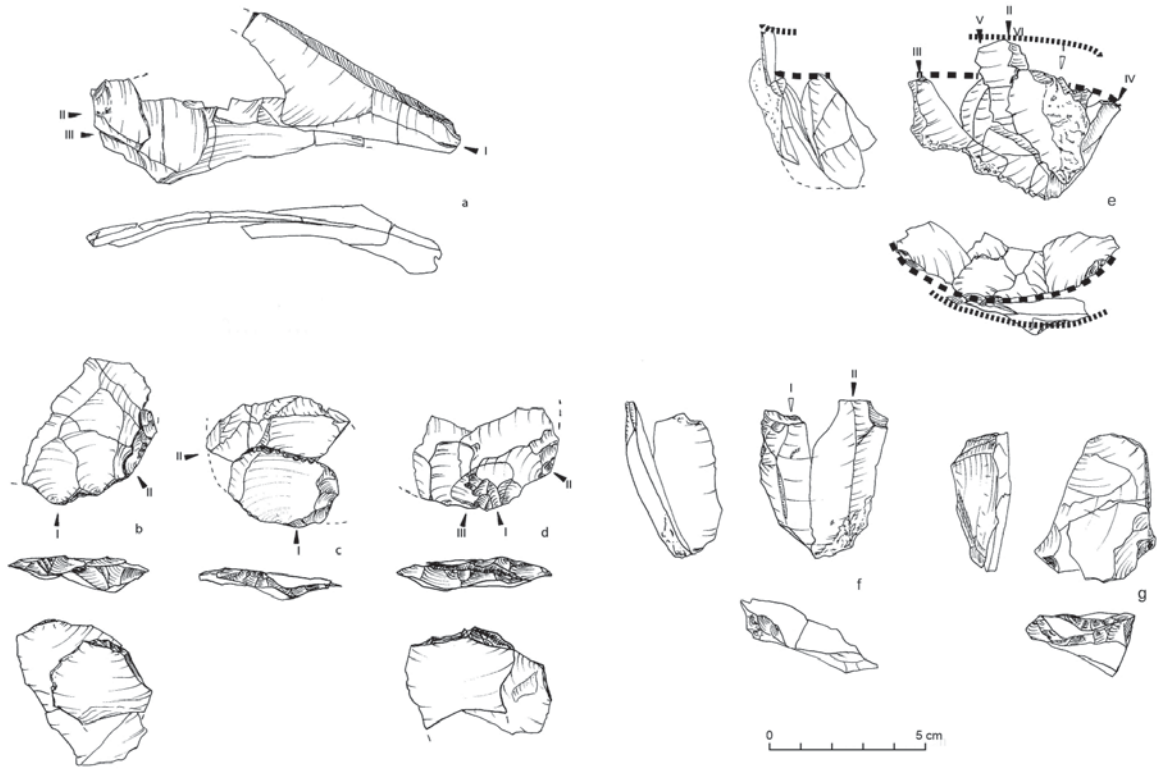

Fig. 4.106. Refitted light-colored chert flakes from site AFD122S: a – opposed direction prepared flaking surface – 38+37(I) + 19(II) + 37+38+37(III); b – two flakes with facetted butts removed in a recurrent schema – 102+54+60 (I) + 26(II); c – two flakes with facetted butts – 63(I) + 57+63(II); d – three flakes with facetted butts removed in a recurrent schema – 24(I) + 27(II) + 62(III); e – sequence of six flakes forming a striking platform (two stages of rejuvenation) – 13(I) + 53+53(II) + 91+69(III) + 87(IV) + 75+75(V) + 99+94(VI); f – two blade-like flakes forming a striking platform(?) – 41(I) + 62(II); g – final Levallois core – 71 and the last removed flake with facetted butt

unretouched Levallois flakes from Affad. Consequently, it is currently assumed that they are the result of either support activities (correcting the parameters of the flaking surface before detaching appropriate Levallois products) or else skill training, in similarity to the evidence from AFD23. This refers to Block 8 from AFD23, in which case a platform was remodeled without repeated shaping of the convexity of the flaking surface, despite the shape and size of the flakes being equally 'non-standard'. However, the application of a preferential schema is supported by refittings forming a platform with two visible stages of reduction of the flaking surface [*Fig. 4.106:f*].

Refitting also concerned a core and a flake with a facetted butt [*Fig. 4.106:g*]. The small dimensions of both artifacts, the debris-like nature (chunk) of the blank and the discovery of both at a distance no greater than 1 m apart supports the training or instructional dimension of this production. This evidence constitutes further reference to the collection from the southwestern sector of AFD23, where the production of tools of standard dimensions exceeding 40–50 mm in length was coupled with technologically similar elements manufactured on a significantly smaller scale and destined for varying purposes rather than actually satisfying the tool needs of a group.

This particular collection of chert artifacts does not include any retouched tools made from Levallois flakes (besides a small number of denticulate tools from an atypical blank; e.g., *Fig. 4.103, 4.104*]. Therefore, one may only speculate whether these forms were taken outside the area under investigation or not detached at all. Although the latter sounds like a paradox, it would find justification were it simply training or experimental processing. However, in the case of the collection from AFD122S (unlike AFD23), there are no additional premises in favor of such a hypothesis. A rational explanation seems more likely, namely that 1) a core already initially shaped which still possessed a large part of its natural cortical surface was brought to the site, 2) a flake (or flakes?) were produced with Levallois methods along with many corrections of the flaking surface, and 3) both tools and cores continued to 'wander'.

The assemblage from AFD122S is supplemented by a broad range of artifacts made of other raw materials [*Table 4.51*] representing both Levallois methods and microlithic bladelets.

Table 4.51. General raw material and technological structure of the collection from site AFD122S

Raw material	Cores	Flakes, chunks	Tools	Total
Ferruginous sandstone	–	126	–	126
Quarzitic sandstone	–	19	–	19
Chert	1	1172	7	1180
Light chert	1	374	3	378
Quartz	–	120	–	120
Agate	–	116	1	117

Unlike AFD23, this particular site was not a workshop site engaged in selection and initial working of cores, but rather a short-term stopover probably involving the use of just a few stone tools. Although such a place could have constituted a central point in the space penetrated in search for food, it did not take on such clear features of a campsite as those observed at AFD23, AFD131 or AFD24.

4.3.5 Site Affad 24 (AFD24)

The location produced an important collection of subfossil animal remains belonging to aurochs among others (see above, Chapter 3), evidence of small cut features, such as postholes and hearth remains (see below, Chapter 5), as well as a collection of lithic artifacts, which included single artifacts of a significantly later, Holocene tradition beside products of Pleistocene date [*Fig. 4.107:q–w*]. As in the case of other sites, this small later component most probably testifies to temporary penetration of this area in the Early Holocene.

Archaeological material on the surface was concentrated within a diameter of approximately 20 m, with single elements dispersed within a circle of 100 m around the central concentration [see below, *Fig. 5.5*]. Excavation in 2016 and 2017 revealed artifacts lying in a sandy surface layer 15 cm deep. Postholes were cut through this layer and into the underlying hard, sterile clayey silt, in similarity to the stratigraphy in the southwestern sector of site AFD23. The original depression

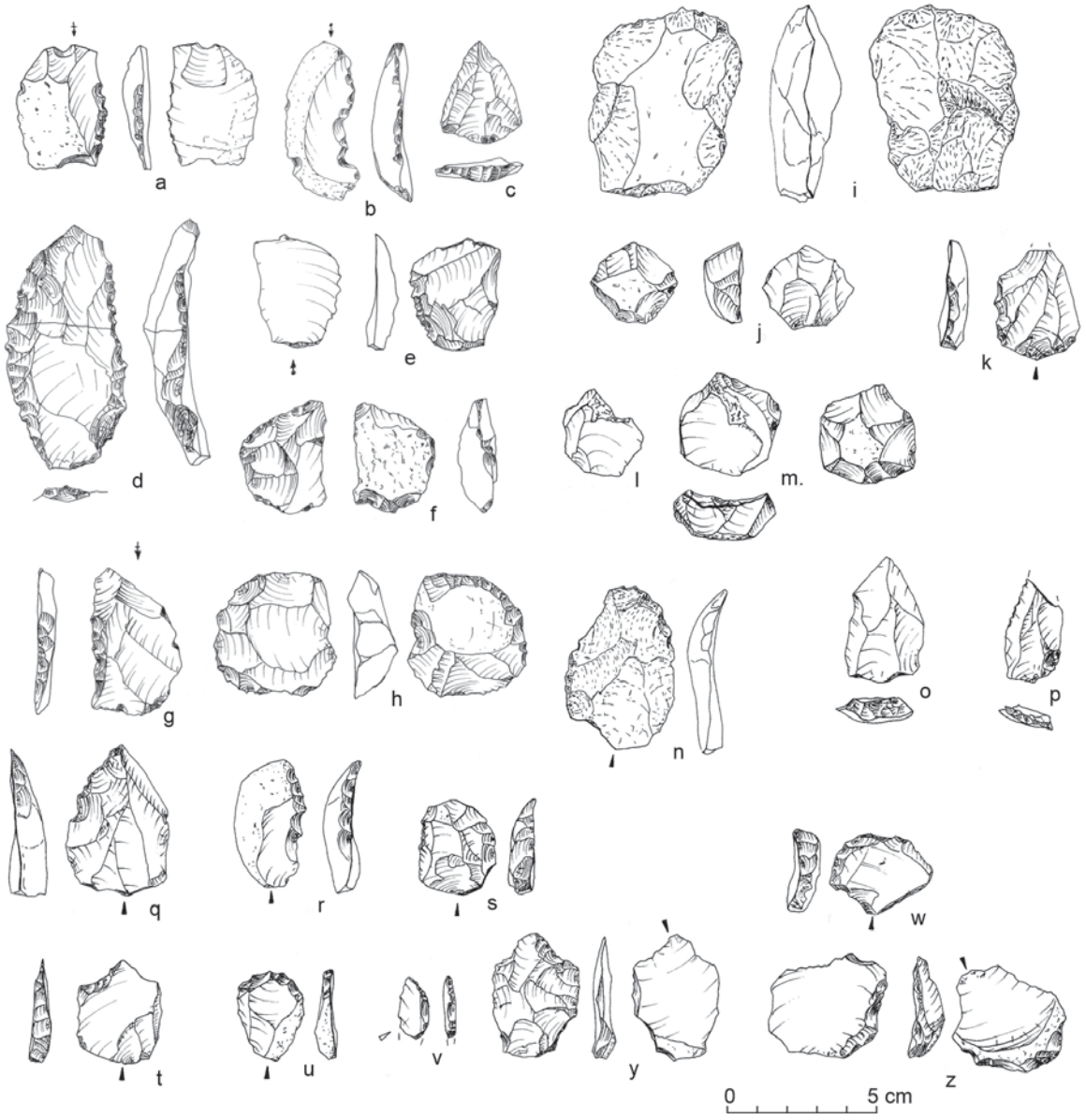

Fig. 4.107. Lithic artifacts from sites AFD24A and AFD24B: a, b, d–g denticulate tools (Ch, A, QS); c – Levallois point (Ch); h – final flake core reused as a scraper (Ch); i, j, l, m – final flake cores (Q, Ch); k, n – denticulated tools (A, QS); o – Levallois point (Ch); p – denticulate tool fragment (Ch); q, r – denticulate tools (Ch); s – scraper (Ch); t – backed tool (Ch); u, w – endscrapers (Ch); v – backed lunate fragment (Ch); y, z – plunging Levallois flakes struck from the final cores (Ch)

of this geomorphological unit had been filled with dust and sand that also contained single lithic artifacts, although they were not recorded in any clear concentrations. A denticulate tool found in such a depression, at a depth of 20–30 cm, revealed traces of soft animal tissue left over from processing meat (see below, Appendix 4.A1). No such remains have been observed on any of the denticulate forms of tools from the Affad Basin, because they could not have been preserved on artifacts lying on the surface. However, this evidence leaves no room for doubt that MSA tools were used primarily for meat processing.

The dating of site AFD24 is in need of a comment. ESR analysis of two ruminant tooth fragments from the site (see above, Appendix 2.A5) indicated a range between 87±6 ka and 160±11 ka, obviously not corresponding to MIS3. It seems unlikely, however, that bones of such age were naturally redeposited in layers dated to MIS3, because all things considered (presence of cut features, refitted nodule of chert) the site shows no evidence of any kind of secondary deposition. It is to be assumed that ESR dates for AFD24 (and AFD23 for that matter) are somehow erroneous, but we are unable for the moment to indicate why these results should seem to be significantly older than they are. Site AFD24 without doubt must be placed in the same stage of formation of this section of the valley, that is, MIS4/MIS3, just like other MSA sites in the Affad Basin.

The raw material make-up of the collection was dominated by chert and similar crypto-crystalline materials (flint, petrified wood, jasper). Single products made of agate, quartz and sandstone were also recorded.

Fig. 4.108. Elements of the chert block worked at site AFD24

Concerning the typological make-up, flakes constituted roughly 75% of the just over 400 artifacts recorded. Only one chert nodule was refitted; the pieces came from Trench B (and an adjacent part of Trench A) [*Fig. 4.108*], from the area of postholes and on overheated floor, indicating the limited extent of tool manufacture at this encampment. Moreover, a refitting of a small Levallois agate core and flake [*Fig. 4.107:l,m*] suggest a training/instructional dimension to this find. Additionally, the large number of cores collected outside the site is proof of intent to use them in an unspecified capacity.

Returning to the refitted chert nodule, it is not complete. Many connecting elements are clearly missing, as well as the residual core itself. However, there is a clearly legible sequences of flakes of technological significance. The first two sequences reflect the formation of the striking surfaces on a core of round shape. The pieces do not connect, but they are undoubtedly from the processing of the same core. The nodule was brought to the site already processed because at least several cortical chips are missing from the assemblages. Given that a number of small elements are missing also from the refitted assemblages, some displacement of small artifacts in the post-depositional stage should also be assumed. The processed nodule was approximately 70 mm long and 45 mm thick. A series of small flakes forming the platform surfaces after the core had been remodeled and significantly reduced in size constitutes an interesting piece of evidence. At the final stage, the core was only 30 mm thick and about 35 mm long. This demonstrates a skillful application of the preferential schema already known from the AFD23 refittings.

The next refitting sequence comprises a series of flakes forming a centripetal flaking surface. Again, although many small pieces are missing, the initial width of the core was determined at approximately 50 mm.

A proximal fragment of a *chapeau-de-gendarme*-type facetted butt is preserved in the collection. While it does not contribute directly to the refitting sequence of formation of the flaking surface or the striking platform, the structure of the raw material clearly suggests that the detachment of this flake (or point) occurred precisely on the side where the nodule was most uniform and devoid of porous inclusions.

Interestingly, a proximal fragment of another facetted-butt flake, detached from an already remodeled core, was also preserved. A small flake from the striking platform formation of this last phase of core reduction was deposited directly with it.

As it turns out, the predetermined products from AFD24 that were produced at the encampment were not intermediate tools intended for use. This applies to both the broken chert flakes and miniature agate flake.

4.3.6 Killing sites AFD110 and AFD124, and fish and mollusk gathering sites AFD113 and AFD34

Four locations that appear not to have been more or less permanent encampments were also investigated in an effort to broaden the data base for studying human adaptation strategies in the Affad Basin microregion in the Late Pleistocene. The subfossil biological material recorded on the surface of these sites included mostly mammals and fish but also, in one case, fresh water mollusk shells. As a rule, these assemblages were accompanied by very few and, at first sight, incidental lithic artifacts that did not occur in concentrations. It was assumed that traces of the use of stone tools could probably be found in the places where animals were killed and initially processed. It goes without saying that the functional and sometimes even chronological relationships between these tools and the animal bone remains often gave rise to reservations, especially when compared to the best studied "outside workshop" zones at AFD 23 (northeastern and southwestern sectors).

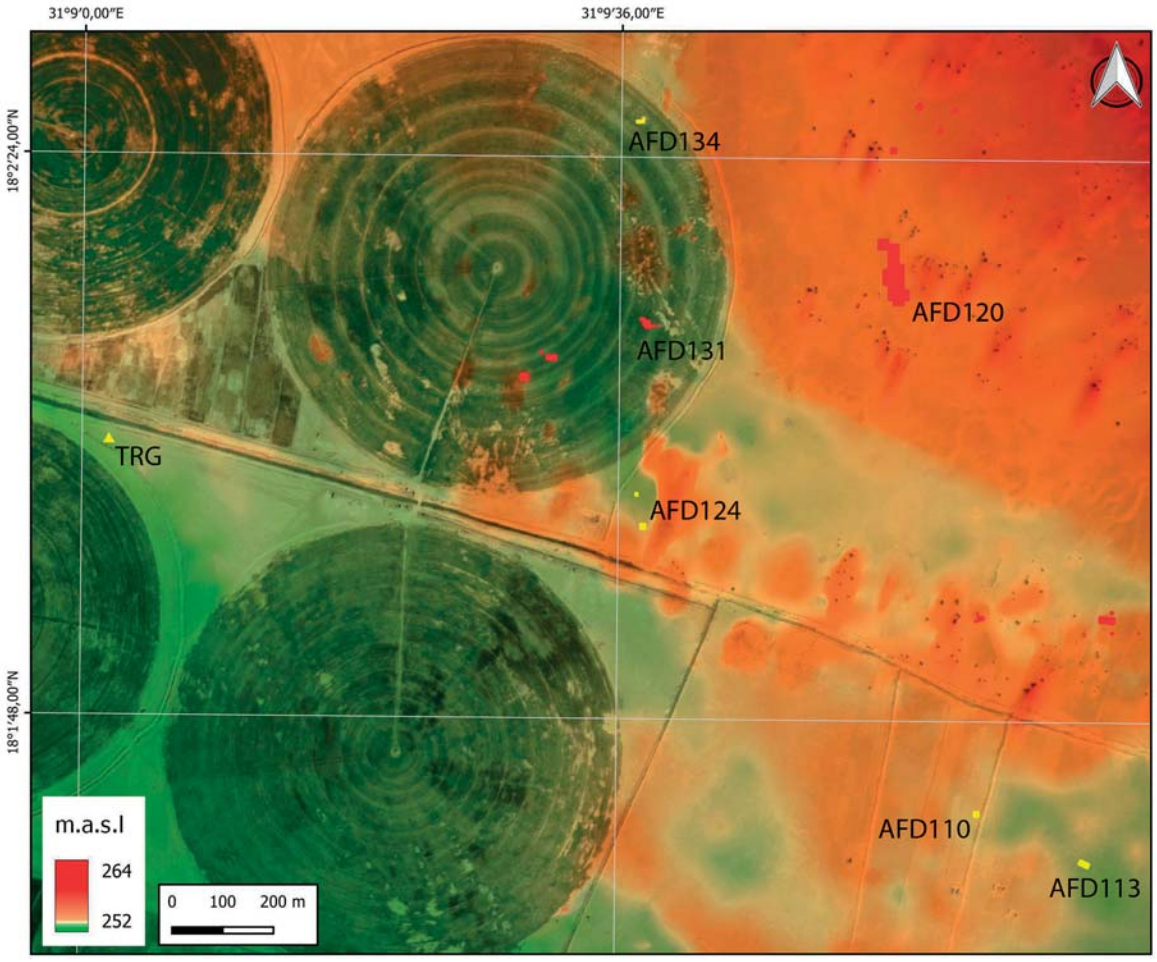

Fig. 4.109. Western part of the Affad Basin with the location of killing sites AFD110 and AFD124, as well as encampment AFD131, and mollusk harvesting locus AFD134 and fish harvesting locus AFD113

Two of the locations were determined to be killing sites, namely AFD110 and AFD124. They were situated in the western sector of the Affad Basin. In both cases, animal bone remains came from single specimens of large ruminants, an auroch in the case of AFD124 and a young buffalo or auroch from AFD110 (see above, Chapter 3). Modelling of the original surface of this area (currently completely transformed and degraded by industrial agriculture) reconstructs a zone on the riverbank of a Nile palaeochannel [*Fig. 4.109*]. Dating is based on the general assumption that this entire area was formed during MIS3, which is confirmed by OSL data from a sediment in which the remains at AFD124 occurred, namely 41.7±4.8 ka (Lub-6434). A surface survey yielded single lithic artifacts [see *Fig. 4.110*]. Their selection, however, may indicate the morphological and metric preferences of hunters regarding the range of stone tools used for processing large hunted prey.

Of interest is the fact that among the forms of flakes with long cutting edges, there were also Levallois cores of significant dimensions, a phenomenon that makes the assemblage from AFD124 resemble the slightly richer collection from the encampment at AFD24. There is also a high proportion of cores in relation to flakes, all brought in from outside, which suggests the use of these artifacts as tools.

A similar collection of Levallois tools was found in the immediate vicinity during the construction of industrial agricultural facilities in 2018, originating presumably from a damaged hunting site of Late Pleistocene data, of which there might have been quite a few on the wide bank of the palaeochannel where large animals were fair game [*Fig. 4.111*].

Fig. 4.110. Assemblage of lithic artifacts found in the immediate vicinity of clusters of auroch bones at site AFD124

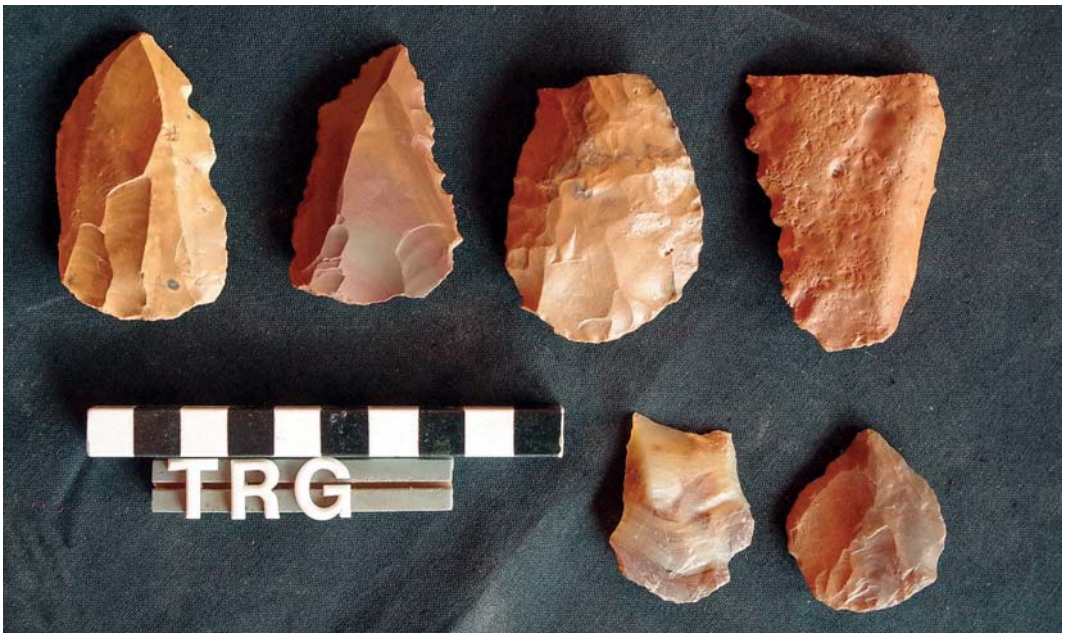

Fig. 4.111. Collection of Levallois tools from a damaged hunting site(?) in the western part of the Affad Basin

Fig. 4.112. Lithic artifacts from site AFD113: top – flakes made of chert; bottom right – flakes made of sandstone; bottom left – small sandstone flakes/chips; center – denticulate tool made of a chert flake

The collection of lithic artifacts found at site AFD113 is different in that it was found among very numerous fish remains of similar size, identified almost exclusively as of the Clariidae family (see above, Chapter 3). Apart from flakes made of various raw materials of a standard size for MSA assemblages, concentrations of small sandstone chips were also discovered [*Fig. 4.112*]. They are construed as evidence of the retouching of a flake blank on the spot, either to make or to repair a denticulate tool. One should add that inasmuch as the larger artifacts bear traces of erosion (smoothing of the edges, a patina), the small chips as a rule are devoid of such marks. Therefore, only the latter are obviously *in situ*, while the presence of other flakes and chunks could be explained in different ways, not excluding natural redeposition in alluvial units.

Last but not least, there is a collection of lithic artifacts from site AFD134 in the palaeochannel zone, an oval concentration of overheated silt, approximately 5 m by 3 m in size, containing a large amount of burnt shells of freshwater mollusks. Dating with two independent methods—TL (Lub-6433: 56.1 ± 6.8 ka) and AMS ^{14}C (Poz-102024: >48 ka)—excluded an early Holocene date in favor of a clear relationship with the Late-Pleistocene settlement horizon. The single lithic artifacts from the surface of this site also represent Middle-Palaeolithic production techniques [*Fig. 4.113*]. They resemble the artifacts from site AFD113: fragments of large sandstone flakes with clear traces of erosion and, at the same time, flakes retouched in a denticulate fashion with exceptionally fresh negative scars.

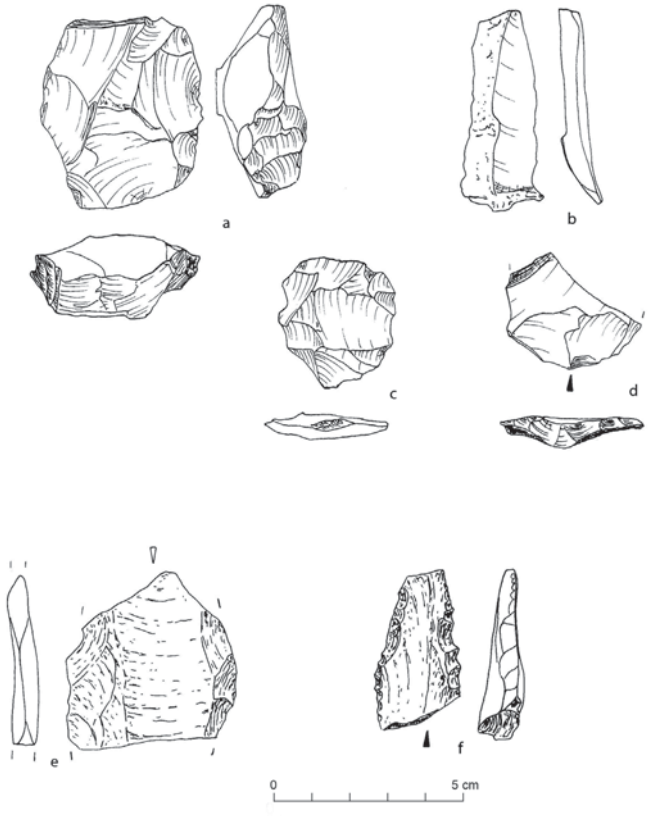

Fig. 4.113. Lithic artifacts collected at site AFD134

4.4 COLLECT OR COPY? TRADITIONAL MSA STRATEGIES FOR PROCURING STONE TOOLS

The Late Pleistocene lithic production in the Affad Basin microregion was examined based on three key categories of assemblages. These are:

– surface assemblages reflecting the location of zones of contemporary settlement remnants, not in all cases identical with primary depositional contexts of the artifacts (e.g., locations in the Tergis district);
– collections of lithic artifacts from the excavation of sectors of sites with confirmed erosion of primary sediments in which they had been deposited (e.g., northern zone of site AFD23, or extensive areas of sites AFD120 and AFD122);
– collections of lithic artifacts from the excavation of sectors of sites with preserved original, vertical and horizontal, stratigraphic relationships.

In the case of the first category of assemblages, a general picture of lithic artifact use can be formed based on objects of defined shape and size, while the presence of pieces not recorded in collections representing the other two categories of assemblages, such as bifacial points known from secondary loci at site AFD108, questions the mutual chronological or functional relationships of these finds. The second category, characteristically, illustrates the later, often intensive transformation of Late Pleistocene landscapes. Erosion of the floor sections of alluvium and aeolian layers was accompanied by an accumulation of material of later origin (gravels and sands brought in during episodes of flushing towards a significantly lowered river bed during the Holocene). Along with these sandy deposits, single artifacts representing occupation in the Early-Holocene period also found their way into Pleistocene sites. Although the most characteristic elements of the microlithic bladelet tradition are easy to recognize, one must also take into account non-distinctive small flakes, chips and chunks of a similar origin that could obscure the picture. Therefore, assessing a given collection from this category, one must take into consideration the possibility of the presence of artifacts representing other than the primary (Pleistocene) system of usage and production.

The third category opens the way to assuming, to a certain degree, the so-called 'Pompeii' premise, meaning that artifact dispersal recreates the functional diversity of particular parts of the encampment. The presence or absence of defined correlates of processes for the production of stone tools reflects for the most part the factor of intentional human activity. One should take into account the possibility of there being 'foreign' products, although in this case the probability of their conscious selection by members of groups inhabiting the site is significantly higher. For example, the most probable explanation for the significant gaps in refitted blocks from the southwestern zone of site AFD23 is that products had been processed away from the encampment and, with the same likelihood, elements such as shaped cores or tools were carried away in the end. In turn, signs of use were noted exclusively on artifacts forming the collections from the southeastern and northeastern sectors of AFD23, which were clearly brought in from beyond these zones.

A reconstruction of a Late Pleistocene stone-tool technological tradition was favored by artifacts forming the third category of collections because they were very well preserved, protected from erosion in the sediments in which they had originally been deposited, dispersed over a small

area and having the advantage of being made of quality raw material (mainly chert). The refitting of more than 40 independent blocks enabled an analysis that revealed three separate methods of stone-tool production, involving a range of Levallois methods.

The most common method was to obtain slightly elongated Levallois flakes from a core with a rectangular flaking surface and opposed-direction initial working. The dimensions of a large part of cores of this kind from the encampment—exceeding 60 mm in length, 50 mm in width and 49 mm in thickness—indicated a certain size standard for cores from which predetermined products could be detached. Given the preferential model of processing which dominated each reconstructed method, the core dimensions were reduced, the smallest of them (less than 49 mm in diameter) signifying in turn the lower limit of nodule size still tolerated by the makers of Levallois flakes from Affad. Some of the refitted blocks also indicate a change of shape of the flaking surface along with a reduction of its size in the end phase, from an initially rectangular and processed in an opposed-direction manner to a circular one that was worked centripetally.

The second method of making tools included unidirectional processing of the core, which corresponded to the model of making a classic Levallois point. In this case also the dimensions of the core were large, with a flaking surface length exceeding 60 mm in the initial processing phases.

The third method was also dedicated to the production of points, but in this case the processing of the flaking surface was carried out from the direction of the sides as well as the one platform, producing a longitudinal convexity (ridge) more or less aligned with the line of symmetry of the prospective tool. In a typological sense, this corresponds to the Nubian II method.

Both of the above methods of making flakes and points were also characterized by a preferential model of reduction. Rejuvenation of the convex shape of the flaking surface was accompanied by a narrowing and shortening of the core. All of the residual forms of cores, which bear negative scars of a correction of the parameters of the flaking surface from the side opposite to the main striking platform, come from the final processing phases and are characterized by small dimensions. It is possible, therefore, that the Nubian I method did not find application in the initial stages of point-making in the Affad Basin, while only those resembling its characteristics (meaning shaping of the tip of the tool from the side opposite the butt) found application in the final phases of reduction.

The collection from the southwestern sector of site AFD23 can be interpreted for the most part as evidence of raw material testing and selection, with many shaped nodules being carried off from the encampment. At the same time, a certain number of nodules exploited *in situ* appears to have been instructional in nature regarding their reduction. Arguing in favor of this idea is the fact that predetermined forms (both points and flakes) were left behind together with the production debris, as is also a significant irregularity of these forms. Moreover, the formation of the platform (*chapeau-de-gendarme*) already in the initial phases of the processing of partly-cortical nodules could also be taken as proof of the training character of the processing performed here, not to mention the thinning of the convexity of the bulb (which makes sense when hafting the point) on opening flakes. The making of small discoidal cores from crude flakes could also have served the purpose of instruction.

Bifacial points are one form that the Late-Pleistocene groups settling the Affad Basin never made. So far, the collections from the investigated sites have yielded no pieces of debris/by-products of such processes. The only, and very rare, examples of bifacial forms come from surface contexts and always bear traces of intensive rolling. One may therefore assume natural or inten-

tional redeposition of these objects, which come from older stages of settlement in the middle part of the Nile Valley (certainly long before the 50th millennium), in sediments dated to MIS3.

The processing of small discoidal cores made from opening flakes is also debatable. These are frequent finds at the Pleistocene sites, although largely from secondary contexts. There does not seem to be any instrumental justification for such slender blanks (detached from the cores on site as indicated by a refitting from AFD24), hence it is likely that the cores themselves were destined to become tools. Or else, the intent was to provide instruction, as already discussed above.

The material studied so far excludes the option of making blade blanks for tools in the Late Pleistocene. Alternative explanations are proposed for the presence of cores, which in a typological sense correspond to a defined prismatic form, and a certain group of flakes with the metric characteristics of blades which could be associated with them. Given the residual character of these cores, the negative scars could be viewed as evidence of rough treatment around the flaking surface, or simply a manifestation of learning the skills required for shaping a nodule with a proper flaking angle. Several of the elongated flakes were refitted, demonstrating that they were always detached from the side edges of a Levallois core with a rectangular shaped flaking surface. This indicates that the purpose in mind was to give a proper degree of flatness to the side fragments of the flaking surface. These flakes could have also been detached from the side edges of a core in an unintentional manner, creating clear ridges. However, the Late-Pleistocene collections from the Affad Basin do not reveal any conscious use of such emerging products and no apparent desire to replicate them. Their slenderness was probably a disadvantageous feature overcome only by mounting them in a frame. Actually, this appears to be one of the fundamental 'discoveries' of the Late-Paleolithic or Late-Stone-Age (LSA) technological traditions.

The Affad collections also revealed a dichotomy of a kind regarding the use of lithic artifacts by the Late-Pleistocene communities. On the one hand, tools were produced using knowledge of and skills required by what is designated today as the Levallois method. On the other hand, a substantially broader range of used products, in terms of tools, was simply production debris from a producer's point of view. Thus, everyday tool requirements seem to have operated independently to an extent of a conscious replication of production schemas of defined tools, which is the definition of a "technological tradition". Moreover, one may only surmise that it constituted a kind of medium of the concept of making 'proper' tools. At the same time, the ancient flakes and points, whether incidentally or deliberately collected, are palpable proof of their presence in the landscape and may, in fact, confirm one's belief in the rationale behind their manufacture.

The tool inventory of the Late Pleistocene Affadians included just a few types. Triangular points, probably constituting spearheads or knives, were recorded in the production debris from the southwestern sector at AFD23, mainly in the form of failed attempts (too crude, as in the case of Block 44). In turn, points or fragments of points known from other locations are significantly more regular and slender in shape. Small negative scars have also been recorded on points from the Affad Basin, testifying to intentional thinning of the base, which is the part of a tool essential for 'hafting', that is, mounting in a wooden shaft or handle. Points could have been prepared for hafting also by the formation of a tang, a technique recorded in a very few cases of tools made of pink quarzitic sandstone at Tergis. However, the relationship of this type of tool formation with Affad sites is uncertain given the significant degree of erosion noted at the Tergis sites. A single example of an analogous artifact was recorded in the northeastern sector of AFD23. Some examples of points also bear numerous traces of damage (in the form of para-burin scars), probably as a result of use.

The most numerous category of stone tools, however, were forms with a long edge retouched in a denticulate manner (both flakes and points resembling a Tayac-type point). Negative scars from retouching frequently show a high degree of regularity. In turn, scraping tools (including racloirs) were recorded with lesser frequency, while perforators were found only incidentally. The results of stone-tool wear analysis confirmed that cutting operations, meaning dividing an animal carcass, were much more important than processing skins. Tools commonly identified with the working of wood—notched forms and burins—were recorded in lesser numbers. Occasional finds included large tools that could have functioned as hoes for gathering activities (of a handaxe or Levallois-core type, suggested by the analysis of the collection from AFD111). Insert forms of knives and sickles also came exclusively from surface contexts and are to be associated with later settlement in the Early Holocene.

Special preferences do not seem to have existed regarding the raw material used for making stone tools. Exclusive use of locally available raw materials is evident: pebbles of chert (or similar cryptocrystalline rock types) at AFD23, ferruginous sandstone at AFD111 and AFD131. Single products of other raw materials, such as the easily identified light-colored chert with external chalk surfaces from AFD122S, justifies the statement that members of groups settling in the Affad Basin forayed over a wider area. Retracing the steps of Affadians in search of primary chert outcrops (limestone formations) in future research will bring into focus the issue of the extent of migration practiced by the Late-Pleistocene and Early-Holocene communities in the Southern Dongola Reach. However, there has been so far no evidence of any importation of raw materials or even single artifacts of raw materials occurring in regions more than 100 km away from Affad, e.g., basalt (the closest outcrops are in the volcanic fields of the Bayuda Desert), Eocene flint (occurring in the Western Desert , corresponding roughly to the distance between the Second and Third Nile Cataracts) or obsidian (upper course of the Blue Nile).

The results of this analysis of lithic artifacts from Late Pleistocene sites in the Affad Basin have justified the decision to consider each of these collections separately despite the relatively small area of investigations. They have highlighted several features that could have otherwise gone unnoticed or not understood had these assemblages been looked at en bloc. At the same time, the results imply a more general regularity concerning MSA tool-procuring strategies in the Middle Nile Valley, which should take into account:

– skills and knowledge of individual toolmakers and tool users, who rarely if ever constitute a monolith;
– availability of suitable raw material; taking cores outside the 'supply' camp may constitute a premise for the idea that access to raw material of a specific quality was not permanent;
– access to ready-made (older) products fulfilling tool expectations;
– function of sites and their seasonal nature, perhaps conditioned by the above-mentioned aspects. In a given group consisting of a small number of adults, hunting trips could have been the prerogative of those capable of producing stone tools, whereas individuals without the skills or unable to make new tools would have stayed behind in the encampment and engaged in gathering ready-made (older) products;
– the provisional nature of most of the tools found at encampment sites is in line with the assumption that most of the 'proper' tools destined to be hunting weapons had been used outside the encampment where they were susceptible to being damaged and subsequently discarded.

APPENDIX 4.A

Wear analysis of siliceous materials from the Affad microregion

Katarzyna Pyżewicz PhD (Faculty of Archaeology, University of Warsaw, Poland)

A wear analysis of siliceous artifacts, including formal tools, cores and deliberately unretouched debris as part of blocks assembled by the use of refitting methods, was performed at the Wear Analysis Workshop of the Institute of Archaeology of the Adam Mickiewicz University in Poznań, Poland.

Methodology

Traces on the surface of lithic artifacts were examined under a metallographic microscope Nikon LV150 adapted to operate in reflected light (with a light intensity change option), giving magnifications from 50× to 100×. Connection with a digital camera allowed images to be transferred to a computer for recording and processing. The actions were conducted at this stage of research due to the possibility of removing traces (e.g., organic traces) from the surface during the washing of the lithics.

Microscopic trace analyses were preceded by a preparation of the surface of the artifacts. Impurities were removed by washing in warm water and detergent. No cleaning tools that could leave any marks on the rock surface were used. Prior to the microscopic analysis artifacts were cleaned with pure acetone aimed at removing any grease left behind as a result of contact with human skin, among other things. Artifacts were viewed at consecutive magnifications of 50×, 100× and 200×, allowing specific marks: damage, cracks and wear, to be identified in detail. A digital photographic record of a selected group of marks was made and subjected to computer processing. Schematic drawings locate the images on individual specimens. Observed traces of use are indicated with schematic drawings as well. Post-depositional and intentional changes of the lithic surface are described in the table below.

Table 4.52. Post-depostitional and intentional changes on the surface of siliceous material from the Affad Microregion

Inv. no.	Post-depositional changes	Wear marks (intentional)
1. Affad 23, refitted elements of Block 8		
1808	Very light, locally glossy patina; remains of glue	No signs of usage or technological marks
1315	Very light, locally glossy patina; remains of glue	No signs of usage or technological marks
26	Very light, locally glossy patina; remains of glue	No signs of usage or technological marks
1324	Locally glossy patina; remains of glue	No signs of usage or technological marks
984	Locally glossy patina; remains of glue	No signs of usage or technological marks

Inv. no.		Post-depositional changes	Wear marks (intentional)
188		Locally glossy patina; remains of glue	No signs of usage or technological marks
186		Locally glossy patina; remains of glue	No signs of usage or technological marks
660 + 474		Intense glossy patina	No signs of usage or technological marks
i/146, 188?, 2013/i/67 – three specimens stuck together		Light, locally glossy patina; remains of glue/glossy patina; remains of glue	No signs of usage or technological marks
?96, 2060, ?, ? – four specimens stuck together		Light, partly locally, glossy patina; remains of glue/intense glossy patina; remains of glue	No signs of usage or technological marks; only on specimen 2060 (2013/i/47, multifaced butt) single marks of wear attributed to an organic raw material(?) located on the butt. Possibly marks of an organic hammerstone or post-depositional marks(?)
1313	i/18	Very light, locally glossy patina; remains of glue	No signs of usage or technological marks
1327 (chip fragment, multi-faced butt)		Very light, locally glossy patina	Single spots of wear attributed to an organic raw material located on the butt; marks of an organic hammerstone(?)
1329		Locally glossy patina	No marks
2690 (multi-faced butt)		Very light, locally glossy patina; remains of glue	No signs of usage or technological marks; single spots of wear attributed to an organic raw material(?) located on the butt, certainly marks of an organic hammerstone
1508		Very light, locally glossy patina	No marks
189		Very intense, locally glossy patina	No marks(?)
1548 + ?		Light, locally glossy patina	No marks (numerous remains of glue on the butt)
1416 + 1314		Light, locally glossy patina	No marks (numerous remains of glue on the butt)
433? + 1314		Light, locally glossy patina	No marks (numerous remains of glue on the butt)
2171		Light, locally glossy patina	No marks
1547		Light, locally glossy patina	No marks (numerous remains of glue on the butt)
1322		Light, locally glossy patina	No marks
490 + 366 + 613		Light, locally glossy patina	No marks (numerous remains of glue on the butt)
Core + single flakes (182, 185, 1323, among others)		Locally glossy patina; remains of glue	No signs of usage or technological marks

Inv. no.		Post-depositional changes	Wear marks (intentional)
2. AFD23, urefitted elements most likely from Block 8 Forms (products of debitage) mainly analysed from a technological viewpoint; covered in remains of glue			
620		Very light, locally glossy patina	No marks
904		Very intense, glossy patina	No marks(?)
2764		Very light, locally glossy patina	No marks
627		Locally glossy patina	No marks
2752 (flake, multi-faced butt)		Very light, locally glossy patina	Single spots of wear attributed to an organic raw material located on the butt, or post-depositional marks(?)
575		Very intense, glossy patina	No marks(?)
1320		Very intense, glossy patina	No marks(?)
2762		Very light, locally glossy patina	No marks
567		Very intense, glossy patina	No marks(?)
1963	2013/i/90	Very light, locally glossy patina	No marks
2763 (flake, multi-faced butt)		Very light, locally glossy patina	Single spots of wear attributed to an organic raw material located on the butt; marks of a hammerstone (?)
2765		Very light, locally glossy patina	No marks (natural butt)
1307		Very light, locally glossy patina	No marks (numerous remains of glue on the butt)
3. AFD23, refitted elements of Block 44 Forms (products of debitage) analyzed mainly from a technological viewpoint; covered in remains of glue			
1882		Light, locally glossy patina	No marks (numerous remains of glue on the butt)
2379? + ?		Light, locally glossy patina	No marks (numerous remains of glue on the butt)
2189 + 2188		Light, locally glossy patina	No marks (numerous remains of glue on the butt)
2498?		Light, locally glossy patina	No marks (numerous remains of glue on the butt)
2472 (flake, multi-faced butt)		Light, locally glossy patina	Single spots of wear attributed to an organic raw material located on the butt, or post-depositional spots(?)
2471 (100% cortical flake, multi-faced butt)		Light, locally glossy patina	Single spots of wear attributed to an organic raw material located on the butt, or post-depositional spots(?)
2474 + 2007 + ? + ? (2474 butt missing; 2007 edge butt)		Light, locally glossy patina	Single spots of wear attributed to an organic raw material located on the butt, or post-depositional spots(?)
1302 (Levallois point) *Fig. 4.114*		Light, locally glossy patina	Line wear and cracking on butt attributed to the use of a hammerstone while shaping the striking platform
2187		Light, locally glossy patina	No marks (numerous remains of glue on the butt)

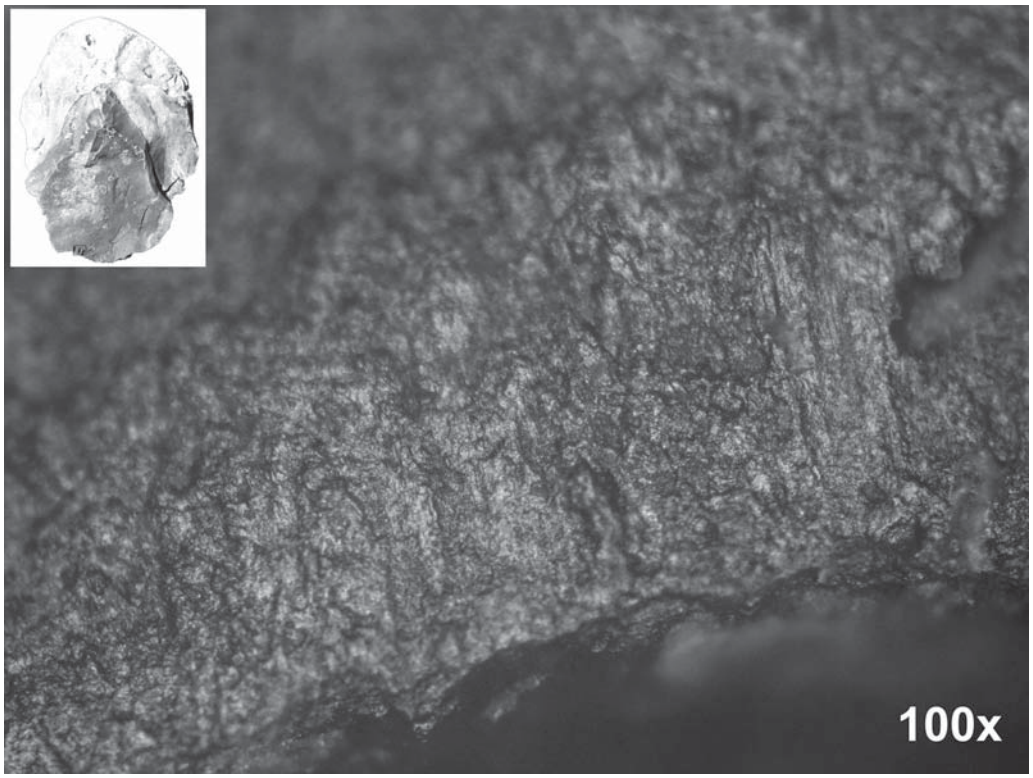

Fig. 4.114. Use-wear traces on a Levallois point 1302 (magnification 100×)

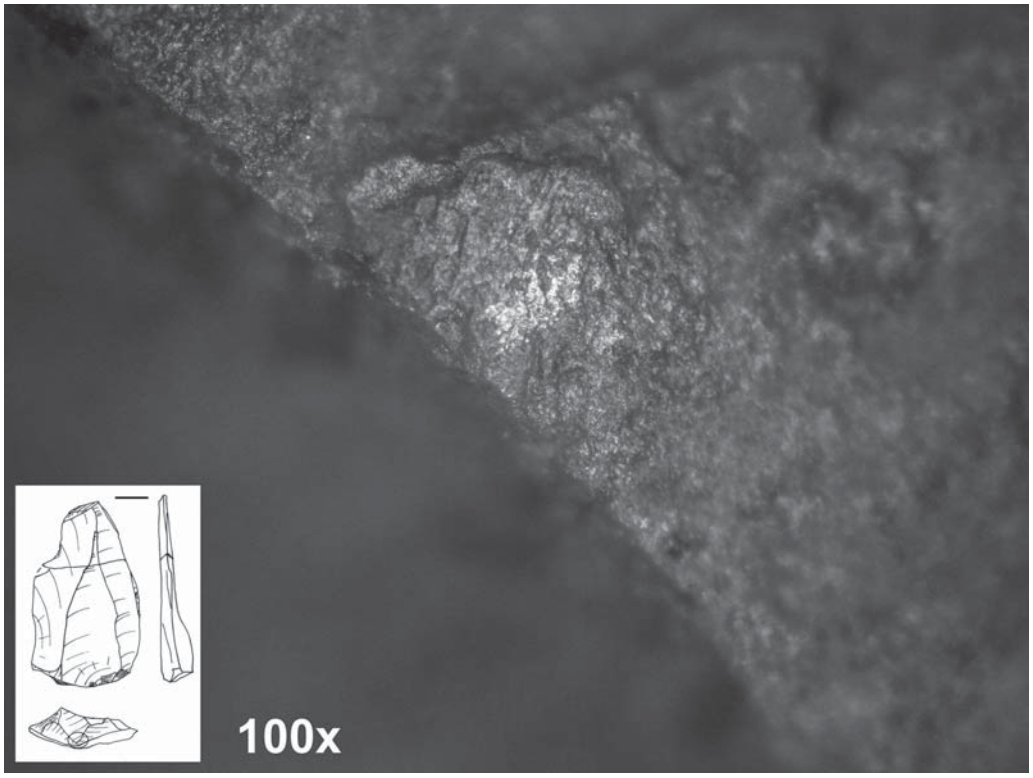

Fig. 4.115. Use-wear traces on a Levallois point 2237 (magnification 100×)

Inv. no.		Post-depositional changes	Wear marks (intentional)
2483		Light, locally glossy patina	No marks (numerous remains of glue on the butt)
1443		Locally glossy patina	No marks
2485 + 2477		Locally glossy patina	No marks (numerous remains of glue on butt)
Core 973 + 2 flakes		Light locally glossy patina	Single spots of wear attributed to an organic raw material located on the butt, or post-depositional spots(?)
4. AFD23/2016, wear analysis			
	2013/G/43 (ID2964)	No patina	No signs of usage or technological marks
1819	2013/i/67	No patina	No signs of usage or technological marks
2450 (Levallois point)	2013/i/38	Light, locally glossy patina	No signs of usage; single spots of wear and cracking on butt attributed to a hammerstone(?)
2237+2238 (Levallois point) *Fig. 4.115*	2013/i/20	Light, locally glossy patina	No signs of usage; single spots of wear and cracking on butt attributed to a hammerstone(?) Straight breakage
2639 (Levallois flake)	2013/i/113	Very light, locally glossy patina	No signs of usage; single spots of wear and cracking on butt related with the use of a hammerstone while detaching the artifact
2891 *Fig. 4.116*	**2013/I/113**	Very intense, locally glossy patina	No signs of usage or technological marks(?)
3036	2013/G/39	Very intense, locally glossy patina	No signs of usage or technological marks(?)
2069	2013/i/111	Very light, locally glossy patina	No wear or technological marks
3067	2013/G/10	Very intense, locally glossy patina	No signs of usage or technological marks(?)
2936	2013/F/18	Very intense, locally glossy patina	No signs of usage or technological marks(?)
2630	2013/i/66	Very light, locally glossy patina	No signs of usage or technological marks
2535	2013/i/84	Very light, locally glossy patina	No signs of usage or technological marks
2658	2013/i/31	Very intense, locally glossy patina (?)	No signs of usage or technological marks
5. Specimens from cut features (2014/i/128)			
3121 **facetted butt**	2013-H-17 Feature H/23	Very light, locally glossy patina	No signs of usage; linear marks on butt and cracking attributed to the use of a hammerstone while detaching the artifact
3122 *Fig. 4.117*		Very light, locally glossy patina	No signs of usage or technological marks
	2014/i/127 Feature 1/25	Very light, locally glossy patina; remains of glue	No signs of usage or technological marks
	1/28 Feature 1/35	Very light, locally glossy patina; remains of glue	No signs of usage or technological marks
	Feature Q5 Part N Q/6	Very light, locally glossy patina, remains of glue	No signs of usage or technological marks

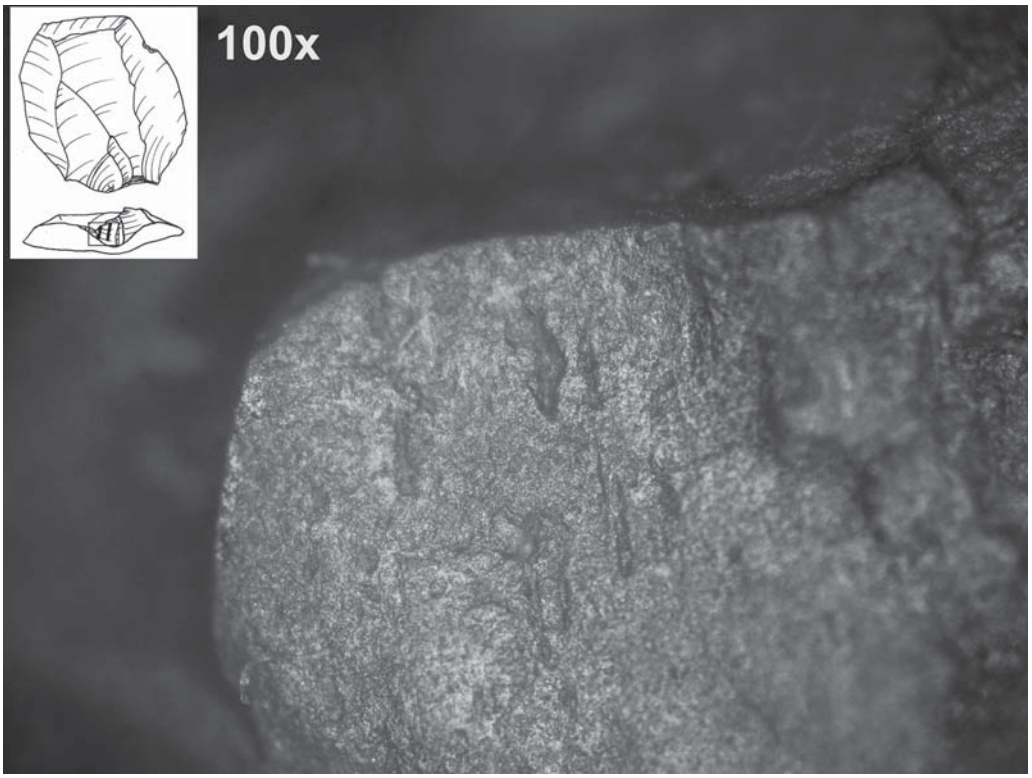

Fig. 4.116. Use-wear traces on a Levallois point 2891 (magnification 100×)

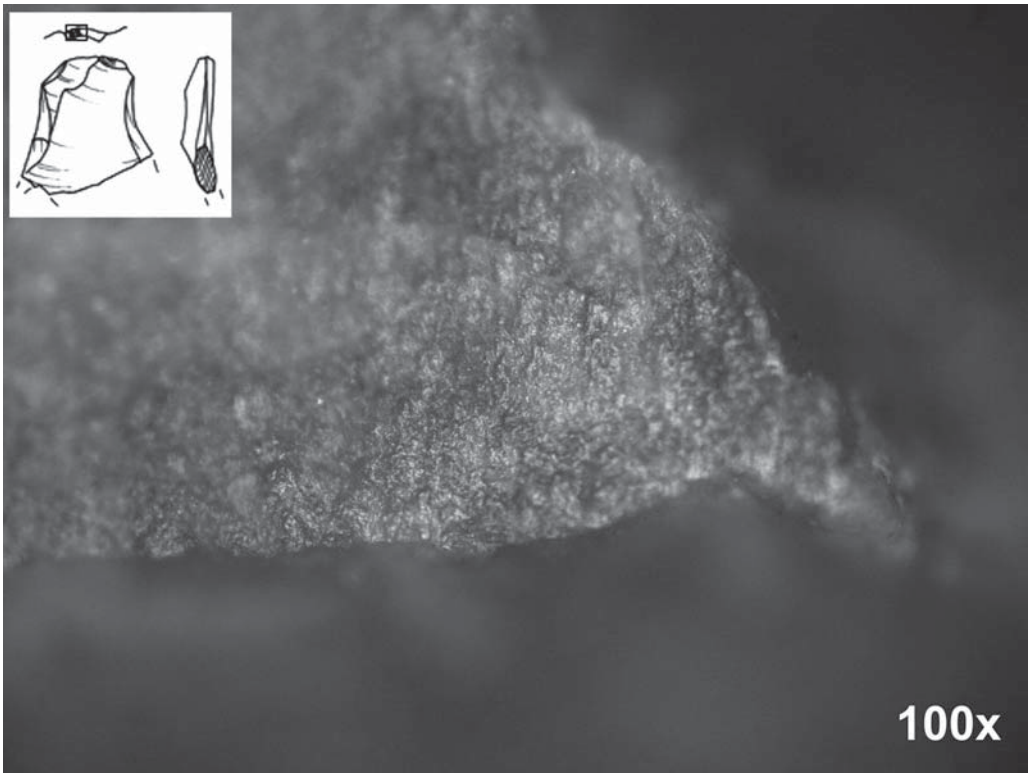

Fig. 4.117. Use-wear traces on a facetted butt 3121 (magnification 100×)

Inv. no.		Post-depositional changes	Wear marks (intentional)
6. AFD24 tools, wear analysis			
AFD24	2016/23	Intense glossy patina	No microscopic signs of usage or technological marks; use wear retouch(?) extends along right-hand edge
AFD24	**W/4 (ID6068 = Levallois flake) W/I/88** *Fig. 4.118*	Locally glossy patina	No technological marks; macroscopic marks extend along both side edges – chipping, as well as microscopic marks – wear attributed to contact with soft tissue, undoubtedly occurring while processing animal carcasses; marks similar to these occurred as a result of processing wood, line wear occurring on the positive side and laterally placed to the working edge, suggesting scraping motions
AFD24	**2016/13** *Fig. 4.119*	Light, locally glossy patina	No technological marks; microscopic marks extend along the left-hand side edge – wear attributed to contact with soft tissue of animals, organic raw material, and undoubtedly occurring while processing animal carcasses
AFD24	**A/II/12 2016/30** *Fig. 4.120*	Light, locally glossy patina	No technological marks; microscopic marks visible along both side edges – wear attributed to contact with soft tissue – skin and bone, undoubtedly occurring while processing animal carcasses; locally situated line wear placed parallel to the working edge, suggesting longitudinal motions, cutting (at least in part)

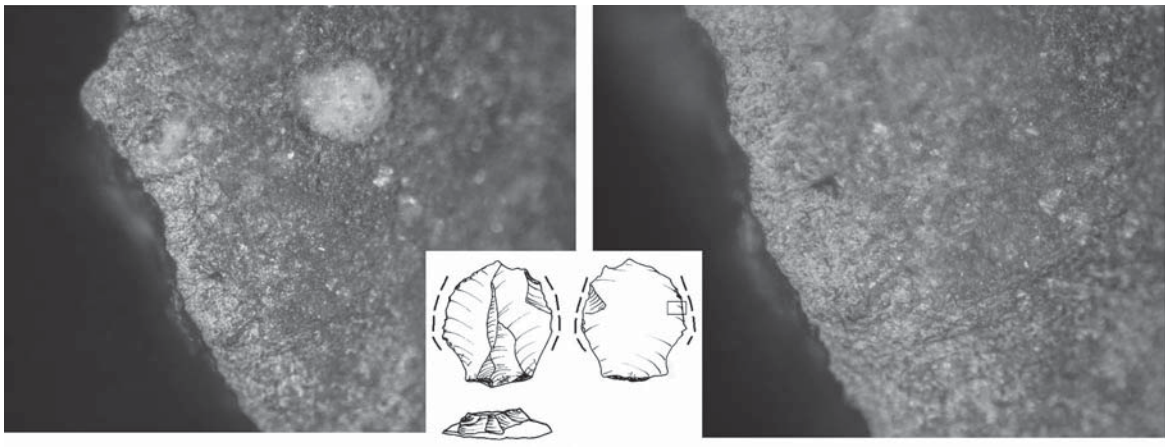

Fig. 4.118. Use-wear traces on a Levallois flake W/4 (magnification 100× left and 200× right)

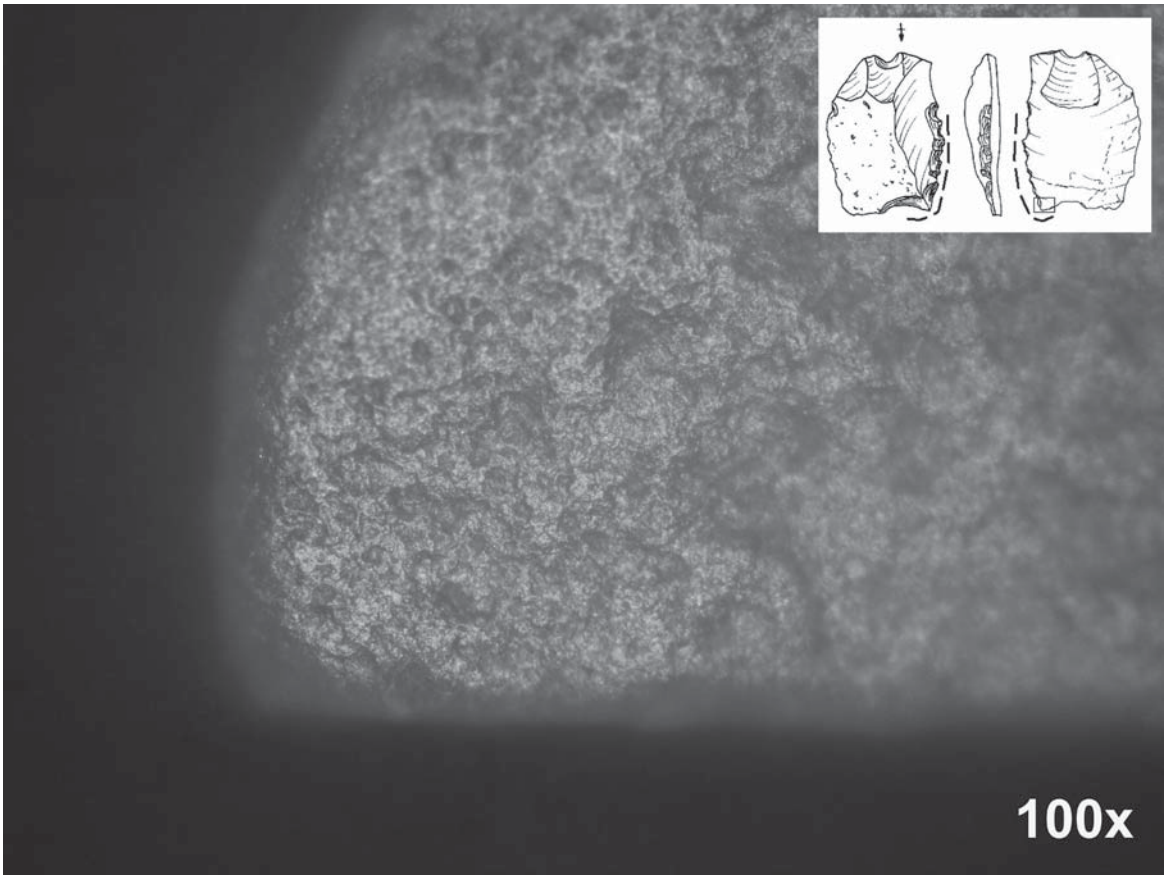

Fig. 4.119. Use-wear traces on 2016/13 (magnification 100×)

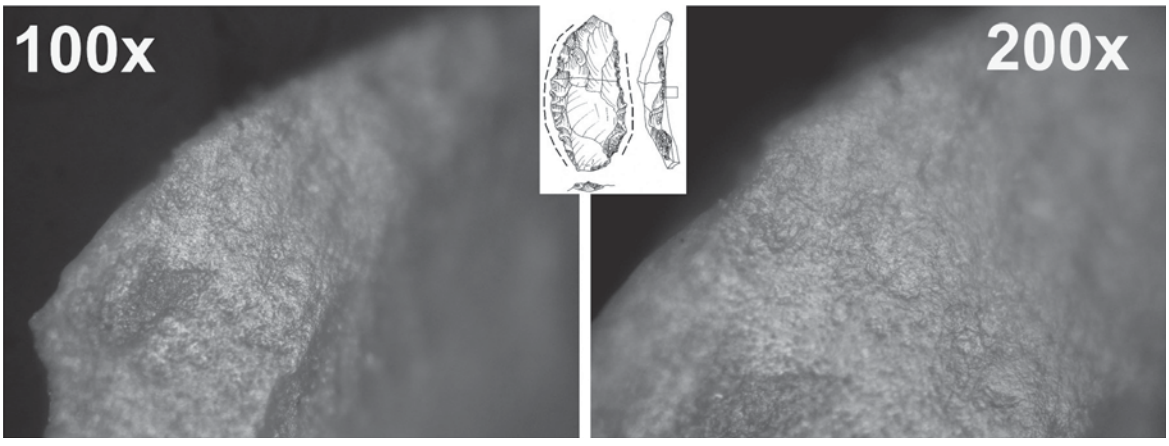

Fig. 4.120. Use-wear traces on 2016/30 (magnification 100× left and 200× right)

Chapter 5

CUT FEATURES RELATED TO MSA SETTLEMENT AT SITES AFD23 AND AFD24

Any presentation of the environmental context and chronology of the MSA communities from Affad will not be complete without a look at some unique anthropogenic features that constitute a behavioral response to the environment. These are features comprising settlement remains—postholes, etc.—and they have been recorded in almost every explored sector at site AFD23 [see *Figs. 3.3, 3.4, 3.5*], as well as at site AFD24 in general. They were located among concentrations of debris from lithic production, as well as animal bone remains. In stratigraphic terms, at AFD23 the cut features were associated with the floor section of sandy deposits described as facies 23.D (see Chapter 2). Some of these (located in ground relief depressions) occurred below a deposit representing facies 23.E.1. Given the meager thickness of sands 23.D.1, the deepest anthropogenic features cut through the top section of clayey silts (facies 23.C). The stratigraphic record from test trench 2013/I/54 (see above, *Fig. 2.6:c* and section E–F) suggests at least two levels of postholes, which would make the sediment dividing the two levels the source of the most precise dating of presumably cyclical (seasonal?) settlement. However, the previously published OSL date of this sediment, UJK-OSL-37: 15.1 ± 1.66 kya (Osypiński et al. 2016), was calculated as the minimum age of the deposit and, according to the current state of knowledge, does not indicate the true age of MSA settlement (Osypiński et al. 2021). Despite this, the finds from Affad 23 and Affad 24 constitute extremely rare evidence considering the published record of Late Pleistocene sites in Northeastern Africa.

5.1 CUT FEATURES FROM AFFAD

The classification of cut features from AFD23 has already been presented in the literature (Osypiński et al. 2016), but it will be reiterated here again at length in order to facilitate the discussion of new finds following the cut-off date of 2014 for the fieldwork results covered in the previous publication.

5.1.1 Site AFD23

The cut features from site AFD23 are divided by size and shape into six basic types [*Table 5.1*, *Fig. 5.1*]. Type I represents small pits (10–15 cm in diameter), with a circular outline and flat bottom. Type II is of analogous shape but greater diameter (around 20 cm). Type III is another variety of smaller pit, but with a triangular (meaning pointed) cross section. Pits of Type IV are, once again, small and circular (10–15 cm in diameter) with rounded bottom. Type V is a variety

Table 5.1. Typology of cut features from site AFD23 (after Osypiński et al. 2016)

Type	∑	Diameter (cm)			Depth (cm)			Fill		
					Bottom parts cutting 23.C.1					
		minimum	maximum	average (*mediana*)	minimum	maximum	total	homogeneous	dual layered	multi-layered
I	52	5	18	12.36 (*-12-*)	1	18	22	37	12	3
II	20	18	30	21.50 (*-20-*)	2	13	>13	18	0	2
III	5	7	16	11.0 (*-12-*)	8	15	>15	5	0	0
IV	44	5	18	11.02 (*-11-*)	2	12	>12	39	2	3
V	8	19	32	23.87 (*-23-*)	5	15	>15	8	0	0
VI	4	20×54	100×125	–	10	23	>23	2	0	2
Total	133							109	14	10

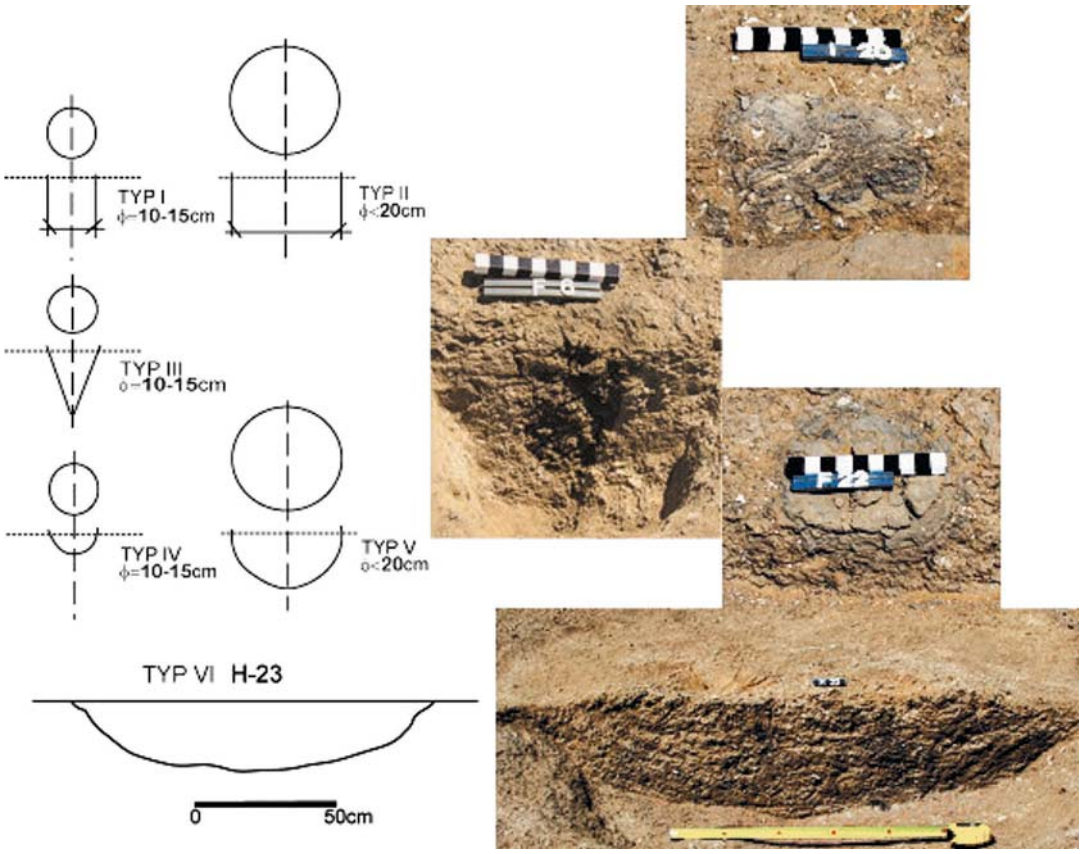

Fig. 5.1. Tentative typology of cut features from site AFD23 illustrated with selected section views of excavated postholes

of Type IV but with greater diameter (around 20 cm). The last kind of pit, Type VI, is the largest of these features; its outlines are polygonal and the bottoms irregular, mostly rounded.

Cut features in the northeastern sector of site AFD23 (trench 2012/B; see *Fig. 3.3*) were recorded only in the clayey-silt top section, because the significant dust content in the fill of these features made observation of the discoloration marking their outline in the main sediment (23.D.1b) difficult at best. The recognized features were mainly small pits (<15 cm) with rounded bottoms (Type IV). Two slightly larger cavities (<20 cm) were also distinguished (Type V), as well as another two with flat bottoms (Type II). The fill of each feature was generally dense, homogeneous and light-colored. Two Type-1 pits possessed layered fill: while laminated dark silt occurred in the bottom parts, the remaining space was filled with loose sand. The cuts could not be fully described, being preserved only in the lower/bottom parts, but their arrangement in a gentle curve, running east–west and extending for about 2 m, was obvious nonetheless [B/2–B/5; see *Fig. 3.3*].

The greatest number of cut features was recorded in the southwestern sector of the site (trench 2013/F-I, 2014/Q and areas explored in 2016) [*Figs 5.2, 5.3*; see also above, *Fig. 3.5*] and here, too, most of them were recorded in the top of the clayey silt layers 23.C.1 or 23.C.2, creating a lightly undulating surface with a visible ground relief depression in the western sector of the explored area. Only three pits were recorded in the floor sections of facies 23.D.1b. Generally, smaller features were found in abundance also in this area (48 of Type I; 5 of Type III; and 37 of Type IV), filled mostly with a light-colored homogeneous fill (82 cases). Only two pits possessed a dual-layer fill, while six more had multilayer lamination, including micro-layers of silt and sand.

Larger features with rounded (Type V) or flat bottoms (Type II) did not form a separate group but were rather dispersed among the small features. The largest pits (Type VI) with simultaneously the greatest depth occurred more or less in the center of the space demarcated by cut features. The fill of feature H/23 (Type VI) was of a laminated character dominated by sand. The other features of this category possessed homogeneous darkish-grey fill (10YR4/1dry, 10YR4/2wet).

The differentiation of the fill reflects the rate at which the features were filled. The multilayered (including dual-layer) nature is explained by water gathering in the negatives/holes left by removed organic elements (posts), as well as windblown sand filling them. It means that at some point a number of these pits actually constituted a physical depression in the ground (after the episode of the wooden installations). In turn, homogeneous fill may reflect a sudden filling of the pits with alluvial silt or a gradual decomposition of the wooden material of the posts themselves left from the settlement period. The zone occupied by the cut features, within the investigated area, forms a strip about 10 m wide, aligned NE–SW.

Small pits have also been recorded among clusters of animal bone remains in the southern sector of the site, even though not all of them could be recognized in full given the significant looseness of the deposit (trench 2013/M; see above, *Fig. 3.4*). Three out of four pits represented Type II features with a relatively small diameter (about 18 cm), hence one is entitled to describe them as larger Type-1 pits. Apart from one pit with a rounded bottom (Type IV), the rest in this zone had flat bottoms. A homogeneous light-colored fill (similar to that from trench 2012/B) was found in all of these pits.

The only artifacts in the fill of cut features from AFD23 were two non-diagnostic flakes in the fill of pit H/23, and single lithic products of Pleistocene knapping in three other pits, that is, I/25, I/35 and Q/5 [*Fig. 5.4*].

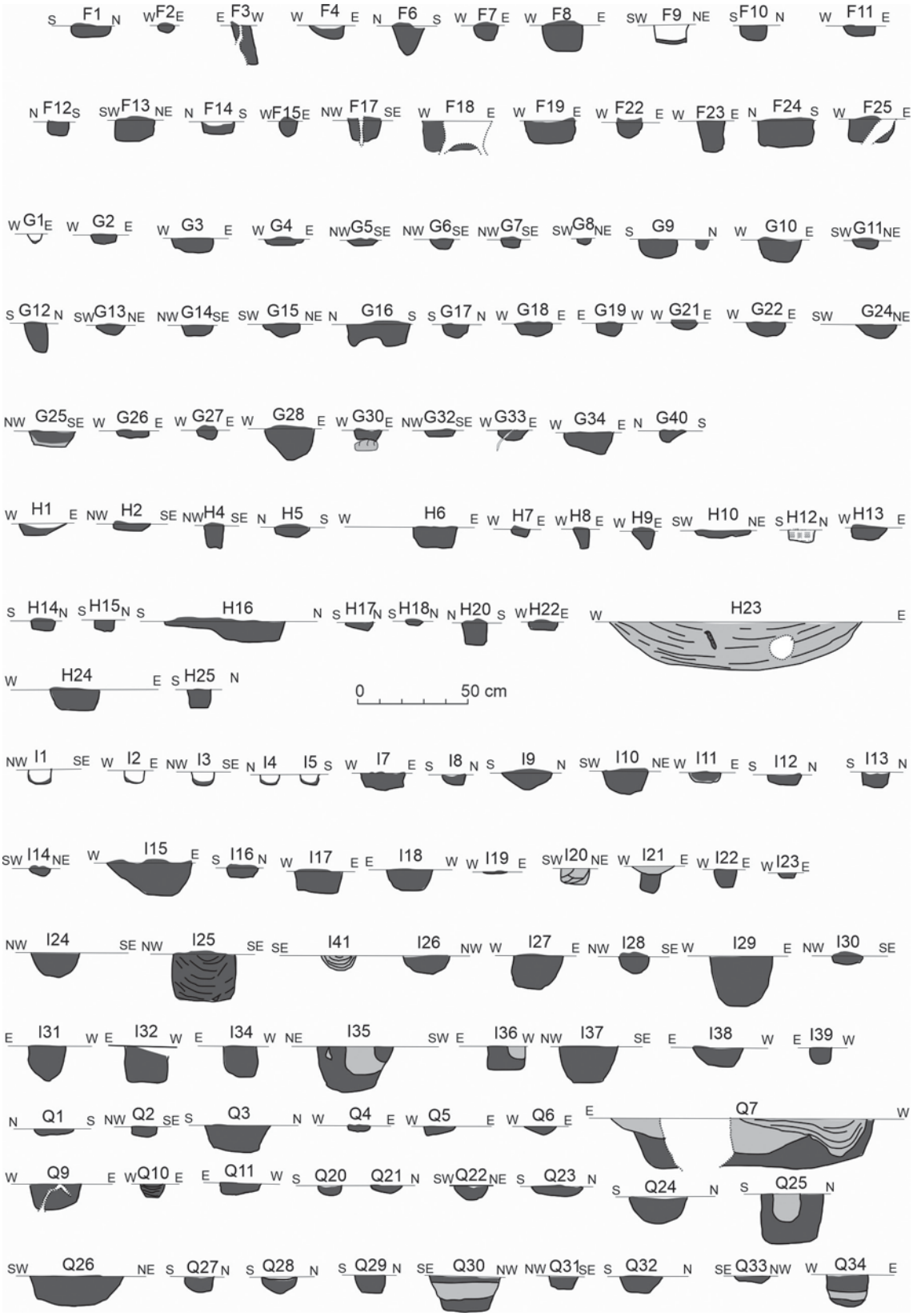

Fig. 5.2. Sections through all of the cut features excavated at site AFD23

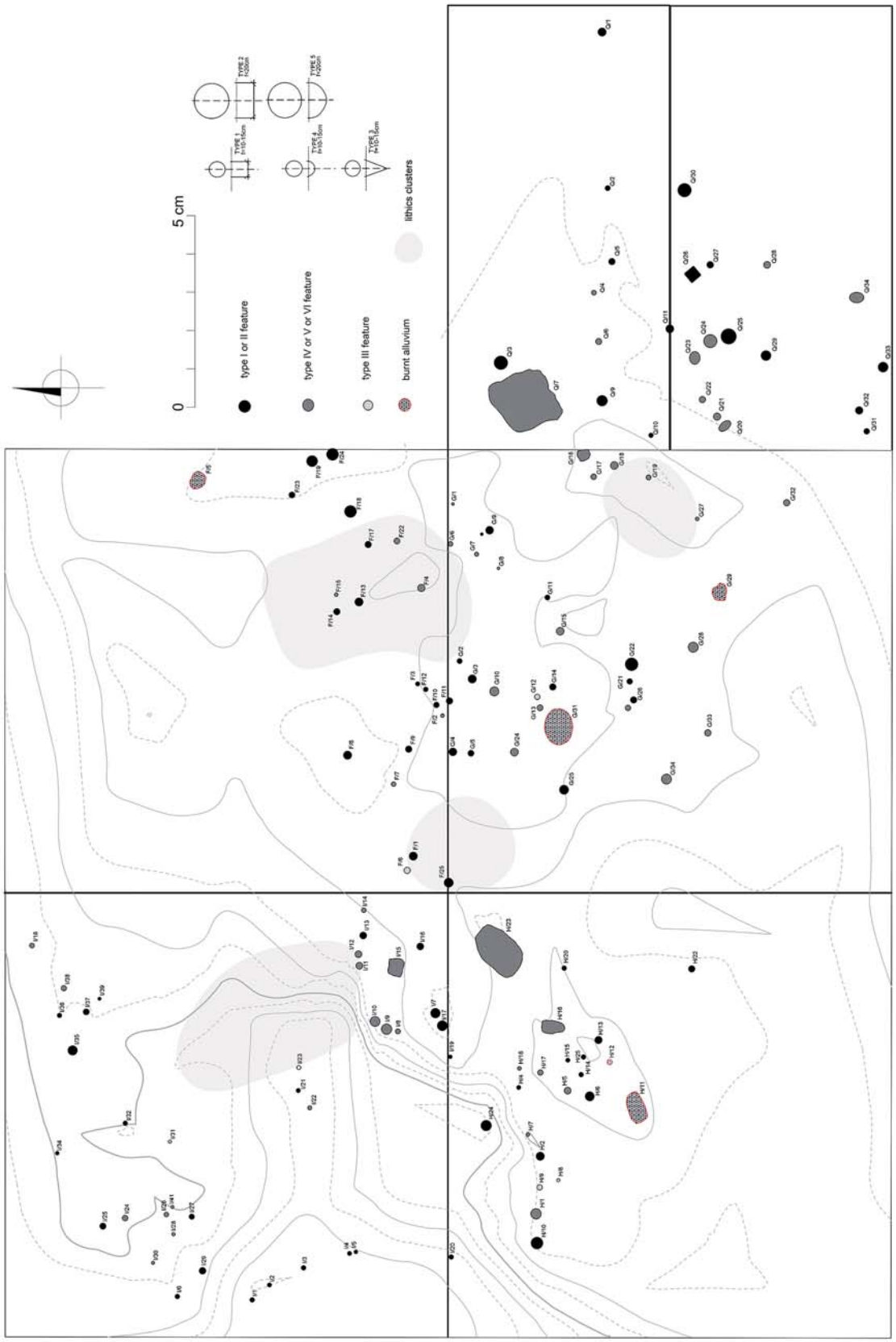

Fig. 5.3. Location of cut features mapped and excavated at site AFD23

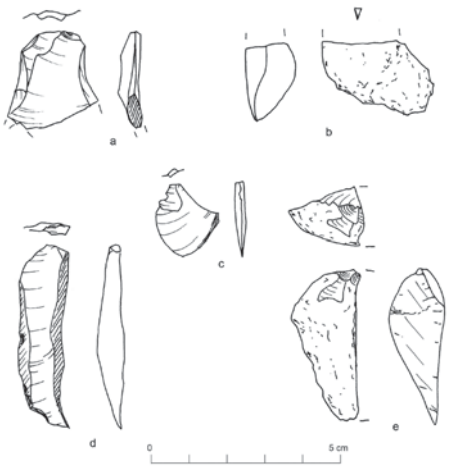

Fig. 5.4. Lithic artifacts from the fill of cut features at site AFD23

5.1.2 Site AFD24

Numerous traces of posthole pits of the same kind as those from AFD23 were evident at site AFD24 right from the start of explorations there in 2016. The set discovered over two seasons of work outlined the most likely boundaries of a lightweight construction belonging to the MSA campsite. The pits are aligned east–west, forming a zone about 10 m wide [*Fig. 5.5*]. The two excavated posthole pits (E5 and E6) turned out to be no more than 5 cm deep, just like the 'empty' postholes from AFD23 where the fill was so loose that it could be removed mechanically once the outline had been traced. Although 24 of the posthole pits at Affad were recorded in the top section of the clayey silt layer, it is more than likely that at the time of MSA settlement the surface was already covered with a layer of sand and dust. This would explain their limited depth in terms of the bottom section embedded in the clayey hard layer below the surface. The presence of pits/hearths was not recorded in the ground relief depressions (as at AFD23). Here, all of the cut features occurred on one level.

Given that most of the posthole pits were not explored, they cannot be either listed or described in terms of their fill. Nonetheless, there is a very strong likelihood that they duplicate the same general scheme known from AFD23. Overall, one should note the remains of at least one hearth in the southern sector of the campsite (area of trench B) with a concentration of small posthole pits around it [see *Fig. 5.5*]. Another cluster of postholes (Type VI) appeared around one of the larger depressions along the boundary between trenches A and E. Smaller clusters of features were noted in other parts of the campsite, for example, a group of three pits of medium size (Type II or V) in the area of trench C, and a linear set of pits in the southern sector of trench B. Overall, 87 small pits (Types I, III, or IV) were recorded in the investigated area, and of these seven revealed a loose dusty fill, while the others presented compact fill of a clearly darker color. The laminated fill of pit E5 was sampled for laboratory analysis of the strontium isotope content (Osypińska et al. 2021).

None of the explored cut features yielded any artifacts.

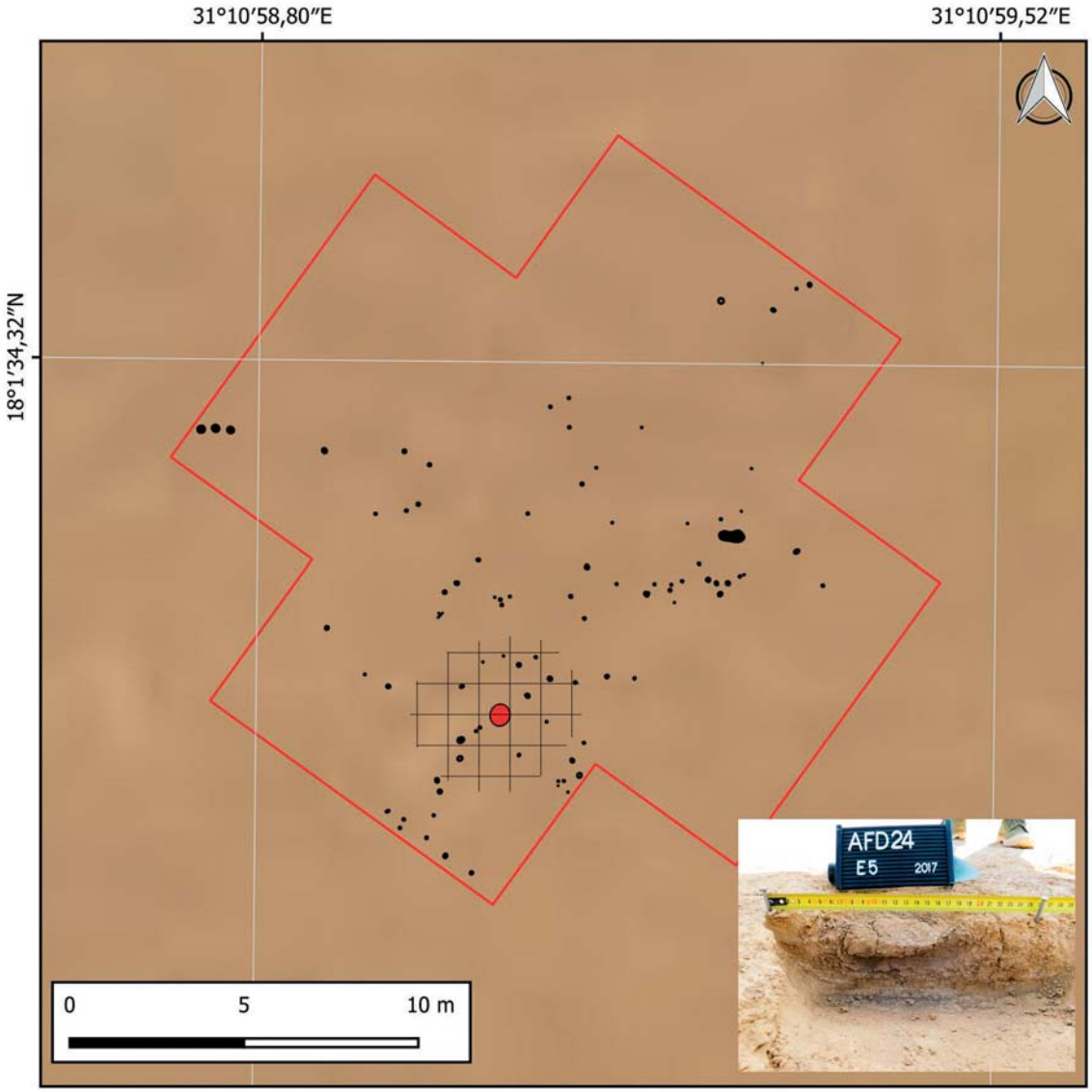

Fig. 5.5. Location of cut features at site AFD24: black – postholes/pits; red – baked alluvium; hatched area – averaged dispersion of refitted lithics; inset, a sectioned posthole

5.2 FUNCTION OF CUT FEATURES

The size, shape and fill of the cut features recorded at AFD23 and AFD24 alone do not identify their function. The spatial context—the mutual spatial relationships of the postholes and other pits, and their relationship to the clusters of lithic products and animal bone remains—has to be considered as well. Very clear evidence of functionality is provided by the data from trench 2012/B at AFD23, where a range of posthole pits and a single hearth occurred alongside antelope bones, indicating meat boning (see above, § 3.4.1). The handling of the meat could thus be linked with consumption on the spot, but it is also possible to suggest further processing, by drying, for example, which is the simplest and most common way of preserving meat. The argu-

ment in favor of meat boning is further supported by the composition of lithic products in this zone and the southern zone of site AFD23 which is attributed a similar function (45% of forms retouched in a denticulate manner within the campsite zone [trenches 2013/F–I,Q], versus up to 75% in the northeastern and southern zones). The drying of fillets (strips) of meat called for the use of simple wooden installations insofar as a given place did not ensure such conditions naturally (for a parallel installation from the Dinder National Park in eastern Sudan see *Fig. 5.6* top left). One may therefore surmise that the posthole pits accompanying numerous concentrations of animal remains and stone tools with confirmed function (e.g., use-wear evidence from site AFD24; see Appendix 4.1) constitute the remnants of simple frames constructed for the purpose

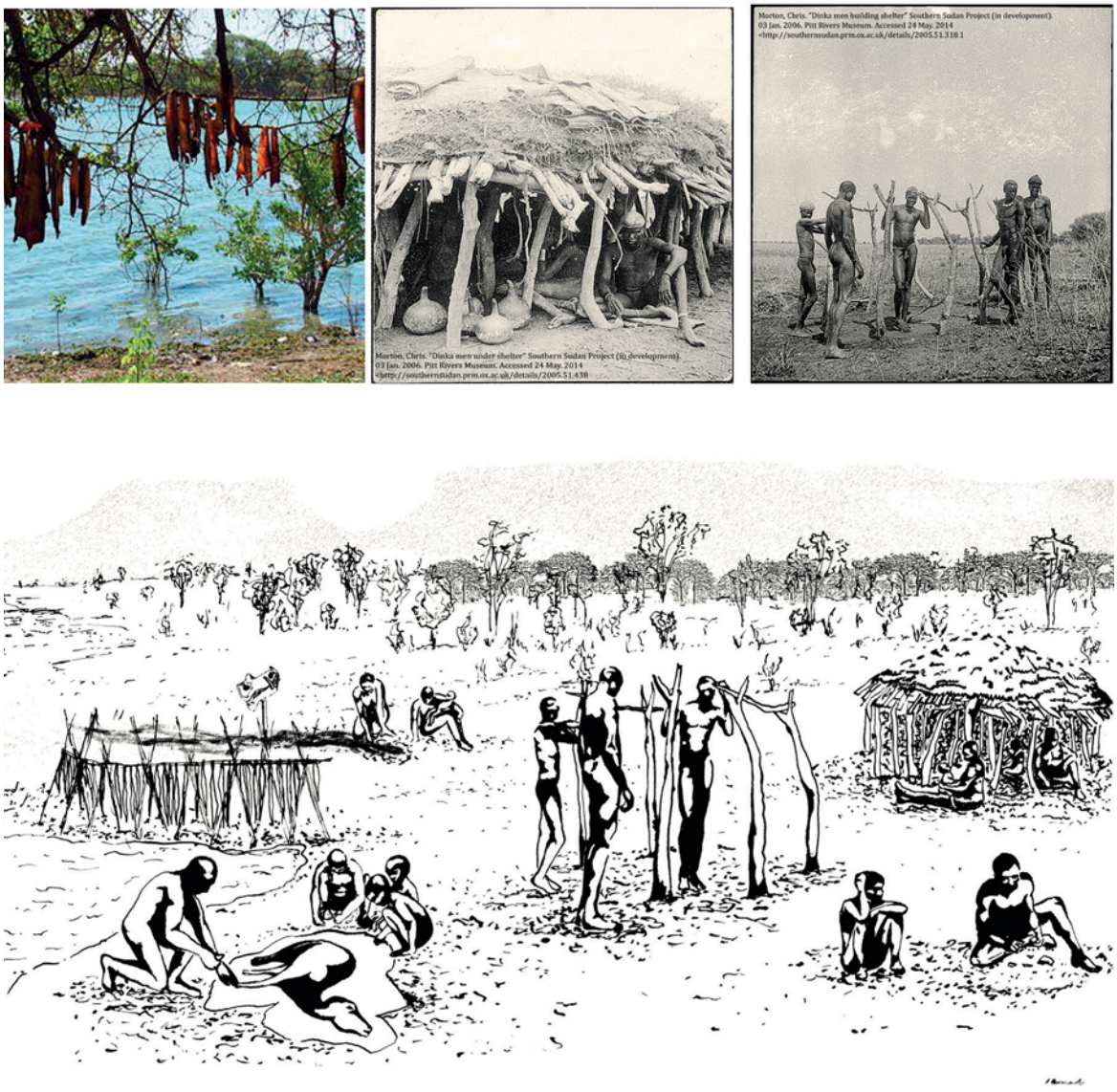

Fig. 5.6. Parallels and functional reconstruction of encampment installations at AFD23: top left, drying meat on branches at Dinder National Park; top center and right, simple irregular shelter of the Dinka people at the beginning of the 20th century; bottom, reconstruction drawing of the campsite at Affad 23

of drying meat. An analogous interpretation for much less numerous posthole pits was proposed for a Late-Pleistocene 'fishing' site in Upper Egypt (Vermeersch, Paulissen, and Huyge 2000).

In turn, the abundance of recorded cut features in the southwestern zone of AFD23 or the area around the hearth feature discovered at AFD24, which evidently acted as a focal point for activities concentrated on the selection and processing of stone raw materials, suggests the central role of these parts of the sites in the functioning of the Late-Pleistocene hunter-gatherer campsites. The small pits seem to reflect irregular technical features of a kind similar to those discovered in the northeastern and southern zones of AFD23. The irregular clusters of posts could suggest a simple screen protecting from the sun and wind, still used today by communities living in the upper course of the Nile [*Fig. 5.6* top center and right].

The larger depressions seem to have had a different function, although the precise purpose (technical? storage?) cannot be indicated. The edges of these cuts are not overheated, hence they could not have functioned as sunken hearths, such as those known from Late-Pleistocene sites at Arkin 5 or Sodmein Cave (Chmielewski 1968; Van Peer et al. 1996; Van Peer and Vermeersch 2007). Similar features are known from several sites of slightly later date in central Egypt, including HK26 at Wadi Kubbaniya (Banks et al. 2015), where numerous posthole pits also occurred in the vicinity.

Archaeological features demonstrating use of fire at AFD23 and AFD24 are known only in the form of locally overheated patches of clayey silt in subsurface sections. This is seen as indicating fires being lighted on the surface of sandy sediments (for example, 23.D.1b) once covering these subsurface layers. One of these overheated places (AFD23, feature P1) is situated in a ground relief depression sealed with another layer of silt and was dated using thermoluminescence to 46.4 ± 4.0 ka (Lub-6432). It is currently one of the more certain indications of the age of the MSA campsite (Osypiński et al. 2021). The small dimensions of these features point to the relatively temporary use of fire at MSA campsites. In the context of potential meat drying, it seems justified to interpret this particular hearth as the main source of smoke meant to ward off insects.

Chapter 6

MSA ADAPTATION STRATEGIES IN THE AFFAD BASIN MICROREGION: TENTATIVE RECONSTRUCTION OF HUMAN BEHAVIOR IN LATE PLEISTOCENE SUB-SAHARAN AFRICA

The Middle Stone Age is central to the emergence of human culture and its expansion beyond Africa and the Great Bend of the Nile, including the Southern Dongola Reach, a key element of the middle section of the Nile Valley. Without detailed research into the prehistory of this region one cannot hope to understand the nature of the human species' first migrations from the plains of the East African lake region northward to the Egyptian section of the Nile valley and the Mediterranean coast. The importance of this geographical relationship has long been recognized by researchers dealing with the prehistory of Africa (Arkell 1949; Marks, Hays, and de Heinzelin 1968; Wendorf and Schild 1992; Van Peer 1998; Goder-Goldberger 2013; Leplongeon, Goder-Goldberger, and Pleurdeau 2020).

The no-longer-active channels of the great tributaries of the Nile, such as Wadi Muqaddam, Wadi el-Melik or Wadi Howar, are widely considered as potential pathways for the spread of early humans. However, the geographical complexity of the Nile Valley, which is quite commonly referred to as the migration "corridor" of the earliest *Homo sapiens*, is compromised by the notion about its transitory character. Taking the metaphor further, looking back through an "Eurasian door" into the "Nile corridor" we see only a relatively well-lit "East African room" from where the first people left. In this research perspective, the Nile Valley area looms as an inhospitable region with climate fluctuations powering a "push-pull" migration mechanism of only slightly milder form compared to that occurring in the neighboring deserts. Yet, a look at human settlement in Nubia from a local perspective (e.g., Wendorf 1968) gives quite the opposite impression, one of a complex process of adaptation of human groups over hundreds of millennia. From this point of view, the "Nile corridor" appears as more than just a passageway to a promised land, indeed, as a place that was actually hospitable and preferential for longtime occupation. It is in this context that the microregion of the Affad Basin, located in the Great Bend of the Nile in Sudan and in the vicinity of the great potential pathways mentioned above, takes on significance as a place where the hydrological network is limited to just the main channel of the Nile extending north toward the Third Nile Cataract.

As it turns out, a favorable coincidence of geological, hydrological and ecological factors in the period after the late Pleistocene turned the complex of archaeological loci discovered by the PalaeoAffad Project in the Affad region into a unique compendium of data on the everyday life and activities of human groups inhabiting the area about 50,000 years ago. Research conducted here over the past few dozen years has significantly supplemented the current state of knowledge on the environment and ecology of early human communities in this region, as well as their adaptation strategies over time. The notable input of this microregional study is threefold, concerning as it does three categories of finds: osteological faunal remains, tangible evidence of human settlement and, last but not least, lithic artifacts providing a window on stone tool production and use

as practiced by the Middle Stone Age (MSA) communities. A "high-resolution", interdisciplinary and multi-faceted analysis of the data coming from the limited area of the Affad Basin has yielded results related to a broader spatial and temporal context. It goes without saying that the present volume is dedicated to the investigation of sites dated to the MSI3 in this microregion, while assemblages of other date await a separate study.

The wealth of faunal material coming from the PalaeoAffad research enabled an archaeozoological study of models of exploitation of the environment, listing the most frequently hunted species and identifying diverse hunting strategies in the context of seasonal variability and availability of specific animal species. Discrete ecological niches explored by humans in the Affad region in the rainy season about 50,000 years ago comprised a woodland savannah with all the richness of its fauna, stretching from the edge of the uplands down to the banks of the river. Incidentally and rather unexpectedly, the research has shown that the African auroch—a species previously not identified this far south in the Nile Valley—was not only an element of the late Pleistocene animal world, but was also an extremely important species in the hunting model of MSA people inhabiting the Great Bend of the Nile. In the dry winter season human settlements drew closer to the channels of the meandering river Nile, while the people explored exposed chert outcrops and riparian forests inhabited by fauna, hunting mainly kob antelopes and other small animals. Large fish were caught and even freshwater clams were harvested for their meat.

Mineralized osteological remains of animals were found in conjunction with settlement remains, that is, places where hearths had burned and features, like postholes and small pits, had been cut. The recording of this second category of finds, which is absolutely unique in this part of north-eastern Africa, has given pioneering insight into the organization of settlement space among early humans from the Late Pleistocene in this area.

A close examination of lithic artifacts found within these settlements and associated with faunal remains has been effective in tracing successive stages of stone tool production and use practiced by the Middle Stone Age (MSA) communities: from ways of obtaining raw materials, through the initial stages of the development of semi-finished products, to the final result, including the distribution of the tools themselves (both in a formal and functional sense). Based on the archaeological data, the presence of stone processing workshops has been proposed, including identification of correlates of the learning processes associated with the working of specific raw materials. The caveat is that these collections represent the output of groups inhabiting a small area. Consequently, the adaptive model presented on these grounds could well be only one of many possible models functioning during the mid-Paleolithic stage of human development.

Levallois technologies have long been considered as long-time "survivors" in the Nile Valley (Vignard 1928; Caton-Thompson 1946; Arkell 1949). The term "epi-Levalloisian" was adopted for Levallois artifacts found in relatively young geological contexts (on the surface of flooding terraces) that could not be dated precisely. Interestingly, an allochthonous southern origin was assumed for some of the defined industries of this type (e.g., Sebilian; Marks 1968d), despite the lack of similarly dated sites from excavations in Sudan. The few "epi-Levalloisian" locations mentioned by Anthony J. Arkell (1949) along almost the entire length of the central section of the Nile Valley represented somewhat incidental, surface collections.

Another important assumption accompanying the idea of Levallois technology surviving south of Nubia is its connection with a humid climate and, therefore, with an environment much richer than that currently present in Egypt or northern Sudan. There is a growing

body of data on this subject coming from the current debate about adaptive models and very limited settlement of semi-desert and desert areas by mid-Palaeolithic communities (e.g., Groucutt and Blinkhorn 2013 with further literature). The palaeo-environmental research in Affad has contributed to this debate a clear picture of the environment of human groups using Levallois tools in this part of the Nile Valley: a wet riparian forest surrounded by a woodland savannah.

6.1 STONE RAW MATERIAL PROCESSING IN THE AFFAD MICROREGION

The Affad collection of stone artifacts comprises finds from the surface and from limited test excavations at site AFD23 (more than 6500 objects) and other sites in its vicinity (altogether more than 10,000 artifacts). State-of-the-art mapping of the finds using DEM models has resulted in a precise projection of mutual spatial relations, as well as the context of other categories of archaeological sources (bone remains, cut features and elements of the topography). This, in turn, has led to a functional identification of given locations, including areas where stone raw materials were processed, such as the southwestern sector of AFD23, among others.

Large chert pebbles constituted the main raw material processed at AFD23. Such pebbles are found in river sediments and they would have been brought to the encampment most likely from the immediate vicinity. The quality of the raw material was tested first as indicated by the numerous examples of nodules with only a few negative scars of detached flakes, interpreted as evidence of testing. Their size usually exceeded several centimeters in diameter. Other rocks were processed only *ad hoc*; one might even venture to say that most of the other raw materials had been brought to AFD23 in ready form. The best example of this are the single ferruginous sandstone products, including prefabricated bifacial forms, probably of significantly older age. Therefore, it should be assumed that chert in the form of large pebbles was the target material that fulfilled the manufacturing (and utility) expectations of the group at AFD23. The large percentage of abandoned nodules, sometimes in the form of initial cores, should be seen as an indication of a stable supply, whether because the preferential raw material was found in abundance in the immediate surroundings of the site or the group had no problems seeking it out. Nodules were collected from natural exposures (river channels); there is no evidence at Affad (or anywhere in Nubia for that matter) of intentional chert extraction by mining.

Analyses of the horizontal stratigraphy of refitted blocks from AFD23 indicated areas of from two to several square meters for individual blocks. Lying on the contemporary surface, in what was a loose sandy sediment prone to erosion, artifacts were more or less dispersed. However, assemblages from sealed layers have revealed surprisingly clear clusters, confirming their non-displaced nature, further substantiated by finds of almost complete antelope limbs retaining an anatomical arrangement. Therefore, given the broad dispersal of chert nodules processed on a small-scale (including refittings of initial cores), it should be assumed that the quality of stone material was being tested in almost every part of the encampment, most probably over a long period. This would constitute circumstantial evidence for concluding that the site in question was a seasonal campsite for a small group of people (judging by the size of the encampment) who returned to it in the dry season more than once to "harvest" chert pebbles from exposed gravel

layers. Needless to say, the postholes interpreted as remains of light wooden installations are a further clue suggesting longer stays in one location. These observations are extremely important from the point of view of modelling the settlement of late Pleistocene groups.

While the handiness of chert raw material seems an obvious factor, it may well be that chert was not the main reason for settling here. Processed products of much smaller size and the absence of any initial cores at a location barely 300 m away from the southwestern "chert" encampment could indicate that in the northern zone all of the necessary stone tools were brought or collected in the immediate vicinity, and that only core forms of a significantly reduced size were processed on the spot. This is obviously an entirely different approach to the task of acquiring stone tools, one that was also observed at a nearby site, AFD24, where the vast majority of tools (and other products) was brought from outside. The two sites with collections dominated by sandstone products, AFD131 and AFD111, are more difficult to interpret. It is not clear (because of erosion of the artifacts which makes their refitting arduous at best) whether nodules were fully processed here, but, in view of the location far from any natural outcrops of this material, the rationale of the Middle Palaeolithic tool users would have been to bring in raw material already tested in terms of its quality, and possibly even pre-processed. Even were we to stop at analysing just the artifact inventories (as is the case with most of the mid-Palaeolithic sites devoid of everything but stone finds), our investigations could still move towards defining different cultural, or at least functional units.

Three basic Levallois-tool production technologies were reconstructed based on the material from Affad. The first of these is related to the production of Levallois flakes from rectangular flaked cores, dressed from two opposite sides in a preferential pattern. Cores of this type had the dimensions of the flaking surface, which allowed for the detachment of a product approximately 50 mm long and 40 mm wide. In the final phases of reduction, the flaking surface of the cores was observed to change from rectangular, with two opposite striking platforms, to centripetal with a circular/omnidirectional platform. The share of each of these two categories of cores in an assemblage could reflect the progress in reduction of core forms rather than an actually different approach to the formation of a flaking surface. Among the refitted nodules of flake cores, only one represented a recurrent pattern, where a series of several flakes was detached from a flaking surface that was not remodeled at any time. However, given the high degree of irregularity of the end products (with striking platforms facetted every time), they were damaged probably already at the manufacturing stage and discarded along with the other production waste. This suggests a training experience, perhaps even "experimental" processing, rather than a well-learned recurrent pattern of intentional creation of a series of flakes, commonly seen as a step in the evolution of Levallois technology toward blade production (e.g., the well-documented refitting series from Taramsa; Van Peer, Vermeersch, and Paulissen 2010).

The second recorded method is a standard production of triangular points from a flaking surface formed from only one side (the actual striking platform). This type of processing was carried out also in a preferential system, remodeling the flaking surface after the detachment of each end product. The refittings did not reveal a single sequence of the repeated use of the same core. Instead, they showed a series of operations performed after a point had been detached, meant to remodel the relief of the flaking surface in the same convention as before.

The third method, reconstructed solely on the basis of observation of the cores and the points themselves, constituted a variation of the so-called "Nubian" method of preparing the core for the detachment of a point. Negative scar fragments forming the axial convexity of the flaking surface

were recorded on several residual cores, starting from the side edges or even from the distal part of the flaking surface. In the case of several points, which, however, could not be reassembled, similar negative scars were also recorded. Since a complete production sequence was not traced in the refittings, it is impossible to say whether this method was used from the very beginning as a different method of forming a flaking surface, or only in the final stages of reduction (as indicated by the already small core forms present in the collection). It should be noted, however, that examples of cores of this type with much larger dimensions are also known from other mid-Palaeolithic sites in Nubia (and not only there).

Several core forms resembling prismatic single-platform cores are not necessarily correlates of blade production methods being practiced at the site. They are relatively large and the processing is of an initial nature, hence they are more likely to be the result of testing the material, if not simply accidental. Blades hypothetically produced in this way were not used to create any tools in a manner recognizable enough to be identified by technological or formal analyses. Flake products that fulfilled the parametric criteria for blades (possessing a length twice their width) came only from working the edge of the flaking surface of Levallois flake cores. Single examples of residual and heavily worn microlithic cores (as well as microliths themselves), recorded at AFD23 in secondary contexts, should most probably be associated with a Holocene settlement in the immediate vicinity of the site.

Small discoidal forms made of crude flakes present a mystery as such. These were not Halfan-type cores (the ones with microchipping in the distal part of the flaking surface), nor has there been any record at the site of any kind of tool being produced from such a small Levallois end product. However, one should assume that the small-sized core forms themselves could have had utility for the toolmakers.

Neither is there any evidence of bifacial tool production at AFD23. The only example of such a processing method comes from the surface and was found very heavily eroded. Since it was made of ferruginous sandstone, it must have been brought to the encampment somewhere from outside as a complete form. It seems that all bifacial points known from the Affad Basin were probably found in the late Pleistocene within even earlier sites in the immediate vicinity (Osypińska and Osypiński 2015).

The study of the stone collections from the Affad Basin has demonstrated a specific dichotomy in the perception of stone products between the producers and the users. Recognizing that in the Paleolithic era everyone used stone tools, but not everyone had the skills to make them, one can adopt a different perspective. The refitted Levallois flakes and points need not have been used at all, or they could have served as provisional tools to be discarded with other production waste. In turn, tool behavior is demonstrated by a whole range of initial flakes or the result of accidental flaking. The dominant form of tool adaptation was denticulate retouching of the longer edge of a blank (flakes and points). In several cases, the presence of burin scars was also noted. The use of such a procedure at the base of a point suggests deliberate thinning for hafting. However, the examples from Affad show that it was applied to irregular flakes. In a few cases, semi-abrupt retouching of crude flakes was also noted, resulting in irregular racloirs/scrapers.

It is proposed for the stone collections in question that they are for the most part the effect of training or even learning of techniques and methods of tool-making in what is now called the "Levallois" tradition. The suggestion is based on observations regarding the supply-based nature of the southwestern zone of site AFD23, the presence of processing remains, and the

treatment of end products of several reconstructed processes (that is, discarding them at the place of production). Failed attempts to thin the bases of starting flakes with the help of a burin-blow procedure, as well as faceting the striking platform in the initial stages of processing, when the dorsal face of a flake had not yet been prepared, constitute further proof in favor of this idea. More research and further refittings, among others, should help to confirm the validity of this hypothesis. It is a question in point just how ancient people familiarized themselves with a whole arsenal of technical procedures that allowed tools to be made for hundreds of millennia in almost unchanged form.

The actual impact of this technological tradition is another issue. Were the techniques of producing Levallois points still being taught 16,000 years ago along the Nile (as suggested by the dating of Nubian industries—Sebilien, Gemaian and Halfan—the stone traditions of which were based on Levallois methods)?[1] Could the myth that accompanied this process have been so long-lasting? Or did the cognitive and psychomotor behaviors of our species in the Middle Palaeolithic always lead to similar results, until and only when the various demographic revolutions gave rise to convergent inventions of microlithization in eastern and southern Africa, as well as Asia?

6.2 HUNTING MODELS AND ADAPTATION STRATEGIES IN THE AFFAD MICROREGION

The often excellent condition of animal bone remains from Affad allowed archaeozoological studies to proceed far beyond a simple list of identified taxa that is the only obtainable result in the case of most open MSA sites in the Nile Valley. The wealth and diversity of faunal data from the Late Pleistocene sites in Affad substantiate the statement that early humans explored every available ecological niche in their surroundings depending on its inherent environmental and seasonal dynamics.

Two basic hunting models appear to have been put in practice in Affad, one for the dry season and the other for the rainy season. In both cases, however, the focus was on capturing animals from the Bovidae family, namely: Bovinae, Reduncinae, Antilopinae and Alcelaphinae.

Hunting in the dry season, when seasonal river channels tended to be low-level and meandering, the MSA hunters concentrated on territorial, middle-sized kob antelopes that inhabited mainly riparian forests and wetlands. However, the gamut of species caught in this season—hippopotamus, grivet, porcupine and dik-dik—reflect a wide range of hunting techniques. Not the least, low water levels, as well as shallows and puddles formed in the dry season, favored meat from sources other than hunted mammals, for example, large and middle-sized fish. Large catfish seem to have been preferred, possibly because fishing techniques were limited to catching by hand or spearing with a simple stick. A single site with preserved, burnt concentrations of Nile oyster shells suggest knowledge of how to consume the meat of these mollusks, which is a valuable source of protein

[1] The AFD23 assemblage is currently dated to the MIS3 period, but the dating of records from Nubia remains unchanged. Moreover, blade industries dating to the Pleistocene period are not known from the region south of the Second Nile Cataract.

and vitamins. Interestingly, there is no record of bird remains at any site in Affad. Either bird-hunting skills were not in place or there was no need to explore the world of the avifauna.

Remains of so-called megafauna, namely elephants and hippopotamuses, deserve separate comment. They were recorded in two contexts: in small clusters on the periphery of the encampments and in large concentrations (always one species at a time) at other loci, classified here as "killing/butchering sites" based on a negligible number of stone artifacts in each case. The Affad evidence in itself does not bear out the possibility of MSA communities having the hunting skills to hunt such large and dangerous animals. Perhaps we are dealing here with instances of taking advantage of accidentally encountered carrion to obtain necessary raw materials, bone in this case.

The other adaptation model was employed in the rainy season when hunters readily explored the slightly drier environment of the savannah, away from the immediate vicinity of the river. High-water levels in the river and the flood zone under water would have forced people to move to higher ground, closer to the edge of the plateau. The findings from Affad suggest slightly different hunting preferences on the part of people inhabiting such an ecosystem. Here, the preferred hunting species seem to have been aurochs, and in the longer term, also other animals inhabiting the woodland savannah, namely giraffes, buffalos, oribi, zebras, but also porcupines and perhaps elephants, hyenas, and the African wild dogs (although the presence of the latter predators may also be associated with their desire to take advantage of waste left behind by people).

Light wooden installations were observed at the encampments, in context with stone processing workshops and animal carcasses suggesting butchering activities. The purpose of hearths and slightly larger cavities/pits found alongside these remains is unclear, possibly technical or storage. With no clear pattern to these remains, it would be misleading to attempt to reconstruct the form of these shelters, the first to be set up perhaps during a seasonal stay at the encampment. Modern ethnographic parallels (e.g., postholes around a fire) often show the ambiguity of such reconstructions. Beyond doubt, however, these MSA communities installed some kind of structures that involved wooden posts being dug into the ground. One can even venture the hypothesis that the skills to build such structures were part of the system of adaptation of groups of people in the era of migration beyond Africa, facilitating, and perhaps even enabling a successful adaptation to new conditions.

* * *

Research at Affad has expanded and deepened significantly the perception of MSA communities living in the Nile Valley and northeastern Africa. The wealth of data and the diverse sources from the Affad sites have granted insight into the cultural package of Middle Palaeolithic hunters and gatherers: their stone processing skills, organization of space, hunting techniques, and not the least, their adaptation strategies to explore different ecological niches. It seems to have been an optimal living environment, offering a great variety of opportunities to obtain food without excessive effort or risk. It is a pity that the Palaeolithic sites at Affad have succumbed to modern progress and are irretrievably lost. One is left with the hope that what was discovered at Affad is a harbinger of other open sites from the period and that the results presented in this study will act as an incentive to other researchers to seek and investigate them.

LIST OF FIGURES AND TABLES

LIST OF FIGURES

Maps, plans, drawings, photos, editing of documentation and data processing by Piotr Osypiński (Palaeo-Affad Project) unless indicated otherwise.
DEM model and editing of images Paweł Wiktorowicz (PalaeoAffad Project).

CHAPTER 4

CHAPTER 5

LIST OF TABLES

CHAPTER 2

CHAPTER 3